

Methods in
Molecular Biology 2636

Springer Protocols

Ava J. Udvardia
James B. Antczak *Editors*



Axon Regeneration

Methods and Protocols

MOREMEDIA



Humana Press

METHODS IN MOLECULAR BIOLOGY

Series Editor

John M. Walker

School of Life and Medical Sciences

University of Hertfordshire

Hatfield, Hertfordshire, UK

For further volumes:

<http://www.springer.com/series/7651>

For over 35 years, biological scientists have come to rely on the research protocols and methodologies in the critically acclaimed *Methods in Molecular Biology* series. The series was the first to introduce the step-by-step protocols approach that has become the standard in all biomedical protocol publishing. Each protocol is provided in readily-reproducible step-by-step fashion, opening with an introductory overview, a list of the materials and reagents needed to complete the experiment, and followed by a detailed procedure that is supported with a helpful notes section offering tips and tricks of the trade as well as troubleshooting advice. These hallmark features were introduced by series editor Dr. John Walker and constitute the key ingredient in each and every volume of the *Methods in Molecular Biology* series. Tested and trusted, comprehensive and reliable, all protocols from the series are indexed in PubMed.

Axon Regeneration

Methods and Protocols

Edited by

Ava J. Udvardia

Department of Biology, Appalachian State University, Boone, NC, USA

James B. Antczak

Office of Technology Development, Medical College of Wisconsin, Milwaukee, WI, USA

Editors

Ava J. Udvardia
Department of Biology
Appalachian State University
Boone, NC, USA

James B. Antczak
Office of Technology Development
Medical College of Wisconsin
Milwaukee, WI, USA

ISSN 1064-3745

ISSN 1940-6029 (electronic)

Methods in Molecular Biology

ISBN 978-1-0716-3011-2

ISBN 978-1-0716-3012-9 (eBook)

<https://doi.org/10.1007/978-1-0716-3012-9>

© The Editor(s) (if applicable) and The Author(s), under exclusive license to Springer Science+Business Media, LLC, part of Springer Nature 2023

This work is subject to copyright. All rights are solely and exclusively licensed by the Publisher, whether the whole or part of the material is concerned, specifically the rights of translation, reprinting, reuse of illustrations, recitation, broadcasting, reproduction on microfilms or in any other physical way, and transmission or information storage and retrieval, electronic adaptation, computer software, or by similar or dissimilar methodology now known or hereafter developed.

The use of general descriptive names, registered names, trademarks, service marks, etc. in this publication does not imply, even in the absence of a specific statement, that such names are exempt from the relevant protective laws and regulations and therefore free for general use.

The publisher, the authors, and the editors are safe to assume that the advice and information in this book are believed to be true and accurate at the date of publication. Neither the publisher nor the authors or the editors give a warranty, expressed or implied, with respect to the material contained herein or for any errors or omissions that may have been made. The publisher remains neutral with regard to jurisdictional claims in published maps and institutional affiliations.

This Humana imprint is published by the registered company Springer Science+Business Media, LLC, part of Springer Nature.

The registered company address is: 1 New York Plaza, New York, NY 10004, U.S.A.

Preface

Axon growth capacity is essential for the establishment of neural circuitry in developing organisms, and for the repair of neural circuitry damaged by injury or disease in mature animals. The capacity for axon growth is acquired by neurons upon terminal differentiation. Interestingly, neurons utilize a molecular toolkit for axon growth and guidance that is remarkably well conserved between central and peripheral neurons over the course of animal evolution. However, despite the high degree of conservation of these mechanisms, the ability of neurons to regenerate axonal connections after axotomy varies widely on the basis of phylogeny and ontogeny.

Developing neurons in both the peripheral nervous systems (PNS) and central nervous systems (CNS) of virtually all animals can regenerate damaged axons. However, among mature neurons with established connections, mammalian CNS neurons do not normally regenerate their axons even though mature PNS neurons retain the capacity for axon regrowth. Amphibians such as frogs display a similar ability for axon regeneration in both CNS and PNS neurons prior to metamorphosis, but post metamorphosis, most CNS neurons lose the ability for axon regeneration with the exception of retinal ganglion cells. In contrast, neotenic amphibians such as axolotls, which reach sexual maturity without metamorphosis, have a lifelong capacity for CNS axon regeneration in the spinal cord and optic nerves. Fish species also demonstrate this lifelong capacity for axon regeneration in the CNS. Understanding the molecular differences between neurons capable of axon regeneration and those lacking this ability poses a fascinating problem for both basic scientists and clinical researchers.

The poor prognosis for functional recovery by patients suffering CNS nerve injuries has fueled the search for therapeutic strategies to promote functional rewiring of disrupted axonal connections. Over the past decade, a number of methodologies and model systems have facilitated the discovery of basic mechanisms regulating axon regeneration. Both *in vitro* and *in vivo* models have been employed to reveal the cellular and molecular apparatuses that promote axon regeneration in the neurons of model systems capable of functional regeneration, and that prevent functional regeneration of axons in the adult mammalian CNS.

The chapters in this book cover a broad range of approaches utilized to decipher cellular and molecular mechanisms enabling successful axon regeneration that in turn may be manipulated to promote functional recovery in human patients. The techniques described employ a variety of model systems including rodent (Chaps. 1, 2, 3, 4, 5, 6, 7, and 8), amphibian (Chaps. 11, 13, 16, and 19), fish (Chaps. 9, 10, 12, 14, 15, 17, 18, 20, 21, 23, and 24), and insect (Chap. 22) models utilizing both *in vivo* and *in vitro* approaches. A variety of physical injury models of the brain, spinal cord, retina, optic nerves, and peripheral neurons are described, including nerve crush, nerve transection, contusion injuries, laser axotomy, chemical damage, light damage, and enucleation. The protocols herein also

describe methods for the isolation/analysis of various macromolecules including mRNA, ncRNA, epigenetic markers, proteins, and lipids isolated from regenerating nervous tissues, including computational methods for various “-seq” analyses including scRNA-seq and TRAP-seq. Finally, methods for live and fixed imaging of regenerating axons and for quantifying behavioral endpoints enable measurements of regenerative success.

Boone, NC, USA
Milwaukee, WI, USA

Ava J. Udvardia
James B. Antczak

Contents

<i>Preface</i>	<i>v</i>
<i>Contributors</i>	<i>ix</i>
1 Defining Selective Neuronal Resilience and Identifying Targets for Neuroprotection and Axon Regeneration Using Single-Cell RNA Sequencing: Experimental Approaches	1
<i>Anne Jacobi and Nicholas M. Tran</i>	
2 Defining Selective Neuronal Resilience and Identifying Targets of Neuroprotection and Axon Regeneration Using Single-Cell RNA Sequencing: Computational Approaches	19
<i>Salwan Butrus, Srikant Sagireddy, Wenjun Yan, and Karthik Shekhar</i>	
3 Retinal Ganglion Cell Axon Fractionation	43
<i>Sean D. Meehan and Sanjoy Bhattacharya</i>	
4 Analysis of Immediate Early Gene Expression Levels to Interrogate Changes in Cortical Neuronal Activity Patterns upon Vision Loss	55
<i>Sara R. J. Gilissen, Maroussia Hennes, and Lutgarde Arckens</i>	
5 Noncoding Regulatory RNAs: Isolation and Analysis of Neuronal Circular RNAs and MicroRNAs	71
<i>Michela Dell’Orco, Grigorios Papageorgiou, Nikolaos Mellios, and Nora I. Perrone-Bizzozero</i>	
6 Transneuronal Delivery of Cytokines to Stimulate Mammalian Spinal Cord Regeneration	85
<i>Daniel Terheyden-Keighley, Marco Leibinger, Charlotte Zeitler, and Dietmar Fischer</i>	
7 Epigenomic Profiling of Dorsal Root Ganglia upon Regenerative and Non-regenerative Axonal Injury	101
<i>Franziska Müller, Jessica S. Chadwick, Simone Di Giovanni, and Ilaria Palmisano</i>	
8 Profiling Locally Translated mRNAs in Regenerating Axons	145
<i>Pabitra K. Sahoo and Jeffery L. Twiss</i>	
9 Analysis of Axonal Regrowth and Dendritic Remodeling After Optic Nerve Crush in Adult Zebrafish	163
<i>An Beckers, Steven Bergmans, Annelies Van Dyck, and Lieve Moons</i>	
10 Assaying Optic Nerve Regeneration in Larval Zebrafish	191
<i>Beth M. Harvey, Melissa Baxter, and Michael Granato</i>	
11 Surgical Methods in Postmetamorphic <i>Xenopus laevis</i> : Optic Nerve Crush Injury Model	205
<i>Alexis M. Feidler, Hieu H. M. Nguyen, and Fiona L. Watson</i>	
12 Generating Widespread and Scalable Retinal Lesions in Adult Zebrafish by Intraocular Injection of Ouabain	221
<i>Diana M. Mitchell and Deborah L. Stenkamp</i>	

13	A Reproducible Spinal Cord Crush Injury in the Regeneration-Permissive Axolotl.	237
	<i>Sarah Walker, Tiago Santos-Ferreira, and Karen Echeverri</i>	
14	Live Imaging of Axonal Dynamics After Laser Axotomy of Peripheral Neurons in Zebrafish	247
	<i>Kadidia P. Adula and Alvaro Sagasti</i>	
15	Rapid Testing of Gene Function in Axonal Regeneration After Spinal Cord Injury Using Larval Zebrafish	263
	<i>Louisa K. Drake, Marcus Keatinge, Themistoklis M. Tsarouchas, Catherina G. Becker, David A. Lyons, and Thomas Becker</i>	
16	Translating Ribosome Affinity Purification (TRAP) and Bioinformatic RNA-Seq Analysis in Post-metamorphic <i>Xenopus laevis</i>	279
	<i>Gregg B. Whitworth and Fiona L. Watson</i>	
17	LCM-Seq for Retinal Cell Layer-Specific Responses During Optic Nerve Regeneration	311
	<i>Wesley Speer and Matthew B. Veldman</i>	
18	Profiling Dynamic Changes in DNA Accessibility During Axon Regeneration After Optic Nerve Crush in Adult Zebrafish	323
	<i>Sumona P. Dhara and Ava J. Udvardia</i>	
19	Quantitative Proteomics of Nervous System Regeneration: From Sample Preparation to Functional Data Analyses.	343
	<i>Dasfne Lee-Liu and Liangliang Sun</i>	
20	Live Cell Imaging of Dynamic Processes in Adult Zebrafish Retinal Cross-Section Cultures	367
	<i>Manuela Lahme and David R. Hyde</i>	
21	PCNA Staining of Retinal Cryosections to Assess Microglial/Macrophage Proliferation.	389
	<i>Anna G. Lovel and Diana M. Mitchell</i>	
22	<i>Drosophila</i> Laser Axotomy Injury Model to Investigate RNA Repair and Splicing in Axon Regeneration.	401
	<i>Qin Wang, Shannon Trombley, Mahdi Rashidzada, and Yuanquan Song</i>	
23	Assessing Rewiring of the Retinal Circuitry by Electroretinogram (ERG) After Inner Retinal Lesion in Adult Zebrafish	421
	<i>Lindsey M. Barrett, Peter C. Meighan, Diana M. Mitchell, Michael D. Varnum, and Deborah L. Stenkamp</i>	
24	Analysis of Visual Recovery After Optic Nerve Crush in Adult Zebrafish	437
	<i>An Beckers, Steven Bergmans, Annelies Van Dyck, and Lieve Moons</i>	
	<i>Index</i>	449

Contributors

- KADIDIA P. ADULA • *Department of Molecular, Cell and Developmental Biology, University of California, Los Angeles, CA, USA*
- LUTGARDE ARCKENS • *Department of Biology & Leuven Brain Institute, KU Leuven, Leuven, Belgium; Laboratory of Neuroplasticity and Neuroproteomics, Katholieke Universiteit Leuven, Leuven, Belgium*
- LINDSEY M. BARRETT • *Department of Biological Sciences, University of Idaho, Moscow, ID, USA*
- MELISSA BAXTER • *Department of Cell and Developmental Biology, Perelman School of Medicine, University of Pennsylvania, Philadelphia, PA, USA*
- CATHERINA G. BECKER • *Centre for Discovery Brain Sciences, University of Edinburgh, Edinburgh, UK; Center for Regenerative Therapies Dresden (CRTD), Technische Universität Dresden, Dresden, Germany*
- THOMAS BECKER • *Centre for Discovery Brain Sciences, University of Edinburgh, Edinburgh, UK; Center for Regenerative Therapies Dresden (CRTD), Technische Universität Dresden, Dresden, Germany*
- AN BECKERS • *Neural Circuit Development and Regeneration Research Group, Animal Physiology and Neurobiology Section, Department of Biology, Leuven Brain Institute, KU Leuven, Leuven, Belgium*
- STEVEN BERGMANS • *Neural Circuit Development and Regeneration Research Group, Animal Physiology and Neurobiology Section, Department of Biology, Leuven Brain Institute, KU Leuven, Leuven, Belgium*
- SANJOY BHATTACHARYA • *Bascom Palmer Eye Institute, Miller School of Medicine at University of Miami, Miami, FL, USA; Miami Integrative Metabolomics Research Center, Miami, FL, USA; Molecular Cellular Pharmacology Graduate Program, University of Miami, Miami, FL, USA*
- SALWAN BUTRUS • *Department of Chemical and Biomolecular Engineering, UC Berkeley, Berkeley, CA, USA*
- JESSICA S. CHADWICK • *Division of Neuroscience, Department of Brain Sciences, Imperial College London, London, UK*
- MICHELA DELL'ORCO • *Department of Neurosciences, University of New Mexico School of Medicine, Albuquerque, NM, USA*
- SUMONA P. DHARA • *Department of Biological Sciences, University of Wisconsin-Milwaukee, Milwaukee, WI, USA*
- SIMONE DI GIOVANNI • *Division of Neuroscience, Department of Brain Sciences, Imperial College London, London, UK*
- LOUISA K. DRAKE • *Centre for Discovery Brain Sciences, University of Edinburgh, Edinburgh, UK*
- KAREN ECHEVERRI • *Eugene Bell Center for Regenerative Biology and Tissue Engineering, Marine Biological Laboratory, University of Chicago, Woods Hole, MA, USA*
- ALEXIS M. FEIDLER • *Department of Biology & Program in Neuroscience, Washington and Lee University, Virginia, USA*

- DIETMAR FISCHER • *Department of Cell Physiology, Faculty of Biology and Biotechnology, Ruhr University of Bochum, Bochum, Germany; Center for Pharmacology, Institute II of Pharmacology, Faculty of Medicine and University Hospital Cologne, University of Cologne, Cologne, Germany*
- SARA R. J. GILISSEN • *Department of Biology & Leuven Brain Institute, KU Leuven, Leuven, Belgium*
- MICHAEL GRANATO • *Department of Cell and Developmental Biology, Perelman School of Medicine, University of Pennsylvania, Philadelphia, PA, USA*
- BETH M. HARVEY • *Department of Cell and Developmental Biology, Perelman School of Medicine, University of Pennsylvania, Philadelphia, PA, USA*
- MAROUSSIA HENNES • *Department of Biology & Leuven Brain Institute, KU Leuven, Leuven, Belgium*
- DAVID R. HYDE • *Department of Biological Sciences, University of Notre Dame, Notre Dame, IN, USA; Center for Stem Cells and Regenerative Medicine, University of Notre Dame, Notre Dame, IN, USA; Center for Zebrafish Research, University of Notre Dame, Notre Dame, IN, USA*
- ANNE JACOBI • *Center for Brain Science and Department of Molecular and Cellular Biology, Harvard University, Cambridge, MA, USA; F.M. Kirby Neurobiology Center, Department of Neurology, Boston Children's Hospital, Harvard Medical School, Boston, MA, USA*
- MARCUS KEATINGE • *Centre for Discovery Brain Sciences, University of Edinburgh, Edinburgh, UK*
- MANUELA LAHNE • *Department of Biological Sciences, University of Notre Dame, Notre Dame, IN, USA; Center for Stem Cells and Regenerative Medicine, University of Notre Dame, Notre Dame, IN, USA; Center for Zebrafish Research, University of Notre Dame, Notre Dame, IN, USA*
- DASFNE LEE-LIU • *Facultad de Medicina y Ciencia, Universidad San Sebastián, Santiago, Chile*
- MARCO LEIBINGER • *Department of Cell Physiology, Faculty of Biology and Biotechnology, Ruhr University of Bochum, Bochum, Germany; Center for Pharmacology, Institute II of Pharmacology, Faculty of Medicine and University Hospital Cologne, University of Cologne, Cologne, Germany*
- ANNA G. LOVEL • *Biological Sciences, University of Idaho, Moscow, ID, USA*
- DAVID A. LYONS • *Centre for Discovery Brain Sciences, University of Edinburgh, Edinburgh, UK*
- SEAN D. MEEHAN • *Bascom Palmer Eye Institute, Miller School of Medicine at University of Miami, Miami, FL, USA; Miami Integrative Metabolomics Research Center, Miami, FL, USA; Molecular Cellular Pharmacology Graduate Program, University of Miami, Miami, FL, USA*
- PETER C. MEIGHAN • *Department of Integrative Physiology and Neuroscience, Washington State University, Pullman, WA, USA*
- NIKOLAOS MELLIOS • *Department of Neurosciences, University of New Mexico School of Medicine, Albuquerque, NM, USA*
- DIANA M. MITCHELL • *Department of Biological Sciences, University of Idaho, Moscow, ID, USA; Biological Sciences, University of Idaho, Moscow, ID, USA*

- LIEVE MOONS • *Neural Circuit Development and Regeneration Research Group, Animal Physiology and Neurobiology Section, Department of Biology, Leuven Brain Institute, KU Leuven, Leuven, Belgium*
- FRANZISKA MÜLLER • *Division of Neuroscience, Department of Brain Sciences, Imperial College London, London, UK*
- HIEU H. M. NGUYEN • *Department of Biology & Program in Neuroscience, Washington and Lee University, Virginia, USA*
- ILARIA PALMISANO  • *Division of Neuroscience, Department of Brain Sciences, Imperial College London, London, UK*
- GRIGORIOS PAPAGEORGIOU • *Department of Neurosciences, University of New Mexico School of Medicine, Albuquerque, NM, USA*
- NORA I. PERRONE-BIZZOZERO • *Department of Neurosciences, University of New Mexico School of Medicine, Albuquerque, NM, USA*
- MAHDI RASHIDZADA • *Raymond G. Perelman Center for Cellular and Molecular Therapeutics, The Children's Hospital of Philadelphia, Philadelphia, PA, USA*
- ALVARO SAGASTI • *Department of Molecular, Cell and Developmental Biology, University of California, Los Angeles, CA, USA*
- SRIKANT SAGIREDDY • *Department of Chemical and Biomolecular Engineering, UC Berkeley, Berkeley, CA, USA*
- PABITRA K. SAHOO • *Department of Biological Sciences, University of South Carolina, Columbia, SC, USA*
- TIAGO SANTOS-FERREIRA • *Roche Pharma Research & Early Development, Roche Innovation Center Basel, F. Hoffmann-La Roche Ltd., Basel, Switzerland*
- KARTHIK SHEKHAR • *Department of Chemical and Biomolecular Engineering, UC Berkeley, Berkeley, CA, USA; Helen Wills Neuroscience Institute, California Institute for Quantitative Biosciences, QB3, Center for Computational Biology, and Biophysics Graduate Program UC Berkeley, Berkeley, CA, USA*
- YUANQUAN SONG • *Raymond G. Perelman Center for Cellular and Molecular Therapeutics, The Children's Hospital of Philadelphia, Philadelphia, PA, USA; Department of Pathology and Laboratory Medicine, University of Pennsylvania, Philadelphia, PA, USA*
- WESLEY SPEER • *Department of Cell Biology, Neurobiology, and Anatomy, Medical College of Wisconsin, Milwaukee, WI, USA*
- DEBORAH L. STENKAMP • *Department of Biological Sciences, University of Idaho, Moscow, ID, USA*
- LIANGLIANG SUN • *Department of Chemistry, Michigan State University, East Lansing, MI, USA*
- DANIEL TERHEYDEN-KEIGHLEY • *Department of Cell Physiology, Faculty of Biology and Biotechnology, Ruhr University of Bochum, Bochum, Germany*
- NICHOLAS M. TRAN • *Center for Brain Science and Department of Molecular and Cellular Biology, Harvard University, Cambridge, MA, USA; Department of Molecular and Human Genetics, Baylor College of Medicine, Houston, TX, USA*
- SHANNON TROMBLEY • *Raymond G. Perelman Center for Cellular and Molecular Therapeutics, The Children's Hospital of Philadelphia, Philadelphia, PA, USA*
- THEMISTOKLIS M. TSAROUCAS • *Centre for Discovery Brain Sciences, University of Edinburgh, Edinburgh, UK*

- JEFFERY L. TWISS • *Department of Biological Sciences, University of South Carolina, Columbia, SC, USA*
- AVA J. UDVADIA • *Department of Biology, Appalachian State University, Boone, NC, USA*
- ANNELIES VAN DYCK • *Neural Circuit Development and Regeneration Research Group, Animal Physiology and Neurobiology Section, Department of Biology, Leuven Brain Institute, KU Leuven, Leuven, Belgium*
- MICHAEL D. VARNUM • *Department of Integrative Physiology and Neuroscience, Washington State University, Pullman, WA, USA*
- MATTHEW B. VELDMAN • *Department of Cell Biology, Neurobiology, and Anatomy, Medical College of Wisconsin, Milwaukee, WI, USA*
- SARAH WALKER • *Eugene Bell Center for Regenerative Biology and Tissue Engineering, Marine Biological Laboratory, University of Chicago, Woods Hole, MA, USA*
- QIN WANG • *Raymond G. Perelman Center for Cellular and Molecular Therapeutics, The Children's Hospital of Philadelphia, Philadelphia, PA, USA*
- FIONA L. WATSON • *Department of Biology & Program in Neuroscience, Washington and Lee University, Virginia, USA; Department of Biology, Washington and Lee University, Lexington, VA, USA*
- GREGG B. WHITWORTH • *Department of Biology, Washington and Lee University, Lexington, VA, USA*
- WENJUN YAN • *Center for Brain Science and Department of Molecular and Cell Biology, Harvard University, Cambridge, MA, USA*
- CHARLOTTE ZEITLER • *Department of Cell Physiology, Faculty of Biology and Biotechnology, Ruhr University of Bochum, Bochum, Germany; Center for Pharmacology, Institute II of Pharmacology, Faculty of Medicine and University Hospital Cologne, University of Cologne, Cologne, Germany*



Chapter 1

Defining Selective Neuronal Resilience and Identifying Targets for Neuroprotection and Axon Regeneration Using Single-Cell RNA Sequencing: Experimental Approaches

Anne Jacobi and Nicholas M. Tran

Abstract

A prevalent feature among neurodegenerative conditions, including axonal injury, is that certain neuronal types are disproportionately affected, while others are more resilient. Identifying molecular features that separate resilient from susceptible populations could reveal potential targets for neuroprotection and axon regeneration. A powerful approach to resolve molecular differences across cell types is single-cell RNA-sequencing (scRNA-seq). scRNA-seq is a robustly scalable approach that enables the parallel sampling of gene expression across many individual cells. Here we present a systematic framework to apply scRNA-seq to track neuronal survival and gene expression changes following axonal injury. Our methods utilize the mouse retina because it is an experimentally accessible central nervous system tissue and its cell types have been comprehensively characterized by scRNA-seq. This chapter will focus on preparing retinal ganglion cells (RGCs) for scRNA-seq and pre-processing of sequencing results.

Key words scRNA-seq, Retina, Retinal ganglion cell, AAV, Neurodegeneration, Axon, Regeneration, Optic nerve crush

1 Introduction

1.1 Basic Strategy

When central nervous system (CNS) axons are damaged, the neurons have limited potential to survive and recover their lost connections. Numerous strategies have been employed to find ways to protect neurons and stimulate axon regeneration including comparing neurons from different developmental stages [1–3] or species that differ in their regenerative potential [4–7]. Another seldom used but complimentary approach would be to compare neuronal types that differ in their resilience to injury. Selective resilience of neuronal types is a phenomenon that is observed in nearly all neurodegenerative conditions. While underlying mechanisms differ by condition, they are expected to involve a combination of intrinsic factors, such as gene expression, physiology, and

morphology, and extrinsic factors, like somal proximity to the site of injury or interactions with glia and immune cells. It stands to reason that parsing the differences between resilient and susceptible populations would reveal factors that mediate survival and could be potential targets for therapy.

A major challenge in identifying determinants of selective resilience is the immense diversity of neuronal cell types in the CNS. For example, the mouse retina comprises approximately 130 neuronal cell types [8–12], and similar complexities have been observed in other regions of the brain [13–16]. While targeted approaches which utilize genetic lines or immune markers to compare neuronal subsets have identified key mediators of survival and axon regeneration [17–19], these approaches are limited by the availability of labeling tools and are not viable for characterizing all cell types at the same time in a complex tissue. To overcome this challenge, we have developed a scalable pipeline which applies single-cell RNA sequencing (scRNA-seq) to comprehensively profile type-specific gene expression across neuronal types before and after an axonal injury [10].

We developed our protocols using mouse retinal ganglion cells (RGCs) as an experimental system to study axonal injury (Fig. 1). RGCs are one of five neuronal classes in the retina. They are the only projection neurons which transmit visual information from the retina to retino-recipient areas of the brain. RGCs offer several practical advantages for modeling nerve injury. First, their axons pass through the optic nerve, creating a pure white matter lesion model independent of other cell types surrounding/influencing white matter tracts in other parts of the CNS. Second, the optic nerve is accessible through the ocular orbital without requiring stereotactic intracranial surgery. Third, prior to performing nerve injury experiments, we developed a comprehensive cellular atlas of RGCs using scRNA-seq, identifying 46 types. This reference atlas served as a critical foundation for determining type-specific expression changes after injury. We applied our approach to track survival of all RGC types after axonal injury and identify genes correlating with resilience and susceptibility. A companion chapter by Butrus et al. (Chap. 2) will describe a computational workflow for mapping cell types after injury and identifying transcriptional differences between resilient and susceptible populations. These approaches provide a practical demonstration of applying scRNA-seq to determine cell type-specific responses to injury.

1.2 Perturbation Model

We used optic nerve crush (ONC) to model acute axonal injury in RGCs [21, 22]. ONC produces a highly stereotyped pattern of RGC loss, resulting in the degeneration of ~85% of RGCs within 2 weeks after injury (Fig. 2) [10, 23]. While most RGCs degenerate, some survive for several months, providing a clear example of selective resilience [19, 24]. In the following experiments, we characterized RGCs at seven time points from 0 to 14 days

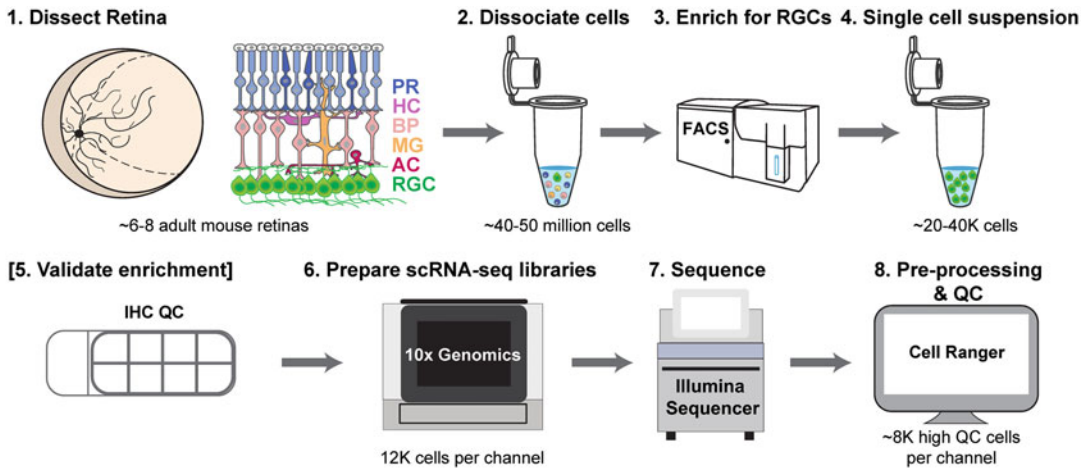


Fig. 1 RGC scRNA-seq workflow. (1) The mouse retina is comprised of five major neuronal classes: photoreceptors (PR), horizontal cells (HC), bipolars (BP), amacrine cells (AC), and retinal ganglion cells (RGCs), which together comprise ~130 cell types. In addition, there are three types of retinal glia: Müller glia (MG), microglia, and astrocytes. For a typical scRNA-seq collection of control adult mouse RGCs, six to eight retinas are dissected from the eye and placed into medium. (2) Retinal cells are dissociated by enzymatic digestion into a single-cell suspension. Cells are then incubated with cell-surface antibodies that detect the target cell population, in this case RGCs. Typical total retinal cell count after **step 2** is ~30–50 million cells (~5–6 million cells/retina). (3–4) RGCs are isolated by fluorescence-activated cell sorting (FACS) and resuspended into a single-cell suspension (expected yield is ~20–40k cells). (5) Enrichment can be verified by immunohistochemistry (IHC) on sorted cells using RGC-specific markers. Due to the limited number of RGCs, it is not recommended to perform enrichment validation for each scRNA-seq collection. (6) Cells are loaded onto the 10× Genomics controller and scRNA-seq libraries are prepared according to the manufacturer’s protocol. (7) scRNA-seq libraries are sequenced on Illumina next-generation sequencing platforms. (8) After demultiplexing and aligning the sequencing data, quality control (QC) is performed to filter for high-quality cells. The expected yield per channel is ~8K high-quality cells. The resulting gene x cell count matrix is utilized for downstream analysis as further described in a companion chapter [20]

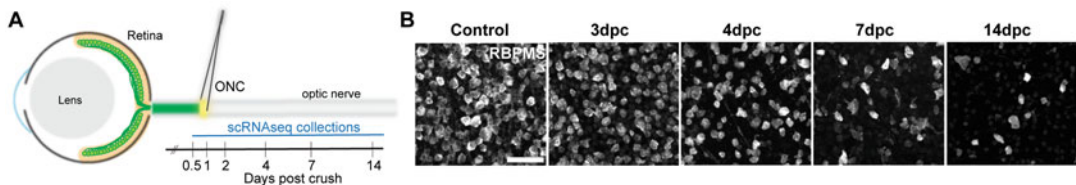


Fig. 2 (a) In Tran et al. [10], RGCs were collected for scRNA-seq from P56 control mice and at six time points following optic nerve crush (ONC) (0.5, 1, 2, 4, 7, 14 days post-ONC). (b) In the ONC model, the axons of RGCs are injured, resulting in progressive RGC degeneration. Whole mount retina IHC micrographs stained with an antibody for the pan-RGC marker RBPMS show RGC loss after ONC, scale bar 50 μm. (Reprinted from Ref. [10], Copyright (2019), with permission from Elsevier)

post-ONC. While our protocols were developed for ONC, they are adaptable to study other perturbations such as models of glaucoma, ischemic injury, or other degenerative conditions.

The ONC model is especially valuable in identifying mediators of axon regeneration. While ONC severs all RGC axons, the pre- and post-lesion optic nerve sheath remains attached, thus leaving a path for regenerating axons to follow. Untreated RGCs exhibit little spontaneous axon regeneration after ONC, but they can be efficiently targeted by adeno-associated virus serotype 2 (AAV2) gene therapy to test the effects of candidate genes on survival and axon regeneration [22]. Several interventions have been identified that boost axon regeneration (Reviewed in [25–27]). Following our scRNA-seq expression screen to identify genes that correlated with resilience and susceptibility, we used AAV2-based approaches to either overexpress putative “resilience” factors or remove “susceptibility” factors by CRISPR-mediated knockdown in RGCs [10]. This identified both positive (*Ucn*, *Timp2*, *Ndnf*, *Prph*) and negative (*Crhbp*, *Mmp9*, *Mmp12*) mediators of survival and axonal regeneration, thereby demonstrating the utility of this approach.

1.3 RGC Purification and scRNA-Seq

This chapter describes protocols for the dissociation and purification of high-quality mouse RGCs for scRNA-seq profiling and pre-processing of scRNA-seq data. Further computational approaches for scRNA-seq analysis are described in a companion chapter by Butrus et al. (Chap. 2) [20]. While our focus is mouse RGCs, the protocols are compatible for collection of other classes of retinal neurons. Since photoreceptors account for ~80% of all retinal neurons [28], it is crucial to enrich for the specific population of interest using approaches such as fluorescence-activated cell sorting (FACS), magnetic cell sorting (MACS), or immunopanning. RGCs in this study were collected by FACS using a combination of Thy1-CD90.2 antibody and *Vglut2-ires-cre; Thy1-stop-YFP Line#15* genetic labeling.

Our cell preparation and purification methods are compatible with both droplet-based (e.g., Drop-seq [8], InDrops [29], 10x Genomics (www.10xgenomics.com), etc.) and plate-based (e.g., Smart-seq2 [30]) scRNA-seq methods. The proper selection of sequencing method is dependent on tissue complexity and desired sequencing depth. Droplet-based approaches enable the profiling of thousands of cells per experiment, but at relatively shallow sequencing depth (target ~50,000 reads per cell). Plate-based approaches like Smart-seq can provide much deeper sequencing depth (target ~1 million reads per cell) but become prohibitively costly and labor intensive for more than a few hundred cells. Since our goal was to characterize expression profiles across the numerous mouse RGC types, we chose droplet-based approaches (10x Genomics). The resulting expression profiles were sufficiently robust to identify cell types and characterize type-specific expression patterns.

2 Materials

2.1 Mouse Strains

Mouse strains are listed below (*see* **Notes 1** and **2**).

1. *C57BL/6J* (JAX # 000664).
2. *Vglut2-ires-cre* (*Slc17a6tm2(cre)Lowl/J* [31], JAX stock #016963).
3. *Thy1-stop-YFP Line#15* (*B6.Cg-Tg(Thy1-EYFP)15Jrs/J* [32], JAX stock #005630).

2.2 Perfusion and Retina Dissection (*See Note 1*)

1. Euthanasia solution: Prepare or purchase a 10× solution containing 390 mg/mL pentobarbital sodium, 50 mg/mL phenytoin sodium to 1× with sterile saline for a 39 mg/mL pentobarbital sodium working solution. Dosage 100–200 mg Euthanasia solution/kg mouse weight.
2. Perfusion pump (peristaltic, including silicone tubing).
3. Small vein infusion set (Butterfly).
4. Surgical scissors (1× fine 22 mm cutting edge, 1× spring scissors 3 mm cutting edge).
5. Hartman Hemostat.
6. Forceps (one pair of straight Adson stainless steel, serrated 1.5 mm tip, two pairs of straight Dumont#5 fine forceps, one pair of curved Dumont#5 fine forceps).
7. 1× PBS (phosphate-buffered saline in ddH₂O), pH 7.4.
8. Disposable transfer pipets (0.8 mL capacity, sterile, polyethylene).
9. Petri dishes (60/15 mm, sterile).
10. Dissecting stereomicroscope (0.63A, 10× ocular).

2.3 Single-Cell Dissociation and RGC Purification

General Note Clean all bench surfaces and instruments when preparing solutions and use filtered tips. Particularly, the inside of the cell culture hood should be cleaned with 70% EtOH beforehand. Wear gloves at all times.

1. Ames' medium powder (*see* **Note 3**).
2. Sodium bicarbonate.
3. ddH₂O.
4. Bovine serum albumin (BSA).
5. 2N–10N NaOH, to adjust pH.
6. Bottle top filtration unit (0.2 PES size).
7. Ovomuroid, 150 mg.
8. DNase I (40,000 U).
9. L-cysteine (152.2 mM).

10. Papain suspension, 100 mg.
11. Calcein blue, 1 mg/mL in DMSO.
12. Trypan blue, stock solution 0.4% (prepared in 0.81% sodium chloride and 0.06% potassium phosphate).
13. 40 μm cell strainer.
14. Millex[®] Syringe Filter Units, sterile, 22 μm .
15. Compressed carbogen gas, oxidizing (5% carbon dioxide USP, 95% oxygen USP).
16. CD90.2 (Thy-1.2) Monoclonal Antibody (53-2.1), APC (Thermo Fisher Scientific, #17-0902-81).
17. Bucket centrifuge capable of 450 $\times g$ spin with 15 mL conical tube inserts, refrigerated to 4 °C.
18. Inverted stereoscope (0.3A, 10 \times objective).
19. Apotome microscope with a differential interference contrast (DIC) filter.
20. Hemacytometer (0.1 mm depth, V-slash loading side, 10 μL loading volume).
21. 15 mL and 50 mL conical centrifuge tubes, polypropylene.
22. 1.7 mL microfuge tube, polypropylene.
23. 4.5 mL fluorescence-activated cell sorting (FACS) collection tubes.

2.3.1 Stock Solutions for Cell Dissociation and RGC Purification

1. Ames' medium: add 8.8 g Ames' medium powder and 1.9 g of sodium bicarbonate to 800 mL of ddH₂O. Stir until fully dissolved and fill up to 1 L with ddH₂O. Filter sterilize through bottle top filtration unit (Subheading 2.3, item 6) and store at 4 °C (*see Note 4*).
2. 4% bovine serum albumin (BSA) stock solution: add 1.8 g BSA to 45 mL Ames' medium, and mix to dissolve completely. Adjust pH to ~7.4 with 2N-10N NaOH. Prepare 1 mL aliquots.
3. 10 \times ovomucoid stock solution (LO): 150 mg BSA, 150 mg ovomucoid, 10 mL Ames' medium, vortex to dissolve. Adjust pH to ~7.4 with 2N NaOH. Prepare 1 mL aliquots.
4. DNase I stock solution: 40,000 units DNase I, 3 mL Ames' medium, vortex to mix. Prepare 50 μL aliquots.
5. L-cysteine (152.2 mM) stock solution: 24 mg L-cysteine, anhydrous, 1 mL ddH₂O. Prepare 50 μL aliquots.

2.3.2 Working Solutions for Cell Dissociation and RGC Purification

General Note Prepare all working solutions fresh on day of use.

1. Prepare oxygenated Ames' medium: Bring ~150 mL filter-sterilized Ames' medium to room temperature. Oxygenate by bubbling with carbogen for at least 15 min (*see Note 5*).

2. Prepare Ames', BSA solution: 27 mL oxygenated Ames' medium, 3 mL 4% BSA stock solution, 3 μ L DNase I stock solution.
3. Prepare 1 \times LO: 1 mL 10 \times ovomucoid stock solution (LO), 9 mL oxygenated Ames' medium, 50 μ L DNase I stock solution.
4. Prepare papain solution: 5 mL oxygenated Ames' medium, 70 μ L papain, 50 μ L DNase I stock solution. Pass through a syringe filter. Add 50 μ L L-cysteine stock solution. Activate at 37 °C for at least 15 min.

2.4 Immunohistochemistry (IHC) and Imaging

1. 1 \times PBS (phosphate-buffered saline in ddH₂O), pH 7.4.
2. Triton X-100, dilute to 10% using 1 \times PBS .
3. Normal donkey serum.
4. Guinea pig polyclonal anti-RBPMS (PhosphoSolutions, #1832-RBPMS).
5. Chicken polyclonal anti-GFP (Abcam, #ab13970).
6. AffiniPure Donkey Anti-guinea pig and Anti-chicken IgG secondary antibodies conjugated to various fluorophores (*see Note 6*).
7. Poly-L-ornithine 0.01%, diluted in molecular grade H₂O.
8. 32% paraformaldehyde, aqueous solution, methanol-free, sealed in 10 mL ampoules.
9. 8-well chamber slide w/removable wells.
10. Slide mounting medium containing DAPI.
11. 22 \times 40 mm glass coverslip, thickness 0.13–0.17 mm.
12. Incubator, temperature set to 62–65 °C.
13. Cell culture incubator with 5% CO₂ saturation, set to 37 °C.
14. Confocal or fluorescent microscope (*see Note 7*).

2.4.1 Working Solutions for IHC

1. Blocking Solution: Add 2.5 mL of rehydrated 100% normal donkey serum, 900 μ L of 10% Triton X-100, and 26.6 mL 1 \times PBS (*see Note 8*).
2. 4% Paraformaldehyde: Add 70 mL of 1 \times PBS to an autoclaved flask, crack open a sealed 10 mL 32% paraformaldehyde (methanol-free) ampoule, add paraformaldehyde to flask, and mix.

2.5 FACS and QC

1. Fluorescence-activated cell sorter (*see Note 9*).
2. ImageJ (Fiji) (<https://imagej.net/Fiji>).
3. Cell ranger (go.10xgenomics.com/scRNA-3/cell-ranger).

3 Methods

General Note The following protocol describes retinal single-cell dissociation, RGC enrichment, and preparation of cells for scRNA-seq. scRNA-seq barcoding and library preparation will vary by method and are not described in this chapter. Experimental examples in this chapter were performed on control RGCs from adult *Vglut2-Cre; Thy1-stop-YFP Line#15* mice for scRNA-seq. For post-injury collections, the number of retinas may need to be increased to account for RGC loss due to injury. Enzymatic dissociation should be limited to ~8 retinas per sample to ensure efficient digestion.

3.1 RGC Single-Cell Dissociation for scRNA-Seq

1. Euthanize ~3–4× mice by intraperitoneal injection of Euthanasia solution or lethal overdose of another approved anesthetic. Confirm deep anesthesia by lack of toe pinch response and transcardially perfuse with ~10 mL 1× PBS until the liver is cleared of blood and draining liquid shows no more blood residues.
2. Enucleate eyes using a curved #5 forceps and place immediately into the oxygenated Ames' medium (*see Note 10*).
3. Dissect out 6–8× retinas in retinas in oxygenated Ames' medium under a stereomicroscope (*see Note 11*). Transfer dissected retinas to a separate dish with oxygenated Ames' medium.
4. Once all retinas are dissected, use a transfer pipet to place retinas into papain solution in a 15 mL conical centrifuge tube, transferring as little oxygenated Ames' medium as possible. Incubate for ~5 min at 37 °C, flick the tube to swirl retinas, and then incubate for an additional ~5 min at 37 °C (Fig. 3a).
5. Remove papain solution, being careful not to disturb retinas, and replace with 2 mL 1× LO solution to stop the enzymatic reaction.
6. Triturate retinal cells plus LO ~10× with a P1000 pipette (Fig. 3b).
7. Let clumps settle for 1–2 min, and transfer 1 mL to a new 50 mL conical centrifuge tube, passing solution through a 40 µm cell strainer.
8. Add 1 mL 1× LO solution to the remaining 1 mL containing cell solution, and triturate ~5–10× with a P1000 pipette.
9. Repeat **steps 7 and 8** until retinal cells plus LO solution appears clear (~4 cycles). Pass remaining 1× LO solution through the 40 µm cell strainer to wash off remaining cells (Fig. 3c).
10. Centrifuge cells at 450 g at 4 °C for 8 min.

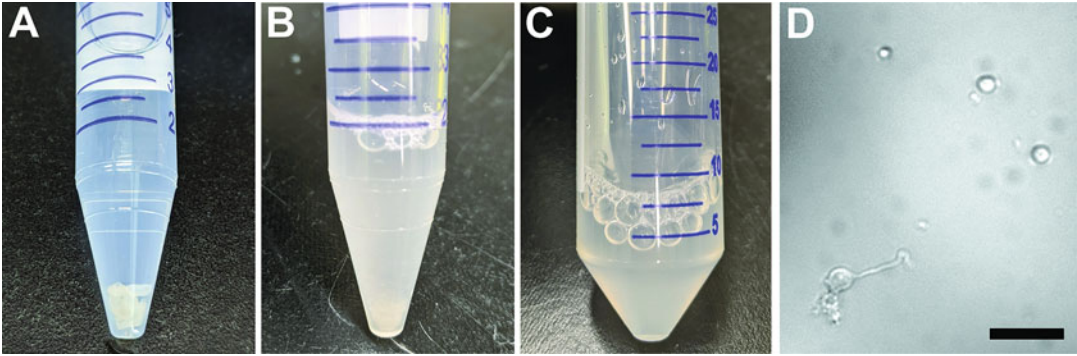


Fig. 3 Retinal cell dissociation. **(a)** Following enzymatic digestion with papain, retinas will still appear “whole.” **(b)** Retinal cells from **(a)** following gentle trituration. **(c)** Retinal cells after LO exchange and filtration; cells should be fully homogenized and no visible clumping present. **(d)** Dissociated retinal cells counterstained with Trypan blue; viable cells will be Trypan blue negative and should generally appear round and vary in size. Some cells will still have attached processes (bottom left cell). Cells were pipetted onto a slide, coverslipped, and imaged on an Apotome microscope, scale bar 100 μm

11. Remove supernatant and resuspend cells in $\sim 300\text{--}500\ \mu\text{L}$ Ames', BSA solution, depending on the initial number of retinas.
12. Use $\sim 4\ \mu\text{L}$ cells diluted $100\times$ in oxygenated Ames' medium to count cells using a hemocytometer. Counterstaining with Trypan blue can be used to assess viability; dilute Trypan blue stock solution 1:10 into cell mixture before loading onto hemocytometer. At this stage, retinal cells should be fully dissociated. Cells will vary in size and most should appear rounded, but some cells will still have attached dendritic or axonal processes (Fig. 3d). The expected yield per retina is approximately five million cells.
13. Dilute cells to 10^7 cells/ $100\ \mu\text{L}$ and mix gently using a $200\ \mu\text{L}$ pipette tip. Add $0.5\ \mu\text{L}$ APC-CD90.2 antibody/ 10^7 cells, mix gently by pipetting, and incubate at RT for 15 min (*see Note 12*).
14. Add 6 mL Ames', BSA solution and centrifuge cells at $450\times g$ at $4\ ^\circ\text{C}$ for 8 min.
15. Remove supernatant and resuspend cells in Ames', BSA solution ($\sim 7\times 10^6$ cells/ $1\ \text{mL}$ Ames', BSA solution).
16. Transfer to 4.5 mL FACS collection tubes by running through a $40\ \mu\text{m}$ cell strainer, add $1\ \mu\text{L}$ Calcein blue/ $1\ \text{mL}$ cell solution, and invert tube to mix.

3.2 FACS

1. Mix cells by vortexing gently.
2. Place the tube onto the FACS machine (*see Note 9*).
3. Place a 1.5 mL microfuge tube containing $150\ \mu\text{L}$ of oxygenated Ames' medium into the collection slot.

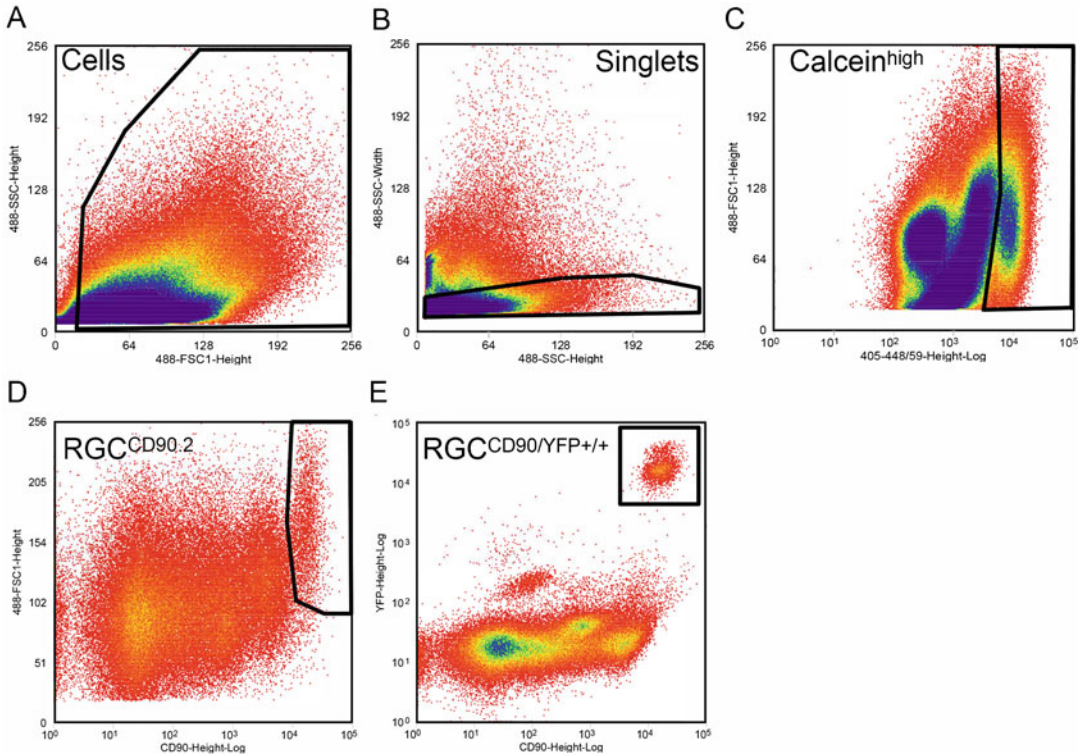


Fig. 4 Example FACS gating for RGC purification. Gates are set to meet the following criteria: **(a)** side scatter (SSC-height) and forward scatter (FSC-height) to select cells from debris; **(b)** SSC-height and SSC-width to select “singlet” cells; **(c)** Calcein “high” population to select viable cells; **(d)** RGCs are identified as “large” CD90.2-positive cells; **(e)** RGCs labeled in the *Vglut2-Cre* reporter line are CD90.2+, YFP+. Gating on A, B, C, and E yielded >95% RGCs. If not using the *Vglut2-Cre* line, gating on A, B, C, and D will yield ~60–70% RGCs

4. Set a FACS gate based on the SSC-height and FSC1-height to identify cells (Fig. 4a).
5. Set a FACS gate based on the SSC-height and SSC-width to identify single cells or “singlets” (Fig. 4b).
6. Set a FACS gate based on the FSC1-height and Calcein blue intensity (405–448/59-height) to select for viable cells (Calcein blue high) (Fig. 4c).
7. Set a FACS gate based on FSC1-height and APC (CD90-height) to select for large CD90+ cells (Fig. 4d).
8. Set a FACS gate based on Yfp-height and APC (CD90-height) to select for Yfp+, CD90+ cells (Fig. 4e).
9. Sort by positive selection using the gates set in **steps 4–8** at a rate of ~2000–5000 events per second, maintaining an efficiency of >80%.
10. Continue sorting through the entire sample before proceeding to either Subheading 3.3 or 3.4 (see **Note 13**).

3.3 Validation of Enrichment (See Note 14)

1. Prior to immunostaining, coat an 8-well chamber slide by adding 250 μL /well of 1:200 poly-L-ornithine in molecular grade H_2O . Dry the slide completely by evaporation in a 62–65 $^\circ\text{C}$ incubator (takes \sim 3 h).
2. Following FACS, spin cells at 450 $\times g$ at 4 $^\circ\text{C}$ for 8 min.
3. Resuspend in 50 μL oxygenated Ames' medium, pipetting up and down to dissolve the pellet.
4. Plate \sim 10,000 cells per well and incubate at 37 $^\circ\text{C}$ in a cell culture CO_2 incubator for 1.5 h to allow cells to settle.
5. Carefully pipet off the medium and fix with 200 μL /well of 4% paraformaldehyde in 1 \times PBS for 20 min at room temperature.
6. Wash twice with 300 μL /well 1 \times PBS for 5 min at room temperature.
7. Add 300 μL of protein blocking solution and incubate for 45 min at room temperature.
8. Incubate with primary antibodies diluted in 300 μL blocking solution (gp αRBPMS 1:1500 dilution, ch αGFP 1:1000 dilution) overnight at 4 $^\circ\text{C}$.
9. Wash twice with 300 μL /well 1 \times PBS for 5 min at room temperature.
10. Incubate with secondary antibodies diluted 1:1000 in 1 \times PBS for 2 h at room temperature (*see Note 15*).
11. Wash twice with 300 μL /well 1 \times PBS for 5 min at room temperature.
12. Add 50–100 μL DAPI Fluoromount-G and coverslip.
13. Image slide by light or confocal microscopy (Fig. 5).

3.4 Single-Cell Sequencing Library Preparation

1. Following FACS, spin cells at 450 $\times g$ at 4 $^\circ\text{C}$ for 8 min.
2. Remove medium and resuspend in \sim 10–20 μL of 1 \times PBS, 0.04% BSA by carefully triturating \sim 15–20 \times (*see Note 16*).
3. Dilute 1 μL of resuspension in 9 μL H_2O and count cells on a hemacytometer. Cells should appear as single isolated cells. If clumping is observed, additional trituration of the resuspension is required.
4. Adjust volume to 1000 cells/ μL .
5. Proceed to single-cell mRNA barcoding and sequencing library preparation (*see Notes 17 and 18*).
6. Sequence scRNA-seq libraries on an appropriate next-generation platform (*see Notes 19 and 20*).

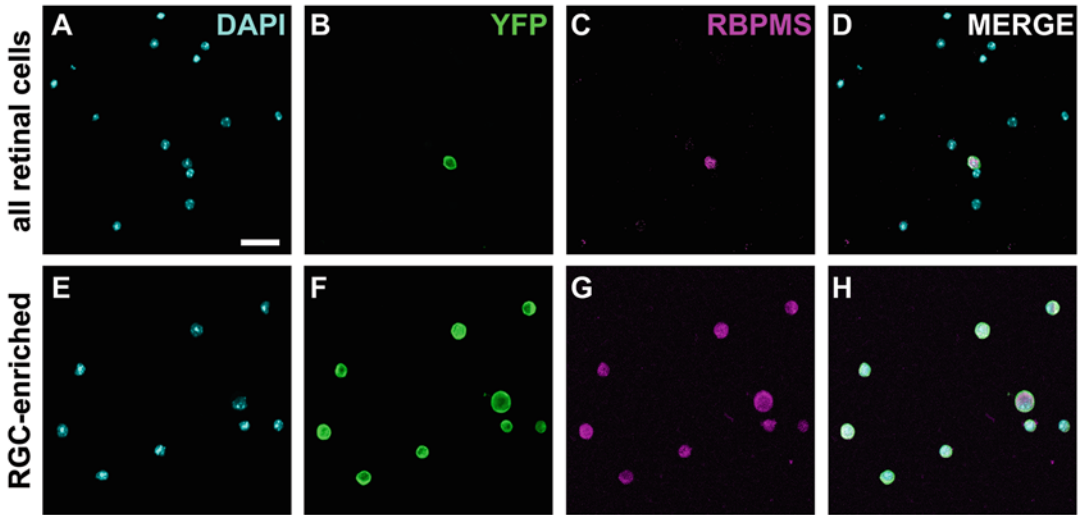


Fig. 5 Validation of RGC enrichment by ICC. (a–d) Staining of all retinal cells (not enriched) collected by FACS with YFP and the RGC-specific marker RBPMS, counterstained with DAPI. <1% of cells are positive for YFP and RBPMS. (e–h) Staining of cells post-RGC enrichment; >95% of cells are double-positive for YFP and RBPMS. Scale bar 50 μm

4 Notes

1. All animal experiments require prior approval by the Institutional Animal Care and Use Committees (IACUC). Each mouse must be euthanized using methods in accordance with the lab's approved IACUC protocol. Experiments performed in this chapter were approved by the IACUC at Harvard University and Children's Hospital, Boston. All experiments were carried out on mice 6–10 weeks including both males and females.
2. In the retina, *Vglut2-ires-cre* specifically expresses Cre recombinase in RGCs. *Thy1-stop-YFP Line#15* is a Cre-dependent conditional line, but when mated to *Vglut2-ires-cre*, Yfp is robustly expressed in RGCs.
3. The formulation of Ames' medium may differ by manufacturer. We recommend using Ames' medium powder from Sigma (Cat. #A1420). The specific formulation of this medium is as follows (all components in g/L): $\text{CaCl}_2 \cdot 2\text{H}_2\text{O}$ 0.169, MgSO_4 0.1488, KCl 0.231, KH_2PO_4 (anhyd) 0.068, NaCl 7.01, L-alanine 0.0024, L-arginine•HCl 0.00421, L-asparagine (anhyd) 0.00084, L-aspartic acid 0.00012, L-cystine•2HCl 0.000065, L-glutamine 0.073, L-glutamic acid•Na 0.001183, glycine 0.00045, L-histidine•HCl• H_2O 0.002513, L-isoleucine 0.00058, L-leucine 0.00144, lysine•HCl 0.003648, L-methionine 0.00039, L-phenylalanine 0.00132,

L-proline 0.00007, L-serine 0.00252, taurine 0.00075, L-threonine 0.00333, L-tryptophan 0.00049, L-tyrosine•2-Na•2H₂O 0.00211, L-valine 0.00176, ascorbic acid•Na 0.01796, D-biotin 0.0001, choline chloride 0.0007, folic acid 0.0001, myoinositol 0.0272, niacinamide 0.0001, D-pantothenic acid•½Ca 0.0001, pyridoxal•HCl 0.0001, riboflavin 0.00001, thiamine•HCl 0.0001, cytidine 0.00073, D-glucose 1.081, hypoxanthine 0.00082, pyruvic acid•Na 0.01333, thymidine 0.00024, uridine 0.00073, sodium bicarbonate 1.9 (add separately)

4. Prepared Ames' medium should be stored at 4 °C and used within 1 week. All stock solutions prepared in Subheading 2.3.1 are using Ames' medium and are then filtered through a sterile Millex[®] Syringe Filter Unit, aliquoted, and frozen at –20 °C until use.
5. Oxygenate Ames' medium prior to preparing working solutions of Ames', BSA solution, 1×LO solution, and papain solution. On the collection day, oxygenate with carbogen (5% carbon dioxide USP, 95% oxygen USP) by attaching a polyethylene tube to a compressed gas tank or other supply and securing a sterile 1 mL pipette tip to the tube ending. Insert tip into the bottle containing Ames' medium, turn on the gas supply to ~500–800 PSI, and bubble for at least 15 min. Proper oxygenation is critical for buffering of cells. We found that oxygenation prior to single-cell dissociation was sufficient to reach the desired pH of 7.4 and reoxygenation was not required. Choosing the appropriate medium is a critical step in protocol optimization. Media are cell type and species-dependent and Ames' medium may not be suitable for non-mouse retinal cells.
6. While various fluorophore conjugates can be used interchangeably, we recommend using a chicken Alexa 488 for detecting anti-Gfp, and either guinea pig Cy3 or Cy5 anti-RBPMS. Select fluorophores that are compatible with your imaging setup.
7. Slides can be imaged with most standard confocal or fluorescent microscope setups. Users should ensure that the lasers and/or fluorescent filters are compatible with the IHC fluorophores. For these experiments, we used a Zeiss 710 and an Olympus FVA with a 20× objective and 405, 488, 568, and 633 lasers.
8. Protein blocking solution can be stored at 4 °C and used for several weeks.
9. For the experiments performed in this chapter, a MoFlo Astrios cell sorter was used; the protocol may need to be optimized for usage on other FACS systems. To execute the sorting as

described, a FACS system with spatially separated lasers that are 405, 488, and 640 nm wavelengths is required. We recommend using a sorting nozzle size of ~100 μm .

10. An optional protocol modification is to add actinomycin D (Millipore Sigma) to suppress novel transcription during cell preparations. Actinomycin D has been shown to reduce the expression of immediate early gene expression (IEG) in scRNA-seq experiments [33, 34]. We found that the addition of 30 μM actinomycin D to solutions in **steps 1–4** and 3 μM to the FACS resuspension buffer 3.1.2 did indeed suppress IEG expression but did not affect clustering or cell assignment [10].
11. Use surgical scissors to remove the cornea and use a curved #5 forceps to remove the lens, separate the retina from the sclera using a straight #5 forceps, cut the sclera along the anterior–posterior axis to the optic nerve head, and peel off the sclera from the retina. Take care to remove vitreous fluid #5 forceps, which will appear as a clear sticky and stringy substance on the inner surface of the retina. Also use a #5 forceps to remove as much of the retinal pigmented epithelium as possible; this pigmented layer will be attached to the outer surface of the retina. Failure to remove the vitreous fluid or retinal pigmented epithelium may cause cells to clump during the dissociation.
12. Required antibody concentrations will vary by target. It is recommended to perform an antibody titration series when optimizing the protocol.
13. The gated population is expected to account for ~0.3% of overall events. The typical FACS yield from 6 \times control retinas collected over ~1–2 h is approximately 20,000–40,000 cells. Yields and collection times will vary in post-ONC collections. After ONC, there is an increased presence of immune/glial cells, some of which may become CD90.2 positive. These cells, however, do not express *Vglut2-Cre* reporter GFP – an advantage when using a reporter line in addition to CD90.2 labeling. They can also be detected during FACS using an antibody against CD45.
14. Confirming enrichment of the target population is an important step to ensuring the efficiency and success of any scRNA-seq experiment. This is especially true when working with low-frequency populations like RGCs, which comprise <1% of total retinal cells. RGC enrichment with this protocol (*Vglut2-cre* reporter line and CD90.2 staining) should yield >95% purity, whereas CD90.2 staining alone yields ~60–70% RGCs. Enrichment can be confirmed by immunocytochemistry on sorted cells using antibodies against GFP and the RGC-specific marker RBPMS. Due to the low yield of RGCs, we recommend performing separate experiments for enrichment validations and scRNA-seq collections.

15. Keep protected from light by wrapping the slide in aluminum foil or placing in a drawer.
16. The cell pellet will likely not be visible after spin down, so it is important to note the orientation of the tube during centrifugation. Approximately 40–50% of cells are lost between the post-FACS and resuspension steps. The resuspension volume should be adjusted to ensure ≥ 1000 cells/ μL concentration, e.g., for a FACS output of 20,000 cells, resuspend in a volume of 10 μL or less. Additionally, since cells are resuspended in $1\times$ PBS, 0.04% BSA instead of medium, it is critical to minimize the timing of **steps 2–5**.
17. scRNA-seq library preparation is not described in this chapter and will differ by platform. User should refer to manufacturer protocols for further instruction (e.g., in this case, 10x Genomics, <https://support.10xgenomics.com/single-cell-gene-expression/library-prep/doc/user-guide-chromium-single-cell-3-reagent-kits-user-guide-v3-chemistry>). Additional equipment and reagents will be required.
18. In Tran et al. [10], scRNA-seq libraries were sequenced on Illumina HiSeq 2500 and Nextseq 500 platforms. The sequencing platform and target read total should be calculated based on the number of libraries and desired sequencing depth. We recommend $\sim 50,000$ reads/cell for RGC scRNA-seq libraries prepared on the 10x Genomics platform. Optimal sequencing depth will vary by target cell type and scRNA-seq library preparation method.
19. Further instructions on the usage of the Cell Ranger software are laid out on the manufacturer’s website (<https://support.10xgenomics.com/single-cell-gene-expression/software/pipelines/latest/what-is-cell-ranger>).
20. To pre-process scRNA-seq data using the Cell Ranger (version 2.1.0, 10X Genomics), use the functions “mkfastq” and “count” to demultiplex scRNA-seq data and align sequencing reads to the appropriate reference genome (e.g., GRCm38 or current version). The output is a gene expression matrix for each library. The Cell Ranger count function has an output file showing basic quality of the data, including total number of reads sequenced, number of reads sequenced per cell, and sequencing saturation; those are useful measures in controlling the depth of the sequencing data. A similar sequencing depth is favorable for data in the same project. Other measures, such as number of reads in cells vs. background and number of genes and transcripts detected per cell, were used for initial cell quality control, but the values could vary depending on Cell Ranger parameters, the cell types captured, and the sequencing methods used. An example Cell Ranger QC report is provided

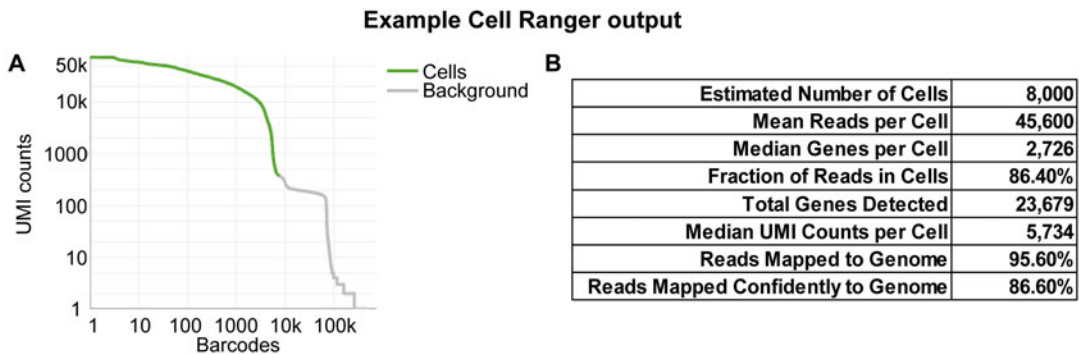


Fig. 6 An example Cell Ranger QC report from a control RGC collection. **(a)** Graph showing the unique molecular identifier (UMI) counts per barcode. Barcoded cells (green) can be distinguished from background (gray) based on a minimum UMI count threshold. For this graph, the estimated number of cells was set to 8000 using the “-forcecells 8000” command based on visual inspection of the graph’s curve. This example is for demonstration purposes only and is not representative of every collection. **(b)** Representative summary statistic ranges from RGC scRNA-seq collections in Tran et al. [10]. Results will vary based on cell type, input cell number, sequencing depth, scRNA-seq library preparation method, etc

in Fig. 6 for demonstration purposes. In Tran et al. [10], a minimum filter of 800 genes/cell was set to remove low-quality cells. For some further information on quality control “best practices,” refer to Hwang et al., Chen et al., and Villani and Shekhar [35–37].

Acknowledgments

We would like to thank Drs. Joshua Sanes and Zhigang He for their mentorship, guidance, and support. We thank Drs. Inbal Benhar and Irene Whitney for their invaluable contributions to the development of retinal cell collection protocols. We also thank Salwan Butrus and Drs. Wenjun Yan and Karthik Shekhar for their critical reading and feedback on this manuscript.

Funding

This work was supported by EY029360 (NIH, NEI) to N.M.T. and Wings for Life Spinal Cord Research Foundation to A.J.

References

- Maclaren RE, Taylor JSH (1997) Regeneration in the developing optic nerve: correlating observations in the opossum to other mammalian systems. *Prog Neurobiol* 53:381–398
- Moore DL, Goldberg JL (2011) Multiple transcription factor families regulate axon growth and regeneration. *Dev Neurobiol* 71:1186–1211. <https://doi.org/10.1002/dneu.20934>
- Goldberg JL, Klassen MP, Hua Y, Barres BA (2002) Amacrine-signaled loss of intrinsic axon growth ability by retinal ganglion cells. *Science* 80(296):1860–1864. <https://doi.org/10.1126/science.1068428>
- Rau A, Dhara SP, Udvadia AJ, Auer PL (2019) Regeneration Rosetta: an interactive web application to explore regeneration-associated gene expression and chromatin accessibility. *G3 Genes Genomes Genet* 9:3953–3959. <https://doi.org/10.1534/g3.119.400729>
- Dhara SP, Rau A, Flister MJ et al (2019) Cellular reprogramming for successful CNS axon regeneration is driven by a temporally changing cast of transcription factors. *Sci Rep* 9:1–12. <https://doi.org/10.1038/s41598-019-50485-6>
- Kizil C, Kaslin J, Kroehne V, Brand M (2012) Adult neurogenesis and brain regeneration in zebrafish. *Dev Neurobiol* 72:429–461. <https://doi.org/10.1002/dneu.20918>
- Van houcke J, Bollaerts I, Geeraerts E et al (2017) Successful optic nerve regeneration in the senescent zebrafish despite age-related decline of cell intrinsic and extrinsic response processes. *Neurobiol Aging* 60:1–10. <https://doi.org/10.1016/j.neurobiolaging.2017.08.013>
- Macosko EZ, Basu A, Satija R et al (2015) Highly parallel genome-wide expression profiling of individual cells using nanoliter droplets. *Cell* 161:1202–1214. <https://doi.org/10.1016/j.cell.2015.05.002>
- Shekhar K, Lapan SW, Whitney IE et al (2016) Comprehensive classification of retinal bipolar neurons by single-cell transcriptomics. *Cell* 166:1308–1323.e30. <https://doi.org/10.1016/j.cell.2016.07.054>
- Tran NM, Shekhar K, Whitney IE et al (2019) Single-cell profiles of retinal ganglion cells differing in resilience to injury reveal neuroprotective genes. *Neuron* 104:1039–1055.e12. <https://doi.org/10.1016/j.neuron.2019.11.006>
- Yan W, Laboulaye MA, Tran NM et al (2020) Mouse retinal cell atlas: molecular identification of over sixty Amacrine cell types. *J Neurosci* 40:5177–5195. <https://doi.org/10.1523/JNEUROSCI.0471-20.2020>
- Rheume BA, Jereen A, Bolisetty M et al (2018) Single cell transcriptome profiling of retinal ganglion cells identifies cellular subtypes. *Nat Commun* 9:2759. <https://doi.org/10.1038/s41467-018-05134-3>
- Yao Z, Nguyen TN, van Velthoven C et al (2020) A taxonomy of transcriptomic cell types across the isocortex and hippocampal formation. *bioRxiv:2020.03.30.015214*. <https://doi.org/10.1101/2020.03.30.015214>
- Tasic B, Yao Z, Graybiuck LT et al (2018) Shared and distinct transcriptomic cell types across neocortical areas. *Nature* 563:72–78. <https://doi.org/10.1038/s41586-018-0654-5>
- Zeisel A, Hochgerner H, Lönnerberg P et al (2018) Molecular architecture of the mouse nervous system. *Cell* 174:999–1014.e22. <https://doi.org/10.1016/j.cell.2018.06.021>
- Saunders A, Macosko EZ, Wysoker A et al (2018) Molecular diversity and specializations among the cells of the adult mouse brain. *Cell* 174:1015–1030.e16. <https://doi.org/10.1016/j.cell.2018.07.028>
- Kaplan A, Spiller KJ, Towne C et al (2014) Neuronal matrix metalloproteinase-9 is a determinant of selective neurodegeneration. *Neuron* 81:333–348. <https://doi.org/10.1016/j.neuron.2013.12.009>
- Bray ER, Yungher BJ, Levay K et al (2019) Thrombospondin-1 mediates axon regeneration in retinal ganglion cells. *Neuron* 103:642–657.e7. <https://doi.org/10.1016/j.neuron.2019.05.044>
- Duan X, Qiao M, Bei F et al (2015) Subtype-specific regeneration of retinal ganglion cells following axotomy: effects of osteopontin and mTOR signaling. *Neuron* 85:1244–1256. <https://doi.org/10.1016/j.neuron.2015.02.017>
- Butrus S, Sagireddy S, Yan W SK (2021) Defining selective neuronal resilience and identifying targets of neuroprotection and axon regeneration using single-cell RNA sequencing – computational Approaches. In: *Methods in molecular biology*. Humana Press Inc., Totowa
- Tang Z, Zhang S, Lee C et al (2011) An optic nerve crush injury murine model to study retinal ganglion cell survival. *J Vis Exp* 2685. <https://doi.org/10.3791/2685>
- Cameron E, Xia X, Galvao J et al (2020) Optic nerve crush in mice to study retinal ganglion

- cell survival and regeneration. *Bioanalysis* 10. <https://doi.org/10.21769/bioprotoc.3559>
23. Galindo-Romero C, Avilés-Trigueros M, Jiménez-López M et al (2011) Axotomy-induced retinal ganglion cell death in adult mice: quantitative and topographic time course analyses. *Exp Eye Res* 92:377–387. <https://doi.org/10.1016/j.exer.2011.02.008>
 24. Pérez de Sevilla Müller L, Sargoy A, Rodriguez AR, Brecha NC (2014) Melanopsin ganglion cells are the most resistant retinal ganglion cell type to axonal injury in the rat retina. *PLoS One* 9:e93274. <https://doi.org/10.1371/journal.pone.0093274>
 25. Yang S-G, Li C-P, Peng X-Q et al (2020) Strategies to promote long-distance optic nerve regeneration. *Front Cell Neurosci* 14:119. <https://doi.org/10.3389/fncel.2020.00119>
 26. Mahar M, Cavalli V (2018) Intrinsic mechanisms of neuronal axon regeneration. *Nat Rev Neurosci* 19:323–337
 27. He Z, Jin Y (2016) Intrinsic control of axon regeneration. *Neuron* 90:437–451
 28. Jeon CJ, Strettoi E, Masland RH (1998) The major cell populations of the mouse retina. *J Neurosci* 18:8936–8946
 29. Klein AM, Mazutis L, Akartuna I et al (2015) Droplet barcoding for single-cell transcriptomics applied to embryonic stem cells. *Cell* 161:1187–1201. <https://doi.org/10.1016/j.cell.2015.04.044>
 30. Picelli S, Faridani OR, Björklund ÅK et al (2014) Full-length RNA-seq from single cells using Smart-seq2. *Nat Protoc* 9:171–181. <https://doi.org/10.1038/nprot.2014.006>
 31. Vong L, Ye C, Yang Z et al (2011) Leptin action on GABAergic neurons prevents obesity and reduces inhibitory tone to POMC neurons. *Neuron* 71:142–154. <https://doi.org/10.1016/j.neuron.2011.05.028>
 32. Buffelli M, Burgess RW, Feng G et al (2003) Genetic evidence that relative synaptic efficacy biases the outcome of synaptic competition. *Nature* 424:430–434. <https://doi.org/10.1038/nature01844>
 33. Wu YE, Pan L, Zuo Y et al (2017) Detecting activated cell populations using single-cell RNA-seq. *Neuron* 96:313–329.e6. <https://doi.org/10.1016/J.NEURON.2017.09.026>
 34. Hrvatin S, Hochbaum DR, Nagy MA et al (2018) Single-cell analysis of experience-dependent transcriptomic states in the mouse visual cortex. *Nat Neurosci* 21:120–129. <https://doi.org/10.1038/s41593-017-0029-5>
 35. Hwang B, Lee JH, Bang D (2018) Single-cell RNA sequencing technologies and bioinformatics pipelines. *Exp Mol Med* 50:96
 36. Chen G, Ning B, Shi T (2019) Single-cell RNA-seq technologies and related computational data analysis. *Front Genet* 10:317
 37. Villani AC, Shekhar K (2017) Single-cell RNA sequencing of human T cells. In: *Methods in molecular biology*. Humana Press Inc., Totowa, pp 203–239



Chapter 2

Defining Selective Neuronal Resilience and Identifying Targets of Neuroprotection and Axon Regeneration Using Single-Cell RNA Sequencing: Computational Approaches

Salwan Butrus, Srikant Sagireddy, Wenjun Yan, and Karthik Shekhar

Abstract

We describe a computational workflow to analyze single-cell RNA-sequencing (scRNA-seq) profiles of axotomized retinal ganglion cells (RGCs) in mice. Our goal is to identify differences in the dynamics of survival among 46 molecularly defined RGC types together with molecular signatures that correlate with these differences. The data consists of scRNA-seq profiles of RGCs collected at six time points following optic nerve crush (ONC) (see companion chapter by Jacobi and Tran). We use a supervised classification-based approach to map injured RGCs to type identities and quantify type-specific differences in survival at 2 weeks post crush. As injury-related changes in gene expression confound the inference of type identity in surviving cells, the approach deconvolves type-specific gene signatures from injury responses by using an iterative strategy that leverages measurements along the time course. We use these classifications to compare expression differences between resilient and susceptible subpopulations, identifying potential mediators of resilience. The conceptual framework underlying the method is sufficiently general for analysis of selective vulnerability in other neuronal systems.

Key words Retinal ganglion cells, Optic nerve crush, Single-cell RNA-sequencing, Machine learning, Supervised classification

1 Introduction

A major hallmark of the mammalian central nervous system is that certain populations of neurons exhibit far greater vulnerability to insults than others. The mechanisms underlying this selective neuronal vulnerability in the context of acute (e.g., traumatic injury) or chronic (e.g., neurodegenerative disease) have been difficult to dissect, but recent advances in scRNA-seq make it possible to compare patterns of gene expression among closely related neuronal types that differ in vulnerability.

We recently explored this strategy in the context of axotomy by analyzing the responses of mouse retinal ganglion cells (RGCs) to optic nerve crush (ONC) [1], a well-studied model of traumatic injury [2]. RGCs are a diverse class of projection neurons, with their diversity in mice comprising >40 discrete types, each with distinct morphological, physiological, and molecular features [3]. Using high-throughput scRNA-seq [4], we derived an *atlas* of 46 molecularly distinct RGC types, a number that is consistent with inventories based on physiology [5] and morphology [6]. Many of these 46 types could be linked 1:1 to previously defined types based on existing molecular knowledge or new histological validation.

Following ONC, ~85% of RGCs die within 2 weeks, and those that survive don't regenerate axons. To determine if specific types are lost at the same or different rates, we profiled RGCs using scRNA-seq from injured retinas at 0, 0.5, 1, 2, 4, 7, and 14 days post crush (dpc) [1]. The companion chapter (please *see* Chap. 1 of this volume) details the experimental methods to profile RGCs using scRNA-seq.

In this chapter, we describe the computational framework introduced in [1] to analyze transcriptomic profiles of injured RGCs over the aforementioned time course aiming to assess type-specific differences in survival and identify gene signatures that correlate with, and may underlie, these differences. Following injury, extensive gene expression changes in RGCs make the inference of type identity challenging. To address this, we devised an iterative supervised classification approach that leverages data from RGCs collected at the intermediate time points. In this approach, transcriptomic signatures of RGC types are successively redefined at each time point to map the cells at the next time point. The underlying method, called iterative-GraphBoost (iGraphBoost), combines a two-step procedure involving gradient boosted trees [7] (**step 1**) and a graph-based voting scheme (**step 2**). This dramatically increases cell type mapping efficiency at later time points and allows us to deconvolve gradual injury-related "state" changes from intrinsic type-specific gene expression programs.

Beginning with an atlas of classified mouse RGCs, we describe a step-by-step workflow to map injured RGCs collected along a time course to the atlas based on their transcriptomic profiles. We quantify the survival dynamics of individual types, identifying resilient and susceptible groups. We then analyze gene expression patterns that correlate with resilience, identifying candidates whose overexpression or knockdown *in vivo* promotes survival and regeneration across RGCs.

2 Materials

We use the Python programming language (version 3.7.4). The source code, together with a Jupyter notebook that reproduces the analysis presented in this chapter, is available in a GitHub repository at https://github.com/shekharlab/mimb_onc_rgc.

2.1 Python Packages

The following Python packages are required and installation instructions are available in the links:

1. Scanpy [8]: a scalable toolkit for single-cell gene expression analysis in Python (<https://scanpy.readthedocs.io/en/stable/>).
2. Harmony [9]: an approach that combines clustering and linear mixture models for single-cell data integration (<https://pypi.org/project/harmony-pytorch/0.1.6/>).
3. XGBoost [7]: a highly effective supervised classification algorithm that combines ensembles of decision trees using gradient boosting (<https://xgboost.readthedocs.io/en/latest/build.html>).
4. Python packages `seaborn`, `sklearn`, `scipy`, `numpy`, and `matplotlib` (*see Note 1*) should be included in standard distributions such as Anaconda (www.anaconda.com) or Miniconda (<https://docs.conda.io/en/latest/miniconda.html>).

2.2 scRNA-seq Datasets

scRNA-seq data are read as sparse matrices of gene expression counts and converted to `AnnData` (Annotated Data) objects using a standard workflow in Scanpy. `AnnData` is a Python class to store and manage annotated data matrices originally introduced in Ref. [8]. Objects of the `AnnData` class are saved on disk in array formats like HDF5 [10] and allow for memory efficient storage and access to large-scale datasets that are increasingly common in scRNA-seq. We use two RGC datasets, both introduced in Ref. [1]:

1. A transcriptomic atlas of uninjured adult RGCs ($n = 35,699$) with each cell identified as a member of one among 45 molecularly defined groups (*see Note 2*). The details underlying data processing, clustering, annotation, and validation are described in [1] and are not covered here.
2. RGCs collected at seven time points following ONC. The time points include 0, 0.5, 1, 2, 4, 7, and 14 days post crush (dpc). Note that the 0dpc dataset serves as an internal negative control to validate the robustness of the inferred transcriptomic signatures in comparison to the atlas [1]. 8456–13,619 RGCs were collected at each of these time points toward a total of 76,646 injured RGCs. Using the atlas as a foundation, we seek to assign type identities to these injured RGCs.

Both datasets are available on the chapter's GitHub page.

3 Methods

We now provide a step-by-step implementation of iGraphBoost. The original analysis in Ref. [1] was performed in the R programming language. Here we reimplement the same in Python using the Scanpy package [8].

3.1 Initializing iGraphBoost with the Adult RGC Atlas

We begin by initializing the Jupyter notebook with the necessary packages.

```
#import general packages
from time import time
import matplotlib.pyplot as plt
import numpy as np
import scanpy as sc
import pandas as pd
from harmony import harmonize
from anndata import AnnData
import anndata
import seaborn as sns
from sklearn.utils import shuffle
import scipy as sp
import matplotlib as mpl
from matplotlib import gridspec
import xgboost as xgb
from sklearn.metrics import confusion_matrix
from random import choices
from typing import Union, Optional, Tuple, Collection, Sequence,
Iterable
from scipy.sparse import issparse, isspmatrix_csr, csr_matrix,
spmatrix
```

Next, we create an AnnData object for the adult RGC atlas, reading in sparse matrices of raw transcript counts and log-normalized expression values (*see Note 3*). We also read in and store metadata corresponding to type identities and experimental batch identifiers as reported in [1].

```
#Read gene expression matrix, cell and gene names corresponding to
row and column identifiers, respectively
adata = sc.read_mtx('atlas.mtx')
atlas_raw = sc.read_mtx('atlas_raw.mtx')

adata = adata.transpose()
adata.layers['raw'] = atlas_raw.X

adata.var_names = pd.read_csv('atlas_vars.csv')['x'].values
adata.obs_names = pd.read_csv('atlas_obs.csv')['x'].values

#Store the type identity and the batch identifier corresponding to
each cell
```

```
adata.obs['Type'] =
pd.Series(pd.read_csv('atlas_type.csv')['x'].values,
dtype='category').values
adata.obs['Batch'] =
pd.Series(pd.read_csv('atlas_batch.csv')['x'].values,
dtype='category').values
```

To visualize the transcriptomic atlas, we perform dimensionality reduction and nonlinear manifold embedding in four steps. First, we identify highly variable genes (HVGs) in the data using the Poisson–Gamma mixture framework [11]. Second, we use these HVGs as features to perform a principal component analysis (PCA), projecting the data onto a lower dimensional subspace whose axes, the so-called principal components (PCs), are linear combinations of the chosen HVGs. The PCs are composite features chosen to maximize the projected variance of the data [12]. Third, to correct for batch effects across biological replicates in the PC space, we use Harmony, an approach that combines maximum diversity clustering and linear mixture models [9]. Fourth, we use Uniform Manifold Approximation and Projection (UMAP) [13] to build a k -nearest neighbor graph in PC space and embed the cells on a 2D projection (*see* Fig. 1a, b). Finally, we visualize the individual genes or combinations of genes identified in Ref. [1] that specifically labeled each type (*see* Fig. 1c).

```
#identify HVGs
from iGraphBoost import meanCVfit
adata.var['highly_variable'] = meanCVfit(adata)

#z-scoring and PCA
adata.raw = adata #store unscaled data for plotting
sc.pp.scale(adata, max_value=10) #scale
sc.tl.pca(adata, svd_solver='arpack') #run PCA

#batch correction using Harmony and visualization using UMAP
Z = harmonize(adata.obsm['X_pca'], adata.obs, batch_key = 'Batch')
adata.obsm['X_harmony'] = Z
sc.pp.neighbors(adata, n_neighbors=25, use_rep='X_harmony')
sc.tl.umap(adata)
```

With the RGC atlas initialized, we now read in the injured RGC dataset.

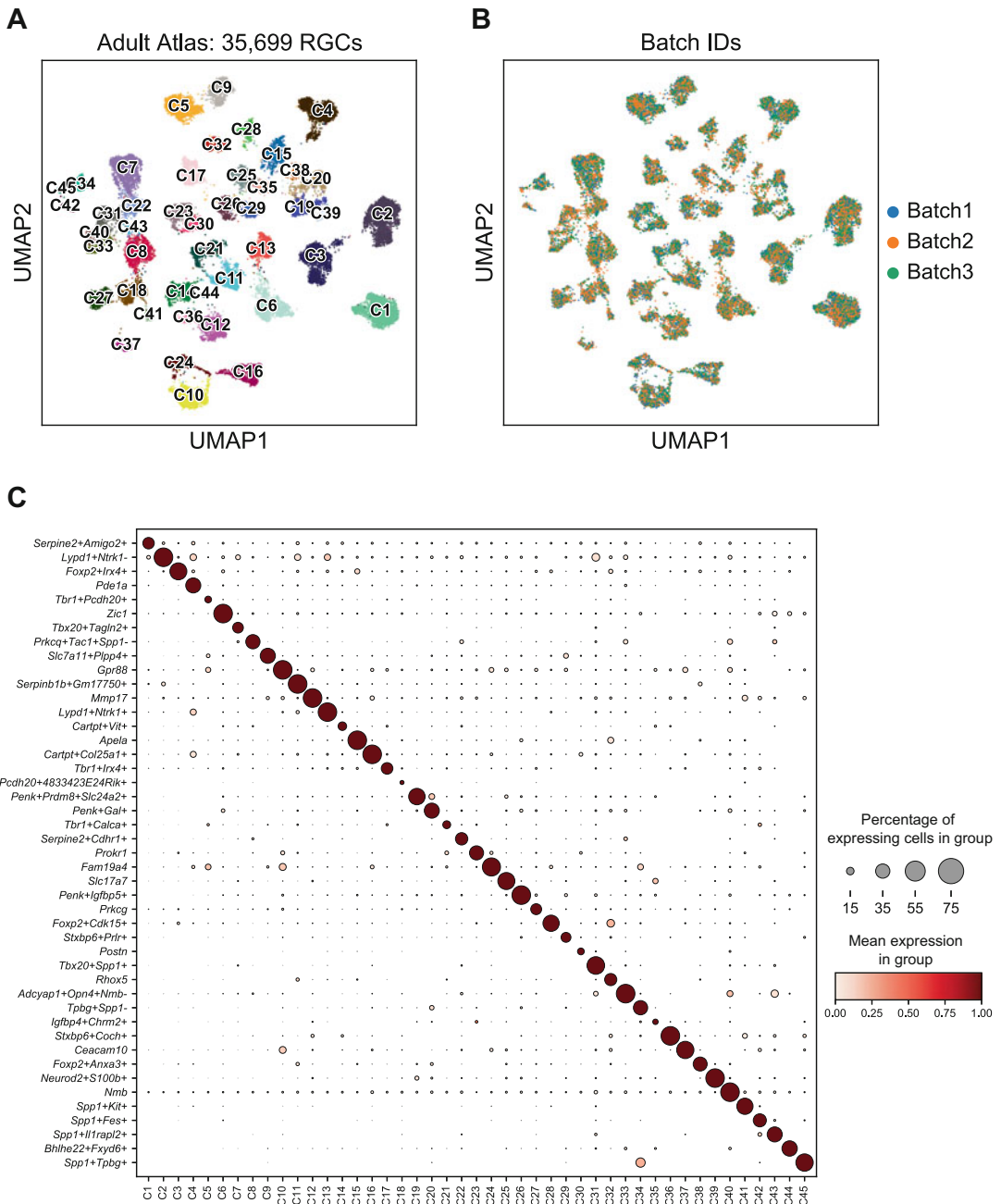


Fig. 1 Adult RGC atlas. **(a)** Transcriptomic diversity of adult RGCs visualized in 2D using UMAP [13]. Each point corresponds to a single RGC, and distance between two cells on the 2D map correlates inversely with their transcriptomic similarity. Colors correspond to RGC types as in the original publication [1]. **(b)** Same as panel a, with cells colored by batch identifier. Each batch corresponds to a biological replicate. **(c)** Dotplot of markers or marker combinations (rows) that uniquely label each of the 45 RGC types (columns). In case of single markers, the size of the circle indicates the percentage of cells expressing the marker, while the color indicates the average normalized expression in the group. Two- or three-marker codes involve the presence of a marker A, and the presence (e.g., $A+B+$ or $A+B+C+$) or absence (e.g., $A+B-$, or $A+B-C+$) of markers B and C. In such cases, the size of the circle indicates the percentage of cells satisfying the expression pattern, and the color depicts the average transcript count of positive markers in the cells, normalized to 1 for each combination

3.2 Read in Injured RGCs as AnnData Objects

The ONC dataset consists of six time points following crush (0.5, 1, 2, 4, 7, and 14dpc) along with a separate control time point (0dpc), expected to resemble the atlas (*see* Fig. 2a). We begin by reading in sparse matrices of raw counts and normalized expression values, each containing all seven ONC time points. The normalized expression values are used for all subsequent analyses except for the feature selection procedure in the function `meanCVfit`, where the raw counts are used. Details on why raw counts are required can be found in Ref. [11] (*see* Note 3).

```
adata = sc.read_mtx(onc_path+'onc.mtx')
adata_raw = sc.read_mtx(onc_path+'onc_raw.mtx')
adata.layers['raw'] = adata_raw.X
adata.var_names = pd.read_csv(onc_path + 'onc_vars.csv')['x'].values
adata.obs_names = pd.read_csv(onc_path + 'onc_obs.csv')['x'].values

adata.obs['Time'] = pd.Series(pd.read_csv(onc_path +
'onc_time.csv')['x'].values, dtype='category').values
```

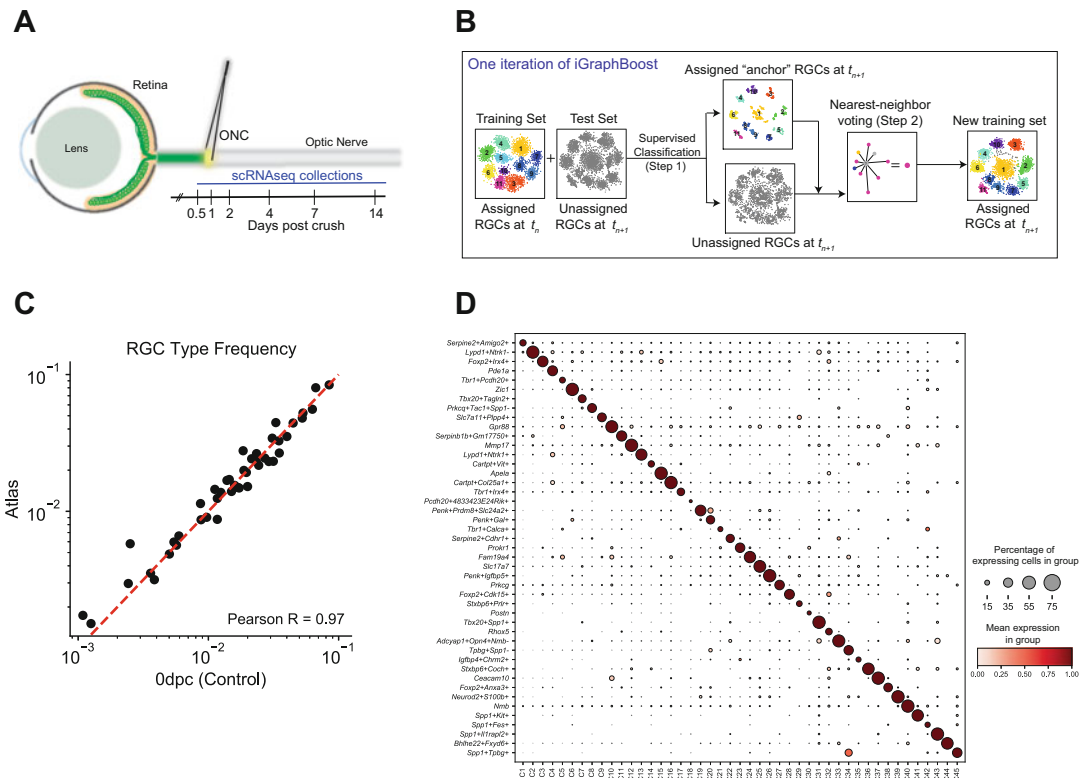


Fig. 2 iGraphBoost overview. (a) scRNA-seq was performed on RGCs collected before and at six times following ONC. 8456–13,619 RGCs were collected at each time point (Adapted from Ref. [1]). (b) Illustration of a single step of the iGraphBoost procedure to classify RGCs collected at time t_{n+1} based on an atlas of RGC types at the previous time point t_n (Adapted from Ref. [1]). (c) Scatter plot of relative frequencies (log–log scale) of each of the 45 types in the atlas (x-axis) and Odpc (y-axis) datasets. (d) Marker dotplot (same as Fig. 1c) in Odpc RGC types, showing consistency with atlas. (a) and (b) are reproduced with permission from Ref. [1])

We then isolate each time point from `adata` and create `AnnData` objects for each time point as shown below for control (0dpc) RGCs, keeping track of experimental batch.

```
ctrl = adata[adata.obs.Time=='Ctrl',:]

#identify and store batch identities
ctrl_batch = []
for i in range(ctrl.shape[0]):
    item = ctrl.obs.index[i].split('_')[0]

    if (item in ['CtC57CD45CD90P1', 'CtC57CD45CD90P2',
'CtC57CD45CD90R1']):
        ctrl_batch.append('CtC57CD45CD90')
    else: ctrl_batch.append(item)

ctrl.obs['Batch'] =
pd.Categorical(ctrl_batch).rename_categories(['Batch1', 'Batch2',
'Batch3', 'Batch4'])

#process in the same way as atlas
ctrl = pre_step1(ctrl)
ctrl.write_h5ad('CtrlONC.h5ad')
```

Here, `ctrl` represents the `AnnData` object for 0dpc RGCs. We repeat this procedure for the data at each of the crush time points to create six objects—`twelveHr` (0.5dpc), `oneday` (1dpc), `twoday` (2dpc), `fourday` (4dpc), `oneweek` (7dpc), and `twoweek` (14dpc). The code for `twelveHr` is shown below, and the code for the other objects, which follow the same template, can be found in the Jupyter notebook in the GitHub repository.

```
twelveHr = adata[adata.obs.Time=='12h',:]

twelveHr_batch = []
for i in range(twelveHr.shape[0]):
    item = twelveHr.obs.index[i].split('_')[0]
    twelveHr_batch.append(item)

twelveHr.obs['Batch'] = pd.Categorical(twelveHr_batch).rename_categories(['Batch1', 'Batch2', 'Batch3', 'Batch4'])

twelveHr = pre_step1(twelveHr)

twelveHr.write_h5ad('twelve_hrONC.h5ad')
```

3.3 iGraphBoost

Overview and

Classification of 0dpc

RGCs

```
#import iGraphBoost functions: available on chapter's GitHub
repository
from iGraphBoost import *
```

iGraphBoost assigns type identities to injured RGCs and is applied successively to each time point. At each time point, we use a two-step procedure to classify RGCs based on a learned taxonomy that leverages information from RGCs classified at preceding time points. This enables the algorithm to deconvolve changes in cell state due to injury from the intrinsic molecular distinction of each RGC type (*see* Fig. 2b).

Briefly, suppose that we have collected injured RGCs at n time points ($t_1 < t_2 < \dots < t_n$) post injury, and we wish to assign type identities (1–45) to each RGC. Beginning with an atlas of uninjured RGCs (denoted as $t_0 < t_1$), iGraphBoost uses a two-step procedure to propagate type labels from the atlas (t_0) to injured RGCs at each time point in successive order. Once classified, injured RGCs at time t_n are used in the classification procedure for RGCs at time t_{n+1} . To demonstrate these steps, we begin by assigning type identities to the first time point—0dpc RGCs (t_1).

3.3.1 Step 1: Supervised Classification

We use XGBoost [7], a gradient-boosted decision tree-based classification framework, to learn a multi-class classifier (denoted C_0) for the adult RGC atlas (t_0) with the aim of using it to classify 0dpc RGCs (t_1). HVGs common to both the atlas and 0dpc RGC datasets are used as features. To learn C_0 , we use a subset of atlas RGCs for training, and use the remaining “held-out” RGCs for validation. The validation subset is used to estimate an empirical test-error rate for the classifier. The classification parameters such as the class weights, number of trees, and the tree depth are chosen to achieve a maximum per-class error rate of less than 5%.

```
atlas = sc.read_h5ad('RGCatlas.h5ad')
ctrl = sc.read_h5ad('CtrlONC.h5ad')

#identify clust-specific atlas genes
atlas_genes = ClusterSpecificGenes(atlas,
                                   genes =
list(atlas.var.index[atlas.var.highly_variable == True]),
                                   obs = 'Type_num')

#subset to genes common b/w atlas and ctrl
var_genes = [i for i in atlas_genes if i in list(ctrl.var.index)]

#train atlas classifier, validate it, then use it to map ctrl
validation_label_train_10, valid_predlabels_train_10,
```

```

test_predlabels = xgbtrainatlas(
    train_anndata = atlas,
    test_anndata = ctrl,
    genes = var_genes
)

#visualize validation results
validationconfmat, validationxticks, validationplot =
plotValidationConfusionMatrix(
    ytrue = validation_label_train_10,
    ypred = valid_predlabels_train_10,
    save_as = 'Atlas_Validation.pdf',
    title = '',
    xaxislabel = 'Predicted',
    yaxislabel = 'True')

```

We next apply C_0 to assign a type identity (1–45) to each of the 0dpc RGCs. For each cell k , C_0 outputs a probability vector $P_{k,0} = (P_{k,0}^1, \dots, P_{k,0}^{45})$, where $P_{k,t}^m$ is the C_0 -assigned probability that cell k belongs to RGC type $m \in (1, 2, \dots, 45)$. Under the hood, this probability is simply the fraction of decision trees in C_0 that vote for class m . Based on $P_{k,0}$, cell k is assigned to class $m_k \in \{1, 2, \dots, 45\}$ such that

$$m_k = \begin{cases} \operatorname{argmax}_m P_{k,0}^m & \text{if } \max(P_{k,0}^m) > \nu \\ \text{"Unassigned"} & \text{otherwise} \end{cases}$$

The parameter ν serves as a decision margin that is chosen as 0.7 for types 1 through 40, and 0.5 for types 41–45. This decision rule is conservative in that it only assigns type identities to cells if the voting margin is much higher than random ($\nu_{\text{random}} = 1/45 \approx 0.023$). We now apply the validated classifier to assign identities to 0dpc RGCs.

```

#store RGC assignments made by classifier
mapping_assignments = []
for i in test_predlabels:
    if i == 45:
        mapping_assignments.append('Unassigned')
    else:
        mapping_assignments.append(str(int(i)+1))

ctrl.obs['Type_iGB'] = mapping_assignments

```

After **step 1**, ~5% of 0dpc RGCs remain unclassified (Fig. 3a). This fraction increases with time as injury-related gene expression changes mask type-specific signatures. This leads us to **step 2**.

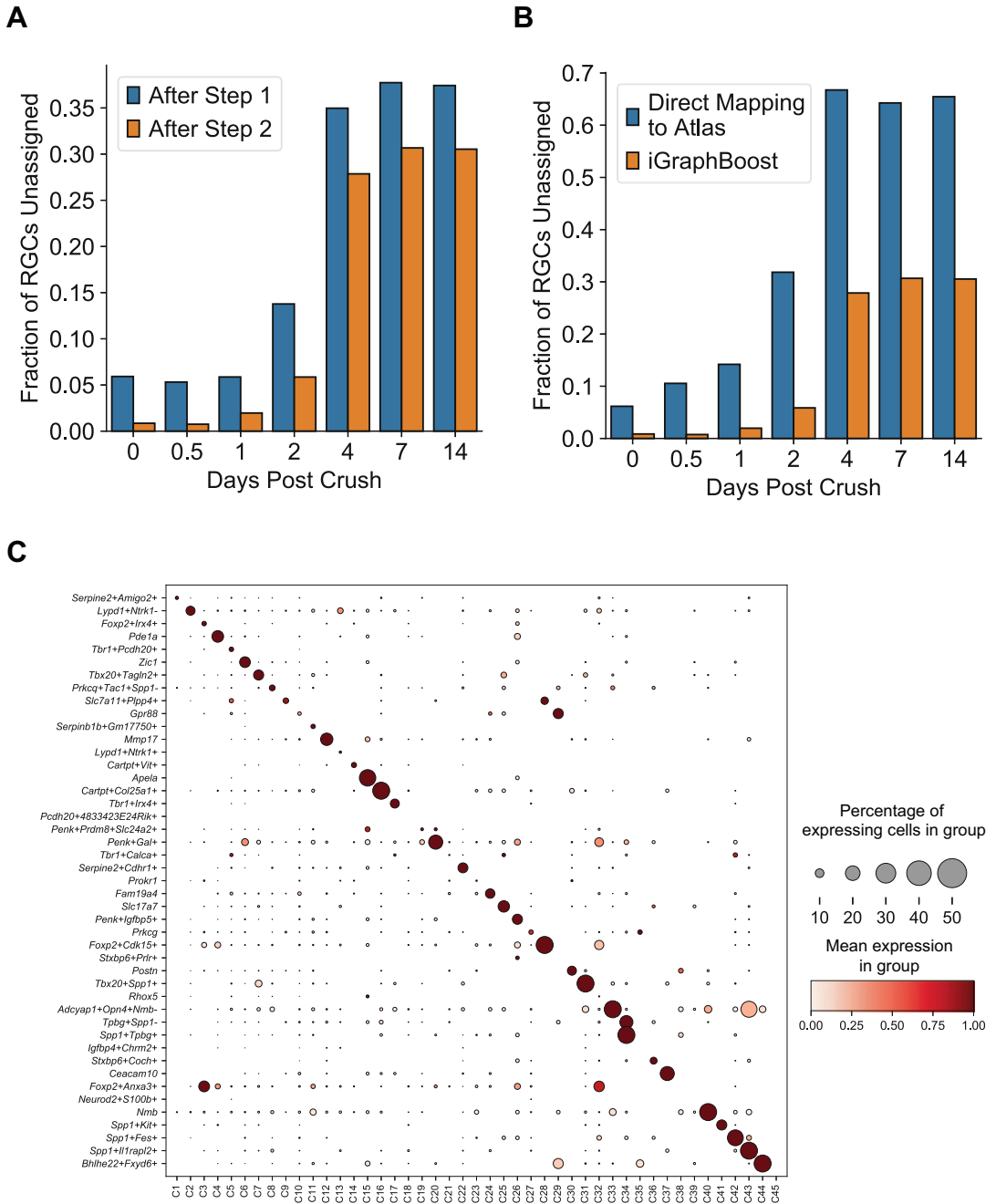


Fig. 3 Performance of iGraphBoost. (a) Contribution of **steps 1** and **2** to the assignment of surviving RGCs at each time point. (b) Fraction of RGCs that remain unassigned at each time point after direct mapping to the atlas or with iGraphBoost. (c) Marker dotplot (same as Fig. 1c) but applied to classified 14dpc RGCs

3.3.2 Step 2: Nearest-Neighbor Voting

In **step 2**, we use the classified cells at 0dpc (t_1) as “anchors” to propagate labels onto the unassigned RGCs by leveraging relationships in a nearest-neighbor (NN) graph (*see* Fig. 2b). We first build a k -NN graph ($k = 15$ neighbors per cell) on the RGCs at t_1 based on the two-dimensional UMAP coordinates (*see* Note 4). As the graph is expected to connect cells with similar transcriptomic profiles, we hypothesized that a cell’s nearest neighbors are likely to be of the same type as that of the cell itself. In practice, we iteratively loop through each unassigned cell from **step 1** and assign it to type m if more than 50% of its 15 neighbors are of type m . Each iteration decreases the fraction of unassigned cells, and the procedure terminates when the change in unassigned cell frequency is less than 0.5%. Continuing from **step 1** for `ctrl`:

```
#run step 2
ctrl = nn_voting(ctrl)
ctrl.write_h5ad('CtrlONC_mapped_iGB.h5ad')
```

Following **step 2**, the fraction of unassigned RGCs at 0dpc is reduced to <2%. As a sanity check, we confirmed that the relative frequency of types among 0dpc RGCs and their patterns of selective marker expression closely matched those of the atlas RGCs, as expected (*see* Fig. 2c, d).

3.4 iGraphBoost Classification of 0.5dpc, 1dpc, and 2dpc RGCs

We now classify RGCs collected at 0.5, 1, and 2dpc, denoted t_2 , t_3 and t_4 , respectively (*see* Fig. 2a). We follow the procedure outlined under Subheading 3.3 with two modifications. First, we exclude as features genes that were upregulated or downregulated broadly across RGCs following injury, identified via a global differential expression (DE) analysis (*see* Ref. [1] for details). This is done to ensure that the classifier learns stable features associated with type identity, and not features that are sensitive to injury. Second, after mapping each t_{n+1} dataset using the classifier C_n trained on the t_n dataset ($n = 1, 2, 3$) in **step 1**, we apply the atlas classifier (C_0) to the remaining unassigned RGCs prior to performing **step 2**. We perform the latter to maximize the amount of information gain from supervised classification. The following code classifies RGCs at 0.5dpc (t_2) using classified 0dpc RGCs (t_1):

```
#identify clust-specific ctrl genes
ctrl = sc.read_h5ad('CtrlONC_mapped_iGB.h5ad')
ctrl_genes = ClusterSpecificGenes(ctrl,
                                  genes =
list(ctrl.var.index[ctrl.var.highly_variable == True]),
                                  obs = 'Type_iGB')

#subset to genes common b/w ctrl and 12h
all_var_genes = [i for i in ctrl_genes if i in
list(twelveHr.var.index)]
```

```

#exclude temporal genes
exclude_genes_df = pd.read_csv('TemporalMarkersONC.txt', header =
None, names = ['Genes'])
exclude_genes = list(exclude_genes_df['Genes'])

var_genes = []
for i in all_var_genes:
    if i not in exclude_genes:
        var_genes.append(i)

#train ctrl classifier using only assigned cells
assigned_cells = []
for i in range(len(ctrl.obs)):
    if ctrl.obs.Type_iGB[i] != 'Unassigned':
        assigned_cells.append(ctrl.obs.index[i])

#train ctrl classifier, validate it, then use it to map 12h
validation_label_train_10, valid_predlabels_train_10,
test_predlabels = xgbtrain(
    train_anndata = ctrl[assigned_cells,:],
    test_anndata = twelveHr,
    genes = var_genes
)

#visualize validation results
validationconfmat, validationxticks, validationplot =
plotValidationConfusionMatrix(
    ytrue = validation_label_train_10,
    ypred = valid_predlabels_train_10,
    save_as = 'Ctrl_Validation.pdf',
    title = '',
    xaxislabel = 'Predicted',
    yaxislabel = 'True'
)

#store RGC assignments made by classifier
mapping_assignments = []
unassigned_index = []
for index, value in enumerate(test_predlabels):
    if value == 45:
        mapping_assignments.append('Unassigned')
        unassigned_index.append(index)
    else:
        mapping_assignments.append(str(int(value)+1))
twelveHr.obs['Type_iGB'] = mapping_assignments

#Mapping remaining unassigned cells at 12h to Atlas
all_var_genes = [i for i in atlas_genes if i in
list(twelveHr.var.index)]

var_genes = []
for i in all_var_genes:

```

```

    if i not in exclude_genes:
        var_genes.append(i)

unassigned_cells = []
for i in range(len(twelveHr.obs)):
    if twelveHr.obs.Type_iGB[i] == 'Unassigned':
        unassigned_cells.append(twelveHr.obs.index[i])

#train atlas classifier, validate it, then use it to map 12h
validation_label_train_10, valid_predlabels_train_10,
test_predlabels = xgbtrainatlas(
    train_anndata = atlas,
    test_anndata = twelveHr[unassigned_cells,:],
    genes = var_genes
)

#visualize validation results
validationconfmat, validationxticks, validationplot =
plotValidationConfusionMatrix(
    ytrue = validation_label_train_10,
    ypred = valid_predlabels_train_10,
    save_as = '',
    title = '',
    xaxislabel = 'Predicted',
    yaxislabel = 'True'
)

#store RGC assignments made by classifier
unassigned_mapping_assignments = []
for i in test_predlabels:
    if i == 45:
        unassigned_mapping_assignments.append('Unassigned')
    else:
        unassigned_mapping_assignments.append(str(int(i)+1))

for index, value in enumerate(unassigned_index):
    mapping_assignments[value] =
unassigned_mapping_assignments[index]

twelveHr.obs['Type_iGB'] = mapping_assignments

#run step 2
twelveHr = step2(twelveHr)

twelveHr.write_h5ad('twelve_hrONC_mapped_iGB.h5ad')

```

We follow an identical procedure to classify 1dpc using classified 0.5dpc RGCs and subsequently use the 1dpc RGCs to classify 2dpc RGCs. Details are omitted here for brevity but may be found in the Jupyter notebook shared in the book chapter's GitHub page. We now classify the three remaining time points.

3.5 *iGraphBoost* Classification of 4d, 7d, and 14d RGCs

In principle, the same procedure outlined above for 0.5, 1, and 2dpc RGCs can be applied to each of 4, 7, and 14dpc RGCs in successive fashion. However, at 4dpc, RGCs exhibit extensive transcriptomic changes preceding a phase of rapid loss between 4 and 14dpc (RGC loss <10% up to 3dpc, *see* Ref. [1]). This may be tackled by sampling additional scRNA-seq data on intermediate time points (e.g. 3dpc or 3.5dpc). As additional data was not available, we opted for a workaround by mapping the 4, 7, and 14dpc RGCs together, pooling them into a single AnnData object `rgc_late` ($t_n + 1$). For training, we combine classified RGCs at 12 h, 1d, and 2d into a single object and learn a t_n classifier, excluding the temporally DE genes as features.

We initiate **step 1** of *iGraphBoost* by training the t_n classifier.

```
rgc_early = twelveHr.concatenate(oneday, twoday)
rgc_late = fourday.concatenate(oneweek, twoweek)

twoday_genes = ClusterSpecificGenes(twoday,
                                     genes =
list(twoday.var.index[twoday.var.highly_variable == True]),
                                     obs = 'Type_iGB')

combined_var_genes = twelvehr_genes + oneday_genes + twoday_genes
var_genes_12h_1d_2d = list(np.unique(combined_var_genes))

all_var_genes = [i for i in var_genes_12h_1d_2d if i in
list(rgc_late.var.index)]

var_genes = []
for i in all_var_genes:
    if i not in exclude_genes:
        var_genes.append(i)

assigned_cells = []
for i in range(len(rgc_early.obs)):
    if rgc_early.obs.Type_iGB[i] != 'Unassigned':
        assigned_cells.append(rgc_early.obs.index[i])

validation_label_train_10, valid_predlabels_train_10,
test_predlabels = xgbtrain(
    train_anndata = rgc_early[assigned_cells,:],
    test_anndata = rgc_late,
    genes = var_genes
)

validationconfmat, validationxticks, validationplot =
plotValidationConfusionMatrix(
    ytrue = validation_label_train_10,
    ypred = valid_predlabels_train_10,
    save_as = 'RGC_Early_Validation.pdf',
    title = '',
    xaxislabel = 'Predicted',
    yaxislabel = 'True'
)
```

We now apply the t_n classifier to the t_{n+1} RGCs (4, 7, and 14dpc).

```
mapping_assignments = []
unassigned_index = []
for index, value in enumerate(test_predlabels):
    if value == 45:
        mapping_assignments.append('Unassigned')
        unassigned_index.append(index)
    else:
        mapping_assignments.append(str(int(value)+1))

rgc_late.obs['Type_iGB'] = mapping_assignments
```

Finally, we also apply the atlas classifier (C_0) to the remaining unassigned t_{n+1} RGCs before proceeding to **step 2**.

```
#Mapping Unassigned cells in rgc_late to Atlas

all_var_genes = [i for i in atlas_genes if i in
list(rgc_late.var.index)]

var_genes = []
for i in all_var_genes:
    if i not in exclude_genes:
        var_genes.append(i)

unassigned_cells = []
for i in range(len(rgc_late.obs)):
    if rgc_late.obs.Type_iGB[i] == 'Unassigned':
        unassigned_cells.append(rgc_late.obs.index[i])

validation_label_train_10, valid_predlabels_train_10,
test_predlabels = xgbtrainatlas(
    train_anndata = atlas,
    test_anndata = rgc_late[unassigned_cells,:],
    genes = var_genes
)

validationconfmat, validationxticks, validationplot =
plotValidationConfusionMatrix(
    ytrue = validation_label_train_10,
    ypred = valid_predlabels_train_10,
    save_as = '',
    title = '',
    xaxislabel = 'Predicted',
    yaxislabel = 'True'
)

unassigned_mapping_assignments = []
for i in test_predlabels:
```

```

if i == 45:
    unassigned_mapping_assignments.append('Unassigned')
else:
    unassigned_mapping_assignments.append(str(int(i)+1))

for index, value in enumerate(unassigned_index):
    mapping_assignments[value] =
unassigned_mapping_assignments[index]

rgc_late.obs['Type_iGB'] = mapping_assignments

```

We now run **step 2** of iGraphBoost for 4, 7, and 14dpc RGCs.

```

#run step 2
fourday = rgc_late[rgc_late.obs.Time=='4d',:]
fourday = step2(fourday)

oneweek = rgc_late[rgc_late.obs.Time=='1w',:]
oneweek = step2(oneweek)

twoweek = rgc_late[rgc_late.obs.Time=='2w',:]
twoweek = step2(twoweek)

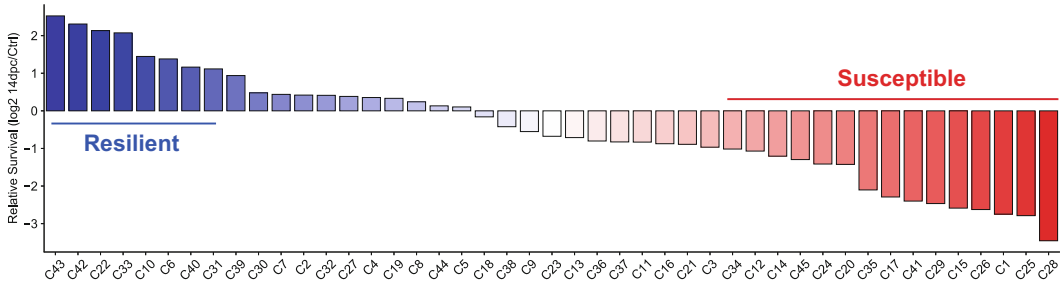
fourday.write_h5ad('fourdayONC_mapped_iGB.h5ad')
oneweek.write_h5ad('oneweekONC_mapped_iGB.h5ad')
twoweek.write_h5ad('twoweekONC_mapped_iGB.h5ad')

```

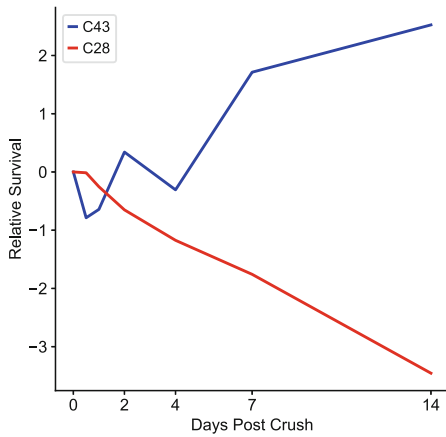
Taken together iGraphBoost results in a sizable improvement in the classification of injured RGCs compared to direct mapping of each time point to the atlas, reducing the proportion of unassigned cells from ~65% to ~30% at 4, 7, and 14dpc (Fig. 3b). As a sanity check, we also verify that classified RGCs at 14dpc maintained type-specific markers, though, as one might expect, some degradation in expression is observed. (compare Figs. 3c to 1c).

Next, we use the iGraphBoost assignments to estimate the relative frequency of the 45 RGC types at each of the six time points. We rank order the types based on their fold difference in relative frequency at 14dpc vs. 0dpc (survival ratio) to identify resilient and vulnerable types (*see* Fig. 4a). The results also allow us to compare survival kinetics between RGC types (*see* Fig. 4b).

A



B



C

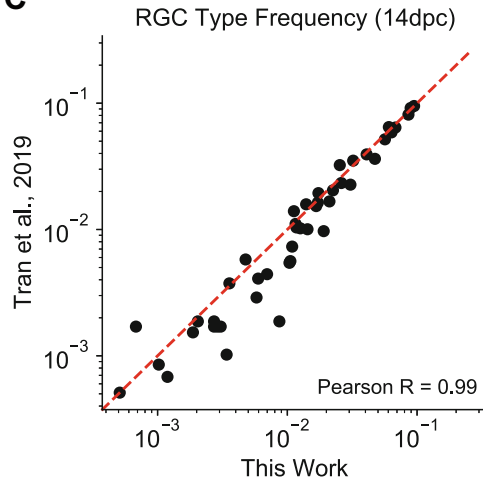


Fig. 4 Differences in survival among RGC types. (a) RGC types (x-axis) rank ordered based on decreasing values of the relative frequency ratio at 14dpc versus control showing variance in resilience among types. (b) Kinetics of relative survival as a function of time of a resilient (C43) and susceptible type (C28). (c) Scatter plot comparing relative frequencies of RGC types at 14dpc obtained in this study (x-axis) and the original publication (y-axis) [1]

```

twoweek = sc.read_h5ad('twoweekONC_mapped_iGB.h5ad')
ctrl = sc.read_h5ad('CtrlONC_mapped_iGB.h5ad')

#Disregard unassigned RGCs
ctrl = ctrl[ctrl.obs.Type_iGB!='Unassigned',:]
twoweek = twoweek[twoweek.obs.Type_iGB!='Unassigned',:]

#Compute survival scores for Figure 4A
twoweek_freqs = twoweek.obs.Type_iGB.value_counts(normalize=True)
ctrl_freqs = ctrl.obs.Type_iGB.value_counts(normalize=True)

surv_scores = dict()
for i in twoweek.obs.Type_iGB.values.categories:
    surv_scores['C'+i] =
    (np.log2(twoweek_freqs[twoweek_freqs.index.get_loc(i)]/ctrl_freqs[ct
rl_freqs.index.get_loc(i)]))
    
```

```

surv_scores_sorted =
pd.Series(surv_scores).sort_values(ascending=False)

#Track the survival score of two types over time (Figure 4B)
onc_objs = [ctrl, twelveHr, oneday, twoday, fourday, oneweek,
twoweek]

onc_freqs = []
for i in onc_objs:
    i = i[i.obs.Type_iGB!='Unassigned',:]
    onc_freqs.append(i.obs.Type_iGB.value_counts(normalize=True))
#43
i='43'
scores43 = []
for j in onc_freqs:

scores43.append(np.log2(j[j.index.get_loc(i)]/ctrl_freqs[ctrl_freqs.
index.get_loc(i)]))
#28
i='28'
scores28 = []
for j in onc_freqs:

scores28.append(np.log2(j[j.index.get_loc(i)]/ctrl_freqs[ctrl_freqs.
index.get_loc(i)]))

```

As another sanity check, we compare the relative frequency of types at each time point estimated in this chapter, with those reported in Ref. [1]. The agreement was excellent, with minor differences that do not impact qualitative conclusions (*see* Fig. 4c and Note 5).

3.6 Identifying Genes Correlated with Resilience and Susceptibility

We defined resilient and susceptible types as those with a survival ratio >2 and <0.5 (log-survival ratio >1 and <-1), respectively. We then sought to identify gene expression patterns that correlate with these differences in survival. First, using a Wilcoxon rank-sum test, we identify DE genes that distinguish resilient and susceptible RGC types based on their baseline transcriptomes at 0dpc (*see* Fig. 5a and Note 6).

```

#remove intermediate types
strength = []
res = list(surv_scores_sorted.index[0:8]) #resilient types
sus = list(surv_scores_sorted[-15:].index) #susceptible types

for i in range(ctrl.shape[0]):
    if ('C' + ctrl.obs.Type_iGB[i] in res):
        strength.append('Resilient')

```

```

    elif('C' + ctrl.obs.Type_iGB[i] in sus):
strength.append('Susceptible')

    else: strength.append('Intermediate')

#add strength identifier and remove intermediates
ctrl.obs['Strength'] = pd.Categorical(strength)
ctrl = ctrl[ctrl.obs.Strength!='Intermediate',:]

#Re-sample each type to 100 cells
subsamped_objs = []
for i in ctrl.obs.Type_iGB.values.categories:
    clust = ctrl[ctrl.obs.Type_iGB==i,:]

    if (clust.shape[0]<100): subsamped_objs.append(subsample(clust,
n_obs=100, copy=True, replace=True))

    else: subsamped_objs.append(subsample(clust, n_obs=100,
copy=True, replace=False))

#the re-sampled object
ctrl_sub = subsamped_objs[0].concatenate(subsamped_objs[1:])

#Perform DE to identify resilience and susceptibility genes
resGenes = DE(ctrl_sub, obs_id='Strength', obs_id_test='Resilient',
ref='Susceptible')
susGenes = DE(ctrl_sub, obs_id='Strength',
obs_id_test='Susceptible', ref='Resilient')

```

The genes *Ndnf* and *Crhbp* were selectively enriched among resilient and susceptible types, respectively (see Fig. 5a). These baseline differences are also maintained at 7dpc (see Fig. 5b). In the original study [1], we hypothesized that in vivo manipulation of these genes in RGCs may broadly improve their survival following ONC. Consistent with this, overexpression (OE) of *Ndnf* or knockout (KO) of *Crhbp* results in increased survival of RGCs (see Fig. 5d). In addition to baseline differences, we can also use iGraphBoost assignments to query genes that are selectively upregulated or downregulated temporally among resilient or susceptible types (see Note 5). We identify *Ucn*, a gene that is selectively upregulated in the two resilient types C42 and C43 (see Fig. 5c). Indeed, in vivo overexpression of *Ucn* enhanced RGC survival (see Fig. 5d). Finally, overexpression of *Ndnf* and *Ucn* along with knockout of *Crhbp* resulted in an unexpected promotion of axon regeneration (see Fig. 5e). This was surprising because our screen was designed to mainly identify genes associated with RGC survival. Taken together, these results illustrate the utility of iGraphBoost in discovering genes that promote neuroprotection and axon regeneration.

In summary, the current and the preceding chapter (please see Chap. 1 of this volume) describe a novel approach to analyze

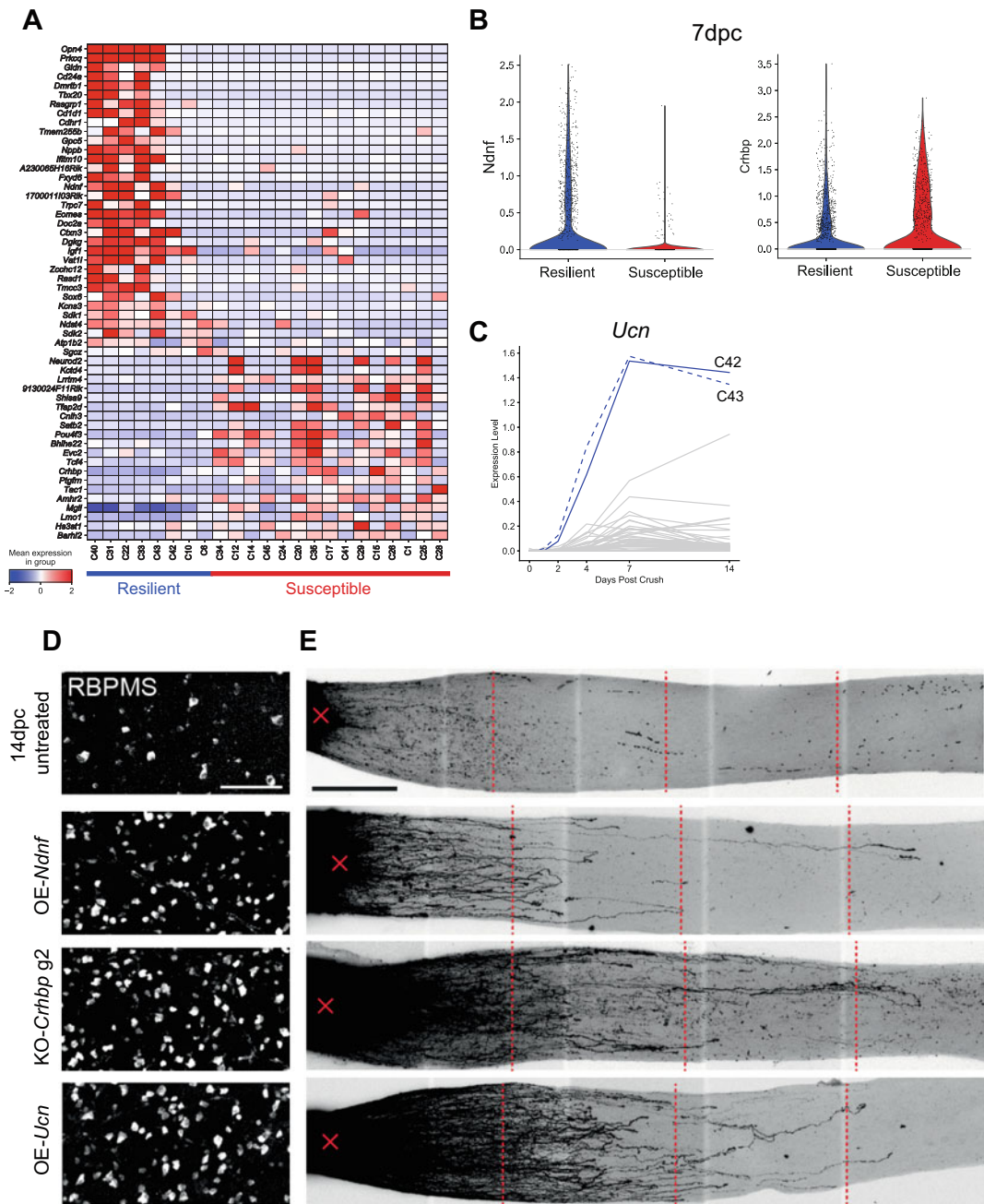


Fig. 5 Gene expression patterns associated with resilience and susceptibility. (a) Heatmap of markers (rows) selectively enriched in resilient and susceptible RGC types (columns) at baseline (0dpc). (b) Violin plot showing expression of a resilient marker, *Ndnf*, and a susceptibility marker, *Crhb3*, from panel a among resilient and susceptible RGC groups at 7dpc. (c) Upregulation of a resilience-associated marker *Ucn* in resilient types C43 and C42 in injured samples. (d) Overexpression of resilience markers *Ndnf* and *Ucn*, and knockout of susceptibility marker *Crhb3*, all result in increased RGC survival at 14dpc. (e) The same interventions as in panel d also promote RGC axon regeneration. (Panels d and e are reproduced with permission from Ref. [1])

selective neuronal vulnerability in the brain with an aim to identify targets that promote neuroprotection. In doing so, we have synthesized experimental approaches utilizing animal models, cellular and molecular biology, and next-generation sequencing together with computational approaches involving machine learning, statistical inference, and data visualization. While our focus was on retinal ganglion cells in the context of optic nerve crush, the approaches can be generalized to other neuronal systems and degeneration models. We hope that these companion chapters inspire researchers to investigate the molecular underpinnings of selective neuronal vulnerability in other systems.

4 Notes

1. `seaborn` and `matplotlib` are graphing and data visualization libraries. `Numpy` and `scipy` are libraries that enable a variety of standard numerical and scientific computation (e.g., matrix multiplication). `sklearn` (also known as scikit-learn) is a suite of machine learning and statistical inference tools in Python.
2. While Ref. [1] identified 46 types of mouse RGCs, two types, the so-called dorsal-preferring and ventral-preferring ON-OFF direction selective RGCs (D- and V-ooDSGCs), are distinguished by a single marker in the adult mouse. We have therefore collapsed these two types into a single cluster (D/V-ooDSGCs) totaling 45 types considered for our classification analyses.
3. The procedure to log-normalize the raw expression matrix of gene counts is described in Ref. [1]. We retain raw counts as they are required for identifying variable genes based on the Poisson–Gamma model introduced in Ref. [11].
4. As an alternative, the neighborhood graph built in principal component (PC) space can also be used in **step 2**. We found that it gives generally similar results to the graph built in UMAP space, but that it is more susceptible to noise due to the larger number of dimensions. We recommend both approaches be attempted for a given dataset to determine the best option.
5. The results of the iGraphBoost implementation outlined in this chapter differ slightly from that reported originally [1]. First the atlas, control, 12 h, 1d, 2d, 4d, 7d, and 14d datasets were subjected to a different scRNA-seq pre-processing computational pipeline from that used in the original work, which implemented the steps in *R*. While the resilient and susceptible types are consistent across both results, there are slight changes

in the rank order of survival which do not change the overall qualitative conclusions.

6. Methods to identify temporally regulated DE genes in the ONC data are described in [1], and not covered here.

Acknowledgments

S.B. would like to acknowledge support from the NSF Graduate Research Fellowship Program (grant DGE 1752814). K. S. acknowledges the support of the National Institutes of Health (grant R00EY028625), Glaucoma Research Foundation (CFC4), and UC Berkeley. We would like to gratefully acknowledge critical feedback from Drs. Anne Jacobi and Nicholas Tran.

References

1. Tran NM, Shekhar K, Whitney IE et al (2019) Single-cell profiles of retinal ganglion cells differing in resilience to injury reveal neuroprotective genes neurosource single-cell profiles of retinal ganglion cells differing in resilience to injury reveal neuroprotective genes. *Neuron* 104:1039–1055. <https://doi.org/10.1016/j.neuron.2019.11.006>
2. Williams PR, Benowitz LI, Goldberg et al (2020) Axon regeneration in the mammalian optic nerve. *Ann Rev Vis Sci* 6:195–213. <https://doi.org/10.1146/annurev-vision-022720-094953>
3. Sanes JR, Masland RH (2015) The types of retinal ganglion cells: current status and implications for neuronal classification. *Annu Rev Neurosci* 38:221–246. <https://doi.org/10.1146/annurev-neuro-071714-034120>
4. Zheng GXY, Terry JM, Belgrader P et al (2017) Massively parallel digital transcriptional profiling of single cells. *Nat Commun* 8. <https://doi.org/10.1038/ncomms14049>
5. Baden T, Berens P, Franke K et al (2016) The functional diversity of retinal ganglion cells in the mouse. *Nature* 529:345–350. <https://doi.org/10.1038/nature16468>
6. Bae JA, Mu S, Kim JS et al (2018) Digital museum of retinal ganglion cells with dense anatomy and physiology. *Cell* 173:1293–1306.e19. <https://doi.org/10.1016/j.cell.2018.04.040>
7. Chen T, Guestrin C (2016) XGBoost: a scalable tree boosting system. *Proc ACM SIGKDD Int Conf Knowl Discov Data Min*, 13–17 August 2016, pp 785–794. <https://doi.org/10.1145/2939672.2939785>
8. Wolf F, Angerer P, Theis F (2018) SCANPY: large-scale single-cell gene expression data analysis. *Genome Biol* 19:15. <https://doi.org/10.1186/s13059-017-1382-0>
9. Korsunsky I, Millard N, Fan J et al (2019) Fast, sensitive and accurate integration of single-cell data with harmony. *Nat Methods* 16:1289–1296. <https://doi.org/10.1038/s41592-019-0619-0>
10. The HDF Group (2000–2010) Hierarchical data format version 5. <http://www.hdfgroup.org/HDF5>
11. Pandey S, Shekhar K, Regev A, Schier AF (2018) Comprehensive identification and spatial mapping of habenular neuronal types using single-cell RNA-Seq. *Curr Biol* 28:1052–1065.e7. <https://doi.org/10.1016/j.cub.2018.02.040>
12. Hotelling H (1933) Analysis of a complex of statistical variables into principle components. *J Educ Psychol* 24:417–441, 498–520
13. McInnes L, Healy J, Melville J (2018) UMAP: uniform manifold approximation and projection for dimension reduction. arXiv



Retinal Ganglion Cell Axon Fractionation

Sean D. Meehan and Sanjoy Bhattacharya

Abstract

Retinal ganglion cell (RGC) axon regeneration in mammals can be stimulated through gene knockouts, pharmacological agents, and biophysical stimulation. Here we present a fractionation method to isolate regenerating RGC axons for downstream analysis using immunomagnetic separation of cholera toxin subunit B (CTB)-bound RGC axons. After optic nerve tissue dissection and dissociation, conjugated CTB is used to bind preferentially to regenerated RGC axons. Anti-CTB antibodies crosslinked to magnetic sepharose beads are used to isolate CTB-bound axons from a nonbound fraction of extracellular matrix and neuroglia. We provide a method of verifying fractionation by immunodetection of conjugated CTB and the RGC marker, Tuj1 (β -tubulin III). These fractions can be further analyzed with lipidomic methods, such as LC-MS/MS to gather fraction-specific enrichments.

Key words Retinal ganglion cell, Optic nerve, Fractionation, Axon regeneration, Immunomagnetic separation

1 Introduction

Retinal ganglion cell (RGC) axon regeneration in the optic nerve is now readily attainable through gene knockouts [1], pharmacological interventions [2, 3], and biophysical stimulation [4]. Over the years, mass spectrometry technology has improved to where sensitivity is less of a limiting factor. Full tissue lipid profiles can be generated easily. As our scientific approaches become more targeted for cell types, such as RGCs, our methods must adapt to provide results with higher specificity. In order to accomplish this, sample complexity must be reduced as it can have significant effects on LC-MS/MS performance and results [5]. With high sample complexity, raw data from the LC-MS/MS is susceptible to high background signals that can drown out target peaks [6, 7]. For example, the use of different digestion protocols can increase the complexity of protein samples as the sheer number of peptides is larger than the number of full-length proteins in the initial sample. Most of our previous “omic” analyses were focused on complete

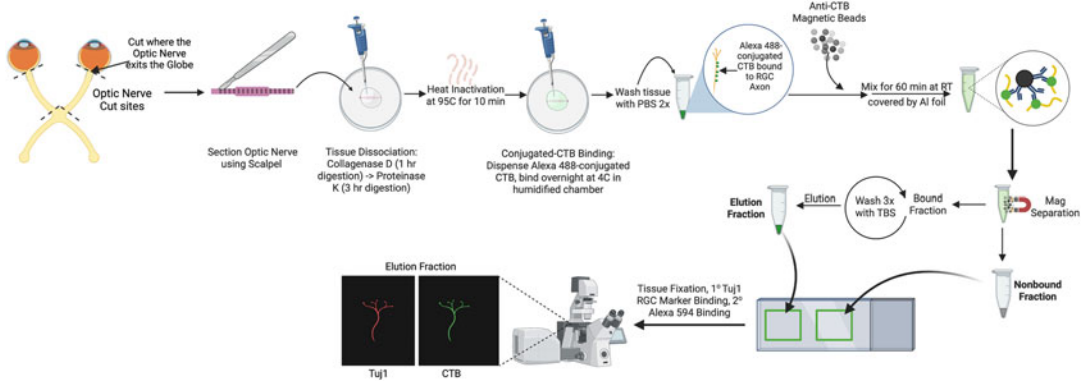


Fig. 1 Overview schematic diagram of RGC axon fractionation protocol

optic nerve tissue analyses. As we begin to identify enriched pathways associated with nerve degeneration and regeneration, our need for cellular fractionation/dissociation has increased. This coincides well with the increase in cell sorting and single-cell technologies. In this published method, we introduce a retinal ganglion cell (RGC) fractionation technique that isolates RGC axons from dissected C57BL/6 mouse optic nerves (Fig. 1). This method can be applied to other mouse types as well. In optic nerve regeneration, a common visualization method involves intravitreally injecting fluorophore-conjugated cholera toxin subunit B (CTB) [8, 9]. CTB selectively binds to the GM1 ganglioside, which is a marker for new RGC axon growth [10, 11]. We decided to take advantage of this selective binding and ubiquitous marker use to develop an immunomagnetic separation technique. Dissected optic nerve tissue is first dissociated using mild protein digestion followed by CTB binding. Separately, anti-CTB antibodies are cross-linked to magnetic sepharose beads. CTB-bound RGC axons are then captured with anti-CTB magnetic beads and collected using a magnetic rack (Fig. 2). Both eluted and nonbound fractions can be collected for future fraction-specific lipidomics. Fractionation efficiency can be evaluated in multiple ways, such as immunoblot or immunodetection of an RGC marker (β -tubulin III) (Fig. 3). We describe here a method to approximate fractionation efficiency using fluorescence microscopy to detect fluorescently conjugated CTB and β -tubulin III immunofluorescence.

2 Materials

1. Magnetic rack with removable magnetic bar, designed to hold 1.5 mL microcentrifuge tubes, for small-scale sample enrichment.
2. 1.5 mL microcentrifuge tubes

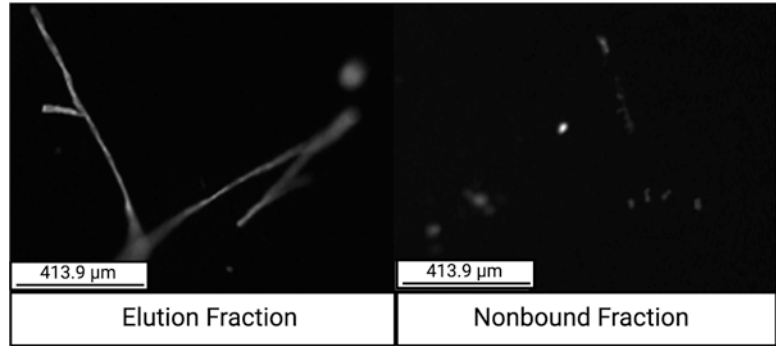


Fig. 2 Visualization of CTB-bound materials in elution and nonbound fractions. Fluorescence microscopy of Alexa 488-conjugated CTB elution and nonbound fractions. Using a Leica AF6000 microscope and GFP laser, the elution and nonbound fractions were evaluated for GFP fluorescent material (shown in white). Long axons can be visualized on the left in the elution fraction. Scale bar: 413.9 μm

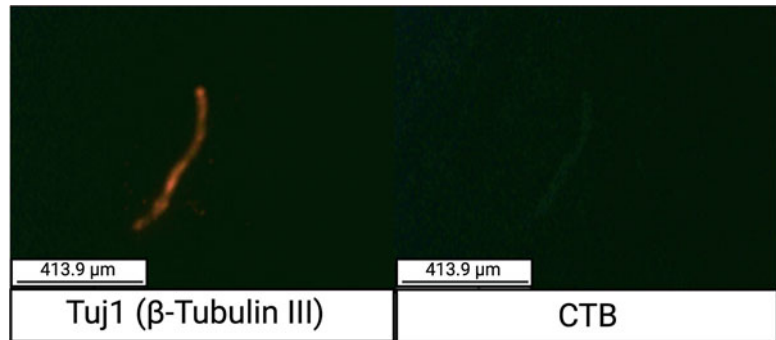


Fig. 3 Fluorescence microscopy of CTB and RGC markers in elution fraction. Using a Leica AF6000 microscope with a GFP and TXR laser, an axon in elution fraction is shown here with Tuj1 (Alexa 594) on the left in red and the conjugated CTB on the right in faded green. Scale bars: 413.9 μm

3. Magnetized sepharose beads conjugated to protein G (subsequently referred to as magnetic beads).
4. TBS: 50 mM Tris-HCl, 150 mM NaCl, pH 7.5.
5. Elution buffer: 0.1 M glycine-HCl, pH 2.9.
6. Neutralizing buffer: 50 mM Tris-HCl, 150 mM NaCl, pH 8.8.
7. Crosslink solution A: 200 mM triethanolamine, adjusted to pH 8.9 by dropwise addition of 1 M HCl.
8. Crosslink solution B: 100 mM ethanolamine, adjusted to pH 8.9 by dropwise addition of 1 M HCl.
9. Crosslink solution C: 50 mM dimethyl pimelimidate dihydrochloride in 200 mM triethanolamine, pH 8.9.

10. Fluorescently tagged cholera toxin subunit B conjugated (e.g., Invitrogen Alexa 488-conjugated CTB, C22841): 2.5 µg/mL in PBS.
11. CTB antibody: Anti-beta subunit cholera toxin antibody, e.g., Abcam ab34992.
12. Euthanized C57BL/6 mouse.
13. Sterile, disposable #10 blade scalpel.
14. Vannas scissors: Micro dissecting spring scissors (3 mm cutting edge, 0.15 mm tip width, 7.62 cm in length), sterilized.
15. Tweezers: Thin tips, 109 mm length, polished, sterilized.
16. Autoclavable petri dish, sterilized, 100 mm diameter × 15 mm height (*see Note 1*).
17. Phosphate-buffered saline (PBS).
18. PBS-T: 0.3% Triton X-100 in PBS.
19. Collagenase D solution: 2 mg/mL in PBS, 3 mM CaCl₂.
20. Proteinase K solution: 3 mg/mL in PBS, 3 mM CaCl₂.
21. Heat block: Temperature range—25 °C to 130 °C.
22. Multipurpose staining chamber/humidified chamber: 39.7 cm × 25.5 cm × 4 cm. This chamber is used to maintain a humid environment during tissue digestion and antibody staining. Otherwise, the tissue will dry out and be unusable. Slides are placed on higher grooves, above the water layer. Maintain water level to cover the entire base level of the chamber. Do not overfill or water could splash onto the slides, if chamber is moved.
23. Rotator: Fixed 23 degrees, 20 orbits/min speed, platform dimensions—30.5 cm × 30.5 cm. The orbital shaker is required for a continuous and uniform mixture of the components. It is used for mixing CTB-bound tissue with the Mag Sepharose Anti-CTB Beads.
24. End-over-end mixer.
25. Microcentrifuge.
26. PAP pen (*see Note 2*).
27. Poly-D-lysine- and laminin-coated glass microscope slides.
28. Tissue fixative: 4% paraformaldehyde in PBS.
29. Blocking solution: 5% bovine serum albumin (BSA) in PBS-T.
30. Primary antibody: Tuj1, a neuron-specific class III beta tubulin antibody, chicken IgY (e.g., Neuromics CH23005), used as a retinal ganglion cell marker.
31. Secondary antibody: Fluorescently labeled goat anti-chicken IgY, (e.g., goat anti-chicken IgY Alexa 594, Abcam).

32. Antibody dilution medium: 1% BSA, PBS-T.
33. Mounting medium, with DAPI (e.g., Vectashield HardSet Antifade Mounting Medium with DAPI, Vector Laboratories).
34. Confocal microscope equipped with compatible lasers for the chosen fluorophores and DAPI (we routinely utilize Alexa 488 and Alexa 594; *see Note 3*).

3 Methods

3.1 Anti-CTB Magnetic Bead Preparation Prior to Optic Nerve Dissection

1. Based on your tissue volume, dispense the appropriate quantity of magnetic beads into a 1.5 mL microcentrifuge tube (*see Note 4*).
2. Place the tube in the magnetic rack with the magnet bar to pull the beads out of the solution, and use a pipette to remove the storage solution from the beads.
3. Remove the magnet bar and resuspend the beads in TBS by inverting the magnetic rack five times.
4. Replace the magnet bar and remove the TBS from the beads using a pipette.
5. Remove the magnet and resuspend the beads in 100 μ L of CTB antibody diluted 1:100 in antibody dilution medium.
6. Rotate the microfuge tube with the antibody and bead solution in the end-over-end mixer for 15 min.
7. Place the tube in the magnetic rack with the magnet bar in place and remove the antibody from the beads using a pipette.
8. Remove the magnet bar and resuspend the beads in 500 μ L of TBS by inverting the magnetic rack five times.
9. Replace the magnet bar and remove the TBS from the beads using a pipette.
10. Remove the magnet bar and resuspend beads in 500 μ L of crosslink solution A by inverting the magnetic rack five times.
11. Replace the magnet bar and remove the crosslink solution A from the beads using a pipette.
12. Remove the tube from magnetic rack and resuspend the beads in crosslink solution C with manual inversion.
13. Place the tube in the end-over-end mixer for 60 min.
14. Replace the tube in the magnetic rack with the magnet bar in place and remove the crosslink solution C from the beads using a pipette.
15. Remove the magnet bar and resuspend the beads in 500 μ L crosslink solution A by inverting the magnetic rack five times.

16. Replace the magnet bar and remove the crosslink solution A from the beads using a pipette.
17. Remove the tube from the magnetic rack and resuspend the beads in 500 μL crosslink solution B with manual inversion.
18. Rotate the microfuge tube with the beads and crosslink solution B in the end-over-end mixer for 15 min.
19. Replace the tube in the magnetic rack with the magnet bar in place and remove crosslink solution B from the beads using a pipette.
20. Remove the magnet bar and resuspend the beads in 500 μL of elution buffer by inverting the magnetic rack five times.
21. Replace the magnet bar and remove the elution buffer from the beads using a pipette.
22. Remove the magnet bar and resuspend the beads in 500 μL TBS by inverting the magnetic rack five times.
23. Replace the magnet bar and remove the TBS from the beads using a pipette.
24. Repeat **steps 23** and **24** twice more, and store the conjugated beads at 4 $^{\circ}\text{C}$ until they are required for RGC axon isolation (*see Note 5*).

3.2 Optic Nerve Isolation and Tissue Dissociation

1. Obtain two dry petri dishes and one petri dish containing PBS.
2. Dissect the eyes from the euthanized mouse and collect them in one dry petri dish (*see Fig. 1*).
3. Separate globe and optic nerve by using scalpel to transect the nerve at the junction of the globe and the optic nerve (optic nerve head).
4. Rinse the dissected optic nerve by dipping it in the petri dish with PBS to wash off any excess blood/tissue. Be careful to not let the optic nerve dry out.
5. Remove the optic nerve from PBS and place on the second dry petri dish using tweezers.
6. Make longitudinal sections along the length of the optic nerve by using a scalpel or one blade of the Vannas scissors. This will lead to thin, sheered optic nerve sections and ultimately create more surface area for tissue digestion.
7. Dispense collagenase D solution to cover the optic nerve (typically 50–100 μL).
8. Digest the tissue in the collagenase D solution for 1 h at room temperature in humidified chamber.
9. Remove the collagenase D solution using a Pasteur pipette while being careful to avoid picking up the optic nerve tissue.

10. Dispense proteinase K solution to cover the optic nerve tissue (typically 50–100 μL).
11. Allow all the tissue to digest in proteinase K solution for 3 h in humidified chamber at room temperature (*see Note 6*).
12. Use heat block or equivalent to inactivate the proteinase K at 95 °C for 10 min. Do not let the tissue dry out during this time by supplementing with extra PBS as necessary.
13. Carefully remove the proteinase K solution from the tissue using a Pasteur pipette.

3.3 Conjugated CTB Binding and Magnetic Separation

1. Dilute Alexa 488-conjugated CTB 1:100 in PBS and dispense it to cover the digested optic nerve
2. Incubate overnight at 4 °C in a humidified chamber, covered from light to allow the labeled CTB to bind to RGC axons.
3. Carefully remove the diluted Alexa 488-conjugated CTB from the tissue using a Pasteur pipette. From this point forward, limit the amount of light exposure to the optic nerve fragments as much as possible to avoid bleaching the fluorophore signal.
4. Wash any residual antibody from the tissue by dispensing 200 μL of PBS onto the optic nerve and then carefully removing it using a Pasteur pipette.
5. Wash the optic nerve two more times with PBS. Collect the last wash including the dissociated optic nerve fragments into a microcentrifuge tube.
6. Spin down the optic nerve fragments at 300 $\times g$ in a microcentrifuge for 5 min.
7. Add the anti-CTB magnetic beads prepared under Subheading 3.1 to the CTB-bound tissue.
8. Mix the solution of tissue and beads on the rotator for 60 min at room temperature, protected from light.
9. Place the tube in magnetic rack with the magnet bar in place to bring the beads out of solution.
10. Use a pipette to remove the solution to a fresh tube labeled “nonbound fraction.” Save this fraction for further analyses.
11. Remove the magnet bar and resuspend the beads in 500 μL wash buffer by inverting the rack five to ten times.
12. Replace the magnet bar and remove the wash buffer from the beads using a pipette.
13. Repeat **steps 11** and **12** twice more.
14. Remove the magnet bar and resuspend the beads in elution buffer (use 3 \times volume of the original anti-CTB magnetic bead volume in **step 8**) by inverting the rack ten times.

15. Allow the beads to incubate in the elution buffer for at least 2 min at room temperature, protected from light.
16. Pulse spin the tube in the microcentrifuge if there is residual solution in the cap of the tube.
17. Replace the tube in the magnetic rack with the magnet bar in place and collect the “elution fraction” in a fresh microcentrifuge tube.
18. Repeat **steps 14–17**, if necessary (*see Note 7*).
19. Add 200 μL of neutralizing buffer to tube containing the elution fraction to neutralize acidic pH.

3.4 Verification of RGC Separation with Immunodetection

1. Immunodetection can be used to visualize the elution and nonbound fractions.
2. Use a PAP pen to delineate two “wells” on a poly-D-lysine- and laminin-coated slide or coverslip encircled using a PAP pen to form the hydrophobic barriers. Designate one well for the elution fraction and the other for the nonbound fraction.
3. Mix the elution fraction using a pipette and then dispense a volume that will fill the designated region onto the slide or coverslip.
4. Repeat **step 3** with the nonbound fraction.
5. Repeat **steps 2 and 3** with a second slide to create a secondary antibody nonspecific binding control.
6. Allow the dispensed solutions to partially dry onto the slides to avoid overflowing.
7. Add tissue fixative to each of the fractions on the slides and incubate for 30 min at room temperature, protected from light. Use a volume that covers but does not overflow the well area designated by the PAP barrier.
8. Remove the tissue fixative solution using a pipette.
9. Wash the slides twice with PBS for 15 min, protected from light.
10. Add blocking solution to each well using a volume that covers the area but does not overflow the hydrophobic barrier delineated with the PAP pen.
11. Incubate for 30 min, in a humidified chamber at room temperature.
12. Remove blocking solution using a pipette.
13. Add the primary antibody (Tuj1), diluted 1:400 in antibody dilution medium, to the wells containing the elution fraction and nonbound fraction. Again, use a volume that covers the area but does not overflow the hydrophobic barrier delineated with the PAP pen.

14. For the wells on the secondary antibody nonspecific binding control slide, add antibody dilution medium instead of the primary antibody.
15. Incubate the control slide and the slide with the primary antibody overnight at 4 °C in a humidified chamber.
16. Remove primary antibody using a pipette.
17. Wash the slides twice with PBS for 15 min, protected from light.
18. Add the secondary antibody to the wells on all slides and incubate at room temperature for 1–2 h in a humidified chamber. Again, use a volume that covers the area but does not overflow the hydrophobic barrier delineated with the PAP pen.
19. Remove secondary antibody from slides using a pipette.
20. Optional: Add appropriate volume of DAPI Vectashield hardening medium to fraction regions, ~15–25 µL. Axons should not have DAPI fluorescence. Place appropriate coverslip size over sample slides. Allow hardening for 15 min at room temperature.
21. Visualize specimens by laser-scanning confocal microscopy (*see* **Notes 3** and **8** and Figs. **2** and **3**).
22. Fractionation efficiency can be evaluated by comparing CTB and Tuj1 labeled materials in the elution and nonbound fractions. Axons will appear as long, thin tissues that are labeled with both CTB and Tuj1 (*see* **Note 9**).

4 Notes

1. Verify that your petri dish is heat tolerant at 95 °C. If not, the protocol can be adapted by carrying out the tissue dissociation in a microcentrifuge tube as well.
2. Beware that PAP pen types may create a fluorescent border that can be seen with microscopy. Be careful to not allow liquid to reside in sample regions, which may result in a false-positive readout. Chamber slides could also be used instead of PAP pens.
3. Fluorophores were chosen to avoid overlapping excitation and emission spectra. Alexa 488 is a green fluorescent dye that uses the 488 nm laser line with an excitation max at 490 nm and an emission max at 525 nm. Alexa 594 is a red fluorescent dye that uses the 561/594 laser line with an excitation max at 590 nm and an emission max at 617 nm. DAPI is a blue fluorescent DNA stain that uses 405 laser line with an excitation max at 350 nm and an emission max at 470 nm.

4. The optimal magnetic bead quantity can be determined using preliminary trials in which increasing quantities of magnetic beads are incubated with the same concentration of the CTB antibody. After preparing the anti-CTB magnetic beads, the protocol can be performed on control tissue samples of equal mass with each magnetic bead concentration at equal volumes. The elution fraction yield can be evaluated using microscopy or western blot for a RGC axonal marker such as Tuj1 and normalized based on the tissue weight. There will be a maximal magnetic bead concentration where the elution fraction yield no longer improves. The lowest concentration with maximal elution fraction yield will be the optimal starting magnetic bead volume.
5. Conjugated beads should be stored at 4 °C and be used within 2–3 weeks. After this, they will begin to lose binding efficiency.
6. If the tissue is not dissociating well, verify that the protein digestion solutions (collagenase D and proteinase K) are prepared fresh and stored properly. You may also increase the digestion time or increase the agitation.
7. To avoid cross-contamination between experiments, it is best to not reuse anti-CTB magnetic beads for multiple fractionation experiments.
8. If Tuj1 fluorescence is low in immunodetection, increase the concentration of Tuj1 primary antibody as described in Sub-heading 3.4, step 13.
9. If the elution fraction efficiency is low, increase the anti-CTB magnetic bead binding time with the dissociated tissue or increase the total quantity of anti-CTB magnetic beads.

References

1. Park KK, Liu K, Hu Y et al (2008) Promoting axon regeneration in the adult CNS by modulation of the PTEN/mTOR pathway. *Science* 322(5903):963–966. <https://doi.org/10.1126/science.1161566>
2. Trzeciecka A, Carmy T, Hackam AS et al (2019) Lipid profiling dataset of the Wnt3a-induced optic nerve regeneration. *Data Brief* 25:103966. <https://doi.org/10.1016/j.dib.2019.103966>
3. Trzeciecka A, Stark DT, Kwong JMK et al (2019) Comparative lipid profiling dataset of the inflammation-induced optic nerve regeneration. *Data Brief* 24:103950. <https://doi.org/10.1016/j.dib.2019.103950>
4. Arcuri J, Liu Y, Lee RK et al (2020) Lipid profile dataset of optogenetics induced optic nerve regeneration. *Data Brief* 31:106001. <https://doi.org/10.1016/j.dib.2020.106001>
5. Mesmin C, van Oostrum J, Domon B (2016) Complexity reduction of clinical samples for routine mass spectrometric analysis. *Proteomics Clin Appl* 10(4):315–322. <https://doi.org/10.1002/prca.201500135>
6. Picotti P, Aebersold R, Domon B (2007) The implications of proteolytic background for shotgun proteomics. *Mol Cell Proteomics* 6(9):1589–1598. <https://doi.org/10.1074/mcp.M700029-MCP200>
7. Hu C, Duan Q, Han X (2020) Strategies to improve/eliminate the limitations in shotgun lipidomics. *Proteomics* 20(11):e1900070. <https://doi.org/10.1002/pmhc.201900070>

8. Smith PD, Sun F, Park KK et al (2009) SOCS3 deletion promotes optic nerve regeneration in vivo. *Neuron* 64(5):617–623. <https://doi.org/10.1016/j.neuron.2009.11.021>
9. Belin S, Nawabi H, Wang C et al (2015) Injury-induced decline of intrinsic regenerative ability revealed by quantitative proteomics. *Neuron* 86(4):1000–1014. <https://doi.org/10.1016/j.neuron.2015.03.060>
10. Baldauf KJ, Royal JM, Hamorsky KT et al (2015) Cholera toxin B: one subunit with many pharmaceutical applications. *Toxins (Basel)* 7(3):974–996. <https://doi.org/10.3390/toxins7030974>
11. Benady A, Freidin D, Pick CG et al (2018) GM1 ganglioside prevents axonal regeneration inhibition and cognitive deficits in a mouse model of traumatic brain injury. *Sci Rep* 8(1): 13340. <https://doi.org/10.1038/s41598-018-31623-y>



Analysis of Immediate Early Gene Expression Levels to Interrogate Changes in Cortical Neuronal Activity Patterns upon Vision Loss

Sara R. J. Gilissen, Maroussia Hennes, and Lutgarde Arckens

Abstract

Mapping immediate early gene (IEG) expression levels to characterize changes in neuronal activity patterns has become a golden standard in neuroscience research. Due to straightforward detection methods such as in situ hybridization and immunohistochemistry, changes in IEG expression can be easily visualized across brain regions and in response to physiological and pathological stimulation. Based on in-house experience and existing literature, *zif268* represents itself as the IEG of choice to investigate the neuronal activity dynamics induced by sensory deprivation. In the monocular enucleation mouse model of partial vision loss, *zif268* in situ hybridization can be implemented to study cross-modal plasticity by charting the initial decline and subsequent rise in neuronal activity in visual cortical territory deprived of direct retinal visual input. Here, we describe a protocol for high-throughput radioactive *zif268* in situ hybridization as a readout for cortical neuronal activity dynamics in response to partial vision loss in mice.

Key words Immediate early genes, *zif268*, Neuronal plasticity, In situ hybridization, Cortical recovery, Monocular enucleation

1 Introduction

Immediate early gene (IEG) expression is established as a readout to assess brain-wide neuronal activity patterns under different physiological and pathological conditions [1–3]. They can be visualized via multiple detection methods such as immunohistochemistry, Western blot, in situ hybridization (ISH), calcium-modulated photoactivatable ratiometric integrator (CaMPARI), and even in vivo imaging [3–5]. The advantage of ISH is the ability to label specific mRNAs while providing region- and cell-specific information. ISH can be carried out via (non)radioactive labeling an oligo-

Authors Sara R. J. Gilissen and Maroussia Hennes have equally contributed to this chapter.

nucleotide, DNA, or RNA probe directed against the IEG of interest. Whereas fluorescence opens up the possibility of multiplexing, radioactivity remains the most sensitive and most effective quantitative detection method because of its unparalleled linear signal range. Radioactive ISH typically consists of a more lengthy protocol, but the results on autoradiographic film can be kept infinite without losing sensitivity. In addition, the same tissue sections can be reused for a cyto-architectural or immunohistochemical staining, precise placement of areal borders, assessment of histological abnormalities, and obtaining (sub)cellular expression information. Several IEGs qualify as neuronal activity reporter, including *c-fos*, *arc*, *homer1*, *zif268/egr1*, and *npas4*. Although all of these IEGs can provide information about neuronal activity, subtle expression differences among them calls for careful consideration when planning an experiment and protocol [6–9]. In the context of assessing the initial impact and subsequent recovery of the visual system after peripheral injury, for example, due to damage to the optic nerve, *zif268* should be the IEG of choice. This IEG namely has the advantage of being expressed at an intermediate baseline level in the absence of specific stimulation, offering the opportunity to detect both decreased and increased neuronal activity levels as a readout of loss or regain of visual stimulation. Furthermore, as *zif68* is broadly expressed, this IEG can be used to study neuronal activity patterns across cortical layers, as well as subcortical structures, including the LGN and the superior colliculus. Interestingly, changes in *zif268* expression levels can also be used to visualize cross-modal brain plasticity [10, 11]. Partial vision loss in mice, for example, where the visual cortex, permanently deprived of retinal inputs, becomes reactivated by inputs from other sensory modalities, can be interrogated using *zif268* labeling (Fig. 1) [12–16]. Moreover, a recent study comparing different IEGs discovered *zif268* expression to be mainly driven by top-down cross-modal neuronal activity, whereas *Arc* expression was primarily driven by bottom-up sensory activity [17], thereby confirming *zif268* as the ideal IEG of choice to study multimodal-driven brain activity and plasticity next to bottom-up sensory activation. Here, we present a standardized protocol for studying the cross-modal plasticity phenomenon by inducing vision loss in mice via monocular enucleation, or the removal of one eye, and assessing loss and regain of neuronal activity in the visually deprived cortex by charting *zif268* expression levels.

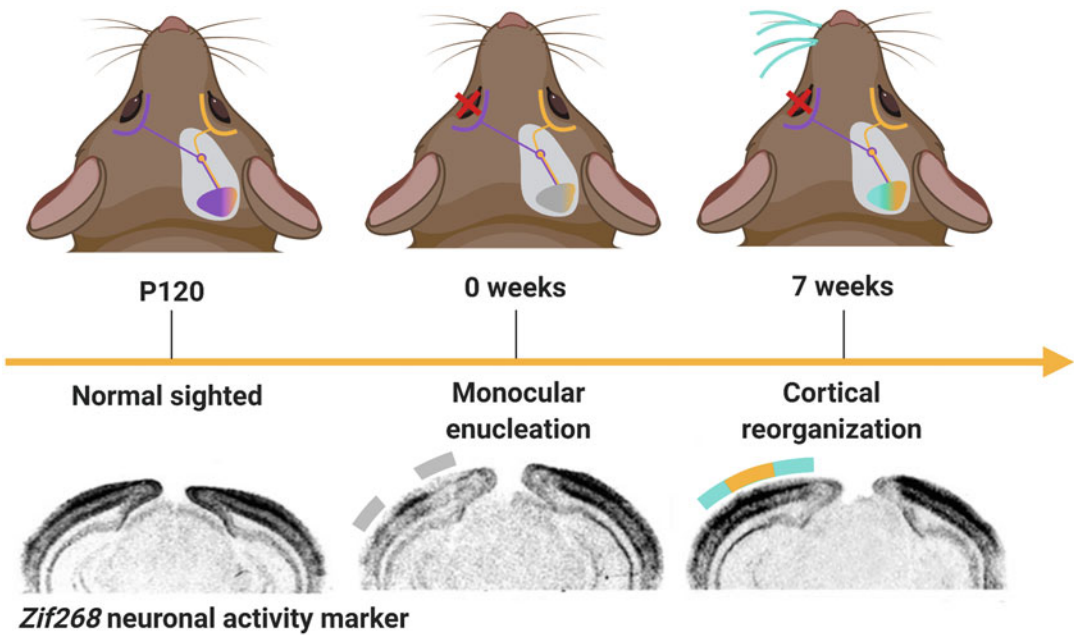


Fig. 1 Mapping of *zif268* expression levels to study the dynamics of cortical plasticity processes upon partial vision loss in adulthood. *Left*: Upon visual stimulation, normal sighted adult mice (P120) show upregulated *zif268* expression in the visual cortex, reflecting normal neuronal activity patterns. *Middle*: Upon monocular enucleation, neuronal activity is reduced and *zif268* expression levels drop significantly in the monocular zone (gray boxes) of the deprived visual cortex. *Right*: During a timeframe of 7 weeks, sensory inputs from the remaining eye and the whiskers drive neuronal reactivation of the deprived binocular (orange box) and monocular (turquoise boxes) visual area, respectively. This regain of neuronal activity is visualized by a restored *zif268* cortical expression pattern

2 Materials

General Note This protocol has been optimized using C57Bl/6j mice, obtained from Janvier Labs, with an age ranging from P45 until P170. It is for labeling *zif268* mRNA with an oligo-cDNA probe (see **Note 1**), labeled with ^{33}P (American Radiolabeled Chemicals Inc., dATP-33P, 1 mCi, ARP-0127A) (see **Note 2**).

1. Autoclaved ultrapure water.
2. Anesthesia solution (0.1 mL/10 g) (i.p.): Mix 0.2 mL medetomidine hydrochloride (1 mg/kg), 0.15 mL ketamine hydrochloride (75 mg/kg), and 1.65 mL sterile 0.9% saline.
3. Anesthesia-reversal solution (i.p.): Mix 100 μL atipamezole hydrochloride (1 mg/kg) and 9.9 mL autoclaved 0.9% saline (see **Note 3**).
4. Analgesics solution (i.p.): Mix 200 μL meloxicam (2 mg/kg) and 800 μL autoclaved 0.9% saline.

5. Ophthalmic ointment.
6. 1× TET buffer: Prepare a solution of 0.1 M Tris–HCl, 0.001 M EDTA, and 0.01 M triethanolamine (TEA) by dissolving 1.211 g Tris, 0.037 g EDTA, and 150 µL TEA in autoclaved ultrapure water. Adjust the pH to 7.7 using 6 N HCl and bring final volume to 100 mL.
7. 10× phosphate-buffered saline (10× PBS): Mix 66.6 mL phosphoric acid, 90 g of NaCl, and 800 mL autoclaved ultrapure water. Adjust the pH to 7.4 by using NaOH crystals until a pH of 6.5–7 is reached. Continue adjusting the pH to 7.4 by using 6 N NaOH. Bring volume up to 1 L and autoclave (*see Note 4*).
8. 1× phosphate-buffered saline (1× PBS): Mix 100 mL 10× PBS buffer and 900 mL autoclaved ultrapure water.
9. 4% formaldehyde: Mix 27 mL formaldehyde solution (37%) and 223 mL 1× PBS buffer.
10. Denhardtts solution: Dissolve 0.5 g Ficoll 400, 0.5 g polyvinylpyrrolidone, and 0.5 g bovine serum albumin (BSA) in 25 mL autoclaved ultrapure water.
11. 0.2 M phosphate buffer: Mix 1.33 mL phosphoric acid and 80 mL autoclaved ultrapure water. Adjust pH to 7.4 using NaOH and bring final volume to 100 mL. Autoclave.
12. 20× saline sodium citrate (SSC) buffer: Prepare a solution of 3 M NaCl and 0.3 M sodium citrate by dissolving 175.3 g NaCl and 88.2 g sodium citrate in 800 mL of autoclaved ultrapure water. Adjust to pH 7 using 6 N HCl, and bring the volume up to 1 L. Autoclave the buffer.
13. Hybridization cocktail: Mix 250 mL formamide, 100 mL of 20× SSC buffer, 5 mL Denhardtts solution, 25 mL 20% sarcosyl (5 g dissolved in 25 mL autoclaved ultrapure water), 50 mL 0.2 M phosphate buffer, and 50 g dextran sulfate. Heat the solution in a 37–42 °C warm water bath and add 20 mL autoclaved ultrapure water. Store at –20 °C aliquoted in 50 mL polypropylene conical tubes.
14. D19 developer: In a 5 L Erlenmeyer flask, mix 4 L distilled water combined with warm tap water until an average temperature of 38 °C is reached or heat the water using a heating plate. Working under a fume hood, add the D19 powder (*see Note 5*) and dissolve the powder using a magnetic stir bar. Add distilled water to 5 L and check for a pH between 9 and 12. Adjust the pH if needed by adding 6 N NaOH to bring it up or 6 N HCl to bring it down. Let the D19 developer cool down and store in a glass bottle.
15. 100% ethanol.

16. Ethanol dilution series (50%–70%–98%): Dilute absolute ethanol to the appropriate concentrations using autoclaved ultrapure water.
17. Chloroform.
18. 2-Methylbutane.
19. *zif268* oligo-cDNA probe.
20. dATP-³³P radioactive ligand (*see Note 2*).
21. Terminal transferase enzyme (Tdt), purified from *E. coli* clone of calf thymus.
22. Liquid scintillation counting solution.
23. DNA, from fish sperm (e.g., 11,467,140,001, Merck).
24. tRNA (e.g., 10,109,495,001, Merck).
25. Oligo-cDNA probe (*see Note 1*).
26. 50% formamide: Mix 50 mL formamide and 50 mL of autoclaved ultrapure water.
27. Heat pads.
28. Curved forceps: Tip width, 0.5 mm; length, 10 cm; tip shape, curved; tip dimensions, 0.5 × 0.4 mm.
29. Large forceps: Tip width, 3.3 mm; length, 16 cm; tip shape, straight; tip dimensions, 3.3 × 1.7 mm.
30. Aluminum foil: multiple 10 × 10 cm sheets.
31. Glassware prebaked at 185 °C: Glass beaker (volume 800 mL), glass slides (25 × 75 mm), glass slide holder, glass slide containers (max volume 250 mL).
32. Poly-L-lysine hydrobromide mol wt > 300,000.
33. Weighing boats (46 × 46 × 8 mm).
34. Cryostat, −20 °C.
35. Heating block: Up to 100 °C with a holder for 0.5 mL and 1.5 mL microcentrifuge tubes.
36. Microcentrifuge tubes (0.5 mL, 1.5 mL).
37. 50 mL conical tubes, polypropylene.
38. Quick spin oligo column (Sephadex G-25).
39. Microcentrifuge.
40. Vortex .
41. β-counter.
42. Scintillation counting tubes for β-counter.
43. Rubber cement.
44. Humidity chamber for immunohistochemistry staining of sectioned samples on glass slides (e.g., Biogear BGHC-024).

45. Tissue paper.
46. Autoradiography film (e.g., hyperfilm Biomax MR).
47. Medical X-ray film cassette.
48. Scanner (e.g., Canon CanoScan 9000F Mark II).
49. Carbon-14 standards on glass slides with an activity range of 0–35 nCi/mg.
50. Computer with ImageJ software and statistical software such as Excel or GraphPad.

3 Methods

3.1 *Monocular Enucleation*

1. Sedate the animal via a 0.2 mL intraperitoneal injection of the anesthesia solution (8 $\mu\text{L/g}$ bodyweight) and keep the animal warm while sedated by using heating pads.
2. Use large forceps to check the tail-pinch reflex to assess the depth of sedation.
3. Apply eye cream to the eye that will not be removed in order to prevent dehydration (*see Note 6*).
4. Sterilize a curved forceps.
5. Place the animal on a smooth and large surface like a table (*see Note 7*) and lay it on its side, with the eye to be removed facing upward.
6. Place the sides of the opened forceps around the eye and press down gently to elevate the eye out of its socket.
7. Bring the forceps behind the eye and close them. Pinch the blood vessel and nerve but not the eyeball (*see Note 8*).
8. Make a small circular movement with the forceps, allowing the animal's body to follow in the same circular movement. Switch from clockwise to counterclockwise rotation when there is any resistance when executing the circular movement (*see Note 9*).
9. Continue fluent circular movements while keeping the forceps tightly closed until the eye detaches from its blood vessel and nerve (*see Note 10*).
10. Reverse sedation via a 0.4 mL i.p. administration of the anesthesia-reversal solution and administer a 0.1 mL subcutaneous injection of analgesics solution.
11. Let the animal recover on a heating pad before returning it to the animal facility.

3.2 Sample Preparation

1. To measure visual cortex activity levels, animals should be placed in a quiet dark room the evening before, and brains should be harvested the next morning upon appropriate sensory stimulation (*see Note 11*).
2. Stimulate the animals during 45 min in bright lighting (*see Note 12*).
3. Fill the bottom of a beaker with 2-methylbutane (± 2 cm liquid to submerge the brains), place on dry ice, and let it cool down to -40 °C (*see Note 13*). Place rectangular pieces of aluminum foil, used to store the brains, on dry ice to cool them in order to prevent tissue damage in **step 5**.
4. Sacrifice the mice via cervical dislocation by applying firm pressure at the base of the skull while pulling the tail backward. Dissect out the brain and place it gently on a small plastic container, i.e., weighing boat. Carefully submerge the plastic container containing the brain in the cooled 2-methylbutane for approximately 5 min.
5. Use forceps to remove the plastic container from the beaker and place the brain on the pre-cooled aluminum foil. Close the aluminum foil and store at -80 °C. (*see Note 14*).
6. Prepare 25 μm brain sections using a cryostat (*see Note 15*). Collect sections on glass slides, baked and pre-coated with poly-L-lysine, and store them at -20 °C (*see Note 16*).

3.3 Labeling and Purification of the Probe

1. Set the heating block at 37 °C.
2. Add 20 μL autoclaved ultrapure water, 8 μL terminal transferase enzyme (Tdt) buffer, 4 μL oligo (40 ng/ μL concentration), 4 μL Tdt (*see Note 17*), and 4 μL ^{33}P -dATP in a 0.5 mL microcentrifuge tube.
3. Incubate the microcentrifuge tube in the heating block at 37 °C for 1.5–2 h.
4. Use a mini Quick spin oligo column (gel filtration chromatography), containing Sephadex G-25 diluted in STE (1 \times) buffer. Carefully tap against the column to resuspend the Sephadex matrix in the buffer (*see Note 18*) and remove the top and bottom part.
5. Place the column on a 1.5 mL microcentrifuge tube and centrifuge using a microfuge at 4000 \times g for 1 min at room temperature.
6. Discard the microcentrifuge tube containing the buffer and place the column into a new microcentrifuge tube.
7. Apply the labeled oligo mixture in the middle of the column and centrifuge using a microfuge at 4000 g force for 4 min at room temperature.
8. Add 200 μL of TET buffer to the microcentrifuge tube, now containing the purified labeled oligo probes.

3.4 Quantifying the Amount of Labeled Oligo Probes

To quantify the amount of radioactively labeled oligo, liquid scintillation counting (Aqua luma) is performed. Radioactivity is expressed in counts per minute (cpm).

1. Place the standard solution (Aqua luma) in the β -counter.
2. Add 2 μL of the labeled oligo to 5 mL Aqua luma and vortex (*see Note 19*). This is done in special scintillation tubes that fit in the available β -counter. The cpm are determined with the software program that fits the chosen isotope (^{33}P).
3. Calculate the amount of labeled oligo (μL) that needs to be added to the hybridization cocktail (*see Note 20*).
4. Store the microcentrifuge tubes of labeled oligo at 4 °C (*see Note 21*).

3.5 Tissue Fixation

1. Take out the frozen glass slides 30 min before fixation and place them on room temperature to dry.
2. Fixate the dry glass slides in 4% formaldehyde for 30 min on 4 °C to inhibit endogenous ribonucleases.
3. Rinse the glass slides two times in 1 \times PBS for 15 min each.
4. Shortly rinse with ultrapure water to remove salts.
5. Dehydrate the tissue on the glass slides by pulling them through a series of solutions with ascending ethanol concentrations: 1' ethanol 50% – 1' ethanol 70% – 1' ethanol 98% – 2' ethanol 100%: Prepare the ethanol dilutions using autoclaved ultrapure water.
6. Delipidate the tissue on the glass slides by submerging them in chloroform for 5'.
7. Shortly rinse in 100% and 98% ethanol to remove the chloroform.
8. Let the glass slides air-dry (*see Note 22*).

3.6 Hybridization

1. Place the hybridization cocktail at 37–42 °C to reduce viscosity (*see Note 23*).
2. Calculate the amount of hybridization cocktail, labeled oligo, DNA, and tRNA required for the complete hybridization solution, based on the number of slides to be stained. Each slide requires 0.5 mL hybridization cocktail, one million cpm of the labeled oligo, 5.5 μL DNA, and 3 μL tRNA (*see Note 24*).
3. Set the heating block to 100 °C. When the right temperature is reached, place the DNA in the heating block and let it boil for at least 10 min to allow denaturation.
4. Prepare a moisturized chamber by adding tissue paper soaked in 50% formamide (*see Note 25*).

5. Surround the sections of each glass slide with rubber cement to create a barrier to keep the hybridization solution on the sections (*see Note 26*).
6. Based on your calculations in **step 2**, combine the hybridization cocktail, DNA, and tRNA in a polypropylene falcon, and vortex.
7. To complete the hybridization solution, add the labeled oligo (as calculated in **step 2**) to the mixture in **step 4** and vortex again.
8. Apply 0.5 mL of the hybridization solution to each glass slide and incubate overnight at 38 °C (*see Note 27*).

3.7 Rinsing and Preparation for Film Exposure

1. Wash the sections with 1× SSC buffer at 43 °C if they were incubated at 38 °C (*see Note 28*).
2. Remove the rubber cement and rinse them again (*see Note 29*).
3. Place the glass slides in a glass slide holder, fill with 1× SSC buffer, and place them in a water bath heated at the same temperature (in this case 43 °C).
4. Rinse four times for 15 min with 1× SSC buffer preheated in the water bath (*see Note 30*).
5. Perform a last short rinse with autoclaved ultrapure water.
6. Dehydrate the tissue sections on the glass slides using an ascending ethanol series, (1' ethanol 50% – 1' ethanol 70% – 1' ethanol 98% – 1' ethanol 100%).
7. Air-dry the glass slides.
8. Take a thick white paper and tape all glass slides on it as well as carbon-14 standards on one of the films (*see Note 31*).
9. Place the autoradiography film (hyperfilm Biomax MR) with its matte side on the glass slides while being in a dark room (presence of red light is allowed) (*see Note 32*). Place the film with glass slides in a medical X-ray film cassette and store it in the dark chamber or in a lighttight closet.
10. Films can be developed after 6 days (*see Note 33*).

3.8 Film Development

1. Take the films out of the cassettes in the dark room.
2. Place the films for 5 min in D19 developer. The films cannot touch each other during development.
3. Rinse the films with (tap) water.
4. Fixate the films for 10 min in Rapid fixer, which is diluted 1/5 (*see Note 34*).
5. Rinse four times in (tap) water (at least 30 s each time, but this can be longer) (*see Note 35*).
6. Rinse with distilled water to avoid calcification stains from the tap water.

7. Air-dry the films by hanging them up, so they can dry on both sides.
8. Once the films are dried, use a scanner (Canon CanoScan 9000F Mark II) to obtain images of each section and the carbon-14 standards for further analysis.

3.9 Analysis

1. Use an image analysis software such as ImageJ to measure IEG expression levels by performing an optical density measurement in the region(s) of interest.
2. Open the image of the carbon-14 standards to calibrate your images.
3. Measure the mean gray background value of each standard/step. Make a rectangular selection that almost covers the entire square of the standard/step that you want to measure. Start on the lightest side and move toward the darkest square. Measure each step (Analyze/Measure). You can adjust the contrast of the image to see the lighter or darker squares more clearly (Image/adjust/Brightness/contrast).
4. Each measurement has been added automatically to the left side of the calibration dialog box (Analyze/Calibrate). Add O.D. values into the right column from 0.00 to 2.60, divided in equal steps (Function: Rodbard – Unit: O.D.).
5. The image is now calibrated to O.D. values and the calibration curve can be saved. The same calibration can be used for all open images by checking “global calibration” at the bottom of the calibrate dialog box.
6. Open the image of the section that you want to analyze.
7. Select the area of interest and measure the OD value (Analyze/measure).
8. Select a background area and measure the OD value (Analyze/measure) (*see Note 36*).
9. Calculate your value with the following formula $((1 - (\text{OD area of interest}/\text{OD background area})) \times 100)$ (*see Note 37*) and save them in an Excel file or statistical program file such as “graphpad.”

4 Notes

1. Depending on the chosen probe, hybridization and rinsing steps will need to be adjusted. Choose an oligonucleotide probe of approximately 45 nucleotides with a similar number of C–G pairs and A–T pairs. The tail and end sequence of the probe should differ from each other to avoid hairpin or loop formations. When performing ISH for a new oligonucleotide

for the first time, you should introduce negative biological and technical controls, by labeling certain sections with a labeled sense probe instead of an antisense probe. A second option is to add excess unlabeled oligo (100×) to the hybridization cocktail. The unlabeled oligo will outcompete the labeled oligo probes. A third option is to destroy all RNA with RNase prior to incubation with labeled probe to check if there is no labeling to DNA [18].

2. We chose ^{33}P radioactive labeling as in our hands it provides the best signal-to-noise ratio for *zif268* ISH based on radiation strength, decay, and hazard for the experimenter. The radioactive isotope can be stored at $-80\text{ }^{\circ}\text{C}$ upon arrival, but it is recommended to start labeling as soon as possible to prevent decay of the radioactivity. It is difficult to find a good supplier; therefore, we would like to share the one that we use: American Radiolabeled Chemicals Inc., dATP- ^{33}P , 1 mCi, ARP-0127A. Other radioactive isotopes have been used for ISH but we do not recommend them due to the following observations: ^{32}P -labeling leads to a poor resolution and ^{32}P has a half-life time of only 14 days. ^{35}S , on the other hand, has a longer half-life time and its labeling provides a slightly better resolution. However, the addition of a reducing agent such as dithiothreitol (DTT) is required to avoid sulfur oxidation, thereby reducing the higher risk of background staining. Moreover, when using ^{35}S , there is an additional risk due to the possibility of aerosol formation. ^3H -labeling would not be ideal as it requires an impractically long autoradiographic exposure time (several months).

When working with radioactivity, make sure the required safety procedures are followed; work in an isolated radioactive room/space, wear a dosimeter to check exposure levels, and wear double pair of gloves, safety goggles, and a dedicated (radioactivity only) lab coat. Radioactivity-contaminated material should be discarded in special waste bins. After finishing the radioactive experiment, make sure to check used material and bench spaces for possible contamination using a Geiger counter.

3. Give double of the amount that you gave to anesthetize (e.g., a mouse of 20 g will receive 0.2 mL anesthesia, i.p. and 0.4 mL anesthesia reversal i.p.).
4. Dissolved NaOH crystals will release heat; use a cold-water bath to cool down the buffer to room temperature or add it in small steps. Store the buffer at room temperature to avoid crystallization.
5. D19 powder can be bought, or you can make it yourself. One bag of D19 powder (normally for 3.8 L) can be used to make 5 L of developer fluid for ISH film development. After usage,

pour developer solution immediately back in the bottle to avoid oxidation. The solution can be reused and stored long-term. The developer works optimally at a room temperature between 16 and 22 °C.

6. Dehydration of the intact eye can occur after 5 min under anesthesia and could lead to visual damage. After applying eye cream to the intact eye, it might be necessary to apply it a second time after removal of the other eye. During eye removal, the animal is faced with the remaining eye toward the table, resulting in loss of the eye cream. If the animal is adequately sedated within the first 5 min, one can choose to add eye cream at the end of the procedure.
7. If the surgery is performed on an uneven surface, the circular movement of the animal will be obstructed and slowed down. This will complicate efficient eye removal and induces a higher risk of bleeding due to inadequate clamping of the nerve and blood vessel.
8. Make sure to pinch the blood vessel and nerve within the arch of the forceps. If you pinch them at the tip of the forceps, the circular movements could lead to detachment between the tissue and forceps, interrupting the twisting of the blood vessel and nerve. Grasping the blood vessel and nerve a second time is not recommended because it will complicate a swift removal and increase the chance of bleeding.
9. In some cases, there will be no resistance felt upon the first turn. In this case, there is no problem in keeping the same circular direction. When there is resistance, the direction of movement should be reversed. This process should be repeated until there is no longer any resistance.
10. Be careful to not lift the forceps too high while making the circular movements; keep them close to the animal and surface. By lifting up the forceps too high, there is a chance to tear the blood vessel and nerve instead of twisting them. A premature tear will lead to bleeding and a longer recovery time.
11. Place the mice in the dark to bring *zif268* levels back to baseline. We dark expose the mice from 5 pm to 9 am. Make sure to not extend the period of dark exposure as this will influence plasticity in the visual cortex.
12. After 45 min of re-exposure to sensory stimulation (light, sound, touch of objects, depending on the experimental question), maximal expression of *zif268* mRNA is reached. For analysis at protein level, maximal expression levels are reached after 60 min.
13. Make sure that the temperature does not go below -50 °C, since this can cause damage to the brain submerged into the liquid.

14. When folding the aluminum foil, make sure that the foil does not touch the top of the cortex. If the foil is not adequately cooled down, the heat of the foil will damage layer 1 of the cortex.
15. Cryosections can be stored up to several years and still be used for ISH. Using sections thicker than 25 μm will not result in a signal intensity increase since maximal tissue penetration by the labeled probe is reached.
16. Poly-L-lysine-coated glass slides can be bought or self-made. They provide adhesion of sections and clear RNases. To coat the glass slides, bake all slides and fluid holders in an oven at 185 °C, while covered in tin foil. Let them cool down and prepare the poly-L-lysine solution, molecular weight > 300,000 (dissolve 100 mg poly-L-lysine hydrobromide powder in 100 mL autoclaved ultrapure water in a pre-baked bottle with an autoclaved lid). Dip the slides in poly-L-lysine solution and let the excessive solution drip off. Place the slides angular at 45° in drying racks. Once dry, place all the slides in boxes and store at -20 °C.
17. Tdt is very temperature sensitive. Place it in a cooling block at -20 °C at all times, even when pipetting.
18. Do not vortex since this could cause damage to the column.
19. Depending on how much oligo you want to radioactively label, you will most likely use more than one microcentrifuge tube. Radioactivity should be measured for each microcentrifuge tube that contains labeled oligo. It is to be expected that each microcentrifuge tube will give a different value. Based on our facilities and equipment, one ISH contains 120 glass slides maximum. Two to three such ISH can be performed based on the amount of radioactively labeled oligo probe.
20. Each glass slide, consisting of six cryosections (mouse brain), needs to be labeled with one million cpm radioactivity. Based on this information, we calculate the amount of labeled oligo that needs to be added to the hybridization buffer.
21. The microcentrifuge tubes with labeled oligo can be stored at 4 °C overnight. It is however also possible to immediately continue with the protocol on the same day.
22. Place the glass slides in holders to avoid any spots on your tissue from dried up water. This should go relatively fast (around 30 min).
23. This can be done before you start fixating your tissue.
24. DNA and tRNA are added to decrease nonspecific binding of the oligo.

25. Adding the formamide is important to avoid condensation droplets to fall on the glass slides, which could dilute the mixture and leave spots with less or no labeling.
26. Apply one rectangle of the rubber cement at the edge of the glass slide, not around each tissue section. Be careful to not place any rubber cement on the tissue sections or the writing part of the glass slides. Use a syringe to apply a 1 mm thick layer of rubber cement. If too much is applied, it will spread upon drying and possibly touch the sections, but when applied too thin, it will be harder to remove in the next step.
27. If the sequence of the labeled oligo matches 100% with the targeted species, the incubation temperature can be set higher. By setting the temperature higher, there will be less aspecific binding. The temperature can however not rise above the melting temperature of the oligo. When the cocktail buffer contains formamide, this will lower the melting temperature. For RNA–DNA hybrids, you can calculate the melting temperature with the following formula: $T_m = 79.8 + 18.5 \log(\text{molarity of monovalent cations}) + 0.58 (\%GC \text{ content of the probe}) + 0.0012 (\%GC \text{ content})^2 - 820 / (\text{length of probe in bases}) - 0.5 (\% \text{ formamide})$.
28. Take the melting temperature of the oligo into account. After overnight incubation, the unbound labeled oligo needs to be rinsed off. This should be done at a temperature 5 °C higher than the incubation step. With negative results, try the experiment again but at a lower temperature.
29. Removing rubber cement can be done with forceps. Use the forceps to grab a corner of the rubber cement. If it was applied in the right consistency, then the rubber cement will come off in one piece when pulled gently.
30. All the waste of each rinsing step should be considered as radioactive waste.
31. Make sure the glass slides do not touch each other when taping them on the white paper. When placing the film and closing the cassette, the glass slides could move a bit leading to them pushing up against each other or even overlap. The film would then not touch the complete glass slide and therefore give unsharp images. The carbon-14 standards are added to be able to make a calibration curve of the optical density (OD) values while analyzing the results. One for each set of simultaneous developed films is enough.
32. The autoradiography hyperfilms (Biomax MR, A4 format) are stored in the fridge at 4 °C. Take them out of the fridge at least 30 min before using them to avoid condensation droplets on the glass slides.

33. Depending on the used oligo, isotope, tissue, and species under study, and on the desired signal intensity, films can be developed after 3 days or up until 4 weeks. Exposure time has to be determined empirically. If the signal is insufficient, new film is applied and a longer developing time is implemented.
34. Always use different tubs for the developer and fixator baths and different spatulas to move the films through the fluid. One is basic while the other is acidic and therefore cannot be mixed together.
35. From this step on, the light can be turned on.
36. Choose a small area to measure the OD value of the background. This does not have to be the same size as the area of interest. Preferably, it is the background of the section so choose an area within the section that is not affected by IEG changes (e.g., white matter underneath the cortical layers).
37. Pure black will have the lowest OD value, but from an experimental viewpoint, it represents the highest expression of your IEG. If you do not transform your values with this formula, you will end up with bar graphs wherein low IEG expression values are represented by high bars and vice versa.

Acknowledgments

We would like to thank Ria Vanlaer for her immense work and input throughout the years in order to optimize this technique.

References

1. Pérez-Cadahía B, Drobic B, Davie JR (2011) Activation and function of immediate-early genes in the nervous system. *Biochem Cell Biol* 89:61–73
2. Gallo FT, Kathe C, Morici JF et al (2018) Immediate early genes, memory and psychiatric disorders: focus on c-Fos, Egr1 and arc. *Front Behav Neurosci* 12:180
3. Franceschini A, Costantini I, Pavone FS, Silvestri L (2020) Dissecting neuronal activation on a brain-wide scale with immediate early genes. *Front Neurosci* 14:596517
4. Xie H, Liu Y, Zhu Y et al (2014) In vivo imaging of immediate early gene expression reveals layer-specific memory traces in the mammalian brain. *Proc Natl Acad Sci U S A*. <https://doi.org/10.1073/pnas.1316808111>
5. Moeyaert B, Holt G, Madangopal R et al (2018) Improved methods for marking active neuron populations. *Nat Commun*. <https://doi.org/10.1038/s41467-018-06935-2>
6. Wisden W, Errington ML, Williams S et al (1990) Differential expression of immediate early genes in the hippocampus and spinal cord. *Neuron*. [https://doi.org/10.1016/0896-6273\(90\)90118-Y](https://doi.org/10.1016/0896-6273(90)90118-Y)
7. Zhang F, Halleux P, Arckens L et al (1994) Distribution of immediate early gene zif-268, c-fos, c-Jun and Jun-D mRNAs in the adult cat with special references to brain region related to vision. *Neurosci Lett*. [https://doi.org/10.1016/0304-3940\(94\)90067-1](https://doi.org/10.1016/0304-3940(94)90067-1)
8. Cullinan WE, Herman JP, Battaglia DF et al (1995) Pattern and time course of immediate early gene expression in rat brain following acute stress. *Neuroscience*. [https://doi.org/10.1016/0306-4522\(94\)00355-9](https://doi.org/10.1016/0306-4522(94)00355-9)

9. Guzowski JF, Timlin JA, Roysam B et al (2005) Mapping behaviorally relevant neural circuits with immediate-early gene expression. *Curr Opin Neurobiol* 15:599–606
10. Zhang F, Vanduffel W, Schiffmann SN et al (1995) Decrease of zif-268 and c-fos and increase of c-Jun mRNA in the cat areas 17, 18 and 19 following complete visual deaf-ferentation. *Eur J Neurosci*. <https://doi.org/10.1111/j.1460-9568.1995.tb01119.x>
11. Arckens L, Van Der Gucht E, Eysel UT et al (2000) Investigation of cortical reorganization in area 17 and nine extrastriate visual areas through the detection of changes in immediate early gene expression as induced by retinal lesions. *J Comp Neurol*. [https://doi.org/10.1002/1096-9861\(20001002\)425:4<531::AID-CNE5>3.0.CO;2-J](https://doi.org/10.1002/1096-9861(20001002)425:4<531::AID-CNE5>3.0.CO;2-J)
12. Van Brussel L, Gerits A, Arckens L (2011) Evidence for cross-modal plasticity in adult mouse visual cortex following monocular enucleation. *Cereb Cortex* 21:2133–2146. <https://doi.org/10.1093/cercor/bhq286>
13. Aerts J, Nys J, Arckens L (2014) A highly reproducible and straightforward method to perform in vivo ocular enucleation in the mouse after eye opening. *J Vis Exp*. <https://doi.org/10.3791/51936>
14. Hennes M, Lombaert N, Wahis J et al (2020) Astrocytes shape the plastic response of adult cortical neurons to vision loss. *Glia*. <https://doi.org/10.1002/glia.23830>
15. Nys J, Aerts J, Ytebrouck E et al (2014) The cross-modal aspect of mouse visual cortex plasticity induced by monocular enucleation is age dependent. *J Comp Neurol* 522:950–970. <https://doi.org/10.1002/cne.23455>
16. Nys J, Smolders K, Laramée M-E et al (2015) Regional specificity of GABAergic regulation of cross-modal plasticity in mouse visual cortex after unilateral enucleation. *J Neurosci* 35: 11174–11189. <https://doi.org/10.1523/JNEUROSCI.3808-14.2015>
17. Mahringer D, Zmarz P, Okuno H et al (2020) Functional correlates of immediate early gene expression in mouse visual cortex. *bioRxiv:2020.11.12.379909*. <https://doi.org/10.1101/2020.11.12.379909>
18. Arckens L, Zhang F, Vanduffelb W et al (1995) Localization of the two protein kinase C- β -mRNA subtypes in cat visual system. *J Chem Neuroanat*. [https://doi.org/10.1016/0891-0618\(94\)00040-Z](https://doi.org/10.1016/0891-0618(94)00040-Z)



Noncoding Regulatory RNAs: Isolation and Analysis of Neuronal Circular RNAs and MicroRNAs

Michela Dell’Orco, Grigorios Papageorgiou, Nikolaos Mellios, and Nora I. Perrone-Bizzozero

Abstract

In addition to expressing a large number of protein-coding transcripts, including alternatively spliced isoforms of the same mRNAs, neurons express a large number of noncoding RNAs. These include microRNAs (miRNAs), circular RNAs (circRNAs), and other regulatory RNAs. The isolation and quantitative analyses of diverse types of RNAs in neurons are critical to understand not only the posttranscriptional mechanisms regulating mRNA levels and their translation but also the potential of several RNAs expressed in the same neurons to regulate these processes by generating networks of competing endogenous RNAs (ceRNAs). This chapter will describe methods for the isolation and analyses of circRNA and miRNA levels from the same brain tissue sample.

Key words RNA isolation, Brain tissues, circRNAs, miRNAs, qRT-PCR

1 Introduction

There are several methods to isolate total RNA from cells, but the most common ones are based on the use of either the chaotropic agent guanidinium thiocyanate combined with phenol and chloroform extraction [1] or a guanidinium salt containing lysis buffer and silica-based columns that bind RNA, followed by elution and alcohol precipitation. The guanidinium thiocyanate–phenol solution, which is commercially available as TRIzol, TRI Reagent, QIAzol, or equivalent kit, disrupts the cells, denatures proteins, and deactivates nucleases and proteases, thereby stabilizing the DNA, RNA, and protein in the sample. The main advantage of this method is the ability to scale up the amount of starting material used from mg to grams of tissue. Disadvantages include the requirement of a chemical hood due to the use of phenol and chloroform.

The column-based methods (e.g., Qiagen RNeasy kit, EZ Tissue/Cell Total RNA Miniprep kit, or similar columns) avoid the use of chemical hoods as they do not use organic chemicals and can be used for low amounts of tissue (10–100 mg), but they cannot be scaled up to grams of tissue. RNA isolation using columns is faster than using organic chemicals. They also minimize DNA contamination by using gDNA Eliminator columns in the RNeasy[®] Plus Kits. Alternatively, DNA can be digested using RNase-free DNase I for in-column digestion or after elution.

Below we describe an RNA isolation protocol using the guanidinium thiocyanate–phenol solution method. After RNA is isolated, the levels of circRNAs and miRNAs can be evaluated using specific cDNA synthesis followed by real-time quantitative PCR (qRT-PCR).

2 Materials

2.1 Reagents and Equipment for Working with RNA

1. RNase decontamination solution, e.g., RNaseZap[™] (*see* **Notes 1** and **2**).
2. RNase-free water (commercially available or DEPC-treated water) (*see* **Note 3**).
3. RNase- and DNase-free microcentrifuge tubes (0.2–1.5 mL) (*see* **Note 3**).
4. Aerosol Barrier Pipet tips (from 10 to 1000 μ L).
5. Micropipettes (from 2 to 1000 μ L) (*see* **Note 1**).
6. 0.2 mL PCR 8-tube strips and set of 8-cap strips.
7. 96- or 384-well PCR plates (e.g., MicroAmp EnduraPlate Optical 96- and 384-well Clear Reaction Plate with Barcode, Applied Biosystems by Life technologies, 4483354 and 4309849) or similar plates from other suppliers.
8. Tube racks for 0.2–1.5 mL tubes.
9. Gloves.
10. Lab coat.
11. Standard thermocycler.
12. Real-time quantitative PCR thermal cycler.
13. Real-time quantitative fast PCR thermal cycler (if available, this is ideal for miRNA assays).
14. Ice.
15. Dry ice.
16. -80 °C freezer.

2.2 RNA Isolation

1. Chemical hood (*see Note 1*).
2. Handheld tissue homogenizer with motor and homogenization pestles (several homogenizers are commercially available to work with RNase-free single-use plastic pestles, e.g., KIMBLE cat# 6HAZ6).
3. Microvolume UV/visible spectrophotometer (e.g., NanoDrop-1000, Thermo Fisher).
4. Fluorometer for nucleic acid quantification (e.g., Qubit, Thermo Fisher).
5. Refrigerated centrifuge at 4 °C and rotor capable of reaching 12,000× *g* for 1.5 mL tubes.
6. Vortex mixer.
7. Water bath or heat block at 37 °C.
8. Surgical stainless-steel tweezers.
9. Chloroform (100%).
10. Ethanol (100%).
11. Diethyl pyrocarbonate (DEPC).
12. 1,4-Dithiothreitol (DTT, 100 mM: 15.4 mg in 1 mL RNase-free water) .
13. RNase-free glycogen (15 mg/mL). *See Note 4*.
14. Reagent for acid guanidinium thiocyanate–phenol–chloroform extraction (e.g., TRIzol, TRI Reagent, QIAzol, or equivalent reagents).
15. RNase inhibitor (e.g., Invitrogen RNaseOUT, 40 U/μL).

2.3 Quantification of circRNAs

1. RNase R (e.g., Epicentre, RNR07250).
2. First-Strand Synthesis System (e.g., SuperScript IV Invitrogen™ by Thermo Fisher, 18091050), or alternative commercially available kits and enzymes such as MultiScribe™ Reverse Transcriptase (Invitrogen™ by Thermo Fisher, 4311235).
3. SuperScript IV First-Strand Synthesis Master Mix for circRNAs (1 μL 50 μM random hexamer primers × number of samples; 1 μL 10 mM dNTP mix × number of samples; 3 μL RNase-free water × number of samples). The use of 10% additional volume of all reagents is recommended to compensate for minor pipetting errors.
4. SuperScript IV RT Master Mix (4 μL SuperScript™ IV RT Reaction Buffer Invitrogen™ 18090050B (*see Note 5*); 1 μL 100 mM DTT × number of samples; 1 μL RNaseOUT Inhibitor 40 U/μL; 0.5 μL SuperScript IV RT; 0.5 μL RNase-free water).
5. SYBR Green Master Mix (e.g., PowerUp™ SYBR™ Green 2X Master mix, A25741, Thermo Fisher).

6. SYBR Green Master Mix for qPCR (33 μL PowerUp™ SYBR™ Green 2X Master mix, Thermo Fisher; 3.3 μL 5 μM forward primer; 3.3 μL 5 μM reverse primer; 22 μL RNase-free water). This amount is enough to run one sample in triplicates.
7. Oligo(dT)_{12–18} Primer, Thermo Fisher, 18418012.

2.4 Quantification of miRNAs

1. TaqMan® MicroRNA Assays or equivalent assays.
2. miRNA RT Master Mix (0.225 μL 100 mM dNTP Invitrogen™, 10297018; 1.5 μL MultiScribe™ Reverse Transcriptase Invitrogen™, 4311235; 2.25 μL 10x RT buffer (*see Note 5*); 0.285 μL RNaseOUT 40 U/ μL ; 4.5 μL primer (5 μM); 6.24 μL RNase-free molecular grade water).
3. TaqMan PCR Master Mix (3.3 μL TaqMan® Small RNA Assay (20X); 33.0 μL TaqMan® Universal PCR Master Mix II (2X); 25.4 μL RNase-free water). This is enough to run each sample in triplicates.

3 Methods

3.1 RNA Isolation from Brain Tissues

1. Assign an “RNA-only” lab space, reagents, and micropipettes and clean all the benches, hood, and tools with RNase decontamination solution (*see Notes 1, 2, and 3*).
2. Keep frozen tissue on dry ice until ready to go to **step 3**. If tissue is freshly dissected, keep tissue cold in saline or phosphate-buffered saline and immediately proceed to **step 3** (*see Note 6*).
3. Calculate weight of samples and reagent amounts: add 1 mL TRIzol™ Reagent per 100 mg of tissue at room temperature.
4. Homogenize tissue in handheld tissue homogenizer with autoclaved or RNase-free disposable pestles. Some tissues may require elimination of bubbles by carefully extruding extracts through a 1 mL syringe.
5. Let homogenized sample incubate at room temperature for 5–10 min.
6. Add 200 μL of 100% chloroform per 1 mL of TRIzol™ Reagent used (*see Note 7*).
7. Vortex vigorously each sample for 30 s. The solution will change color from bright pink to opaque light pink.
8. Allow samples to sit at room temperature for 3 min. Phase separation will start at this point.
9. Centrifuge at 4 °C for 15 min at 12,000 $\times g$. Prepare new batch of 1.5 mL tubes while samples are in the centrifuge.

10. Hold sample tube at a slight angle, and collect upper, clear aqueous phase containing the RNA. Use 200 μL pipette tips to transfer the aqueous layers to new microfuge tubes. To minimize DNA contamination, avoid touching the white interphase and check the pipette tips for any contamination before transferring the aqueous phase to new tubes.
11. Then add 3 μL of 15 mg/mL RNase-free glycogen solution (*see Note 4*) and mix by vortexing. After that, add 500 μL of 100% isopropanol per 1 mL TRIzol™ Reagent and mix by inverting the tubes several times.
12. Incubate at $-20\text{ }^{\circ}\text{C}$ for 30 min or overnight for higher yield.
13. Centrifuge samples at $4\text{ }^{\circ}\text{C}$ for 15 min at $12,000\times g$, noting the side of the tube where the RNA pellets will be collected.
14. Check the presence of a light blue RNA pellet if using Glyco-Blue™ or a white pellet if using regular RNase-free glycogen and carefully discard the isopropanol.
15. Wash the pellet with 1 mL 75% ethanol. For better RNA quality, prepare fresh ethanol solution before washing.
16. Discard ethanol and use a 200 μL micropipette to carefully remove all the supernatant. Let tubes sit open in a chemical hood or bench counter until ethanol is fully evaporated but do not let the pellet overdry (*see Note 8*).
17. Resuspend the pellet in 25–100 μL of DNase-/RNase-free distilled water by pipetting the pellet up and down multiple times. If the pellet is not completely resuspended, incubate the samples at $37\text{--}50\text{ }^{\circ}\text{C}$ for 10 min to solubilize the RNA.
18. Quantify the amount of RNA using both a Qubit fluorometer and Nanodrop (Thermo Fisher) or UV/visible spectrophotometer to assess RNA quality and concentration following the manufacturer's instructions (*see Note 9*).
19. Store samples at $-80\text{ }^{\circ}\text{C}$ or proceed to cDNA synthesis.

3.2 circRNA cDNA Synthesis

1. Digest 100–500 ng of isolated RNA in a solution of 1 μL 10x RNase R (Epicentre®, RNR07250) reaction buffer and 1 μL of RNase R (20 U/ μL) adjusting the volume to 10 μL with RNase-free molecular grade water (for details on RNase R, *see Note 10*).
2. Incubate at $37\text{ }^{\circ}\text{C}$ for 30 min in a thermocycler or water bath.
3. Place a 96-well plate place on ice, and add calculated concentration of RNA so that each well has a total of 8 μL of RNA to begin with.
4. In a 1.5–2 mL tube mix SuperScript IV First-Strand Synthesis Master Mix as described in the Materials section.

5. Add 5 μL of SuperScript IV First-Strand Synthesis Master Mix into each well with the initial 8 μL for a total of 13 μL in each well.
6. Cover wells with strip caps and vortex and centrifuge the plate (*see Note 11*).
7. Place plate in regular or quantitative PCR thermal cycler with the machine programmed as follows: Lid, 105 °C; volume, 13 μL ; **step 1**, 65 °C for 5 min; **step 2**, 4 °C for ∞ .
8. While **step 7** is ongoing, prepare the SuperScript IV RT Master Mix as described in the Materials section. Do not vortex master mix, but simply pipet up and down to mix.
9. Once **step 7** is completed, take plate out of thermal cycler and vortex and centrifuge again.
10. Place on ice and slowly uncap wells.
11. Add 7 μL of SuperScript IV RT Master Mix to each well and cap again.
12. Slightly vortex plate and centrifuge.
13. Place well plate in a thermal cycler (please note that this reaction can be run using a standard thermocycler) with the machine programmed as follows: Lid, 105 °C; volume, 20 μL ; **step 1**, 23 °C for 10 min; **step 2**, 50 °C for 10 min; **step 3**, 80 °C for 10 min; **step 4**, 4 °C for ∞ .
14. Once **step 13** is completed, take plate out of thermal cycler and store at -20 °C until needed for PCR amplification.

3.3 circRNA qRT-PCR, Primers' Design, and Validation

1. Find detailed information on the circRNA of interest in circRNA-related databases such as circBase (<http://www.circbase.org/>) [2] or circInteractome (<https://circinteractome.nia.nih.gov/>) [3] and identify its full sequence, including the exons and/or introns it contains.
2. Design primers that span the circRNA backspliced junction via primer design software, such as NCBI primer and/or primer3 [4]. For exonic circRNAs with small-sized introns, try to have the primer within the exons that comprise the backspliced junction.
3. Validate primers and calculate amplification slopes. For details on primer validation and primer slope determination, *see Note 12*. An example of primer validation is shown in Fig. 1.
4. After the PCR reaction, run the PCR product in an agarose gel and note its size. PCR products can be cut and gel purified, so that they can be processed for Sanger sequencing for sequence validation.

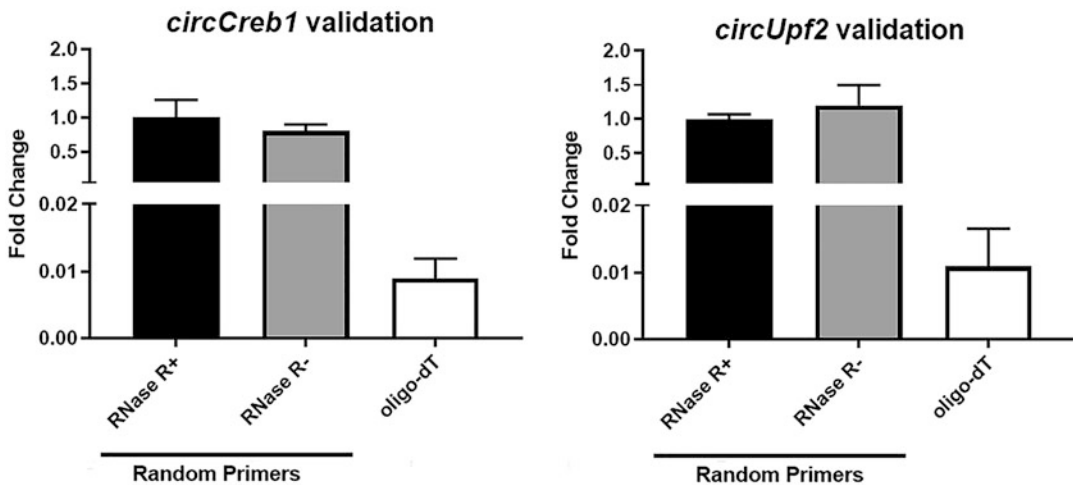


Fig. 1 Validation of circRNA-specific qRT-PCR. Examples of validation of qRT-PCR reactions for *circUpf2* and *circCreb1*; re-printed with permission from Dell’Orco et al., 2020 [7]. To assess the specificity, reactions were run in parallel with the same RNA samples that were either treated with RNase R (RNase R+) or left untreated (RNase R-). In addition, instead of using random primers for the reverse transcription reactions, the same RNA was used for cDNA synthesis in the presence of oligo-dT primers. If the primers only recognize the circRNA and not the linear mRNA, there should be no significant difference between the results of RNase R+ and RNase R- reactions. Finally, the oligo-dT reactions should show minimal or no amplification as shown by the 100-fold lower amplification of the oligo-dT vs. random primers cDNA synthesis reactions for the circRNAs. Please note that the scales have been divided to show the minimal circRNA amplification from the qRT-PCR reactions using oligo-dt primer. Fold-changes are relative to the RNase R+ condition

3.4 circRNA Quantification by qRT-PCR

circRNA qRT-PCR is performed as previously described in Zimmerman et al. (2020) [5].

1. Take the 96-well plate stored in -20°C after cDNA synthesis and let it thaw at room temperature. Once thawed vortex and centrifuge.
2. Dilute cDNA from plate at a 1:10 and 1:200 ratio (*see Note 12*).
3. Take diluted cDNA and make 4.4 μL aliquots for each sample ($\sim 1.33 \text{ uL} \times 3.3$ to allow for enough cDNA for all triplicates plus 10% more for pipetting corrections).
4. Make SYBR Green Master Mix as described in the Materials section.
5. Add master mix last and immediately place on ice after vortexing and centrifuging.
6. Add 61.6 μL of the SYBR Green Master Mix to each sample and place on ice immediately.
7. After adding the master mix to all the samples, gently vortex the plate and centrifuge, placing on ice immediately again.

8. Take another tub of ice and place 384-well plate making sure it is evenly set on the ice.
9. Pipet 20 μL of each sample into each well making sure to pipet three wells per sample.
10. Once all samples have been pipetted in triplicates, use adhesive film to seal well plate.
11. Vortex and centrifuge sealed plate to get rid of any bubbles (*see Note 11*).
12. Once no bubbles are visible, place plate in PCR machine, which should be set to the following settings prior to placing plate in machine as indicated below.
13. Set the thermal cycling conditions using the standard cycling mode: **step 1**, UDG activation, 50 °C 2 min, hold; **step 2**, Dual-Lock™ DNA polymerase 95 °C 2 min, hold; **step 3**, denature 95 °C for 15 s and anneal/extend 60 °C 1 min, 40 cycles. Dissociation curve conditions (melt curve stage): 1.6 °C/s at 95 °C for 15 s, 1.6 °C/s at 60 °C for 1 min, and 0.15 °C/s at 95 °C for 15 s.
14. Run PCR as follows:
 - PCR machine: Always choose the Comparative Curve analysis setting if available except when determining the slope of the PCR amplification curve, where you need to choose the standard curve option.
 - Choose appropriate reagent (SYBR Green) and make sure that the reaction volume per well is set up to 20 μL .
15. Calculate the concentration of each circRNA relative to the reference circRNA (*see Note 13*).

3.5 miRNA-Specific cDNA Synthesis

1. Clean working area with RNase decontamination solution (*see Notes 1 and 2*).
2. Defrost all samples and reagents, except the enzymes, on ice and keep them on ice.
3. Dilute RNA samples to 2 ng/ μL in UltraPure™ DNase-/RNase-free distilled water (Invitrogen™, 10977015) or equivalent RNase-free molecular grade water (*see Note 3*).
4. Prepare the miRNA RT Master Mix using TaqMan® MicroRNA Reverse transcription kit and TaqMan® MicroRNA Assay primers (Life Technologies) as described in the Materials section (*see Note 14*).
5. Dispense 15 μL master mix into each tube.
6. Dispense 7.5 μL of RNA diluted to 2 ng/ μL into each tube.
7. Set the thermocycler as follows: **step 1**, 16 °C 30 min; **step 2**, 42 °C 30 min; **step 3**, 85 °C 5 min; hold 4 °C ∞ .
8. Store cDNA at -20 °C or proceed to miRNA qRT-PCR.

3.6 miRNA-Specific Quantification by qRT-PCR

1. Dilute all cDNA samples 1:100 with RNase-free water and run in triplicate for each miRNA analyzed.
2. Prepare the TaqMan PCR Master Mix for each miRNA as described in the Materials section. This will prepare enough master mix to run reactions in triplicates.
3. Dispense the master mix into tubes for each sample.
4. Add 1.33 μL cDNA template or RNase-free water for the no-template controls (NTC) to each tube.
5. Vortex and then briefly centrifuge to remove bubbles by centrifugation (*see Note 11*).
6. Dispense 20 μL per well (three wells for each sample, for each miRNA).
7. Cover the plate with a thermal adhesive sealing film and spin down to prevent bubbles.

Load plate into a fast real-time qPCR machine (if available as this allows to run reactions in half as much time as in regular qPCR machines) or regular real-time qPCR machine: select FAM as detector, set solution volume to 20 μL , and run the following protocol: **step 1**, 50 °C, 2 min 1 cycle; **step 2**, 95 °C, 20 s, 1 cycle; **step 3**, 95 °C, 1 s and 60 °C, 20 s, 40 cycles.

8. Calculate miRNA levels relative to U6 snRNA or another control miRNA that does not change between samples using the comparative $2^{-\Delta\text{Ct}}$ method [8, 9] (*see Note 15*).

4 Notes

1. Separate working area for RNA extraction from that used for tissue dissection or protein work to avoid contamination with RNases from animal tissues and protein extracts. Also, use a separate set of micropipettes and pipet tips with barrier filters.
2. Before starting any RNA extraction, both the working area and micropipettes need to be cleaned with an RNase Decontamination Solution, e.g., RNaseZap™, Invitrogen™, AM9780, RNase AWAY™, Thermo Fisher Scientific 10328011, or similar solution prepared in the laboratory. Besides commercially available reagents, disinfecting solutions can be prepared using the following chemicals in distilled water: mandelic acid (1%), lactic acid (1%), hydrogen peroxide (5%), sodium dodecyl sulfate (SDS, 1–2%), and EDTA (1%) as described in patent numbers US4448750A, EP0109279A2, and WO1996020737A1. Also, spray your gloves with RNaseZap™ before handling the samples and remember to avoid breathing close to the tubes as saliva has high content of RNases.

3. All reagents and tubes need to be RNase-free by purchasing them as such or by pretreating with DEPC-treated dH₂O, which can be used as an alternative to commercially available RNase-free water. DEPC is prepared at a concentration of 0.1% in double distilled water. Glassware and plastic ware need to be treated with 0.1% DEPC-water at 37 °C for at least 1 h. DEPC-treated water is also incubated for at least 1 h at 37 °C. After this, it is important to autoclave both the tubes and water to destroy residual DEPC for at least 15 min, as this reagent inactivates not only RNases but also other enzymes that have histidines in the catalytic site. DEPC can also react with lysine, cysteine, and tyrosine residues although with less efficiency.
4. Be sure to add glycogen before the ethanol precipitation to recover mRNAs, circRNAs, and small RNAs such as miRNAs as shown above. RNase-free glycogen can be purchased already prepared (e.g., GlycoBlue™ Coprecipitant, Invitrogen™, AM9516) or prepared in the laboratory. To prepare RNase-free glycogen solution (15 mg/mL), add 150 mg of glycogen to 10 mL of double distilled water and stir until the glycogen is fully dissolved. This will take about 1–2 h. Transfer aliquots to 2 mL microcentrifuge tubes. Add an equal volume of phenol–chloroform to the glycogen solution and vortex thoroughly. Centrifuge at 12,000× *g* for 10 min at 4 °C and transfer the upper aqueous phase (containing glycogen) into new 2 mL tubes. Add an equal volume of cold (4 °C) chloroform/isoamyl alcohol (50:1 vol: vol) into the glycogen phase and vortex thoroughly. After vortexing and letting phase separation, the chloroform phase should be the lower phase. Centrifuge at 12,000× *g* for 10 min at 4 °C and transfer the upper aqueous phase (containing glycogen) into new 2 mL tubes. Freeze aliquots at –20 °C or –80 °C for long-term storage.
5. 10X RT buffers are commercially available (Promega, A3561) or can be easily prepared with 500 mM Tris–HCl (pH 8.3), 750 mM KCl, and 30 mM MgCl₂.
6. If tissues are larger than 100 mg, they will need to be broken apart in liquid nitrogen using a ceramic mortar and pestle. Then let liquid nitrogen evaporate and keep pulverized tissue frozen on dry ice or –80 °C. TRIzol RNA extraction can be used for small tissues as described in Bastle et al. (2017) [9]. Briefly, whole brains are flash frozen and dissected using a brain matrix kept at –20 °C. Regions of interest can be dissected using 1.25 and 2 mm brain punches.
7. For tissues with high myelin content (e.g., cerebellum), double the amount of chloroform.

8. Remove supernatant with a pipet tip. Quickly centrifuge the tube to collect any remaining 75% ethanol to the bottom. Remove as much of the remaining ethanol with a pipet tip and air-dry the RNA pellet by leaving the tubes open on the counter for approximately 15–30 min. When the pellet is dry, there must be no visible ethanol in the tube. Do not overdry the pellet as it may be difficult to resuspend.
9. While a Qubit fluorometer (Thermo Fisher) gives a more accurate quantification of the RNA, a NanoDrop 1000 Spectrophotometer (Thermo Fisher) can be used to assess the quality of the isolated RNA samples and the presence of contaminations. The Qubit fluorometer uses specific dyes for RNA, DNA or protein while the NanoDrop quantification is based on UV absorbance at 260 nm (nucleic acids' peak absorbance). However, the Qubit does not provide any information about RNA purity. In a NanoDrop instrument, an A260/A230 ratio lower than 2.0 may be the result of residual phenol, residual guanidine, or glycogen used for precipitation. Finally, an A260/A280 ratio lower than 1.8 indicates high level of protein contamination. RNA quality can also be assessed running RNAs on denaturing agarose gels or using a 2100 Bioanalyzer Instrument (Agilent). Good quality RNA will show clear 18 s and 28 s bands, while DNA contamination will be seen as an intense high molecular weight band. The Bioanalyzer also provides RNA integrity numbers (RIN). High-quality RNA has a RIN >8.
10. RNase R is 3' to 5' exoribonuclease that digests all linear RNAs except double-stranded RNAs leaving all circular RNAs intact. Keep RNase R (and all enzymes) in a cold block kept at -20°C while using it to avoid deactivation. The RNase R treatment does not need to be repeated after primer validations [6, 7].
11. If a centrifuge for spinning plates is not available, there are very cheap alternatives as using a salad spinner (see <https://bitesizebio.com/3200/how-to-build-a-plate-centrifuge-for-25/> for instructions of how to make one of these).
12. For primer validation and slope determination, include serial dilutions of cDNA from random hexamer reverse transcription in addition to cDNA derived from RNase R-treated total RNA, cDNA derived from oligo-dT reverse transcription, as well as no-template negative controls using all the reagents minus the cDNA. Visualize melting curves and calculate primer slopes. To determine the best concentration of cDNA to use in your qPCR reaction, prepare serial dilutions of the cDNA and select a concentration in a range where the amplification is proportional to the cDNA amount. Only primers that generate a single PCR product with a unique melting curve and appropriate size and primer slope (typically 3 ± 0.5 cycles/log cDNA

concentration) should be selected. Expression of the circRNA product should be maintained or increased following RNase R treatment, but greatly diminished following oligo-dT reverse transcription (Fig. 1). Sanger sequencing should confirm that the primers amplify the unique circRNA backspliced junction.

13. For quantification of circRNAs, we utilize the following formula: relative circRNA expression = $E^{Ct^{\text{circRNA}}}$ / $E^{Ct^{\text{normalizer}}}$, where $E = 10^{-(1/\text{primer slope})}$. When multiple circRNA normalizers are used, the geometric mean of their average Ct values was calculated instead. If no circRNA normalizers are available, housekeeping genes such as GAPDH or 18S rRNA can be used instead. Also, *CDR1as* and *circTulp4* are good normalizers for brain tissues.
14. Please note that TaqMan[®]-based assays described above are listed only as examples of the protocols used in our laboratories, and products from other suppliers can be used as alternatives or prepared in house. The TaqMan[®] technology, also known as fluorogenic 5' nuclease chemistry, is preferable for these determinations as miRNAs are very short and the use of an internal fluorogenic probe increases the specificity of the detection. In addition, TaqMan[®] MicroRNA Assays have the advantage of being highly specific for mature miRNAs and do not detect precursor miRNAs, as there are separate assays for these. Due to their high sensitivity, they only require 1–10 ng of total RNA. Earlier versions of TaqMan[®] MicroRNA Assays use a target-specific stem-loop primer during cDNA synthesis requiring a miRNA-specific RT. In contrast, the new TaqMan Advanced miRNA Assays include a polyadenylation step for the miRNAs and use a universal RT step.
15. Besides using U6 snRNA, other endogenous control snRNAs, snoRNAs, and miRNAs have been identified to be used as normalizers with TaqMan[®] MicroRNA Assays (<https://www.gene-quantification.de/AB-microRNA-endog-controls.pdf>). You can also select any miRNA that does not change in any of the samples and conditions that you are studying.

Acknowledgments

This work was supported by NIH, R01DA034097, and R21 DA048651 grants to N.P.B. as well as a mentored PI grant as part of an P20 grant from the NIGMS (1P20GM121176-01, N. M.), a NIAAA R01 grant (R01AA026583, N.M. and G.P.), a NARSAD Young Investigator Grant (FP00000839, N.M.) by the Brain & Behavior Research Foundation, and a high priority short-term R56 award from the NIMH (1R56MH119150-01, N.M.).

References

1. Chomczynski P, Sacchi N (1987) Single-step method of RNA isolation by acid guanidinium thiocyanate-phenol-chloroform extraction. *Anal Biochem* 162:156–159. [https://doi.org/10.1016/0003-2697\(87\)90021-2](https://doi.org/10.1016/0003-2697(87)90021-2)
2. Glažar P, Papavasileiou P, Rajewsky N (2014) CircBase: a database for circular RNAs. *RNA* 20:1666–1670. <https://doi.org/10.1261/rna.043687.113>
3. Dudekula DB, Panda AC, Grammatikakis I et al (2016) CircInteractome: a web tool for exploring circular RNAs and their interacting proteins and microRNAs. *RNA Biol* 13:34–42. <https://doi.org/10.1080/15476286.2015.1128065>
4. Untergasser A, Cutcutache I, Koressaar T et al (2012) Primer3-new capabilities and interfaces. *Nucleic Acids Res* 40. <https://doi.org/10.1093/nar/gks596>
5. Zimmerman AJAJ, Hafez AKAK, Amoah SKSK et al (2020) A psychiatric disease-related circular RNA controls synaptic gene expression and cognition. *Mol Psychiatry* 25. <https://doi.org/10.1038/s41380-020-0653-4>
6. Panda A, Gorospe M (2018) Detection and analysis of circular RNAs by RT-PCR. *Bio-Protocol* 8. <https://doi.org/10.21769/bioprotoc.2775>
7. Dell’Orco M, Oliver RJ, Perrone-Bizzozero N (2020) HuD binds to and regulates circular RNAs derived from neuronal development- and synaptic plasticity-associated genes. *Front Genet* 11. <https://doi.org/10.3389/fgene.2020.00790>
8. Livak LJ, Schmittgen TD (2001) Analysis of relative gene expression data using realtime quantitative PCR and the 2^{-ΔΔCT} method. *Methods* 25:402–408. <https://doi.org/10.1006/meth.2001.1262>
9. Bastle RM, Oliver RJ, Gardiner AS et al (2017) In silico identification and in vivo validation of miR-495 as a novel regulator of motivation for cocaine that targets multiple addiction-related networks in the nucleus accumbens. *Mol Psychiatry* 23:434–443. <https://doi.org/10.1038/mp.2016.238>



Transneuronal Delivery of Cytokines to Stimulate Mammalian Spinal Cord Regeneration

Daniel Terheyden-Keighley, Marco Leibinger, Charlotte Zeitler, and Dietmar Fischer

Abstract

The spinal cord contains multiple fiber tracts necessary for locomotion. However, as a part of the central nervous system, they are extremely limited in regenerating after injury. Many of these key fiber tracts originate from deep brain stem nuclei that are difficult to access. Here we detail a new methodology that achieves functional regeneration in mice after a complete spinal cord crush, describing the crushing procedure itself, intracortical treatment application, and a set of appropriate validation steps. The regeneration is achieved by the one-time transduction of neurons in the motor cortex with a viral vector expressing the designer cytokine hIL-6. This potent stimulator of the JAK/STAT3 pathway and regeneration is transported in axons and then transneuronally delivered to critical deep brain stem nuclei via collateral axon terminals, resulting in previously paralyzed mice walking again after 3–6 weeks. With no previously known strategy accomplishing this degree of recovery, this model is well suited to studying the functional impact of compounds/treatments currently only known to promote anatomical regeneration.

Key words Crush, SCI, Functional, Recovery, Intracortical, Mouse, hIL-6, AAV, Raphe, Model

1 Introduction

The spinal cord is essential for receiving incoming sensory information from the peripheral nervous system, in addition to processing and outputting motor information from the brain. However, as vital as it is to locomotion, the spinal cord's ability to regenerate after injury is almost nonexistent [1]. Up until now, the large variety of treatment strategies designed to aid functional recovery after complete spinal cord lesions have failed to yield approved therapies [1, 2]. One of the aspects that make this endeavor so challenging is the sheer number of barriers to functional recovery, meaning that multiple problems must be solved simultaneously for success. Key among these are (a) the inhibitory environment of the central nervous system (CNS) [3], (b) the lack of an active

regeneration program in the damaged nerves [4], and finally, (c) the lack of proper synapsing and circuit formation [5–7]. Moreover, functional recovery likely requires the regeneration of multiple trajectories originating in different brain nuclei, some challenging to target. The overwhelming majority of experimental compounds and therapies do not show any functional readout because of a failure to address one or more of the aforementioned barriers, making it difficult to assess their true potential in aiding functional regeneration.

Here we present a new methodology that stimulates axon regeneration of several tracts simultaneously and achieves functional recovery of hind limb locomotion after complete spinal cord crush, finally providing a model for testing the efficacy of additional compounds for combinatorial treatments in improving functional regeneration [8]. Using safe, non-integrating viral vectors, a designer cytokine known as hyper-interleukin-6 (hIL-6) is transduced into layer V neurons of the primary motor cortex. In addition to detailing the spinal cord crush procedure, precise instructions for performing the intracortical injections are also provided, along with a set of validation steps for ensuring the quality of the operations.

The use of hIL-6 circumvents the need for IL-6 receptor expression by the target neurons, as it is a fusion protein of the soluble IL-6 receptor that is covalently bound to its ligand. Thus, hIL-6 potently and efficiently activates its downstream regenerative effector: signal transducer and activator of transcription 3 (STAT3) [9, 10]. Furthermore, hIL-6 treatment overcomes the inhibitory effects of myelin [10]. Significantly, hIL-6 is secreted at the transduced neurons' axon terminals, resulting in the transneuronal activation of STAT3 in secondary nuclei such as the raphe or red nucleus [8]. Key among these are the serotonergic hindbrain nuclei of the medulla, as this group of neurons is responsible for the resulting functional regeneration [11]. STAT3 activation transforms these neurons into a regenerative state, allowing them to extend their axons within the CNS and presumably to form direct or indirect connections with crucial neurons of the hind limb locomotive central pattern generators.

The unique aspect addressed by this methodology is that by targeting the output layer of the upstream motor cortex, the crucial downstream motor tracts are simultaneously stimulated by being collateral targets. Recovery peaks after just 3–6 weeks, with the model returning a clear readout using either Catwalk gait analysis or Basso mouse scale (BMS) testing [12]. Compared to control mice whose hind limbs are limited to ankle movement (BMS: ≤ 2), AAV2-hIL-6-treated mice can achieve plantar paw placement, support their hindquarters, and take steps (BMS: ≥ 4). The model produces a clear leap over control animals and leaves ample room for improvement, providing fertile ground for demonstrating improved recovery after concomitant treatment with other test compounds and strategies.

2 Materials

2.1 Animals and Animal Care

1. Mice: Wild-type C57BL/6 J housed for at least 10 days under the same conditions before beginning the experiments, including a 12 h/12 h light/dark cycle with ad libitum access to food and water. Males and females show an equal regeneration response to hIL-6 treatment. Take care to have all experimental procedures approved by the local animal care committee and conduct them in compliance with federal and state guidelines for animal experiments.
2. 1 mg/mL carprofen.
3. 1 mg/mL gentamicin.
4. Eye gel: nose and eye gel.
5. Anesthetic: Isoflurane administered via an isoflurane vaporizer set to 1.5% with a flow rate of 1 liter of oxygen per minute (*see Note 1*).
6. Isoflurane vaporizer.

2.2 Surgical Tools for Crush

1. Iris forceps (e.g., FST: 11064-07).
2. Straight-bladed scalpel (e.g., FST: #11, 10011-00).
3. Scalpel handle #3 (e.g., FST: 1003-12).
4. Fine scissors (e.g., FST: 14060-09).
5. Tissue-spreader: Colibri retractors (e.g., FST: 17000-02) (*see Note 2*).
6. Rongeurs, 0.5 mm (e.g., FST: 16221-14 Friedman-Pearson Rongeurs).
7. Bone scissors: Noyes (e.g., Dimeda 09.111.12).
8. Wound clips, 7 mm (e.g., FST: 12032-07).
9. Clip applier, 7 mm (e.g., Agnathos: 204-1000).
10. Sutures: Ethicon Ethilon II blue 5-0 (non-resorbable) and Ethicon Monocryl violet monofil 5-0 (resorbable).
11. Needle holder (e.g., FST: 91201-12).
12. Fine forceps: Dumont #5 (e.g., FST: 11254-20).
13. Crush forceps: #5 forceps hand-filed down to 0.15 mm width for at least 5 mm in length for a uniform crush size over the dorsoventral axis of the spinal cord.

2.3 Tools and Supplies for Intracortical Injection

1. Stereotaxic instrument (e.g., Kopf: model 940).
2. Mouse anesthesia mask (e.g., Kopf: model 907).
3. Microdrill and 0.5 mm bit (5000 RPM-capable).
4. Microfluidic injector (e.g., Drummond Scientific, Nanoject III or II).

5. Capillary puller (e.g., Zeitz DMZ universal electrode puller).
6. Micropipette beveler (e.g., World Precision Instruments, 48000).
7. 50 μm diameter pulled capillaries with 45-degree beveled tips (*see Note 3*).

2.4 Viruses

1. AAV2 with hIL-6 under the control of a CMV promotor, IRES-driven GFP as a reporter system (produced in-house and available from Fischer lab [8]).
2. Control virus: AAV2-GFP; both viruses should have a titer of 1×10^{13} virus genomes/mL (produced in-house and available from Fischer lab) [8] (*see Note 4*).

2.5 Validation

1. Phosphate-buffered saline (PBS).
2. Paraformaldehyde (PFA) (4% in PBS).
3. Sucrose (30% in water).
4. Acetone.
5. Dry ice.
6. Cyro-embedding medium (e.g., Tissue-Tek, Sakuraus).
7. Cryotome (e.g., Leica CM3050).
8. Microscope slides.
9. Pstat3 antibody (1:200) RRID: AB_2491009.
10. GFP antibody (1:500) RRID: AB_10128178.
11. 5HT antibody (1:5000) RRID: RRID:AB_572262, RRID: AB_572263.
12. GFAP antibody (1:500, ab53554 Abcam).
13. Secondary antibodies including anti-mouse, anti-goat, and anti-rabbit conjugated to Alexa Fluor 405 (1:500, Jackson ImmunoResearch), 488, or 594 (1:1000, Invitrogen).
14. Streptavidin Alexa Fluor 405, 488, or 594 conjugate (Thermo Fischer).
15. Biotinylated dextran amine (BDA) 10% solution in water (Invitrogen, D1956).
16. Blocking solution (5% donkey serum, 2% bovine serum albumin in PBS + 0.05% Tween 20).
17. Methanol.
18. Embedding medium.
19. 70% ethanol.

3 Methods

3.1 T8 Spinal Cord Crush

1. Anesthetize the adult mouse with 1.5% isoflurane (*see Note 1*) and shave a 2 cm wide strip along the back from the spine's crest up to the ears and the scalp from between the ears up to eye level. Apply eye gel to prevent them from drying out. Wipe down both shaved areas with 70% ethanol to remove hairs and clean the surgery area.
2. Administer carprofen (5 mg/kg) and gentamicin (5 mg/kg) in PBS subcutaneously and as separate injections.
3. Drape the mouse over a 2–3 cm diameter cylinder (*see Note 5*).
4. After checking for reflexes, make a midline incision approximately 2 cm in length from the level of the shoulder blades in the caudal direction (*see Fig. 1a* and **Note 6**).
5. Separate the surrounding skin from the underlying tissue by inserting closed pointy scissors and then opening them to spread the tissue apart (blunt dissection) (*Fig. 1b*).
6. Pinch and lift the most caudal edge of the fat pad at the midline using iris forceps, and then make a small incision in the fat's caudal edge before inserting scissors to blunt dissect open a large hole (*see Fig. 1c, d* and **Note 7**).
7. Carefully cut along the lateral edges of this fat pad to create a loose sheet that can then be folded back toward the head to reveal a large blood vessel entering the spine (*Fig. 1d, e*).
8. This blood vessel is located above the spine between T5 and T6 and is thus an ideal landmark. Using the iris forceps, feel along the midline from T6, counting spinous processes to identify the T7 process, and then grip it to stabilize the mouse until after the crush (*Fig. 1e*).
9. Using a straight-bladed scalpel, cut two 1 cm long incisions on the left and right side next to spinous processes along the T7–T9 vertebra using flat strokes until the blade is scraping along the underlying bone. Try to stay as close to the midline (spinous processes) as possible when cutting either side (*Fig. 1e*).
10. Insert a small tissue spreader into the muscle incisions for better visibility and access to the spine (*see Fig. 1f* and **Note 8**).
11. Using the flat edge of 0.5 mm cup rongeurs, excavate the T8 vertebra. This will inevitably also remove the T8 spinous process (*Fig. 1g, h*).
12. Using the pointed end of the rongeurs at a flat angle, gently pinch the area between T8 and T9 to remove the ligament but be careful not to cut too deep and damage the dura mater (*Fig. 1i*).

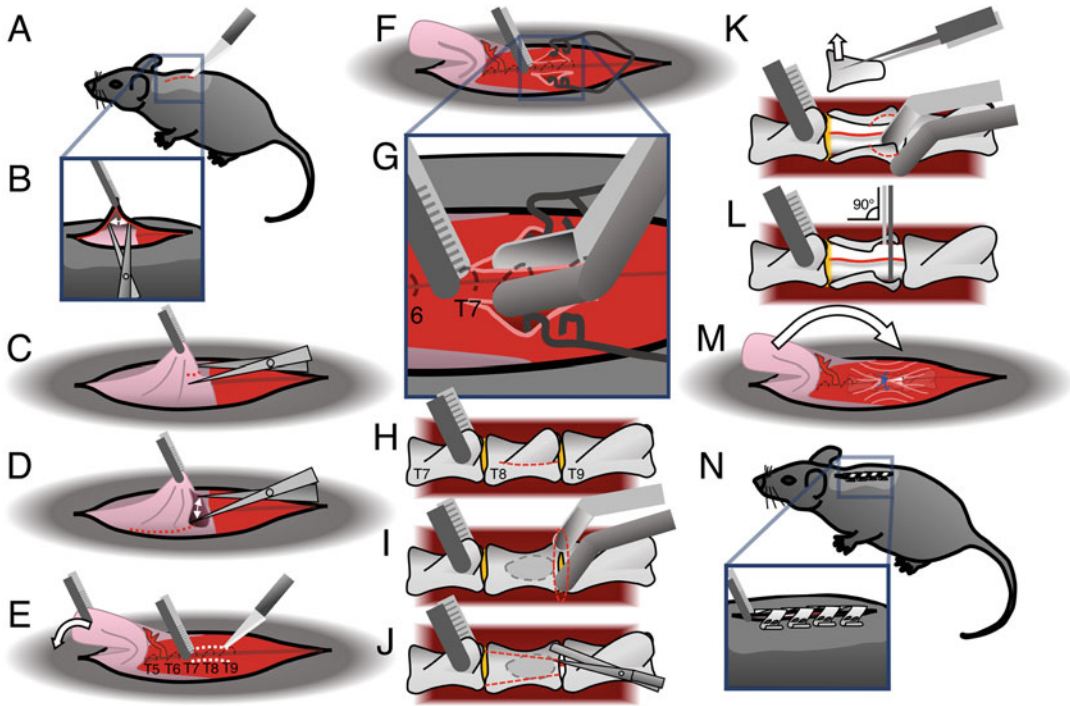


Fig. 1 Spinal cord crush procedure. (a) Mouse with shaved back and 2 cm midline incision to reveal (b) fat pad and muscle tissue, where scissors are used to bluntly dissect the surrounding skin. (c) Caudal incision into the fat pad. (d) Blunt dissection to enlarge the hole, followed by lateral cutting (red dotted line) on both sides. (e) Folding back the fat flap to reveal a large blood vessel between T5 and T6 and lateral incisions adjacent to T8 through the muscle tissue (white dotted lines) while supporting from T7. (f) Insertion of a tissue-spreader into the longitudinal back muscles, followed by (g) excavation of the T8 vertebra using the flat edge of 0.5 mm rongeurs, removing the muscle tissue, and (h) T8 spinal process. (i) Removal of the T8–T9 ligament by gentle scraping with the tip of the rongeurs. (j) Lateral cutting of the T8 lamina with fine bone scissors, followed by (k) removing the T8 lamina and nipping off remaining edges with rongeurs. (l) Insertion of crush forceps to execute the spinal cord crush at a 90-degree angle to the spinal cord. (m) Adjacent longitudinal muscles sutured together over the crush site with a single resorbable suture, followed by the fat pad’s return to its original position and (n) closing of the skin with two to four wound clips

13. Using fine bone scissors, gently insert the sharp edge at a very shallow angle under the bone where the ligament was, in the cranial direction. Cut the lamina arcus laterally to the left and right of the midline (*see* Fig. 1j and Note 9).
14. These cuts should span the T8 vertebra, resulting in a rectangle of bone becoming free. Discard this using fine forceps (Fig. 1k).
15. This might leave sharp remaining parts of the T8 vertebra on either side of where the bone previously was. Using the rongeurs, very carefully pinch off these protrusions and avoid touching the spinal cord (Fig. 1k).

16. If any periosteum is visible covering the spinal cord (a pink/red membrane), carefully remove this with fine forceps to not interfere with the crush.
17. Now that the spinal cord is free, insert the crushing forceps at a 90-degree angle to the spinal cord, lowering the tips until they touch the bottom of the spinal canal, gently scraping along the bone (Fig. 1l).
18. In a controlled manner, pinch the forceps together for 1–2 s, ensuring that only enough force is applied to close the forceps fully (*see Note 10*).
19. Now that the crush is complete, remove the spreader and suture the two sides of the back muscles together to cover the exposed spinal cord. Use a single resorbable suture (Fig. 1m).
20. Finally, pull the fat pad back over the operated vertebra and close the skin using two to four wound clips (*see Fig. 1n and Note 11*) and allow the mouse to recover in an oxygenated, 37 °C cage.
21. If there is no further surgery planned (e.g., intracortical injection), allow the mouse to recover in an oxygenated, 37 °C cage for 10 min.
22. Treat the mice with appropriate amounts of painkiller and antibiotic subcutaneously. Provide intraperitoneal injections of 0.5 mL PBS for the next 5 days. Also, manually express their bladders, check the urine pH, and weigh them daily for the rest of their lives (*see Note 15*).

3.2 Intracortical Injections

1. Directly after performing the spinal cord crush, make a midline incision on the scalp from the level of the eyes, 1 cm in the caudal direction (centered over bregma, Fig. 2a).
2. Transfer the mouse into the stereotaxic frame, which also provides oxygenated isoflurane at the same 1.5% (*see Note 1*) via an appropriate anesthesia mask.
3. Free the skin around the incision, and then gently scratch over the area with a sharp scalpel to shred and remove the loose connective tissue covering the skull (*see Fig. 2b, c and Note 12*).
4. Scratch a 2 × 1 mm rectangle into the skull using fine forceps parallel to the midline and 0.5 mm lateral from it while being centered adjacent to bregma (Fig. 2d).
5. Using an electronic fine crafts drill, gently mill this traced outline until the rectangle's center becomes loose (Fig. 2e). Lift this away with fine forceps (*see Fig. 2f and Note 13*).

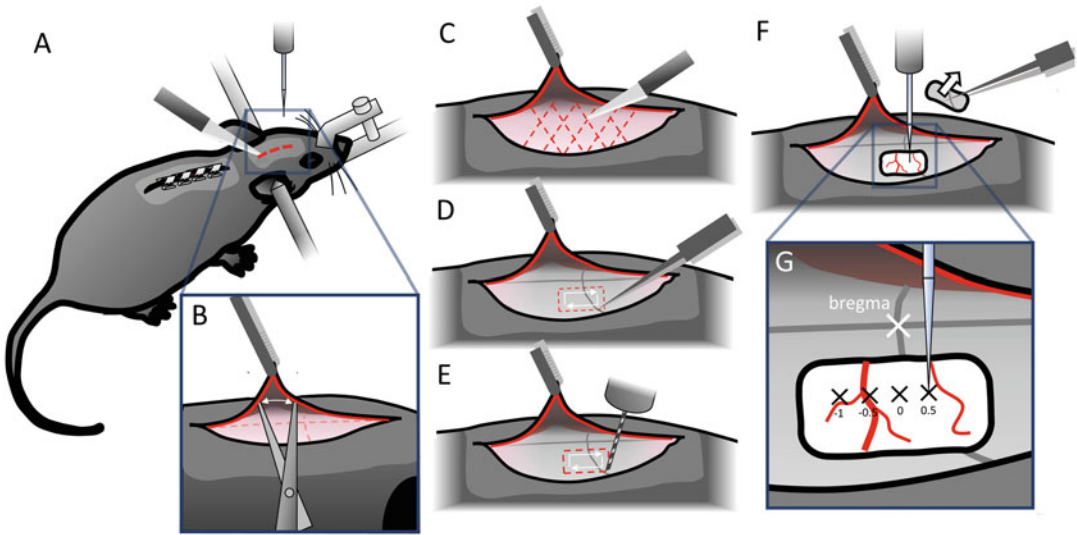


Fig. 2 intracortical injections' procedure. (a) Mouse with shaved head mouth-fixed to a stereotactic frame with midline skin incision over bregma. (b) Skin freed from the skull by blunt dissection with scissors. (c) Removing underlying soft connective tissue with gentle scalpel scraping. (d) Scratching the outline of the skull window adjacent to bregma over the future injection sites. (e) Slowly milling away the bone by repeatedly tracing over the scratched outline with a fine drill until the bone is thin enough to (f) remove with fine forceps. (g) Viral injection into the motor cortex 1.5 mm lateral from bregma. Bregma should not be confused with the more caudal skull bone intersection known as lambda (not visible here)

6. Using the stereotaxic device and a programmable micro-injector fitted with a virus-filled beveled glass capillary with a 50 μm diameter tip, inject hIL-6 AAV2 into the following four coordinates: +0.5 mm, 0 mm, -0.5 mm, and -1.0 mm anterior, all 1.5 mm lateral from bregma (Fig. 2g). A positive coordinate indicates a location cranial from bregma. Use a depth of 0.6 mm for each injection. Allow 1 min after needle insertion and another min after each injection to stabilize the tissue. Use the following micro-injector settings: volume, 100 nL; rate, 10 nL/s; cycles, 5; time (delay), 10 s. This will result in 500 μL of virus solution being injected per site, and thus 2 μL total per hemisphere. Only one hemisphere needs hIL-6 treatment to achieve robust functional recovery of hind limb locomotion (*see Note 14*).
7. Once the injections have been done, close the skin with three to four sutures and allow the mouse to recover in an oxygenated, 37 $^{\circ}\text{C}$ cage.
8. Treat the mice with appropriate amounts of painkiller and antibiotic subcutaneously and provide intraperitoneal injections of 0.5 mL PBS for the next 5 days. In addition, manually express their bladders, check the urine pH, and weigh them daily for the rest of their lives (*see Note 15*).

3.3 Validation Steps

The model presented here requires practice and has the potential for small mistakes, which could prevent functional regeneration. To help troubleshoot these issues and ensure a certain quality standard, we have listed here a collection of histological validation steps for both the crush and injection procedures. For the crush, these include checking for spared axons and measuring the lesion size, whereas for the injections, they examine virus efficacy, injection depth, and transneuronal stimulation. All tissue processing is carried out using the following standard protocols at room temperature unless specified otherwise:

3.3.1 Tissue Preparation

1. Anesthetize and then sacrifice the mice via transcardial perfusion with PBS (10 mL), followed by 4% PFA (25 mL).
2. Dissect out the entire CNS via laminectomy of the spine and lateral cutting open of the skull. Post-fixate the CNS in 4% PFA overnight at 4 °C, followed by 5 days of incubation in 30% sucrose at 4 °C (*see Note 16*).
3. Cut the CNS into five chunks: spinal cord for analysis of anatomical axon regeneration (3 mm rostral to 8 mm caudal from crush site), distal spinal cord for validation of spared axons (8–10 mm caudal from the lesion site), proximal spinal cord for validation of axonal staining (3–5 mm rostral from the lesion site), the medulla, and the motor cortex including all injection sites.
4. Submerge tissues in cryo-embedding solution and freeze chunks other than the cortex and medulla into tissue blocks at –20 °C for sectioning.
5. Snap-freeze the cortex and medulla by first equilibrating acetone on dry ice, and then folding aluminum foil into a cube-shaped beaker for lowering the cortex and medulla suspensions into the acetone, rapidly freezing them into tissue blocks (*see Note 17*).
6. Cryosection all tissue into 20 µm thick sections of the appropriate orientation, and mount onto microscope slides and store at –20 °C.

3.3.2 Immunostaining

1. Air-dry sections at room temperature for at least 15 min after removal from the freezer.
2. Remove embedding medium with 10-min incubation in PBS.
3. Permeabilize for 10 min in methanol.
4. Block sections for at least 1 h in blocking solution.
5. Incubate sections overnight with the primary antibody diluted in blocking solution at 4 °C in a moist container.
6. Wash 3× 10 min in PBS.

7. Apply the secondary antibody and/or fluorophore-conjugated streptavidin diluted in a blocking solution for 1 h in a dark, moist container.
8. Wash 3× 10 min in PBS.
9. Embed, then coverslip the slides, and store them at 4 °C until imaged.

3.3.3 Crush Quality: Spared Axons

All animals in a complete spinal cord crush regeneration study must be checked for spared axons. We recommend checking multiple spinal cord tracts for axons 8–10 mm caudal to the lesion site, as after 8 weeks, this is longer than the furthest regeneration distance.

1. Starting with the CST, inject 10% BDA 2 weeks before sacrifice into the same coordinates as the virus injections.
2. Stain transverse sections using a fluorophore-conjugated streptavidin (1:500).
3. Second, stain serotonergic fibers with anti-5HT (1:5000) antibodies in the same sections (*see* Fig. 3a, b and **Note 18**).

3.3.4 Crush Quality: Lesion Size

Lesion size is a crucial metric to monitor due to its effect on regeneration. Control mice must have a similar average lesion size to treated mice to allow for valid regeneration comparisons. Lesion sites that are too large will likely result in no regeneration [13]. Quantification of the site of the lesion is therefore recommended. To this end:

1. Immunostain longitudinal sections containing the lesion site and the central canal with anti-GFAP (1:500) allowing the visualization of the lesion borders.
2. Trace this outline with ImageJ to obtain the approximate lesion size (*see* Fig. 3c and **Note 19**).

3.3.5 Intracortical Injection Quality: Virus Efficacy

Successful viral transduction is measured by examining the IRES-based GFP expression in transduced cortical neurons and pSTAT3-positive nuclei in the transduced cells that surround these neurons and indicate the secretion of active hIL-6.

1. Stain coronal sections of the cortex for pSTAT3 (1:200), GFP (1:500), and also streptavidin-405 (1:500) to visualize BDA injection locations (*see* **Note 20**).
2. All three stains should line up with a GFP cloud in the middle, surrounded by a larger pSTAT3-positive cloud and BDA cloud (*see* Fig. 3d–f and **Note 21**).

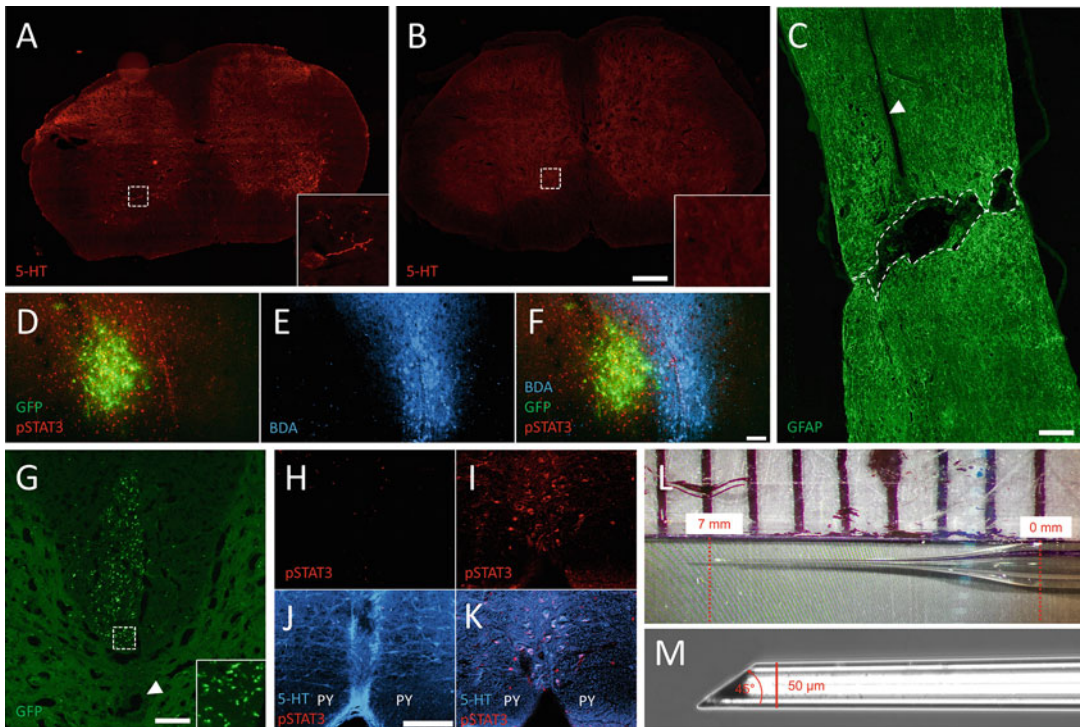


Fig. 3 Validation steps. (a) Transverse section 8–11 mm distal from an incomplete crush with spared serotonergic axons (5-HT-positive) and (b) a successful crush without spared axons. The dashed box indicates an area of enlargement. Scale bar: 200 μ m. (c) Longitudinal section from a successfully regenerated mouse showing the crush site stained for GFAP with the dotted line representing the lesion border to be measured 8 weeks after lesion. Arrowhead indicates the central canal. Scale bar: 200 μ m. (d) Coronal section through a cortical injection site for hIL-6 virus validation. pSTAT3-positive neurons surrounding the virally transduced GFP-positive cells. (e) BDA injection visualization from panel d. (f) Overlay of panels d and e: example of BDA injection missing the AAV-hIL-6 injection location resulting in the labeling of non-stimulated CST fibers. (g) Transverse spinal cord section proximal to the lesion site showing successful unilateral cortical layer V transduction resulting in GFP-positive axons on the CST's contralateral side relative to the injected hemisphere. Arrowhead indicates the central canal. The dashed box indicates an area of enlargement. Scale bar: 50 μ m. (h, j) Negative control showing no pSTAT3-positive serotonergic raphe neurons, whereas (i, k) show pSTAT3/5-HT double-positive cells, indicating successful transneuronal stimulation of these neurons in an AAV2-h-IL6-treated mouse. PY: pyramidal tract (l). Needles for intracortical injection are around 7–10 mm in length and (m) 50 μ m in diameter with a 45-degree beveled tip

3.3.6 Intracortical Injection Quality: Layer V Transduction

The 0.6 mm injection depth corresponds with layer V of the sensory-motor cortex, where the pyramidal neurons with axons projecting to the pyramidal tract/CST reside. To confirm their successful transduction:

1. Stain coronal brain sections containing the motor cortex with injection sites and transverse spinal cord sections from 3 to 5 mm cranial from the lesion site for GFP (1:500).
2. Transduced layer V pyramidal neurons result in GFP-positive axons visible in the dorsal CST (*see* Fig. 3g and Note 22).

3.3.7 *Intracortical
Injection Quality:
Transneuronal hIL-6
Delivery*

The most crucial aspect of this methodology is the transneuronal stimulation of deep brain stem nuclei with hIL-6, particularly the raphe nuclei's serotonergic neurons. To validate their stimulation:

1. Stain coronal sections of the medulla with pSTAT3 (1:200) and 5-HT (1:500) antibodies.
2. Positive raphe-neuronal nuclei should be seen clustered along the ventral midline above the pyramidal tracts (*see* Fig. 3h–k and Note 20).

4 Notes

1. The isoflurane percentage can vary strongly between manufacturers and use cases. Therefore, we recommend experimenting to see the lowest setting that results in reflex-free anesthesia with the setup used. When mouth-fixed for intracortical injections, use the appropriate anesthesia mask for the stereotaxic frame. However, for the spinal cord crush procedure, cut the conical end of a 50 mL tube into a funnel shape for placing the mouse into, with a hole cut into the conical tip for connecting the isoflurane tube.
2. Use wire clippers to trim off half of the loop portion from the tissue spreaders, resulting in two-wire hooks (Fig. 1f). Then insert just the end hooks into the longitudinal muscle when spreading.
3. Capillary tip should be 0.7–1 cm long and, most notably, 50 μm in diameter as thinner capillaries do not allow for filling, and thicker ones do not penetrate well through the dura mater. We find that grinding the tips on a beveler at a 45-degree angle for 20 min produce ideal capillaries. Inspect the quality of each tip under a microscope (Fig. 3l, m).
4. Virus titer determined via qPCR by comparing against a known copy number plasmid dilution series. Damaged/non-packaged virus genomes are eliminated via DNase treatment before titer determination.
5. This helps straighten the mouse's S-shaped spine; else, manipulating T7 to operate on T8 becomes difficult as T7 lies within this furrow. We find that rolled up tissues held together with some tape to be adequate.
6. This should produce an opening where the cranial half is white (fat), and the caudal half is red (muscle).
7. Be very careful not to snag the large landmark blood vessel used later between T5 and T6, which causes severe bleeding.

8. At this point, we clean up any blood with some sterile wadding cut into thin wedge shapes. These can be left in the wound to wick away blood to maintain clear visibility. With more experience, we find the procedure to generate less and less bleeding.
9. Each cut should be composed of multiple smaller cuts to reduce the scissors' penetration depth to avoid squeezing the spinal cord.
10. By exerting the minimum force necessary to avoid spared axons, a narrower crush site should be formed and thus a higher chance of axons crossing.
11. If the fat pad has dried out at this time point, then apply a drop of sterile PBS to allow for manipulation.
12. This loose connective tissue can very easily catch in the drill bit if not thoroughly removed. This will result in a sudden tug on the drill bit, which might cause the mouse severe brain injury if it occurs at an inopportune moment.
13. The drilling of the skull is a very delicate procedure. Here, we recommend going around the traced outline with very little pressure to establish a groove, then slightly more pressure to remove material. Aim to get the bone so thin as to be transparent, and then the rest can be quickly snapped when lifting it away with forceps. Use sterile wadding to stop any bleeding after removing the skull piece.
14. If a large blood vessel is blocking an injection site, then use the closest possible location and record the new coordinates for when administering the BDA injections later. If fluid leakage is seen around the injection site, then this would hint at the capillary being either blunt or too thick, with the resulting hole being too big. Alternatively, this could be a sign that the dura mater was damaged during drilling, in which case the needle also has a hard time creating a seal. However, the brain surface should also not become too dry, and so the skin from the initial incision can be briefly wiped over the brain to keep it moist between injections.
15. Care must be taken when expressing bladders, as applying too much pressure can result in bladder rupture or backflow of urine into the kidneys, resulting in a swift death. Bladders are especially fragile in the first few days after surgery. Male bladders are more challenging to express and suffer more from bladder infections.
16. For CNS extraction, help fold the mouse's head under its torso to straighten its s-shaped spine. This is particularly important during laminectomy (aiming to cut at 10 and 2 on a clock dial when viewing the spinal canal side-on, dorsal side up), and later when peeling out the spinal cord and cutting each of the nerve

roots. Aim to finish CNS extraction under ~ 30 min after perfusion, as then the CNS can be placed on a strip of nitrocellulose membrane to post-fixate in a straightened form. This is useful later for obtaining straight longitudinal tissue sections. If the spinal cord is left in PFA longer than ~ 30 min, it becomes challenging to correct its s-shape.

17. Snap-freezing prevents the formation of ice crystals, reducing the number and size of holes in brain tissue sections. Do not let acetone spill over into the brain suspension, as this will cause it to crack.
18. Serotonergic axons are more likely to be spared and are also known to contribute to functional recovery. Spared axons tend to be straight and found in their canonical tracts. An early indication of spared axons is a BMS score greater than zero on the first day after crush.
19. In our experience, the average lesion size is around $0.1\text{--}0.2\text{ mm}^2$. It has been reported that lesion widths larger than 0.5 mm prevent any regeneration [13].
20. Staining pSTAT3 is challenging due to a relatively weak signal. To combat high background, block sections for at least 2 h in blocking solution. Use the non-transduced hemisphere in the coronal cortical sections as a negative control to compare against.
21. If the BDA stain does not align with the GFP/pSTAT3 stain, it will suggest that different locations were identified as bregma for viral and BDA injection. BDA overlap with pSTAT3 is crucial for the correctly targeted evaluation of affected CST axons. When opening the skin on the skull after 6 weeks for BDA injection, a thick layer of connective tissue will have been deposited over the bone. To better identify bregma, this should be very carefully removed with fine forceps without scratching the bone so as not to camouflage the cranial bone edges.
22. An alternative way of checking injection depth is that GFP-positive cells in the cortical sections should lie approximately midway between the brain surface and the corpus callosum. A more accurate location can be achieved by overlaying the sections with a brain atlas.

Acknowledgments

The German Research Foundation supported this work.

References

1. Tran AP, Warren PM, Silver J (2018) The biology of regeneration failure and success after spinal cord injury. *Physiol Rev* 98(2): 881–917. <https://doi.org/10.1152/physrev.00017.2017>
2. Zhang N, Fang M, Chen H, Gou F, Ding M (2014) Evaluation of spinal cord injury animal models. *Neural Regen Res* 9(22):2008–2012. <https://doi.org/10.4103/1673-5374.143436>
3. Cregg JM, DePaul MA, Filous AR, Lang BT, Tran A, Silver J (2014) Functional regeneration beyond the glial scar. *Exp Neurol* 253: 197–207. <https://doi.org/10.1016/j.expneurol.2013.12.024>
4. Lu Y, Belin S, He Z (2014) Signaling regulations of neuronal regenerative ability. *Curr Opin Neurobiol* 27:135–142. <https://doi.org/10.1016/j.conb.2014.03.007>
5. Duan Y, Panoff J, Burrell BD, Sahley CL, Muller KJ (2005) Repair and regeneration of functional synaptic connections: cellular and molecular interactions in the leech. *Cell Mol Neurobiol* 25(2):441–450. <https://doi.org/10.1007/s10571-005-3152-x>
6. Oliphint PA, Alieva N, Foldes AE, Tytell ED, Lau BY, Pariseau JS, Cohen AH, Morgan JR (2010) Regenerated synapses in lamprey spinal cord are sparse and small even after functional recovery from injury. *J Comp Neurol* 518(14): 2854–2872. <https://doi.org/10.1002/cne.22368>
7. Yang B, Zhang F, Cheng F, Ying L, Wang C, Shi K, Wang J, Xia K, Gong Z, Huang X, Yu C, Li F, Liang C, Chen Q (2020) Strategies and prospects of effective neural circuits reconstruction after spinal cord injury. *Cell Death Dis* 11(6):439. <https://doi.org/10.1038/s41419-020-2620-z>
8. Leibinger M, Zeitler C, Gobrecht P, Andreadaki A, Gisselmann G, Fischer D (2021) Transneuronal delivery of hyper-interleukin-6 enables functional recovery after severe spinal cord injury in mice. *Nat Commun* 12(1):391. <https://doi.org/10.1038/s41467-020-20112-4>
9. Leibinger M, Andreadaki A, Diekmann H, Fischer D (2013) Neuronal STAT3 activation is essential for CNTF- and inflammatory stimulation-induced CNS axon regeneration. *Cell Death Dis* 4:e805. <https://doi.org/10.1038/cddis.2013.310>
10. Leibinger M, Andreadaki A, Gobrecht P, Levin E, Diekmann H, Fischer D (2016) Boosting central nervous system axon regeneration by circumventing limitations of natural cytokine signaling. *Mol Ther* 24(10): 1712–1725. <https://doi.org/10.1038/mt.2016.102>
11. Fabbiani G, Rehmann MI, Aldecosea C, Trujillo-Cenoz O, Russo RE (2018) Emergence of serotonergic neurons after spinal cord injury in turtles. *Front Neural Circuits* 12:20. <https://doi.org/10.3389/fncir.2018.00020>
12. Basso DM, Fisher LC, Anderson AJ, Jakeman LB, McTigue DM, Popovich PG (2006) Basso mouse scale for locomotion detects differences in recovery after spinal cord injury in five common mouse strains. *J Neurotrauma* 23(5): 635–659. <https://doi.org/10.1089/neu.2006.23.635>
13. Zukor K, Belin S, Wang C, Keelan N, Wang X, He Z (2013) Short hairpin RNA against PTEN enhances regenerative growth of corticospinal tract axons after spinal cord injury. *J Neurosci* 33(39):15350–15361. <https://doi.org/10.1523/JNEUROSCI.2510-13.2013>



Epigenomic Profiling of Dorsal Root Ganglia upon Regenerative and Non-regenerative Axonal Injury

Franziska Müller, Jessica S. Chadwick, Simone Di Giovanni, and Ilaria Palmisano 

Abstract

RNA sequencing (RNA-seq), chromatin immunoprecipitation sequencing (ChIP-seq), and assay for transposase-accessible chromatin sequencing (ATAC-seq) are genome-wide techniques that provide information relative to gene expression, chromatin binding sites, and chromatin accessibility, respectively. Here we describe RNA-seq, H3K9ac, H3K27ac and H3K27me3 ChIP-seq, and ATAC-seq in dorsal root ganglia (DRG) after sciatic nerve or dorsal column axotomy, to characterize the transcriptional and epigenetic signatures of DRG upon regenerative vs non-regenerative axonal lesion.

Key words DRG, Axonal regeneration, Epigenetics, Transcription, Chromatin accessibility, RNA-seq, ChIP-seq, ATAC-seq

1 Introduction

The dorsal root ganglia (DRG) contain the cell bodies of pseudounipolar sensory neurons projecting a peripheral regeneration-competent axonal branch within the peripheral nerves and a central regeneration-incompetent axonal branch that enters the dorsal columns in the spinal cord (Fig. 1a). Sciatic nerve axotomy (SNA) and dorsal column axotomy (DCA) provide models of regenerative and non-regenerative axonal lesion, respectively. The development of high-throughput techniques, such as RNA sequencing (RNA-seq), chromatin immunoprecipitation sequencing (ChIP-seq), and assay for transposase-accessible chromatin sequencing (ATAC-seq), has been critical for the understanding of the complexity of the transcriptome and its regulation via epigenetic mechanisms [1–3]. The integration of data from ATAC-seq, ChIP-seq, and RNA-seq represents a powerful approach for establishing how information encoded in chromatin results in changes in gene expression. We applied RNA-seq, H3K9ac, H3K27ac and

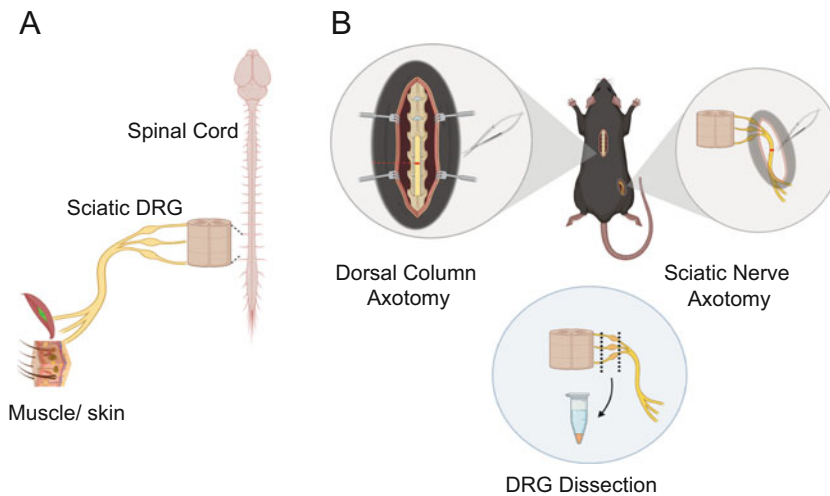


Fig. 1 In vivo anatomy and surgeries. **(a)** Spinal cord and dorsal root ganglia anatomy. The sciatic dorsal root ganglia (DRG) pseudounipolar neuronal bodies extend one branch into the ascending tracts of the dorsal column in the spinal cord, and one branch into the sciatic nerve of the hind limb, innervating muscle and skin. **(b)** Dorsal column axotomy (DCA) and sciatic nerve axotomy (SNA) surgeries. Following either DCA or SNA, the sciatic DRG are dissected, collected and processed for downstream analysis

H3K27me3 ChIP-seq, and ATAC-seq in DRG after SNA or DCA, to characterize the transcriptional and epigenetic signatures of DRG upon regenerative versus non-regenerative axonal lesion. We found that successful axon regeneration relies on the capability to initiate a transcriptional response to injury, characterized by a more accessible chromatin state with increased occupancy of active histone marks at gene promoters and enhancers [4–6].

In this chapter, we present laboratory protocols for SNA and DCA injuries, DRG dissection, RNA-seq, ChIP-seq, and ATAC-seq library preparation.

1.1 *Peripheral and Central Axonal Injury and Sciatic DRG Dissection*

For SNA, the sciatic nerve is exposed by blunt dissection of the biceps femoris and gluteus superficialis, and axotomy is carried out ~20 mm distally from sciatic DRG. In control mice (Sham), the sciatic nerve is exposed without axotomy. For DCA, the spinal cord is exposed via a T9 laminectomy ~20 mm from sciatic DRG, the dura mater is removed, and a dorsal hemisection up to the central canal is performed. For the control laminectomy surgery (Lam), the dura mater is removed without performing the hemisection. Twenty-four hours after injury, animals are sacrificed and DRG are collected and processed for downstream analysis (Fig. 1b).

1.2 *Total RNA Extraction from DRG Tissue*

RNA-seq, in addition to other information, provides evidence about the genes that are differentially expressed in different biological conditions [7]. For DRG transcriptional profiling (Fig. 2a), we used sciatic DRG from mice that underwent SNA vs Sham or DCA vs Lam 24 h earlier ($N = 3$ biological replicates).

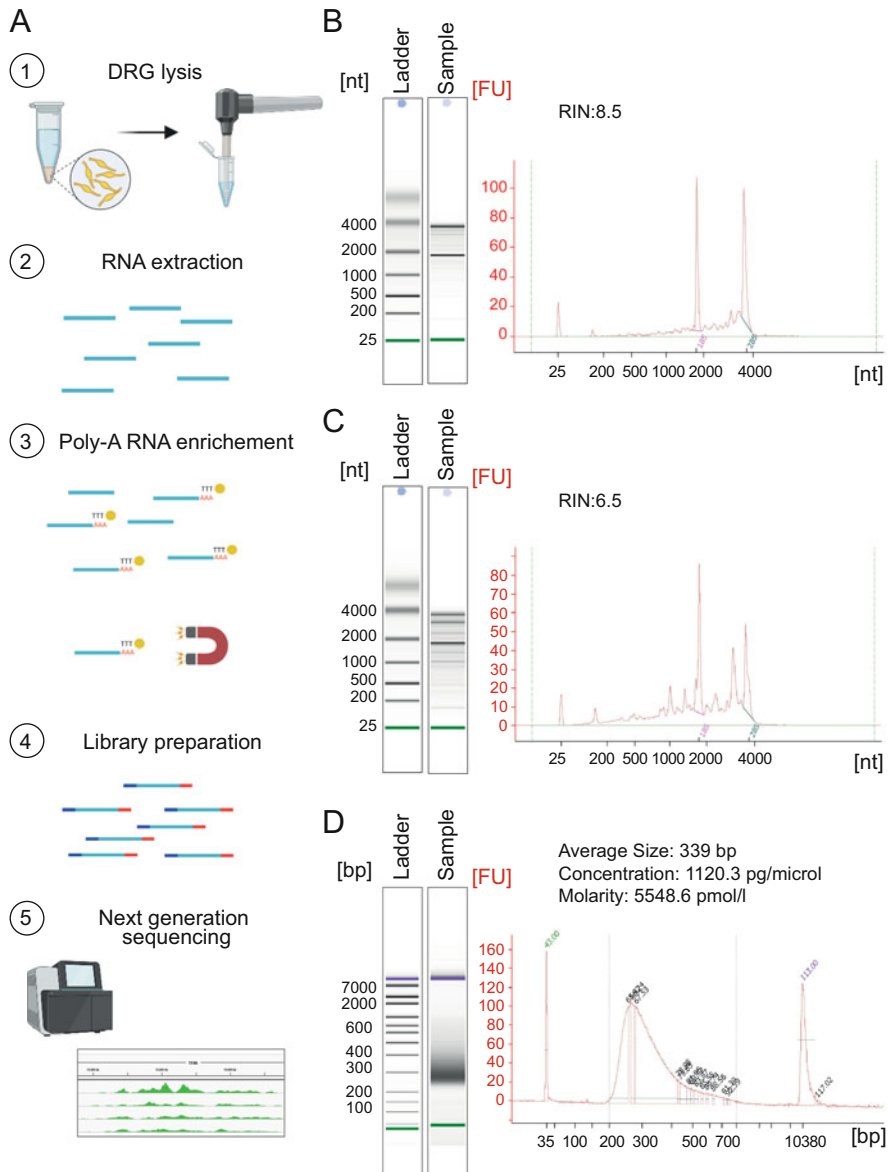


Fig. 2 RNA-seq. **(a)** Schematic of the RNA-seq procedure. **(b)** Bioanalyzer trace showing an optimal RNA preparation, with RNA Integrity Number (RIN) > 8.0. **(c)** Bioanalyzer trace showing a degraded RNA preparation, with a low RIN. **(d)** Bioanalyzer trace showing a library preparation. For intact RNA samples, the expected average fragment length is ~300–400 bp

Samples are lysed in the presence of guanidine–thiocyanate to inactivate RNase. Ethanol is added to ensure binding conditions and samples are loaded on a silica-based membrane column, which enables the binding of RNA molecules longer than 200 nucleotides. After DNase I digestion and washing to remove contaminants, RNA is eluted in water.

1.3 RNA-Seq Library Preparation

For library preparation, poly-A-enriched RNA is sheared and converted to a library of short cDNA fragments carrying sequencing adapters at both ends. The use of specific index primers enables library multiplexing. Libraries are pooled and sequenced to obtain short sequences from one or both ends. These reads are aligned to the reference genome and used for transcript identification and quantification. The read counts are used for differential expression analysis, providing information about the genes that are differentially regulated in regenerative vs non-regenerative axonal lesion [4, 6].

1.4 Chromatin Immunoprecipitation from DRG Tissue

ChIP provides context to the binding sites of proteins, such as histones, transcription factors, and chromatin remodelers in relation to the chromatin [2]. We performed ChIP-seq for H3K9ac and H3K27ac (markers of active promoters and enhancers) and H3K27me3 (marker of repressed chromatin) in sciatic DRG from mice that underwent SNA vs Sham or DCA vs Lam 24 h earlier ($N = 2$ biological replicates) (Fig. 3a). The procedure is based on

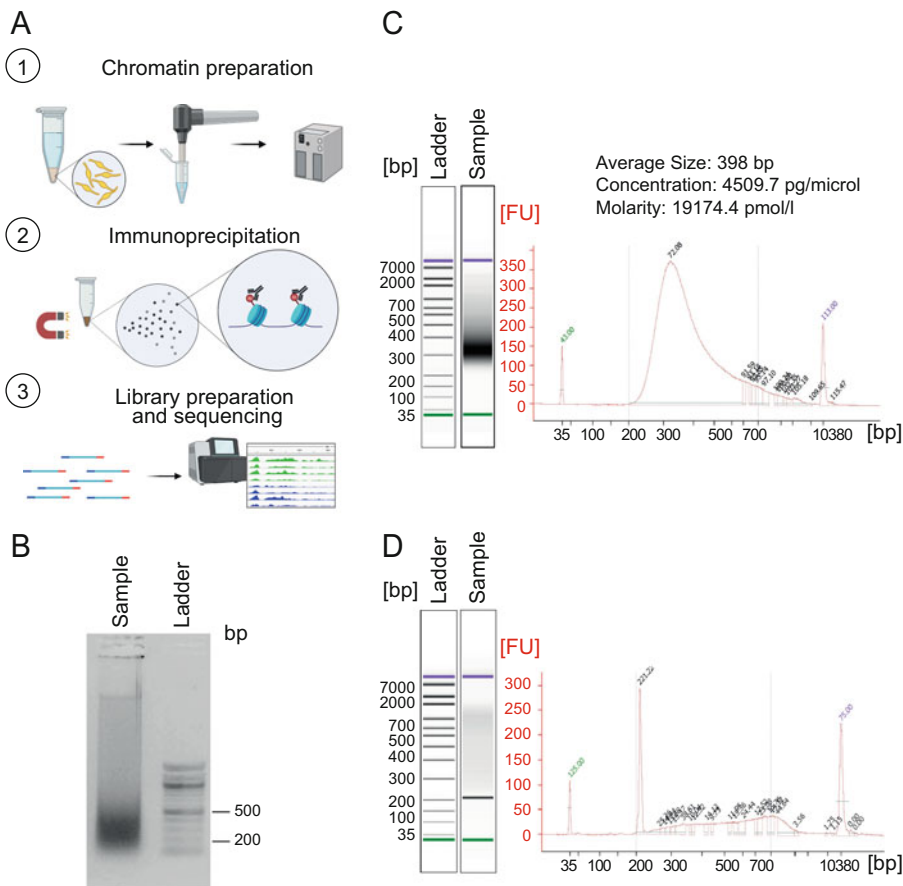


Fig. 3 ChIP-seq. (a) Schematic of the ChIP-seq procedure. (b) Agarose gel run showing the result of chromatin sonication with DNA fragments in the range of 200–800 bp. (c) Bioanalyzer trace showing a successful library preparation. (d) Bioanalyzer trace showing a failed library preparation, presenting also adapter contamination

Schmidt et al. [2] with some adjustments. Protein–DNA interactions are stabilized by cross-linking. After lysis, chromatin is fragmented by sonication and incubated with bead-bound antibodies against the protein of interest. After elution and reverse cross-linking, the purified DNA can be used for real-time polymerase chain reaction (RT-PCR) or library preparation for sequencing.

1.5 ChIP-Seq Library Preparation

Library preparation involves end repair, ligation of the adapters, and PCR amplification. The use of specific index primers enables sample multiplexing. The reads obtained from sequencing are aligned to the reference genome and used for peak identification and quantification. The read counts are used for differential occupancy analysis, providing information about the gene promoters and enhancers that are differentially occupied by H3K9ac, H3K27ac, and H3K27me3 in regenerative vs non-regenerative axonal lesion [5, 6]. Recently, alternative methodologies to ChIP-seq have been published, which require a lower amount of starting material [8].

1.6 ATAC-Seq from DRG Tissue

ATAC-seq provides information about the accessibility of the chromatin, via the use of a genetically engineered hyperactive Tn5 transposase that simultaneously cuts and ligates sequencing adapters preferentially at regions of open chromatin [3]. To perform ATAC-seq in DRG (Fig. 4a), we used sciatic DRG from mice that underwent SNA vs Sham or DCA vs Lam 24 h earlier ($N = 3$ biological replicates). After cell lysis, the chromatin is incubated with the Tn5 transposase for DNA tagmentation. Upon cleanup, the DNA is used for library preparation with index primers, which enable sample multiplexing, and paired-end sequencing is performed to uniquely map the open regions. The reads are then aligned to the reference genome and used for open chromatin region identification and quantification. The read counts are used for differential accessibility analysis, providing information about the gene promoters and enhancers that are differentially accessible in regenerative vs non-regenerative axonal lesion [6]. Since accessible chromatin is partially protected from the activity of the Tn5 transposase by bound transcription factors, the analysis of a particular ATAC-seq feature, called “footprint” [9], provides information about transcription factor occupancy.

2 Materials

General Note Prepare all solutions using nuclease-free water and molecular biology grade reagents. Prepare all the working buffers fresh and store them at room temperature (unless indicated otherwise). Do not leave the reagent bottles or the sample tubes open longer than necessary. Use and change gloves frequently. Use

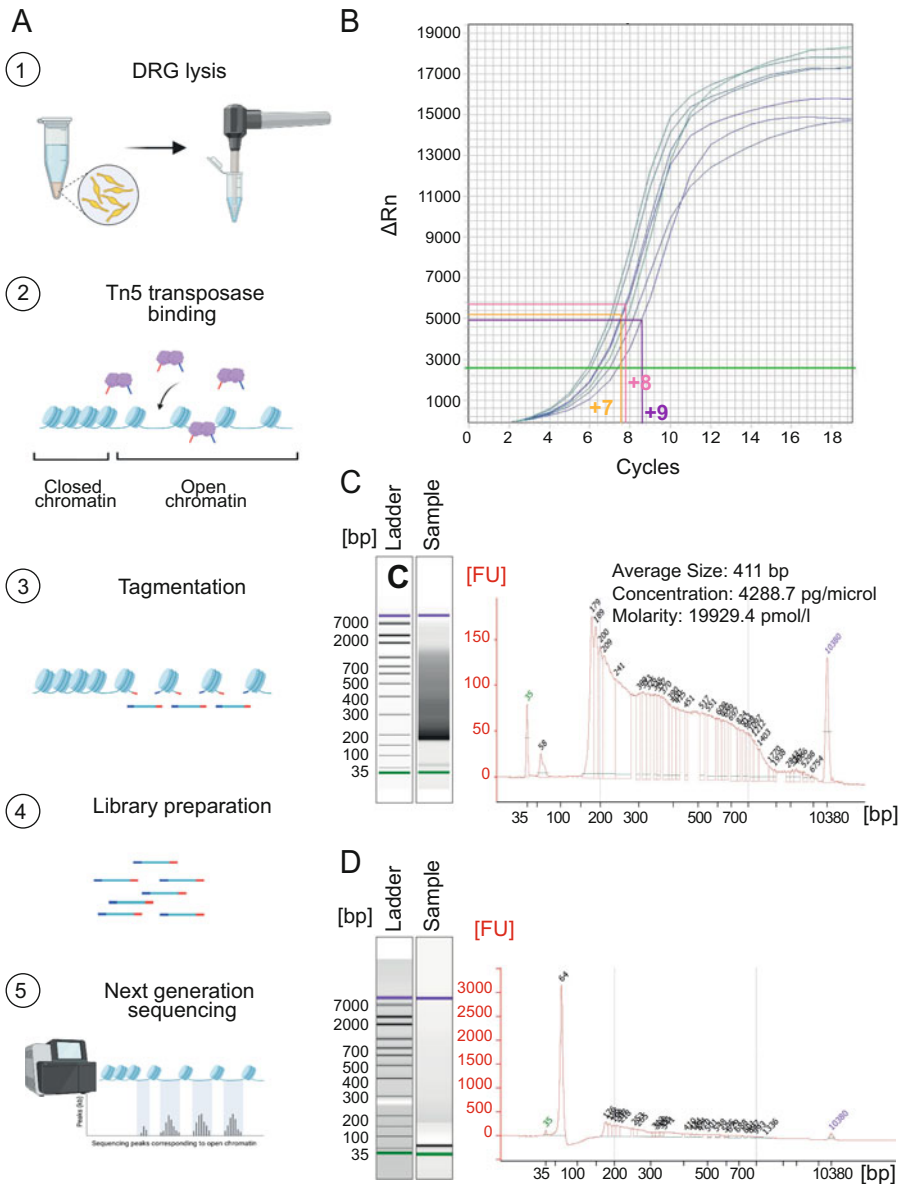


Fig. 4 ATAC-seq. **(a)** Schematic of the ATAC-seq procedure. **(b)** qPCR to determine the appropriate number of PCR cycles to avoid GC bias. Extrapolate the Ct values corresponding to one third or one fourth of the maximum Rn. If Ct values of two traces are similar, use the cycle number from the lower Rn (pink and yellow). If the cycle number falls between two integers, select the smaller integer (yellow and purple). **(c)** Bioanalyzer trace showing a successful library preparation from DRG, with sloping curve of PCR fragment sizes between ~150 and 1000 bp, with periodicity of ~200 bp. **(d)** Bioanalyzer trace showing a failed library preparation, presenting also adapter contamination

disposable nuclease-free plasticware. Follow all waste disposal regulations when disposing waste materials. When working with RNA, make sure you maintain a RNase-free environment, by cleaning the working station, the pipettes, the surgical tools, the tube racks, and the centrifuge with an RNase decontamination solution (e.g., RNaseZap, Invitrogen). When working with DNA, make sure you maintain a DNase-free environment, by cleaning the working station, the pipettes, the tube racks, and the centrifuge with water first, and then with 70% ethanol.

2.1 Common Materials

1. Ice.
2. Tube racks.
3. Micropipettes and filter tips.
4. 15 and 50 mL polypropylene conical tubes.
5. Serological pipettes, nuclease-free, individually wrapped.
6. Motorize pipette controller (e.g., Corning Stripettor).
7. 1.5 mL RNase-free microtubes for DRG collection (e.g., Anachem; *see Note 1*).
8. 1.5 mL microcentrifuge tubes, low adsorption, nuclease-free (e.g., DNA LoBind tubes, Eppendorf).
9. Cordless motor for pellet pestle (e.g., Kimble).
10. Disposable pellet pestles for 1.5 mL microtubes (e.g., Anachem; *see Note 1*).
11. 0.22 μ M syringe filters and syringes.
12. 0.22 μ M bottle filters.
13. Tabletop centrifuge with plate rotor.
14. Microcentrifuge.
15. Thermocycler.
16. Thermoblock (e.g., Eppendorf, Thermomixer, T range 15–100 °C).
17. Vortex mixer.
18. 96-well PCR plates, low adsorption (e.g., Eppendorf twin.tec PCR Plates LoBind).
19. Clear PCR plate sealing films, adhesive (e.g., BioRad Microseal “B”).
20. Magnetic stands for 96-well plates and for microtubes.
21. Chip-based capillary electrophoresis platform (e.g., Agilent 2100 Bioanalyzer).
22. Hank’s Balanced Salt Solution (HBSS). Store at 4 °C.
23. Nuclease-free water.
24. 99.8% ethanol.

25. 70 and 80% ethanol in nuclease-free water made fresh.
26. Paramagnetic bead-based nucleic acid cleanup kit (e.g., AMPure XP beads). Store at 4 °C. Place at room temperature for at least 30 min prior to use.

2.2 Sciatic DRG Axonal Injury and Dissection

1. Male C57BL/6J mice (6–8 weeks old) between 20 and 30 g, housed on a 12-h light/dark cycle with water and standard chow available ad libitum.
2. Standard mouse chow.
3. Saline: 0.9% sodium chloride physiological solution. Filter with 0.22 µM bottle filter units.
4. Carprofen small animal solution: 1 mg/mL diluted in saline, prepared fresh the day of surgery.
5. Buprenorphine hydrochloride small animal solution: 0.03 mg/mL diluted in saline, prepared fresh the day of surgery.
6. Isoflurane 100% w/w inhalation vapor.
7. Antiseptic agent (e.g., 70% ethanol) and wipes.
8. Antiseptic solution: povidone-iodine 10% w/w cutaneous solution in sterile water.
9. 1 mL syringes.
10. Microlances 30G for injection and 20G for dissection.
11. Sterile cotton swabs.
12. Hair trimmer.
13. Sterile drapes.
14. Sterile transparent drapes.
15. Heat mat.
16. Eye lube.
17. Anesthetic induction chamber with flow gas tubing and scavenge tubing.
18. Anesthetic induction chamber with flow gas tubing and scavenge tubing connected to a nose cone of a non-rebreathing circuit.
19. Anesthetic scavenging unit.
20. Stereo microscope.
21. Technical scale (capacity 1500 g, resolution 0.01 g).
22. MicroAdson forceps with fenestrated handle, 1 × 2 teeth.
23. LaGrange scissors ToughCut 11.5 cm.
24. Spinal cord hook 12 cm.
25. Vannas spring micro scissors straight 2.5 mm cutting edge.
26. Dumont #7 fine forceps.

27. Reflex 7 mm wound clips.
28. Reflex 7 mm wound clip applicator.
29. Anesthesia recovery chamber.
30. Water.
31. Student scalpel handle #3 and sterile surgical blades.
32. Friedman-Pearson rongeur straight 1 mm cup.
33. Noyes spring scissors straight.
34. Narrow Pattern forceps straight 12 cm.
35. Olsen-Hegar needle holder.
36. Vicryl suture 6-0|RB-2 45 cm undyed.
37. Student scissors straight SharpSharp 14.5 cm.
38. Styrofoam board.
39. Student Dumont #5 forceps standard Inox.
40. Student Vannas spring scissors straight.
41. 1.5 mL microtubes.
42. RNA stabilization solution (e.g., RNAlater).

**2.3 Total RNA
Extraction from DRG
Tissue**

1. RNase decontamination solution (e.g., RNaseZap, Invitrogen).
2. RNA stabilization solution (e.g., RNAlater).
3. RNA isolation kit (e.g., Qiagen RNeasy mini kit, containing RLT, RW1, and RPE buffers, RNeasy spin column, collection tubes, RNase-free water; *see Note 2*).
4. DNase I enzyme (e.g., Qiagen; *see Note 3*).
5. RLT lysis mix: add 6 μL of 2-mercaptoethanol to 600 μL of RLT lysis buffer (included in the RNeasy mini kit); use 600 μL per sample. Calculate the number of samples (N) and prepare RLT lysis mix for N+1 samples. Prepare fresh.
6. DNase I Master Mix: add 10 μL Qiagen DNase I stock solution to 70 μL Qiagen RDD buffer; 80 μL per sample. Prepare DNase I Master Mix for N+1 samples. Prepare fresh.
7. Kit for chip-based capillary electrophoresis for RNA samples, 25–500 ng/ μL (e.g., RNA 6000 Nano Kit, Agilent).
8. Microvolume spectrophotometer (e.g., NanoDrop).

**2.4 RNA-Seq Library
Preparation**

1. Reverse transcriptase with reduced RNaseH activity (e.g., Superscript II, Invitrogen). Store at $-20\text{ }^{\circ}\text{C}$. Thaw on ice prior to use.
2. Library pooling buffer: 10 mM Tris-HCl (pH 8.5) with 0.1% Tween 20. Prepare fresh.

3. Reverse Transcription Master Mix: 7 μL FSM, 1 μL reverse transcriptase; 8 μL total per sample. Pipette up and down at least ten times to mix the components. Pulse the Reverse Transcription Master Mix in the microcentrifuge at $600\times g$ for 5 s to collect the liquid at the bottom of the tube.
4. Illumina TruSeq stranded mRNA Library Prep Kit (*see Note 4*). Store the components according to manufacturer's instructions.
5. EPF (Elute, Prime, Fragment mix): included in the TruSeq stranded mRNA Sample Preparation Kit. Thaw at room temperature prior to use.
6. BBB (Bead Binding Buffer): included in the TruSeq stranded mRNA Sample Preparation Kit. Thaw at room temperature prior to use.
7. BWB (Bead Washing Buffer): included in the TruSeq stranded mRNA Sample Preparation Kit. Thaw at room temperature prior to use.
8. ELB (Elution Buffer) included in the TruSeq stranded mRNA Sample Preparation Kit. Thaw at room temperature prior to use.
9. RPB (RNA Purification Beads) included in the TruSeq stranded mRNA Sample Preparation Kit. Place at room temperature for 30 min.
10. FSM (First Strand Master Mix): included in the TruSeq stranded mRNA Sample Preparation Kit. Thaw at room temperature. Make small aliquots to be stored at $-20\text{ }^{\circ}\text{C}$ if you do not anticipate to using the entire mix.
11. RSB (Resuspension Buffer): included in the TruSeq stranded mRNA Sample Preparation Kit. Thaw at room temperature prior to use.
12. SSM (Second Strand Master Mix): included in the TruSeq stranded mRNA Sample Preparation Kit. Thaw at room temperature.
13. ERP (End Repair Mix): included in the TruSeq stranded mRNA Sample Preparation Kit. Thaw at room temperature prior to use.
14. CTE (End Repair Control): included in the TruSeq stranded mRNA Sample Preparation Kit. Thaw at room temperature and then keep on ice. Centrifuge CTE at $600\times g$ for 5 s and dilute it 1:100 in RSB.
15. ATL (A-tailing Mix): included in the TruSeq stranded mRNA Sample Preparation Kit. Thaw at room temperature.

16. CTA (A-Tailing Control): included in the TruSeq stranded mRNA Sample Preparation Kit. Thaw at room temperature and keep on ice. Centrifuge CTA at $600\times g$ for 5 s and dilute it 1:100 in RSB.
17. RNA Adapter Indexes: included in the TruSeq stranded mRNA Sample Preparation Kit. Thaw at room temperature. Centrifuge at $600\times g$ for 5 s.
18. CTL (Ligase Control): included in the TruSeq stranded mRNA Sample Preparation Kit. Thaw at room temperature. Centrifuge at $600\times g$ for 5 s. Dilute 1:100 in RSB.
19. STL (Stop Ligase Mix): included in the TruSeq stranded mRNA Sample Preparation Kit. Thaw at room temperature. Centrifuge at $600\times g$ for 5 s.
20. LIG (DNA Ligase mix): included in the TruSeq stranded mRNA Sample Preparation Kit. Thaw just before use.
21. PMM (PCR Master Mix): included in the TruSeq stranded mRNA Sample Preparation Kit. Thaw at room temperature and keep on ice. Centrifuge at $600\times g$ for 5 s.
22. PPC (Primer PCR Cocktail) contained in the TruSeq stranded mRNA Sample Preparation Kit. Thaw at room temperature and keep on ice. Centrifuge at $600\times g$ for 5 s.
23. 96-well 0.3 mL PCR plate labeled with the RNA Bead Plate (ABP) barcode label.
24. 96-well 0.3 mL PCR plate labeled with the cDNA Plate (CDP) barcode label.
25. 96-well 0.3 mL PCR plate labeled with the Insert Modification Plate (IMP) barcode label.
26. 96-well 0.3 mL PCR plate labeled with the Adapter Ligation Plate (ALP) barcode label.
27. 96-well 0.3 mL PCR plate labeled with the Clean UP ALP Plate (CAP) barcode labels.
28. 96-well 0.3 mL PCR plate labeled with the Polymerase Chain Reaction Plate (PCR) barcode label.
29. 96-well 0.3 mL PCR plate labeled with the Target Sample Plate (TSP1) barcode label.
30. Fluorescent-based double-stranded DNA quantification kit (e.g., Invitrogen Qubit kit).
31. Fluorometric quantitation platform (e.g., Qubit 2.0).
32. Kit for chip-based capillary electrophoresis DNA analysis to detect 5–500 pg/ μ L concentrations of DNA (e.g., Agilent High Sensitivity DNA Assay)

2.5 Chromatin Immunoprecipitation from DRG Tissue

1. Solution A: 1% formaldehyde, 50 mM HEPES-KOH pH 7.5, 100 mM NaCl, 1 mM EDTA pH 8.0, 0.5 mM EGTA pH 8.0 in nuclease-free water; 400 μ L per sample. Prepared fresh each day (*see Note 5*).
2. 2.5 M glycine: Dissolve 93.8 g of glycine in 500 mL of nuclease-free water. Filter with 0.22 μ M bottle filter units. May be stored at room temperature for up to 6 months.
3. Protease inhibitor cocktail (e.g., cOmplete EDTA-free protease inhibitor cocktail, Roche): Add one tablet of cOmplete EDTA-free protease inhibitor cocktail to 50 mL of PBS. Prepare fresh prior to use. Keep on ice.
4. Lysis buffer 1 (LB1): 50 mM HEPES-KOH pH 7.5, 140 mM NaCl, 1 mM EDTA pH 8.0, 10% glycerol, 0.5% NP-40, 0.25% Triton X-100 in nuclease-free water; 10 mL per sample. Add commercially available EDTA-free protease inhibitor tablet to manufacturer's specification (e.g., one tablet of Roche cOmplete EDTA-free protease inhibitor cocktail/50 mL of solution) and filter with 0.22 μ M filters. Prepare fresh prior to use. Keep on ice.
5. Lysis buffer 2 (LB2): 10 mM Tris-HCl pH 8.0, 200 mM NaCl, 1 mM EDTA pH 8.0, 0.5 mM EGTA pH 8.0 in nuclease-free water; 10 mL per sample. Add commercially available EDTA-free protease inhibitor tablet to manufacturer's specification (e.g., one tablet of Roche cOmplete EDTA-free protease inhibitor cocktail/50 mL of solution) and filter with 0.22 μ M filters. Prepare fresh prior to use. Keep on ice.
6. Lysis buffer 3 (LB3): 10 mM Tris-HCl pH 8.0, 100 mM NaCl, 1 mM EDTA pH 8.0, 0.5 mM EGTA pH 8.0, 0.1% Na-deoxycholate, 0.5% N-lauroylsarcosine in nuclease-free water; 0.6 mL per sample. Add commercially available EDTA-free protease inhibitor tablet to manufacturer's specification (e.g., one tablet of Roche cOmplete EDTA-free protease inhibitor cocktail/50 mL of solution) and filter with 0.22 μ M filters. Prepare fresh prior to use. Keep on ice.
7. NaHCO₃/SDS mix: 0.1 M NaHCO₃, 1% SDS in nuclease-free water.
8. Proteinase K solution: 20 mg/mL in nuclease-free water. Store at -20 °C.
9. 5 M LiCl: Dissolve 10.59 g of LiCl in 50 mL of water and mix on a rocker. Filter with 0.22 μ M filters and store at room temperature.
10. 1% agarose gel: Weigh 1 g of agarose and add 100 mL ddH₂O, and microwave until completely solubilized. Add 3 μ L of 10 mg/mL ethidium bromide and pour the solution to prepare the gel according to the electrophoresis system manufacturer's guidelines (*see Note 6*).

11. 6× DNA loading buffer (e.g., New England Biolabs). Store at 4 °C.
12. 100 bp DNA ladder. Store at 4 °C.
13. 1.5 mL TPX polymethylpentene microtubes (e.g., Diagenode).
14. Bath sonicator (e.g., Diagenode, Bioruptor).
15. Chemical fume hood.
16. Rotator.
17. Agarose gel electrophoresis apparatus.
18. Liquid nitrogen.
19. LB3/Triton: 10 mM Tris-HCl pH 8.0, 100 mM NaCl, 1 mM EDTA pH 8.0, 0.5 mM EGTA pH 8.0, 0.1% Na-deoxycholate, 0.5% N-lauroylsarcosine, 1% Triton X-100 in nuclease-free water; 0.4 mL per sample. Add commercially available EDTA-free protease inhibitor tablet to manufacturer's specification (e.g., one tablet of Roche cOmplete EDTA-free protease inhibitor cocktail/50 mL of solution) and filter with 0.22 μM filters. Prepared fresh. Keep on ice.
20. 10% Triton X-100 in nuclease-free water. Filter with 0.22 μM filters.
21. Magnetic separation beads (e.g., Invitrogen, Dynabeads). Store at 4 °C.
22. Blocking solution: 0.5% Bovine Serum Albumin (BSA) (w/v) in nuclease-free water (*see Note 7*); 10 mL per sample.
23. Primary antibody of choice for the protein of interest (*see Note 8*).
24. ChromPure IgG (e.g., Jackson ImmunoResearch). The IgG are required only for ChIP-PCR and when testing antibodies (*see Note 8*).
25. RIPA buffer: 50 mM HEPES-KOH pH 7.5, 500 mM LiCl, 1 mM EDTA pH 8.0, 1% NP-40, 0.7% Na-deoxycholate in nuclease-free water; 6 mL per sample. Filter with 0.22 μM filters. Prepared fresh. Keep on ice.
26. Tris-buffered saline (TBS): 20 mM Tris-HCl (pH 7.6), 150 mM NaCl in nuclease-free water; 1 mL per sample. Filter with 0.22 μM filters. Prepare fresh prior to use.
27. Elution buffer: 50 mM Tris-HCl pH 7.8, 10 mM EDTA pH 8.0, 1% SDS in nuclease-free water; 0.35 mL per sample. Filter with 0.22 μM filters. Prepare fresh prior to use.
28. Tris-EDTA buffer (TE): 50 mM Tris-HCl pH 7.8, 10 mM EDTA pH 8.0 in nuclease-free water; 0.2 mL per tube. Filter with 0.22 μM filters. Prepare fresh prior to use.

29. PCR purification kit, (e.g., Qiagen Qiaquick containing PB and PE buffers, Qiaquick spin column, and collection tubes). Store at room temperature (*see Note 9*).
30. 3 M sodium acetate, pH 5.0.
31. Picogreen dsDNA assay. Store at 4 °C. Dilute 20× TE buffer supplied in the kit to 1× in nuclease-free water. Prepare the Picogreen reagent by diluting 200-fold the concentrated DMSO solution in 1× TE buffer. Protect from light with foil. Dilute the 100 µg/mL lambda DNA standard in 1× TE buffer to 20 µg/mL.
32. Plate fluorometer.
33. Black 96-well plate for fluorescent samples.

2.6 ChIP-Seq Library Preparation

1. DNA Library Prep Kit for Illumina (e.g., NEBNext Ultra; *see Note 10*). Store at −20 °C
2. End prep enzyme mix and 10× End repair reaction buffer (supplied in the NEBNext Ultra DNA Library Prep Kit). Thaw on ice prior to use.
3. End Prep Master Mix: 3.0 µL of End prep enzyme mix and 6.5 µL of End repair reaction buffer 10×; 9.5 µL per sample. Calculate the number of samples (N) and prepare End Prep Master Mix for N+1 samples. Pipette up and down at least ten times to mix the components. Pulse the End Prep Master Mix in the microcentrifuge at 600× *g* for 5 s to collect the liquid at the bottom of the tube.
4. NEBNext Adaptor for Illumina (supplied in the NEBNext Ultra DNA Library Prep Kit at 15 mM). Dilute the Adaptor 1:10 in nuclease-free water to 1.5 mM immediately before use. If starting from a lower amount of DNA, for example, 5 ng of DNA, dilute the Adaptor 1:20.
5. Adaptor Master Mix: 15 µL of Blunt/TA Ligase Master Mix, 1 µL of Ligation Enhancer, and 2.5 µL of diluted NEBNext Adaptor for Illumina (add the Adaptor last); 18.5 µL per sample. Blunt/TA Ligase Master Mix and Ligation Enhancer are supplied in the NEBNext Ultra DNA Library Prep Kit and do not need to be thawed, but should be kept on ice. Prepare Adaptor Master Mix for N+1 samples. Pipette up and down at least ten times to mix the components. Pulse the Adaptor Master Mix in the microcentrifuge at 600× *g* for 5 s to collect the liquid at the bottom of the tube.
6. USER enzyme (supplied in the NEBNext Ultra DNA Library Prep Kit).
7. NEBNext Q5 Hot Start HiFi PCR Master Mix.

8. Amplification Master Mix: 2 μL of Universal PCR Primer (supplied in the NEBNext Ultra DNA Library Prep Kit), 25 μL of NEBNext Q5 Hot Start HiFi PCR Master Mix, and 6 μL of nuclease-free water; 33 μL per sample (*see Note 11*). Prepare Amplification Master Mix for N+1 samples. Pipette up and down at least ten times to mix the components. Quickly spin to collect the liquid at the bottom of the tube.
9. Index primers (e.g., NEBNext Multiplex Oligos for Illumina). Store at -20°C .
10. 10 mM Tris-HCl, pH 8.5. Store at room temperature.
11. Library pooling buffer: 10 mM Tris-HCl, pH 8.5, with 0.1% Tween 20. Prepare fresh.
12. Fluorescent-based double-stranded DNA quantification kit (e.g., Invitrogen Qubit kit).
13. High Sensitivity DNA Kit (Agilent) store according to manufacturer's instructions.
14. Fluorometric quantitation platform (e.g., Qubit 2.0).

**2.7 ATAC-seq
Library Preparation
from DRG Tissue**

1. Lysis buffer: 10 mM Tris-HCl (pH 7.5), 10 mM NaCl, 3 mM MgCl_2 , 0.1% NP-40 in nuclease-free water; 0.5 mL per sample. Add one tablet of cOmplete, EDTA-free protease inhibitor cocktail to 50 mL of lysis buffer before use. Filter with 0.22 μM filters and keep on ice.
2. Methyl green-pyronin.
3. Tagmentation enzyme kit (e.g., Illumina Tagment DNA Enzyme and Buffer kit; *see Note 12*). Store at -20°C .
4. Transposition Master Mix: Thaw the 2 \times TD buffer and TDE1 Tagment DNA Enzyme (included in Illumina Tagment DNA Enzyme and Buffer kit) on ice. Combine 25 μL of TD buffer, 2.5 μL of TDE1 Tagment DNA Enzyme, and 22.5 μL of nuclease-free water. Calculate the number of samples (N). Prepare Transposition Master Mix for N+1 samples. Pipette Transposition Master Mix up and down at least ten times to mix the components. Quickly spin to collect the liquid at the bottom of the tube.
5. Silica membrane-based DNA purification kit (e.g., Qiagen MinElute Purification kit, including the PB and PE buffers, MinElute spin column, and collection tubes). Store at room temperature (*see Note 13*).
6. 3 M sodium acetate, pH 5.0.
7. Hemocytometer.
8. Microscope.
9. High-Fidelity PCR Master Mix (e.g., NEBNext HF 2 \times PCR Master Mix; *see Note 14*). Store at -20°C .

10. 25 μM PCR Primer 1 (Ad1_noMX; *see* Table 1). Desalted oligos are resuspended in nuclease-free water at 100 μM and aliquoted. Prepare a 25 μM working dilution in nuclease-free water.
11. 25 μM PCR barcoded primers (Ad2; *see* Table 1). Desalted oligos are resuspended in nuclease-free water at 100 μM and aliquoted. Prepare a 25 μM working dilution in nuclease-free water.
12. SYBR Green I Nucleic Acid Gel Stain 100 \times . Dilute commercially available 10,000 \times SYBR Green I in TE 1:100 to obtain 100 \times working solution.
13. PCR Master mix 1: 25 μL of NEB Next HF 2 \times PCR Master Mix, 2.5 μL of 25 μM PCR Primer Ad1_noMX, 0.3 μL of 100 \times SYBR Green I, and 9.7 μL of nuclease-free water; 37.5 μL per sample. Prepare a master mix for N+1 samples. Pipette up and down at least ten times to mix the components. Quickly spin to collect the liquid at the bottom of the tube.
14. PCR Master mix 2: 5 μL of NEB Next HF 2 \times PCR Master Mix, 0.25 μL of 25 μM PCR Primer Ad1_noMX, 0.06 μL of 100 \times SYBR Green I, and 4.44 μL of nuclease-free water; 9.75 μL per sample. Prepare a master mix for N+1 samples. Pipette up and down at least ten times to mix the components. Quickly spin to collect the liquid at the bottom of the tube.
15. qPCR machine.
16. Qiagen EB Buffer. Store at room temperature.
17. Qiagen EB Buffer with 0.1% Tween 20. Prepare fresh.
18. High Sensitivity DNA Kit. Store according to manufacturer's instructions.

3 Methods

3.1 *Peripheral and Central Axonal Injury and Sciatic DRG Dissection*

All animal work should be authorized by the appropriate institutional animal care committees.

3.1.1 *Animal Preparation*

1. Wipe the preparation area and surgical area with antiseptic agent (e.g., 70% ethanol).
2. Place heat mats in the preparation and surgery areas to maintain animal body temperature at 30 $^{\circ}\text{C}$ and cover with sterile drapes.
3. Set up the preparation area by placing cotton swabs, eye lube, povidone-iodine solution, analgesics, and syringes with needles on the sterile drapes.

Table 1**Table of PCR primers for ATAC-seq library preparation (based on Buenrostro et al. [3])**

Ad1_noMX	AATGATACGGCGACCACCGAGATCTACACTCGTCGGCAGCGTCAGATGTG
Ad2.1_TAAGGCGA	CAAGCAGAAGACGGCATAACGAGATTCGCCTTAGTCTCGTGGGC TCGGAGATGT
Ad2.2_CGTACTAG	CAAGCAGAAGACGGCATAACGAGATCTAGTACGGTCTCGTGGGC TCGGAGATGT
Ad2.3_AGGCAGAA	CAAGCAGAAGACGGCATAACGAGATTTCTGCCTGTCTCGTGGGC TCGGAGATGT
Ad2.4_TCCTGAGC	CAAGCAGAAGACGGCATAACGAGATGCTCAGGAGTCTCGTGGGC TCGGAGATGT
Ad2.5_GGACTCCT	CAAGCAGAAGACGGCATAACGAGATAGGAGTCCGTCTCGTGGGC TCGGAGATGT
Ad2.6_TAGGCATG	CAAGCAGAAGACGGCATAACGAGATCATGCCTAGTCTCGTGGGC TCGGAGATGT
Ad2.7_CTCTCTAC	CAAGCAGAAGACGGCATAACGAGATGTAGAGAGGTCTCGTGGGC TCGGAGATGT
Ad2.8_CAGAGAGG	CAAGCAGAAGACGGCATAACGAGATCCTCTCTGGTCTCGTGGGC TCGGAGATGT
Ad2.9_GCTACGCT	CAAGCAGAAGACGGCATAACGAGATAGCGTAGCGTCTCGTGGGC TCGGAGATGT
Ad2.10_CGAGGCTG	CAAGCAGAAGACGGCATAACGAGATCAGCCTCGGTCTCGTGGGC TCGGAGATGT
Ad2.11_AAGAGGCA	CAAGCAGAAGACGGCATAACGAGATTGCCTCTTGTCTCGTGGGC TCGGAGATGT
Ad2.12_GTAGAGGA	CAAGCAGAAGACGGCATAACGAGATTCCTCTACGTCTCGTGGGC TCGGAGATGT
Ad2.13_GTCGTGAT	CAAGCAGAAGACGGCATAACGAGATATCACGACGTCTCGTGGGC TCGGAGATGT
Ad2.14_ACCACTGT	CAAGCAGAAGACGGCATAACGAGATACAGTGGTGTCTCGTGGGC TCGGAGATGT
Ad2.15_TGGATCTG	CAAGCAGAAGACGGCATAACGAGATCAGATCCAGTCTCGTGGGC TCGGAGATGT
Ad2.16_CCGTTTGT	CAAGCAGAAGACGGCATAACGAGATACAAACGGGTCTCGTGGGC TCGGAGATGT
Ad2.17_TGCTGGGT	CAAGCAGAAGACGGCATAACGAGATACCCAGCAGTCTCGTGGGC TCGGAGATGT
Ad2.18_GAGGGGTT	CAAGCAGAAGACGGCATAACGAGATAACCCCTCGTCTCGTGGGC TCGGAGATGT
Ad2.19_AGGTTGGG	CAAGCAGAAGACGGCATAACGAGATCCCAACCTGTCTCGTGGGC TCGGAGATGT
Ad2.20_GTGTGGTG	CAAGCAGAAGACGGCATAACGAGATCACCACACGTCTCGTGGGC TCGGAGATGT

(continued)

Table 1
(continued)

Ad2.21_TGGGTTTC	CAAGCAGAAGACGGCATAACGAGATGAAACCCAGTCTCGTGGGC TCGGAGATGT
Ad2.22_TGGTCACA	CAAGCAGAAGACGGCATAACGAGATTGTGACCAGTCTCGTGGGC TCGGAGATGT
Ad2.23_TTGACCCT	CAAGCAGAAGACGGCATAACGAGATAGGGTCAAGTCTCGTGGGC TCGGAGATGT
Ad2.24_CCACTCCT	CAAGCAGAAGACGGCATAACGAGATAGGAGTGGGTCTCGTGGGC TCGGAGATGT

4. Set up the surgical area by placing sterile surgery tools on sterile drapes
5. Place a stereo microscope in the surgical area to visualize the lesion site. This is particularly relevant for central lesion surgery.
6. In the preparation area, gently remove the mouse from the cage, weigh the animal, and record the weight.
7. Place the animal in the anesthetic induction chamber. Ensure the flow gas tubing and the scavenge tubing are connected properly to the chamber.
8. Induce anesthesia by turning the oxygen flow meter to 1.5 L/min flow rate and the isoflurane machine to 4%.
9. Once the mouse has lost its pedal reflex and the breathing has become deeper, gently transfer the mouse to the nose cone of a non-rebreathing circuit. Ensure the flow gas tubing and the scavenge tubing are connected properly to the circuit.
10. Maintain anesthesia by turning the oxygen flow meter to 1.5 L/min flow rate and the isoflurane machine to 2%.
11. Check again pedal reflex and apply eye lube to the eyes to prevent drying. Shave the surgery site using a hair trimmer and swab the area with antiseptic povidone-iodine solution for skin disinfection.
12. Administer analgesics (carprofen 5 mg/kg and buprenorphine 0.1 mg/kg) via subcutaneous injection. For a 30 g mouse, use 0.15 mL of 1 mg/mL carprofen and 0.1 mL of 0.03 mg/mL buprenorphine. Inject the analgesics separately, in a site which does not interfere with the surgery (e.g., into the loose skin over the neck, when performing sciatic nerve injury or over the flank, when performing a spinal cord injury).
13. Gently transfer the anesthetized animal to the surgery area. Place the mouse dorsal side up to the nose cone of a non-rebreathing circuit. Ensure the flow gas tubing and the scavenge tubing are connected properly to the circuit.

Maintain on 2% isoflurane for the duration of surgery. Monitor breathing throughout surgery to ensure that anesthesia is maintained (*see Note 15*). Cover mouse with transparent sterile drape with hole exposing surgery area to ensure sterility and visibility of the area. Check pedal reflex and continue with SNA or DCA.

3.1.2 Sciatic Nerve Axotomy Surgery

1. Lift the skin using a MicroAdson forceps and make a small skin incision below the hip bone with using LaGrange scissors.
2. Blunt dissect the biceps femoris and gluteus maximus to expose the sciatic nerve between the femur bone and tendon using LaGrange scissors.
3. Lift the sciatic nerve using a surgical spinal cord hook.
4. Cut the nerve using Vannas spring scissors. Using the reference in **step 2**, the cut will be approximately 20 mm distally from the sciatic DRGs. Skip this step if sham injury is performed.
5. Following injury, let the nerve fall back into place once released. Gently place the muscles over the top.
6. Holding the skin together using Dumont #7 curved forceps, clip the skin together using a 7 mm wound clip applier and 7 mm suture clips.
7. Repeat **steps 1–6** on the other sciatic nerve for a bilateral injury.
8. Turn the isoflurane machine off and gently place the animal to recover in a 30 °C recovery chamber. Once recovered, transfer the mouse to the cage. Provide a dish of standard chow food soaked with water in the cage to ensure food availability.

3.1.3 Dorsal Column Axotomy Surgery

1. Place a small, rolled cylinder of tissue 2 cm in diameter underneath the chest of the mouse to raise the spinal cord into an arc. This will make the surgery site easier to identify and access. Pull skin of the upper back using a MicroAdson forceps to provide tension and perform a midline incision with a scalpel at the thoracic level spanning from about T8 to T12 to expose the vertebrae. Cut and move aside the superficial interscapular fat to enable muscle tissue dissection, taking care not to touch the cervical vessel.
2. Below the cervical vessel, you find lamina T5/6. Use this as reference. Remove the muscle over T9–11 using a Friedman-Pearson rongeur to expose laminae.
3. Slowly and carefully insert one blade of the Noyes spring scissors into the gap between the vertebrae and perform a T9 laminectomy, making sure the orientation of the blade is always away from the cord. With Narrow Pattern forceps, carefully remove the vertebrae (*see Note 16*).

4. Repeat **step 3** on the other side of the T9 vertebrae.
5. Carefully puncture the dura mater above T9 using the tip of a 30G needle horizontal to the cord, holding it with the Olsen-Hegar needle holder.
6. Perform a dorsal column axotomy at T9 to a depth of 0.5 mm with Vannas spring micro scissors. Skip this step if sham injury is performed.
7. Apply Vicryl sutures separately to the connective and muscle tissue, and then apply 7 mm suture clips to the skin.
8. Turn the isoflurane machine off and gently place the animal to recover in a 30 °C recovery chamber. Once recovered, transfer the mouse to the cage. Provide a dish of standard chow food soaked with water in the cage to ensure food availability.

3.1.4 Sciatic DRG Dissection

1. Twenty-four hours following SNA or DCA, cull the mice via cervical dislocation, with exsanguination as the secondary confirmation method.
2. Spray hair with 70% ethanol, and then cut the head off using Student scissors straight. Place the cadaver dorsal side facing up. Remove the skin by creating a midline incision from the neck to the tail. Gently peel the skin starting at the forelimbs, pulling all the way back to the hind limbs and tail. Place the cadaver ventral-side facing upward, cut part of the ribcage, and remove all the internal organs. Pin the cadaver with 20G needles to a Styrofoam board ventral-side facing upward, by the top of the spine and the hind limbs.
3. Set up a stereo microscope for better visualization of the dissection area.
4. Pull away the muscle covering the vertebrae with Dumont #5 forceps (*see Note 17*).
5. Lift and cut away the vertebrae using a Student Vannas spring scissors and pull the vertebrae away to reveal the spinal cord and DRG (*see Note 18*).
6. Using Dumont #5 forceps, lift the peripheral branch of the sciatic DRG, careful not to touch the DRG itself. Using Vannas spring micro scissors, cut with the central and then the peripheral axonal branch (*see Note 19*).
7. Collect the DRG directly into either HBSS on ice or RNAlater at room temperature depending on the subsequent procedure.

3.2 Total RNA Extraction from DRG Tissue and RNA-Seq

General Note We used sciatic DRG from mice that underwent SNA vs Sham or DCA vs Lam 24 h earlier ($N = 3$ biological replicates). We usually pool 6–12 sciatic DRG from one to two mice/replicate. Although RNA from DRG can be prepared using TRIzol extraction method, we find that silica-based membrane and

microspin technology provides better quality RNA. All the procedures and centrifugations for RNA extraction are performed at room temperature unless otherwise specified. Do not allow the centrifuge to go below 20 °C. Perform all the procedures quickly but handle the column gently to avoid loss of the sample.

3.3 RNA Preparation

1. Dissect sciatic DRGs (*see* Subheading 3.1.4) and immediately collect them in a 1.5 mL microtube containing 100 μ L of RNAlater (*see* Note 20).
2. Allow complete penetration of RNAlater in the DRG tissue by incubating DRG in the reagent overnight at 4 °C. *PAUSE POINT*: the RNA in the tissue is stable for up to 1 week at room temperature and 4 weeks at 4 °C, or it can be stored at lower temperature for longer time (the reagent does not usually freeze at -20 °C. If crystals are formed, make sure you removed them).
3. Spin down the DRG at 800 rpm for 15 s. Aspirate the RNAlater and add 100 μ L of RLT lysis mix.
4. Disrupt the tissue by homogenization with the motorized pestle until disappearance of clumps.
5. Add extra 500 μ L RLT lysis mix and pipette three to four times, until few or no clumps left.
6. Spin at 18,000 $\times g$ for few seconds and transfer the supernatant in a new RNase-free 1.5 mL microtube.
7. Add 600 μ L of 70% ethanol (1 volume), and mix well by pipetting. Precipitates might form but do not centrifuge.
8. Load the lysate on the RNeasy spin column (supplied in the RNeasy mini kit). Since the maximum loading volume of the column is 700 μ L, you need to do this twice. Centrifuge at 18,000 $\times g$ for 15 s and discard the flow-through every time.
9. Wash the column by adding 350 μ L RW1 buffer (supplied in the RNeasy mini kit). Centrifuge at 18,000 $\times g$ for 15 s. Discard the flow-through.
10. Add 80 μ L of the freshly made DNase I incubation mix to the RNeasy spin column membrane and incubate at room temperature for 15 min. Ensure you add the mix in the center of the membrane to avoid inefficient DNase treatment due to the DNase I sticking to the wall or on the o-ring of the column.
11. Wash the column by adding 350 μ L RW1 buffer to the column. Centrifuge at 18,000 $\times g$ for 15 s. Discard the flow-through.
12. Wash the column by adding 500 μ L of RPE buffer. Centrifuge at 18,000 $\times g$ for 15 s. Discard the flow-through. Be careful to avoid touching the tube with the column to avoid ethanol carryover as it might affect downstream analysis.

13. Wash the column by adding 500 μL of RPE buffer. Centrifuge at $18,000\times g$ for 2 min. Discard the collection tube.
14. Place the column into a new 2 mL collection tube (supplied in the kit). Centrifuge at full speed for 1 min to dry the column. Discard the tube.
15. Place the RNeasy spin column in a new 1.5 mL collection tube (supplied in the kit). Add 30 μL RNase-free water (supplied in the kit) to the column making sure it goes directly on top of the spin column membrane. Incubate for 1 min at room temperature. Centrifuge at $20,000\times g$ for 1 min to elute the RNA. You will recover 28 μL of RNA.
16. Take an aliquot of 4 μL for quality control and quantification. Store the remaining RNA at -80°C for downstream analysis.
17. Check the RNA concentration on the NanoDrop (*see Note 21*).
18. Check the RNA integrity on the Agilent 2100 Bioanalyzer using an RNA Nano chip (*see Note 22* and Fig. 2b–c).

3.3.1 mRNA Purification and Fragmentation

1. Dilute 2 μg of total RNA of each sample in nuclease-free water to a final volume of 50 μL in separate wells of the RBP plate.
2. Vortex the RPB beads to resuspend them and add 50 μL of RPB beads to each well by pipetting up and down at least six times until complete resuspension. Seal the RBP plate with a Microseal “B” adhesive seal making sure the plate is fully sealed.
3. Place in a thermocycler, with heated lid at 100°C , and run the following program to perform RNA denaturation: 5 min at 65°C , and then hold at 4°C .
4. Retrieve the plate from the thermocycler and incubate for 5 min at room temperature to allow mRNA binding to the oligo-dT RPB beads.
5. Place the plate on a magnetic stand and leave it for 5 min or until complete separation of the beads.
6. Remove the adhesive seal, and then aspirate and discard the supernatant, being careful not to disturb the beads.
7. Remove the plate from the magnetic stand. Add 200 μL BWB to each well, and then mix by gently pipetting up and down at least six times until complete resuspension.
8. Place the plate on a magnetic stand and leave for 5 min or until complete separation of the beads.
9. Centrifuge ELB at $600\times g$ for 5 s.
10. Aspirate and discard the supernatant, containing mainly ribosomal RNA and non-messenger RNA, being careful not to disturb the beads.

11. Remove the plate from the magnetic stand. Add 50 μ L ELB to each well, and then mix by pipetting up and down at least six times until complete resuspension. Seal the RBP plate with a Microseal “B” adhesive seal making sure the plate is fully sealed.
12. Place in a thermocycler, with heated lid at 100 °C, and run the following program to perform mRNA elution: 2 min at 80 °C, and then hold at 25 °C.
13. Centrifuge BBB at $600\times g$ for 5 s.
14. Retrieve the plate from the thermocycler. Remove the seal and add 50 μ L BBB to each well, and then mix by pipetting up and down at least six times until complete resuspension to allow mRNA rebinding to the beads.
15. Incubate for 5 min at room temperature.
16. Place the plate on a magnetic stand and leave it for 5 min or until complete separation of the beads.
17. Aspirate and discard the supernatant, being careful not to disturb the beads. Remove the plate from the magnetic stand. Add 200 μ L BWB to each well, and then mix by pipetting up and down at least six times until complete resuspension.
18. Place the plate on a magnetic stand and leave it for 5 min or until complete separation of the beads.
19. Aspirate and discard the supernatant, being careful not to disturb the beads.
20. Remove the plate from the magnetic stand. Add 19.5 μ L EPF mix, containing random hexamers for RT priming, to each well, and then mix by pipetting up and down at least six times until complete resuspension. Seal the RBP plate with a Microseal “B” adhesive seal making sure the plate is fully sealed.
21. Place in a thermocycler, with heated lid at 100 °C, and run the following program to perform elution, fragmentation, and priming: 8 min at 94 °C, and then hold at 4 °C.
22. Retrieve the plate from the thermocycler and spin down quickly to collect any liquid at the bottom of the plate.

3.3.2 First Strand cDNA Synthesis

1. Place the RBP plate on a magnetic stand and leave it for 5 min or until complete separation of the beads.
2. While on magnetic stand, remove the seal and transfer 17 μ L supernatant of each well to the corresponding well of a new 0.3 mL plate labeled with CDP barcode, being careful not to carry over the beads.
3. Add 8 μ L of the Master mix 1 in each well of the CDP plate and then mix by pipetting up and down at least six times until complete resuspension. Seal the plate with a Microseal “B”

adhesive seal making sure the plate is fully sealed and spin down quickly to collect any liquid at the bottom of the plate.

4. Place in a thermocycler, with heated lid at 100 °C, and run the following program to perform first strand cDNA synthesis: 10 min at 25 °C, 50 min at 42 °C, 15 min at 70 °C, and then hold at 4 °C.

3.3.3 Second Strand cDNA Synthesis

1. Centrifuge the SSM mix at $600\times g$ for 5 s.
2. Retrieve the plate from the thermocycler, remove the seal, and add 25 μL of SSM in each well of the CDP plate and then mix by pipetting up and down at least six times until complete resuspension. Seal the plate with a Microseal “B” adhesive seal making sure the plate is fully sealed.
3. Place in a thermocycler, with heated lid at 30 °C, and run the following program to perform second strand cDNA synthesis: 60 min at 16 °C.
4. Retrieve the plate from the thermocycler, let it reach room temperature, and remove the seal. Vortex the AMPure XP Beads to resuspend them and add 90 μL of beads to each well of the CDP plate by pipetting up and down at least 15–20 times until complete resuspension.
5. Incubate for 15 min at room temperature.
6. Place the well plate on a magnetic stand and leave it for 5 min or until complete separation of the beads.
7. Aspirate and discard 135 μL of the supernatant, being careful not to disturb the beads.
8. While the plate is still on the magnetic stand, wash the beads with 200 μL of 80% ethanol. Incubate for 30 s at room temperature and carefully aspirate and discard the supernatant.
9. Repeat this wash once, making sure to remove any residual ethanol.
10. Air-dry the beads for 10–15 min while the plate is still on the magnetic stand (*see Note 23*).
11. Remove the plate from the magnetic stand. Elute the cDNA from the beads by adding 52.5 μL of RSB. Mix by pipetting up and down 15 times until complete resuspension of the beads.
12. Incubate 2 min at room temperature.
13. Place the well plate on a magnetic stand and leave it for 5 min to achieve separation of the beads.
14. Retrieve 50 μL of supernatant being careful not to carry over any beads and transfer in a new PCR plate with the IMP barcode. *PAUSE POINT*: the plate can be sealed, and double-stranded cDNA can be frozen at $-20\text{ }^{\circ}\text{C}$ for 1 week.

3.3.4 *End Repair*

1. In case the IMP plate was stored, retrieve it from the freezer, let it reach room temperature, and spin down quickly.
2. Remove the seal from the plate and add 10 μL of the diluted CTE and 40 μL of the ERP in each well of the IMP plate and then mix by pipetting up and down at least ten times until complete resuspension. Seal the plate with a Microseal “B” adhesive seal making sure the plate is fully sealed.
3. Place in a thermocycler, with heated lid at 30 °C, and run the following program to perform end repair: 30 min at 30 °C.
4. Retrieve the plate from the thermocycler and remove the seal. Vortex the AMPure XP Beads to resuspend them and add 160 μL of beads to each well of the IMP plate by pipetting up and down at least 15–20 times until complete resuspension.
5. Incubate for 15 min at room temperature.
6. Place the well plate on a magnetic stand and leave it for 5 min or until complete separation of the beads.
7. Aspirate and discard 127.5 μL of the supernatant, twice, being careful not to disturb the beads.
8. While the plate is still on the magnetic stand, wash the beads with 200 μL of 80% ethanol. Incubate for 30 s at room temperature and carefully aspirate and discard the supernatant.
9. Repeat this wash once, making sure to remove any residual ethanol.
10. Air-dry the beads for 10–15 min while the plate is still on the magnetic stand (*see Note 23*).
11. Remove the plate from the magnetic stand. Elute the cDNA from the beads by adding 17.5 μL of RSB. Mix by pipetting up and down 15 times until complete resuspension of the beads.
12. Incubate for 2 min at room temperature
13. Place the well plate on a magnetic stand and leave it for 5 min to achieve separation of the beads.
14. Retrieve 15 μL of supernatant being careful not to carry over any beads and transfer in a new PCR plate with the ALP barcode. *PAUSE POINT*: the plate can be sealed and frozen at –20 °C for 1 week.

3.3.5 *3' Ends Adenylation*

1. Add 2.5 μL of the diluted CTA in each well of the ALP plate and then mix by pipetting up and down at least ten times until complete resuspension.
2. Add 12.5 μL of the ATL and seal the plate with a Microseal “B” adhesive seal making sure the plate is fully sealed.
3. Place in a thermocycler, with heated lid at 100 °C, and run the following program: 30 min at 37 °C.
4. Retrieve the plate from the thermocycler.

3.3.6 Adapter Ligation

1. Remove the seal from the ALP plate. Add 2.5 μL of the LIG, 2.5 μL of the diluted CTL, and 2.5 μL of each RNA Adapter Index in each well of the ALP plate and then mix by pipetting up and down at least ten times until complete resuspension. Seal the plate with a Microseal “B” adhesive seal making sure the plate is fully sealed. If multiplexing libraries, each library should be generated with a different index.
2. Place in a thermocycler, with heated lid at 30 °C, and run the following program to perform adapter ligation: 10 min at 30 °C.
3. Retrieve the plate from the thermocycler and remove the seal.
4. Add 5 μL of the STL in each well of the ALP plate to stop ligation and then mix by pipetting up and down at least ten times until complete resuspension.
5. Vortex the AMPure XP Beads to resuspend them and add 42 μL of beads to each well of the ALP plate by pipetting up and down at least 15–20 times until complete resuspension.
6. Incubate for 15 min at room temperature.
7. Place the well plate on a magnetic stand and leave it for 5 min or until complete separation of the beads.
8. Aspirate and discard 79.5 μL of the supernatant, being careful not to disturb the beads.
9. While the plate is still on the magnetic stand, wash the beads with 200 μL of 80% ethanol. Incubate for 30 s at room temperature and carefully aspirate and discard the supernatant.
10. Repeat this wash once, making sure to remove any residual ethanol.
11. Air-dry the beads for 10–15 min while the plate is still on the magnetic stand (*see Note 23*).
12. Remove the plate from the magnetic stand. Elute the DNA from the beads by adding 52.5 μL of RSB. Mix by pipetting up and down 15 times until complete resuspension of the beads.
13. Incubate for 2 min at room temperature.
14. Place the well plate on a magnetic stand and leave it for 5 min to achieve separation of the beads.
15. Retrieve 50 μL of supernatant being careful not to carry over any beads and transfer in a new PCR plate with the CAP barcode.
16. Vortex the AMPure XP Beads to resuspend them and add 50 μL of beads to each well of the CAP plate for a second clean up by pipetting up and down at least 15–20 times until complete resuspension.
17. Incubate for 15 min at room temperature.

18. Place the well plate on a magnetic stand and leave it for 5 min or until complete separation of the beads.
19. Aspirate and discard 95 μL of the supernatant, being careful not to disturb the beads.
20. While the plate is still on the magnetic stand, wash the beads with 200 μL of 80% ethanol. Incubate for 30 s at room temperature and carefully aspirate and discard the supernatant.
21. Repeat this wash once, making sure to remove any residual ethanol.
22. Air-dry the beads for 15 min while the plate is still on the magnetic stand (*see Note 23*).
23. Remove the plate from the magnetic stand. Elute the cDNA from the beads by adding 22.5 μL of RSB. Mix by pipetting up and down 15 times until complete resuspension of the beads.
24. Incubate for 2 min at room temperature.
25. Place the well plate on a magnetic stand and leave it for 5 min to achieve separation of the beads.
26. Retrieve 20 μL of supernatant being careful not to carry over any beads and transfer in a new PCR plate with the PCR barcode. *PAUSE POINT*: the plate can be sealed and frozen at $-20\text{ }^{\circ}\text{C}$ for 1 week.

3.3.7 PCR Library Amplification

1. In case the PCR plate was stored, retrieve it from the freezer, let it reach room temperature, and spin down quickly.
2. Remove the seal from the PCR plate and add 5 μL of the PPC and 25 μL of the PMM in each well of the PCR plate and then mix by pipetting up and down at least ten times until complete resuspension. Seal the plate with a Microseal “B” adhesive seal making sure the plate is fully sealed.
3. Place in a thermocycler, with heated lid at $100\text{ }^{\circ}\text{C}$, and run the following program to perform PCR amplification: 1 cycle at $98\text{ }^{\circ}\text{C}$ for 30 s; then 15 cycles ($98\text{ }^{\circ}\text{C}$ for 10 s; $60\text{ }^{\circ}\text{C}$ for 30 s; $72\text{ }^{\circ}\text{C}$ for 30 s); finally, 1 cycle at $72\text{ }^{\circ}\text{C}$ for 5 min. Hold at $4\text{ }^{\circ}\text{C}$.
4. Retrieve the plate from the thermocycler and remove the seal.
5. Vortex the AMPure XP Beads to resuspend them and add 50 μL of beads to each well of the PCR plate by pipetting up and down at least 15–20 times until complete resuspension.
6. Incubate for 15 min at room temperature.
7. Place the well plate on a magnetic stand and leave it for 5 min or until complete separation of the beads.
8. Aspirate and discard 95 μL of the supernatant, being careful not to disturb the beads.
9. While the plate is still on the magnetic stand, wash the beads with 200 μL of 80% ethanol. Incubate for 30 s at room temperature and carefully aspirate and discard the supernatant.

10. Repeat this wash once, making sure to remove any residual ethanol.
11. Air-dry the beads for 10–15 min while the plate is still on the magnetic stand (*see Note 23*).
12. Remove the plate from the magnetic stand. Elute the DNA from the beads by adding 32.5 μL of RSB. Mix by pipetting up and down 15 times until complete resuspension of the beads.
13. Incubate for 2 min at room temperature.
14. Place the well plate on a magnetic stand and leave it for 5 min to achieve separation of the beads.
15. Retrieve 30 μL of supernatant being careful not to carry over any beads and transfer in a new PCR plate with the TSP1 barcode.
16. Save an aliquot of 4 μL for further quantification and quality check. *PAUSE POINT*: the plate can be sealed, and libraries can be frozen at $-20\text{ }^{\circ}\text{C}$ for 1 week.
17. Check the library concentration using Qubit assay.
18. Check the library size on the Agilent 2100 Bioanalyzer using a DNA High Sensitivity chip, after diluting the libraries at the required concentration (Fig. 2d).
19. Pool the libraries for sequencing in Qiagen EB buffer containing 0.1% Tween 20 (*see Note 24*). We usually sequence at an average of 60 million read pairs per sample (75–100 bp length) (*see Note 25*).

3.4 Chromatin Immunoprecipitation from DRG Tissue

General Note We used sciatic DRG from mice that underwent SNA vs Sham or DCA vs Lam 24 h earlier ($N = 2$ biological replicates). We usually pool sciatic DRGs from ten mice/replicate for histone ChIP. For transcription factors, more input material might be required.

3.4.1 Chromatin Preparation

1. Dissect sciatic DRGs (*see Subheading 3.1.4*) and immediately collect them on ice in a 1.5 mL tube containing 1 mL of cold HBSS (*see Note 1*).
2. Spin down at 1000 rpm for 2 min at room temperature, remove HBSS, and flash-freeze in liquid nitrogen. Store at $-80\text{ }^{\circ}\text{C}$. *PAUSE POINT*: DRG can be stored at $-80\text{ }^{\circ}\text{C}$ for a few months (*see Note 26*).
3. Crush the frozen pellet with the motorized pestle to reduce the DRG pellet into smaller pieces. First add 100 μL of solution A, crush with the motorized pestle, and then add an extra 300 μL , recovering any leftover on the pestle surface.
4. Incubate for 15 min at room temperature (*see Note 27*).
5. Add 1/20 volume of 2.5 M glycine, mix, and incubate for 5 min at room temperature to quench formaldehyde.

6. Centrifuge at $2500\times g$ at $4\text{ }^{\circ}\text{C}$ for 3 min.
7. Aspirate the supernatant and wash with 1 mL of cold PBS supplemented with protease inhibitors.
8. Centrifuge at $2500\times g$ at $4\text{ }^{\circ}\text{C}$ for 3 min.
9. Aspirate the supernatant and repeat PBS washes three more times. Remove the supernatant.
10. Resuspend the pellet in 100 μL of LB1 by pipetting. Crush the pellet gently with the pestle, and then add 900 μL of LB1 to wash the pestle and the tube wall. Recover everything and transfer into 15 mL Falcon tubes. Add LB1 up to 10 mL.
11. Rock gently at $4\text{ }^{\circ}\text{C}$ for 10 min. In this step, cell lysis occurs.
12. Centrifuge at $2000\times g$ for 5 min at $4\text{ }^{\circ}\text{C}$.
13. Aspirate the supernatant carefully and resuspend the pellet in 10 mL of LB2 to wash the pellet. Rock gently at $4\text{ }^{\circ}\text{C}$ for 10 min.
14. Centrifuge at $2000\times g$ for 5 min at $4\text{ }^{\circ}\text{C}$ to pellet nuclei.
15. Aspirate the supernatant carefully and resuspend the pellet in 600 μL of LB3 for nuclear lysis.
16. Split in two TPX microtubes (300 μL each) and sonicate the suspension with a Bioruptor sonicator for 30 min at high intensity, 0.5 cycle (30 s on, 30 s off). Tubes are placed on the dedicated adapter and immersed in the cold-water bath. This is achieved by either placing the Bioruptor in a cold room or connecting the sonicator to a cold-water circuit to avoid heating of the samples. After sonication, lysate should be clear (*see Note 28*).
17. Pool the content of the two tubes and save an aliquot of 20 μL for the sonication check. Flash-freeze the samples in liquid nitrogen and store at $-80\text{ }^{\circ}\text{C}$. *PAUSE POINT*: the samples can be processed after a few days.
18. To check sonication efficiency, extract DNA by adding 34 μL of the NaHCO_3 /SDS mix and 1 μL of 20 mg/mL Proteinase K to the saved aliquot.
19. Incubate for 1 h at $55\text{ }^{\circ}\text{C}$ using a thermoblock.
20. Precipitate DNA by adding 2.4 μL 5 M LiCl and 367 μL 99.8% ethanol and centrifuge at 14,000 rpm for 15 min at $4\text{ }^{\circ}\text{C}$.
21. Wash with 0.5 mL 70% ethanol and centrifuge at 14,000 rpm for 15 min at $4\text{ }^{\circ}\text{C}$.
22. Air-dry the pellet and resuspend in 10 μL of nuclease-free water.
23. Add 2 μL of $6\times$ loading buffer and load on a 1% agarose gel to check the size of the DNA. Average size should be 200–800 bp (Fig. 3b).

3.4.2 Immuno-precipitation

1. Thaw the lysate on ice. Add 10% Triton X-100 to a final concentration of 1%, and spin at max speed in microcentrifuge for 10 min at 4 °C to pellet debris.
2. Transfer the supernatant into a new tube, and add LB3/Triton up to 1 mL for each sample. Save 5% (50 µL) of the lysate and store it at -20 °C.
3. In the meantime, set up two new 1.5 mL microtubes per sample. Put 1 mL of blocking solution in the tubes and add Dynabeads: 50 µL of Dynabeads in one tube (for lysate pre-clearing) and 100 µL in the other tube (for antibody binding) by pipetting up and down (*see Note 29*).
4. Collect the beads using magnetic stand. Remove supernatant.
5. Wash beads in 1 mL blocking solution two more times, resuspending the beads by flicking the tube each time. Remove the washing buffer each time.
6. Incubate the lysate with the washed 50 µL beads (the beads for pre-clearing) for 6 h on a rotator at 4 °C (*see Note 30*).
7. Resuspend the washed 100 µL beads (the beads for antibody binding) in 250 µL blocking solution by flicking the tube. Add 10 µg of antibody and incubate for 6 h on a rotator at 4 °C (*see Note 8*).
8. After the antibody incubation, collect the beads using a magnetic stand and wash them in 1 mL of blocking solution as described in **steps 4–5**. Wash for a total of three times.
9. Resuspend the beads in 100 µL of blocking solution: these are ready-to-use beads.
10. After the lysate pre-clearing, collect the beads at the bottom of the tube with the magnetic stand. Recover the lysate and add each lysate to the 100 µL antibody/magnetic bead mix.
11. Incubate overnight on rotator at 4 °C.

3.4.3 Washing, Elution, and Cross-Linking Reversal

1. Perform all the following steps in a cold room.
2. Collect the beads using magnetic stand. Remove the supernatant. To remove the supernatant from the lid of the tubes, spin the tubes at low speed for a few seconds. Place the tubes back on the magnetic stand and remove the residual supernatant.
3. Resuspend the beads with 1 mL of RIPA buffer by gently flicking the tubes.
4. Place the tubes on a rotator for 5 min to wash the beads. Collect the beads using magnetic stand and remove the supernatant.
5. Repeat **steps 3–4** five times more (total of six washes) (*see Note 31*).

6. After removing the last wash, to remove the wash buffer from the lid of the tubes, spin the tubes at low speed for a few seconds. Place the tubes back on the magnetic stand and remove the residual wash buffer.
7. Wash the beads with 1 mL TBS. Collect the beads using magnetic stand and remove the TBS buffer.
8. Spin beads at $960\times g$ for 3 min at $4\text{ }^{\circ}\text{C}$, place the tubes back on the magnetic stand, and remove any residual TBS buffer.
9. Add 200 μL of Elution buffer.
10. Thaw the 50 μL of Input, add 150 μL of Elution buffer, and mix.
11. Incubate the Input and ChIP tubes on a thermoblock set at $65\text{ }^{\circ}\text{C}$ overnight to elute and reverse cross-link. In the first 15 min, resuspend beads every 5 min by vortexing hard.

3.4.4 DNA Purification and Quantification

1. Place the ChIP tubes on the magnetic stand and transfer the supernatant into new tubes. Remove beads.
2. Proceed in parallel with the ChIP and Input tubes. Add 200 μL of TE buffer.
3. Add 8 μL of 1 mg/mL RNase A and incubate at $37\text{ }^{\circ}\text{C}$ for 45 min to remove RNA.
4. Add 4 μL of 20 mg/mL Proteinase K and incubate at $55\text{ }^{\circ}\text{C}$ for 1.5 h to remove proteins.
5. Purify DNA with Qiagen columns using the Qiaquick PCR kit following the procedure below (manufacturer's instructions). Briefly, the DNA is absorbed by the silica membrane in the presence of the high concentration of salts provided by the buffers, while proteins and contaminants are washed away. DNA is finally eluted in water.
6. Split each sample in two tubes, add five volumes of PB buffer (supplied in the kit) and 1 μL of 3 M sodium acetate pH 5.0 (*see Note 32*). Incubate at $37\text{ }^{\circ}\text{C}$ for 30 min.
7. Load the content of both tubes on a single Qiaquick column placed in a 2 mL collection tube. Since the maximum loading volume of the column is 800 μL , you need to do this in three steps. Centrifuge at $18,000\times g$ for 60 s every time. Discard the flow-through every time.
8. Wash the column by adding 750 μL of PE buffer (supplied in the kit). Centrifuge at $18,000\times g$ for 60 s. Discard the collection tube. Be careful to avoid touching the tube with the column to prevent ethanol carryover as it might affect downstream analysis.
9. Place the column in a new 2 mL collection tube and centrifuge at $18,000\times g$ for 60 s to dry the column. Discard the collection tube.

10. Place the column in a new 1.5 mL tube. Add 50 μL nuclease-free water to the column making sure it goes directly to the spin column membrane. Incubate for 1 min at room temperature. Centrifuge at $20,000\times g$ for 1 min to elute the DNA. You will recover 48 μL of DNA. *PAUSE POINT*: DNA can be stored at $-20\text{ }^{\circ}\text{C}$. Take an aliquot of 5 μL for quantification.
11. Quantify DNA with Picogreen assay: set up a DNA standard curve from 20 to 0.002 $\mu\text{g}/\text{mL}$ via serial dilutions. Pipette 10 μL of each standard in duplicate in a black 96-well plate for fluorescence analysis. Pipette 1 μL of each Input sample and 4 μL of each ChIP sample in triplicate and add $1\times$ TE buffer up to 10 μL . As a blank control, pipette 10 μL of $1\times$ TE buffer. Add 190 μL of diluted Picogreen reagent into each well and mix. Incubate the plate for 5 min at room temperature, protected from light. Read at 490 nm using a fluorimeter.
12. Subtract the fluorescence of the blank from that of all the other wells (samples and standard curve) and average the background corrected fluorescence among the duplicates (standard curve) or triplicates (sample). Build the standard curve by plotting the obtained fluorescence values versus the DNA amount in each well. Determine the amount of sample DNA in each well by interpolating the sample fluorescence values in the standard curve. Determine the DNA concentration of the samples by dividing the DNA amount by the volumes of sample used in each well (1 μL for Input samples and 4 μL for the ChIP samples). We normally get concentrations in the range of 3–10 $\text{ng}/\mu\text{L}$ for the ChIP samples.

3.5 ChIP-Seq Library Preparation

1. Prepare a 96-well PCR plate on ice by pipetting 30–40 ng of DNA and nuclease-free water up to 55.5 μL .
2. Add 9.5 μL of the Master mix 1 in the wells containing the DNA and water. Pipette up and down at least ten times to mix the components. Seal the plate with adhesive films making sure the sealing is complete. Quickly spin to collect the liquid at the bottom of the plate.
3. Place in a thermocycler, with a heated lid at $95\text{ }^{\circ}\text{C}$, and run the following program to perform the end repair: 30 min at $20\text{ }^{\circ}\text{C}$, then 30 min at $65\text{ }^{\circ}\text{C}$, hold at $4\text{ }^{\circ}\text{C}$.
4. Retrieve the plate from the thermocycler and spin down quickly to collect any liquid at the bottom of the plate.
5. Carefully remove the sealing from the plate and on ice add 18.5 μL of the Master mix 2 in each well. Pipette up and down at least ten times to mix the components. Seal the plate with adhesive films making sure the sealing is complete. Quickly spin to collect the liquid at the bottom of the plate.
6. Place in a thermocycler with a heated lid on and incubate for 15 min at $20\text{ }^{\circ}\text{C}$.

7. Without removing the plate from the thermocycler, carefully remove the sealing from the plate and add 3 μL of the USER enzyme in each well. Pipette up and down at least ten times to mix the components. Seal the plate with adhesive films making sure the sealing is complete.
8. Incubate for 15 min at 37 °C to perform adaptor ligation.
9. Quickly spin the plate and carefully remove the sealing from the plate. Perform size selection (*see Note 33*). Add 13.5 μL of nuclease-free water to each well to reach a final volume of 100 μL . Vortex the AMPure XP Beads to resuspend them and add 55 μL of beads to each well by pipetting up and down at least 15–20 times until complete resuspension.
10. Incubate for 5 min at room temperature.
11. Place the well plate on a magnetic stand and leave it for 5 min or until complete separation of the beads.
12. Remove and transfer the supernatant containing the selected DNA into a new PCR plate, being careful not to carry over any beads. The plate with the beads can be discarded.
13. Vortex the AMPure XP Beads to resuspend them and add 25 μL of beads to each well by pipetting up and down at least 15–20 times until complete resuspension.
14. Incubate for 5 min at room temperature.
15. Place the well plate on a magnetic stand and leave it for 5 min or until complete separation of the beads.
16. Aspirate and discard the supernatant, being careful not to disturb the beads.
17. While the plate is still on the magnetic stand, wash the beads with 200 μL of 80% ethanol. Incubate for 30 s at room temperature and carefully aspirate and discard the supernatant.
18. Repeat this wash once, making sure to remove any residual ethanol.
19. Air-dry the beads for 5–10 min while the plate is still on the magnetic stand (*see Note 23*).
20. Remove the plate from the magnetic stand. Elute the DNA from the beads by adding 17 μL of Qiagen EB buffer. Mix by pipetting up and down 15 times until complete resuspension of the beads. Incubate for 2 min at room temperature.
21. Place the well plate on a magnetic stand and leave it for 5 min to achieve separation of the beads.
22. Retrieve 15 μL of supernatant being careful not to carry over any beads and transfer in a new PCR plate.
23. Add 33 μL of the Master mix 3 in each well of the PCR plate. Add 2 μL of a different Index Primer in each well. This procedure will allow multiplexing of the samples, as each sample will

be identified by a different index primer. Please refer to the kit manual for compatible index combinations. Pipette up and down at least ten times to mix the components. Seal the plate with adhesive films making sure the sealing is complete. Quickly spin to collect the liquid at the bottom of the plate.

24. Place in a thermocycler, with heated lid on, and run the following program to perform library PCR amplification: 1 cycle at 98 °C for 30 s, then 10 cycles (*see Note 34*) (98 °C for 10 s, 65 °C for 75 s), then 1 cycle at 65 °C for 5 min. Hold at 4 °C.
25. Quickly spin the plate and carefully remove the sealing from the plate. Perform library cleanup. Vortex the AMPure XP Beads to resuspend them and add 45 µL of beads to each well by pipetting up and down 15–20 times until complete resuspension.
26. Incubate for 5 min at room temperature.
27. Place the well plate on a magnetic stand and leave it for 5 min or until complete separation of the beads.
28. Aspirate and discard the supernatant, being careful not to disturb the beads.
29. While the plate is still on the magnetic stand, wash the beads with 200 µL of 80% ethanol. Incubate for 30 s at room temperature and carefully aspirate and discard the supernatant.
30. Repeat this wash once, making sure to remove any residual ethanol.
31. Air-dry the beads for 5 min while the plate is still on the magnetic stand (*see Note 23*).
32. Remove the plate from the magnetic stand. Elute the DNA from the beads by adding 33 µL of Qiagen EB buffer. Mix by pipetting up and down 15 times until complete resuspension of the beads. Incubate for 2 min at room temperature.
33. Place the well plate on a magnetic stand and leave it for 5 min to achieve separation of the beads.
34. Retrieve 28 µL of supernatant being careful not to carry over any beads and transfer in a new PCR plate. If needed, perform the cleanup twice (*see Note 35*).
35. Save an aliquot of 4 µL for further quantification and quality check. *PAUSE POINT*: the libraries can be frozen at –20 °C.
36. Check the library concentration using Qubit assay.
37. Check the library size on the Agilent 2100 Bioanalyzer using a DNA High Sensitivity chip, after diluting the libraries at the required concentration (Fig. 3c, d).
38. Pool the libraries for sequencing in Qiagen EB buffer containing 0.1% Tween 20 (*see Note 24*). We usually sequence at a depth of 20–30 million single-ended reads per sample (50 bp length) (*see Note 36*).

3.6 ATAC-Seq from DRG Tissue

3.6.1 Cell Preparation and Transposition Reaction

General Note We used sciatic DRG from mice that underwent SNA vs Sham or DCA vs Lam 24 h earlier ($N = 3$ biological replicates). We usually use sciatic DRGs from one mouse/replicate.

1. Dissect sciatic DRGs (*see* Subheading 3.1.4) and immediately collect them on ice in a 1.5 mL tube containing 1 mL of cold HBSS (*see* Note 1).
2. Aspirate HBSS, then add 100 μ L of cold lysis buffer, and crush the DRG tissue with the motorized pestle.
3. Add an extra 400 μ L of cold lysis buffer, washing the pellet pestle. Incubate for 10 min on ice (*see* Note 37).
4. Transfer 50,000 nuclei in a new nuclease-free microtube and centrifuge for 10 min at $500\times g$ at 4 °C to pellet the nuclei. Discard the supernatant and place nuclear pellet on ice.
5. Add 50 μ L of Transposition mix to each sample and gently pipette to resuspend nuclei on ice.
6. Incubate transposition reaction at 37 °C for 30 min using a thermoblock.
7. Immediately after the transposition, purify with Qiagen MinElute PCR Purification following manufacturer's instructions. Briefly, the DNA is absorbed by the silica membrane in the presence of the high concentration of salts provided by the buffers, while proteins and contaminants are washed away. DNA is finally eluted in water.
8. Add 5 volumes of PB buffer (supplied in the kit) and 1 μ L of 3 M sodium acetate pH 5.0 (*see* Note 32).
9. Load the content on a MinElute column placed in of a 2 mL collection tube. Centrifuge at $18,000\times g$ for 60 s. Discard the flow-through.
10. Wash the column by adding 750 μ L of PE buffer (supplied in the kit). Centrifuge at $18,000\times g$ for 60 s. Discard the collection tube. Be careful to avoid touching the tube with the column to prevent ethanol carryover, as it might affect downstream analysis.
11. Place the column in a new 2 mL collection tube and centrifuge at $18,000\times g$ for 60 s to dry the column. Discard the collection tube.
12. Place the column in a new 1.5 mL nuclease-free collection tube. Add 14 μ L nuclease-free water to the column making sure it goes directly onto the spin column membrane. Incubate for 1 min at room temperature Centrifuge at $20,000\times g$ for 1 min to elute the DNA. You will recover 12 μ L of DNA. **PAUSE POINT:** DNA can be stored at -20 °C.

3.6.2 Library Amplification

1. Thaw the eluted DNA on ice in case it has been stored at -20°C .
2. Pipette $37.5\ \mu\text{L}$ of the PCR Master mix 1 per sample to a PCR plate.
3. Add $10\ \mu\text{L}$ of the transposed DNA and $2.5\ \mu\text{L}$ of specific barcoded $25\ \mu\text{M}$ PCR Primer Ad2 in each well (*see* Table 1). This procedure will allow multiplexing of the samples as each sample will be identified by a different index primer. Pipette up and down to mix the components. Seal the plate with adhesive films making sure the sealing is complete.
4. Quickly spin to collect the liquid at the bottom of the plate.
5. Place in a thermocycler, with heated lid on, and run the following program to perform partial library PCR amplification (*see* **Note 38**): 1 cycle at 72°C for 5 min, followed by 1 cycle at 98°C for 30 s, then 5 cycles (98°C for 10 s, 63°C for 30 s, 72°C for 60 s). Hold at 4°C .
6. Retrieve the PCR plate from the thermocycler and leave it on ice.
7. Pipette $9.75\ \mu\text{L}$ of the PCR Master mix 2 per sample to a PCR plate.
8. Add $5\ \mu\text{L}$ of the partially amplified library and $0.25\ \mu\text{L}$ of barcoded PCR Primer Ad2. Pipette up and down to mix the components. Seal the plate with adhesive films making sure the sealing is complete. Quickly spin to collect the liquid at the bottom of the plate.
9. Using a qPCR machine, run the following program: 1 cycle at 98°C for 30 s, then 25 cycles (98°C for 10 s, 63°C for 30 s, 72°C for 60 s). Hold at 4°C .
10. To calculate the number of additional PCR cycles needed, plot linear R_n vs Cycle Number and then calculate the number of cycles that corresponds to one third or one fourth of the maximum fluorescence intensity (*see* Fig. 4b and **Note 39**).
11. After calculating the additional number of cycles, run the remaining $45\ \mu\text{L}$ of PCR reaction to complete library amplification cycle as follows: 1 cycle at 98°C for 30 s, then x cycles (calculated additional # of cycles) (98°C for 10 s, 63°C for 30 s, 72°C for 60 s). Hold at 4°C . **PAUSE POINT**: DNA can be stored at -20°C .

3.6.3 Library Purification

1. Thaw the plate in case it has been stored at -20°C . Quickly spin the plate and carefully remove the sealing from the plate.
2. Add $5\ \mu\text{L}$ of nuclease-free water to the PCR reaction to bring the total volume to $50\ \mu\text{L}$.
3. Perform library cleanup using AMPure XP Beads (*see* **Note 40**). Vortex to resuspend them and add $80\ \mu\text{L}$ of beads ($1.6\times$, left side selection to remove primer dimers) to each well by pipetting up and down 15–20 times until complete resuspension.

4. Incubate for 10 min at room temperature.
5. Place the well plate on a magnetic stand and leave it for 5 min or until complete separation of the beads.
6. Aspirate and discard the supernatant, being careful not to disturb the beads.
7. While the plate is still on the magnetic stand, wash the beads with 200 μL of 80% ethanol. Incubate for 30 s at room temperature and carefully aspirate and discard the supernatant.
8. Repeat this wash once, making sure to remove any residual ethanol.
9. Air-dry the beads for 5–10 min while the plate is still on the magnetic stand (*see Note 23*).
10. Remove the plate from the magnetic stand. Elute the DNA from the beads by adding 25 μL of Qiagen EB buffer. Mix by pipetting up and down 15 times until complete resuspension of the beads. Incubate for 2 min at room temperature.
11. Place the well plate on a magnetic stand and leave it for 5 min or until complete separation of the beads.
12. Retrieve 23 μL of supernatant being careful not to carry over any beads and transfer in a new PCR plate. One cleanup is usually enough to remove all primer dimers.
13. Save an aliquot of 4 μL for further quantification and quality check. *PAUSE POINT*: the libraries can be frozen at $-20\text{ }^{\circ}\text{C}$.
14. Check the library concentration and size on the Agilent 2100 Bioanalyzer using a DNA High Sensitivity chip, after diluting the libraries at the required concentration (Fig. 4c, d and **Note 41**).
15. Pool the libraries in Qiagen EB buffer containing 0.1% Tween 20 for sequencing (*see Note 24*). We usually sequence at 80 million (>50) read pairs per sample (75–100 pb length) (*see Note 42*).

4 Notes

1. We recommend using the 1.5 mL Anachem microtubes fitting the Anachem pellet pestle. We found that the motorized pestle ensures the perfect homogenization of the DRG tissue. Inefficient lysis will bring lower yield.
2. Other kits can be used; however, we find that Qiagen RNeasy mini kit gives optimal results. The kit should be stored at room temperature and is stable at least 9 months. Binding capacity of the column is 30 mg of tissue and 100 μg of RNA. The first time you use the kit, add four volumes of 99.8% ethanol

(vol/vol) to the concentrated RPE buffer. Label the bottle. Do not leave the bottle open for too long, as the ethanol will evaporate.

3. DNase I lyophilized enzyme and the RDD buffer are stored at 4 °C and can be kept for at least 9 months. To prepare stocks, dissolve the DNase I in 550 µL of RNase-free water. DNase I is especially sensitive to physical denaturation. Mix gently by inverting. Do not vortex. Aliquot in RNase-free tubes and store at –20 °C for up to 9 months. Thawed aliquots can be stored at 2–8 °C for up to 6 weeks.
4. We used Illumina TruSeq stranded mRNA Library Prep Kit; however, alternative kits are also available. The procedure might change if alternative kits are used. Please refer to manufacturer's manual.
5. Formaldehyde is flammable, toxic by inhalation, and by contact with skin, it can cause burns and is potentially carcinogenic. Formaldehyde should be handled with appropriate safety equipment and used under chemical hood.
6. Ethidium bromide is toxic and mutagenic and should be stored according to the manufacturer's instructions, handled with appropriate safety equipment, and used under chemical hood. Safer alternatives are also available.
7. We recommend using IgG-Free Protease-Free BSA (e.g., Jackson ImmunoResearch).
8. The choice of the antibody is critical for efficient ChIP. We recommend using ChIP grade antibodies, and testing them before using them for ChIP-seq. When testing, positive and negative controls are needed. We performed ChIP-seq for H3K9ac and H3K27ac (markers of active promoters and enhancers) and H3K27me3 (marker of repressed chromatin). We have successfully used H3K27ac (Ab4729, Abcam), H3K9ac (Ab10812, Abcam), or H3K27me3 (C15410195, Diagenode) antibodies with consistent enrichment, and those can be used as positive controls. A negative control is created by setting up an extra tube per sample where the same amount of IgG of the same species is added instead of the specific antibody. The bound DNA, after purification, is then tested by qPCR and enrichment over Input is calculated. We found that 10 µg of antibodies is enough for histone ChIP. For transcription factors, a higher amount of antibody is usually needed.
9. Other kits can be used. The kit is stable for up to 12 months at room temperature. Before use, check the buffers for any precipitate, and redissolve at 37 °C if needed. The binding capacity of the column is 10 µg. If it is the first time you are using PE buffer, add four volumes of 99.8% ethanol (vol/vol) to the concentrated PE buffer. Label the bottle. Do not leave the bottle open for too long, as the ethanol will evaporate.

10. There are many commercially available library preparation kits. We have provided instructions based on our experience with the NEBNext Ultra library preparation kit. A more recent version of the library kit has been produced. If you are using a different kit, we recommend following the manufacturer's instructions.
11. The volumes of the primers might change as each kit lot might have different primer concentrations. Please refer to each lot instructions.
12. There are many commercially available tagmentation kits. We have provided instructions based on our experience with the Illumina Tagment DNA Enzyme and Buffer kit.
13. There are many commercially available DNA purification kits that enable elution of purified DNA in small volumes. We have provided instructions based on our experience with the Qiagen MinElute Purification kit. The kit is stable for up to 12 months. At the arrival, store the MinElute spin columns at 4 °C. Before use, check the buffers for any precipitate, and redissolve at 37 °C if needed. The binding capacity of the column is 5 µg. The first time you use the kit, add four volumes of 99.8% ethanol (vol/vol) to the concentrated PE buffer. Label the bottle. Do not leave the bottle open for too long, as the ethanol will evaporate.
14. There are many commercially available high-fidelity PCR master mixes. We have provided instructions based on our experience with the NEBNext HF 2× PCR Master Mix.
15. Increase isoflurane flow if breathing quickens and decrease is breathing slows. Ideally maintain a rate of 1–1.5 breaths per second.
16. Should the laminectomy cause bleeding, take a cotton swab and apply pressure to the site until the bleeding has stopped. This may take several minutes. If the mouse has lost up to 500 µL of blood, inject 1000 µL of saline subcutaneously to aid erythrocyte production and maintenance of blood volume. Monitor the mouse carefully in the post-recovery period.
17. Be careful not to drag the forceps either side of the spinal cord, as you will catch the peripheral axonal branches that enter here, and damage the DRG. Keep the forceps on the bone itself.
18. Cut vertically and not at an angle so as not to catch the underlying DRG. If there is bone remaining which covers the DRG, remove this gently using forceps.
19. The L6 DRG are smaller and more difficult to identify. Gently pull away muscle or move the spinal cord to the side to find it underneath. The DRG sometimes have a black speckled membrane, which covers their surface that can be used to identify them.

20. At least 10 μL of RNAlater are recommended for 1 mg of tissue. The procedure for tissue collection should be as quick as possible to avoid RNA degradation. Although RNA from DRG can be prepared immediately after DRG extraction, or after liquid nitrogen flash freezing, we found that RNA stabilization in RNAProtect Tissue Reagent o.n. preserves RNA integrity better. Do not use RNAProtect Tissue Reagent with frozen tissue.
21. The A260/280 and A260/230 ratios provide an idea of the purity of the RNA. A260/280 should be ~ 2.0 and A260/230 ~ 2.0 – 2.2 . Abnormal ratios usually indicate contamination of proteins or other reagents in the extraction protocol. Non-optimal ratios may also be faced at very low concentrations of nucleic acids. However, with this procedure, we have always had a good yield of high-quality RNA. Starting from 6–12 sciatic DRGs from one to two mice, the RNA concentration is in the range of 100–200 ng/ μL .
22. The bioanalyzer provides a measure of RNA integrity by measuring an RNA Integrity Number (RIN), which is based on the ratio between the 18S and 28S ribosomal subunits. A RIN > 8.0 is expected with this procedure (Fig. 2b); however, RIN > 7.5 are sometimes accepted. We found that treatment of the tissue with RNAProtect Tissue Reagent o.n. greatly improves the RIN score. In case of low RIN (Fig. 2c), repeat the RNA preparation, being aware of the possible sources of RNase contaminations.
23. Do not overdry the beads as this might result in low sample recovery. The bead pellet should not crack, as this means it is too dry.
24. Calculate the molar concentration of each library and dilute the more concentrated libraries to put them in line with the less concentrated ones. Pool the same amount (nmols) of each library, aiming for a final concentration of 5–10 nM. If the index primers are different for each sample, you can pool all the libraries in one single pool to avoid batch effects. Sequence the pool multiple times until the required depth. Do not dilute and pool all the libraries, as you might need to run them again. Be accurate in pipetting and try to avoid pipetting very small volumes.
25. For sequencing analysis and differential expression analysis, several tools are available [7]. In our analysis [6], after quality control, reads were aligned to the mm10 mouse reference genome using TopHat v.2.0.12 [10] running Bowtie2 v.2.2.3 [11]. A transcriptome index was built using gene structure annotations corresponding to the Ensembl (<https://www.ensembl.org/index.html>) annotation of the mm10 genome

sequence and provided to TopHat during the alignment step. Read counts were obtained from mapped reads using HTSeq v.0.6.1 (<https://pypi.python.org/pypi/HTSeq/0.6.1>), and differential expression analysis was performed using EdgeR v.3.8.6 [12], using limma v.3.22.7 [13] in R v.3.1.1. Differential expression testing was performed on the normalized output from EDASeq using EdgeR.

26. An alternative approach would be to fix the fresh tissue immediately after collection, quench, wash (following protocol until **step 9** under Subheading 3.4.1), and then flash-freeze it at -80°C , until ready for the experiment. Although we have never directly compared the two approaches, we found that freezing the tissue at the collection time, without any further processing, gives good results. Moreover, it is time convenient when a large number of mice have to be handled.
27. Cross-linking time and conditions can be optimized for different proteins and for different tissues. However, we have found that these conditions and times work well in DRG tissue. Insufficient cross-linking can result in loss of DNA–protein contacts, and over-cross-linking can result in difficulty in sonication and in denaturation of the protein of interest.
28. Sonication is needed for nuclear lysis and shearing of the chromatin. After sonication, the cloudy lysate should turn clear. Under-sonication, with generation of large fragments, will result in loss of resolution of the binding events. Sonication might require some optimization depending on the sample type and amount, and on the sonicator being used. We have found that the described settings using the Bioruptor sonicator work well for sciatic DRG tissue from ten mice. For the Bioruptor, PTX tubes are used, as their hard plastic improves the transmission of the ultrasounds to the sample. A successful sonication will result in DNA fragments in the range of 200–800 bp (Fig. 3b). Insufficient shearing can be troubleshooted by additional cycles of sonication or reducing the fixation time. If using a tip sonicator, be careful to keep the sample tubes on ice at all times and the tip centered in the tube.
29. Before using Dynabeads, ensure proper bead resuspension by tilting, rotating, and flicking the vial. Do not vortex. To make sure to pipette the right amount of beads, pipette very slowly and wash the tip by pipetting up and down a few times in blocking solution. Dynabead protein G have a high affinity for most rabbit and mouse antibodies; however, refer to the datasheet to check the affinity for different species/classes of antibodies.
30. Dynabeads have low nonspecific binding; however, we perform the preclearing step anyway.

31. We find that these washing conditions work well in general. The number of washes and the composition of the RIPA wash buffer can be optimized depending on the antibody used. For less stringent washes, the number of washes can be decreased, and/ or the concentration of detergents can be reduced.
32. The addition of 3 M sodium acetate pH 5.0 is to ensure that pH conditions are optimal for DNA binding. DNA binding to the silica membrane requires pH < 7.5. We do not add pH indicator to the PB buffer, as it might interfere with following library preparation steps.
33. Although the kit manual does not recommend size selection when starting from <100 ng of DNA, we find size selection essential to ensure the correct library size. The protocol refers to a library size of 200 bp. We use AMPure XP beads; however, SPRIselect beads can also be used.
34. The number of cycles depends on the starting amount of DNA. We use 10 cycles for 30 ng and 12 cycles for 5 ng. Further adjustments may be required for different DNA input amount.
35. We found that two cleanup rounds are needed to remove any residual traces of adaptors.
36. For ChIP-seq analysis, several tools are available [14]. In our analysis [6], after quality control, reads were aligned to the mm10 reference genome and used for peak calling using the AQUAS histone ChIP-seq pipeline (https://github.com/kundajelab/chipseq_pipeline). Genomic bins of 1000 bp upstream and downstream of each transcription start site for each gene were created using the same gene annotation as used for the RNA-seq data. Read counts per genomic bin (for gene analysis) or peak (for enhancer analysis) were obtained from the mapped reads using HTSeq-0.6.1 (<https://pypi.python.org/pypi/HTSeq/0.6.1>), and subsequently, differential binding testing was conducted using EdgeR-3.8.6 [12].
37. Take an aliquot of 20 µL in a tube and add 20 µL of methyl green-pyronin to check lysis efficiency under the microscope. Nuclei of lysed cells will be counterstained in green. Count the nuclei using a hemocytometer. We usually get 125,000 nuclei from sciatic DRG of one mouse.
38. Only five cycles are applied at first. Reaction is then monitored using qPCR to enable the amplification to be stopped before saturation. The appropriate number of PCR cycles is determined in order to avoid GC and size bias during PCR amplification.
39. The goal of the qPCR is to generate libraries with the minimum number of PCR cycles. If two samples have similar Ct values, calculate the cycle number from the sample with smaller fluorescence intensity (Fig. 4b, pink and yellow). If the number

of cycles to be added is in between two cycles, use the smaller integer (Fig. 4b, yellow and purple samples). We normally perform six extra cycles (not exceeding 11 cycles).

40. We found that column purification of the libraries does not remove primer–dimers. Therefore, we recommend magnetic bead purification rather than column purification.
41. Bioanalyzer trace should show a sloping curve of PCR fragment sizes between ~ 150 and 1000 bp, with periodicity of ~200 bp (Fig. 4c). Additional peaks at ~78 bp may be seen and represent excess PCR primers dimers (Fig. 4d). If a high molecular weight contamination is present, a second AMPure XP bead cleanup using a 0.3× ratio can be applied (right-side selection); however, it is most often not needed.
42. For ATAC-seq analysis, some tools are available [15]. In our analysis [6], quality control, read alignment, signal track generation, and peak calling were performed using the Kundaje lab’s ATAC-seq processing pipeline (https://github.com/kundajelab/atac_dnase_pipelines) running Bowtie2 [11] and MACS2 (<https://pypi.org/project/MACS2/>). Genomic bins of 1000 bp upstream and downstream of each transcription start site for each gene were created using the same gene annotation as used for the RNA-seq data. Read counts per genomic bin (for gene analysis) or peak (for enhancer analysis) were obtained from the mapped reads using HTSeq-0.6.1 (<https://pypi.python.org/pypi/HTSeq/0.6.1>), and, subsequently, differential accessibility testing was conducted in EdgeR-3.8.6 [12]. ATAC-seq footprints were generated using HINT [16]. Differential footprinting analysis was performed using BaGFoot [17] at the level of promoters and enhancers.

Acknowledgments

The work has been supported by the Wings for Life (SDG), Rose-trees Trust (SDG), Leverhulme Trust (SDG), International Spinal Research Trust (SDG), Brain Research UK (SDG), and Medical Research Council (SDG). The schematics have been generated using BioRender (BioRender.com).

References

1. Wang Z, Gerstein M, Snyder M (2009) RNA-seq: a revolutionary tool for transcriptomics. *Nat Rev Genet* 10(1):57–63. <https://doi.org/10.1038/nrg2484>
2. Schmidt D, Wilson MD, Spyrou C, Brown GD, Hadfield J, Odom DT (2009) ChIP-seq: using high-throughput sequencing to discover protein–DNA interactions. *Methods* 48(3):240–248. <https://doi.org/10.1016/j.ymeth.2009.03.001>
3. Buenrostro JD, Giresi PG, Zaba LC, Chang HY, Greenleaf WJ (2013) Transposition of

- native chromatin for fast and sensitive epigenomic profiling of open chromatin, DNA-binding proteins and nucleosome position. *Nat Methods* 10(12):1213–1218. <https://doi.org/10.1038/nmeth.2688>
4. Hervera A, De Virgiliis F, Palmisano I, Zhou L, Tantardini E, Kong G, Hutson T, Danzi MC, Perry RB, Santos CXC, Kapustin AN, Fleck RA, Del Rio JA, Carroll T, Lemmon V, Bixby JL, Shah AM, Fainzilber M, Di Giovanni S (2018) Reactive oxygen species regulate axonal regeneration through the release of exosomal NADPH oxidase 2 complexes into injured axons. *Nat Cell Biol* 20(3):307–319. <https://doi.org/10.1038/s41556-018-0039-x>
 5. Hervera A, Zhou L, Palmisano I, McLachlan E, Kong G, Hutson TH, Danzi MC, Lemmon VP, Bixby JL, Matamoros-Angles A, Forsberg K, De Virgiliis F, Matheos DP, Kwapis J, Wood MA, Puttagunta R, Del Rio JA, Di Giovanni S (2019) PP4-dependent HDAC3 dephosphorylation discriminates between axonal regeneration and regenerative failure. *EMBO J*. <https://doi.org/10.15252/embj.2018101032>
 6. Palmisano I, Danzi MC, Hutson TH, Zhou L, McLachlan E, Serger E, Shkura K, Srivastava PK, Hervera A, Neill NO, Liu T, Dhrif H, Wang Z, Kubat M, Wuchty S, Merckenschlager M, Levi L, Elliott E, Bixby JL, Lemmon VP, Di Giovanni S (2019) Epigenomic signatures underpin the axonal regenerative ability of dorsal root ganglia sensory neurons. *Nat Neurosci* 22(11):1913–1924. <https://doi.org/10.1038/s41593-019-0490-4>
 7. Conesa A, Madrigal P, Tarazona S, Gomez-Cabrero D, Cervera A, McPherson A, Szczesniak MW, Gaffney DJ, Elo LL, Zhang X, Mortazavi A (2016) A survey of best practices for RNA-seq data analysis. *Genome Biol* 17:13. <https://doi.org/10.1186/s13059-016-0881-8>
 8. Kaya-Okur HS, Wu SJ, Codomo CA, Pledger ES, Bryson TD, Henikoff JG, Ahmad K, Henikoff S (2019) CUT&Tag for efficient epigenomic profiling of small samples and single cells. *Nat Commun* 10(1):1930. <https://doi.org/10.1038/s41467-019-09982-5>
 9. Li Z, Schulz MH, Look T, Begemann M, Zenke M, Costa IG (2019) Identification of transcription factor binding sites using ATAC-seq. *Genome Biol* 20(1):45. <https://doi.org/10.1186/s13059-019-1642-2>
 10. Kim D, Pertea G, Trapnell C, Pimentel H, Kelley R, Salzberg SL (2013) TopHat2: accurate alignment of transcriptomes in the presence of insertions, deletions and gene fusions. *Genome Biol* 14(4):R36. <https://doi.org/10.1186/gb-2013-14-4-r36>
 11. Langmead B, Salzberg SL (2012) Fast gapped-read alignment with Bowtie 2. *Nat Methods* 9(4):357–359. <https://doi.org/10.1038/nmeth.1923>
 12. Robinson MD, McCarthy DJ, Smyth GK (2010) edgeR: a bioconductor package for differential expression analysis of digital gene expression data. *Bioinformatics* 26(1):139–140. <https://doi.org/10.1093/bioinformatics/btp616>
 13. Ritchie ME, Phipson B, Wu D, Hu Y, Law CW, Shi W, Smyth GK (2015) limma powers differential expression analyses for RNA-sequencing and microarray studies. *Nucleic Acids Res* 43(7):e47. <https://doi.org/10.1093/nar/gkv007>
 14. Nakato R, Sakata T (2021) Methods for ChIP-seq analysis: a practical workflow and advanced applications. *Methods* 187:44–53. <https://doi.org/10.1016/j.ymeth.2020.03.005>
 15. Yan F, Powell DR, Curtis DJ, Wong NC (2020) From reads to insight: a hitchhiker's guide to ATAC-seq data analysis. *Genome Biol* 21(1):22. <https://doi.org/10.1186/s13059-020-1929-3>
 16. Gusmao EG, Allhoff M, Zenke M, Costa IG (2016) Analysis of computational footprinting methods for DNase sequencing experiments. *Nat Methods* 13(4):303–309. <https://doi.org/10.1038/nmeth.3772>
 17. Baek S, Goldstein I, Hager GL (2017) Bivariate genomic footprinting detects changes in transcription factor activity. *Cell Rep* 19(8):1710–1722. <https://doi.org/10.1016/j.celrep.2017.05.003>



Profiling Locally Translated mRNAs in Regenerating Axons

Pabitra K. Sahoo and Jeffery L. Twiss

Abstract

Spatial and temporal regulation of protein expression plays important roles in many cellular functions, particularly for highly polarized cell types. While the subcellular proteome can be altered by relocalizing proteins from other domains of the cell, transporting mRNAs to subcellular domains provides a means to locally synthesize new proteins in response to different stimuli. Localized protein synthesis is a critical mechanism in neurons that extend dendrites and axons long distances from their cell bodies. Here, we discuss methodologies that have been developed to study localized protein synthesis using axonal protein synthesis as an example. We provide an in-depth method using dual fluorescence recovery after photobleaching to visualize sites of protein synthesis using reporter cDNAs that encode two different localizing mRNAs along with diffusion-limited fluorescent reporter proteins. We show how this method can be used to determine how extracellular stimuli and different physiological states can alter the specificity of local mRNA translation in real time.

Key words Localized protein synthesis, FRAP, mRNA translation, Axonal protein synthesis

1 Introduction

Localization of mRNAs coupled with synthesis of proteins at subcellular sites or domains is a characteristic feature of all polarized eukaryotic cells, including neurons [1–3]. Neurons are extremely polarized, and they transport mRNAs and needed translational machinery into their axons and dendrites. This provides an “on-demand” means to generate multiple copies of the encoded protein from a single mRNA rather than transporting individual proteins from the cell body into the axons and dendrites. Seminal works showing that dendrites and axons can autonomously synthesize proteins have led to questions on functions for that protein synthesis, which proteins are locally synthesized, and how is mRNA transport into and translation within dendrites and axons regulated [3, 4]. We focus on that last question in this article. Our objective is to present methodologies used to visualize and quantitate localized mRNA translation that have been developed using cultured

neurons. These approaches provide platforms for dissecting the mechanisms that regulate the specificity of localized neuronal protein synthesis without contamination from other cellular sources. We typically utilize dorsal root ganglion (DRG) neurons as our model system, since these neurons rapidly extend axons for hundreds of microns over 1–3 days in culture, so they provide definitive spatial resolution of distal axons from the cell body. Since the DRGs can be cultured from adult rodents, they provide a model to evaluate regeneration of axons. However, these approaches can and have been extended to other neuronal populations and can be modified for use *in vivo* [5–7].

Methodologies for studying mRNA translation in axons have largely relied on (1) directly labeling nascent peptide chains, (2) isolating ribosomes with bound mRNAs, and (3) using reporter mRNAs as surrogates for endogenous transcripts. Puromycylation is an example of directly labeling nascent peptide chains [8] (*see Note 1*). Ribosomes can also be isolated with bound mRNAs to provide an assessment of mRNA translation (*see Note 2*). Puromycylation assay and ribosome/polysome fractionation techniques can provide unbiased analyses for local mRNA translation when axons can be completely isolated from the neuronal soma. We focus this article on the use of reporter mRNAs as surrogates for endogenous transcripts in axons. Several studies have used fluorescence recovery after photobleaching (FRAP) approach to study localized translation of specific mRNAs [9–14]. FRAP was initially developed to study protein motility in living cells [15]. This classic FRAP approach uses high-intensity laser light to photobleach an area of a cell to fully deplete fluorescence, and then recovery of fluorescence is followed in this region of interest (ROI) to track protein motility. The faster it recovers, the more mobile a protein is. To study localized protein synthesis, fluorescent reporter protein cDNAs are tagged with a membrane-localizing epitope (e.g., myristoylation (MYR)), which markedly limits diffusion of the nascently synthesized proteins from sites of translation (Fig. 1) [5]. Axonal localization and translational control motifs are largely restricted to untranslated regions (UTRs) of mRNAs [3]. RNA localization motifs typically reside in the 3' UTR, with the 5' UTR typically contributing to translational regulation [16]. Thus, subcellular localization of a fluorescent reporter mRNA can often be driven by 3' UTR of an axonal mRNA, and translational regulation of the localized reporter mRNA can be driven by 5' UTR of that axonal mRNA. So, cloning the 5' and 3' UTRs of candidate mRNAs flanking the initiation codon and stop codons, respectively, of the coding sequence of a diffusion-limited GFP cDNA (GFP^{MYR}) or mCherry cDNA (mCH^{MYR}) provides a surrogate for transport and translational regulation of the endogenous

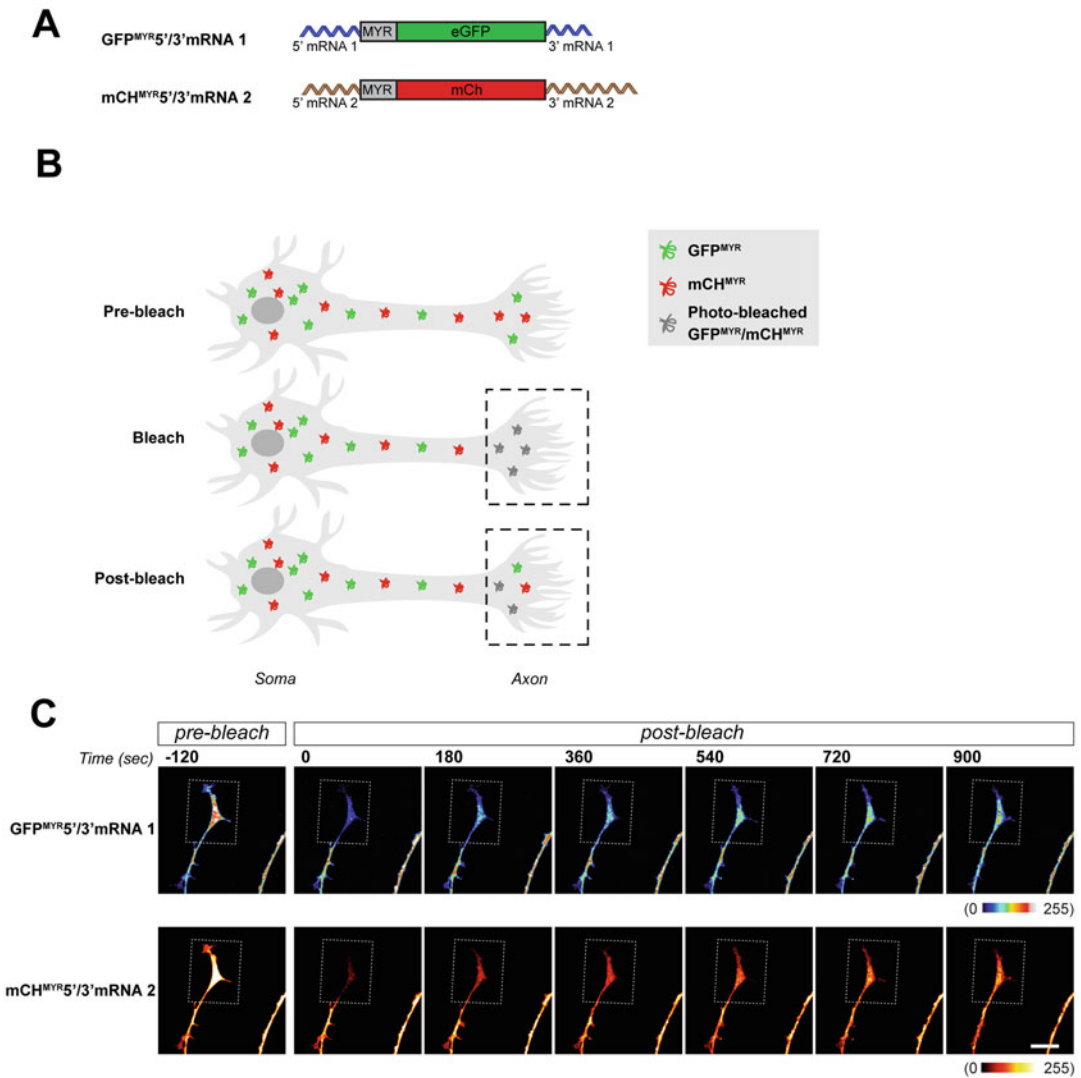


Fig. 1 Fluorescence recovery after photobleaching for visualizing intra-axonal translation of multiple mRNAs. (a) Schematics of translation reporters used in dual FRAP are shown. 5'-3' UTRs of mRNA 1 are tagged with GFP^{MYR} and 5'-3' UTRs of mRNA 2 are tagged with mCH^{MYR}. (b) Illustrations of FRAP sequences are shown. As the neurons are transfected with two translation reporters simultaneously, GFP^{MYR} reporter is shown in green and mCH^{MYR} reporter is shown in red (pre-bleach, top panel). After exposing the ROI with high-energy lasers, fluorescence signals are bleached out (middle panel). Post bleaching the fluorescence signal recover over time (bottom panel). (c) Representative images of an example dual FRAP sequences are shown. Scale bar = 20 μ m

mRNA. Consequently, one can use such reporters to test for axonal localization and local translation activity. By co-transfecting with GFP^{MYR} and mCH^{MYR} reporters bearing 5'/3' UTRs of different localizing mRNAs, one can simultaneously assess translation of different mRNA surrogates in response to stimuli and physiological conditions [11].

Within limited duration post-bleach periods, the recovery of the MYR-tagged translation reporters after photobleaching in axons and dendrites provides a surrogate for localized translation of endogenous mRNAs over space and time. Although the FRAP technique is not nearly as high throughput as puromycylation, AHA, *RiboTag*, and TRAP methods, FRAP provides fast readout, delivers spatial resolution, and eliminates the contamination issue from surrounding cells. Moreover, we have successfully tracked translation of multiple reporters simultaneously to address specificity of mRNA translation [11, 12]. Thus, FRAP provides a powerful tool to validate locally translating mRNAs from the puromycylation or *RiboTag* screens and, as we outline below, can be extended to address specificity for translation of different mRNAs in response to stimuli. Though we describe the use of FRAP for regenerating axons of adult DRG neurons, the reader should take note that it is readily adaptable to other neurons and with care could be used in subcellular domains of smaller cells depending on available instrumentation. Also note that we present the transfection methods that we have optimized for the adult rat and mouse DRG neurons [17], but the reader can use any transfection method that works for their cell of interest. The methods we offer below can be used to study localized translation of specific transcripts in axons. Since these methods require exogenous expression, this approach is not without limitations as it can result in overexpression of the surrogate mRNA relative to the endogenous mRNA. To further validate the mRNA's axonal translation, other techniques should also be used in combination with FRAP. For example, puromycylation assays can be done in isolated nerves *ex vivo* followed by affinity isolation of labeled proteins and immunoblotting for protein of interest to see if that protein is axonally synthesized [8, 11]. Also, puromycylation can be combined with proximity ligation assays (PLA) using antibodies to puromycin and the protein of interest to both validate intra-axonal translation of that protein and visualize sites of translation along the axon.

2 Materials

2.1 DRG Cell Culture and Transfections

1. Isolated dorsal root ganglia (DRG) neurons (*see Note 3*).
2. Glass bottom dishes for live cell imaging.
3. 10 cm tissue culture plates.
4. Autoclaved sterile phosphate-buffered saline (PBS), pH 7.4.
5. Cell culture tested poly-L-lysine prepared in sterile tissue culture grade water (50 $\mu\text{g}/\text{mL}$), mol wt 70,000–150,000, store at 4 $^{\circ}\text{C}$.
6. 200 $\mu\text{g}/\text{mL}$ mouse laminin: Prepare a 200 $\mu\text{g}/\text{mL}$ stock solution of mouse laminin in sterile PBS and store frozen at -20°C .

7. Fetal bovine serum (FBS).
8. Dulbecco's Modified Eagle Medium (DMEM).
9. DMEM, without phenol red.
10. Ham's F-12 medium.
11. Ham's F-12 medium, without phenol red.
12. 1:1 DMEM/F12 cell culture medium: Using DMEM and Ham's F-12 media that contain phenol red, prepare by mixing Dulbecco's Modified Eagle Medium (DMEM) 1:1 with Ham's F-12 medium.
13. 1:1 DMEM/F12 cell culture medium without phenol red: Using media that do not contain phenol red, prepare by mixing DMEM 1:1 with Ham's F-12 medium.
14. 10 mM cytosine arabinoside (AraC): Prepare 10 mM stock solution of AraC in sterile tissue culture grade water and store frozen at -20°C .
15. N1 medium supplement (100 \times).
16. 100 \times L-glutamine supplement (200 mM).
17. DRG growth medium: 1:1 DMEM/F12 cell culture medium (with phenol red), containing 1 \times N1 medium supplement, 1 \times L-glutamine, 100 μM AraC, and 10% FBS.
18. DRG growth medium without phenol red: 1:1 DMEM/F12 cell culture medium without phenol red, containing 1 \times N1 medium supplement, 1 \times L-glutamine, 100 μM AraC, and 10% FBS.
19. 0.2% bovine serum albumin (BSA): Prepare 0.2% BSA in sterile PBS and store at 4°C until used.
20. Hibernate A medium.
21. Penicillin–streptomycin (P/S), 10,000 IU/mL, sterile.
22. PBS+P/S: Add 100 units/mL of P/S to PBS and keep at room temperature (prepare after DRG isolations) to be used during DRG culture.
23. DRG serum-supplemented wash medium: 1:1 DMEM/F12 cell culture medium, supplemented with 10% FBS, and 100 units/mL of P/S.
24. P/S wash medium: 1:1 DMEM/F12 cell culture medium, supplemented with 100 units/mL of P/S.
25. DRG collection medium: Hibernate A medium, with N1 medium supplemented to 1 \times .
26. Sterile, tissue culture grade dH_2O .
27. Molecular biology grade ethanol.
28. Dimethyl sulfoxide (DMSO).

29. 50 units/ μL Collagenase Type II: Prepare 50 units/ μL stock solution of Collagenase Type II in PBS and store frozen at $-80\text{ }^{\circ}\text{C}$.
30. 5 3/4" glass pipettes: Fire-polished to decrease cell damage during trituration (*see Note 4*).
31. Straight micro-scissors (7 cm long, 0.1 mm tips, 3 mm blades).
32. Electroporator with high transfection efficiency for neurons (e.g., Lonza Nucleofector; *see Note 14*).
33. AmaxaTM Rat Neuron Nucleofector Kit (Lonza, Cat # VPG-1003; includes cuvettes).
34. AmaxaTM Basic Neuron SCN Nucleofector Kit (Lonza, Cat # VSPI-1003; includes cuvettes).
35. Diffusion-limited GFP cDNA (GFP^{MYR}) or mCherry cDNA (mCH^{MYR}) plasmid constructs (*see Note 5*).
36. High-quality, endotoxin-free DNA (*see Note 6*).
37. $37\text{ }^{\circ}\text{C}$, 5% CO_2 incubator.
38. Lab tape.
39. 15 mL conical tubes.
40. 50 mL conical tubes.
41. Centrifuge with swinging bucket rotors.
42. 1.5 mL microfuge tubes.
43. 1 mL pipettes.
44. Confocal microscope with $63\times/1.4$ NA oil immersion objective and FRAP module.

2.2 Study of Local Translation Using FRAP

See Subheading 3.4, steps 1–3, before preparing any of the following materials:

1. 10 ng/ μL mouse 2.5S nerve growth factor (NGF): Prepare 10 ng/ μL stock solution of NGF in sterile 0.2% BSA and store frozen at $-80\text{ }^{\circ}\text{C}$.
2. 10 ng/ μL brain-derived neurotrophic factor (BDNF): Prepare 10 ng/ μL stock solution of BDNF in sterile 0.2% BSA and store frozen at $-80\text{ }^{\circ}\text{C}$.
3. 10 ng/ μL neurotrophin 3 (NT3): Prepare 10 ng/ μL stock solution of NT3 in sterile water and store frozen at $-80\text{ }^{\circ}\text{C}$.
4. 150 $\mu\text{g}/\mu\text{L}$ cycloheximide: Prepare 150 $\mu\text{g}/\mu\text{L}$ stock solution of cycloheximide in ethanol and store frozen at $-80\text{ }^{\circ}\text{C}$.
5. 100 mM anisomycin: Prepare 100 mM stock solution of anisomycin in ethanol and store frozen at $-80\text{ }^{\circ}\text{C}$.
6. 1 mM thapsigargin: Prepare 1 mM stock solution of thapsigargin in DMSO and store frozen at $-80\text{ }^{\circ}\text{C}$.
7. 3 mM BAPTA-AM: Prepare 3 mM stock solution of BAPTA-AM in DMSO and store frozen at $-80\text{ }^{\circ}\text{C}$.

2.3 Fluorescence Recovery After Photobleaching (FRAP) and Data Analysis

1. Confocal microscope with argon lasers (*see Note 7*).
2. Live cell imaging chamber with CO₂ and temperature control.
3. FRAP module in image acquisition software (*see Note 8*).
4. Data analysis in Microsoft Excel (<https://www.microsoft.com/en-us/microsoft-365/excel>).

3 Methods

3.1 Preparation of Glass Bottom Dishes

1. The day before culturing, put the glass bottom dishes in 10 cm plates, and add approximately 2 mL of poly-L-lysine (50 µg/mL) into each glass bottom dish.
2. Leave poly-L-lysine on plates for 60 min at 37 °C.
3. Remove poly-L-lysine (*see Note 9*), wash twice (5 min each) with sterile tissue culture grade dH₂O, and air-dry the glass bottom dishes in the hood for at least 30 min. Inspect to ensure that the glass bottom dishes are dry. If not, continue drying until no visible liquid remains.
4. Cover the glass bottom dishes with 2.0 mL of laminin (5 µg/mL in PBS).
5. Incubate overnight at 4 °C with gentle rocking to ensure complete coverage of the surface of the glass bottom dishes (*see Note 10*).
6. Next remove laminin and wash glass bottom dishes twice (5 min each) with sterile PBS + P/S.
7. Add 2 mL of DRG growth medium to the glass bottom dishes and let the plates sit in 37 °C incubator until the neurons are ready to be plated.

3.2 DRG Culture

1. Collect all DRGs from rats in the DRG collection medium and place all the isolated DRGs into one well of a 12-/24-well plate containing 1 mL of DRG collection medium (*see Note 11*).
2. After all the DRGs have been removed, wash them briefly by moving them from well to well through six wells containing 0.5 mL of P/S wash medium (*see Note 12*).
3. After the rinses in **step 2**, transfer the DRGs into a fresh well containing 0.5 mL of DRG serum-supplemented wash medium.
4. Snip the DRGs using a pair of micro-scissors to get three to four pieces from each DRG (approximately 0.2–0.4 mm diameter each).
5. Add 50 units/µL Collagenase Type II to a final concentration of 2000 units/mL and incubate at 37 °C, 5% CO₂ for 20 min.

6. Triturate the DRG cell suspension 15–20 times by gently pipetting up and down using a fire-polished pipette to break apart the ganglia. Return to the 37 °C, 5% CO₂ for 5 min (*see Note 4*).
7. Triturate the cell suspension before transferring to a 15 mL conical tube.
8. Add 8.5 mL of DRG serum-supplemented wash medium to the cell suspension.
9. Pellet the cells at 160× *g* for 5 min in a swinging bucket rotor at room temperature.
10. Aspirate the medium. Add 1 mL of DRG serum-supplemented wash medium to the pellet and triturate 15–20 times with a fire-polished Pasteur pipette until the tissue is fully dissociated.
11. Add 8 mL of DRG serum-supplemented wash medium to the dissociated pellet, invert to mix, and then centrifuge at 160× *g* for 5 min.
12. Repeat **steps 10–11** two additional times for a total of three washes.
13. After the final wash, resuspend cells from 10–12 DRGs in Amaxa™ Rat Neuron Nucleofector Kit buffer (100 µL per transfection).
14. Add 10 µg of diffusion-limited GFP^{MYR} or mCH^{MYR} cDNA plasmid constructs to each 1.5 microfuge tubes.
15. Add 100 µL of the resuspended cells to each tube containing plasmid, mix well, and transfer to the cuvettes provided in the Nucleofector kit (*see Note 13*).
16. Transfect DRGs in the Lonza Nucleofector using the G013 rat DRG high-efficiency protocol (*see Note 14*).
17. Add 500 µL of warmed DRG growth medium (*see Note 15*).
18. Transfer transfected cells to a 1.5 mL microfuge tube using the pipettes provided in Amaxa™ Rat Neuron Nucleofector Kit.
19. Resuspend the cells well using a 1 mL pipette and add a volume equivalent to three to four DRGs to each glass bottom dish with DRG growth medium (prepared in Subheading 3.1).
20. Culture the cells overnight in the tissue culture incubator at 37 °C, 5% CO₂.
21. On the next day, replace the medium with 500 µL of fresh DRG growth medium.
22. FRAP is performed 36–60 h after transfections.
23. Four hours before starting FRAP, DRG growth medium is replaced with DRG growth medium without phenol red (*see Note 16*).

3.3 FRAP

1. Turn on the CO₂ controller (set at 5%) and temperature controller (set at 37 °C) of the live cell imaging chamber, 2 h before starting the FRAP experiment.
2. Place the glass bottom dishes with DRG neurons in the live cell imaging chamber and locate transfected neurons under the microscope.
3. Turn on argon lasers and white light lasers and set those at 70% energy level.
4. Set pinhole to three Airy units to ensure full-thickness bleaching and acquisition of the axon (63×/1.4 NA oil immersion objective) [17].
5. Find a region of interest (ROI) for FRAP. We generally focus on terminal axons/growth cones (GC), which are at least 200 μm away from the soma (*see Note 17*).
6. Set up FRAP sequences as follows: (i) pre-bleach, imaged every 60 s for 2 min; (ii) bleach, pulsed every 0.82 s for 80 frames; and (iii) post-bleach, imaged every 30 s for 15 min.
7. Use 488 nm and 514 nm laser lines on Leica SP8X confocal microscope to bleach GFP^{MYR} and mCH^{MYR} signals, respectively, at 100% power.
8. For both pre-bleach and post-bleach sequences, use white light lasers set at 15% laser power, 498–530 nm for GFP^{MYR}, and 565–597 nm for mCH^{MYR} emissions, respectively.
9. Start FRAP and acquire images at the abovementioned laser powers (*see schematics in Fig. 1b* and representative example images in Fig. 1c) (*see Note 18*).

3.4 Study Effect of External Environment on Local Translation Using FRAP

1. If the translation reporters are locally translated, inhibition of protein synthesis will show significant reduction in fluorescence recovery. To determine if fluorescence recovery in axons was from translation, DRG cultures are treated with translation inhibitors such as 100 μM anisomycin or 150 μg/mL cycloheximide for 30 min prior to photobleaching (*see Note 19*).
2. During development neurotrophic factors regulate axon growth and guidance by controlling local translation of specific mRNAs in distal axons. To test if trophic factors control local synthesis of translation reporters, DRG cultures are treated with neurotrophic factors, such as NGF/BDNF/NT3 for 3 h. These trophic factors can be used individually or together depending on the focus of your work.
3. Immediately after nerve injury, increases in intra-axoplasmic Ca²⁺ regulates translation of specific axonal mRNAs [8, 11]. To test if Ca²⁺ signaling plays a role in regulating localized protein synthesis of the translation reporters, DRG

cultures can be treated for 1 h with 1 μM thapsigargin (blocks Ca^{2+} uptake in endoplasmic reticulum, increasing cytoplasmic Ca^{2+} level), 3 μM BAPTA-AM (chelates intracellular Ca^{2+}), or 50 μM EGTA (chelates extracellular and intracellular Ca^{2+}).

3.5 Quantification of FRAP Data

1. Fluorescent intensities in the bleached ROIs are calculated using the Leica LASX software.
2. Export the ROI signal intensities for each and every time point as an Excel file (*see* Table 1).
3. The ROI signal intensity in the first image of post-bleach sequence is then deducted from pre-bleach and post-bleach image intensities to set the first post-bleach signal intensity to zero. This is done to normalize across experiments, so that the fluorescence intensity value at $t = 0$ min post-bleach from each image sequence is set as 0% (*see* Table 1).

Table 1
Collection and analysis of dual FRAP data

A



Time (sec)	ROI Intensity	0 sec post-bleach set to zero	% Recovery
-120	23.8	8.5	100
0	15.3	0	0
30	15.4	0.1	1.3
60	15.6	0.3	3.7
90	15.7	0.4	4.9
120	16.0	0.8	9.2
150	16.4	1.1	12.7
180	16.4	1.1	13.0
210	16.5	1.2	14.1
240	16.4	1.2	13.6
270	16.2	1.0	11.3
300	16.5	1.2	14.1
330	16.9	1.6	19.0
360	17.1	1.9	21.8
390	17.1	1.9	22.1
420	17.1	1.8	21.6
450	17.4	2.2	25.4
480	17.6	2.3	27.2
510	17.6	2.3	27.3
540	17.6	2.3	27.3
570	17.6	2.3	27.6
600	17.7	2.4	28.7
630	17.7	2.5	28.9
660	18.1	2.8	33.0
690	18.2	3.0	34.8
720	18.1	2.8	33.1
750	17.9	2.7	31.3
780	18.0	2.7	32.2
810	18.0	2.7	32.0
840	18.2	3.0	34.7
870	18.2	2.9	34.6

B



Time (sec)	ROI Intensity	0 sec post-bleach set to zero	% Recovery
-120	23.1	19.4	100
0	3.8	0	0
30	5.1	1.3	6.9
60	5.9	2.1	10.8
90	6.3	2.5	13.0
120	7.0	3.2	16.6
150	7.3	3.6	18.4
180	7.8	4.0	20.6
210	8.0	4.2	21.5
240	8.2	4.4	22.8
270	8.5	4.7	24.4
300	8.8	5.0	25.7
330	9.0	5.2	26.9
360	9.5	5.7	29.6
390	9.6	5.8	30.0
420	9.9	6.2	31.8
450	10.2	6.4	33.0
480	10.1	6.4	32.8
510	10.4	6.6	34.2
540	10.4	6.6	34.1
570	10.6	6.9	35.4
600	10.7	6.9	35.6
630	10.8	7.0	36.2
660	11.2	7.4	38.2
690	11.2	7.5	38.4
720	11.1	7.3	37.6
750	11.1	7.3	37.7
780	11.2	7.4	38.4
810	11.3	7.5	38.6
840	11.6	7.8	40.1
870	11.8	8.0	41.2

Raw pixel intensities in the ROI from pre-bleach (-120 s) and post-bleach (0-870 s) sequences for mRNA 1 are shown in **a** and for mRNA 2 are shown in **b** (column 2). Pixel intensities at 0 s is deducted from all the time points to normalize expression difference between neurons (column 3). The percentage of fluorescence recovery at each time point after photobleaching is then calculated by normalizing relative to the pre-bleach fluorescence intensity set at 100% (column 4)

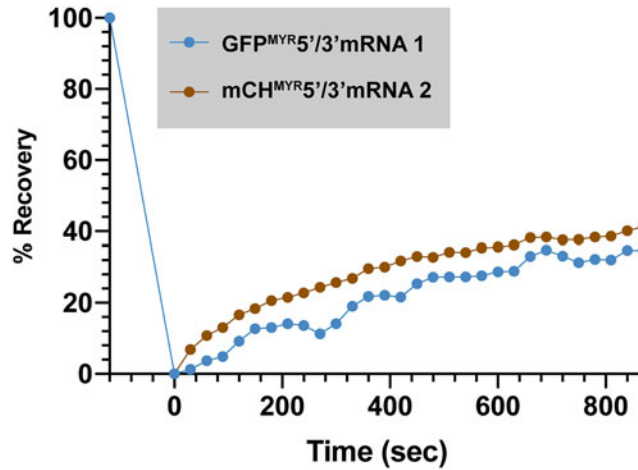


Fig. 2 Representation of FRAP quantification data. Percentage fluorescence recoveries of both the translation reporters after photobleaching are shown over time

4. The percentage of fluorescence recovery at each time point after photobleaching is then calculated by normalizing relative to the pre-bleach fluorescence intensity (set at 100%; see Table 1).
5. Three to five FRAP sequences are acquired from each biological replicate and are repeated over three biological replicates.
6. Mean \pm SEM for each time point is then plotted in a XY graph, and fluorescence recovery between different treatment groups are compared for statistical significance by using appropriate analysis of variance (ANOVA; see Fig. 2).

4 Notes

1. Puromycin is a tyrosyl-tRNA mimic that blocks mRNA translation by getting incorporated into nascently elongating polypeptide chains, resulting in release of a puromycin-labeled peptide chain from translating ribosomes [18]. Puromycin-specific antibodies are used to detect the labeled peptides in vivo by immunofluorescence. If a suitable preparation can isolate axons to purity, puromycylated proteins can be affinity purified (immunoaffinity or avidin-biotin systems (see below)) followed by immunoblotting for specific proteins or mass spectrometry for an unbiased assessment of axonal protein synthesis [18]. The commercially available puromycin analog O-propargyl-puromycin (OPP) can be used to label nascently synthesized proteins, followed by *Click-It* chemistry with

fluorescent tags for visualization in fixed cells or biotinylation of lysates for affinity purifications [8]. Labeling with L-azidohomoalanine, a methionine analog that also has *Click-It* capability, has similarly been used to directly label newly synthesized proteins in axons and dendrites [19, 20]. These direct peptide labelings are powerful tools for visualizing sites of localized protein synthesis and bring the potential for unbiased analyses. However, the methods are limited to static time points of total protein synthesis, so the dynamics of responses can only be addressed through taking multiple time points after a stimulation. Recent reports also show that labeled peptides can diffuse away from ribosomes upon release [21], so localized translation of individual mRNAs may be higher than assessed with these labeling approaches. Also, the unbiased assessments require highly purified axonal contents to avoid contamination from non-neuronal cells and neuronal cell bodies.

2. Isolation of polysomes using sucrose gradients has been used for both synaptosome preparations (initially targeting dendritic protein synthesis) and axonal isolates [14, 22]. These analyses were limited to discontinuous polysome gradient centrifugations that did not allow distinguishing number of ribosomes bound to an mRNA—continuous gradients allow one to estimate numbers of ribosomes per mRNA, but the yields from axonal preparations have been too limited for that technique in our experience. New methods rely on precipitating ribosomes that are “frozen” in place on the mRNAs and then extracting mRNAs for analyses. The *RiboTag^{fl/fl}* mouse, where the ribosomal large subunit protein 22 (Rpl22) is tagged with hemagglutinin (HA), is one of these approaches where cellular specificity is driven by expression of Cre recombinase [23]. Using HA-specific antibodies, HA-Rpl22 protein is immunoprecipitated and ribosome-associated mRNAs are analyzed [24]. This technique can be used both for cultured neurons and in vivo. Similarly, “translating ribosome affinity purification” (TRAP) relies on expression of GFP-tagged Rpl10a [25, 26]. Since cell-specific expression of the Rpl10a-GFP and HA-Rpl22 is used, these are less limited by contamination from other cellular elements than puromycylation. However, these techniques also precipitate mRNAs with stalled ribosomes in addition to the actively translating ribosomes. Recent studies show that in neuropil ribosomal proteins (RP) are synthesized locally and associate with translating mRNAs [27]. This local incorporation of RPs into the ribosome was found to be dependent on location and cellular environment [27], which could be missed depending on which RP is used for precipitation.

3. We describe this approach based on our experience with primary neurons isolated from adult rat DRGs, but this can easily be extrapolated to other neuronal types and species. For each FRAP experiment, we typically transfect single cell suspended neurons collected from ten DRGs.
4. Fire polishing the glass pipettes removes the sharp edges and decreases the diameter of the opening. This helps to mechanically dissociate the DRGs by triturating. We repeat the trituration (15–20 times) until the DRG suspension is homogenous (*see* DRG culture method for details).
5. 5' and 3' UTRs of candidate mRNAs are identified using NCBI gene tools. Gene-specific primers are used to specifically amplify the 5' UTR and 3' UTR. These are cloned upstream and downstream of GFP^{MYR} or mCH^{MYR} cDNA, respectively (*see* schematics in Fig. 1a). All cDNA sequences are validated by Sanger sequencing prior to use.
6. High-quality plasmid DNAs of concentration are isolated to yield $\geq 0.5 \mu\text{g}/\mu\text{L}$ and 260/280 ratio ≥ 1.8 . We use the maxi-prep kit from Qiagen but any other kit should also work as long as you can obtain high-quality, endotoxin-free DNA.
7. We use the Leica SP8X confocal microscope with 488 nm and 514 nm argon laser lines for photobleaching (set at 70% power). Variability between confocal setups necessitates that you optimize parameters such as laser energy used and timing for photobleaching for your microscopy system.
8. Confocal microscopes with FRAP capability generally have the FRAP module in the image acquisition software. We use SP8X confocal microscope with the LAX software, which has the FRAP software module.
9. We generally reuse poly-L-Lysine three to four times (maintaining sterility) stored at 4 °C.
10. We place the glass bottom dishes in 10 cm plates for ease of transfer to and from the incubator, hood, and microscope. Lab tape tabs can be placed along the edge to secure the lid and avoid contamination if care is taken to not completely seal the plate or to dislodge adherent cells.
11. We use ten DRGs per transfection for the AmaxaTM Rat Neuron Nucleofector Kit. Three to four DRGs are seeded per glass bottom dish. For few ganglia, we have used the AmaxaTM Basic Neuron SCN Nucleofector Kit with three to four DRGs per transfection.
12. Micro-scissors are used to move the ganglia one by one instead of forceps, which tend to crush the ganglia and reduce yields of viable neurons (this also helps by nicking the epineurium so P/S medium, and later dissociation enzymes, can fully infiltrate the ganglia).

13. Avoid air bubbles while transferring the cell-transfection buffer mix into the cuvettes or else the nucleofection fails or efficiency falls.
14. Transfection efficiency and cell health following transfection are key variables, so any transfection method that optimizes these variables in your cell of interest should suffice. We use the Nucleofector II from Lonza to transfect neurons; more recent Nucleofector versions from Lonza will work equally well with optimization.
15. Be ready with 500 μ L of DRG growth medium in a 1 mL pipette before placing the cells into the nucleofection apparatus. In our hands, adding warmed growth medium to the cells immediately after nucleofection substantially increases survival of the transfected neurons.
16. Using phenol red-free medium in live cell imaging reduces background fluorescence.
17. Since the protein synthesis can be monitored in real time with FRAP, this approach provides both spatial and temporal resolution for analyses. For axons and dendrites, care needs to be taken to choose an ROI sufficiently separated from the neuronal cell body to avoid the complication of diffusion and transport of fluorescent protein from axon segments outside of the ROI. This also requires limiting the duration of post-bleach analyses to be certain that recovery signals derive from locally synthesized reporter protein. We generally assess growth cones/terminal axons for FRAP as these are sites of active protein synthesis in culture and as diffusion/transport is restricted to the regions proximal to the ROI. However, more proximal axon shaft and branch points can also be used as ROIs as indicated for your mRNAs of interest.
18. Like transcription, translation of individual mRNAs can be turned on or turned off by different physiological stimuli. Translation of multiple candidate RNA reporters can be tracked simultaneously. Here, we have present methods to dissect the translational regulation of two mRNAs simultaneously in axons, but this could easily be extended to three or four mRNA surrogates depending on microscopy setup and available reporter constructs. Ability to co-transfect primary neurons is also a limitation for extending to more plasmids. For two plasmids, we use 5 μ g of each reporter DNA for transfection—co-transfection efficiency will likely decrease with three or more plasmids. We have also focused on translational control in regenerating PNS axons, but this can be extended to any neuron type provided the axon can be distinguished. Finally, this FRAP approach can also be used to define mRNA localization and translational control motifs by modifications of the UTRs in the reporters (e.g., deletion analyses).

19. The MYR sequence in the GFP and mCH reporters used here allows for a covalent co-translational modification of the nascently synthesized protein by myristoylation, which increases membrane localization for reporter protein synthesized in neurites [5]. Though this modification limits diffusion of the locally synthesized reporter, there can be diffusion within the cell membrane from regions outside of the bleached ROI as well as transport of reporter linked to vesicles from cell body-synthesized protein [13]. Both of these events are stochastic, but start to accumulate signals over longer imaging sequences (more than 30 min in our hands). Measured fluorescence recovery can be largely (or completely) restricted to locally translated reporter by limiting the post-bleach recovery period to less than 30 min for a ROI separated from the soma by ≥ 200 μm . By pretreating with protein synthesis inhibitors (e.g., anisomycin, cycloheximide), one can confirm that the recovery is translation-dependent. Monitoring the bleached ROI section immediately adjacent to the edge of the ROI allows for detection of recovery that results from diffusion or transport from axonal regions outside of the ROI.

Acknowledgments

This work was supported by grants from the National Institutes of Health (R01NS089633 and R01NS117821 to JLT), National Science Foundation (MCB-1020970 to JLT), the Dr. Miriam and Sheldon G. Adelson Medical Research Foundation (to JLT), and South Carolina Spinal Cord Injury Research Fund (2019-PD-02 to PKS). JLT is the incumbent SmartState Chair in Childhood Neurotherapeutics at the University of South Carolina.

References

- Smith TP, Sahoo PK, Kar AN, Twiss JL (2020) Intra-axonal mechanisms driving axon regeneration. *Brain Res* 1740:146864. <https://doi.org/10.1016/j.brainres.2020.146864>
- Sahoo PK, Smith DS, Perrone-Bizzozero N, Twiss JL (2018) Axonal mRNA transport and translation at a glance. *J Cell Sci* 131(8): jcs196808. <https://doi.org/10.1242/jcs.196808>
- Dalla Costa I, Buchanan CN, Zdradzinski MD, Sahoo PK, Smith TP, Thames E, Kar AN, Twiss JL (2021) The functional organization of axonal mRNA transport and translation. *Nat Rev Neurosci* 22(2):77–91. <https://doi.org/10.1038/s41583-020-00407-7>
- Namjoshi SV, Raab-Graham KF (2017) Screening the molecular framework underlying local dendritic mRNA translation. *Front Mol Neurosci* 10:45. <https://doi.org/10.3389/fnmol.2017.00045>
- Aakalu G, Smith WB, Nguyen N, Jiang C, Schuman EM (2001) Dynamic visualization of local protein synthesis in hippocampal neurons. *Neuron* 30(2):489–502. [https://doi.org/10.1016/S0896-6273\(01\)00295-1](https://doi.org/10.1016/S0896-6273(01)00295-1)
- Holt CE, Martin KC, Schuman EM (2019) Local translation in neurons: visualization and function. *Nat Struct Mol Biol* 26(7):557–566. <https://doi.org/10.1038/s41594-019-0263-5>

7. Papandreou ME, Palikaras K, Tavernarakis N (2020) Assessment of de novo protein synthesis rates in *Caenorhabditis elegans*. *J Vis Exp* 163. <https://doi.org/10.3791/61170>
8. Terenzio M, Koley S, Samra N, Rishal I, Zhao Q, Sahoo PK, Urisman A, Marvaldi L, Oses-Prieto JA, Forester C, Gomes C, Kalinski AL, Di Pizio A, Doron-Mandel E, Perry RB, Koppel I, Twiss JL, Burlingame AL, Fainzilber M (2018) Locally translated mTOR controls axonal local translation in nerve injury. *Science* 359(6382):1416–1421. <https://doi.org/10.1126/science.aan1053>
9. Perry RB, Doron-Mandel E, Iavnilovitch E, Rishal I, Dagan SY, Tsoory M, Coppola G, McDonald MK, Gomes C, Geschwind DH, Twiss JL, Yaron A, Fainzilber M (2012) Subcellular knockout of importin beta1 perturbs axonal retrograde signaling. *Neuron* 75(2):294–305. <https://doi.org/10.1016/j.neuron.2012.05.033>
10. Perry RB, Rishal I, Doron-Mandel E, Kalinski AL, Medzhradszky KF, Terenzio M, Alber S, Koley S, Lin A, Rozenbaum M, Yudin D, Sahoo PK, Gomes C, Shinder V, Geraisy W, Huebner EA, Woolf CJ, Yaron A, Burlingame AL, Twiss JL, Fainzilber M (2016) Nucleolin-mediated RNA localization regulates neuron growth and cycling cell size. *Cell Rep* 16(6):1664–1676. <https://doi.org/10.1016/j.celrep.2016.07.005>
11. Sahoo PK, Kar AN, Samra N, Terenzio M, Patel P, Lee SJ, Miller S, Thames E, Jones B, Kawaguchi R, Coppola G, Fainzilber M, Twiss JL (2020) A Ca^{2+} -dependent switch activates axonal casein kinase 2alpha translation and drives G3BP1 granule disassembly for axon regeneration. *Curr Biol* 30(24):4882–4895 e4886. <https://doi.org/10.1016/j.cub.2020.09.043>
12. Sahoo PK, Lee SJ, Jaiswal PB, Alber S, Kar AN, Miller-Randolph S, Thames E, Taylor EE, Smith T, Singh B, Ho TS-Y, Urisman A, Chand S, Pena EA, Burlingame AL, Woolf CJ, Fainzilber M, English AW, Twiss JL (2018) Axonal G3BP1 stress granule protein limits axonal mRNA translation and nerve regeneration. *Nat Commun* 9:3358. <https://doi.org/10.1038/s41467-018-05647-x>
13. Yudin D, Hanz S, Yoo S, Iavnilovitch E, Willis D, Gradus T, Vuppalachandi D, Segal-Ruder Y, Ben-Yaakov K, Hieda M, Yoneda Y, Twiss JL, Fainzilber M (2008) Localized regulation of axonal RanGTPase controls retrograde injury signaling in peripheral nerve. *Neuron* 59(2):241–252. <https://doi.org/10.1016/j.neuron.2008.05.029>
14. Zheng JQ, Kelly TK, Chang B, Ryazantsev S, Rajasekaran AK, Martin KC, Twiss JL (2001) A functional role for intra-axonal protein synthesis during axonal regeneration from adult sensory neurons. *J Neurosci* 21(23):9291–9303. <https://doi.org/10.1523/jneurosci.21-23-09291.2001>
15. Axelrod D, Koppel DE, Schlessinger J, Elson E, Webb WW (1976) Mobility measurement by analysis of fluorescence photobleaching recovery kinetics. *Biophys J* 16(9):1055–1069. [https://doi.org/10.1016/S0006-3495\(76\)85755-4](https://doi.org/10.1016/S0006-3495(76)85755-4)
16. Gomes C, Merianda TT, Lee SJ, Yoo S, Twiss JL (2014) Molecular determinants of the axonal mRNA transcriptome. *Dev Neurobiol* 74(3):218–232. <https://doi.org/10.1002/dneu.22123>
17. Willis DE, Twiss JL (2011) Profiling axonal mRNA transport. *Methods Mol Biol* 714:335–352. https://doi.org/10.1007/978-1-61779-005-8_21
18. Koppel I, Fainzilber M (2018) Omics approaches for subcellular translation studies. *Mol Omics* 14(6):380–388. <https://doi.org/10.1039/c8mo00172c>
19. Dorrbaum AR, Alvarez-Castelao B, Nassim-Assir B, Langer JD, Schuman EM (2020) Proteome dynamics during homeostatic scaling in cultured neurons. *elife* 9. <https://doi.org/10.7554/eLife.52939>
20. Kar AN, Macgibeny MA, Gervasi NM, Gioio AE, Kaplan BB (2013) Intra-axonal synthesis of eukaryotic translation initiation factors regulates local protein synthesis and axon growth in rat sympathetic neurons. *J Neurosci* 33(17):7165–7174. <https://doi.org/10.1523/JNEUROSCI.2040-12.2013>
21. Enam SU, Zinshteyn B, Goldman DH, Cassani M, Livingston NM, Seydoux G, Green R (2020) Puromycin reactivity does not accurately localize translation at the subcellular level. *elife* 9. <https://doi.org/10.7554/eLife.60303>
22. Weiler IJ, Spangler CC, Klintsova AY, Grossman AW, Kim SH, Bertaina-Anglade V, Khaliq H, de Vries FE, Lambers FA, Hatia F, Base CK, Greenough WT (2004) Fragile X mental retardation protein is necessary for neurotransmitter-activated protein translation at synapses. *Proc Natl Acad Sci U S A* 101(50):17504–17509. <https://doi.org/10.1073/pnas.0407533101>
23. Sanz E, Yang L, Su T, Morris DR, McKnight GS, Amieux PS (2009) Cell-type-specific isolation of ribosome-associated mRNA from complex tissues. *Proc Natl Acad Sci U S A* 106(33):

- 13939–13944. <https://doi.org/10.1073/pnas.0907143106>
24. Rozenbaum M, Rajman M, Rishal I, Koppel I, Koley S, Medzihradzky KF, Oses-Prieto JA, Kawaguchi R, Amieux PS, Burlingame AL, Coppola G, Fainzilber M (2018) Translatome regulation in neuronal injury and axon regrowth. *eNeuro* 5(2). <https://doi.org/10.1523/ENEURO.0276-17.2018>
25. Doyle JP, Dougherty JD, Heiman M, Schmidt EF, Stevens TR, Ma G, Bupp S, Shrestha P, Shah RD, Doughty ML, Gong S, Greengard P, Heintz N (2008) Application of a translational profiling approach for the comparative analysis of CNS cell types. *Cell* 135(4): 749–762. <https://doi.org/10.1016/j.cell.2008.10.029>
26. Ostroff LE, Santini E, Sears R, Deane Z, Kanadia RN, LeDoux JE, Lhakhang T, Tsirigos A, Heguy A, Klann E (2019) Axon TRAP reveals learning-associated alterations in cortical axonal mRNAs in the lateral amygdala. *elife* 8. <https://doi.org/10.7554/eLife.51607>
27. Fusco CM, Desch K, Dörrbaum AR, Wang M, Staab A, Chan ICW, Vail E, Villeri V, Langer JD, Schuman EM (2021) Neuronal ribosomes dynamically exchange ribosomal proteins in a context-dependent manner. *bioRxiv:2021.2003.2025.437026*. <https://doi.org/10.1101/2021.03.25.437026>



Analysis of Axonal Regrowth and Dendritic Remodeling After Optic Nerve Crush in Adult Zebrafish

An Beckers, Steven Bergmans, Annelies Van Dyck, and Lieve Moons

Abstract

Neurodegenerative diseases and central nervous system (CNS) injuries are frequently characterized by axonal damage, as well as dendritic pathology. In contrast to mammals, adult zebrafish show a robust regeneration capacity after CNS injury and form the ideal model organism to further unravel the underlying mechanisms for both axonal and dendritic regrowth upon CNS damage. Here, we first describe an optic nerve crush injury model in adult zebrafish, an injury paradigm that inflicts de- and regeneration of the axons of retinal ganglion cells (RGCs), but also triggers RGC dendrite disintegration and subsequent recovery in a stereotyped and timed process. Next, we outline protocols for quantifying axonal regeneration and synaptic recovery in the brain, using retro- and anterograde tracing experiments and an immunofluorescent staining for presynaptic compartments, respectively. Finally, methods to analyze RGC dendrite retraction and subsequent regrowth in the retina are delineated, using morphological measurements and immunofluorescent staining for dendritic and synaptic markers.

Key words Axonal regrowth, Dendritic remodeling, Optic nerve crush, Retinotectal system, Retina, Zebrafish, Neurobiology

1 Introduction

Over the past decades, extensive progress has been made in the search for axonal regenerative treatments using different animal models, and both extrinsic and intrinsic factors, underlying the failure of axonal regrowth in the mammalian CNS, have been identified [1, 2]. Besides axonal damage, neurodegenerative diseases and CNS trauma are also characterized by dendrite pathology, including dendritic shrinkage and loss of dendritic tree complexity, as shown in both animal models and patients [3–8]. Strikingly however, dendrites have been overlooked for many decades in the neuroregenerative field, and therefore it remains largely elusive if and how neurons are able to regrow dendrites after damage [9, 10].

Zebrafish possess a robust CNS regeneration capacity in adulthood and show full functional recovery after axonal injury. Therefore, they form the ideal model organism to tackle these research questions and unravel the underlying mechanisms of successful axonal and dendritic regeneration [10–12]. More specifically, our research group has been using the zebrafish visual system, comprising the retina, optic nerve, optic chiasm, optic tract, and the visual target areas in the brain, in zebrafish mainly being the optic tectum (Fig. 1a). A major advantage of the retinotectal system is that only one neuronal cell type from the retina, i.e., the retinal ganglion cells (RGCs), sends information to the brain. Moreover, the distinct localization of RGC dendrites and axons, i.e., inside the inner plexiform (IPL) layer of the retina and in the retinal nerve fiber layer (NFL)/optic projection, respectively (Fig. 1b), creates the opportunity to use the same model system for deciphering the pathways/molecules underlying both axon and dendrite regrowth. Therefore, the teleost retinotectal system is ideally suited to study a potential interplay between axons and dendrites during CNS repair.

In this chapter, we first describe a mild, acute optic nerve crush (ONC) injury model, in which all of the RGC axons are disrupted simultaneously (Fig. 1c) (Subheading 3.1). This model, which is widely used in rodents as well, exclusively damages the RGC axons without hindering ocular blood flow or inducing a massive inflammatory response in the vitreous.

Two methods are outlined to study axonal outgrowth initiation and early regrowth. The first one is based on the use of biocytin, a neuroanatomical tracer that is easily absorbed by neurons and travels bidirectionally (antero- and retrogradely) via passive transport. Applying biocytin posterior to the injury site can be used to visualize the RGCs inside the retina that regenerated their axons past the ONC site (retrograde tracing) (see Subheadings 3.2, 3.8, and 3.9) [13]. A second method to study early axonal regrowth is measuring the growth distance of axons in the optic nerve using horizontal visual system cryosections of Tg (*gap-43:eGFP*) zebrafish (see Subheading 3.10) [13]. This transgenic reporter line is characterized by the expression of enhanced green fluorescent protein (eGFP) regulated by the *growth-associated protein 43* (*gap-43*) promoter, thereby labeling growing axons [13–16]. A later stage of axonal regeneration, being tectal reinnervation, can be studied by applying biocytin anterior to the ONC site (see Subheadings 3.2, 3.6, and 3.11). In this way, the regrowing axons running inside the projection areas in the brain, mainly being the fibrosum et griseum superficiale (SFGS) and stratum opticum (SO) of the optic tectum (Fig. 1d), are traced (anterograde tracing) [13, 17–20]. Upon optic tectum reinnervation, the regenerated RGC axons will eventually reform synapses with their target neurons in the brain, which can be visualized using immunofluorescent labeling of synaptotagmin 2, a Ca^{2+} sensor involved in neurotransmitter release, present in RGC

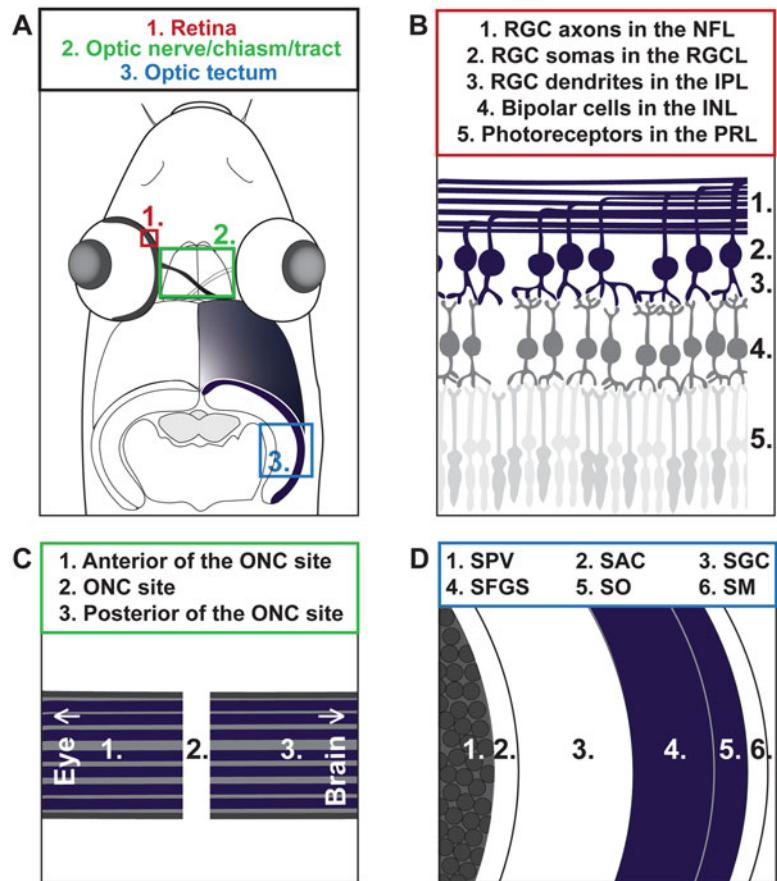


Fig. 1 Schematic visualization of the zebrafish retinotectal system. **(a)** Overview of the three main parts of the retinotectal system being (1) the retina; (2) the optic projections forming optic nerves, optic chiasm, and optic tracts; and (3) the main RGC projection area in the brain, the optic tectum. The gray-colored butterfly-shaped brain structure contains the torus longitudinalis and the valvula cerebelli and is often used to recognize central optic tectum sections. **(b)** The major route of electrical information flow in the retina is formed by the photoreceptor–bipolar–RGC neuronal chain. The dendrites of the RGCs are located within the INL, while the axons, in contrast, bundle inside the NFL and form the optic projection. **(c)** Visualization of an injured optic nerve, in which the ONC site is indicated, as well as the anterior and posterior position relative to the injury site. **(d)** The zebrafish optic tectum can be divided into two main areas: the SPV, containing the majority of tectal cell bodies, and the synaptic neuropil area, in which the SO and SFGS contain most RGC axons. *INL* inner nuclear layer, *NFL* nerve fiber layer, *ONC* optic nerve crush, *RGC* retinal ganglion cell, *RGCL* retinal ganglion cell layer, *SAC* stratum album centrale, *SFGS* stratum griseum centrale, fibrosum et griseum superficiale, *SGC* stratum griseum centrale, *SM* stratum marginale, *SO* stratum opticum

presynaptic terminals (*see* Subheadings 3.8 and 3.13) [18, 21, 22]. In uninjured control fish, most RGC axons, projecting toward the optic tectum, make synapses in the SFGS (80%) or the SO (15%), while the remaining RGC axons (5%) project into the stratum griseum centrale (SGC) and a projection zone (S/S) between the stratum album centrale (SAC) and stratum periventriculare (SPV) (Fig. 1d) [18, 23].

In addition to methods for analyzing axonal regeneration, this chapter will also delineate techniques to study RGC dendrite remodeling processes, an overlooked topic within regeneration studies. An indirect way for this is to measure IPL thicknesses on retinal cryo- or paraffin sections (*see* Subheadings 3.7 and 3.12). Thinning and regaining thickness of this layer can indeed provide valuable information regarding neuronal process disintegration/shortening and dendrite regrowth, respectively [18, 24]. It is for instance well-known that IPL thickness is significantly reduced in the early stages of glaucoma and that this thinning becomes more pronounced over disease progression. The glaucoma-induced IPL thinning is linked with RGC dendritic retraction and loss of synapses, known to manifest early after disease onset, as observed in primate, cat, and rodent glaucoma models, as well as in human glaucomatous retinas [24–28]. To obtain direct insights into retinal dendritic changes after ONC, the spatiotemporal expression pattern of microtubule-associated protein 2 (Map 2) can be characterized on retinal sections, as Map 2 is a validated marker for (IPL) dendrites and known to be essential for dendritic stabilization and outgrowth in vertebrates (*see* Subheadings 3.8 and 3.13) [29–32]. Finally, visualization of synaptic de- and regeneration can be performed using immunostaining for the postsynaptic density (Psd) marker Psd-95, which is a protein attached to the postsynaptic membrane and involved in anchoring synaptic proteins (Subheadings 3.8 and 3.13) [6, 33]. Additional staining for synaptotagmin 2 can strengthen the findings regarding synapse loss and synaptogenesis in the IPL of the retina (*see* Subheadings 3.8 and 3.13).

2 Materials

Prepare all solutions with distilled, deionized water, unless indicated otherwise. Store reagents as instructed by the manufacturer.

2.1 Optic Nerve Crush (ONC)

1. Zebrafish of similar size and age (*see* **Note 1**).
2. Two forceps with fine tips. Apply a 0.5 mm mark measured from the tip on one of the forceps, to allow immediate measurement of distance from the optic nerve head while crushing. This can be done using a stereomicroscope, millimeter paper, and an iron file.
3. 70% ethanol.

4. Tricaine stock solution: Dissolve tricaine powder 0.3% w/v (MS-222) in 20.6 mM Tris-HCl made in ultrapure water and adjusted to pH7.0 with 1 M HCl. The 0.3% tricaine stock solution can be stored at 4 °C up to 6 weeks if kept in the dark.
5. Anesthetic solution 1: Dilute 7 mL of the tricaine stock solution in 93 mL aquarium system water in a 250 mL glass beaker (0.02% tricaine). Diluted tricaine can be kept at 4 °C maximally for 1 week (*see Note 2*).
6. Aquarium fishnet.
7. Small fish holder: Plastic Pasteur pipette (3 mL) from which half of the upper part (pipette bulb) is removed by making a longitudinal cut using scissors. In this way, a convenient small fishnet/holder is created to take out fish from a narrow beaker. A tiny fishnet can be used as well, if available.
8. Lid of a petri dish with a maximum height of 1 cm (*see Note 3*).
9. Tissue paper.
10. Recovery fish tank.
11. Dissecting stereomicroscope (minimum 30× magnification) with an upper light source.

2.2 Biocytin-Soaked Gelfoam Clot Preparation and Application

1. Biocytin.
2. Gelfoam.
3. Parafilm.
4. Dissection needles.
5. Small petri dishes (± 3 cm diameter).
6. Tin foil.
7. Sylgard-coated dissection plate or petri dish (*see Note 4*).
8. Dissection scissors (2.5 mm blades straight).

2.3 Perfusion and Tissue Dissection

1. Anesthetic solution 2: Dilute 33 mL of the tricaine stock solution in 67 mL aquarium system water in a 250 mL glass beaker (0.1% tricaine). Diluted tricaine can be stored at 4 °C maximally for 1 week.
2. 1× phosphate-buffered saline (PBS): First prepare a 10× PBS stock solution consisting of 80 mM Na₂HPO₄·2H₂O, 1.5 M NaCl, 20 mM KH₂PO₄, 30 mM KCl. The 10× stock solution should be prepared in distilled, deionized water and adjusted to pH 7.4 with 10 M NaOH. To obtain a 1× working solution of PBS, dilute the 10× PBS stock solution 1/10 with distilled, deionized water, taking care to maintain the pH at 7.4 prior to bringing the working solution up to the final dilution volume.
3. Mask for dust.

4. 4% paraformaldehyde (PFA): While weighing PFA, always wear a dust mask. Add 4 g of PFA in approximately 80 mL of 1× PBS in a glass beaker. Use a spinning magnet and a stirring plate to gently stir and heat the PFA (until ± 60 °C) inside a ventilated hood to dissolve the powder. Cool down the solution and adjust the volume to 100 mL with 1× PBS in a volumetric flask. Store it at 4 °C for maximum 1 week. Always use 4% PFA at RT, unless indicated differently.
5. 25 mL syringes.
6. Butterfly needles (21G 0.8 × 19 mm).
7. Horizontal glass capillary puller.
8. Glass capillaries (outer diameter 1.3–1.4 mm, length 75 mm).
9. Dissection scissors (4 mm blades straight).
10. Pinheads.
11. Fume hood.
12. Storage buffer: First prepare a 10× stock solution consisting of 80 mM Na₂HPO₄·2H₂O, 20 mM KH₂PO₄, 1.5 M NaCl, 30 mM KCl, 0.4% NaN₃. The 10× solution should be prepared in distilled, deionized water and adjusted to pH 7.4 with 5 M NaOH. To obtain a 1× working solution of storage buffer, mix one volume of the 10× stock solution with nine volumes of distilled, deionized water. Check the pH prior to bringing the working solution up to the final dilution volume and adjust as necessary to maintain the pH at 7.4.

2.4 Cryo-preservation, Embedding, and Cryostat Sectioning

1. Sucrose solutions: 10, 20, and 30% in 1× PBS.
2. Embedding molds (e.g., disposable plastic base molds 15 mm × 15 mm) or small petri dishes.
3. Microwave.
4. Agarose–sucrose embedding medium: Make a suspension of 1.25 g agarose, 30 g sucrose in 100 mL 1× PBS in an Erlenmeyer flask. Heat it using a microwave until it boils to dissolve the agarose. Dissolved agarose can be used and reheated for maximum two times, and stored for 1 month at 4 °C.
5. Dissection needles.
6. Tissue paper.
7. Scalpel or razor blade.
8. Optimum cutting temperature (OCT) compound.
9. Cryostat.
10. Fine paint brushes (maximum 0.5–1 cm width).
11. Adhesion slides (*see* **Note 5**).

2.5 Embedding and Vibratome Sectioning

1. Vibratome.
2. Superglue.
3. Cutting buffer: First prepare a 10× stock solution consisting of 80 mM $\text{Na}_2\text{HPO}_4 \cdot 2\text{H}_2\text{O}$ and 20 mM KH_2PO_4 . The 10× solution should be prepared in distilled, deionized water and adjusted to pH to 7.4 with 5 M NaOH. Store the 10× stock at 4 °C up to 1 year. To obtain a 1× working solution of cutting buffer, mix one volume of the 10× stock solution with nine volumes of distilled, deionized water. Check the pH prior to bringing the working solution up to the final dilution volume and adjust as necessary to maintain the pH at 7.42.
4. 24-well plates with net inserts.

2.6 Hematoxylin and Eosin (H&E) Staining

1. Oven.
2. 50%, 96%, and absolute ethanol (>99%).
3. Hematoxylin solution according to Mayer.
4. 1% eosin.
5. Xylene.
6. Dibutylphthalate polystyrene xylene (DPX) mounting medium.
7. Coverslips.

2.7 Diamino-benzidine Tetrahydrochloride (DAB) Staining

1. Shaking table.
2. 3,3'-diaminobenzidine tetrahydrochloride (DAB) tablets.
3. 0.1% phosphate-buffered saline with Triton X-100 (PBST): 100 μL Triton X-100 in 100 mL 1× PBS. Always make fresh.
4. 10× glycine solution: 190 mg glycine in 5 mL 0.1% PBST. Can be stored for maximum 4 weeks at 4 °C.
5. VECTASTAIN Elite ABC system (Vector Laboratories) (*see Note 6*).
6. 1% NiCl_2 . Can be stored for 1 year at 4 °C.
7. 1% CoSO_4 . Can be stored for 1 year at 4 °C.
8. 35% H_2O_2 .
9. Gelatin-coated glass slides.
10. Acetone.
11. Acetate buffer: 75 mL 0.1 N sodium acetate with 50 mL 0.1 N acetic acid, adjusted to pH 4.8. Can be stored for 1 year at 4 °C.
12. 1% neutral red: 1 g of neutral red in 100 mL distilled, deionized water. Filter it using a filter paper (general-purpose filter papers, grade 601). Can be stored for 1 year at 4 °C.
13. Neutral red staining solution: Add 4 mL acetate buffer to 100 mL of the 1% neutral red solution. This can be stored at RT for maximum 6 months and reused 15 times.

2.8 *Immuno-fluorescent Staining*

1. Humidified slide staining chamber.
2. Glass or plastic staining jars.
3. Hydrophobic barrier pen.
4. 1X Tris(hydroxymethyl)aminomethane-buffered saline with Triton X-100 (TBST): First prepare a 10× stock solution in distilled, deionized water composed of 0.1 M tris (hydroxymethyl)aminomethane, 15 M NaCl, and 0.015 M Triton X-100. The 10× stock solution should be prepared in distilled, deionized water and adjusted to pH 7.6 with 1 M HCl. To obtain a 1× working solution of cutting buffer, mix one volume of the 10× stock solution with nine volumes of distilled, deionized water. Check the pH prior to bringing the working solution up to the final dilution volume and adjust as necessary to maintain the pH at pH 7.6.
5. Citrate buffer: First prepare a 10× stock solution consisting of 100 mM citric acid and 0.5% Tween 20. The 10× stock solution should be prepared in distilled, deionized water and adjusted to pH 6.0 with 10 M NaOH. To obtain a 1× working solution of citrate buffer, mix one volume of the 10× stock solution with nine volumes of distilled, deionized water. Check the pH prior to bringing the working solution up to the final dilution volume and adjust as necessary to maintain the pH at 6.0.
6. 1X Tris–NaCl-blocking (TNB) buffer: First prepare a 10× stock solution consisting of 0.5% blocking reagent (Perking Elmer) dissolved in 1× TBST. To obtain a 1× working solution of TNB, mix one volume of the 10× stock solution with nine volumes of distilled, deionized water.
7. Methanol.
8. Normal donkey serum.
9. Bovine serum albumin (BSA).
10. Mouse anti-synaptotagmin 2 (znp-1) (Developmental Studies Hybridoma Bank).
11. Mouse anti-Map 2 (M1406, Sigma-Aldrich).
12. Mouse anti-Psd-95 (ab2723, Abcam).
13. Alexa Fluor conjugated to streptavidin.
14. Donkey anti-mouse Alexa Fluor-conjugated secondary antibody.
15. Streptavidin conjugated to horseradish peroxidase (HRP).
16. Tyramide signal amplification kit.
17. Donkey anti-mouse biotin-conjugated secondary antibody.
18. 0.1% 4',6-diamidino-2-phenylindole (DAPI) in 1× PBS.
19. Anti-fade fluorescence mounting medium.

2.9 Microscopy and Quantification

1. Fluorescence microscope with a 20× objective.
2. Confocal microscope with a 20× and 60× objective.
3. Bright field microscope with a 10× objective.
4. Fiji image processing software program (*see Note 7*).

3 Methods

3.1 Optic Nerve Crush (ONC)

1. Place one layer of tissue paper, immersed in the anesthetic solution 1, on the petri dish lid.
2. Sterilize the forceps using 70% ethanol.
3. Use an aquarium fishnet to catch a fish from the tank and put it in the beaker with anesthetic solution 1 (*see Note 8*).
4. Wait until the fish is sufficiently sedated. The gill movement should be decreased to a minimum and the fish will have lost its balance and lay on its back (*see Note 9*).
5. Transfer the sedated fish using the small fish holder to the center of the petri dish lid with its tail toward you. Place it on its right lateral side so that its left side is facing upward (*see Note 10*). Place one layer of tissue paper soaked in anesthetic solution 1 on top of the fish, including the gills, but without covering the eye.
6. Remove the dermal layer of the cornea covering the eye using the sterile forceps (Fig. 2a). Grab this transparent layer by closing the forceps at the edge of the eyeball and remove it by making an upward circular movement.

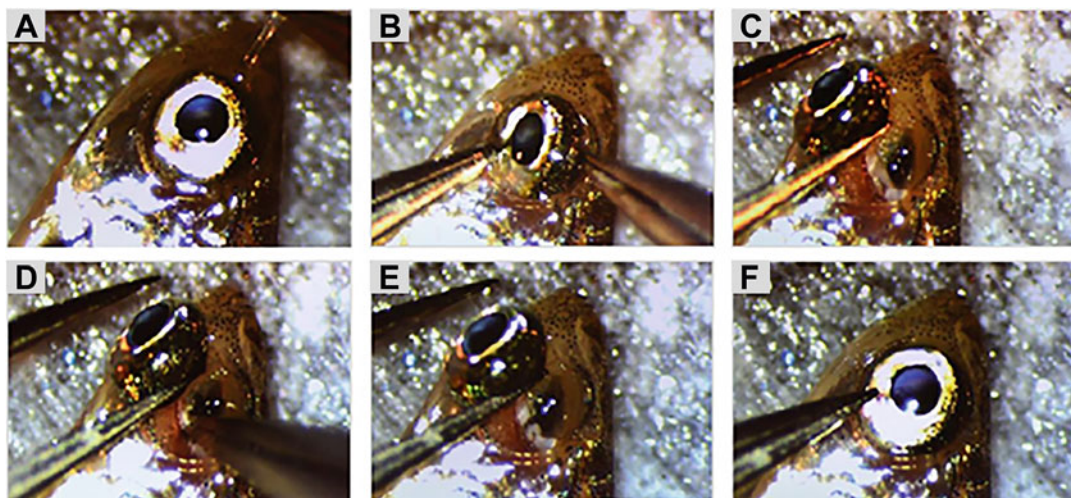


Fig. 2 Steps of an ONC procedure. (a) First, the dermal layer of the outer cornea is removed, (b and c) after which the eye is lifted out of the orbit and (d) the optic nerve is crushed. (e) A successful ONC is indicated by a transparent interruption of the optic nerve. (f) After performing this injury model, the eye is put back into the orbit. *ONC* optic nerve crush

7. Gently tilt the eye out of its orbit. For this, place the left forceps (almost completely pinned together, 0.5 mm apart) in the middle of the ventral side of the eye and gently push down in order to lift the dorsal side upward. Insert the right forceps (pinned together up to 0.5 mm) carefully in the dorsal side of the orbital cavity, just below the eyeball (Fig. 2b). Cautiously tilt the eye with the right forceps and stabilize it with the left forceps so it stays external from the eye socket (Fig. 2c) (*see Note 11*).
8. If present, carefully remove any fat tissue inside the orbital cavity with the right forceps to expose the white optic nerve (*see Note 12*).
9. While still stabilizing the eye with the left forceps, crush the optic nerve firmly with the right pincer for 10 s at a distance of 0.5 mm from the optic nerve head, measured using the mark on the forceps tip (Fig. 2d) (*see Note 13*). Take care not to damage the ophthalmic artery running parallel to the nerve. Remove the animal from the experiment in case of a hemorrhage, as the regeneration process might be affected. At the crush site, an interruption of the optic nerve is visible as a see-through mark (Fig. 2e), but the two optic nerve parts should still be connected via a transparent dural sheet.
10. Remove the left, stabilizing forceps in order to place the eye back into its orbit. Due to the extraocular muscles, the eye will spontaneously reposition in the correct orientation (Fig. 2f).
11. Awaken the fish by providing a water stream across its gills to remove the anesthesia. Gently hold the fish with two fingers by its tail and move it inside the water of the recovery tank until the fish shows signs of regaining awareness (*see Note 14*).

3.2 Biocytin-Soaked Gelfoam Clot Preparation and Application for Anterograde and Retrograde Tracing

1. Take a small petri dish (± 3 cm diameter) and place a piece of parafilm to cover the bottom of the dish. Dissolve 10 mg of biocytin in 500 μ L of distilled, deionized water on the parafilm-covered petri dish while keeping it as much as possible in the dark. Resolve any remaining biocytin clumps using pipette tips or dissection needles, to obtain a homogenous and saturated biocytin solution.
2. Cut a 2 cm \times 2 cm part of the gelfoam into smaller pieces and let them take up the biocytin solution. Use extra gelfoam if there is still fluid left. Tear the biocytin-soaked gelfoam into multiple clots of around 1 mm \times 1 mm \times 1 mm (approximately similar to the diameter of the zebrafish optic nerve) using two sharp objects (e.g., old forceps or dissection needles).
3. Divide the clots over multiple petri dishes with a parafilm-covered bottom. The number of clots on a single petri dish is ideally the maximum quantity used in one experiment. Let the

clots dry overnight in the petri dish, wrapped in tin foil, at room temperature (RT) and store afterward at -20°C . These clots can be stored up to 1 year.

4. Allow the fish to recover from ONC (*see* Subheading 3.1) until the preferred time post-injury when early axonal regeneration or tectal reinnervation needs to be quantified (*see* **Note 15**).
5. Sedate the fish in anesthetic solution 1 and position it on the Sylgard-coated dissection plate. Stabilize the left eye with the forceps, after removing the dermal layer of the cornea (*see* **Note 16**).
6. Cut the optic nerve between the eye and the ONC site, or between the ONC site and the brain, for anterograde or retrograde tracing, respectively. Use the small dissection scissors, located in your right hand to make the cut. Avoid harming the ophthalmic artery.
7. Place a biocytin-soaked gelfoam clot at the location of the cut (Fig. 1c) (*see* **Note 17**). The size of the clot cannot exceed the diameter of the optic nerve too much. If necessary, make the clot smaller by pinching it with a forceps.
8. Place the eye back in its socket and revive the fish. Write down the recovery time at the end of this step for every fish (*see* **Note 18**).
9. Perfuse the fish 3 h after biocytin application (*see* Subheading 3.3).

3.3 Transcardial Perfusion and Tissue Dissection and Fixation

1. Fill one syringe with $1\times$ PBS and one with 4% PFA.
2. Cut off the needle part from the butterfly needle and connect the remaining tubing with the syringe.
3. Make the glass needles with the puller using the following settings: heater 80°C , sub magnet 30, main magnet 70.
4. Insert the capillary needle in the plastic tubing from the previous step.
5. Test the infusion device on flow-through and if no fluid runs out of the needle, pinch off an extra part of the glass capillary tip (*see* **Note 19**).
6. Perform all subsequent steps for perfusion under a fume hood due to the PFA toxicity, so place all the equipment, including the dissection microscope, underneath it.
7. Euthanize the fish in anesthetic solution 2 and place it horizontally with its head pointing to the left on the Sylgard plate.
8. Balance the fish with a forceps on its back.

9. Insert the large scissors in the anus, located anterior to the anal fin and posterior to the pelvic fin. Make a 2 cm T-shaped incision with the horizontal base from the left lateral side to the right lateral side, and the vertical part from the anus toward the head.
10. Use two pinheads to fix the zebrafish at both sides of the anal fin.
11. Turn the dissection plate/dish 90° to position the fish with its tail toward you.
12. Carefully open up the upper body cavity to expose the heart using two pairs of forceps.
13. Fully stabilize the animal by placing two pinheads inside the body cavity, at the height of the heart.
14. Switch to a high magnification (at minimum 30×) in order to have a detailed overview of the zebrafish heart.
15. Perforate the atrium using the small dissection scissors by making some small cuts in the muscle.
16. Take the syringe with 1× PBS and point the needle toward the ventricle, in the direction of the bulbus arteriosus. Start pumping the fluid even before touching the ventricle and pierce the ventricle with a steady force. In case of a successful perfusion, blood will become visible and leaves the body via the perforated atrium (*see Note 20*). Remove all circulating blood by injecting ±1 mL of 1× PBS.
17. Start the fixation process by injecting ±1 mL of 4% PFA, in the same way as described in the previous step (*see Notes 21 and 22*). Remove the perfusion fluids and blood on the dissection plate with tissue paper. Remove all the pinheads.
18. To dissect the left eye, place the fish on its right lateral side and tilt the crushed eye out of its socket. Cut the exposed optic nerve with dissection scissors and gently remove the eye by grabbing the remaining optic nerve attached to the eye with a forceps and making an upward movement. Of note, the optic nerve will already be cut if a retro- or anterograde tracing was performed previously.
19. To dissect the brain, remove both eyes, as described in the previous step. Place one pinhead just posterior to the skull to fix the animal on its ventral side. A heart-shaped part, covering the optic tecti, can be recognized in the skull. Take two forceps and place them at the base of the skull, located at the edge of the spine and skull. Gently lift the skull, without touching the brain tissue underneath. Remove some extra tissue at the level of the spine. The complete (white and thus successfully perfused) brain should now be visible. Grab the brain at the edge

of the spine and the skull. Gently lift out the brain while cutting the fiber connections with small scissors.

20. To dissect the complete visual system, do not remove the eyes. Place the fish on its ventral side and remove the skull. Remove the telencephalon and olfactory bulbs, using the small scissors. Make a vertical cut at the edge of the olfactory bulbs and optic tecti and take the telencephalon and olfactory bulbs out using forceps. Discard all the remaining tissue surrounding the complete visual system at the lateral and anterior sides using dissection equipment. Remove the mouth, jaws, eye sockets, as well as the gills, until the visual system is completely liberated. Grab the brain at the transition brain/spinal cord and lift it slightly while simultaneously cutting the remaining fiber connections with small scissors. Position the right forceps horizontally underneath the brain, the optic projections, and the eyes (ventral side of the visual system). Make an upward movement with this forceps to remove the complete visual system. Never remove a visual system without supporting the eyes, as the weight of the eyes could otherwise easily break the optic nerves/tracts (*see Note 23*).
21. Post-fix the tissues overnight in 4% PFA at 4 °C (in a 24-well plate or in an Eppendorf tube). Eyes harvested to make cryosections for immunofluorescent stainings are only fixed for 1 h (*see Note 24*). Eyes specifically harvested to make sections for Psd-95 staining are only fixed for 30 min in ice-cold 4% PFA at 4 °C.
22. Rinse the fixed tissues three times for 10 min in 1× PBS. Tissue storage can be prolonged by the use of storage buffer.

3.4 Cryo-preservation, Embedding, and Cryostat Sectioning

1. Incubate the tissues for cryosectioning in increasing concentrations of sucrose (10, 20%, 30% sucrose solution for three consecutive nights) (*see Note 25*).
2. Place the tissues in a small petri dish or embedding mold. Transfer the zebrafish eyes/brains/visual systems using a plastic Pasteur pipette from which part of the tip is cut to enlarge the opening. Transfer as little PBS as possible. Dry the tissues carefully with tissue paper.
3. Warm the agarose (freshly made or reheated) at a temperature of ± 55 °C and gently pour it inside the embedding device, preferably at a corner and not directly onto the tissue.
4. Position the tissues correctly using dissection needles, without touching them directly. Instead, move/turn the tissues by moving the agarose in the surrounding area. Continue to check the orientation, and if needed, reposition the tissues, until the agarose is solidified.

5. Orientate eyes in such a way that from the top view, (1) both the dorsal side of the eye, which is black-colored, and ventral side, which is silver-colored, are visible (1:1 ratio) and (2) the cornea is located to the right and thus the optic nerve to the left.
6. Orientate brains vertically (so standing upwards) with the olfactory bulbs pointing toward the sealing and the dorsal side (showing the optic tecti) facing you. Make sure that the brains do not tilt and that both optic tecti are positioned in a straight line (*see Note 26*).
7. Position visual systems horizontally. Make sure that the optic nerves/tracts are positioned in a horizontal line and that they are not bend due to the weight of the eyes.
8. Take out the agarose holding the tissues, by going around all edges with a dissection needle. Reduce the size of the agarose block to a cube of $\pm 0.5 \text{ cm}^3$ for eyes/brains or 1 cm^3 for visual systems.
9. Use the following settings on the cryostat: $10 \mu\text{m}$ section thickness, $50 \mu\text{m}$ trim thickness, $-25 \text{ }^\circ\text{C}$ for the knife temperature, $-27 \text{ }^\circ\text{C}$ for the specimen temperature.
10. Put the specimen disk inside the chamber of the cryostat on the quick freeze spot and apply a circle of OCT freezing medium in the center of the disk. Wait until the medium is almost completely frozen (white color) and place the agarose block on the small remaining wet OCT area. Let the agarose block freeze completely (*see Note 27*). Orient the agarose block on the specimen disk so that sagittal retinal sections, coronal brain sections, or horizontal visual systems sections are made.
11. Clamp the specimen disk in the object head of the cryostat.
12. Trim the agarose blocks with the eyes until the sections contain a half-moon-shaped, completely layered central retina (check under a microscope). Remove the first sections in which the retina macroscopically looks like a circle (periphery). Trim the agarose blocks with the visual systems until you reach the sections containing the optic nerves/tracts. As this is rather difficult to see with the naked eye, catch the trimmed sections on a glass slide and check them under a microscope to follow up the sectioning progress through the tissue.
13. Collect the $10 \mu\text{m}$ sections serially on eight (retina and brain) or four (visual system) glass slides kept at RT. Sectioning the central part of the adult zebrafish retina and the optic tectum will yield ± 12 sections per glass slide (about 100 sections in total). Sectioning the visual system will yield $\pm 4\text{--}5$ sections containing the optic nerves/tract on each slide (so in total $\pm 15\text{--}20$ sections).

3.5 Embedding and Vibratome Sectioning

1. Embed the zebrafish brains using the embedding molds and 4% agarose, as described in Subheading 3.4.
2. Reduce the size of the agarose block by making a pyramid with its large square base being the posterior side of the brain (the side of the spinal cord) and the smaller top containing the olfactory bulbs. Make the pyramid as small as possible, without damaging the brain (*see Note 28*). Cut one corner of the pyramid, for example, always the one closest to the left optic tectum, as a marking point in order to distinguish the left from the right optic tectum later on.
3. Glue the brain-containing agarose pyramid with its large base on the sample chuck of the vibratome using the superglue.
4. Place the sample chuck with the brain in the chuck holder and if necessary, adjust the position of the sample chuck in this way that the optic tecti are positioned in one straight horizontal line. The brain is now oriented in the correct way to make coronal sections through the optic tecti.
5. Add ice-cold cutting buffer and a cooling element straight out of a freezer in the buffer tray of the vibratome.
6. Use the following settings on the vibratome: 50 μm section thickness, 100 μm trimming thickness, 0.6 mm amplitude, 100 Hz frequency, 1.7 mm/s sectioning speed.
7. Trim until the optic tecti. Bring the first five to six 50 μm sections in one well of a 24-well plate filled with 1 \times PBS. These sections represent the most anterior levels of the optic tecti, which are normally not used for the DAB staining in our lab but kept as spare sections. The next six sections contain the center of the optic tecti and can be recognized as they contain the torus longitudinalis and valvula cerebelli, which form a butterfly shape in these brain sections (Fig. 1a). Place these sections in one net well of another 24-well plate filled with 1 \times PBS. The last more posterior sections are again placed together with the spare anterior ones (*see Note 29*). Repeat these steps for the other brains but use different wells of the plates to deposit the sections.

3.6 DAB Staining

1. Perform the DAB staining, used to visualize the biocytin-traced axons, in 24-well plates with the net wells containing the vibratome sections with the center of the optic tecti. Place the well plate on a shaking table set on a low speed for the different steps. For all subsequent steps, use 4 mL of liquid/well.
2. Quench the endogenous peroxidases in the tissue by adding 2% hydrogen peroxide in 0.1% PBST for 20 min (*see Note 30*). Perform this step in the dark as hydrogen peroxide is light sensitive.

3. Prepare the ABC staining solution by adding one drop of A and B each per 12 mL 0.1% PBST (thus for three wells). Vortex thoroughly and let stand for 30 min, in the dark (*see Note 31*).
4. Add 0.1% glycine in 0.1% PBST for 20 min to the sections. Glycine will react with the leftover PFA and stop the fixation process.
5. Add the ABC staining solution, containing the avidin–HRP complex to the wells and incubate for 90 min in the dark.
6. Perform two washing steps using 1× PBS for 15 min each.
7. Make the DAB staining solution by dissolving one DAB tablet in 20 mL 1× PBS (*see Note 32*). When dissolved, add 40 μL 1% NiCl₂ and 40 μL 1% CoSO₄ (*see Note 33*). Right before the staining reaction, supplement this DAB solution with H₂O₂ (1:1000).
8. Fill an extra 24-well plate with the DAB solution and place it underneath a hood, close to a microscope.
9. Start the DAB step and check the staining reaction via the microscope, preferably in the wells with sections harvested from uninjured control animals. After ±1 min, the staining reaction normally has developed sufficiently, which is visible as a brown precipitation in the right optic tectum in the complete SFGS and SO where RGC axons run (Fig. 1a, c).
10. Stop the staining reaction by rinsing the sections in another plate filled with distilled, deionized water. Inspect the stained sections one more time, at your leisure, to ensure that the staining reaction was successful and has developed sufficiently. If so, rinse the sections a second time in distilled, deionized water (*see Note 34*).
11. Using a paintbrush, place the sections on a gelatin-coated glass slide (*see Note 35*). Carefully remove excess liquid by using a tissue paper and finally let the slides dry in an oven (37 °C) for at least 30 min.
12. To visualize cell nuclei, perform the neutral red counterstain. Rehydrate the sections with a 2 min rehydration step in distilled, deionized water.
13. Submerge the sections for 10 s in the neutral red staining and rinse two times in distilled, deionized water.
14. Incubate the sections in an increasing concentration of ethanol (50, 70, 96% ethanol, 3 min each) for dehydration, followed by two times for 15 s in pure acetone.
15. Degrease the sections by submerging them two times for 3 min in xylene.
16. Mount the sections using a coverslip and DPX mounting medium. Avoid air bubbles.
17. Let the slides dry overnight in a ventilation hood. Store the slides in a slide box at RT.

3.7 H&E Staining

1. Dry the slides containing the retinal sections for IPL measurements in an oven at 37 °C, and rehydrate them for 5 min in distilled, deionized water.
2. Submerge the sections for 3 min in the hematoxylin solution, which will result in a blue–purple staining of the nuclei.
3. Rinse the sections thoroughly for 5 min under running tap water, followed by incubation in the eosin staining for 10 s. Eosin gives the cytoplasm a pink color.
4. Perform a dehydration step (rinse in 50, 70, and 96% ethanol, followed by two times 5 min in absolute ethanol) and degrease the slides using xylene (two times 5 min).
5. Mount using DPX.

3.8 Fluorescent Stainings

1. Perform the different stainings on cryosections using the standard protocol which includes the following steps: drying, rehydration, heat-mediated antigen retrieval, blocking with serum, overnight primary antibody incubation, secondary antibody incubation, DAPI staining and mounting. Modifications compared to the standard protocol are mentioned in the different steps for the specific antibody. To visualize regenerated RGCs, use the retinal cryosections made after retrograde biocytin tracing. To visualize synaptic/dendritic degeneration/recovery in the retina, perform an immunostaining for synaptotagmin 2, Psd-95, or Map 2. Anti-synaptotagmin 2 can also be used on optic tectum cryosections.
2. Dry the slides in an oven at 37 °C for 10 min.
3. Submerge the sections for 5 min in distilled, deionized water, followed by 5 min in 1× TBST (*see Note 36*).
4. Preheat the citrate buffer in the microwave until it obtains a cloudy, opaque appearance (*see Note 37*). Submerge the sections in the warm buffer and place them in an oven at 95 °C for 20 min, after which they need to cool down at RT for 20 min. No heat-mediated antigen retrieval step is necessary for the staining using anti-Psd-95. For anti-Map 2, the antigen retrieval step is executed within a microwave and not an oven. Start with cold citrate buffer and perform two 5-min heating steps at 700 W and one at 500 W. Add buffer in between heating in case not enough fluid is left due to spilling during the boiling process.
5. Rinse the sections three times for 5 min in 1× TBST.
6. Quench the activity of endogenous peroxidases for the synaptotagmin 2 staining, as the secondary antibody amplification step here is based on the catalytic activity of HRP. Incubate the sections in 0.3% H₂O₂ in methanol for 20 min, performed in the dark, followed by three washing steps in 1× TBST.

7. Perform a 2-h blocking step with pre-immune donkey serum (1:5) in 1× TNB (*see Note 38*). Perform the blocking step with 0.3% Triton X-100, 3% BSA, 10% normal donkey serum in 1× PBS for the anti-Psd-95 staining.
8. Incubate the slides overnight with the primary antibody on RT, except for anti-Psd-95 (4 °C). Use the following dilutions: 1:1000 znp-1 in 10% normal donkey serum in 1× TNB, 1:2000 anti-Map 2 in 1× TNB, 1:500 anti-Psd-95 in 0.3% Triton X-100, 1% BSA and 3% normal donkey serum in 1× PBS. For visualizing the regenerated RGCs inside the retina after retrograde biocytin tracing, no primary antibody is added. Biocytin is immediately visualized by incubation with fluorescently-labelled streptavidin (*see step 10*).
9. Rinse the sections three times for 5 min using 1× TBST, to remove the excess of primary antibody (*see Note 39*).
10. Perform a 2-h incubation step with a donkey anti-mouse Alexa Fluor-conjugated secondary antibody, diluted 1:300 in 1× TNB. For the staining with znp-1, an amplification method using the tyramide signal amplification system is used to increase signal intensity of the staining. Perform a 45-min incubation step with donkey anti-mouse secondary antibody conjugated to biotin (1:300 in 1× TNB), followed by 30 min of streptavidin–HRP (1:100 in 1× TNB). Incubate the sections with the tyramide signal amplification reagent, according to manufacturer's protocol (*see Note 40*). To visualize the regenerating RGCs after biocytin tracing, add the labeled streptavidin (Alexa Fluor conjugated to streptavidin, 1:200 in 1× TNB) and incubate for 2 h.
11. Rinse the sections three times for 5 min with 1× PBS.
12. Counterstain the nuclei using the DAPI solution for 30 min.
13. Rinse using 1× PBS and mount the slides using an anti-fade fluorescence mounting medium (*see Note 41*). The slides can be stored at 4 °C.

3.9 Microscopic Visualization and Quantification of the Biocytin-Traced RGCs

1. Take fluorescent pictures of the stained retinas after retrograde biocytin tracing. Use a fluorescence microscope and a 20× objective.
2. Define the central retinal section on the slides by identifying the location of the optic nerve head. Image six central retinal sections adjacent to this central section, so at 80, 160, and 240 μm distance at either side of the optic nerve head.
3. Using FIJI and the cell counter plug-in (analyze > cell counter), count the absolute number of biocytin-positive cells in the complete retinal ganglion cell layer of all six sections.

4. Make an average per fish for the number of biocytin-positive cells per retinal section.
5. Analyze three to five fish per condition.

3.10 Microscopic Visualization and Quantification of Axonal Regeneration in the Optic Nerve

1. Image the visual system cryosections of the Tg(*gap-43:eGFP*) fish using a confocal microscope using a 20× objective. Use at minimum four sections containing the complete optic nerve tract.
2. Determine the distance grown by the eGFP-positive axons, being the length between the crush site and the axonal growth tips, using FIJI.
3. Make an average per fish.
4. Use five to six fish per condition.

3.11 Microscopic Visualization and Quantification of Tectal Reinnervation

1. Take light microscopy images of the DAB-stained vibratome brain sections after anterograde biocytin tracing using a 10× objective. Focus on the black-stained axons, reinnervating the superficial layers of the optic tectum (SFGS and SO).
2. To semi-quantify tectal reinnervation, open a picture of an uninjured control zebrafish brain in FIJI (*see Note 42*). Outline the area of innervation, being the SFGS and SO, using the polygon selection tool. This is most obvious and straightforward to do in the uninjured condition as here this innervation area is completely filled with axons.
3. Duplicate the selected area of innervation (image > duplicate, or control + shift + D) and clear everything outside your selected area (edit, clear outside). Measure the surface of the area (analyze > measure, or control + M).
4. Manually set a threshold to quantify the biocytin-positive area inside the SFGS and SO using the threshold tool (image > adjust > threshold, or control + shift + T for Windows). Use the bottom sliding bar in order to only select the biocytin-positive area (*see Note 43*). Apply this threshold (apply in the threshold tool), select the threshold area (edit > selection > create selection), and finally measure this area (analyze > measure, or control + M for Windows).
5. Define the axonal density as the ratio of the biocytin-positive area to the area of reinnervation, being the SO and SFGS of the optic tectum.
6. Analyze tectal reinnervation on at minimum five sections containing the central optic tecti per fish. Determine the average value for each fish. Use the tectal reinnervation values of the uninjured fish as a reference value and set as 100%. Express the reinnervation values for the injury conditions in %, relative to this reference control (*see Notes 44 and 45*).

**3.12 Microscopic
Visualization and
Quantification of
Dendritic
Degeneration/
Recovery Using IPL
Thickness
Measurements**

1. Take pictures of six central H&E-stained sections (three at 80, 160, and 240 μm distance at either side of the optic nerve head) using a bright-field microscope and a 20 \times objective.
2. Measure the IPL thickness, as well as the photoreceptor layer (Fig. 1b) at about 300 μm on both sides of the optic nerve using FIJI. The thickness of the photoreceptor layer (PRL) is used as a correction factor, e.g., for small orientation/embedding differences between different retinas.
3. Calculate the IPL/PRL ratios and average per fish (*see Note 46*).
4. Use at minimum three fish per condition.

**3.13 Microscopic
Visualization and
Quantification of
Synaptic and Dendritic
Degeneration/
Recovery Using
Fluorescent Stainings**

1. Take images of the synaptotagmin 2-stained brain and retinal sections, the Psd-95-stained retinal sections, and Map 2-stained retinal sections with a confocal microscope using a 60 \times objective. Take pictures of at least five sections with the central right optic tectum (containing the butterfly-shaped torus longitudinalis and valvula cerebelli, Fig. 1a) and six central retinal sections (three at 80, 160, and 240 μm distance at either side of the optic nerve head).
2. Quantify the immunopositive area/region of interest (IPL or optic tectum area) in the same way as previously described (*see Subheading 3.11*) (*see Note 47*).
3. Average the obtained values for each fish and use at least five fish per condition.

4 Notes

1. For standard research questions, we use 5–7-month-old zebrafish, which are approximately 2.5 cm. We prefer not to give excessive amounts of food to our fish so that they remain slim, as obese fish have substantial fat tissue in their eye orbits, which complicates the execution of an ONC.
2. Never use anesthetic solutions coming straight out of the fridge (4 $^{\circ}\text{C}$) as this will result in a cold shock. Warm it to 28 $^{\circ}\text{C}$ using a water bath. Protect both the tricaine stock solution and anesthetic solutions from light to avoid degradation and thereby the production of toxic by-products.
3. If the height of the petri dish lid exceeds 1 cm, it hinders your hand movements and thus complicates the operative procedure.
4. Sylgard is a clear polymer which has the ideal hardness to perform dissections on: it is soft enough to insert, e.g., pinheads and does not damage dissection material, but sufficiently

hard to support the animal. You can buy pre-made Sylgard-filled petri dishes or make it yourself following manufacturer's guidelines.

5. Specialized adhesion slides have excellent adhesive properties for cryosections, and their use minimizes tissue loss during the staining process. If electrostatic effects hinder the collection of cryosections, place a slightly moist tissue paper underneath the glass slides.
6. In our lab, we always use the VECTASTAIN Elite ABC system from Vector Laboratories. It is possible to buy the required compounds for visualization separately (avidin and biotinylated peroxidase), but we do not have experience with this working method.
7. FIJI is freely available via this link: <https://imagej.net/Downloads>. For counting the regenerated RGCs after biocytin tracing, use the cell counter plug-in, which is automatically available after program installation.
8. Be careful not to transfer too much water in the anesthetic solution when transferring the fish, to avoid diluting it. Therefore, first hold the aquarium fishnet containing the caught animal against the side of the tank above the water level so that a lot of water drips down.
9. Adequate sedation can be evaluated by slightly tapping the beaker on the table or gently pinching the zebrafish tail with a forceps. Absence of a response/movement indicates that the fish is sufficiently sedated.
10. In our lab, we normally crush unilaterally and always use the left eye for this. It is possible to perform an ONC on the right optic nerve as well, but then it is easier to position the fish in the opposite direction (head toward you, tail facing away).
11. If tilting the eye out of its orbit is executed too roughly, it is possible that you; break extraocular muscles and that the eye is lost after this operation, tear the ophthalmic artery resulting in major bleeding or stretch/the optic nerve and that the optic nerve damage is not similar as in a well-executed ONC. It is also important that the forceps are not used in a closed position within this step, as too much force is then applied on a single position with the risk of pinching through the sclera.
12. Removing fat tissue should be executed in a gentle way, as it could otherwise cause bleeding inside the orbit that hinders sight during further surgery.
13. In 5–7-month old fish, the distance of 0.5 mm of the optic nerve head is located in the middle of the exposed optic nerve, while in older fish it is, in relative terms, more positioned toward the optic nerve head.

14. If a fish does not recover from the anesthesia as expected, e.g., due to a prolonged operative duration and thus a longer sedation period, gently provide additional aquarium system water over the gills using a Pasteur pipette.
15. If early axonal regeneration or tectal reinnervation needs to be measured on different time points after injury, it is more convenient to plan the ONC at different days so that the more labor-intensive biocytin tracing and perfusion steps can be performed at one single day for the different conditions.
16. The dermal layer of the cornea starts to restore from 2 dpi and regains its pre-injury thickness around 6 dpi.
17. For retrograde biocytin tracing experiments, the biocytin clot is always placed posterior to the ONC site. In this way, the RGCs inside the retina that have regenerated their axons past the injury are traced. For quantifying tectal reinnervation, the clots are placed anterior to the crush site. If we would place the biocytin for anterograde tracing posterior to the injury site, accidentally spared axons due to an incomplete ONC are also traced. Of note, in our hands, no axons are visible using this anterograde tracing technique in the right optic tectum immediately after a left ONC, which is a proof that we disrupt all axons and do not have spared ones left.
18. Do not put more than two/three fish in one recovery tank at this point. It is important that the biocytin tracing step takes equally long (3 h) for every fish so you need to be able to separate the different individuals. If you put more than one fish in a tank, write down a recognizable physical characteristic (color, gender, size) together with the time of biocytin application in order to distinguish them.
19. Obtaining the correct size of the needle opening is of utmost importance and requires some experience. While needles with large openings are inconvenient to insert in the small zebrafish ventricle, too small openings obstruct the flow and come together with a wobbly tip that bends under pressure. Therefore, we break the tip of the capillary needle at the point where it is not flexible anymore.
20. Always aim the needle toward the bulbus arteriosus. In this way, when you would apply too much force, the needle will end up in the bulbus and the fluid will still run inside the vascular system. If you puncture the ventricle from the side and slip, the needle will exit the ventricle at the other side, and perfusion fails.
21. PFA cross-links proteins and is therefore a widely used fixative. The fixation process is visible during the perfusion as the tail of the fish can move from one side to the other fiercely. For injecting the different fluids (PBS and PFA), you have two possibilities: (1) the use of two different syringes and injection

tubes, with the disadvantage that you need to insert a needle at the same place two times, or (2) the use of one injection tube but two different syringes so that the needle can stay in between changing syringes. With the latter option, make sure to rinse sufficiently in between two fish so that you always start with PBS in the injection tube.

22. To be completely safe, wear a mask that protects against organic vapors, even if you work under a fume hood, as PFA fumes can be carcinogenic.
23. In case there is still some tissue attached to the visual system at this point, you can place it in a petri dish with some PBS and remove the extra, unwanted tissue using small scissors.
24. Tissues harvested for immunofluorescent staining using antibodies are only fixed for 1 h in 4% PFA at RT. This in contrast to the tissues obtained after biocytin tracing or to perform histological staining onto, which are fixed overnight. Antibody-based stainings have a higher success rate when performed on lightly fixed tissues, as strong fixation can mask the epitopes. For IPL thickness measurements, it is of crucial importance that the morphology of the retina is perfectly maintained. As such, PFA fixation should definitely be performed overnight to ensure retinal layer thickness preservation. A superior method to preserve morphology is the use of Bouin Hollande as a fixative in combination with paraffin sectioning.
25. Cryopreservation with sucrose is important to prevent formation of ice crystals during the freezing process, which could result in tissue damage.
26. To our experience, embedding the brains vertically is easier than embedding them in a horizontal position.
27. Never place the agarose block containing the tissues immediately in the OCT compound, as it will sink in the still soluble medium which will complicate the sectioning process. Indeed, the knife will encounter different harnesses (OCT compound, agarose, tissue, agarose, OCT compound), and this is disadvantageous to make sections. OCT is thus only used as a glue here.
28. Reducing the size of the agarose pyramid will result in smaller sections, which are easier to place on glass slides.
29. In our lab, the spare sections are normally not stained, unless the DAB staining failed. In that case, you can still stain the spare anterior/posterior sections to get an indication of the results of the experiment. Nevertheless, the most anterior sections are interesting to use when interested in early tectum reinnervation, as in these anterior sections the axons arrive first (in our lab around 4 days post-ONC).

30. Quenching endogenous peroxidases is important as the staining method used here is based on the catalytic activity of the enzyme HRP and active peroxidases inside the tissue could produce false-positive results.
31. The component A and B of the ABC kit contain avidin and biotinylated HRP, respectively, which will bind to each other with a high affinity in this step.
32. When working with DAB, be careful and take all necessary precautions (lab coat, double gloves, dust mask) as it is highly carcinogenic.
33. To intensify the staining and increase the contrast, NiCl_2 and CoSO_4 are used to create a gray–black staining, compared to a brown (DAB) one, due to a metal precipitation.
34. As DAB is a potential carcinogen, keep the 24-well plates that came into contact with it as dedicated equipment for DAB stainings, or always use new ones. Avoid putting the used plates in the normal lab circulation.
35. The sections or the surrounding agarose cannot overlap on the slides as this is detrimental for microscopy visualization later on. In case you want to put sections of different fish on one slide, make sure to physically separate them into groups.
36. Rehydration and washing steps can be performed in plastic or glass staining jars. Steps with more expensive products (antibodies, pre-immune serum, DAPI) are better performed directly on the slides inside a humidity chamber as the used volume can be substantially reduced. Put the humidity chambers on a shaking table to ensure equal incubation and spreading of the fluid. In our hands, 400 μL is enough to cover the glass slides for an overnight incubation period in a humidity chamber, without the slides drying out. However, we do use a PAP pen to draw a thin hydrophobic barrier around the area on the glass slide containing all sections, in order to reduce the surface that needs to be incubated with the antibody.
37. A heat-mediated antigen retrieval step is often performed in immunofluorescent stainings to reveal epitopes that were potentially masked due to the formalin fixation.
38. A blocking step using serum will saturate all binding sites in a tissue and is important prior to antibody incubation in order to prevent aspecific binding of the used primary/secondary antibodies.
39. Ideally, the first part of a staining is started in the afternoon, while the second part is performed the day after in the morning. In this way, the risk of dried sections is minimized. For financial considerations, it is possible to recuperate the primary antibody after overnight incubation. Store it at 4 °C for maximum 1 week and reuse it for another staining on a new batch of slides.

40. As the tyramide signal amplification reagent is expensive, we reuse it in one and the same staining. Therefore, divide the slides in two groups, perform the incubation step for the first group, recuperate the solution, and reuse it for the second group. Make sure that all slides are incubated with tyramide signal amplification reagent for exactly the same time. Otherwise, false intensity differences between slides could be produced.
41. The easiest way to mount slides according to our experience is to add ± 90 μL of mounting medium in a straight line on the coverslip itself. Position one side of the coverslip in a $\pm 45^\circ$ angle against the slide and then gently lower the coverslip to prevent air bubbles from forming. Remove excess of water and the mounting medium carefully using tissue paper before putting the slide in the slide folder.
42. In our lab, we created a macro to run in FIJI which guides you through the different steps of this analysis method. This macro can be downloaded via this link: <https://gitlab.com/NCDRIlab/tectal-reinnervation-zebrafish>. To run it, go to Plug-ins > Macro > Run and select the macro, after which the analysis is explained in different steps.
43. Quantifying tectal reinnervation using anterograde biocytin tracing is a semiquantitative method as you manually set the threshold to define the biocytin-positive axons. At this point, it is important to check every part of the SO/SFGS and decide the ideal threshold value for the complete region. In our hands, it is common that the peripheral parts of the brain show more dark areas of axons than the center part, so use a threshold value that is in between the ideal value for the different regions. The threshold step requires focus and practice as you should always do it in the same way for every section separately.
44. Outlining the area of reinnervation (SO/SFGS) is more difficult in sections of zebrafish subjected to an ONC, as here this is only partly filled with (regenerated) axons. Estimate this surface as good as possible, based on the outlining steps performed on the brain sections of uninjured fish. Again, this requires some experience.
45. Besides using this DAB staining, the biocytin inside the reinnervated axons can also be visualized using the same fluorescent staining protocol as described in Subheading 3.8, in this case performed on 10 μm coronal cryosections of the optic tecti. Analysis of tectal reinnervation can be performed in the same way as for the DAB-stained sections. As an alternative for visualizing the axons using anterograde biocytin tracing, *Tg (gap-43:eGFP)* zebrafish could be used, in which the regrowing axons are detectable due to the eGFP expression under the regulation of the *gap-43* promoter.

46. Although the IPL thickness can give valuable information regarding dendritic disintegration/regeneration, we are aware that directly imaging and measuring the length of the RGC dendrites would be more accurate. However, sparse labeling of RGCs and their dendrites is then necessary, as imaging a single RGC and its dendrites is impossible when all RGCs are fluorescently tagged. However, no zebrafish line is available at the moment in which there is only sparse labeling of the RGCs in the adult stage, so therefore we use these IPL measurements to have a first indication of possible dendritic remodeling processes ongoing after ONC.
47. Quantification of the immunopositive area/IPL is less straightforward as for the optic tectum, since there is IPL thinning after ONC and this can influence the results of your quantification. Make sure to keep this in mind when interpreting the results.

Acknowledgments

We thank present and former lab members of the Neural Circuit Development and Regeneration (NCDR) group, especially the ones forming the zebrafish research team, who have helped to develop these techniques over the years. This work was financially supported by fellowships and project grants from the Research Foundation-Flanders (FWO), FWO Flanders-Quebec bilateral research grant, the KU Leuven Research Council, and L'Oréal/UNESCO (For Women in Science).

References

1. Benowitz LI, He Z, Goldberg JL (2017) Reaching the brain: advances in optic nerve regeneration. *Exp Neurol* 287:365–373
2. Berry M, Ahmed Z, Logan A (2019) Return of function after CNS axon regeneration: lessons from injury-responsive intrinsically photosensitive and alpha retinal ganglion cells. *Prog Retin Eye Res* 71:57–67. <https://doi.org/10.1016/j.preteyeres.2018.11.006>
3. Di Polo A (2015) Dendrite pathology and neurodegeneration: focus on mTOR. *Neural Regen Res* 10:559–561
4. Johnston D, Frick A, Poolos NP (2016) Dendrites and disease. In: Stuart G, Spruston N, Häusser M (eds) *Dendrites*, 3rd edn. Oxford Academic, Oxford, p 677–702. <https://doi.org/10.1093/acprof:oso/9780198745273.001.0001>
5. Emoto K (2011) Dendrite remodeling in development and disease. *Develop Growth Differ* 53:277–286
6. Della SL, Inman DM, Lupien CB et al (2013) Differential progression of structural and functional alterations in distinct retinal ganglion cell types in a mouse model of glaucoma. *J Neurosci* 33:17444–17457. <https://doi.org/10.1523/JNEUROSCI.5461-12.2013>
7. Frankfort BJ, Kareem Khan A, Tse DY et al (2013) Elevated intraocular pressure causes inner retinal dysfunction before cell loss in a mouse model of experimental glaucoma. *Investig Ophthalmol Vis Sci* 54:762–770. <https://doi.org/10.1167/iovs.12-10581>
8. Morquette B, Morquette P, Agostinone J et al (2015) REDD2-mediated inhibition of mTOR promotes dendrite retraction induced by axonal injury. *Cell Death Differ* 22:612–625. <https://doi.org/10.1038/cdd.2014.149>

9. Peterson SL, Benowitz LI (2018) Mammalian dendritic regrowth: a new perspective on neural repair. *Brain* 141:1891–1894
10. Beckers A, Moons L (2019) Dendritic shrinkage after injury: a cellular killer or a necessity for axonal regeneration? *Neural Regen Res* 14: 1313–1316
11. Bollaerts I, Veys L, Geeraerts E et al (2018) Complementary research models and methods to study axonal regeneration in the vertebrate retinofugal system. *Brain Struct Funct* 223: 545–567
12. Becker T, Becker CG (2014) Axonal regeneration in zebrafish. *Curr Opin Neurobiol* 27: 186–191
13. Van Houcke J, Bollaerts I, Geeraerts E et al (2017) Successful optic nerve regeneration in the senescent zebrafish despite age-related decline of cell intrinsic and extrinsic response processes. *Neurobiol Aging* 60:1–10. <https://doi.org/10.1016/j.neurobiolaging.2017.08.013>
14. Udvardi AJ (2008) 3.6 kb Genomic sequence from Takifugu capable of promoting axon growth-associated gene expression in developing and regenerating zebrafish neurons. *Gene Expr Patterns* 8:382–388. <https://doi.org/10.1016/j.gep.2008.05.002>
15. Dhara SP, Rau A, Flister MJ et al (2019) Cellular reprogramming for successful CNS axon regeneration is driven by a temporally changing cast of transcription factors. *Sci Rep* 9:1–12. <https://doi.org/10.1038/s41598-019-50485-6>
16. Diekmann H, Kalbhen P, Fischer D (2015) Characterization of optic nerve regeneration using transgenic zebrafish. *Front Cell Neurosci* 9. <https://doi.org/10.3389/fncel.2015.00118>
17. Van Dyck A, Bollaerts I, Beckers A et al (2021) Müller glia–myeloid cell crosstalk accelerates optic nerve regeneration in the adult zebrafish. *Glia*. <https://doi.org/10.1002/glia.23972>
18. Beckers A, Van Dyck A, Bollaerts I et al (2019) An antagonistic axon-dendrite interplay enables efficient neuronal repair in the adult zebrafish central nervous system. *Mol Neurobiol* 56:3175–3192. <https://doi.org/10.1007/s12035-018-1292-5>
19. Bollaerts I, Van Houcke J, Andries L et al (2017) Neuroinflammation as fuel for axonal regeneration in the injured vertebrate central nervous system. *Mediat Inflamm* 2017: 9478542
20. Lemmens K, Bollaerts I, Bhumika S et al (2016) Matrix metalloproteinases as promising regulators of axonal regrowth in the injured adult zebrafish retinotectal system. *J Comp Neurol* 524:1472–1493. <https://doi.org/10.1002/cnc.23920>
21. Liu Q, Londraville R, Marrs JA et al (2008) Cadherin-6 function in zebrafish retinal development. *Dev Neurobiol* 68:1107–1122. <https://doi.org/10.1002/dneu.20646>
22. Fox MA, Sanes JR (2007) Synaptotagmin I and II are present in distinct subsets of central synapses. *J Comp Neurol* 503:280–296. <https://doi.org/10.1002/cnc.21381>
23. Nevin LM, Robles E, Baier H, Scott EK (2010) Focusing on optic tectum circuitry through the lens of genetics. *BMC Biol* 8:126
24. Aref AA, Sayyad FE, Mwanza JC et al (2014) Diagnostic specificities of retinal nerve fiber layer, optic nerve head, and macular ganglion cell-inner plexiform layer measurements in myopic eyes. *J Glaucoma*. <https://doi.org/10.1097/IJG.0b013e31827b155b>
25. Greenberg BM, Frohman E (2010) Optical coherence tomography as a potential readout in clinical trials. *Ther Adv Neurol Disord* 3: 153–160
26. Miki A, Medeiros FA, Weinreb RN et al (2014) Rates of retinal nerve fiber layer thinning in glaucoma suspect eyes. *Ophthalmology*. <https://doi.org/10.1016/j.ophtha.2014.01.017>
27. Kim EK, Park HYL, Park CK (2017) Segmented inner plexiform layer thickness as a potential biomarker to evaluate open-angle glaucoma: dendritic degeneration of retinal ganglion cell. *PLoS One*. <https://doi.org/10.1371/journal.pone.0182404>
28. Chua J, Tan B, Ke M et al (2020) Diagnostic ability of individual macular layers by spectral-domain optical coherence tomography in different stages of glaucoma. *Ophthalmol Glaucoma*. <https://doi.org/10.1016/j.ogla.2020.04.003>
29. Riederer B, Matus A (1985) Differential expression of distinct microtubule-associated proteins during brain development. *Proc Natl Acad Sci U S A* 82:6006–6009. <https://doi.org/10.1073/pnas.82.17.6006>
30. Lieven CJ, Millet LE, Hoegger MJ, Levin LA (2007) Induction of axon and dendrite formation during early RGC-5 cell differentiation. *Exp Eye Res* 85:678–683. <https://doi.org/10.1016/j.exer.2007.08.001>

31. Kim Y, Jang YN, Kim JY et al (2020) Microtubule-associated protein 2 mediates induction of long-term potentiation in hippocampal neurons. *FASEB J* 34:6965–6983. <https://doi.org/10.1096/fj.201902122RR>
32. Cho T, Kashiwagi Y, Okabe S (2019) Temporal sequences of synapse disintegration triggered by afferent axon transection, time-lapse imaging study of presynaptic and postsynaptic molecules. *eNeuro* 6. <https://doi.org/10.1523/ENEURO.0459-18.2019>
33. Meyer MP, Trimmer JS, Gilthorpe JD, Smith SJ (2005) Characterization of zebrafish PSD-95 gene family members. *J Neurobiol* 63:91–105. <https://doi.org/10.1002/neu.20118>



Assaying Optic Nerve Regeneration in Larval Zebrafish

Beth M. Harvey, Melissa Baxter, and Michael Granato

Abstract

Zebrafish have a remarkable capacity for spontaneously regenerating their central nervous system. Larval zebrafish are optically transparent and therefore are widely used to dynamically visualize cellular processes *in vivo*, such as nerve regeneration. Regeneration of retinal ganglion cell (RGC) axons within the optic nerve has been previously studied in adult zebrafish. In contrast, assays of optic nerve regeneration have previously not been established in larval zebrafish. In order to take advantage of the imaging capabilities in the larval zebrafish model, we recently developed an assay to physically transect RGC axons and monitor optic nerve regeneration in larval zebrafish. We found that RGC axons rapidly and robustly regrow to the optic tectum. Here, we describe the methods for performing the optic nerve transections, as well as methods for visualizing RGC regeneration in larval zebrafish.

Key words Larval zebrafish, Optic nerve regeneration, Retinal ganglion cell neurons

1 Introduction

Due to the poor regenerative capacity of the mammalian central nervous system, diseases that damage retinal ganglion cell (RGC) bodies and their axons within the optic nerve can ultimately result in irreversible blindness [1–3]. Regeneration of the mammalian optic nerve is mostly insufficient due to limited RGC axonal regrowth and massive RGC death [4–6]. Although studies have identified signaling pathways that enhance RGC survival and increase axonal growth after injury, RGC axons often fail to reach their original targets [7–15]. Therefore, model systems that complement mammalian axonal regeneration studies can further identify mechanisms that promote optic nerve regeneration.

In contrast to most mammals, lower vertebrates such as zebrafish have a remarkable capacity to regenerate their central nervous system [16]. Cellular and molecular mechanisms that mediate the spontaneous regeneration of both the optic nerve and spinal cord have been studied using adult zebrafish [17–27]. Additionally, zebrafish have been used for decades to extensively study the

development of the spinal cord and visual system, both at the cellular and molecular genetic levels (reviewed in [28–30]). However, only recently have assays been established to study spinal cord regeneration in the larval zebrafish [31–35]. As larvae are optically transparent, such studies have provided dynamic *in vivo* insights into cellular behaviors and injury responses [36–38]. Conversely, robust assays using larval zebrafish for optic nerve regeneration have been absent.

We sought to take advantage of the larval zebrafish system to assay optic nerve regeneration in 5-day-old zebrafish. Larval zebrafish at 5 days post fertilization possess a functional visual system, in which RGC axons exit the eye and cross at the optic chiasm to project solely to the contralateral optic tectum (Fig. 1a–c) [39–43]. Furthermore, several behavioral assays are well established to probe visual system function [41, 42, 44–47]. We therefore developed a rapid and robust assay to monitor regeneration of RGC axons using the transgenic line *Tg(isl2b:GFP)* that labels RGCs and their axons [48]. We perform optic nerve transections using a sharpened tungsten needle to transect the RGC axons distal to where they exit the eye but proximal to the optic chiasm (Fig. 1c) [49]. We have observed that by 96 h post injury, RGC axons robustly regrow to the optic tectum [49]. Here, we describe the methods for performing the optic nerve transection, as well as visualizing RGC regeneration, either directly with immunostaining or labeling with lipophilic dyes.

2 Materials

2.1 RGC Axon Transection in Larval Zebrafish

1. *Tg(isl2b:GFP)* transgenic line (*see Note 1*).
2. E3 medium: 5 mM NaCl, 0.17 mM KCl, 0.33 mM CaCl₂•2H₂O, 0.33 mM MgSO₄. Store at room temperature for up to a month, and then consider making fresh to prevent contamination.
3. E3 medium with 0.2 mM phenylthiourea (PTU): 5 mM NaCl, 0.17 mM KCl, 0.33 mM CaCl₂•2H₂O, 0.33 mM MgSO₄, 0.2 mM PTU. Store in the dark at 29 °C for up to a month.
4. Fluorescent stereomicroscope.
5. 1 M Tris–HCl, pH 9.0.
6. 0.4% tricaine: Dissolve tricaine in distilled water, then pH to 7.0 using 1 M Tris–HCl pH 9.0. For long-term storage, store in 1 mL aliquots at –20 °C.
7. Anesthetic solution: Make fresh for each experiment by diluting 0.4% tricaine to 0.0053% tricaine in E3 medium.
8. Glass Pasteur pipet, 1.5 mm tip.

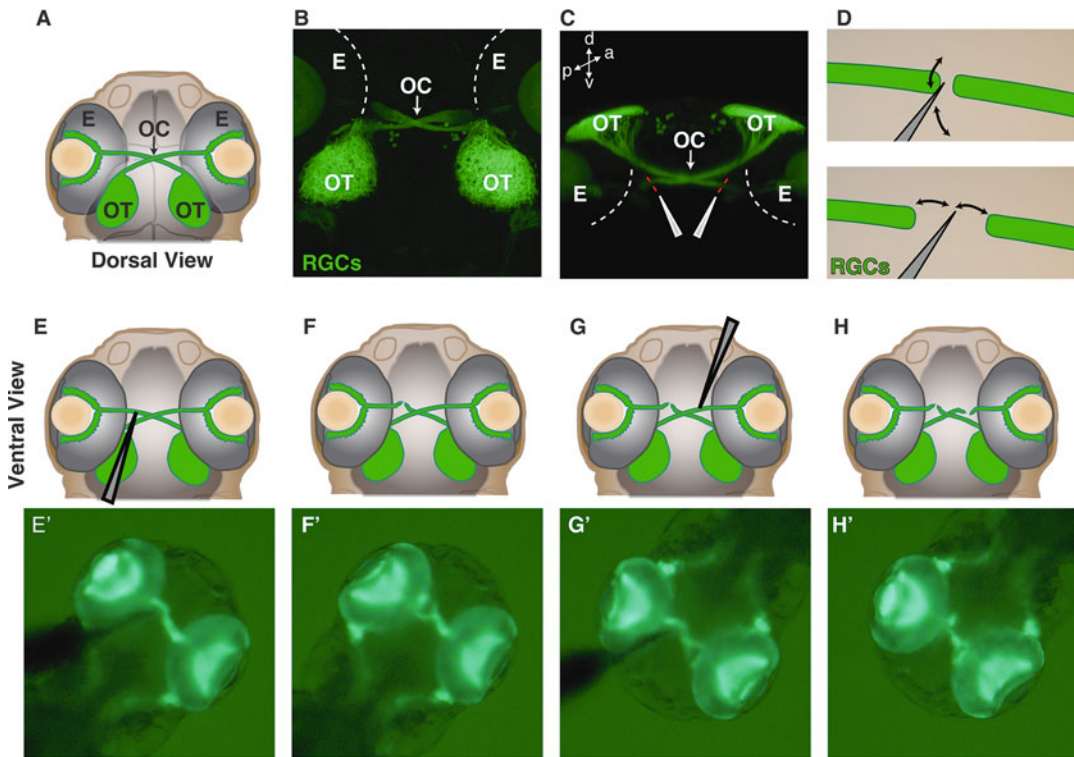


Fig. 1 Transecting RGC axons in larval zebrafish with a sharpened tungsten needle. **(a)** Diagram of the retinotectal projection in *Tg(isl2b:GFP)* larval zebrafish from a dorsal view. The cell bodies of RGCs are in the innermost layer of the retina. RGC axons exit the eye (E), cross solely contralaterally at the optic chiasm (OC) and terminate in the optic tectum (OT). **(b)** Confocal image stacks represented as maximum intensity projection of the retinotectal projection in a *Tg(isl2b:GFP)* larva at 5 days post fertilization. Eyes are outlined by dashed lines. **(c)** Image of confocal stack from **(b)** rotated 90 degrees into the page. The transection site, indicated by red dashed lines, is distal to the region where RGC axons exit the eye, yet proximal to the optic chiasm. Eyes are outlined by dashed lines. *d* dorsal, *v* ventral, *a* anterior, *p* posterior. **(d)** RGC axons are transected by using very precise up and down, as well as back and forth motions with the sharp tip of the tungsten needle. **(e–e')** After mounting larvae ventral-up, a sharpened tungsten needle is inserted through the jaw to reach the transection site. **(f–f')** Following transection, the RGC axons are clearly severed. **(g–g')** Based on preference of the person performing the transection, the larva can be reoriented to transect the RGC axons of the second eye. **(h–h')** RGC axons of both eyes are transected. **(e'–h')** Images were acquired on an Olympus SZX16 fluorescent microscope

9. Low-melt agarose: Using a microwave, dissolve 2.5% low-melt agarose (*see Note 2*) in E3 medium. Stocks of 50 mL can be stored at room temperature for up to about 3 months. For each transection experiment, use a microwave to remelt and aliquot 500 μ L of low-melt agarose in 1.5 mL microcentrifuge tubes with final concentration 0.016% tricaine. Keep these tubes of melted agarose at 42 $^{\circ}$ C.
10. Microscopy slides, 3 inches 1 inch by 1 mm.

11. Tungsten needle: Tip diameter 0.001 mm, rod diameter 0.125 mm.
12. 5 N NaOH.
13. Ringer's medium with 0.2 mM PTU: 116 mM NaCl, 2.9 mM KCl, 1.8 mM CaCl₂, 5 mM HEPES, 0.2 mM PTU. Adjust to pH 7.2 using 5 N NaOH.
14. Glass depression plate.
15. Fluorescent compound microscope, such as a Zeiss Axio Imager M1.

2.2 Immunostaining Tg(isl2b:GFP) Larvae

1. Phosphate-buffered saline (PBS).
2. 4% paraformaldehyde (PFA): Make fresh each time by diluting 16% PFA in PBS (*see Note 3*).
3. PBT: 0.25% Triton X-100 detergent dissolved in PBS .
4. 150 mM Tris-HCl, pH 9.0
5. 0.05% trypsin-EDTA.
6. Blocking solution: 1% bovine serum albumin (BSA), 2% normal goat serum (NGS), and 1% dimethylsulfoxide (DMSO) in PBT.
7. Antibody binding solution: 1% BSA and 1% DMSO in PBT.
8. Anti-GFP primary antibodies (Takara Cat# 632381, *see Note 4*).
9. Green fluorescing secondary antibody.
10. Non-hardening antifade mounting medium.

2.3 Using Lipophilic Dyes to Label RGC Axons

1. Capillaries, 4 inch in length, 1.0 mm outer diameter with filament.
2. Micropipette puller (e.g., Sutter Instrument, Model P-87).
3. Coverslips, 22 mm × 22 mm and 9 mm × 9 mm.
4. Coverslip sealant or clear nail polish.
5. Micromanipulator.
6. Lipophilic dyes (*see Note 5*). Dissolve 0.5% lipophilic dyes such as DiI or DiD, in dimethylformamide (DMF). Dyes can be stored protected from light at -80 °C for at least 6 months.
7. 1.5% low-melt agarose: Using a microwave, dissolve 1.5% low-melt agarose in PBS and aliquot into 1.5 mL microcentrifuge tubes. While mounting larvae for imaging, keep these tubes of melted agarose at 42 °C.

3 Methods

3.1 RGC Axon Transection in Larval Zebrafish

1. Collect *Tg(isl2b:GFP)* embryos in E3 medium. Begin incubating embryos at shield stage in E3 medium with 0.2 mM PTU at 29 °C in the dark to inhibit melanocyte pigmentation (*see Note 6*).
2. Change the E3 medium with 0.2 mM PTU daily until larvae are 5 days post fertilization.
Use a fluorescent microscope to sort for larvae with fluorescently labeled RGCs.
3. Anesthetize larvae at 5 days post fertilization in anesthetic solution.
4. Use a glass Pasteur pipet to transfer anesthetized larvae to low-melt agarose (*see Note 7*).
5. Transfer larvae in some low-melt agarose onto a microscopy slide. Orient the larvae ventral-up and centered within a dome of low-melt agarose (*see Note 8*). Allow the low-melt agarose to completely harden for a few minutes before performing the transections.
6. After the low-melt agarose has completely solidified, add a small drop of anesthetic solution onto the dome of low-melt agarose (*see Note 9*).
7. Perform optic nerve transections on a fluorescent stereomicroscope. Begin by inserting the tungsten needle through the pharyngeal arches (*see Note 10*).
8. Position the tip of the needle distal to the region where RGC axons exit the eye, yet proximal to the optic chiasm (Fig. 1c, e-e', g-g'; *see Note 11*).
9. Use small up and down, as well as back and forth motions with the sharp tip of the needle to create a transection across the axons (Fig. 1d; *see Notes 12–14*). The transection should appear distinct with a clear separation between a proximal stump and the portion of axons distal to the injury site (Fig. 1f-f', h-h').
10. After performing the transections, release the larvae from the dome of low-melt agarose by gently breaking away the low-melt agarose from around the larvae with forceps.
11. Transfer the larvae to a dish of Ringer's medium with 0.2 mM PTU for about 1 h to recover from the procedure. Then change the medium to E3 with 0.2 mM PTU and incubate at 29 °C in the dark (*see Note 15*).
12. Sort larvae for complete optic nerve transections at 16–18 h post injury on a fluorescent microscope using a glass depression plate (*see Note 16*). Keep larvae in E3 with 0.2 mM PTU at

29 °C in the dark until desired timepoints for visualization of regeneration or fixation.

13. To monitor axonal regeneration at any timepoint following transections, larvae can be placed into a glass depression plate and observed on a fluorescent dissecting microscope, or anesthetized in anesthetic solution, mounted in low-melt agarose and observed on a fluorescent compound microscope.

3.2 Immunostaining Tg(isl2b:GFP) Larvae (See Note 17)

1. Fix larvae that are 5–9 days post fertilization in 4% PFA in a 1.5 mL microcentrifuge tube overnight at 4 °C using gentle rocking or a rotating mixer.
2. Discard the fix in and wash larvae in PBT for about 5 min at room temperature.
3. Repeat the 5-min PBT wash for a total of three washes using gentle rocking or a rotating mixer.
4. For antigen retrieval, incubate larvae in 150 mM Tris–HCl pH 9.0 for 5 min at room temperature.
5. Transfer to 70 °C and incubate for 15 min.
6. Wash larvae in PBT for 5 min twice at room temperature using gentle rocking or a rotating mixer.
7. For permeabilization, incubate larvae in 0.05% trypsin–EDTA for 5 min on ice (*see Note 18*).
8. Wash and remove PBT twice to remove most of the 0.05% trypsin–EDTA .
9. Perform a 10-min wash in PBT at room temperature using gentle rocking or a rotating mixer.
10. Block for 1 h at room temperature in blocking solution using gentle rocking or a rotating mixer.
11. Remove blocking solution. Then incubate larvae in primary anti-GFP antibody at 1:200 dilution in antibody binding solution overnight at 4 °C using gentle rocking or a rotating mixer.
12. Wash in PBT for 10 min using gentle rocking or a rotating mixer.
13. Repeat **step 12** at least three times (*see Note 19*).
14. Incubate larvae in secondary antibody at a 1:500 dilution in antibody binding solution overnight at 4 °C using gentle rocking or a rotating mixer.
15. Repeat **step 12** at least three times (*see Note 19*).
16. Remove PBT and add non-hardening antifade mounting medium to larvae. Store larvae at 4 °C until mounted for imaging (*see Note 20*).

3.3 Using Lipophilic Dyes to Label RGC Axons

1. Fix larvae in 4% PFA overnight at 4 °C (*see* **Notes 21** and **22**).
2. Discard fix and wash larvae in PBS.
3. Use a micropipette puller to prepare capillary needles with short tapers (*see* **Note 23**).
4. Pipet or backfill pulled capillary needles with lipophilic dyes.
5. Use coverslip sealant or clear nail polish to secure a 22 mm × 22 mm coverslip angled on top of stacks of three 9 mm × 9 mm coverslips on a microscopy slide (Fig. 2a).
6. Lay larvae against the 22 mm × 22 mm coverslip so that the desired retina is angled toward the injection needle. Larvae can be laid lengthwise along the coverslip, or on top of the coverslip slightly hanging off the edge (Fig. 2b). Keep larvae moist with PBS (*see* **Note 24**).
7. Break the tip of the capillary needle by grazing the tip of the capillary needle with forceps (*see* **Note 25**).
8. Use a micromanipulator to insert the capillary needle into the space between the lens and the RGC layer (Fig. 2c). Inject retinas with more or less lipophilic dye to either fully fill the RGC layer or label specific regions of RGCs in the retina.
9. Keep larvae overnight in PBS at room temperature to allow lipophilic dyes to diffuse along RGC axons.
10. Mount larvae in non-hardening antifade mounting medium or 1.5% low-melt agarose to image using fluorescent microscopy.

4 Notes

1. The *Tg(isl2b:GFP)* transgenic line [48] is available through the Zebrafish International Resource Center (ZIRC; ID ZDB-ALT-100322-2; <https://zebrafish.org/home/guide.php>).
2. We specifically recommend using SeaPlaque (Lonza) low-melt agarose, which has an optimal gel strength for immobilizing larvae and performing transections as described in this method.
3. PFA is a hazardous toxic chemical and should be handled under a fume hood with personal protective equipment, including gloves, a lab coat, and safety glasses and should be disposed of following your institutions hazardous waste procedures.
4. We have also immunostained *Tg(isl2b:GFP)* larvae using anti-GFP antibodies from other vendors, such as Life Technologies and Aves labs at 1:500 dilutions.
5. Lipophilic dyes incorporate into lipid membranes and diffuse laterally to fluorescently label entire cellular membranes. When

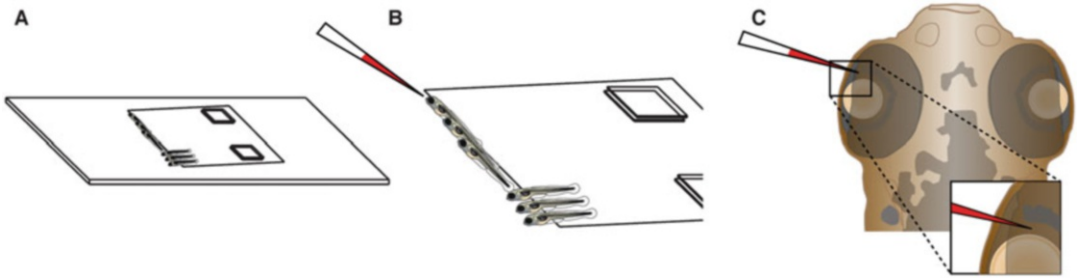


Fig. 2 Injecting lipophilic dyes into retinas of larval zebrafish. (a) A glass coverslip is secured at an angle on stacks of spacer coverslips on a microscopy slide. (b) Larvae are laid against the coverslip or on top of the coverslip to orient the eye toward the injection needle. (c) To label the RGC layer, the needle is inserted into the space between the lens and the RGC layer and dye is injected

applied onto neurons, the dyes can diffuse along axons, allowing for the visualization of these neuronal projections.

6. Shield stage is a distinct developmental timepoint characterized by when the embryonic shield structure becomes visible. This typically occurs 6 h post fertilization, but the timing can vary depending on the temperature embryos are kept during early development. PTU has been shown to negatively affect enzymes other than the tyrosinase enzyme that drives production of melanin, when added at or before 24 h post fertilization [50–52]. However, in our protocol, we add PTU once embryos reach shield stage to maximize the reduction of pigmentation. Ultimately, we observe robust RGC axonal regrowth using our PTU conditions.
7. Take care to avoid adding additional anesthetic solution along with larvae to the microcentrifuge tube of low-melt agarose, as to not greatly dilute the concentration of low-melt agarose. Once larvae are added, gently mix the low-melt agarose by pipetting up and down to prevent larvae from settling for too long at the bottom of the tube and to homogenize the low-melt agarose and anesthetic solution. Briefly rinse the pipet by pipetting E3 medium after transferring larvae to prevent low-melt agarose from solidifying in the pipet.
8. Pipet and orient about one to three larvae into each dome of low-melt agarose. When transections are efficient, as many as about 20 larvae can be mounted at a time on the microscopy slide to be transected. When orienting the larvae in the low-melt agarose, use a probe to gently push the larvae into the dome of agarose all the way down to the microscopy slide to keep larvae secured deep within the low-melt agarose dome during transections.
9. This will prevent larvae mounted in low-melt agarose from drying out and help to visualize the larvae during the

transection. However, too much anesthetic solution can cause the low-melt agarose to lift off from the microscopy slide. Only just moisten the low-melt agarose and avoid getting anesthetic solution beneath the agarose.

10. Depending on your handedness or personal preference, the orientation of the larvae and needle as you perform the transection can vary. The person performing the transections in Fig. 1e'–h' is left-handed and inserts the needle from the left. Determine with practice the best angle for yourself to insert the needle into the larvae to get efficient transections.
11. For robust regeneration, it is critical that the location of the transection not be exactly where the RGC axons exit the eye, but distal to the region where RGC axons exit the eye and proximal to the optic chiasm.
12. For robust regeneration, try not to displace the RGC axons from their original path while performing the transection.
13. Larval lethality during optic nerve transection is most commonly caused by an overly aggressive injury with the tungsten needle. Take care to not insert the needle too deeply or multiple times. Use very precise movements.
14. The tungsten needles are not significantly dulled from performing transections. More often the needle becomes bent or dulled by accidentally touching a hard surface. For efficient transections, consider replacing bent or dull tungsten needles for new sharp needles.
15. Transection throughput increases with practice. A person who is experienced in performing transections can mount in low-melt agarose, transect both optic nerves, and remove from the low-melt agarose an average of about 20 larvae in an hour, mounting about one to three larvae in each dome of low-melt agarose.
16. Completely transected nerves have no visible intact axons remaining from the eye to the optic tectum. The degeneration of RGC axons will cause the optic tecta to have marked reduced fluorescence [49].
17. The immunostaining method to stain larvae was modified from a protocol described previously [53].
18. Keep larvae in trypsin for no longer than 5 min on ice. Longer trypsinization has been shown to deform the optic tecta [54].
19. Additional washes or longer durations in PBT can reduce background signal from primary or secondary antibodies.
20. Completely removing all PBT from the larvae before adding non-hardening antifade mounting medium such as Vectashield (VectorLabs) can cause the larvae to shrivel and deform.

Depending on how many larvae are stained in a microcentrifuge tube, keep about 50 μL of PBT in the tube and then add about 100 μL non-hardening antifade mounting medium.

21. We have observed the GFP signal remain fluorescent after fixing *Tg(isl2b:GFP)* larvae, allowing the GFP to be imaged along with the lipophilic dyes.
22. Detergents will disrupt cellular membranes and prevent the diffusion of lipophilic dye along axonal projections. It is critical that larvae are not incubated in solutions with any detergents when using lipophilic dyes to label RGC axons.
23. Make sure to obtain proper training to use your own specific micropipette puller. Pulled capillary needles with short tapers are best for injecting into retinas since longer tapers would be too flexible and are more likely to bend before penetrating the eye.
24. Take care to prevent touching the capillary needle with lipophilic dye to any PBS surrounding the larvae so as not to stain any part of the larvae other than inside the retina.
25. Since the lipophilic dyes are dissolved in volatile liquids, the capillary needle will dry and clog easily. Keep periodically ejecting from the capillary needle to prevent it from clogging. Avoid breaking the capillary needle too much; otherwise, the volume of lipophilic dye ejected may become too great.

Acknowledgments

We would like to thank the members of the Granato laboratory for their comments and discussion. BMH was supported by a University of Pennsylvania Postdoctoral Fellowship for Academic Diversity. This work was supported by grants from the National Institutes of Health to Michael Granato (EY024861 and NS097914).

References

1. Calkins DJ, Pekny M, Cooper ML et al (2017) The challenge of regenerative therapies for the optic nerve in glaucoma. *Exp Eye Res* 157:28–33. <https://doi.org/10.1016/j.exer.2017.01.007>
2. Case LC, Tessier-Lavigne M (2005) Regeneration of the adult central nervous system. *Curr Biol* 15:R749–R753. <https://doi.org/10.1016/j.cub.2005.09.008>
3. Silver J, Miller JH (2004) Regeneration beyond the glial scar. *Nat Rev Neurosci* 5: 146–156. <https://doi.org/10.1038/nrn1326>
4. Villegas-Pérez MP, Vidal-Sanz M, Rasminsky M et al (1993) Rapid and protracted phases of retinal ganglion cell loss follow axotomy in the optic nerve of adult rats. *J Neurobiol* 24:23–36. <https://doi.org/10.1002/neu.480240103>
5. Berkelaar M, Clarke DB, Wang YC et al (1994) Axotomy results in delayed death and apoptosis of retinal ganglion cells in adult rats. *J Neurosci* 14:4368–4374
6. Goldberg JL, Espinosa JS, Xu Y et al (2002) Retinal ganglion cells do not extend axons by

- default: promotion by neurotrophic signaling and electrical activity. *Neuron* 33:689–702. [https://doi.org/10.1016/s0896-6273\(02\)00602-5](https://doi.org/10.1016/s0896-6273(02)00602-5)
7. Park KK, Liu K, Hu Y et al (2008) Promoting axon regeneration in the adult CNS by modulation of the PTEN/mTOR pathway. *Science* 322:963–966. <https://doi.org/10.1126/science.1161566>
 8. Moore DL, Blackmore MG, Hu Y et al (2009) KLF family members regulate intrinsic axon regeneration ability. *Science* 326:298–301. <https://doi.org/10.1126/science.1175737>
 9. Smith PD, Sun F, Park KK et al (2009) SOCS3 deletion promotes optic nerve regeneration in vivo. *Neuron* 64:617–623. <https://doi.org/10.1016/j.neuron.2009.11.021>
 10. Sun F, Park KK, Belin S et al (2011) Sustained axon regeneration induced by co-deletion of PTEN and SOCS3. *Nature* 480:372–375. <https://doi.org/10.1038/nature10594>
 11. de Lima S, Koriyama Y, Kurimoto T et al (2012) Full-length axon regeneration in the adult mouse optic nerve and partial recovery of simple visual behaviors. *Proc Natl Acad Sci U S A* 109:9149–9154. <https://doi.org/10.1073/pnas.1119449109>
 12. Duan X, Qiao M, Bei F et al (2015) Subtype-specific regeneration of retinal ganglion cells following axotomy: effects of osteopontin and mTOR signaling. *Neuron* 85:1244–1256. <https://doi.org/10.1016/j.neuron.2015.02.017>
 13. Norsworthy MW, Bei F, Kawaguchi R et al (2017) Sox11 expression promotes regeneration of some retinal ganglion cell types but kills others. *Neuron* 94:1112–1120.e4. <https://doi.org/10.1016/j.neuron.2017.05.035>
 14. Kurimoto T, Yin Y, Omura K et al (2010) Long-distance axon regeneration in the mature optic nerve: contributions of oncomodulin, cAMP, and pten gene deletion. *J Neurosci* 30:15654–15663. <https://doi.org/10.1523/JNEUROSCI.4340-10.2010>
 15. Pernet V, Joly S, Jordi N et al (2013) Misguidance and modulation of axonal regeneration by Stat3 and Rho/ROCK signaling in the transparent optic nerve. *Cell Death Dis* 4:e734. <https://doi.org/10.1038/cddis.2013.266>
 16. Rasmussen JP, Sagasti A (2017) Learning to swim, again: axon regeneration in fish. *Exp Neurol* 287:318–330. <https://doi.org/10.1016/j.expneurol.2016.02.022>
 17. Becker T, Wullmann MF, Becker CG et al (1997) Axonal regrowth after spinal cord transection in adult zebrafish. *J Comp Neurol* 377:577–595
 18. Hui SP, Dutta A, Ghosh S (2010) Cellular response after crush injury in adult zebrafish spinal cord. *Dev Dyn* 239:2962–2979. <https://doi.org/10.1002/dvdy.22438>
 19. Ma L, Yu Y-M, Guo Y et al (2012) Cysteine- and glycine-rich protein 1a is involved in spinal cord regeneration in adult zebrafish. *Eur J Neurosci* 35:353–365. <https://doi.org/10.1111/j.1460-9568.2011.07958.x>
 20. Goldshmit Y, Sztaf TE, Jusuf PR et al (2012) Fgf-dependent glial cell bridges facilitate spinal cord regeneration in zebrafish. *J Neurosci* 32:7477–7492. <https://doi.org/10.1523/JNEUROSCI.0758-12.2012>
 21. Hui SP, Sengupta D, Lee SGP et al (2014) Genome wide expression profiling during spinal cord regeneration identifies comprehensive cellular responses in zebrafish. *PLoS One* 9:e84212. <https://doi.org/10.1371/journal.pone.0084212>
 22. Mokalled MH, Patra C, Dickson AL et al (2016) Injury-induced ctgfa directs glial bridging and spinal cord regeneration in zebrafish. *Science* 354:630–634. <https://doi.org/10.1126/science.aaf2679>
 23. Becker CG, Meyer RL, Becker T (2000) Gradients of ephrin-A2 and ephrin-A5b mRNA during retinotopic regeneration of the optic projection in adult zebrafish. *J Comp Neurol* 427:469–483
 24. Veldman MB, Bembem MA, Thompson RC, Goldman D (2007) Gene expression analysis of zebrafish retinal ganglion cells during optic nerve regeneration identifies KLF6a and KLF7a as important regulators of axon regeneration. *Dev Biol* 312:596–612. <https://doi.org/10.1016/j.ydbio.2007.09.019>
 25. Zou S, Tian C, Ge S, Hu B (2013) Neurogenesis of retinal ganglion cells is not essential to visual functional recovery after optic nerve injury in adult zebrafish. *PLoS One* 8:e57280. <https://doi.org/10.1371/journal.pone.0057280>
 26. Kaneda M, Nagashima M, Nunome T et al (2008) Changes of phospho-growth-associated protein 43 (phospho-GAP43) in the zebrafish retina after optic nerve injury: a long-term observation. *Neurosci Res* 61:281–288. <https://doi.org/10.1016/j.neures.2008.03.008>
 27. Saul KE, Koke JR, García DM (2010) Activating transcription factor 3 (ATF3) expression in the neural retina and optic nerve of zebrafish during optic nerve regeneration. *Comp Biochem Physiol, Part A Mol Integr Physiol* 155:172–182. <https://doi.org/10.1016/j.cbpa.2009.10.042>

28. Bollmann JH (2019) The zebrafish visual system: from circuits to behavior. *Annu Rev Vis Sci* 5:269–293. <https://doi.org/10.1146/annurev-vision-091718-014723>
29. Culverwell J, Karlstrom RO (2002) Making the connection: retinal axon guidance in the zebrafish. *Semin Cell Dev Biol* 13:497–506
30. Lewis KE, Eisen JS (2003) From cells to circuits: development of the zebrafish spinal cord. *Prog Neurobiol* 69:419–449. [https://doi.org/10.1016/s0301-0082\(03\)00052-2](https://doi.org/10.1016/s0301-0082(03)00052-2)
31. Briona LK, Dorsky RI (2014) Radial glial progenitors repair the zebrafish spinal cord following transection. *Exp Neurol* 256:81–92. <https://doi.org/10.1016/j.expneurol.2014.03.017>
32. Briona LK, Poulain FE, Mosimann C, Dorsky RI (2015) Wnt/ β -catenin signaling is required for radial glial neurogenesis following spinal cord injury. *Dev Biol* 403:15–21. <https://doi.org/10.1016/j.ydbio.2015.03.025>
33. Ohnmacht J, Yang Y, Maurer GW et al (2016) Spinal motor neurons are regenerated after mechanical lesion and genetic ablation in larval zebrafish. *Development* 143:1464–1474. <https://doi.org/10.1242/dev.129155>
34. Wehner D, Tsarouchas TM, Michael A et al (2017) Wnt signaling controls pro-regenerative Collagen XII in functional spinal cord regeneration in zebrafish. *Nat Commun* 8:126. <https://doi.org/10.1038/s41467-017-00143-0>
35. Anguita-Salinas C, Sánchez M, Morales RA et al (2019) Cellular dynamics during spinal cord regeneration in larval zebrafish. *Dev Neurosci* 41:112–122. <https://doi.org/10.1159/000500185>
36. Rosenberg AF, Wolman MA, Franzini-Armstrong C, Granato M (2012) In vivo nerve-macrophage interactions following peripheral nerve injury. *J Neurosci* 32:3898–3909. <https://doi.org/10.1523/JNEUROSCI.5225-11.2012>
37. Ducommun Priest M, Navarro MF, Bremer J, Granato M (2019) Dynein promotes sustained axonal growth and Schwann cell remodeling early during peripheral nerve regeneration. *PLoS Genet* 15:e1007982. <https://doi.org/10.1371/journal.pgen.1007982>
38. Gribble KD, Walker LJ, Saint-Amant L et al (2018) The synaptic receptor Lrp4 promotes peripheral nerve regeneration. *Nat Commun* 9:2389. <https://doi.org/10.1038/s41467-018-04806-4>
39. Stuermer CA (1988) Retinotopic organization of the developing retinotectal projection in the zebrafish embryo. *J Neurosci* 8:4513–4530
40. Burrill JD, Easter SS (1994) Development of the retinofugal projections in the embryonic and larval zebrafish (*Brachydanio rerio*). *J Comp Neurol* 346:583–600. <https://doi.org/10.1002/cne.903460410>
41. Brockerhoff SE, Hurley JB, Janssen-Bienhold U et al (1995) A behavioral screen for isolating zebrafish mutants with visual system defects. *Proc Natl Acad Sci U S A* 92:10545–10549
42. Easter SS, Nicola GN (1996) The development of vision in the zebrafish (*Danio rerio*). *Dev Biol* 180:646–663
43. Gahtan E, Tanger P, Baier H (2005) Visual prey capture in larval zebrafish is controlled by identified reticulospinal neurons downstream of the tectum. *J Neurosci* 25:9294–9303. <https://doi.org/10.1523/JNEUROSCI.2678-05.2005>
44. Orger MB, Baier H (2005) Channeling of red and green cone inputs to the zebrafish optomotor response. *Vis Neurosci* 22:275–281. <https://doi.org/10.1017/S0952523805223039>
45. Burgess HA, Schoch H, Granato M (2010) Distinct retinal pathways drive spatial orientation behaviors in zebrafish navigation. *Curr Biol* 20:381–386. <https://doi.org/10.1016/j.cub.2010.01.022>
46. Bianco IH, Kampff AR, Engert F (2011) Prey capture behavior evoked by simple visual stimuli in larval zebrafish. *Front Syst Neurosci* 5:101. <https://doi.org/10.3389/fnsys.2011.00101>
47. Temizer I, Donovan JC, Baier H, Semmelhack JL (2015) A visual pathway for looming-evoked escape in larval zebrafish. *Curr Biol* 25:1823–1834. <https://doi.org/10.1016/j.cub.2015.06.002>
48. Pittman AJ, Law M-Y, Chien C-B (2008) Pathfinding in a large vertebrate axon tract: isotypic interactions guide retinotectal axons at multiple choice points. *Development* 135:2865–2871. <https://doi.org/10.1242/dev.025049>
49. Harvey BM, Baxter M, Granato M (2019) Optic nerve regeneration in larval zebrafish exhibits spontaneous capacity for retinotopic but not tectum specific axon targeting. *PLoS One* 14:e0218667. <https://doi.org/10.1371/journal.pone.0218667>
50. Li Z, Ptak D, Zhang L et al (2012) Phenylthiourea specifically reduces zebrafish eye size. *PLoS One* 7:e40132. <https://doi.org/10.1371/journal.pone.0040132>
51. Elsalini OA, Rohr KB (2003) Phenylthiourea disrupts thyroid function in developing zebrafish. *Dev Genes Evol* 212:593–598. <https://doi.org/10.1007/s00427-002-0279-3>

52. Bohnsack BL, Gallina D, Kahana A (2011) Phenothiourea sensitizes zebrafish cranial neural crest and extraocular muscle development to changes in retinoic acid and IGF signaling. *PLoS One* 6:e22991. <https://doi.org/10.1371/journal.pone.0022991>
53. Randlett O, Wee CL, Naumann EA et al (2015) Whole-brain activity mapping onto a zebrafish brain atlas. *Nat Methods* 12:1039–1046. <https://doi.org/10.1038/nmeth.3581>
54. Marquart GD, Tabor KM, Horstick EJ et al (2017) High-precision registration between zebrafish brain atlases using symmetric diffeomorphic normalization. *Gigascience* 6:1–15. <https://doi.org/10.1093/gigascience/gix056>



Surgical Methods in Postmetamorphic *Xenopus laevis*: Optic Nerve Crush Injury Model

Alexis M. Feidler, Hieu H. M. Nguyen, and Fiona L. Watson

Abstract

Many human optic neuropathies lead to crippling conditions resulting in partial or complete loss of vision. While the retina is made up of several different cell types, retinal ganglion cells (RGCs) are the only cell type connecting the eye to the brain. Optic nerve crush injuries, wherein RGC axons are damaged without severing the optic nerve sheath, can serve as a model for traumatic optical neuropathies as well as some progressive neuropathies such as glaucoma. In this chapter, we describe two different surgical methods for establishing an optic nerve crush (ONC) injury in the postmetamorphic frog, *Xenopus laevis*. Why use the frog as an animal model? Mammals lose the ability to regenerate damaged CNS neurons, but amphibians and fish retain the ability to regenerate new RGC bodies and regrow RGC axons following an injury. In addition to presenting two different surgical ONC injury methods, we highlight their advantages and disadvantages and discuss the distinctive characteristics of *Xenopus laevis* as an animal model for studying CNS regeneration.

Key words Optic nerve crush, Optic nerve injury model, Retinal ganglion cells, Regeneration, Glaucoma, CNS regeneration injury model

1 Introduction

Optic nerve crush (ONC) injury paradigms in established animal models are useful for studying traumatic optic neuropathies and progressive neurodegenerative eye diseases. An optic nerve crush injury is generated by manually severing the RGC axons in the optic nerve without severing the optic sheath that surrounds the RGC axons. Not only does the crush injury method provide a good tool for studying regeneration and neural protection, but it also provides a useful model for studying the degenerative patterns that occur during progressive neurodegeneration following a trauma. Coupling disease and injury models with cell type-specific reporters such as green fluorescent protein (GFP) under control of an RGC-driven promoter such as Thy-1 in mammals or islet 2b in amphibians is particularly helpful as it provides a way to visually

track RGC loss, axonal damage, and any subsequent regrowth in relation to specific molecules of interest [1, 2]. Amphibians and other anamniotes are able to regenerate axons within their optic nerve well into adulthood, thus providing a useful model to study the mechanisms and genetic programs that govern the processes of regeneration, degeneration, and neural protection from cell death [3]. The South African clawed frog, *Xenopus laevis*, is particularly well suited as an animal model for regenerative studies because following metamorphosis from its larval form into its limbed adult form, this animal loses its capacity to regenerate all its CNS neurons with the exception of those in the retina [4]. This unique postmetamorphic partial loss of CNS regenerative capacity highlights how the ONC injury model in *Xenopus* can serve to answer some of the most fundamental questions in regeneration within the same species as well as between species.

Here we provide a stepwise methodological description of two different optic nerve crush injuries in postmetamorphic *Xenopus laevis*. While the two methods differ in their surgical approach, in both ONC injuries, we use forceps to squeeze the optic nerve and sever the RGC axons without penetrating the optic sheath surrounding the nerve. The ventral or buccal ONC surgery requires the crushing forceps to approach the optic nerve ventrally through a cut in the buccal cavity [5]. Using this approach, the optic nerve is crushed 3–5 mm from the optic disc, a location midway between the optic chiasm and eye orbit. The dorsal ONC surgery requires the crushing forceps to approach the optic nerve dorsally through a cut in the conjunctiva surrounding the eye [6]. This surgery is most similar to injury models of glaucoma performed in mice and zebrafish [7, 8]. In this dorsal ONC surgery, the conjunctiva is carefully and partially cut away from the eye and the eye is rolled/tilted forward, while a crush is made approximately 2 mm from the optic nerve head. One advantage of the ventral/buccal ONC surgery is that it produces long nerve sections both distal and proximal to the crush injury that can be easily harvested and imaged. However, the ventral/buccal ONC surgery is more variable in terms of the distance of the crush injury from the optic nerve head, a variability that is likely attributed to individual differences in the blood vessels used as landmarks for initiating the first cut combined with variability in overall differences in individual frog size. In addition, because the distance from the ON head cannot be measured precisely until the experimental endpoint, it can be difficult to locate the site of the ONC injury in post-injury frogs with longer recovery time points because the RGC axons have regenerated. This issue is of particular concern for studies interested in tracking regrowth events occurring locally at the ONC injury site. The dorsal ONC surgery generates a more consistent and reproducible crush in terms of the distance from the ON head regardless of the frog size. One disadvantage is that these surgeries are more

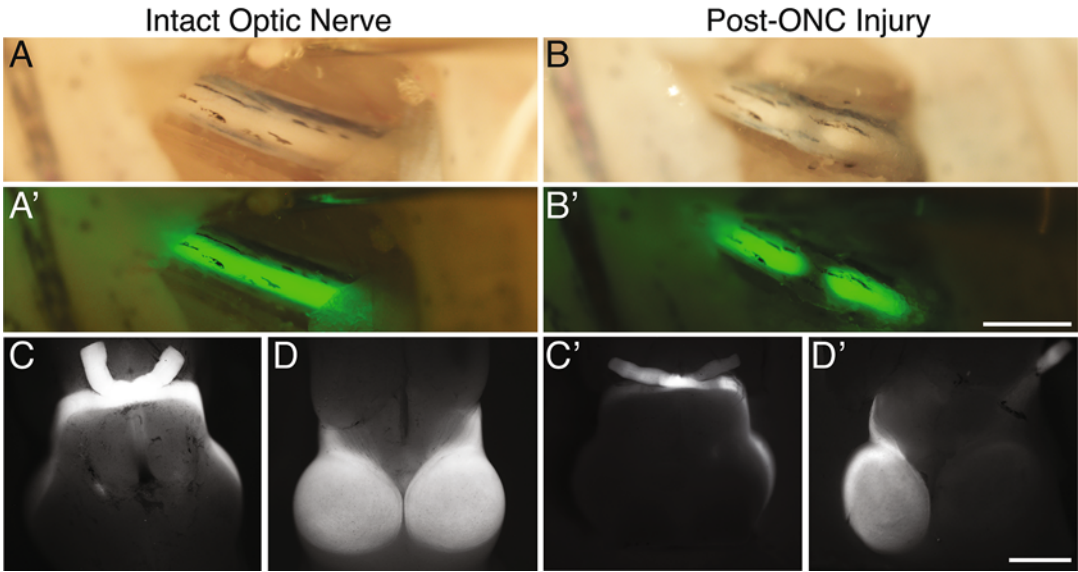


Fig. 1 GFP fluorescence can be used to identify the optic nerve and validate success of the ONC injury. Forceps are used to crush the retinal ganglion cell axons without severing the optic nerve sheath or damaging the blood supply. Representative images from a ventral ONC surgery show an intact optic nerve from a *Tg(islet2b:GFP)* transgenic frog taken using a standard stereoscopic dissecting microscope with white light (**a**), under fluorescence (**a'**), and following a 3 s ONC injury under white light and fluorescence, respectively (**b**, **b'**). Transgenic frog lines expressing endogenous GFP in RGC axons are useful for tracking RGC axon regrowth. In the intact frog, axons can be imaged along the nerve (**b**, **b'**), at the optic chiasm (**c**, **c'**), and in the tectum (**d**, **d'**). Representative images using an epifluorescence dissecting microscope of a naïve (**c**, **d**) and post-ONC injury day 7 (**c'**, **d'**) frog brain show the dorsal side of the optic tectum with the optic chiasm visible (**c**, **c'**) and the ventral side of the optic tectum showing entry of the RGC axons into the tectal area (**d**, **d'**). By post-ONC injury day 7, GFP is no longer visible in the RGC axons in the right optic nerve chiasm (**c'**) or tectum (**d'**). Scale bars = 1 mm (**a–b'**) and 2 mm (**c–d'**) (see **Note 1**)

difficult to perform due to the smaller surgical incision, the presence of increased vasculature at the surgical area that must be avoided, and the possibility of stretching the optic nerve when the eye is rolled forward. Regardless of the surgical approach adopted, working with transgenic animals expressing a GFP reporter in RGC axons provides the opportunity to easily verify the crush by visually observing a loss of fluorescence in the axons at the crush site at the time of the ONC injury (see Fig. 1**b**, **b'**). A loss of GFP fluorescence in the axons at the optic chiasm (see Fig. 1**c**, **c'**) and in the optic tectum can provide additional validation at the experimental endpoint (see Fig. 1**d**, **d'**). Finally, the experimental design and surgical controls merit thoughtful consideration. While individual eyes connect exclusively with the contralateral optic tectum in fish and frog, cross talk between the eyes exist and use of the unoperated eye as a control should, when possible, be avoided [9]. Because *Xenopus laevis* relies on post-injury neural protection mechanisms and regrowth of damaged RGC axons instead of neurogenesis to

restore sight, including both naïve (no surgery) and sham (received an ON surgery without the crush injury) sibling animals will provide the controls necessary to tease apart the inflammatory and immune effects related to the surgery from those related to regeneration.

2 Materials

1. Adult *Xenopus laevis* (see **Note 1**).
2. Forceps Dumont #55, straight.
3. Forceps Dumont #5/45, angled.
4. Forceps Dumont #5, straight.
5. Scalpel handle.
6. Scalpel blades #11.
7. Vannas-Tübingen spring scissors (iris scissors).
8. Insect pins size 000.
9. Dissecting pins.
10. Vinyl, rubber or silicone dissecting pad (~15 cm × 10 cm) (see **Note 2**).
11. Surgical foam, medical gauze, or paper towels (pre-cut into 0.2 cm²) (see **Note 3**).
12. Anesthesia tank or container (see **Note 4**).
13. Recovery tanks (~11 cm × 20 cm) (see **Note 5**).
14. Paper towels.
15. Plastic ruler (15 cm).
16. 10× MMR: 1 M NaCl, 20 mM KCl, 10 mM MgSO₄, 20 mM CaCl₂, 50 mM HEPES (pH 7.8) in RO water. Adjust solution to pH 7.4 using 5 N NaOH (see **Note 6**).
17. 0.1× MMR: Prepare a 100-fold dilution of the 10× MMR stock using RO water. Adjust the solution to pH 7.4 using 5 N NaOH (final concentrations: 0.01 M NaCl, 0.2 mM KCl, 0.1 mM MgSO₄, 0.2 mM CaCl₂, 0.5 mM HEPES) (see **Note 6**).
18. 10× anesthesia: 0.5% Ethyl 3-aminobenzoate methanesulfonate (MS-222/tricaine). Prepare a 0.5 g per 100 mL of 0.1× MMR. Adjust solution to pH 7.4 using 5 N NaOH. Initially this solution is very acidic. Adjust the pH slowly as it tends to jump quickly as you pass pH 4.5.
19. *Xenopus* adult 5× anesthesia: Prepare a 5× strength anesthesia by diluting a 10× anesthesia twofold using 0.1× MMR or RO water. Verify that the pH is maintained near 7.4. Store at 4 °C. This anesthetic can be reused.

20. Recovery solution: Prepare a solution of 0.1× MMR and autoclave.
21. 1× PBS: 137 mM NaCl, 2.7 mM KCL, 10 mM Na₂HPO₄, 1.8 mM KH₂PO₄, 1 mM CaCl₂, 0.5 mM MgCl₂.
22. Stereoscopic dissecting microscope (*see Note 1*).
23. Dual gooseneck microscope illuminators.

3 Methods

3.1 Anesthetization

1. Fill anesthesia tank or container with *Xenopus* adult 5× anesthesia (*see Note 4*).
2. Place the frog in the anesthesia tank until fully immersed and immediately cover the top with a lid to avoid escape.
3. Prepare a recovery tank containing 1–5 cm optimized frog water or 0.1× MMR for postsurgical recovery (*see Note 5*).
4. Leave the frog in *Xenopus* adult 5× anesthesia until the frog is fully unresponsive to a toe pinch.
5. When the frog is fully anesthetized, measure and record its length from cloaca to snout by removing the frog from anesthesia and placing it ventral side down on a ruler (*see Note 7*).
6. Proceed to either the ventral/buccal surgery (Subheading 3.2) or the dorsal surgery (Subheading 3.3).

3.2 Ventral or Buccal Optic Nerve Crush Injury

1. Become familiar with the anatomy of the adult frog eye (*see Note 8*).
2. Determine whether the right or left eye will receive an ONC injury (*see Note 9*).
3. Place frog's ventral side up on a flexible rubber, vinyl, or silicone mat with the frog's head facing the researcher (*see Fig. 2a*).
4. To prevent the frog's skin from drying out, drape a wet paper towel pre-soaked 0.1× MMR or optimized frog water and cover the frog's entire body leaving only the head exposed. Use a plastic transfer pipette to periodically wet the frog's ventral side with frog water to maintain moisture in their skin (*see Note 10*).
5. Place sturdy dissecting pins on either side of the frog's head on each side of the jaw and stake them to the mat near the jawline (*see Fig. 2a*).
6. Gently thread one thin insect pin (size# 000) through the skin of frog's lower jaw. (*see Fig. 2a*).
7. To expose the top of the buccal cavity and hold the mouth open with the lower jaw out of the way, tether the horizontal

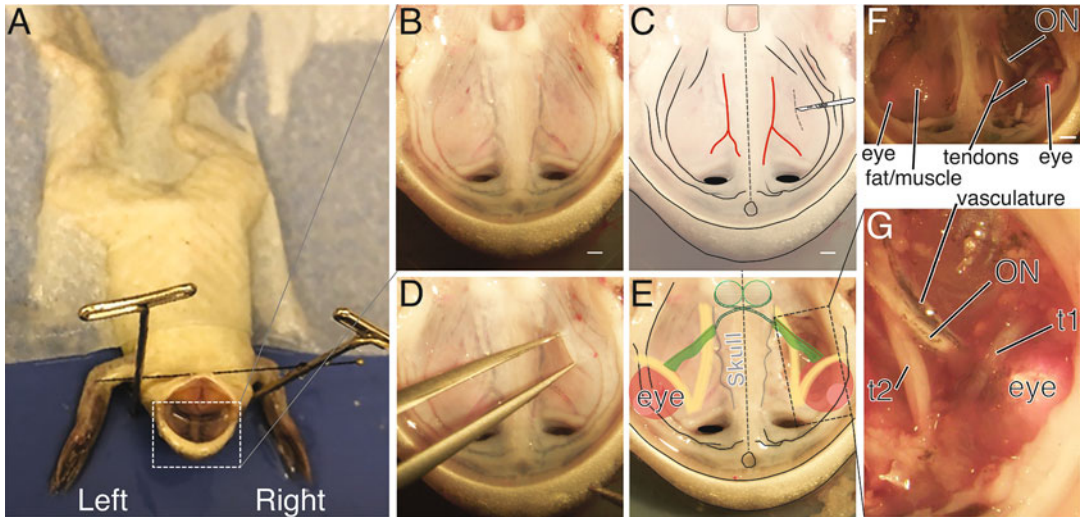


Fig. 2 Ventral/buccal ONC surgery (right ONC). The frog is placed ventral side up on a vinyl dissecting mat (left and right refer to the frog's orientation) (a). A simple three-pin placement stabilizes the frog to provide access to the buccal cavity (a). The vasculature (red) running parallel to midline (dashed line) and the creases in the buccal dermal tissue surrounding the buccal cavity (black lines) emanating from the internal nares (black ovals) provide landmarks to inform the position of the initial surgical incision (b, c). A scalpel can be used to make a shallow incision, and blunt forceps (#5) are used to lift the dermal tissue and expand the incision without damaging the underlying tissue (d). A diagram shows the location of the eyes (red), tendons (yellow), and optic nerve sheath (green) containing the RGC axons with the overlying vasculature (e). Note that as the optic nerve crosses through the bones of the skull into the brain, the thick optic nerve dural sheath is absent (e). The RGC axons from each eye cross at the optic chiasm and synapse with tectal cells in the optic tectum which lies on the underside of the brain. Note that the optic nerve is no longer surrounded by the optic sheath upon entry into the skull (e). Panel f, left of midline, shows the fat and muscles located beneath the buccal dermal layer, while to the right of midline a dissection with the fat and muscles removed reveals the optic nerves and tendons (f). Panel g shows a close-up of the optic nerve (ON), tendons (t1, t2), vasculature (vasc.), and eye. Scale bar = 1 mm (see Note 7)

insect pin attached to the lower jaw using the two dissecting pins (see Fig. 2a, b and Note 11).

8. Using the midline as a guide to distinguish left and right, locate the two prominent blood vessels in the dermal layer at the surface of the buccal cavity (see Fig. 2b, c).
9. In this dermal layer, locate the creases that extend along the jawline from the internal nares (see Fig. 2c).
10. Between the buccal creases and the vasculature that runs parallel to midline, use the scalpel to make a small shallow incision through the dermal layer (see Fig. 2c).
11. Use the forceps to hold pre-cut pieces of surgical foam and absorb any liquid from or near the wound (see Note 12).
12. Using the #5 blunt-ended forceps, expand the incision area by inserting the closed forceps into the slit and gently releasing the

forceps to expand the incision area. Open and close the forceps gently several times to expand the incision area (*see* Fig. 2d and **Note 13**) and continue to use surgical foam as required to absorb any excess fluid.

13. Use a pair of forceps to gently remove any fat overlying the optic nerve (*see* **Note 14**). Continue to use the surgical foam to absorb any excess fluid.
14. To locate the optic nerve lying beneath the muscles, use a pair of #5 forceps to penetrate the muscle fibers and gently move them aside along the length of the muscle fibers (*see* Fig. 2f—compare left and right sides).
15. Once the optic nerve is located, switch to #55 forceps and crush the optic nerve by squeezing the nerve between the tip of the forceps and holding them closed for 5 s (*see* **Note 15**).
16. Proceed to Recovery and Postsurgical Care (*see* Subheading 3.4).

3.3 Dorsal Optic Nerve Crush Injury

1. Become familiar with the anatomy of the adult frog eye before proceeding (*see* **Note 8**).
2. Determine whether the right or left eye will receive an ONC injury (*see* **Note 9**).
3. Place frog's dorsal side up on to a flexible rubber, silicone, or vinyl mat with the frog's snout facing the researcher.
4. To prevent the frog's skin from drying out, immerse a paper towel in optimized frog water or 0.1× MMR and cover the frog's entire body leaving only the head exposed (*see* Fig. 3a). Use a plastic transfer pipette to periodically wet the dorsal side of the frog with water to maintain skin moisture (*see* **Note 10**).
5. Use the forceps in one hand to pull the eyelid and conjunctiva upward (the conjunctiva is the membrane that lines the eye and eyelid) (*see* Fig. 3c and **Note 8**).
6. At the same time, using a scalpel in your other hand, make a small incision on the taught conjunctiva at the top of the eye (*see* Fig. 3c).
7. Use either a pair of forceps or the scalpel to gently separate the conjunctival membrane normally sealed to the eye by approximately 140°–180° around the eye, i.e., the top half of the eye (*see* Fig. 3b, c and **Note 16**).
8. To examine the dermal layer beneath the skin, use iris scissors to make a dorsal cut in the surface epidermal layer (i.e., the skin) at a 45° angle relative to midline (*see* Fig. 3d and **Note 17**).
9. Examine the underlying dermal layer, and locate and avoid any vasculature embedded within this layer (*see* Fig. 3e, f and **Note 18**).

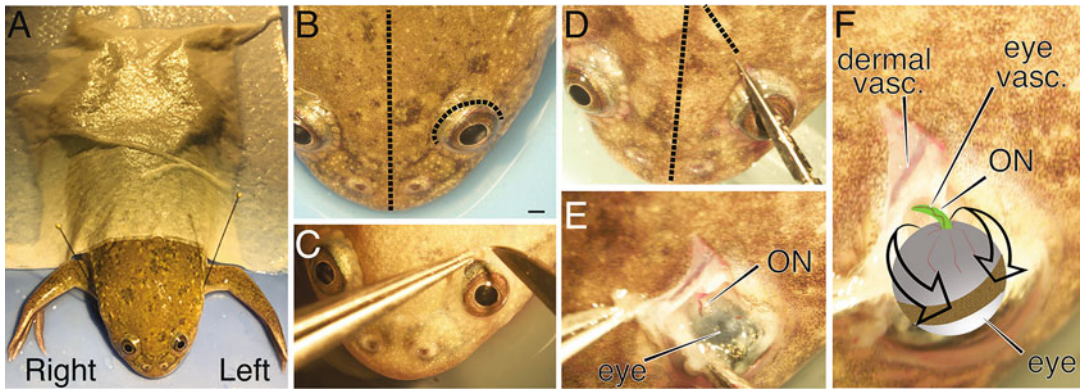


Fig. 3 Dorsal ONC surgery (left ONC). The postmetamorphic frog is placed dorsal side up on a dissecting mat, and pins are placed on either side of the head to limit movement (left and right refer to the frog's orientation) (a). Forceps and/or a scalpel is used to tease away the conjunctival tissue of the eyelid 180° around the eye (b, c). A pair of iris scissors are used to first cut the skin at a 45° angle to midline (d) to locate the vasculature (vasc.) in the dermal layer beneath the skin (e, f). The dermal layer underlying the skin is then cut while avoiding the vasculature so as to expose the eye cavity behind the eye (e). As surgical skills improve, the dermal layer will no longer need to be cut and forceps can be inserted between the eye and dermal layer and used to widen the gap. Blunt forceps are used to gently move the musculature, while a second pair of forceps is used to grasp the conjunctiva above the eye and roll/tilt the eye forward and to the side in order to expose the optic nerve (ON green) which is attached to the base of the eye (e, f). While holding the eye forward with one hand, with the other hand, use sharp #55 or #5/45° angled forceps to crush the optic nerve (ON) for 3 s approximately 2 mm from the eye orbit (e). Crushing the nerve from an angle beneath the optic nerve helps ensure the eye vasculature remains intact. The eye diagram in panel f illustrates the movement of the eye rotation, the optic nerve inside the ON sheath (green), and the eye blood vasculature (red). Scale bar = 1 mm (see Note 7)

10. Slip the tip of the iris scissors or sharp forceps between the dermal layer and the eye and widen the space between the dermal layer and the eye (see Fig. 3d and Note 19).
11. Use a pair of #55 forceps to grasp the conjunctiva and gently roll the eye forward and away from the nasal cavity. This will open the cavity behind the eye and reveal the optic nerve which is located deep at the base of the eye (see Fig. 3e, f and Note 19).
12. If the rectus muscles overlying the eye are obscuring the optic nerve, use blunt-ended forceps in your other hand to penetrate through the layer of muscle fibers and gently move these aside until the optic nerve can be revealed.
13. While maintaining a grasp on the conjunctiva, switch to a pair of sharp 45° angled #55 forceps.
14. Extend the angled forceps into the space behind the frog eye, straddle the optic nerve with the tips of forceps, and squeeze the optic nerve 2 mm away from the optic nerve head firmly for 5 s (see Note 20).

15. Once the optic nerve is crushed, tilt the eye forward again to verify the ONC injury (*see* Fig. 1 and **Note 21**).
16. Use the forceps to gently tip the eye back into the eye socket and return the skin to cover the wound (*see* **Note 22**).
17. Proceed to Recovery and Postsurgical Care (*see* Subheading 3.4).

3.4 Recovery and Postsurgical Care

1. After the surgical procedure is completed, rinse the frog in a bath of optimized frog water or 0.1× MMR to remove any residual anesthesia from the frog's skin.
2. Place the frog in a recovery tank prepared with sufficient optimized frog water or 0.1× MMR to partially immerse frog while leaving its snout and nares exposed to air.
3. Drape a wet paper towel over the frog leaving its snout exposed to air (*see* **Note 5**).
4. Once the frog recovers from anesthesia and is able to move in response to touch, remove the paper towel and either fill the tank completely with water so the frog is fully immersed or move the frog to a maintenance tank.

4 Notes

1. Use of all animal experiments should be carried out in accordance with procedures approved by the Institutional Animal Care and Use Committee (IACUC). The frog genotype should be carefully considered. Wild-type (non-transgenic) frogs can be acquired with naturally pigmented green skin or as albinos which lack the pigmentation in the skin, chromatophores, and the black retinal pigment epithelium (RPE) of the retina. The optic nerve sheath of naturally pigmented frogs is covered in chromatophores and thus facilitates the identification of the optic nerve. However, these chromatophores change in size and location and, if not removed during the dissection, can obscure fluorescence imaging of axonal RGCs in the optic nerve and tectum. To circumvent this problem, albino *Xenopus* are often used to facilitate subsequent imaging of fluorescence in the optic nerve and tectum. However, the absence of chromatophores in albino frogs necessitates the use of additional anatomical landmarks to distinguish the optic nerve from the tendons (*see* **Note 8**). Use of transgenic animals expressing GFP in the retinal ganglion cell (RGC) axons (*Tg(Islet2b:GFP-Cyto)*) can provide many advantages: First, use of these frogs facilitates surgical training as GFP expression in RGC axons can be used to readily identify the optic nerve and allow the quality of the crush injury to be more readily verified at the time of surgery (*see* Fig. 1b, b').

Second, GFP fluorescence in RGC axons terminating in the optic tectum is lost by post-surgery day 7 and does not begin to be expressed in the regenerating RGCs until post-surgery day 35 [2]. Thus, in crush injuries between post-injury day 7 and 35, it is possible to examine the optic tectum (Fig. 1d, d') using a fluorescence dissecting microscope at the experimental endpoint and quickly confirm whether the ONC was full, partial, or failed. In addition to being able to exclude samples that have not been fully crushed, this feedback helps refine the surgical skills of the individual performing the crush injuries and helps build the confidence necessary to achieve a 95–100% surgical success rate. Third, the GFP in degenerating RGC axons appears as large green puncta in the RGC axons extending from the crush site to the tectum. Used in conjunction with other molecular reagents such as *in situ* probes or antibodies to study regeneration, this punctate pattern can provide valuable feedback during the imaging phase of experiments. While the use of transgenic frog lines can be advantageous, visualization of fluorescence requires a fluorescent stereoscopic dissecting microscope, a cost that can be prohibitive. Published transgenic frog lines are fully characterized [2, 10] and available upon request either from the author or purchased through the National Xenopus Resource (NXR, RRID:SCR_013731, <http://www.mbl.edu/xenopus>).

2. Use of a mat is particularly important for the ventral or buccal ONC injury as dissecting pins are inserted into the mat and used to tether the mouth open. Thus, the mat should be thick enough to hold large dissecting pins vertically and withstand sufficient pressure to hold the jaw open.
3. Surgical foam is preferable to paper towels or gauze as a very small amount of surgical foam can absorb more liquid than paper towel or gauze and does not shred.
4. For small- to medium-sized adult frogs (cloaca to snout lengths up to 8 cm), a 500 mL plastic beaker filled with anesthesia is sufficient. The beaker should be placed in a lidded secondary container to help contain any anesthesia splashed by the frog.
5. To avoid any possibility of drowning while the frogs are fully anesthetized, prepare a recovery tank with sufficient water to partially immerse the frog without immersing its external nares in the snout. After the surgery, immediately rinse the frog in a container of water to remove any residual anesthesia, and place the frog in the recovery tank. To keep the frog's skin moist, drape a wet towel over its body making sure that the head is not covered.

6. Reverse osmosis (RO) water or other filtered water that removes chlorine and other chemical contaminants must be used to make reagents in which frogs will be immersed. If available, water optimized for frogs with water parameters that include pH and conductivity [11] can be used in lieu of $0.01\times$ MMR.
7. Placing a ruler atop of a clean rubber/vinyl mat in a tray limits water puddling in the lab.
8. Frog anatomy: The surface of the buccal cavity consists of a dermal layer (*see* Fig. 2b, c) beneath which the sclera, the tough opaque outer layer of tissue protecting the eye orbit, can be seen (*see* Fig. 2e, f left of midline). The sclera of the eye transitions posteriorly into the optic nerve dural sheath, a thick and tough sheath containing the optic nerve that extends from the back of the eye to the skull (*see* Fig. 2e–g). In the area between the skull and eye, two tendons (ligaments) can also be observed. These tendons can be distinguished from the optic nerve based on their attachment sites and their appearance. The tendon of membrana nictitans (t1) overlays the base of the eye and can be easily avoided as it is oriented perpendicular to the optic nerve (*see* Fig. 2f, g). A second tendon (t2) runs at a parallel angle to the optic nerve but extends beneath the optic nerve sheath (*see* Fig. 2e–g). Tendons can also be distinguished from the optic nerve based on their coloring and texture. Typically, tendons appear opaque (white with a yellowish tint), whereas the optic nerve sheath of frogs with natural green pigmentation is opaque (white with a gray tint) and is covered with chromatophores, making the optic nerve easily distinguishable from the tendons. A large blood vessel is located at the surface of the optic sheath and can be used to further distinguish the optic nerve from the tendons. To facilitate fluorescence imaging of the optic nerve and tectum during the analysis phase of the experiment, albino frogs are often used instead of naturally pigmented frogs because the chromatophores are absent. Performing ONC injuries on albino *Xenopus* requires additional skill because the identification of the optic nerve relies primarily on anatomical landmarks and differences in tissue coloration and texture. Increasing the magnification of the dissecting microscope along with practice will help in the identification of optic nerves lacking chromatophores. In addition to the tendons, a layer of fat and muscles (rectus muscles) are attached to the eye. The muscles are anchored to the bones and sclera at either end and surround the optic nerve (*see* Fig. 2f left eye). These muscle fibers appear as white translucent fibrous tissues and readily distinguishable from the optic nerve, while the fat appear as large fatty globular cells.

9. It is critical to define the left and right optic nerve. Typically, the left optic nerve is defined as the frog's left side when it is lying on its ventral side facing away from the researcher (*see* Figs. 2a and 3a). The choice of which optic nerve to crush is important as all subsequent experiments will likely be performed on this same side. The choice will largely depend on the skill of the individual(s) performing the surgeries and whether this individual is right- or left-handed.
10. The frog skin is very delicate and should remain wet/moist at all times. Periodically monitor the skin of the frog. If the surgery is taking longer than a few minutes, use a plastic transfer pipette to wet the towel overlaying the frog to avoid drying of the skin. Instead of draping the frog with a wet towel, the frog can be wrapped in a wet towel with its head poking out of the towel "envelope."
11. A thick vinyl or rubber mat can help anchor the dissecting pins securely to the mat. Anchoring the pins to the mat is especially important since the thin horizontal pin will be used to wedge open the mouth and can strain the vertical dissecting pins (*see* Fig. 2a).
12. Depending on the size of the wound, a significant amount of fluid can accumulate in the space overlying the optic nerve making the optic nerve hard to locate. Use forceps to hold a small pre-cut piece of surgical foam to absorb the excess fluid. This procedure may have to be repeated until all the excess fluid is removed.
13. As you expand the incision area using the forceps, lift the dermal layer so as not to damage any of the underlying tissues (Fig. 2d). An improvement of the surgical skills will lead to a decrease in the incision size. Depending on the size of the frogs, the incision can expand up to 0.5–1 cm in length.
14. Large adult frogs have more fat than newly metamorphosed juvenile frogs. The fat can lie atop of the optic nerve within the muscle fibers making it difficult to locate the optic nerve. The fat can be readily distinguished from the muscle as it appears as large fatty globules, while the muscle appears as long thick fibrous tissue. Partial removal of the fat may be required to locate the optic nerve. The fat, easily removed using forceps, will not lead to any bleeding. There will however be an accumulation of fluid which can be absorbed using surgical foam.
15. Squeezing the optic nerve will also temporarily squeeze the vasculature supplying blood to the retina. The RGC axons are fragile and can be severed without damaging the optic nerve sheath or the overlying vasculature. The blood supply to the eye should resume following the optic nerve crush. The crush requires a balance of sufficient force to sever the axons without

permanently damaging or tearing the overlying blood supply or damaging the optic nerve sheath. If the vasculature ruptures, abort the surgery as the retina will be damaged due to prolonged lack of blood supply and/or pooling of blood. At the experimental endpoint, a quick examination of the retina can exclude any retinæ that have either been damaged by too much blood or a lack of blood.

16. Clearing the conjunctival membrane surrounding the eye facilitates tilting the eye forward. However, do not exceed cutting the conjunctival tissue from the eye more than halfway around the eye (180°). Clearing the tissue surrounding the entire eye can lead to the loss of the entire eyeball during the recovery period.
17. The frog skin is supplied by many small blood vessels. These can be easily seen and avoided in the skin of the albino frog but may be more difficult to see and avoid in naturally pigmented frogs. As the skill of the surgery is mastered, this dorsal optic nerve crush surgery can be performed without the need to cut the skin (as shown in Fig. 3d). Instead, once the conjunctiva between the eye and dermal layers is cut, the skin can simply be pulled back and the forceps are inserted directly into the gap behind the eye to access the optic nerve (*see Note 20*). If a blood vessel is cut, use forceps to apply pressure to the wound using small pre-cut pieces of surgical foam. The bleeding will not be excessive and should not interfere with the surgery.
18. The dermal layer beneath the skin is highly vascularized. A large blood vessel that is part of a larger network of blood vessels is oriented along the perimeter of the top of the eye and is embedded into the dermal layer (*see Fig. 3e, f*). It is critical to avoid the vasculature in the overlying dermal layer as blood from these blood vessels can flood into the area surrounding the eye and seep into the exposed eye cavity making it difficult to locate the optic nerve. If this occurs, surgical foam may be used to apply pressure to the wound to stop the bleeding. However, if the bleeding persists or if the cavity behind the eye is filled with blood, we recommend aborting the surgery because the excessive blood may damage the retina and compromise the experiment.
19. The iris scissors or forceps can be inserted between the dermal layer and the sclera surrounding the eye without damaging the dermal vasculature. Once inserted, release the forceps or iris scissors to widen the gap between the sclera and the dermal tissue. The gap should be sufficient to peer into the cavity and locate the optic nerve once the eye is tilted forward.

20. The optic nerve is located at the base of the eye (towards the frog's ventral side) opposite the lens so the optic nerve cannot be accessed without rolling the eye forward. Because the optic nerve is located so deep, it can be difficult to see. It is important to distinguish between the optic nerve and the tendons (*see Note 8*). Depending on the size of the frog, the optic nerve may be obscured by the rectus muscles attached to the eye. In small juvenile frogs, there is little fat and the nerve can be readily identified. In large adult frogs, locating the nerve is more difficult as the nerve may lie beneath the musculature and fat. Tip the eye forward and angle the eye away from the snout and examine the area carefully. Leaving a small amount of conjunctival tissue above the eye can be useful to help grasp the eye to roll the eye forward. Switch between the low- and high-powered magnification to help locate the optic nerve and visualize the crush. If the rectus muscle attached to the eye obscures the optic nerve, use the forceps to penetrate and move aside the muscle along the length of the fiber so as to minimize any muscle fiber damage. Use the forceps to open a space leading to the back of the eye. This part of the surgery requires practice as it can be tricky to hold the eye tilted forward; see the optic nerve and perform the crush. Visualizing the optic nerve at the same time as manually crushing it without making a large surgical incision is the most challenging part of the surgery. When learning to perform the optic nerve crush injury, we rely on visual confirmation of the crush. Thus, the initial crushes may have large injuries. As this technical skill is mastered, one can visually identify the nerve and then switch to using the tactile senses to accurately position the forceps around the nerve and then crush it using the tips of the forceps without the need for cutting the dermal layer. After the crush, tip the head forward to validate the crush. This skill will improve until the individual performing the surgery can visually see the optic nerve, hold the eye in situ, and rely on the tactile senses to "feel" the location of the optic nerve with the forceps and perform the crush. Inserting a wet paper towel that has been tightly rolled up into a cylindrical shape into the frog's mouth can project the eye outward and make it easier to locate the optic nerve. Use the tips of the forceps to squeeze the nerve. Be consistent in terms of the position of the tips used to squeeze the nerve, the time, and the distance from the eye as these parameters can increase experimental variability.
21. A successful optic nerve crush should appear as a translucent and flattened stretch of nerve (*see Fig. 1a, a'*). In transgenic frogs expressing GFP in RGC axons, a break in the fluorescence at the site of the crush injury should be visible (*see Fig. 1b, b'*).
22. The skin heals nicely of its own accord without any incidences of infection.

Acknowledgments

Many thanks to Mr. Dave Pfaff and Cleveland Candle for their design help with Illustrator.

References

1. Dratviman-Storobinsky O, Hasanreisoglu M, Offen D et al (2008) Progressive damage along the optic nerve following induction of crush injury or rodent anterior ischemic optic neuropathy in transgenic mice. <http://www.molvis.org/molvis/v14/a254/>. Accessed 2 Mar 2021
2. Whitworth GB, Misaghi BC, Rosenthal DM et al (2017) Translational profiling of retinal ganglion cell optic nerve regeneration in *Xenopus laevis*. *Dev Biol* 426:360–373. <https://doi.org/10.1016/j.ydbio.2016.06.003>
3. Phipps LS, Marshall L, Dorey K, Amaya E (2020) Model systems for regeneration: *Xenopus*. *Development* 147:dev180844. <https://doi.org/10.1242/dev.180844>
4. Belrose JL, Prasad A, Sammons MA et al (2020) Comparative gene expression profiling between optic nerve and spinal cord injury in *Xenopus laevis* reveals a core set of genes inherent in successful regeneration of vertebrate central nervous system axons. *BMC Genomics* 21:540. <https://doi.org/10.1186/s12864-020-06954-8>
5. Szaro BG, Loh YP, Hunt RK (1985) Specific changes in axonally transported proteins during regeneration of the frog (*Xenopus laevis*) optic nerve. *J Neurosci* 5:192–208
6. Zhao Y, Szaro BG (1994) The return of phosphorylated and nonphosphorylated epitopes of neurofilament proteins to the regenerating optic nerve of *Xenopus laevis*. *J Comp Neurol* 343:158–172. <https://doi.org/10.1002/cne.903430112>
7. Tang Z, Zhang S, Lee C et al (2011) An optic nerve crush injury murine model to study retinal ganglion cell survival. *J Vis Exp* 2685. <https://doi.org/10.3791/2685>
8. Liu Q, Londraville RL (2003) Using the adult zebrafish visual system to study cadherin-2-expression during central nervous system regeneration. *Methods Cell Sci* 25:71–78. <https://doi.org/10.1023/B:MICS.0000006854.18378.fc>
9. Ananthakrishnan L, Szaro BG (2009) Transcriptional and translational dynamics of light neurofilament subunit RNAs during *Xenopus laevis* optic nerve regeneration. *Brain Res* 1250:27–40. <https://doi.org/10.1016/j.brainres.2008.11.002>
10. Watson FL, Mills EA, Wang X et al (2012) Cell type-specific translational profiling in the *Xenopus laevis* retina. *Dev Dyn Off Publ Am Assoc Anat* 241:1960–1972. <https://doi.org/10.1002/dvdy.23880>
11. McNamara S, Wlzlza M, Horb ME (2018) Husbandry, general care, and transportation of *Xenopus laevis* and *Xenopus tropicalis*. In: Vleminckx K (ed) *Xenopus*. Springer, New York, pp 1–17



Generating Widespread and Scalable Retinal Lesions in Adult Zebrafish by Intraocular Injection of Ouabain

Diana M. Mitchell and Deborah L. Stenkamp

Abstract

Zebrafish regenerate functional retinal neurons after injury. Regeneration takes place following photic, chemical, mechanical, surgical, or cryogenic lesions, as well as after lesions that selectively target specific neuronal cell populations. An advantage of chemical retinal lesion for studying the process of regeneration is that the lesion is topographically widespread. This results in the loss of visual function as well as a regenerative response that engages nearly all stem cells (Müller glia). Such lesions can therefore be used to further our understanding of the process and mechanisms underlying re-establishment of neuronal wiring patterns, retinal function, and visually mediated behaviors. Widespread chemical lesions also permit the quantitative analysis of gene expression throughout the retina during the period of initial damage and over the duration of regeneration, as well as the study of growth and targeting of axons of regenerated retinal ganglion cells. The neurotoxic Na⁺/K⁺ ATPase inhibitor ouabain specifically offers a further advantage over other types of chemical lesions in that it is scalable; the extent of damage can be targeted to include only inner retinal neurons, or all retinal neurons, simply by adjusting the intraocular concentration of ouabain that is used. Here we describe the procedure through which these “selective” vs. “extensive” retinal lesions can be generated.

Key words Regeneration, Retina, Zebrafish, Ouabain, Lesion, Central nervous system, Müller glia, Eye, Intravitreal injection

1 Introduction

The zebrafish has emerged as an outstanding model organism for the study of tissue regeneration. Zebrafish have the capacity to functionally regenerate appendages, cardiac and skeletal muscle, bone, the pancreas, the liver, hair cells of the lateral line, and tissues of the central nervous system including the spinal cord, brain, and retina (reviewed by [1]). In addition, zebrafish are amenable to genetic manipulations, high-throughput screens, and the transgenic expression of molecule- and cell-specific fluorescent reporters, permitting investigators to interrogate the mechanisms

underlying regeneration and to visualize the regenerative process (reviewed by [2]). Insights derived from tissue regeneration in zebrafish are rapidly being applied to mammalian model systems (reviewed by [3]), with the ultimate goal of translating this knowledge for human therapeutics to treat human retinal disease and trauma (reviewed by [4]).

The study of zebrafish retinal regeneration in particular has contributed to the key findings that the primary glial cells of the retina—Müller glia—act as the stem cells that produce neural progenitors that repopulate the retina with neurons lost due to the original damage [5–9]. The field of zebrafish retinal regeneration is currently focused upon understanding the genetic and epigenetic changes that take place in Müller glia to promote regeneration [10–19], the roles of the inflammatory response/microglia in regulating regeneration [20–23], as well as the restoration of retinal architecture [24–27], circuitry [28–30], and visual function [25, 26, 29]. To gain these and other advancements, and to facilitate future objectives, investigators have incorporated a broad array of retinal lesioning approaches, each with specific advantages for the investigators' aims.

In our laboratories, we use a chemical lesion approach to injure the zebrafish retina with intraocular injection of the neurotoxin ouabain [21, 22, 25, 26, 29, 30]. Our method was adapted from that of previous investigators studying retinal regeneration in goldfish [31–33], carp [34], and trout [35] and has seen considerable use by others who study zebrafish retinal regeneration [9, 24, 36, 37]. Ouabain is an inhibitor of the Na⁺/K⁺ ATPase enzyme found in abundance on neurons [38], and the poisoning of this enzyme by ouabain leads to death of retinal neurons [21, 24, 25]. Because ouabain is injected into the vitreal chamber, this lesioning strategy results in widespread destruction of retinal neurons, such that visual function is measurably impaired [25, 26, 29]. A widespread and tissue-disruptive lesion, rather than targeted destruction of a selected cell type, or region of the retina [27, 28, 39, 40], facilitates the quantitative evaluation of global transcriptional and protein changes over time [26, 36, 41], the examination of inflammatory responses [21, 22], the study of the restoration of retinal architecture [24–26], circuitry [29, 30], and axon outgrowth and pathfinding of the regenerated neurons [26] and permits the evaluation of functional recovery with behavioral and electrophysiological analyses [25, 26, 29]. A further advantage to the use of ouabain for chemical lesioning of the zebrafish retina is that it is scalable; a reduced concentration of the injected ouabain solution results in the destruction of fewer retinal neuronal layers [24–26], allowing researchers to examine regeneration of selected cell types.

2 Materials

2.1 Solutions

1. 0.4% MS-222 stock solution: Prepare a 0.4% (w/v) MS-222 stock solution by adding 0.8 g pharmaceutical grade tricaine methane sulfonate (MS-222) to 4.2 mL 1 M Tris-HCl, pH 7.5 buffer in ultrapure water (*see Note 1*). In fish-safe glassware (*see Note 2*), bring volume to 200 mL with ultrapure water. Adjust the pH to 7.0 with 1 M NaOH added dropwise. Prepare 4.25 mL aliquots and freeze for future use.
2. Anesthetic solution: Prepare a fresh solution of 0.1% MS-222 (163 mg/L) by adding 4.25 mL of thawed, 0.4% MS-222 stock solution (4 mg MS-222/mL) to 100 mL of zebrafish system water in a 250 mL glass beaker reserved only for zebrafish handling.
3. 6.5% (w/v) NaCl solution: Add 0.65 g of NaCl to a 15 mL conical tube (or other appropriate fish-safe glassware; *see Note 2*), bring to 10 mL with ultrapure water, and mix until dissolved. Sterilize the solution by passing through a 0.22 μ m filter.
4. 0.65% NaCl solution: Add 1 mL of the 6.5% NaCl solution to 9 mL of ultrapure water and mix. Sterilize the solution by passing through a 0.22 μ m filter.
5. 2 mM ouabain stock solution: Prepare by adding 7.2875 mg ouabain octahydrate to 5 mL ultrapure water (*see Note 3* for safety precautions). Sterilize the solution by passing through a 0.22 μ m filter (*see Note 2*).
6. 200 μ M ouabain solution: 200 μ M ouabain, 0.65% NaCl. Combine 1 mL of 2 mM ouabain stock solution with 1 mL of 6.5% NaCl solution and 8 mL ultrapure water (*see Notes 2, 3, and 4*).
7. 40 μ M ouabain solution: Prepare 1 mL of 40 μ M ouabain by mixing 200 μ L of 200 μ M ouabain solution with 800 μ L of 0.65% NaCl solution (*see Notes 2, 3, and 4*).
8. Zebrafish system water: One or more 1–4 L tanks with system water from the zebrafish facility will be needed for recovery of each fish following the procedure.
9. 70% EtOH in a squirt bottle.
10. 100% ultrapure water in a sterile plastic beaker.

2.2 Supplies

1. Dial calipers.
2. Sapphire microknife (SS Handle, 13 cm, retractable with 0.75 mm blade).
3. Blunt-end 10 μ L Hamilton syringe, 26 s gauge, point style 3 (Hamilton CAL80075 1701 N PT3, calibrated).

4. Fish transfer net.
5. Nitrile gloves.
6. Plastic transfer pipettes.
7. Spoon for handling adult fish.
8. Plastic wrap.
9. Paper towels.
10. Kimwipes.

2.3 Equipment

1. Stereomicroscope, (5 \times , with 220 mm working distance objective is effective).
2. Fiber-optic light source to illuminate fish undergoing procedure.
3. Micromanipulator, preferably a manual, bar-mounted 3-axis coarse micromanipulator with additional X-axis fine control (e.g., Narishige MN-153).

3 Methods

3.1 Preparation of the Workspace

1. Protect stereomicroscope stage by covering it completely with plastic wrap. Wet the paper towels with system water to provide a damp surface upon which to place the anesthetized fish. Place the paper towels on top of the plastic wrap on the microscope stage.
2. Briefly create a vortex within the prepared ouabain solution to ensure it is well mixed. Load the 10 μ L Hamilton syringe with either 40 μ M or 200 μ M ouabain solution, for selective or extensive lesion. Ensure that there are no air bubbles.
3. Install the Hamilton syringe into the fine X-axis mount of the micromanipulator. Micromanipulator should be set such that this “X-axis” points the syringe tip downward at approximately 45° angle. Check the field of view from the oculars to ensure that this view will encompass the size of the zebrafish head and that the very tip of the syringe needle is visible. You will also need to ensure that you are able to manipulate the syringe in the X and Z direction sufficiently to allow smooth entry into and out of the eye when injecting while maintaining an appropriate field of view.
4. Rinse the sapphire knife with 70% EtOH, allow to air-dry, close it, and store in the plastic beaker of water or on a clean surface.
5. Prepare a fresh 100 mL of working concentration (163 mg/L) MS-222 solution in system water, in a glass beaker specifically for fish use.

3.2 Intraocular Injection of Ouabain

1. Using a fish transfer net, transfer a single zebrafish to the MS-222 solution and allow it to remain there until spontaneous movement has ceased, opercular movement is not evident, and the fish shows no startle response (does not move in response to tapping the beaker). The fish should be anesthetized within 30 s.
2. Transfer the fish, using the spoon, to the damp paper towel on the microscope stage such that it is lying on its side. Orient the fish with tail toward the micromanipulator (*see Note 5* and *Fig. 1*), with the eye to be injected facing upward, toward the objective. Illuminate the eye with the fiber-optic light source. Flush the fish briefly with MS-222 solution, using a plastic transfer pipette.
3. Using the dial calipers, measure the eye's diameter along the dorsal–ventral axis, at its widest point. Record this diameter and determine the volume of ouabain solution to inject based on *Table 1*. These volumes are intended to result in final intraocular concentrations of 2–4 μM for selective lesion and 10–20 μM for extensive lesion, depending on concentration of the working solution used, and based upon calculations for the spherical geometry of the eye [*32, 42*], and the results of pilot studies for each investigator (*see Notes 4, 5, and 6*).
4. Depress the plunger of the Hamilton syringe until a small droplet of liquid is visible at the tip of the needle, and then absorb the droplet onto a Kimwipe, in order to expel any trapped air from the needle.
5. Using the sapphire microknife (the sharpest edge is marked with a black dot; *see Note 7*), make an incision in the cornea, parallel with the dorsal–ventral axis of the eye, with the midpoint of the incision between the center of the eye and the most temporal point of the eye (*see Fig. 1*). The incision must be deep enough to penetrate the zonule fibers/tissues separating the anterior and posterior chambers but must not damage the retina itself (*see Note 8*). Avoid cutting the iris.
6. Using the micromanipulator, introduce the tip of the Hamilton syringe through the incision into the vitreal chamber. The tip of the needle must be behind the lens and well into the vitreous space in order to obtain consistent results (*see Note 4*). However, the needle must also not do direct damage to the retina. This may require manipulating the syringe in both the X and Z direction.
7. Inject the appropriate volume of ouabain solution, as determined upon eye diameter in *step 3*, *Table 1*. *See Fig. 1* for illustration of *steps 5–7*. Note that the eye may visibly increase slightly in size due to the additional intravitreal volume.

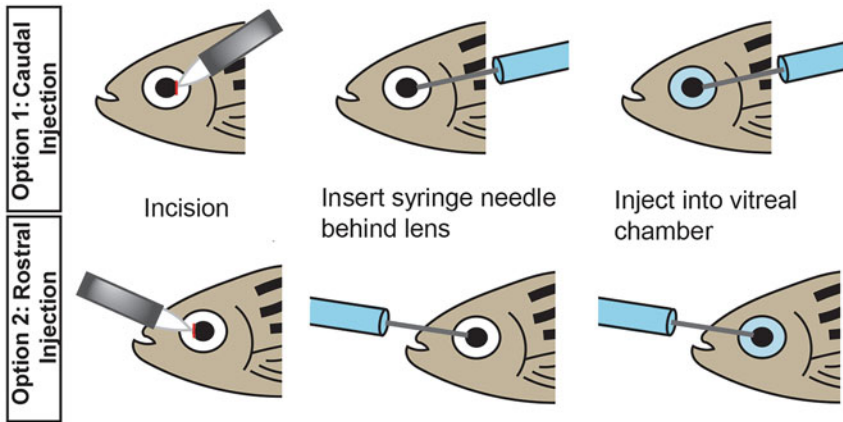


Fig. 1 Illustration of steps 5–7 (corneal incision–injection)

Table 1

Volumes of ouabain working stocks to inject, based upon eye diameter, calculations from spherical geometry, and recent experience within our laboratories

Eye diameter	Volume to inject ^a (using either 40 μM or 200 μM ouabain solution)
2.0–2.1 mm	0.4 μL
2.1–2.2 mm	0.48 μL
2.3 mm	0.64 μL
2.4 mm	0.72 μL
2.5 mm	0.82 μL

^aFor selective lesion, use indicated volume of 40 μM working stock to obtain 2–4 μM estimated intraocular concentration; for extensive lesion, use indicated volume of 200 μM working stock to obtain 10–20 μM estimated intraocular concentration (*see Note 4*)

8. Wait 10 s, and carefully withdraw the needle. Wait another 10–30 s until the edges of the corneal incision realign, and then transfer the fish to a tank of clean system water to recover from the anesthesia (*see Note 9*).
9. If additional fish will be undergoing this procedure, wet the sapphire knife and tip of the needle with 70% EtOH, allow each to air-dry, and close and store knife in plastic beaker of ultra-pure water or on clean surface in-between procedures.

3.3 Recovery

1. In the event that the fish does not resume opercular movements, respiration can be assisted by gently passing a stream of system water through the mouth and across the gills using a plastic transfer pipette. The MS-222 will diffuse out of the bloodstream and the fish will recover from anesthesia.

2. If the fish shows external signs of damage, tetracycline (0.3 g/L) may be added to the system water during recovery (*see Note 10*).
3. Monitor fish for 2 h, checking every 30 min after the procedure and before returning to the zebrafish facility (*see Note 11*). Check on fish at least once daily for the first 5–7 days following the procedure (*see Note 12*).
4. Eject any remaining ouabain solution from the syringe into a small storage tube and dispose according to institutional environmental health and safety guidelines (*see Note 13*). Flush the syringe with ultrapure water several times, and then with 100% EtOH, and allow to dry, prior to storage.
5. Rinse the sapphire knife with 70% EtOH, and then with water, close it, and then place into the water beaker for approximately 5 min. Rinse with 100% EtOH before storing.

4 Notes

1. Preparation of MS-222 stock from the crystalline solid requires the use of nitrile gloves, protective clothing, chemical safety goggles, and an N95 mask and should be done in a fume hood or sealed container.
2. Detergent residues can adversely affect the gills and protective external mucus layer of fish. Therefore, glassware used in preparing solutions to be used with live fish should be washed only with bleach and hot water, without the use of detergents, and rinsed thoroughly.
3. Ouabain is a potent neurotoxin [38]. Preparation of the 2 mM ouabain solution from crystalline solid ouabain requires the use of an N95 mask. The 2 mM ouabain concentrated stock can be stored in aliquots at -20°C for up to 6 months, and then thawed for later use in preparing fresh working dilutions.
4. The 40 μM Ouabain solution is for generating a “selective” lesion that destroys inner retinal neurons but spares photoreceptors and glia, while the 200 μM working stock is for generating an “extensive” lesion that destroys all retinal neurons but spares glia. Ours and other laboratories have reported the use of a range of ouabain concentrations and/or injection volumes that each reliably resulted in the desired type of damage for a particular investigator [9, 21, 22, 24–26, 29, 30, 36]. The concentrations and volumes provided in Table 1 are on the higher end of this range. A number of factors may account for these apparent methodological inconsistencies, including the following: Individual investigators may prefer different needle tip positions within the eye, resulting in either

more localized distribution of the injected ouabain, or injection predominantly into the anterior chamber of the eye with limited availability to the retina. Such preferences may lead to unreliable damage outcomes, localized damage rather than widespread damage, and/or an apparent need to use higher concentrations of the ouabain working solution. Additional factors underlying this apparent methodological inconsistency may be the commercial source of ouabain, variability in overall eye size of adult zebrafish, and potential effects of background strain on eye morphology, with investigators taking eye size-related variability into account using different approaches. One approach is to (i) assume the eye is close enough to spherical in shape for the purposes of volume calculations, (ii) use a ratio of lens to eye diameter of $\sim 1:2$ (e.g., [43], but note that axial diameters, rather than external eye diameters, are provided in this reference) to estimate lens diameter and then calculate lens volume, and (iii) subtract lens volume from eye volume to obtain intraocular volume into which the injected volume will be diluted. These calculations also assume that injected ouabain diffuses through intraocular tissues other than the lens [32]. Note that this approach results in *estimated* intraocular concentrations, which are subject to inaccuracies and potential variability in outcome, as was previously observed for goldfish intraocular injections [32, 35]. Therefore, we recommend that each investigator establish, through sufficient pilot studies, the concentration and volume of intraocular ouabain that reliably results in the desired outcome—selective vs. extensive lesion, using histological analyses. Analyses for extensive damage can be seen in references [24–26]; analyses for selective damage can be seen in references [21, 22, 24, 29], and some of these are illustrated in Fig. 2. After pilot studies reveal appropriate and reliable concentrations and injection volumes, investigators may use the strategies described in *see* **Note 12** and illustrated in Fig. 3 for evaluating effective lesioning in live zebrafish for subsequent experimental purposes.

5. Orientation of the fish and the direction of entry of the Hamilton syringe needle will depend on investigator preference (Fig. 1).
6. We recommend against the use of zebrafish with eyes smaller than 2.0 mm in diameter. In our experience, injection of fish with eyes smaller than 2.0 mm diameter results in highly inconsistent lesioning results.
7. The tip of the sapphire microknife is fragile and must only be touched to the zebrafish eye and nothing else.
8. It may help to hold the eye steady with sterile curved forceps while making this incision. Holding the sapphire blade almost perpendicular to the surface of the cornea, in a dorsal–ventral

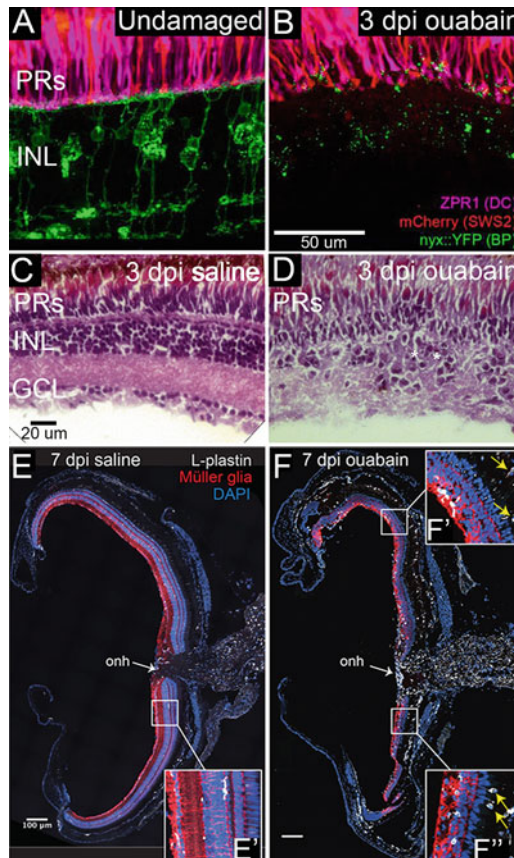


Fig. 2 Examples of verification of ouabain-mediated selective damage to inner retinal neurons of zebrafish retina, using histological methods on fixed retinal tissues. **(a, b)**. Verification using transgenic reporters (*sws2:mCherry*+ blue-sensitive cones and *nyx::mYFP*+ bipolar neurons; BP) and immunofluorescence (*zpr1*+ double cones; DC), in undamaged control retina **(a)** and 3 days post-injection (dpi) with intraocular ouabain **(b)**. Both retinas **(a, b)** display *mCherry*+ (red) and *zpr1*+ (magenta) cone photoreceptors (PRs); undamaged control retina **(a)** shows *mYFP*+ BPs (yellow) within the inner nuclear layer (INL), while these are missing at 3 dpi **(b)**. GCL, ganglion cell layer. **(a and b)** were modified from Fig. 1 in McGinn et al. (2018) [29]. **c, d**. Verification using hematoxylin and eosin (H&E) staining, at 3 days after intraocular saline **(c)** and 3 days after intraocular ouabain **(d)**. Both retinas show H+ PR layers **(c, d)**. Saline control retina **(c)** also shows H+ (purple) INL and GCL, and E+ plexiform layers, while these layers are considerably disrupted at 3 dpi ouabain **(d)**, and instead show pyknotic nuclei (asterisks). **(c and d)** were modified from Fig. 6 in Mitchell et al. (2018) [21]. **e, f**. Verification of widespread and consistent response to inner retinal damage across entire retina, using immunofluorescence (glutamine synthetase+ Müller glia; L-plastin+ immune cells) and a nuclear label (DAPI). Retina of saline-injected eye **(e)** shows DAPI+ (blue) retinal nuclear layers, radially organized glutamine synthetase+ Müller glia (magenta), and occasional L-plastin+ (white) immune cells (**e'**), at 7 dpi. Retina of ouabain-injected eye **(f)** shows a consistent, DAPI+ photoreceptor layer, disorganized inner retinal layers, hypertrophied Müller glia, and increased numbers and changes in morphology of immune cells (**f, f', f''**) at 7 dpi. Immune cells can be seen within the optic nerve head (onh; **f**) and appearing in regions apical to the retina (arrows in **f', f''**), suggesting the invasion of immune cells from outside the retina. **(e and f)** were modified from Fig. 1 in Mitchell et al. (2019) [22]

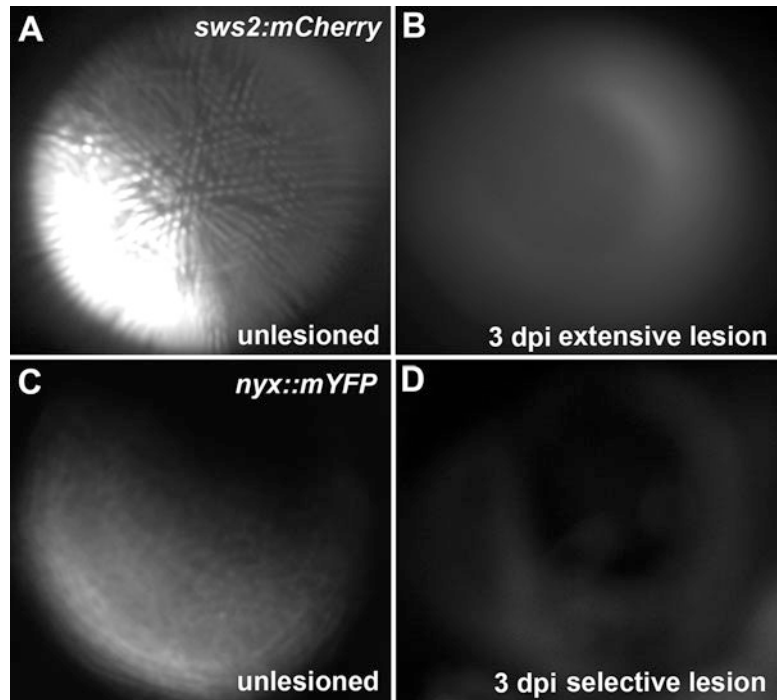


Fig. 3 Verification of extensive and selective lesions using anesthetized, *sws2:mCherry* (a, b) transgenic fish, *nyx::mYFP* (c, d) transgenic fish, and an epifluorescence stereomicroscope; images are views of the photoreceptor layer of a control, undamaged retina (a), and a retina subjected to extensive lesion (b), 4 days post-injury, and of the YFP+ bipolar neurons of an undamaged control retina (c), and a retina subjected to selective lesion (d), 3 days post-injury. Images are views through the cornea and lens of the eye

orientation, will facilitate making the incision. The incision may nick the iris of the eye. Such an incision facilitates visualization of the incision site for introducing the Hamilton syringe, but also increases the likelihood of bleeding, and should be avoided.

9. Alternatively, flush the fish briefly with MS-222 solution, and then turn the zebrafish onto its opposite side to repeat the procedure for the contralateral eye. An example of when bilateral retinal damage is needed is when one of the experimental endpoints is a visually mediated behavior [25, 26]. As another alternative, some investigators routinely inject the contralateral eye with sterile saline as the within-fish control. Such an approach requires a duplicated syringe and/or micromanipulator arrangement to minimize the time that the fish is under anesthesia and out of water, and any carryover of ouabain from the loaded solution. For analysis of neurons, we favor the use of an undamaged control eye for a number of reasons, including

that a sham (saline) injection does inflict damage to other eye tissues, and this damage can prompt cellular responses within the retina of the control eye. However, for analysis of immune responses including microglia, we prefer a sham (saline) single eye injection control from separate fish.

10. In our experience, this has not been needed. However, Institutional Animal Care and Use Committees generally indicate that some treatment be available should the fish show external signs of injury.
11. If space and equipment permit, the intraocular injection of ouabain procedure can be done in a “procedures” area within an animal facility. Our equipment is currently set up within a research laboratory setting. Therefore, because the fish are outside of the zebrafish facility for a few hours, when they return, they must be housed separately from fish that only remain within our main recirculating, monitored system. We provide this separate housing in a freestanding recirculating rack-and-tank unit that is independent of the main system and is dedicated to regeneration studies.
12. Once a series of pilot experiments have confirmed the intended damage outcome through histological assessment, intended damage outcomes can be verified in subsequent experiments in numerous ways, without the need to sacrifice the zebrafish and obtain fixed tissues. The use of transgenic reporter lines with fluorescent proteins in targeted retinal cell types will allow the investigator to examine the retina of a live, anesthetized zebrafish with an epifluorescence stereomicroscope [29, 30, 44]. For example, the *sws2:mCherry*; *nyx::mYFP* dual transgenic [45, 46] can be examined for the absence of the row mosaic of mCherry+ blue-sensitive cones (Fig. 3a, b) and YFP+ bipolar neurons to verify extensive damage (vs. the presence of these neurons in an undamaged contralateral eye). The same dual transgenic can be examined for the presence of the row mosaic [47] of mCherry+ cones and absence of YFP+ bipolar neurons to verify selective damage (Fig. 3c, d). In our experience, 4 days post-injection (dpi) appears optimal for verification of extensive damage, and 3 dpi appears optimal for selective damage. Damage outcome may also be verified through behavioral assays such as a place-preference assay [26, 48] or escape-response assay [25]. These approaches require that both retinas be damaged and cannot distinguish between selective and extensive lesion. Alternatively, unilateral retinal damage can be verified by the presence of an abnormal dorsal light reflex (DLR)—the zebrafish will swim in a “tilted” manner such that the lesioned eye appears to look upward toward a source of downwelling light [25]. This approach

also cannot distinguish between selective and extensive lesion and is far easier to incorporate when using larger-bodied, non-shoaling, and less active fish such as goldfish [33, 49].

13. As an example of institutional guidelines regarding safe disposal of a toxic material such as ouabain, unused ouabain solution is ejected into a small storage tube or bottle, labeled with the contents and concentrations, labeled as toxic, assigned a container number, investigator name and contact information, sealed, and temporarily maintained within a designated space of a fume hood. Solid waste (such as plastic tubes and pipette tips) that were used with ouabain solutions are also collected in a similar manner. Our Environment, Health, and Safety (EHS) office provides us with stickers for entering this information on each new container used. As additional experiments are performed, we add more unused ouabain solution into the same container, and either enter onto the sticker the additional amounts and concentrations added or maintain a separate log sheet for the container if there is insufficient space on the sticker. When the container is nearly full, we submit a waste collection request form to EHS and one of their personnel will come to the lab to pick up the waste for disposal.

Acknowledgments

Retinal regeneration studies in our laboratories using the approaches described have been supported by NIH R01 EY012146 (DLS), NIH R01 EY030467 (DMM), and NIH R21 EY026814 (DLS and DMM). We are also grateful for support in the form of pilot grants and other funding from Idaho INBRE (NIH P20 GM103408). We thank past and present members of the Stenkamp and Mitchell laboratories, particularly Ruth Frey for zebrafish husbandry and Lindsey Barrett for the images shown in Fig. 3a, b.

References

1. Massoz L, Dupont MA, Manfroid I (2021) Zebra-fishing for regenerative awakening in mammals. *Biomedicine* 9(1). <https://doi.org/10.3390/biomedicines9010065>
2. Gao H, Luodan A, Huang X, Chen X, Xu H (2021) Muller glia-mediated retinal regeneration. *Mol Neurobiol* 58:2342. <https://doi.org/10.1007/s12035-020-02274-w>
3. Konar GJ, Ferguson C, Flickinger Z, Kent MR, Patton JG (2020) miRNAs and Muller glia reprogramming during retina regeneration. *Front Cell Dev Biol* 8:632632. <https://doi.org/10.3389/fcell.2020.632632>
4. Lahne M, Nagashima M, Hyde DR, Hitchcock PF (2020) Reprogramming Muller glia to regenerate retinal neurons. *Annu Rev Vis Sci* 6:171–193. <https://doi.org/10.1146/annurev-vision-121219-081808>
5. Yurco P, Cameron DA (2005) Responses of Muller glia to retinal injury in adult zebrafish. *Vis Res* 45(8):991–1002

6. Fausett BV, Goldman D (2006) A role for alpha1 tubulin-expressing Muller glia in regeneration of the injured zebrafish retina. *J Neurosci* 26(23):6303–6313
7. Bernardos RL, Barthel LK, Meyers JR, Raymond PA (2007) Late-stage neuronal progenitors in the retina are radial Muller glia that function as retinal stem cells. *J Neurosci* 27(26):7028–7040
8. Thummel R, Kassen SC, Montgomery JE, Enright JM, Hyde DR (2008) Inhibition of Muller glial cell division blocks regeneration of the light-damaged zebrafish retina. *Dev Neurobiol* 68(3):392–408
9. Nagashima M, Barthel LK, Raymond PA (2013) A self-renewing division of zebrafish Muller glial cells generates neuronal progenitors that require N-cadherin to regenerate retinal neurons. *Development* 140(22):4510–4521. <https://doi.org/10.1242/dev.090738>
10. Fausett BV, Gumerson JD, Goldman D (2008) The proneural basic helix-loop-helix gene *ascl1a* is required for retina regeneration. *J Neurosci* 28(5):1109–1117
11. Qin Z, Barthel LK, Raymond PA (2009) Genetic evidence for shared mechanisms of epimorphic regeneration in zebrafish. *Proc Natl Acad Sci U S A* 106(23):9310–9315
12. Ramachandran R, Reifler A, Parent JM, Goldman D (2010) Conditional gene expression and lineage tracing of tuba1a expressing cells during zebrafish development and retina regeneration. *J Comp Neurol* 518(20):4196–4212. <https://doi.org/10.1002/cne.22448>
13. Ramachandran R, Zhao XF, Goldman D (2011) *Ascl1a*/Dkk/beta-catenin signaling pathway is necessary and glycogen synthase kinase-3beta inhibition is sufficient for zebrafish retina regeneration. *Proc Natl Acad Sci U S A* 108(38):15858–15863
14. Powell C, Grant AR, Cornblath E, Goldman D (2013) Analysis of DNA methylation reveals a partial reprogramming of the Muller glia genome during retina regeneration. *Proc Natl Acad Sci U S A* 110(49):19814–19819. <https://doi.org/10.1073/pnas.1312009110>
15. Powell C, Elsaedi F, Goldman D (2012) Injury-dependent Muller glia and ganglion cell reprogramming during tissue regeneration requires Apobec2a and Apobec2b. *J Neurosci* 32(3):1096–1109. <https://doi.org/10.1523/JNEUROSCI.5603-11.2012>
16. Nelson CM, Ackerman KM, O'Hayer P, Bailey TJ, Gorsuch RA, Hyde DR (2013) Tumor necrosis factor-alpha is produced by dying retinal neurons and is required for Muller glia proliferation during zebrafish retinal regeneration. *J Neurosci* 33(15):6524–6539. <https://doi.org/10.1523/JNEUROSCI.3838-12.2013>
17. Lenkowski JR, Qin Z, Sifuentes CJ, Thummel R, Soto CM, Moens CB, Raymond PA (2013) Retinal regeneration in adult zebrafish requires regulation of TGFbeta signaling. *Glia* 61(10):1687–1697. <https://doi.org/10.1002/glia.22549>
18. Wan J, Zhao XF, Vojtek A, Goldman D (2014) Retinal injury, growth factors, and cytokines converge on beta-catenin and pStat3 signaling to stimulate retina regeneration. *Cell Rep* 9(1):285–297. <https://doi.org/10.1016/j.celrep.2014.08.048>
19. Nagashima M, D'Cruz TS, Danku AE, Hesse D, Sifuentes C, Raymond PA, Hitchcock PF (2020) Midkine-a is required for cell cycle progression of Muller glia during neuronal regeneration in the vertebrate retina. *J Neurosci* 40(6):1232–1247. <https://doi.org/10.1523/JNEUROSCI.1675-19.2019>
20. White DT, Sengupta S, Saxena MT, Xu Q, Hanes J, Ding D, Ji H, Mumm JS (2017) Immunomodulation-accelerated neuronal regeneration following selective rod photoreceptor cell ablation in the zebrafish retina. *Proc Natl Acad Sci U S A* 114(18):E3719–E3728. <https://doi.org/10.1073/pnas.1617721114>
21. Mitchell DM, Lovel AG, Stenkamp DL (2018) Dynamic changes in microglial and macrophage characteristics during degeneration and regeneration of the zebrafish retina. *J Neuroinflammation* 15(1):163. <https://doi.org/10.1186/s12974-018-1185-6>
22. Mitchell DM, Sun C, Hunter SS, New DD, Stenkamp DL (2019) Regeneration associated transcriptional signature of retinal microglia and macrophages. *Sci Rep* 9(1):4768. <https://doi.org/10.1038/s41598-019-41298-8>
23. Conedera FM, Pousa AMQ, Mercader N, Tschopp M, Enzmann V (2019) Retinal microglia signaling affects Muller cell behavior in the zebrafish following laser injury induction. *Glia* 67(6):1150–1166. <https://doi.org/10.1002/glia.23601>
24. Fimbel SM, Montgomery JE, Burket CT, Hyde DR (2007) Regeneration of inner retinal neurons after intravitreal injection of ouabain in zebrafish. *J Neurosci* 27(7):1712–1724
25. Sherpa T, Fimbel SM, Mallory DE, Maaswinkel H, Spritzer SD, Sand JA, Li L, Hyde DR, Stenkamp DL (2008) Ganglion cell regeneration following whole-retina

- destruction in zebrafish. *Dev Neurobiol* 68(2): 166–181
26. Sherpa T, Lankford T, McGinn TE, Hunter SS, Frey RA, Sun C, Ryan M, Robison BD, Stenkamp DL (2014) Retinal regeneration is facilitated by the presence of surviving neurons. *Dev Neurobiol* 74(9):851–876. <https://doi.org/10.1002/dneu.22167>
 27. Powell C, Cornblath E, Elsaedi F, Wan J, Goldman D (2016) Zebrafish Muller gliaderived progenitors are multipotent, exhibit proliferative biases and regenerate excess neurons. *Sci Rep* 6:24851. <https://doi.org/10.1038/srep24851>
 28. D’Orazi FD, Zhao XF, Wong RO, Yoshimatsu T (2016) Mismatch of synaptic patterns between neurons produced in regeneration and during development of the vertebrate retina. *Curr Biol* 26(17):2268–2279. <https://doi.org/10.1016/j.cub.2016.06.063>
 29. McGinn TE, Mitchell DM, Meighan PC, Partington N, Leoni DC, Jenkins CE, Varnum MD, Stenkamp DL (2018) Restoration of dendritic complexity, functional connectivity, and diversity of regenerated retinal bipolar neurons in adult zebrafish. *J Neurosci* 38(1):120–136. <https://doi.org/10.1523/JNEUROSCI.3444-16.2017>
 30. McGinn TE, Galicia CA, Leoni DC, Partington N, Mitchell DM, Stenkamp DL (2019) Rewiring the regenerated zebrafish retina: reemergence of bipolar neurons and cone-bipolar circuitry following an inner retinal lesion. *Front Cell Dev Biol* 7:95. <https://doi.org/10.3389/fcell.2019.00095>
 31. Maier W, Wolburg H (1979) Regeneration of the goldfish retina after exposure to different doses of ouabain. *Cell Tissue Res* 202(1): 99–118
 32. Raymond PA, Reifler MJ, Rivlin PK (1988) Regeneration of goldfish retina: rod precursors are a likely source of regenerated cells. *J Neurobiol* 19(5):431–463. <https://doi.org/10.1002/neu.480190504>
 33. Mensinger AF, Powers MK (1999) Visual function in regenerating teleost retina following cytotoxic lesioning. *Vis Neurosci* 16(2): 241–251
 34. Kastner R, Wolburg H (1982) Functional regeneration of the visual system in teleosts. Comparative investigations after optic nerve crush and damage of the retina. *Z Naturforsch C Biosci* 37(11–12):1274–1280. <https://doi.org/10.1515/znc-1982-11-1229>
 35. Kurz-Isler G, Wolburg H (1982) Morphological study on the regeneration of the retina in the rainbow trout after ouabain-induced damage: evidence for dedifferentiation of photoreceptors. *Cell Tissue Res* 225(1): 165–178. <https://doi.org/10.1007/BF00216226>
 36. Eastlake K, Heywood WE, Tracey-White D, Aquino E, Bliss E, Vasta GR, Mills K, Khaw PT, Moosajee M, Limb GA (2017) Comparison of proteomic profiles in the zebrafish retina during experimental degeneration and regeneration. *Sci Rep* 7:44601. <https://doi.org/10.1038/srep44601>
 37. Thomas JL, Morgan GW, Dolinski KM, Thummel R (2018) Characterization of the pleiotropic roles of Sonic Hedgehog during retinal regeneration in adult zebrafish. *Exp Eye Res* 166:106–115. <https://doi.org/10.1016/j.exer.2017.10.003>
 38. Lees GJ, Lehmann A, Sandberg M, Hamberger A (1990) The neurotoxicity of ouabain, a sodium-potassium ATPase inhibitor, in the rat hippocampus. *Neurosci Lett* 120(2):159–162. [https://doi.org/10.1016/0304-3940\(90\)90027-7](https://doi.org/10.1016/0304-3940(90)90027-7)
 39. Fraser B, DuVal MG, Wang H, Allison WT (2013) Regeneration of cone photoreceptors when cell ablation is primarily restricted to a particular cone subtype. *PLoS One* 8(1): e55410. <https://doi.org/10.1371/journal.pone.0055410>
 40. D’Orazi FD, Suzuki SC, Darling N, Wong RO, Yoshimatsu T (2020) Conditional and biased regeneration of cone photoreceptor types in the zebrafish retina. *J Comp Neurol* 528(17): 2816–2830. <https://doi.org/10.1002/cne.24933>
 41. Medrano MP, Bejarano CA, Battista AG, Venera GD, Bernabeu RO, Faillace MP (2017) Injury-induced purinergic signalling molecules upregulate pluripotency gene expression and mitotic activity of progenitor cells in the zebrafish retina. *Purinergic Signal* 13(4):443–465. <https://doi.org/10.1007/s11302-017-9572-5>
 42. Easter SS Jr, Johns PR, Baumann LR (1977) Growth of the adult goldfish eye—I: optics. *Vis Res* 17(3):469–477. [https://doi.org/10.1016/0042-6989\(77\)90041-4](https://doi.org/10.1016/0042-6989(77)90041-4)
 43. Collery RF, Veth KN, Dubis AM, Carroll J, Link BA (2014) Rapid, accurate, and non-invasive measurement of zebrafish axial length and other eye dimensions using SD-OCT allows longitudinal analysis of myopia and emmetropization. *PLoS One* 9(10): e110699. <https://doi.org/10.1371/journal.pone.0110699>
 44. Duval MG, Chung H, Lehmann OJ, Allison WT (2013) Longitudinal fluorescent

- observation of retinal degeneration and regeneration in zebrafish using fundus lens imaging. *Mol Vis* 19:1082–1095
45. Sifuentes CJ, Kim JW, Swaroop A, Raymond PA (2016) Rapid, dynamic activation of Muller glial stem cell responses in zebrafish. *Invest Ophthalmol Vis Sci* 57(13):5148–5160. <https://doi.org/10.1167/iops.16-19973>
 46. Schroeter EH, Wong RO, Gregg RG (2006) In vivo development of retinal ON-bipolar cell axonal terminals visualized in *nyx::MYFP* transgenic zebrafish. *Vis Neurosci* 23(5):833–843. <https://doi.org/10.1017/S0952523806230219>
 47. Allison WT, Barthel LK, Skebo KM, Takechi M, Kawamura S, Raymond PA (2010) Ontogeny of cone photoreceptor mosaics in zebrafish. *J Comp Neurol* 518(20):4182–4195. <https://doi.org/10.1002/cne.22447>
 48. Sherpa T, Hunter SS, Frey RA, Robison BD, Stenkamp DL (2011) Retinal proliferation response in the buphthalmic zebrafish, *bugeye*. *Exp Eye Res* 93(4):424–436. <https://doi.org/10.1016/j.exer.2011.06.001>
 49. Lindsey AE, Powers MK (2007) Visual behavior of adult goldfish with regenerating retina. *Vis Neurosci* 24(3):247–255



A Reproducible Spinal Cord Crush Injury in the Regeneration-Permissive Axolotl

Sarah Walker, Tiago Santos-Ferreira, and Karen Echeverri

Abstract

Following injury, axolotls are able to functionally regenerate their spinal cord, regaining both motor and sensory control. In contrast, humans respond to severe spinal cord injury by forming a glial scar, which prevents further damage but also inhibits any regenerative growth, resulting in loss of function caudal to the injury site. The axolotl has become a popular system to elucidate the underlying cellular and molecular events that contribute to successful CNS regeneration. However, the experimental injuries (tail amputation and transection) that are utilized in axolotls do not mimic the blunt trauma that is often sustained in humans. Here, we report a more clinically relevant model for spinal cord injuries in the axolotl using a weight-drop technique. This reproducible model allows precise control over the severity of the injury by regulating the drop height, weight, compression, and position of the injury.

Key words Axolotl, Spinal cord, Crush injury

1 Introduction

Spinal cord injuries are severely debilitating conditions that have profound impacts on neurological function and quality of life. In humans, traumatic injury to the spinal cord results in irreversible neuronal cell death and damage, leading to the loss of motor and sensory function [1]. The inability for humans to repair their spinal cord has thus placed particular emphasis on understanding the events that underlie neuronal repair and for developing clinically relevant animal models to investigate spinal cord injury.

Unlike mammals, a few species are able to regenerate their spinal cord following injury. In these regenerating species, two models of spinal cord injury have been widely utilized, including spinal cord transection [2–6] or tail amputation [7–9]. Although

Supplementary Information The online version contains supplementary material available at https://doi.org/10.1007/978-1-0716-3012-9_13.

these techniques have offered valuable insight into the events underlying spinal cord repair, amputation and transection are often not reflective of spinal cord injuries sustained in humans. These findings have thus emphasized the importance and requirement of a more clinically relevant spinal cord injury model.

Several animal models of spinal cord injury have been developed to more accurately reflect injuries sustained in humans. In non-regenerating mammalian systems such as mice and rats, research efforts have focused upon crush or contusion injuries [10, 11]. In contrast, tail amputation and spinal cord transection remain prevalent in species capable of CNS repair [7, 2, 12, 13]. Recently, however, crush or contusion injuries have been developed in both zebra fish [5] and the axolotl [14] to represent a more relevant model for spinal cord injury in regeneration-competent species.

The Mexican axolotl, known as a champion of regeneration, exhibits a remarkable capacity for regenerative repair as an adult. However, no studies to date have provided a detailed methodology for spinal cord crush injuries in this species. Here, we present a reproducible model for performing axolotl spinal cord crush injuries. We utilize a weight-drop technique that enables precise control over the age/size of axolotl, severity of injury (through drop height, and mass), and the duration of the compression. In this chapter, we also provide protocols for two downstream applications following spinal cord crush injuries, including histological Acid Fuchsin Orange G (AFOG) staining, which can be used to detect scar formation, or RNA extraction to look at gene expression.

2 Materials

2.1 *Axolotl Care*

1. 40% Holtfreter's solution: Dissolve 62 g reef salts, 4 g alkaline buffer, 4 g calcium carbonate, and 0.7 g acid buffer into 1 L of deionized water. Add the 1 L salt solution into a 40 L carboy and fill to a final volume of 40 L with deionized water. Adjust the pH within 7.0–8.0 range.
2. 10% benzocaine stock: Dissolve 10 g of benzocaine in 100 mL of absolute ethanol (*see Note 1*). Dilute the 10% stock to 0.01% working solution using 40% Holtfreter's solution (*see Note 2*).

2.2 *Weight Drop Apparatus for Spinal Crush Injury (Fig. 1)*

1. Weights: For our apparatus, we use weights with a length of 2 cm, whereas the height varies depending on the mass. While we primarily use a 10 g weight in experiments, heavier weights also fit into the apparatus, including 20 g and 50 g.
2. Plastic cap for weights.
3. Filter paper or paper towels.

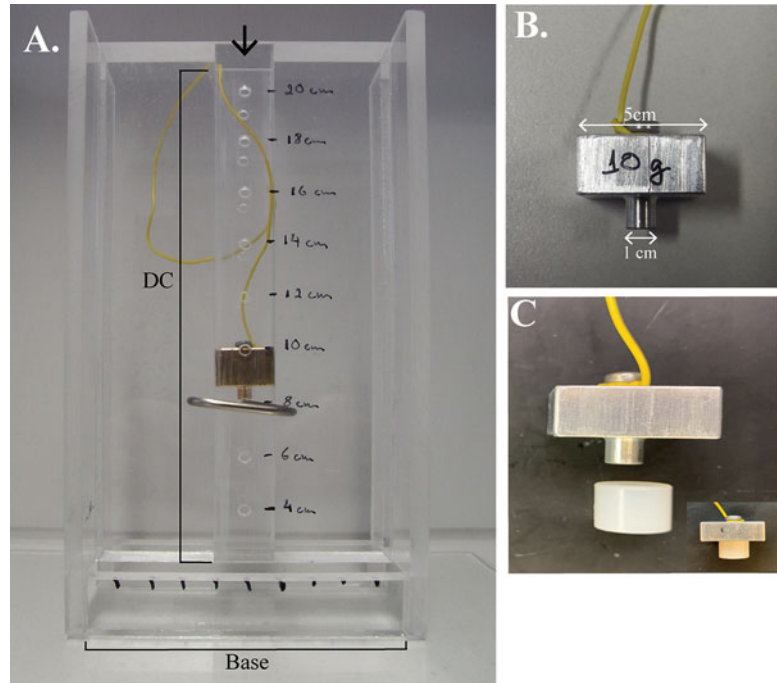


Fig. 1 Spinal cord crush injury model. (a) Apparatus to control the drop height (indicated in cm on drop column). Arrow indicates original placement of the weight into the drop column (DC). (b) Approximate size of weight that fits into the drop column. (c) Plastic cap used on the weight to disperse the impact and prevent piercing through the tissue

4. Rope attached to the weight to lower it to the apparatus—length can be variable.

2.3 Visualization of Lesion Site Using AFOG Staining

1. 1× phosphate buffered saline (PBS), pH 7.4.
2. 4% paraformaldehyde: Weigh 2 g of paraformaldehyde powder into a 50 mL conical tube. Add 50 mL of 1× phosphate buffered saline (PBS), and incubate at 60 °C until the powder has dissolved. Shake the tube periodically to help the powder into solution. After the paraformaldehyde powder has successfully dissolved, store at 4 °C for up to 1 week (*see Note 3*).
3. Ethanol: Dilute absolute ethanol to 25%, 50%, and 75% using 1× PBS for tissue dehydration. In addition, dilute ethanol to 96%, 70%, and 40% using distilled water for rehydration steps.
4. Paraffin wax.
5. Tissue embedding molds.
6. Microtome for paraffin sectioning.
7. Superfrost Plus microscope slides (25 × 75 mm).
8. Xylene.

9. Bouin's solution.
10. AFOG histological staining solution: Dissolve 1 g aniline blue, 2 g Orange G, and 3 g acid fuchsin in 200 mL distilled water. Adjust pH to 1.09 using concentrated HCl (*see Note 4*).
11. 1% phosphomolybdic acid: Add 1 mL of phosphomolybdic acid to 100 mL of distilled water.
12. Anti-fade specimen mounting medium.
13. Coverslips (24 × 60 mm).

2.4 RNA Extraction

1. Guanidinium, thiocyanate–phenol–chloroform-based RNA extraction reagent (e.g., TRIzol, Invitrogen).
2. Chloroform.
3. Isopropanol.
4. 75% ethanol: Dilute absolute ethanol to 75% in RNase-free water.
5. RNase-free water.
6. Refrigerated microcentrifuge.
7. Tissue homogenizer (*see Note 5*).

3 Methods

3.1 Apparatus Preparation

1. Determine the appropriate axolotl size suitable for experiment of interest and the desired height, weight, and time of compression (*see Table 1*).
2. Soak filter paper or paper towel in 40% Holtfreter's solution, and place at the base of the weight-drop apparatus (Fig. 1a). The filter paper/paper towel will keep the axolotl in the desired position during the experiment.
3. Place a plastic cap covering over top of the weight (Fig. 1c). This plastic cap better disperses the impact of the weight, preventing piercing of the tissue.
4. Insert a pin into the drop column to hold the weight at the desired height. Slowly lower the weight (10 g) into the drop column (Fig. 1a, indicated by arrow).

3.2 Spinal Cord Crush Injury

1. Anesthetize the axolotls in 0.01% benzocaine or higher concentration depending on the size of the axolotl (*see Note 6*).
2. Place the axolotl on top of the moist filter paper or paper towel at the base of the apparatus. Ensure the axolotl is in the appropriate position under the weight-drop column.
3. Quickly pull the pin out of the drop column, allowing the weight to fall on the axolotl spinal cord.

Table 1
Apparatus parameters for spinal cord crush injury

Drop height (cm)	Weight (g)	Time of compression(s)	Degree of injury
8	10	120	Full SC transection plus severe damage to surrounding tissue
6	10	120	Full SC transection plus severe damage to surrounding tissue
4	10	120	Full SC transection, less damage to surrounding tissue
4	10	60	Full SC transection, damage to skin on muscle on contact side only
4	10	30	Full SC transection, damage to skin on muscle on contact side only

Included parameters were experimentally validated to cause severe damage to the spinal cord (SC) of axolotls 4–5 cm in length

4. Once the weight has reached the base of the apparatus, time the weight compression on the axolotl.
5. After the desired compression time, gently transfer the axolotl into an individual recovery tank filled with 40% Holtfreter's solution (*see Note 7*).
6. Once the axolotl has regained consciousness, gently run a pair of forceps over the tail downstream of the injury site (*see Videos 1 and 2*). If the injury was successful in causing severe damage to the spinal cord, the axolotl will not respond to stimulus caudal to the injury site once it has recovered from the anesthesia.
7. Monitor the recovery of each axolotl and continue to check their responsiveness downstream of the injury site. We use a tail touch assay to determine when functional recovery has occurred (*see Videos 1 and 2*).

3.3 Paraffin Wax Tissue Processing

1. At desired time point following injury, anesthetize axolotls in 0.01% benzocaine.
2. Identify the injury site, and using a scalpel cut the tail tissue ~1 mm upstream and downstream of the injury. The injury site is easily identified as the skin and muscle bundles above the spinal cord are also damaged, the disrupted tissue is easily visualized under the dissecting microscope, and sometimes a blood clot is visible in the injured area.
3. Fix tissues in fresh 4% paraformaldehyde overnight at 4 °C (*see Note 3*).
4. The next day, wash tissues twice in 1× PBS for 10 min.

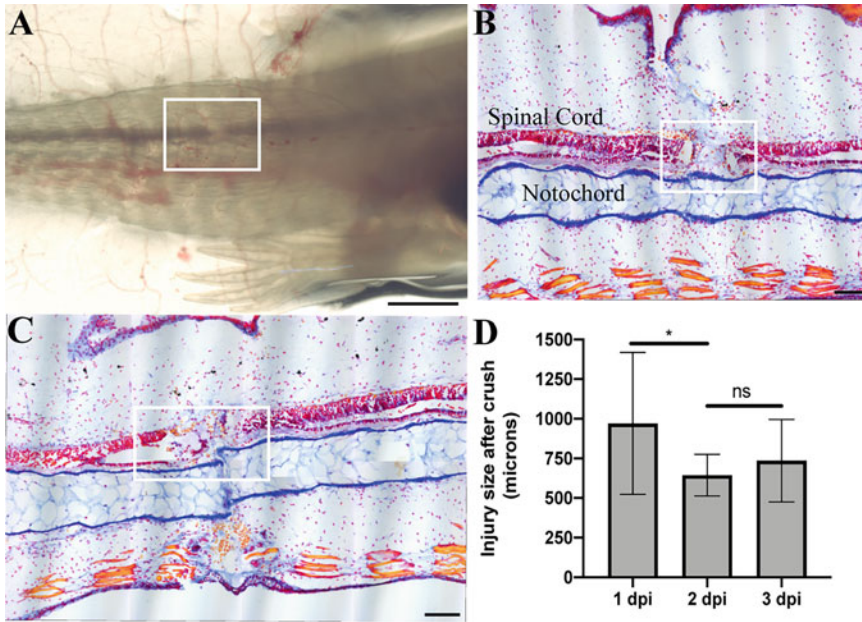


Fig. 2 Histological AFOG staining of the axolotl spinal cord after crush injury. Axolotls 4.5–5 cm in length were used for histological analyses, and the apparatus parameters included 10 g weight, 8 cm drop height, and 2.0 min compression. (a) Image of the animal directly after impact. Scale bar = 2 mm. (b) Histological staining at 1 day post-injury (dpi); only the spinal cord is damaged. NC, notochord. SC, spinal cord. Scale bar = 500 μm . (c) Histological staining at 1 day post-injury, 3 min compression time which also leads to damage to surrounding tissue like the notochord. White rectangle indicates region of injury. Scale bar = 500 μm . (d) Graph displays the average length of the injury site (μm) at 1 dpi ($n = 11$), 2 dpi ($n = 8$), and 3 dpi ($n = 9$). After injury, a significant reduction in the size of the lesion was detected between 1 dpi and 2 dpi ($p = 0.03$), which is indicative of regenerative repair. No significant difference was detected between 2 dpi and 3 dpi ($p = 0.19$), indicating a lack of cellular die back

5. Gradually dehydrate tissues in 25%, 50%, 75%, and 100% ethanol diluted in 1 \times PBS for 10 min.
6. Incubate tissues for 20 min in xylene (*see Note 8*).
7. Change the xylene and incubate samples for an additional 10 min.
8. Using forceps, gently transfer the samples into melted paraffin wax at 60 $^{\circ}\text{C}$ overnight.
9. The next day, embed samples in tissue embedding molds using paraffin wax. Leave embedded samples at 4 $^{\circ}\text{C}$ for 2–3 h before removing from molds (*see Note 9*).
10. Let samples come to room temperature before sectioning.
11. Cut 30 μm sections to visualize the spinal cord both upstream and downstream of the injury site (Fig. 2b–c).
12. After sectioning, allow slides to dry overnight at room temperature before proceeding to staining procedures (*see Note 10*).

3.4 AFOG Staining

1. Incubate the slides for 10 min in xylene in a glass Coplin jar to remove the paraffin. Repeat (*see Note 8*).
2. Completely submerge the slides in 100% ethanol for 5 min to remove the xylene.
3. Gradually rehydrate the sections in a series of graded ethanol dilutions in distilled water. Wash the sections twice in each dilution of 96%, 70%, and 40% ethanol for 1 min each.
4. Wash the slides for 1 min in distilled water to rehydrate the sections. Repeat.
5. Preheat Bouin's solution for 30 min at 60 °C in an incubator.
6. Incubate the slides in a Coplin jar filled with pre-heated Bouin's solution for 2 h at 60 °C in an incubator (*see Note 11*).
7. Remove the Coplin jar from the incubator, and cool to room temperature for 1 h.
8. Gently wash the slides under running distilled water for 30 min (*see Notes 12 and 13*).
9. Incubate the sections in 1% phosphomolybdic acid for 4.5 min.
10. Wash the slides under gently running distilled water for 5 min.
11. Incubate the slides in AFOG staining solution for 4.5 min.
12. Gently rinse the sections under running distilled water for 2 min.
13. Quickly rinse slides in 96% ethanol for 10 s. Repeat (*see Note 14*).
14. Rinse the slides in 100% ethanol for 10 s. Repeat.
15. Quickly rinse the slides in xylene for 10 s. Repeat (*see Note 8*).
16. Mount slides in mounting medium with a coverslip.

3.5 RNA Extraction

1. Anesthetize the axolotls in 0.01% benzocaine or higher concentration depending on the size of the axolotl (*see Note 6*).
2. Dissect out the tissue of interest or cut out the tissue area of interest.
3. Place the tissue directly into 1 mL of RNA extraction reagent in a fume hood (*see Note 15*), or if you wish to store the tissue for processing later, place directly into a tube in liquid nitrogen.
4. Use 1 mL of RNA extraction reagent per 100 mg of tissue.
5. Homogenize the tissue directly in RNA extraction reagent (*see Note 15*).
6. Mix the sample by pipetting up and down with a P1000; use a fresh tip for each sample.
7. Add 0.2 mL chloroform (*see Note 16*) per 1 mL RNA extraction reagent.

8. Close the tubes and shake vigorously for 15 s in the fume hood.
9. Incubate for 3 min at room temperature.
10. Centrifuge at $11,000\times g$ for 15 min at 2–8 °C.
11. Collect the upper aqueous phase and place into a new tube; discard the rest in the appropriate waste disposal area.
12. Add 0.5 mL isopropanol to the solution and incubate at room temperature for 10 min.
13. Centrifuge the samples at $10,000\times g$ for 10 min at 2–8 °C; a gel-like pellet should form.
14. Carefully remove the supernatant and add 1 mL of 75% ethanol diluted in RNase-free water. Briefly vortex.
15. Spin again in a centrifuge at $10,000\times g$ for 5 min at 2–8 °C.
16. Remove the supernatant and air-dry the pellet for 5 min.
17. Dissolve the pellet in 50–100 μ l of RNase-free water. To help dissolve the RNA, samples can be heated to 55 °C for 10 min.

4 Notes

1. Benzocaine is toxic and should only be handled in a fume hood.
2. The 10% benzocaine stock solution should be stored at 4 °C, whereas the working 0.01% solution may be stored at room temperature.
3. Paraformaldehyde is toxic and should only be handled in a fume hood.
4. AFOG staining is a common histological technique that can be used to visualize cell and tissue morphology. This staining technique can be used on tissue sections to better visualize the injury site following crush injury, or at later time points to visualize regenerative repair. In general, AFOG stains cartilage blue, cell nuclei brown/black, and the spinal cord pink.
5. We routinely use a Pellet Pestle Cordless Motor Tissue Disruptor from Kimble Chase or DWK Life Sciences Kimble Kontes all-glass Duall Tissue Grinders. For extracting RNA from big pieces of tissue from adult animals, we often freeze the tissue in liquid nitrogen and grind the tissue up in a frozen mortar and pestle in the presence of liquid nitrogen and then proceed to the RNA extraction step.
6. Depending on the age and size of the axolotl, different concentrations of benzocaine may be required to anesthetize the animals. In general, larval animals (2–3 cm) can be anesthetized in 0.01% benzocaine, whereas adult animals are anesthetized in 0.02% benzocaine.

7. After spinal cord injury, we suggest allowing the axolotls to recover in smaller individual tanks. This will make it much easier to monitor individual animals and to identify any unsuccessful injuries.
8. Xylene is toxic and must be handled in a fume hood. Xylene also degrades plastic and should only be used in glass Coplin jars.
9. After samples have been embedded in paraffin wax, the tissue molds containing each sample can be wrapped in Saran Wrap and stored at 4 °C until required for sectioning.
10. Sections may be stored at room temperature in a slide box for several weeks.
11. Alternatively, samples may be incubated overnight in Bouin's solution. If planning an overnight incubation, do not preheat solution to 60 °C, and perform the incubation at room temperature.
12. Rinsing the sections under a running tap can often lead to the sections dislodging from the slides if the water pressure is too strong. Position a plastic container on an angle directly under the faucet flow; then allow this slower runoff to rinse the slides.
13. In the event that distilled water from a faucet is not available, regular tap water is an adequate substitution.
14. Rinses in 96% ethanol, 100% ethanol, and xylene for **steps 13–15** must be accurately timed for only 10 s; otherwise tissue sections will become discolored.
15. RNA extraction reagents are toxic chemicals; use in a fume hood. Wear safety glasses, gloves, and a lab coat when handling.
16. Chloroform is toxic; pipette under the fume hood.

References

1. Ahuja CS, Wilson JR, Nori S, Kotter MRN, Druschel C, Curt A, Fehlings MG (2017) Traumatic spinal cord injury. *Nat Rev Dis Primers* 3:17018. <https://doi.org/10.1038/nrdp.2017.18>
2. Sabin KZ, Jiang P, Gearhart MD, Stewart R, Echeverri K (2019) AP-1(cFos/JunB)/miR-200a regulate the pro-regenerative glial cell response during axolotl spinal cord regeneration. *Commun Biol* 2:91. <https://doi.org/10.1038/s42003-019-0335-4>
3. Noorimotlagh Z, Babaie M, Safdarian M, Ghadiri T, Rahimi-Movaghar V (2017) Mechanisms of spinal cord injury regeneration in zebrafish: a systematic review. *Iran J Basic Med Sci* 20(12):1287
4. Diaz Quiroz JF, Tsai E, Coyle M, Sehm T, Echeverri K (2014) Precise control of miR-125b levels is required to create a regeneration-permissive environment after spinal cord injury: a cross-species comparison between salamander and rat. *Dis Model Mech* 7(6):601–611. <https://doi.org/10.1242/dmm.014837>
5. Hui SP, Dutta A, Ghosh S (2010) Cellular response after crush injury in adult zebrafish spinal cord. *Dev Dyn* 239(11):2962–2979. <https://doi.org/10.1002/dvdy.22438>
6. Hanslik KL, Allen SR, Harkenrider TL, Fogerson SM, Guadarrama E, Morgan JR (2019) Regenerative capacity in the lamprey spinal cord is not altered after a repeated transection.

- PLoS One 14(1):e0204193. <https://doi.org/10.1371/journal.pone.0204193>
7. Monaghan JR, Walker JA, Page RB, Putta S, Beachy CK, Voss SR (2007) Early gene expression during natural spinal cord regeneration in the salamander *Ambystoma mexicanum*. *J Neurochem* 101(1):27–40. <https://doi.org/10.1111/j.1471-4159.2006.04344.x>
 8. Walker SE, Nottrodt R, Maddalena L, Carter C, Spencer GE, Carlone RL (2018) Retinoid X receptor α downregulation is required for tail and caudal spinal cord regeneration in the adult newt. *Neural Regen Res* 13(6):1036–1045. <https://doi.org/10.4103/1673-5374.233447>
 9. Echeverri K, Tanaka EM (2003) Electroporation as a tool to study in vivo spinal cord regeneration. *Dev Dyn* 226(2):418–425. <https://doi.org/10.1002/dvdy.10238>
 10. Deep A, Adeeb N, Hose N, Rezaei M, Fard SA, Tubbs RS, Yashar P, Liker MA, Kateb B, Mortazavi MM (2015) Mouse models of spinal cord injury and stem cell transplantation. *Transl Res Anat* 1:2–10. <https://doi.org/10.1016/j.tria.2015.10.001>
 11. Minakov AN, Chernov AS, Asutin DS, Konovalov NA, Telegin GB (2018) Experimental models of spinal cord injury in laboratory rats. *Acta Nat* 10(3):4–10
 12. Rodrigo Albers A, Tazaki A, Rost F, Nowoshilow S, Chara O, Tanaka EM (2015) Planar cell polarity-mediated induction of neural stem cell expansion during axolotl spinal cord regeneration. *elife* 4:e10230. <https://doi.org/10.7554/eLife.10230>
 13. Rost F, Rodrigo Albers A, Mazurov V, Brusch L, Deutsch A, Tanaka EM, Chara O (2016) Accelerated cell divisions drive the outgrowth of the regenerating spinal cord in axolotls. *elife*:5. <https://doi.org/10.7554/eLife.20357>
 14. Thygesen MM, Lauridsen H, Pedersen M, Orłowski D, Mikkelsen TW, Rasmussen MM (2019) A clinically relevant blunt spinal cord injury model in the regeneration competent axolotl (*Ambystoma mexicanum*) tail. *Exp Ther Med* 17(3):2322–2328. <https://doi.org/10.3892/etm.2019.7193>



Live Imaging of Axonal Dynamics After Laser Axotomy of Peripheral Neurons in Zebrafish

Kadidia P. Adula and Alvaro Sagasti

Abstract

Axon severing results in diverse outcomes, including successful regeneration and reestablishment of function, failure to regenerate, or neuronal cell death. Experimentally injuring an axon makes it possible to study degeneration of the distal stump that was detached from the cell body and document the successive steps of regeneration. Precise injury reduces damage to the environment surrounding an axon, and thereby the involvement of extrinsic processes, such as scarring or inflammation, enabling researchers to isolate the role that intrinsic factors play in regeneration. Several methods have been used to sever axons, each with advantages and disadvantages. This chapter describes using a laser on a two-photon microscope to cut individual axons of touch-sensing neurons in zebrafish larvae, and live confocal imaging to monitor its regeneration, a method that provides exceptional resolution.

Key words Axotomy, Transient transgenesis, Somatosensory, Regeneration, Axon, Zebrafish, Live imaging

1 Introduction

Outcomes of axon injury are variable. A severed axon may regenerate to reinnervate its correct target, fail to regenerate altogether, regenerate but grow in the wrong direction, or die. Successful axon regeneration is dictated by both intrinsic and extrinsic factors that integrate a balance of positive and negative cues [1–4]. Intrinsic factors refer to the state of signaling pathways in the injured neuron itself, while extrinsic factors are signals from nearby cells and the extracellular matrix. For example, in the mammalian central nervous system, glial and immune cells release a myriad of both positive and negative factors [5]. These extrinsic cues make it difficult to experimentally disambiguate the contribution of intrinsic growth pathways from those of external factors in the axon regeneration process. Methods that use scissors or forceps to create injuries, including spinal cord, sciatic nerve, and optic nerve crushes, as

well as traumatic brain injury models, damage multiple axons and surrounding tissues and are thus more likely to trigger extrinsic cells to participate in the axon injury response.

Determining an individual neuron's contribution to the repair process is essential for understanding the heterogeneous outcomes of repair responses. MicroPoint UV pulsed lasers and femtosecond lasers mounted on two-photon microscopes can be used to target individual axons, but the latter offer more control and thus more precisely limit damage to the target [6–15]. Zebrafish (*Danio rerio*) is an excellent model organism in which to ask these questions because both its central and peripheral nervous systems are permissive to axon regrowth [1, 16]. Moreover, transient transgenesis can be used to label and image individual neurons in living animals. Zebrafish larvae have been used to elucidate mechanisms of Wallerian degeneration, axon regeneration, and engulfment of axonal debris and to characterize physiological changes during these processes [17–21]. This chapter describes precise axotomies in zebrafish using a laser mounted on a two-photon microscope. Although this protocol focuses specifically on severing the peripheral axons of larval sensory neurons, called Rohon–Beard (RB) neurons [22, 23], with different transgenes, this approach can be easily adapted to study other types of zebrafish peripheral neurons, including motor and lateral line neurons.

2 Materials

2.1 Somatosensory Neuron Labeling

1. Zebrafish: 3–18-month-old-type male and female fish (e.g., ZFIN: ZDB-GENO-960809-7). Fish are kept in a 14/10 dark/light cycle. Embryos are raised in a 28.5 °C incubator until 5 dpf.
2. 20 ng/uL of Tg(isl1[ss]: Gal4-VP16,UAS:DsRed) or Tg(isl1[ss]:Gal4-VP16,UAS:GFP) plasmids [24].
3. Pulled borosilicate glass needles (with a filament): 10 cm in length, inner diameter 0.78 mm, outer diameter 1.0 mm.
4. Injection mold (2% agarose, molecular biology grade): Add 0.8 g of agarose and 50 mL of 1× E3 embryo buffer in a 500 mL Erlenmeyer flask. Obstruct the opening of the flask with a crumpled paper towel. Microwave the flask for 2 min, stopping every 20 s to swirl the flask (*see Note 1*), or until the agarose is fully dissolved. Cool until warm to the touch. Pour the agarose gel into a 10 cm plate. Place a plastic microinjection mold with straight ridges on top of the gel and press gently (*see Note 2*). Wait for the gel to solidify. Remove the plastic mold and store the 2% agarose gel at 4 °C.

2.2 Fish Embryo Cultivation

1. 60× E3 embryo buffer (1 L): Dissolve 17.2 g NaCl, 0.76 g KCl, 2.9 g CaCl₂·2H₂O, and 4.9 g MgSO₄·7H₂O in deionized (ddH₂O) water [25]; use 0.1 M NaOH to bring to pH 7.2. Autoclave.
2. 1× E3 embryo buffer: In a 20 L carboy, mix 333 mL of 60× E3 embryo buffer with 19.667 L of ddH₂O and 12 drops of 0.05 wt. % methylene blue aqueous solution. Store at room temperature (*see Note 3*).

2.3 Preventing Pigment Development

1. 50× PTU solution: Dissolve 0.3 g of 1-phenyl 2-thiourea (PTU) in 200 mL of 1× E3 embryo buffer in a chemical hood. Heat the solution to 60 °C on a hot plate with a magnetic stirrer until dissolved. Divide the 50× stock solution (10 mM) into 10 mL aliquots and store at −20 °C.
2. E3P (E3 buffer with 0.2 mM PTU): Thaw 20 mL 50× PTU aliquot; mix with 980 mL of 1× E3 embryo buffer. Heat the 1 L diluted solution to 60 °C. Cool down to room temperature before use (*see Note 4*).

2.4 Anesthetizing Fish

1. Tricaine stock solution (MS-222 or 3-amino benzoic acid ethyl ester): Make a 0.4% stock solution of tricaine by dissolving 400 mg of tricaine methanesulfonate in 97.9 mL of ddH₂O, 2.1 mL of 1 M Tris–HCl (pH 9.0), 0.1 M NaOH, pH to 7.0. Make 50 mL aliquots and store at −20 °C. Keep an aliquot at 4 °C when in use.
2. E3P + tricaine: Dilute tricaine stock solution 1:5 in E3P to obtain a 0.08% working solution.

2.5 Mounting Embryos for Imaging

1. 5-mm-thick Delrin rings (*see Note 5*): Oval ring (inner diameter 12 mm × 23 mm, outer diameter 19 mm × 30 mm); circular ring (inner diameter 12 mm, outer diameter 16 mm) (Fig. 2).
2. Microscope cover glass: 24 × 60 mm.
3. Pre-cleaned and single frosted end glass slides: 75 × 25 × 1 mm.
4. Dow Corning High Vacuum Grease.
5. A curved probe: Insert a black enameled insect pin into a microdissecting needle holder. Manually curve the insect pin tip.
6. For 1% agarose (molecular biology grade): Add 0.5 g of low melting agarose and 50 mL of 1× E3 embryo buffer in a 500 mL Erlenmeyer flask. Obstruct the opening of the flask with a crumpled paper towel. Microwave the flask for 2 min, stopping every 20 s to swirl the flask (*see Note 1*), or until the agarose is fully dissolved. Cool until warm to the touch and aliquot 1 mL of melted agarose into 1.5 mL tubes. Store the tubes in a 42 °C heat block with a cover to maintain temperature uniformity.

3 Methods

These instructions use Zeiss 800 series microscopes for laser axotomy and imaging, but this procedure can be adapted to any confocal microscope, imaging software, or standard operating parameters.

3.1 Injections

1. Set up zebrafish crossing tanks with adult male and female zebrafish in the evening. Separate males and females with a divider.
2. The next morning, remove the divider to allow the fish to breed. After ~20 min collect freshly fertilized eggs using a tea strainer and wash into a petri dish.
3. Bring the 2% agarose gel injection mold to room temperature. Gently load embryos into the mold (as described elsewhere in detail [26]). Fill the mold with 1× E3 embryo buffer.
4. Load 20 ng/μL of Tg(isl1[ss]: Gal4-VP16,UAS:DsRed) plasmid into a pulled glass needle (*see Note 6*).
5. Inject embryos at the one- to four-cell stage (Fig. 1) with 5 nL of this plasmid (for details see [26]). Injecting plasmids into larvae at this stage results in transient expression. Since extra-chromosomal plasmids are inherited unequally during cell division, this approach results in mosaic labeling of touch-sensing neurons (TSN) in the skin, making it possible to screen for animals with expression in isolated neurons (*see Note 7* and Fig. 1).
6. Maintain embryos in 1× E3 embryo buffer and raise them in a 28.5 °C incubator.

3.2 Screening Embryos

1. At 22–23 h postfertilization (hpf), exchange the medium for E3P (E3 + PTU). Pigment cells interfere with laser axotomy and make it difficult to image neuronal arbors; PTU inhibits pigmentation, enabling embryos to remain transparent (Fig. 2, upper right panel) (*see Note 8*).
2. A few hours before axotomy, manually dechorionate embryos using forceps (*see Note 9*).
3. To immobilize larvae, in a 10 cm dish with E3P, add ten drops of tricaine stock solution (for a final concentration of ~0.08%) with a 3 mL plastic Pasteur pipette, and monitor them under a microscope to confirm that they stop moving.
4. Screen through embryos to find animals with isolated labeled neurons, using a dissecting or compound fluorescence microscope (e.g., Zeiss, Axioskop 2 Fs Plus). For our experiments, we identified larvae with a single labeled neuron innervating the tail (*see Note 10* and Fig. 1).

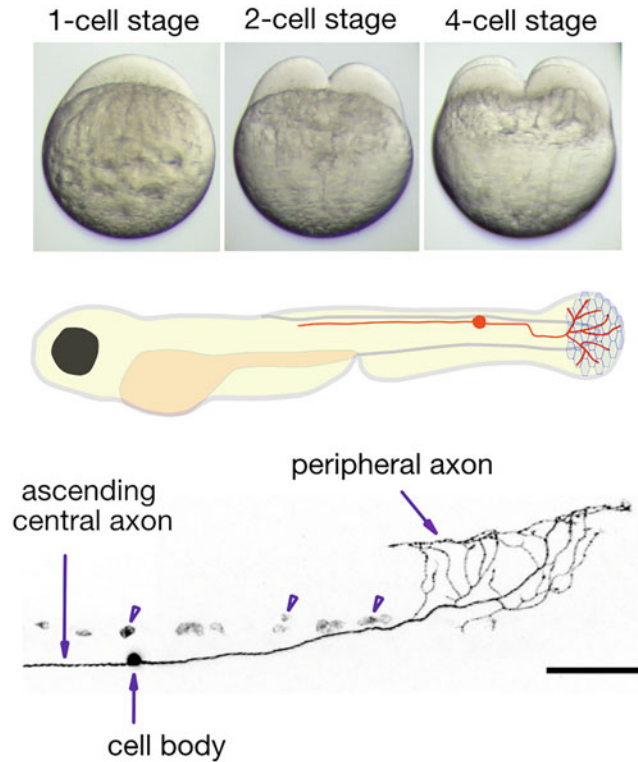


Fig. 1 *Upper panels:* Zebrafish embryo at the one-, two-, and four-cell stages. *Middle panel:* Cartoon of zebrafish larva with a single tail-innervating RB neuron depicted in red. RB cell bodies are located in the dorsal spinal cord. The peripheral axon, after exiting the spinal cord, arborizes upon reaching the skin. *Lower panel:* A tail-innervating RB neuron, with the cell body, the ascending central axon in the spinal cord, and the peripheral axon indicated. Arrowheads point to PTU-resistant pigment cells. The image was converted to gray scale and inverted. (Scale bar, 100 μm)

5. Transfer screened larvae to a small petri dish. Label each dish, indicating whether the identified axon innervates the right or left side of the body. Animals must be mounted so that the side with the identified axon faces the coverslip, since laser illumination for severing and imaging does not penetrate through the animal.
6. Once screening is complete, replace media with E3P. Place the larvae in a 28.5 °C incubator until they reach the 48 hpf stage.

3.3 Mounting

1. Using a micropipette tip, collect and apply a thin layer of vacuum grease on one side of an oval mounting ring (*see Note 11*), and press the ring onto a clean cover glass (Fig. 2, top left panel).

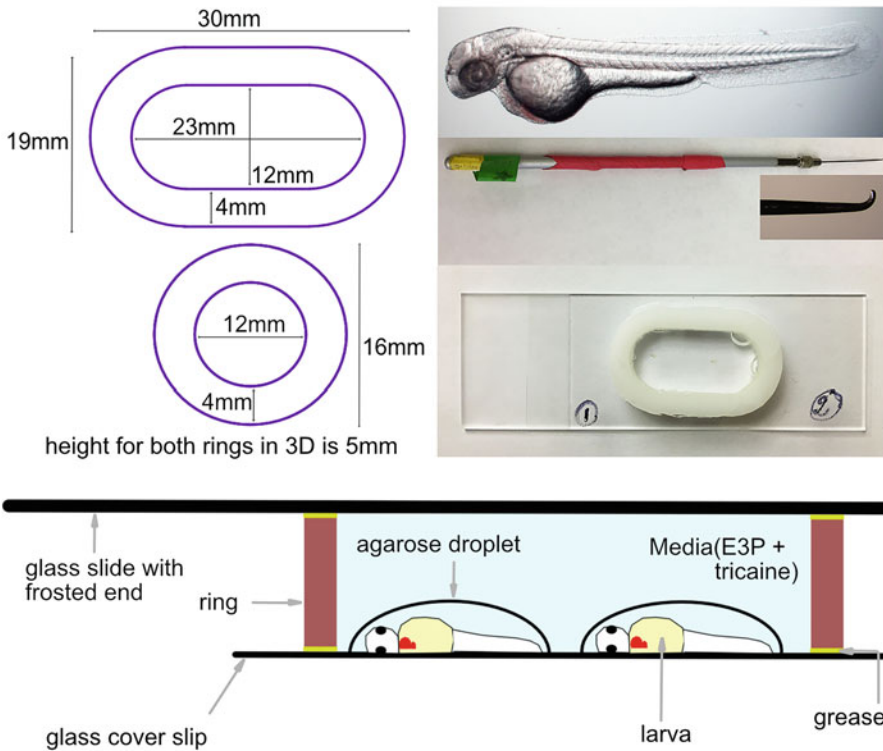


Fig. 2 *Left panel:* Schematic of oval and circular rings with dimensions indicated. *Upper right panel:* Zebrafish larva at 48 h postfertilization. The larva was anesthetized with E3P + tricaine. *Middle right panel:* Manually curved probe. *Lower right panel:* Two larvae mounted against a microscope cover slide. The larvae were sealed in an oval mounting ring, which was sandwiched between the microscope cover glass and a glass slide. The chamber was filled with E3P + tricaine. *Bottom panel:* Labeled cartoon with a side view of larvae mounted in an oval ring

2. Anesthetize larvae at 48 hpf (Fig. 2, top right panel) with tricaine. For larvae in a 10 cm petri dish, ten drops (or ~0.08%) of tricaine stock solution are sufficient. If the larvae are in a 6 cm petri dish, add fewer drops of tricaine stock solution. Confirm that the animals have stopped moving.
3. Mix in one drop of tricaine stock solution into the 1% melted agarose tube. Use a glass Pasteur pipette inserted into a pump pipette (see Note 12) to pick up one anesthetized embryo with as little E3P + tricaine as possible, and transfer it to a tube containing 1% low melting agarose. Use the pipette to transfer the larvae along with melted agarose onto the cover glass, inside the mounted ring (see Note 13). Rinse the inside of the glass pipette a few times with E3P + tricaine to remove residual agarose.

4. Arrange the animal in the molten agarose under a dissecting light microscope. Use a curved probe (Fig. 2, second right panel) to gently press the larva (the side with the labeled neuron), as close to the cover glass as possible (Fig. 2, third right panel and bottom panel). To target touch-sensing neurons in the tail, larvae should be mounted horizontally (on their sides), and the two eyes should be aligned when viewed from above. If the larva floats away from the coverslip, gently push it back down with the curved probe. The agarose should reach $\sim 1/3$ of the mounting ring in height. Wait ~ 15 min for the agarose to solidify (*see* **Note 14**).
5. Grease the other side of the mounted ring and fill the rest of the chamber with E3P + tricaine.
6. Press the microscope slide with the frosted end against the greased ring. Clean off any excess water around the mounted ring with Kimwipes (Fig. 2, third right panel and bottom panel).

3.4 Pre-axotomy Imaging

1. Use a confocal microscope to collect images of the target neurons from living larvae (Fig. 3). Imaging parameters for acquisition with a Zeiss LSM-800 (or LSM 880) upright microscope and the Zen Blue 2.3 software are as follows: Under the “Acquisition Mode” tab, optimize imaging parameters, including bits per pixel, image frame size, pixel dwell time, averaging, image size, and pixel size. We usually use an 8 bits per pixel format, an image frame size of 512×512 , a 1.52 μs pixel dwell time, a 1.86 s scan time, an averaging number of 2, and a 1.25 μm pixel size. Under the “Channels” tab, choose the appropriate laser wavelengths, gain, and pinhole diameter to image the neurons. For eGFP or DsRed, we use 488 nm and 561 nm laser lines, respectively, and a master gain of 650 V. We set a pinhole diameter to an Airy unit of 1, which maximizes confocality.
2. Start the Zen Blue 2.3 software to visualize cells. If the system is being used for the first time that day, the stage and focus should be calibrated to avoid accidents (*see* **Note 15**). After hardware initialization is complete, a “Stage/Focus not calibrated” dialog window will appear. Select “Calibrate Now.” Calibration will take less than a minute. Maintain the stage at a 28.5 °C temperature with a heated stage or objectives.
3. Go to the “Acquisition” window and open your protocol. Go to the “Locate” window and under “Reflected Light” activate the “On” tab. Under “Favorites” select the “DsRed” configuration setting. Using the eyepiece, find the larva with the 10 \times objective (Plan-Neofluar, NA = 0.3) and center it in the field of view. Switch to a 20 \times (Plan-Apochromat, NA = 0.8) objective and focus on the axon.

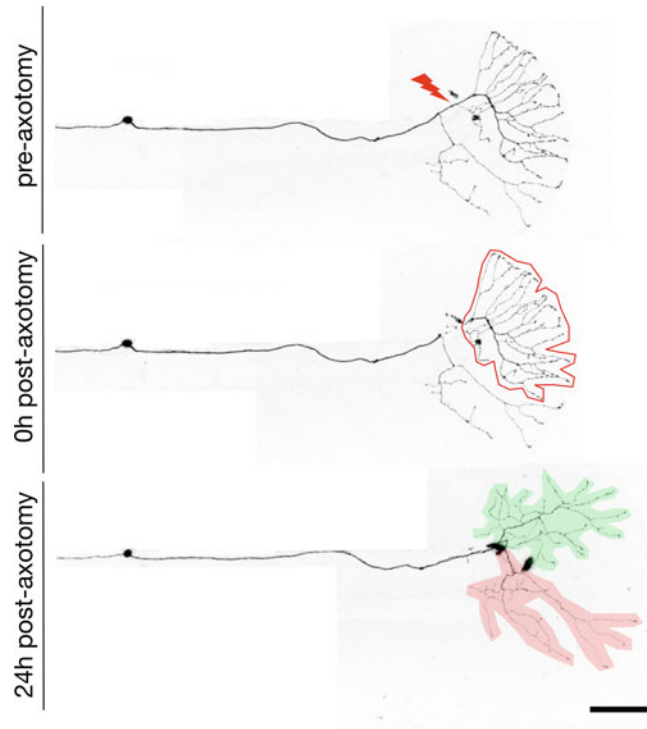


Fig. 3 At 48 h postfertilization, a touch-sensing neuron innervating the tail was imaged before axotomy. Using a laser mounted on a two-photon microscope, its peripheral arbor was cut at the second branching point and imaged again within the hour. The detached distal axon branch, outlined in red, underwent Wallerian degeneration a few hours after the injury. At 24 h post-axotomy, the neuron was imaged again to assess regeneration. Regeneration from the injury site is shaded in green, and the spared branch is shaded in red. The ability to distinguish injury site regeneration from spared branches illustrates the clarity provided by labeling and injuring a single neuron. For display purposes, the image was converted to a maximum projection and inverted. (Scale bar, 100 μm)

4. Go to the “Acquisition” window. Open the DsRed fluorescent beam by checking and highlighting the “DsRed track” sub-tab in the “Channels” tab. Return to the protocol tab and press the “Live” tab to see the neuron on the screen. In the “Acquisition Mode” tab, you may adjust the zoom. Press the “Live” sub-tab in the protocol tab to image and center the axon (*see Note 16*).
5. Under the “Z-Stack” tab, optimize your “slice interval”; we usually set ours at 1 μm . Use the manual focus knob, and the manual monitor to set the range of your z-stack by selecting a “Set First” slice position and a “Set Last” slice position. In the protocol tab, exit the “Live” mode. Press the “Start Experiment” tab to acquire the pre-axotomy image (*see Note 17*). As the image is acquired, a stack-by-stack 2D projection will be displayed on the monitor (*see Note 18*). Save the image as a “.czi” file.

3.5 Axotomies with a Two-Photon Microscope

1. For axotomies, we use a LSM 880 inverted confocal/two-photon microscope equipped with a laser (Chameleon, 690–1064 nm) for two-photon imaging and Zen Black 2.1 SP3 software, but this procedure can be adapted to any equivalent microscope. To begin, turn the key on the two-photon laser box from “Standby” to “On.” Let the power ramp up. Wait until the screen on the laser box displays the following messages: “Power: 3960 mV,” “813 nm,” and “Status: Ok.”
2. Start the Zen Black 2.1 SP3 software to visualize the neuron. Go to the “Locate” window and under “Reflected Light” activate the “On” tab. Under “Configuration” select “DsRed.” Locate and center your sample through the objectives, starting with a 10× objective (Plan-Apochromat, NA = 0.45) to find the larva. Center the larva in the field of view before switching to a 20× objective (Plan-Apochromat, NA = 0.8) to focus on the axon.
3. Go to the “Acquisition” window. Activate the DsRed fluorescent laser by checking and highlighting the “DsRed track” sub-tab in the “Channels” tab. Return to the protocol tab and press the “Live” tab to see the neuron on the screen. In the “Acquisition Mode” tab, adjust the zoom to 1× zoom and center the peripheral axon in the field of view. Press the “Live” tab a second time to exit the “Live” mode, and use the “Crop” tab to zoom into the area of the target axon. Zoom to a minimum of 100×. Ensure that DsRed fluorescence is below saturation by reducing the gain. Exit “Live” mode in the protocol tab. Imaging parameters for the axon severing protocol are as follows: Under the “Acquisition Mode” tab, optimize imaging parameters including image frame size, pixel dwell time, scanning time, averaging, and pixel size. Use the imaging parameters described under Subheading 3.4. Under the “Channels” tab, choose the appropriate laser wavelengths, gain, pinhole diameter, and slice interval for your neurons.
4. Activate the two-photon laser (813 nm) by checking and highlighting the “2-photon track” tab (*see Note 19*). Start with 5.0% laser power. In the protocol tab, press “Live” again for 1 s; a burst of fluorescence indicates damage to the axon. Exit “Live” mode. Turn off the two-photon laser beam (813 nm) by unchecking and deselecting the “2-photon track” tab. Switch back to the “DsRed track” and return to 1× zoom to see if the axon is cut. It may take a few moments for the axon to be severed. Axon beading adjacent to the target site is a good indication that it will be severed. If the axon remains uncut, raise the two-photon laser power in 0.5% increments and repeat, until cutting is successful (*see Note 20*).

5. At the end of the microscopy session, exit the program. A “Laser Off” window will appear. Turn off all the lasers and press “OK.”
6. Take a “post-axotomy” confocal image using the same settings as described for pre-axotomy under Subheading 3.4. Within a few hours post-axotomy, the detached branch will degenerate by Wallerian degeneration (Fig. 3, middle panel).

3.6 Larva Recovery

1. Recover zebrafish larvae under a dissecting light microscope. Separate the cover slide from the mounting ring. The agarose might remain attached to the cover glass or detach to float in the E3P + tricaine-filled chamber formed by the mounting ring. In either case, use a glass pipette to remove media around the agarose. Remove the mounting ring.
2. Use a thin metal spatula or a razor blade to trim away the agarose surrounding the larva. Use two sets of forceps to carefully push away the remaining agarose from the larva. Pay particular attention not to puncture the yolk or damage the tail.
3. Once the larva is free, add a few drops of E3P. Use a glass pipette to transfer the larva from the glass slide to an individually labeled small petri dish. Fill the petri dish with E3P.
4. Allow 5–10 min for the larva to recover. When it responds to touch, put the petri dish back into the 28.5 °C incubator. After 24 h, remount the larva and take a 24-h post-axotomy image.

3.7 Post-regeneration Imaging and Time-Lapse Movies

1. Remount larvae to assess regeneration after the desired time interval (*see* Subheading 3.3). We typically assess RB neuron regeneration 24 h after axotomy. Image the neuron with the same confocal settings as described under Subheading 3.4.
2. In addition to taking static images of peripheral axons at specific time points, time-lapse movies of the regeneration process can be recorded. To record the first 12 h post-injury, start the movie immediately after axotomy (do not recover animals from the agarose). To record later phases of regeneration, recover the larva after axotomy (*see* Subheading 3.6), and remount it later (*see* **Note 21**). Set up imaging acquisition as described above, but add additional sections to the z-stack, both above and below the axon, to accommodate potential drift of the stage or neurons as the larva continues to grow. Using the “Time-series” option under the “Acquisition” tab, you can collect a single movie for up to 12 h, without harming the animal. We typically collect movie frames at 5-min intervals for 144 cycles (12 h). Using the “Tiles” option allows the recording of several movies within the same time period. To capture dynamics of an entire peripheral arbor, movies can be made using a 20× air or water objective. To focus on growth cone dynamics, use a 40–63× oil objective.

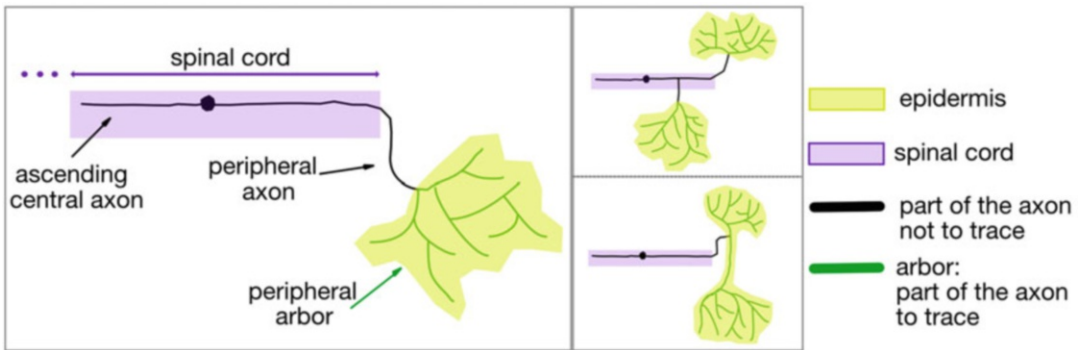


Fig. 4 *Left panel:* Cartoon depicting a RB neuron with a single peripheral arbor. The spinal cord is usually at a deeper focal plane than the peripheral arbor. *Upper right panel:* A RB neuron with two peripheral arbors. *Lower right panel:* A RB neuron with a single peripheral arbor with one significantly longer branch. The Simple Neurite Tracer plug-in in Fiji was used to trace all images in a z-stack format

3.8 Peripheral Axon Arbor Tracing

1. Most RB neurons have a single peripheral arbor (Fig. 4, left panel) which extends from the cell body and leaves the spinal cord to penetrate the skin, at which point it branches between epithelial cells, like the arbors of a tree [22, 23]. We compare arbor sizes pre-axotomy to arbor sizes immediately after axotomy and 24 h post-axotomy. For tracing, use the Simple Neurite Tracer (SNT) plug-in in Fiji [27] with the images in a z-stack format. SNT is part of Fiji's Neuroanatomy suite (see Note 22).

3.9 Post-imaging Processing

1. For presentation and analysis, use ImageJ (Fiji) or other image processing software to produce maximum projections of the .czi files. We convert images to gray scale and invert them before saving them as TIFF images to maximize contrast. Multiple images of large neurons can be stitched together to create a complete representation.

4 Notes

1. Remove the crumpled paper towel and orient the flask away from you before swirling to release pressure. Reinsert the crumpled paper towel and return the flask to the microwave for the next 20-s heating cycle.
2. To make the agarose injection mold, a plastic mold is placed on the gel before it solidifies. For specific dimensions, see [26]. We use molds with straight ridges to make trenches into our 2% agarose injection molds. Trenches are used to align the embryos and secure the chorions in place for ease of injection. Plastic molds can imprint various shapes onto agarose gels, including spirals and linear trenches.

3. Ringer's solution optimized for zebrafish may also be used to grow zebrafish embryos [28].
4. PTU crystals form during freezing and may not dissolve completely once thawed. Heating the solution to 60 °C will dissolve them. Let the solution cool to room temperature before use. If making several bottles of E3P, leave one out at room temperature for use, and store the rest at 4 °C.
5. A white Delrin acetal resin sheet, 5 mm thick, was laser cut to fashion mounting rings. Alternatively, mounting rings can be 3D printed or cut from other materials. If you plan to treat mounted larvae with drugs during imaging, you may want to use rings made with sheets 2 mm in thickness. These shorter rings will reduce the volume of the imaging chamber and thus require less medium to fill the chamber. A 22 mm × 22 mm microscope cover glass may also be used.
6. Other transgenes can be used to label different neuron types (e.g., [29, 30]).
7. To achieve sparser labeling, and thus maximize the probability of labeling single neurons, inject the plasmid into the yolk between the two- and four-cell stages, rather than the one-cell stage.
8. PTU specifically prevents the formation of the pigment melanin in zebrafish melanophores, which can obstruct neurons during imaging. Embryos should be switched to PTU-containing medium before the onset of melanogenesis in the skin. Alternatively, mutant embryos lacking pigment cells can be used [31, 32].
9. To dechorionate embryos, use two forceps. Under the light microscope, being careful not to poke and injure the larva, pinch and hold the top of the chorion with the first forceps. Pinch the chorion with the second forceps, close to the first forceps, and gently pull the forceps apart to rip the chorion and free the wriggling larvae.
10. The cell body of a tail-innervating neuron may be anywhere in the caudal spinal cord, but its peripheral arbor typically arborizes at or posterior to the cloaca. Moreover, a tail-innervating neuron has an ascending central axon but no descending central axon.
11. A 10 mL syringe, with a Luer-Lok Tip, filled with vacuum grease can be used to facilitate the application of grease onto the sides of a mounting ring.
12. A pump pipette offers more control than a bulb for transferring liquids with a glass Pasteur pipette.

13. Several larvae can be simultaneously mounted within a ring; however, to keep track of individual larvae and facilitate rescue, mount a single larva in a circular ring and a maximum of two larvae in an oval ring.
14. If you are mounting larvae to record a time-lapse movie, wait more than 15 min for the agarose to solidify or until wrinkles can be seen over the surface of the agarose drop with the naked eye. This extra polymerization time ensures the solidity of the agarose, preventing the larva from drifting out of z-stack range.
15. To avoid crushing slides and potentially damaging objective lenses, the first user of the day should calibrate both the stage and the focus.
16. The “Stage” tab can be used to change the position of the neuron on the monitor with the mouse instead of using the manual knob. By clicking on the arrowheads of the “x-position” and the “y-position,” the neuron can be moved to the left and right, or upward and downward, respectively.
17. It can be useful, for presentation purposes, to collect separate images of the cell body and peripheral axon, since the spinal cord and the skin are at different focal depths. The images can then be collaged and stitched together using Fiji or Photoshop to create a complete representation of the neuron.
18. To see a preview of your image as a maximum projection before saving your image as a “.czi” file, go to the “Ortho tab,” select the “Ortho-Display” sub-tab, and select “Maximum Intensity Projection.”
19. At 813 nm, the two-photon laser beam is out of the visible spectrum. Although the beam cannot be seen, the damage it inflicts can. Choose any wavelength to visualize the fluorescent debris resulting from the two-photon laser damage; if severing is successful, a burst of light will appear across the screen.
20. It is essential to be patient at this step and switch back to the “DsRed track” to check for axonal damage after each 0.5% increase of the two-photon laser (813 nm), whether or not there is a burst of fluorescence indicating the scattering of debris. Depending on how a larva is mounted, 5–8% of two-photon laser power should be sufficient to cut an axon innervating the skin. As mounting between individual larvae varies slightly, starting at 5.0% for each larva is important. If more power is required to cut an axon, remount the larva. If remounting does not solve the issue, the two-photon laser may need to be realigned.
21. In our experiments, we observed a slower axon regeneration rate for larvae that were in tricaine during 12-h movies, in comparison with freely moving, unanesthetized larvae that

were remounted after 12 h. While tricaine does not block axon regeneration, the slowed growth rate could be related to its effect on a neuron's electrical activity.

22. Note that a small number of RB neurons have more than one peripheral arbor; for example, a peripheral axon can branch in the spinal cord, creating a neuron with two separate peripheral arbors innervating the skin. We measure total arbor length for such neurons by adding together the lengths of the two arbors. The point at which an axon exits the spinal cord is often detectable as a kink in the axon's trajectory. Lengths between branches of peripheral arbors can vary considerably, which can sometimes make a single arbor appear to be two separate arbors (Fig. 4, lower right panel).

Acknowledgments

KPA was supported by a Cota-Robles fellowship, Bridge to the Doctorate Fellowship, and NIH fellowship F31NS106742-02. This work was supported by NIH grant R01AR064582 (to AS).

References

1. Rasmussen JP, Sagasti A (2016) Learning to swim, again: axon regeneration in fish. *Exp Neurol* 287:318–330
2. Mahar M, Cavalli V (2018) Intrinsic mechanisms of neuronal axon regeneration. *Nat Rev Neurosci* 19:323–337
3. Huebner EA, Strittmatter SM (2009) Axon regeneration in the peripheral and central nervous systems. *Results Probl Cell Differ* 48:339–351
4. Uyeda A, Muramatsu R (2020) Molecular mechanisms of central nervous system axonal regeneration and remyelination: a review. *Int J Mol Sci* 21:8116
5. Giger RJ, Hollis ER 2nd, Tuszynski MH (2010) Guidance molecules in axon regeneration. *Cold Spring Harb Perspect Biol* 2:a001867
6. Stone MC, Albertson RM, Chen L et al (2014) Dendrite injury triggers DLK-independent regeneration. *Cell Rep* 6:247–253
7. Wlaschin JJ, Gluski JM, Nguyen E et al (2018) Dual leucine zipper kinase is required for mechanical allodynia and microgliosis after nerve injury. *elife* 7:e33910
8. O'Brien GS, Rieger S, Martin SM et al (2009) Two-photon axotomy and time-lapse confocal imaging in live zebrafish embryos. *J Vis Exp* 16(24):1129. <https://doi.org/10.3791/1129>
9. Burgess HA, Granato M (2007) Sensorimotor gating in larval zebrafish. *J Neurosci* 27:4984–4994
10. Yanik MF, Cinar H, Cinar HN et al (2004) Neurosurgery: functional regeneration after laser axotomy. *Nature* 432:822
11. Hammarlund M, Jorgensen EM, Bastiani MJ (2007) Axons break in animals lacking beta-spectrin. *J Cell Biol* 176:269–275
12. Ylera B, Ertürk A, Hellal F et al (2009) Chronically CNS-injured adult sensory neurons gain regenerative competence upon a lesion of their peripheral axon. *Curr Biol* 19:930–936
13. Jackson J, Canty AJ, Huang L et al (2015) Laser-mediated microlesions in mouse neocortex to investigate neuronal degeneration and regeneration. *Curr Protoc Neurosci* 73:2.24.1–2.24.17
14. Allegra Mascaro AL, Sacconi L, Pavone FS (2010) Multi-photon nanosurgery in live brain. *Front Neuroenerg* 2:21
15. Bormann P, Zumsteg VM, LWA R et al (1998) Target contact regulates GAP-43 and alpha-tubulin mRNA levels in regenerating retinal ganglion cells. *J Neurosci* 18(4):405–419
16. Bastmeyer M, Beckmann M, Schwab ME et al (1991) Growth of regenerating goldfish axons is inhibited by rat oligodendrocytes and CNS myelin but not but not by goldfish optic nerve

- tract oligodendrocyte like cells and fish CNS myelin. *J Neurosci* 11:626–640
17. Vargas ME, Yamagishi Y, Tessier-Lavigne M et al (2015) Live imaging of calcium dynamics during axon degeneration reveals two functionally distinct phases of calcium influx. *J Neurosci* 35:15026–15038
 18. Rasmussen JP, Sack GS, Martin SM et al (2015) Vertebrate epidermal cells are broad-specificity phagocytes that clear sensory axon debris. *J Neurosci* 35:559–570
 19. Lewis GM, Kucenas S (2013) Motor nerve transection and time-lapse imaging of glial cell behaviors in live zebrafish. *J Vis Exp*. <https://doi.org/10.3791/50621>
 20. Rosenberg AF, Wolman MA, Franzini-Armstrong C et al (2012) In vivo nerve-macrophage interactions following peripheral nerve injury. *J Neurosci* 32:3898–3909
 21. Rieger S, Sagasti A (2011) Hydrogen peroxide promotes injury-induced peripheral sensory axon regeneration in the zebrafish skin. *PLoS Biol* 9:e1000621
 22. Palanca AMS, Lee S-L, Yee LE et al (2013) New transgenic reporters identify somatosensory neuron subtypes in larval zebrafish. *Dev Neurobiol* 73:152–167
 23. Katz HR, Menelaou E, Hale ME (2021) Morphological and physiological properties of Rohon-Beard neurons along the zebrafish spinal cord. *J Comp Neurol* 529:1499–1515
 24. Sagasti A, Guido MR, Raible DW et al (2005) Repulsive interactions shape the morphologies and functional arrangement of zebrafish peripheral sensory arbors. *Curr Biol* 15:804–814
 25. Cold Spring Harbor Laboratory Press (2021) 1559–6095. <http://cshprotocols.cshlp.org>. Accessed 13 May 2021
 26. Rosen JN, Sweeney MF, Mably JD (2009) Microinjection of zebrafish embryos to analyze gene function. *J Vis Exp*. <https://doi.org/10.3791/1115>
 27. Schindelin J, Arganda-Carreras I, Frise E et al (2012) Fiji: an open-source platform for biological-image analysis. *Nat Methods* 9: 676–682
 28. The Zebrafish Information Network (1994–2021). <https://zfin.atlassian.net>. Accessed 13 May 2021
 29. Stil A, Drapeau P (2016) Neuronal labeling patterns in the spinal cord of adult transgenic zebrafish. *Dev Neurobiol* 76:642–660
 30. Satou C, Kimura Y, Hirata H et al (2013) Transgenic tools to characterize neuronal properties of discrete populations of zebrafish neurons. *Development* 140:3927–3931
 31. Lister JA, Robertson CP, Lepage T et al (1999) nacre encodes a zebrafish microphthalmia-related protein that regulates neural-crest-derived pigment cell fate. *Development* 126: 3757–3767
 32. D’Agati G, Beltre R, Sessa A et al (2017) A defect in the mitochondrial protein Mpv17 underlies the transparent casper zebrafish. *Dev Biol* 430:11–17



Rapid Testing of Gene Function in Axonal Regeneration After Spinal Cord Injury Using Larval Zebrafish

Louisa K. Drake, Marcus Keatinge, Themistoklis M. Tsarouchas, Catherina G. Becker, David A. Lyons, and Thomas Becker

Abstract

Larval zebrafish show axonal regrowth over a complex spinal injury site and recovery of function within days after injury. Here we describe a simple protocol to disrupt gene function in this model using acute injections of highly active synthetic gRNAs to rapidly detect loss-of-function phenotypes without the need for breeding.

Key words Zebrafish larvae, Axon regeneration, CRISPR/Cas9 mutagenesis, Spinal cord injury

1 Introduction

In mammals, spinal cord injuries are permanent and can lead to lifelong disability. In contrast, anamniotes (fish and salamanders) undergo complete functional recovery after spinal cord transection. Axon growth across the lesion site is essential for this recovery [1].

Zebrafish larvae are a useful model for investigating molecular pathways which promote axonal growth over an injury site (“bridging”) after spinal cord injury. Whereas adult zebrafish functionally regenerate their spinal cord in 4–6 weeks [2, 3], 3-day-old larvae only need 48 h [4]. In addition, since zebrafish larva is transparent, transgenic reporter lines allow visualization of cell types of interest in the regenerating spinal cord of live animal. Using larvae also allows the researcher to observe most regenerative processes before potential pain sensation develops and larvae become protected under the law (by 5 days postfertilization in Europe). Experiments on larvae can thus be considered a relative replacement in the sense of the 3Rs of humane animal research (reduction, replacement, and refinement) [5].

Synthetic CRISPR gRNAs (sCrRNAs) have recently been shown to be a highly efficient tool to obtain almost complete somatic gene disruption when these are injected into one-cell stage zebrafish embryos [6–9]. The resulting phenotypes usually reflect those obtained in stable mutant lines for the genes of interest. However, additional controls should always be considered [6]. Raising sCrRNA-injected embryos to generate stable lines is one of these.

Here we describe combining the advantages of the zebrafish model with sCrRNA injections into one streamlined testing protocol for investigating genes involved in axon bridging after spinal cord injury. First, sCrRNAs targeting a molecule of interest are microinjected into the one-cell stage zebrafish embryo and quality-controlled at 1 day of development using restriction fragment length polymorphism (RFLP) analysis. At 3 days of development, the spinal cord of the larva is completely transected. Finally, the live fish are checked for the presence or absence of an axonal bridge using a fluorescence microscope at 1 and 2 days post-injury (or other timepoints of interest). In this way, loss-of-function phenotypes can be obtained in a complex in vivo injury situation within days and inform follow-on analyses of the targeted genes' functions in successful spinal cord regeneration.

2 Materials

2.1 CRISPR/Cas9 Microinjections

1. Zebrafish: Tg(*Xla.Tubb:DsRed*) or other transgenic line allowing visualization of axons in the spinal cord (*see Note 1*).
2. Dissecting microscope.
3. Microinjector.
4. Micromanipulator.
5. Pasteur pipettes—regular and fine-tip.
6. 90 mm petri dishes.
7. E3 medium: 5 mM NaCl, 0.17 mM KCl, 0.33 mM CaCl₂, 0.33 mM MgSO₄, 0.1% methylene blue.
8. 0.4% Fast Green FCF dye in H₂O.
9. Cas9 nuclease diluted to 7 μM (*see Note 2*).
10. Synthetic trans-activating CRISPR RNA (tracrRNA) (*see Note 3*).
11. Bespoke or pre-designed sCrRNAs targeting genes of interest (*see Subheading 3.1 and Note 13 for design guidance and Note 3 for storage information*).
12. Control sCrRNA with sequence 5'- TTACCTCAGTTA CAATTTAT-3' (*see Note 4*).
13. Adjustable pipette (1–10 μL) with gel-loading tips.

14. Needle puller (e.g., Sutter P97).
15. Injection needles: Use needle puller to make injection needles from borosilicate glass capillaries containing a filament (*see Note 5*).
16. No. 5 Watchmaker's forceps (0.02 × 0.05 mm tips).
17. Stage micrometer with graduations of 0.01 mm.
18. Mineral oil.
19. Standard microscope slide.

**2.2 Quality Control
by Restriction
Fragment Length
Polymorphism**

1. 0.2 mL PCR tubes.
2. 50 mM NaOH.
3. 1M Tris-HCl, pH 8.0.
4. 2× Taq polymerase in ready to use mixture (e.g., BioMix Red, Biotline).
5. Custom primers (10 μM) to amplify region of interest (*see Notes 6 and 15* and Subheading 3.1, step 5).
6. Restriction enzymes corresponding to design of sCrRNAs (*see Subheading 3.1 and Note 13*).
7. 100 bp DNA ladder.
8. 1× TAE buffer: 242 g Tris-HCl, 57.1 mL glacial acetic acid, 100 mL 0.5 EDTA solution (pH 8.0). Add distilled H₂O up to 1 L. Dilute 1:50 in deionized H₂O.
9. Nucleic Acid Stain (e.g., Sigma GelRed).
10. Agarose gel mold.
11. Agarose gel combs.
12. 2% agarose gel prepared on day of use: Dissolve 3 g agarose powder (molecular grade) in 150 mL 1× TAE buffer and heat in microwave until clear and bubbling. Let cool for 5 min and then add 7.5 μL Nucleic Acid Stain. Pour into gel mold with gel combs in place (*see Note 7*).
13. Gel tank.
14. Electrophoresis power supply.
15. UV transilluminator (*see Note 8*).

**2.3 Larval Spinal
Cord Lesions**

1. Anesthetic: 0.4 g MS-222 in 100 mL PBS (*see Note 9*).
2. 30 ½ G syringe needle attached to 1 mL syringe to allow for stability and greater control.
3. Agarose plates prepared on day of use: Add 4 g agarose (any grade) to 100 mL PBS and then heat in microwave to melt. Pour approximately 15 mL into lid of 90 mm petri dish, and allow to set for 20 min at room temperature (or shorter time at 4 °C) (*see Note 10*).

4. Fluorescence microscope with filter to visualize DsRed (~580 nm; or other fluorophore which allows visualization of axons in your chosen transgenic strain).

3 Methods

3.1 Designing sCrRNAs (See Note 11)

1. Identify the gene of interest (GOI) from Ensembl genome browser using the search tool.
2. Copy and paste the sequence of coding exons with some flanking intronic material individually into SnapGene Viewer (*see Note 12*).
3. Identify sCrRNA sites (*see Note 13* and Fig. 1).
4. Once designed, the sCrRNA can be ordered from a commercial supplier (*see Notes 2* and *14*).
5. Design primer pairs to amplify region containing the sCrRNA-targeted site (*see Note 15*).

3.2 Microinjection of CRISPR/Cas9 grNA (See Note 16)

1. On the evening before injections, separate male and female *Xla.Tubb:DsRed* fish.
2. On the morning of injections, prepare injection mix(es): 1 μL of each sCrRNA (up to total of 4 μL), 1 μL TracrNA, 1 μL Cas9, and 1 μL 0.4% Fast Green FCF dye.
Gently pipette up and down to mix using filter tips. Keep on the mix on ice until loaded into the tip.
3. Transfer 3 μL of injection mix to an injection needle using a pipette fitted with a gel loading tip (*see Note 17*).
4. Attach the injection needle to a micromanipulator connected to the microinjector.
5. Position the needle in the center of the field of view under of stereomicroscope, and pinch off the tip with fine forceps to make an opening in pulled needle (*see Note 18*).
6. Prepare the stage micrometer by adding one drop of mineral oil (approximately 100 μL) directly onto the micrometer.
7. Use the microinjector to expel a droplet of injection mix from needle into mineral oil on stage micrometer and measure diameter of droplet. Ideally, droplet should be 15–20 microns in diameter (*see Note 19*).
8. Repeat **steps 3–7** to prepare needles for the control and any additional injection mixes if different samples are to be injected in the same session (*see Note 20*).
9. After needles are prepared (or shortly before), allow male and female fish to mix again in a mating tank (*see Note 21*).

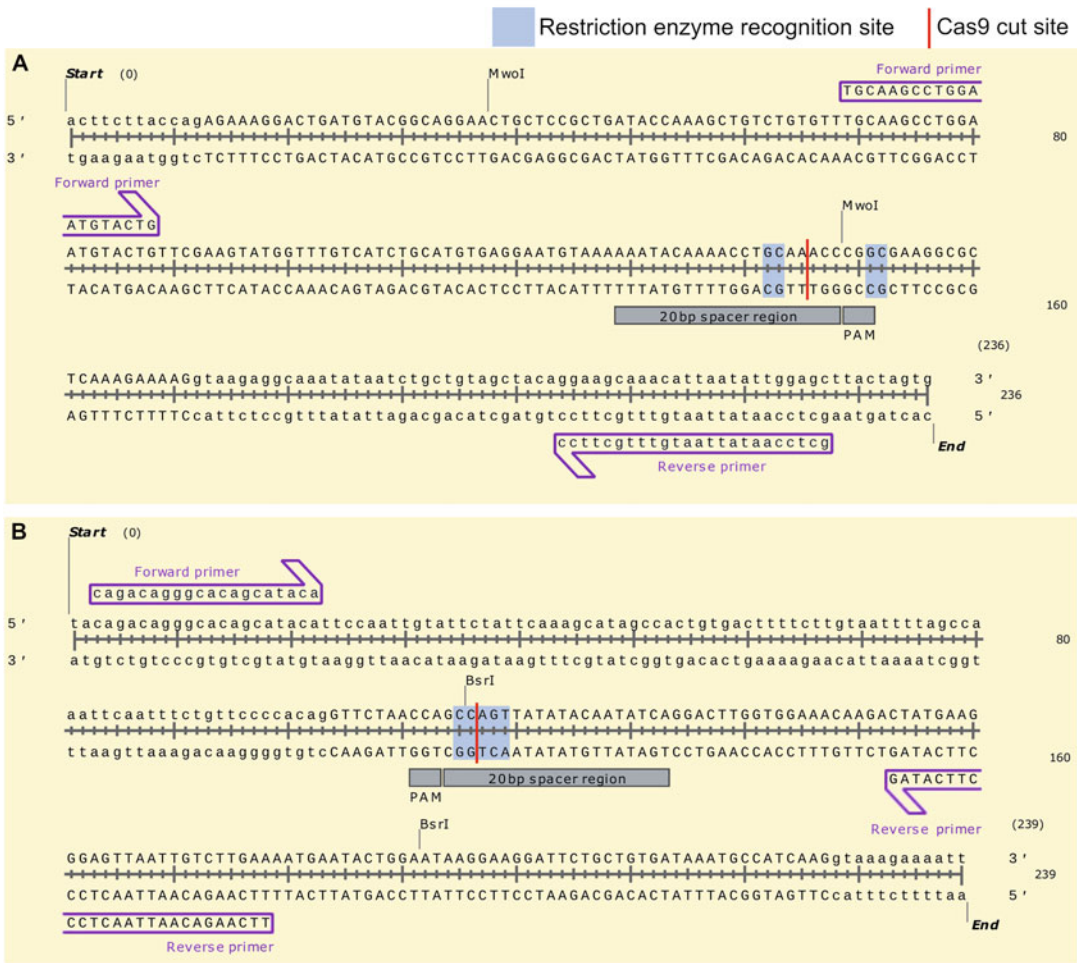


Fig. 1 Examples of sCrRNA designs. Shown are extracts from the sequences of two different genes in SnapGene Viewer, *tnfrsf1b* in (a) and *tnfrsf1a* in (b). Intronic sequences are shown in lower case and exon sequences in upper case. For the sake of clarity, only the restriction enzyme sites used in this design are shown. (a) shows a PAM site in the sense strand. The Cas9 cut site is 3 bp upstream to the NGG (shown as a red line in the figure). This cut site coincides with the recognition site for MwoI (shown in blue in the figure). (b) Here, the NGG is present in the antisense strand. Therefore, the Cas9 cut site is 3 bp downstream of CCN (complement to NGG), which coincides with the recognition site of BsrI. (c) The sequences of the sCrRNA and primers which would be ordered based on the designs in (a) and (b)

10. Collect the recently fertilized embryos (ideally within 20 min of being laid). Use a Pasteur pipette to line up embryos in a straight line against a glass slide on a petri dish lid. Use glass slides to allow embryos to line up in a straight line (*see Note 22*).
11. Center the line of embryos in the microscope's field of view, at the highest magnification (we use 50 \times).
12. Use the micromanipulator to move the needle to pierce the chorion and yolk.
13. Expel one measure of injection mix into yolk.
14. Repeat **steps 12** and **13** until the entire line of embryos have been injected.
15. Return embryos to a dish of E3 medium and keep at 28.5 °C at a density of 30–40 embryos per 50 mL petri dish (*see Note 23*).
16. Later the same day, remove embryos which are clearly dead or in which the dye has not successfully been incorporated into the embryo cell mass (*see Fig. 2a*).
17. Remove dead/dying embryos every day and replace E3 medium as necessary.

**3.3 Quality Control
Using RFLP for
Injected Larvae (See
Note 24)**

1. Select eight sCrRNA-injected and four control-injected embryos for DNA extraction.
2. Place each individual into a separate PCR tube and remove as much E3 medium as possible. It is important to not pool individuals, as some may be better injected than others (*see Note 25*).
3. Add 100 μ L 50 mM NaOH to each tube and boil at 95 °C for 10 min.
4. Briefly vortex to dissolve the embryos.
5. Neutralize with 10 μ L 1 M Tris–HCl. These homogenates are your DNA samples for the subsequent PCR reaction.
6. Test the success and/or efficiency of sCrRNA injection by amplifying the selected region using PCR. Prepare the following PCR master mix to test the activity of one sCrRNA in all DNA samples: 100 μ L BioMix Red, 41 μ L nuclease-free H₂O, 18 μ L 10 μ M forward primer, and 18 μ L 10 μ M reverse primer (primers designed in Subheading 3.1, **step 5**).
7. Add 18 μ L of above master mix individually to four empty PCR tubes.
8. Add 9 μ L to another eight empty PCR tubes.
9. Add 2 μ L of control-injected DNA to each tube from **step 7** to a total of 20 μ L and mix. Each tube should have a different DNA sample.

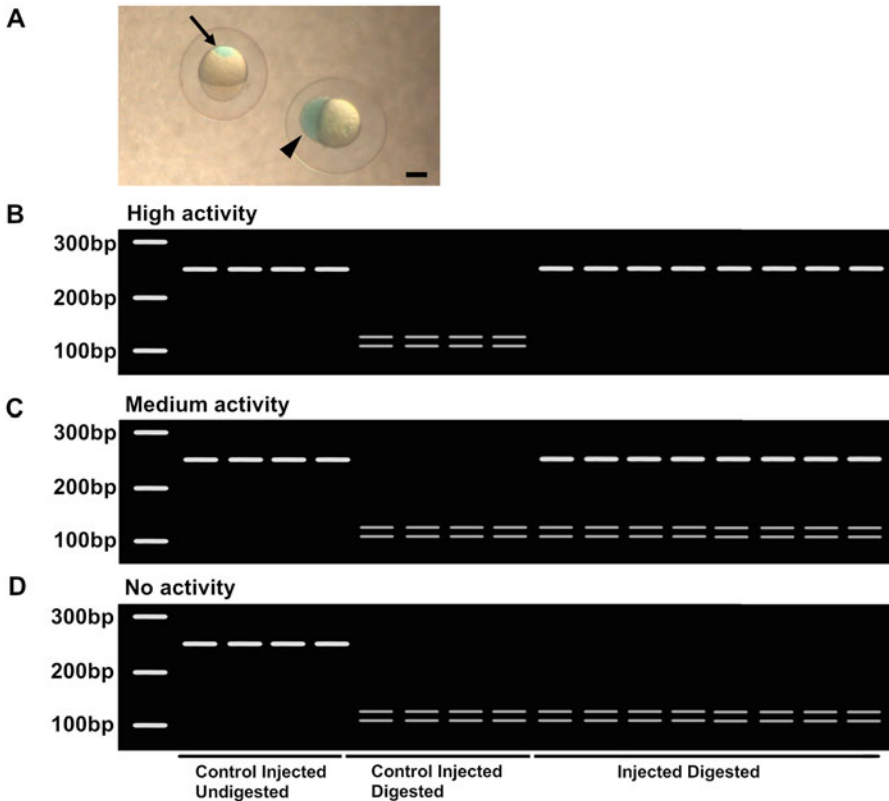


Fig. 2 Injection and RFLP analysis for haCr. **(a)** An unsuccessfully injected embryo (left) and a successfully injected embryo (right) are shown. Arrowhead points to green dye in the cell mass on top of the yolk, indicating successful injection. Arrow points to bolus of green dye at the bottom of the yolk that has not been transported into the cell mass. **(b–d)** Diagrammatic representations of the RFLP assay, in the typical arrangement we use in the laboratory. Note that each lane represents one embryo. On the left-hand side of each gel is a DNA ladder. Following this, the PCR product of the undigested samples of four control-injected embryos is run. Next are the four samples of control-injected embryos that have been digested. Finally, the eight digested samples of active sCrRNA-injected embryos are loaded. Scale bar in **a** is 250 μm

10. To the eight tubes from **step 8**, add 1 μL of sCrRNA-injected DNA sample and mix, to a total of 10 μL . Each tube should have a different DNA sample.
11. Load all 12 samples into thermocycler and set program: Heat to 95 $^{\circ}\text{C}$ for 180 s, 95 $^{\circ}\text{C}$ for 30 s, 55 $^{\circ}\text{C}$ for 30 s (*see Note 26*), and 72 $^{\circ}\text{C}$ for 60 s; repeat **steps 2–4** 35 times, 72 $^{\circ}\text{C}$ for 300 s; hold at 4 $^{\circ}\text{C}$.
12. Once the thermocycler run has finished, transfer 10 μL of each of the four control-injected PCR products (from **step 9**) into four empty tubes. These are the undigested PCR products—set to the side at room temperature.

13. With the 12 tubes from **steps 8** and **9**, use a pipette with filter tips to add 1 μL of the appropriate restriction enzyme directly to PCR product, and mix gently.
14. Heat sample to optimal temperature of restriction enzyme for 120 min (*see Note 27*).
15. Place 2% agarose gel into gel tank and remove comb.
16. Load samples into gel. Start by loading 10 μL of 100 bp DNA ladder into leftmost well. Continue by adding the entirety ($\sim 10 \mu\text{L}$) of the first control-injected undigested sample to the next well (from **step 12**). Continue so that all four of the control-injected undigested samples are loaded into separate consecutive wells. Next, add the four control-injected digested samples to the following four wells in the same manner. Finally, add the eight digested injected samples to the following eight wells. See Fig. 2 for a visual representation of this setup.
17. Run the gel at 100 V for 60–90 min (*see Note 28*).
18. View gel using UV lightbox.
19. Compare sizes of bands between control-injected and sCrRNA-injected samples to determine guide efficiency (*see Notes 29–32* and Fig. 2b–d).
20. Two sCrRNAs with mutation rates of $>90\%$, representing highly active sCrRNAs (haCRs), are optimal. If none are found in the initial four sCrRNAs tested, redesign.

3.4 Spinal Cord Injury of 3-Day Postfertilization Larvae

1. Add 0.4% MS-222 to a petri dish with 3-day postfertilization larvae to a final concentration of 0.01% (we use 1 mL of 0.4% MS-222 in 40 mL of medium). Leave for 2–3 min until all larvae stop responding to touch stimuli.
2. Use Pasteur pipette to place anesthetized larva on agar plate (*see Note 33*).
3. Place larvae in the center of dissecting microscope field of vision with light source on. Use the sharpest point of the syringe needle to fully transect spinal cord (avoiding injury to the underlying notochord) at the level of the 15th myotome. Try to use one smooth motion to create the lesion. Ideally the resultant damage will appear V shaped (*see Fig. 3a* and **Note 34**).
4. Displace lesioned fish from agar plate into petri dish with E3 medium (and no anesthetic) (*see Note 35*).
5. Keep at a density of 30–40 fish per 50 mL petri dish at 28.5 °C. Remove any fish which have damage to their notochord (Fig. 3b).

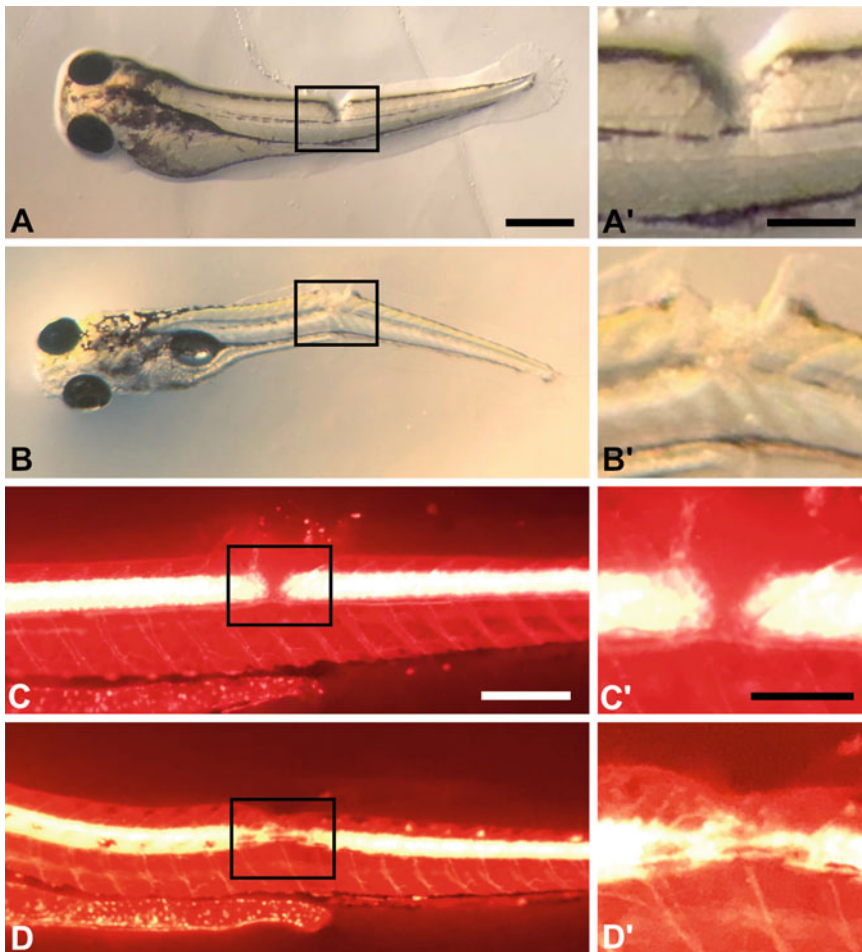


Fig. 3 Successful injury and repair. All panels show images of larvae sucked to an agarose surface by minimizing the water film covering the larvae and are imaged under a stereomicroscope as we do in our routine experiments. Rostral is left and dorsal is up. **(a)** A 3-day-old larva, shown immediately after successful lesion. **(b)** A 4-day-old larva, shown 24 h after lesion. This is an example of a fish whose notochord has been injured and should therefore be discarded. This is apparent by the bent shape of the larva, as well as the visible damage to the notochord, which becomes most obvious at some time after injury. **(c)** and **(d)** show lesioned *XlaTubb:DsRed* transgenic larvae viewed under a fluorescent stereomicroscope. **(c)** is an example of a larva with a fresh injury site (boxed) showing complete severance of axon connections (injury at 3 days postfertilization). **(d)** A larva at 24 h after injury at 3 days postfertilization shows an axonal bridge across the lesion site (boxed). **(a'–d')** are close-ups of the areas boxed in **(a–d)**, respectively. Scale bar in **a** is 500 μm and applies to **a** and **b**. Scale bar in **a'** is 200 μm and applies to **a'** and **b'**. Scale bar in **c** is 300 μm and applies to **c** and **d**. Scale bar in **c'** is 100 μm and applies to **c'** and **d'**

3.5 Bridging Assay for Regenerative Success

1. At 24 h post-injury, use a Pasteur pipette to place fish on the agar plate and remove excess medium.
2. Use a fluorescence microscope at high magnification to determine whether an axon bridge is present in each fish. Keep a tally of the number of fish with and without axon bridges. We

consider an axon bridge to be present when at least one continuous axon fascicle traverses the lesion site (*see* Fig. 3c–d for examples of bridged and unbridged lesion sites and **Note 36**).

3. Return the fish to the petri dish with E3 medium at 28.5 °C.
4. Repeat **step 2** at 48 h post-injury (or other timepoint of interest), and note down the presence or absence of a bridge at this timepoint for each group. Compare the frequency of successful bridging in the injected group to the control group (*see* **Note 37**).

4 Notes

1. The *Xla.Tubb:Dsred* line was created by [10]. The red fluorescing protein DsRed is expressed in all neuronal structures under the control of the promoter region of the neuron-specific beta-tubulin gene.
2. For storage of Cas9 at –20 °C, use a buffer which contains 50% glycerol to dilute (e.g., NEB Diluent Buffer B: 300 mM NaCl, 10 mM Tris–HCl, 0.1 mM EDTA, 1 mM DTT, 500 µg/mL BSA, 50% glycerol, pH 7.4 at 25 °C).
3. We order unmodified sCrRNAs, purified using HPLC at a 2 nmol concentration from Sigma (Merck KGaA, Darmstadt). sCrRNAs (including tracrRNA) come as a lyophilized powder at room temperature. Upon arrival, briefly spin for 2–3 s in a microcentrifuge; then resuspend sCrRNA/Tracr with 100 µL of nuclease-free water to achieve a 20 µM concentration. Gently pipette up and down to mix with a filter tip. If not injecting straight away, they can be stored aliquoted at –20 °C.
4. This sequence is based on the standard control sequence used for morpholino studies. We use a control-injected group whenever we are using the guides as part of an experiment, but this is not necessary when just assessing the efficiency of your guides (here, uninjected embryos can be used instead).
5. We use injection needles with an outer diameter of 1 mm and an inner diameter of 0.58 mm. To pull the needles, we use the following settings: heat 580, pull 250, velocity 55, time 100, and air pressure 400.
6. We buy 25 nmole of each primer and keep them frozen as 100 µM stock solutions in nuclease-free water at –20 °C. Working solutions at 10 µM in nuclease-free water can be stored at 4 °C or at room temperature for short periods of time.
7. Comb should create at least 18 wells. Comb teeth should be thin and wide for optimal separation. Square teeth are not appropriate for restriction digestion.

8. At minimum, the UV transilluminator needs to allow visualization of the different band sizes run on the gel. Ideally, this would also be fitted with a camera for easy analysis of efficiency, allowing the user to refer back to previous gels easily (e.g., to check for a decrease in sCrRNA efficiency).
9. Anesthetic solution can be made in advance and stored at 4 °C for up to a week.
10. If you allow agar to cool for approximately 5 min before pouring into petri dish, the agar plate will have fewer bubbles and will therefore make lesioning easier.
11. Several sCrRNAs must be designed and tested to identify a pair of highly active sCrRNAs (haCrS) with >90% mutation rate. In the first instance, we design four sCrRNAs for each gene. We rarely have to test more than eight individual sCrRNAs to identify a pair of haCrS.
12. Where possible, initially design four sCrRNAs to four different exons for the initial sCrRNA activity testing phase. If only a single exon is present or a small number, design multiple sCrRNAs to the same exon. Targeting early exons and those coding for functional regions is optimal. Final exons should be avoided when possible.
13. sCrRNA sites are made up of a 20 bp “spacer region” connected to a 3 bp protospacer adjacent motif (PAM). The spacer region is the DNA sequence which the sCrRNA recognizes and binds to and is 20 nucleotides of redundant sequence 5' to the PAM sequence, in other words 5' N₂₀NGG or 5' CCNN₂₀ if targeting the opposite strand (see Fig. 1). In order to use RFLP to assay the sCrRNA activity (*see* Subheading 3.3), a suitable restriction enzyme site must cross the Cas9 cut, 3 bp 5' of the PAM site (Fig. 1). Suitable restriction enzymes are those which function fully in the PCR mix of choice. We use New England Biolabs enzymes and BioMix Red for this reason—we also prefer BSL1/BSTXI and XCM1 as they are cheap, have large recognition sequences of mostly redundant sequence, function in BioMix without buffers, and have inbuilt PAM sites allowing either strand to be targeted.
14. Always check with the manufacturer that the “sense” of your sCrRNA sequence is correct. The PAM site, although needed for the Cas9 to function, is not included in the physical sCrRNA itself.
15. Primers must be designed so that the region of interest can be amplified and digested and undigested bands can readily be differentiated from digested ones. We recommend designing PCR products which are between 150 and 300 bp in length. If

there are multiple recognition sites for the same enzyme within the chosen exon, the primers must be designed to amplify a region including only one of these recognition sites.

16. To identify highly active (haCrS), we initially co-inject four different guides targeting the same gene of interest, as designed in Subheading 3.1. We then perform the RFLP assay as described in Subheading 3.3 to identify two haCrS for functional gene targeting. Occasionally, further four guides might need to be designed and co-injected to find two haCrS. Once two haCrS are identified, we co-inject just those two guides for the lesion assay to maximize guide efficiency while minimizing off-target effects.
17. Sometimes this introduces bubbles which block the pulled needle. To avoid this, place the pipette tips as far into the glass needle as possible, and gently push the pipette pump. Expelling the liquid too fast may result in incomplete transfer of liquid and/or bubbles through the delicate tip.
18. Making an opening of the required size requires practice. For first-time users, start by pinching off just a small length of needle and repeat until an opening is created.
19. The time and pressure settings on the microinjector can be used to fine-tune the droplet size.
20. Adjust pressure/time settings on microinjector to fine-tune droplet size to ensure equivalent injection volume for each needle.
21. To increase the likelihood of obtaining high-quality embryos, mixing of males and females should be timed to coincide with the beginning of the light phase of the light–dark cycle (we pull out a tank divider that previously separated males and females for the preceding night).
22. Excess water should be removed to allow for easier injecting. Removing the water can be done by allowing it to run underneath the glass slide, or alternatively by using a fine-tip pipette.
23. You might also like to keep one group of embryos as uninjected controls, particularly if not using a control-injected group.
24. Here we describe how to perform RFLP for one injected guide. We perform this method on all designed sCrRNAs targeting a particular gene of interest (usually four in the first instance). This allows us to identify two haCrS for functional studies. We then co-inject these two guides only and use the injected fish for the lesion experiment and bridging assay. However, we continue to perform RFLP for each of the two guides on eight injected fish out of every batch of injections as an internal control to check for continued sCrRNA efficiency and injection success.

25. We usually perform this stage at 1 day postfertilization. Successfully injected individuals should have a green hue throughout their body and yolk sac. Embryos do not need dechorionating.
26. This program works for the majority of our primer designs. However, if amplification is unsuccessful, you may want to adjust this setting based on the melting temperatures (T_m) of your custom primer pairs (this information is usually provided by the manufacturer).
27. We use a thermocycler to easily heat to the desired temperature. Some enzymes only need 60–90 min to undergo complete restriction digestion, but if you are unfamiliar with the enzyme, it is best to start with 120 min.
28. The length of time the gel is run for depends on specific dimensions of gel. The important thing is to run the gel long enough to allow for clear resolution of similar-sized bands but without running the bands off the gel completely.
29. If the injections have been successful (and guides are highly efficient), the size of the band(s) in the sCrRNA-injected samples should be equal to those in the control undigested sample (if the targeting has been successful, the restriction enzyme recognition site will no longer be present, so the restriction digestion will have been unsuccessful). See Fig. 2b for an example of this.
30. Occasionally, highly active guides will show a smear-like band at the same height as the undigested controls and may also have a second band slightly higher than an undigested band. These show the guide works well and is causing the formation of heteroduplexes.
31. If guides are inefficient (or not properly injected), the size of the band(s) in the sCrRNA-injected samples will be equal to those in the control-digested sample. See Fig. 2d for an example of this.
32. Sometimes you will get dual bands—one at the position of the control undigested and another at the position of the control digested. This indicates that guides are not 100% efficient. You can compare the relative intensities of the bands to approximate efficiencies. See Fig. 2c for an example of this.
33. It is easier to lesion the fish when the agar plate surrounding the fish is dry (to prevent fish moving under pressure of needle), so remove as much excess medium as possible using a fine-tip Pasteur pipette.
34. The difficulty here is fully transecting the spinal cord without damaging the notochord. This can be made easier for beginners by using the maximum possible magnification (we use 50 \times), and using a microscope that has a light source

illuminating the fish from both below and above, in order to be able to see the notochord boundary clearly. It may also benefit beginners to begin by lesioning the fish under a fluorescent microscope (allowing the user to see the axons) to understand the extent of the lesion necessary to allow complete spinal cord transection.

35. To remove the fish from the agar plate without causing excessive mechanical strain to the lesion site, we use a Pasteur pipette to direct a stream of E3 medium at the larva on the agar plate to dislodge it and wash it into the petri dish.
36. It may be worthwhile for beginners to screen for complete transection soon after lesion is performed (~2 h allows for optimal visibility of lesion site). This allows users to remove false positives (e.g., larvae which would otherwise be counted as bridged at 24 h post-lesion but instead were never completely transected).
37. In our hands, we routinely see ~40% of larvae with bridges at 24 h post-lesion and ~80% at 48 h post-lesion.

Acknowledgments

This work was supported by the EU Cofund ERANET NEURON consortium NEURONICHE with contributions from MRC (MR/R001049/1), Spinal Research, and Wings for Life to CGB, a project grant from the BBSRC (BB/R003742/1) to TB, by a Wellcome Trust Senior Research Fellowship (102836/Z/13/Z) to DAL and by Biogen who provided funding via a scientific research agreement with DAL. LKD was funded by a BBSRC Eastbio PhD studentship.

References

1. Becker CG, Lieberoth BC, Morellini F, Feldner J, Becker T, Schachner M (2004) L1.1 is involved in spinal cord regeneration in adult zebrafish. *J Neurosci* 24(36):7837–7842. <https://doi.org/10.1523/JNEUROSCI.2420-04.2004>
2. Becker T, Wullmann MF, Becker CG, Bernhardt RR, Schachner M (1997) Axonal regrowth after spinal cord transection in adult zebrafish. *J Comp Neurol* 377:577–595. [https://doi.org/10.1002/\(sici\)1096-9861\(19970127\)377:4<577::aid-cne8>3.0.co;2-#](https://doi.org/10.1002/(sici)1096-9861(19970127)377:4<577::aid-cne8>3.0.co;2-#)
3. van Raamsdonk W, Maslam S, de Jong DH, Smit-Onel MJ, Velzing E (1998) Long term effects of spinal cord transection in zebrafish: swimming performances, and metabolic properties of the neuromuscular system. *Acta Histochem* 100:117–131. [https://doi.org/10.1016/S0065-1281\(98\)80021-4](https://doi.org/10.1016/S0065-1281(98)80021-4)
4. Wehner D, Tsarouchas TM, Michael A, Haase C, Weidinger G, Reimer MM, Becker T, Becker CG (2017) Wnt signaling controls pro-regenerative Collagen XII in functional spinal cord regeneration in zebrafish. *Nat Commun* 8(1):126. <https://doi.org/10.1038/s41467-017-00143-0>
5. Tannenbaum J, Bennett BT (2015) Russell and Burch's 3Rs then and now: the need for clarity in definition and purpose. *J Am Assoc Lab Anim Sci* 54(2):120–132
6. Keatinge M, Tsarouchas TM, Munir T, Porter NJ, Larraz J, Gianni D, Tsai HH, Becker CG, Lyons DA, Becker T (2021) CRISPR gRNA

- phenotypic screening in zebrafish reveals pro-regenerative genes in spinal cord injury. *PLoS Genet* 17(4):e1009515. <https://doi.org/10.1371/journal.pgen.1009515>
7. Hoshijima K, Juryneć MJ, Klatt Shaw D, Jacobi AM, Behlke MA, Grunwald DJ (2019) Highly efficient CRISPR-Cas9-based methods for generating deletion mutations and F0 embryos that lack gene function in zebrafish. *Dev Cell* 51(5):645–657.e644. <https://doi.org/10.1016/j.devcel.2019.10.004>
 8. Klatt Shaw D, Mokalled MH (2021) Efficient CRISPR/Cas9 mutagenesis for neurobehavioral screening in adult zebrafish. *G3* (Bethesda). <https://doi.org/10.1093/g3journal/jkab089>
 9. Kröll F, Powell GT, Ghosh M, Gestri G, Antinucci P, Hearn TJ, Tunbak H, Lim S, Dennis HW, Fernandez JM, Whitmore D, Dreosti E, Wilson SW, Hoffman EJ, Rihel J (2021) A simple and effective F0 knockout method for rapid screening of behaviour and other complex phenotypes. *elife* 10. <https://doi.org/10.7554/eLife.59683>
 10. Peri F, Nusslein-Volhard C (2008) Live imaging of neuronal degradation by microglia reveals a role for v0-ATPase a1 in phagosomal fusion in vivo. *Cell* 133(5):916–927. <https://doi.org/10.1016/j.cell.2008.04.037>



Translating Ribosome Affinity Purification (TRAP) and Bioinformatic RNA-Seq Analysis in Post-metamorphic *Xenopus laevis*

Gregg B. Whitworth and Fiona L. Watson

Abstract

Recent technical advances provide the ability to isolate and purify mRNAs from genetically distinct cell types so as to provide a broader view of gene expression as they relate to gene networks. These tools allow the genome of organisms undergoing different developmental or diseased states and environmental or behavioral conditions to be compared. Translating ribosome affinity purification (TRAP), a method using transgenic animals expressing a ribosomal affinity tag (ribotag) that targets ribosome-bound mRNAs, allows for the rapid isolation of genetically distinct populations of cells. In this chapter, we provide stepwise methods for carrying out an updated protocol for using the TRAP method in the South African clawed frog *Xenopus laevis*. A discussion of the experimental design and necessary controls and their rationale, along with a description of the bioinformatic steps involved in analyzing the *Xenopus laevis* transcriptome using TRAP and RNA-Seq, is also provided.

Key words TRAP, Expression profiling, *Xenopus laevis*, RNA-Seq analysis

1 Introduction

The goal of many translational profiling studies is to compare the transcriptome or transcriptome of genetically distinct cell types from organisms undergoing developmental, behavioral, and environmental changes. Early advances for creating cell-type-specific translational profiles for CNS cells have been difficult due to their highly complex and heterogeneous organization. The morphologically indistinct and physical intermixing of heterogeneous tissues has made their isolation particularly challenging, and the tissue extraction and processing methods risk changing the profiles themselves [1, 2]. In addition, the amount of total RNAs present in a cell includes noncoding RNAs (ncRNAs), ribosomal RNAs (rRNAs), transfer RNAs (tRNAs), microRNAs (miRNAs), as well as the mRNAs destined for translation into proteins. The difference

between the populations of ribosomal-bound and non-ribosomal-bound RNAs is further complicated by RNAs and ribonucleoproteins (RNPs) present in the cell that are tied up in stress granules or undergoing degeneration [3]. Thus teasing apart the transcriptional profiles based on total cellular RNAs (transcriptome) from the translational profiles based on mRNAs destined for translation (translatome) presents additional challenges [3].

Translating ribosome affinity purification (TRAP), a method first devised for translational profiling in mice, relies on the use of TRAP transgenic mouse lines that express cell-type-specific promoters to drive expression of a ribosomal tag that can then be used to capture and isolate ribosomes and their associated mRNAs [4, 5]. This method resolves the challenges of needing to (a) rapidly isolate genetically distinct cell types without the burden of physically dissociating and isolating them and (b) isolating actively translating mRNAs from the total RNAs, by using a cell-type-specific promoter to target a single cell type and by stalling and capturing only those mRNAs bound to ribosomes. In essence, this method “TRAPs” mRNAs in their *in vivo* conditions where previous methods required lengthy cell purification steps such as fluorescence-activated cell sorting (FACS) and immunopanning, processes that would likely change their expression profiles [1, 2]. The TRAP-extracted or “TRAPed” RNA samples will also include rRNA and tRNAs, both of which are easily identifiable and can be excluded from analysis. Because the TRAP method specifically targets mRNAs bound to tagged ribosomes, this protocol provides a closer representation of the pool of mRNAs destined for translation [6].

Specifically, the original TRAP method [4] relies on the use of transgenic animals that express an enhanced green fluorescent protein (EGFP) fused to a ribosomal protein (rpl10a or L10a) chosen for its location on the surface of the large ribosomal subunit. A linker sequence is introduced between the EGFP and L10a protein to enhance protein folding and facilitate incorporation of L10a into the large ribosomal subunit. In this way, the transgene’s EGFP protein is expressed on the surface of the ribosome, exposed to the cytoplasm and readily accessible to antibody recognition. The method hinges on the use of transgenic TRAP animal lines with cell-type-specific promoters to drive expression of the EGFP-L10a transgene in distinct populations of cells. In this way, tissues can be rapidly dissected and homogenized into lysates, and only tagged ribosomes from the targeted cell type are isolated, thus circumventing the need for lengthy dissections. Addition of cycloheximide to the buffers inhibits translation elongation, in essence “TRAPping” ribosomes *in situ* on mRNAs. The purified lysates are incubated with an affinity matrix consisting of anti-EGFP antibodies conjugated to biotinylated protein L-coated magnetic beads that bind the EGFP-L10a ribosomal tag. A simple magnet is then used to

capture these EGFP-tagged ribosomes along with their associated mRNAs. Sequential washes clear the lysates of proteins, enzymes, salts, and other reagents from the ribosome–mRNA complexes. At the final step in the TRAP protocol, mRNAs are purified using standard commercial RNA isolation procedures. Qualitative and quantitative assessment of the TRAP-extracted RNAs is crucial to determine whether these TRAPed RNAs can be used for downstream application that includes RNA-Seq, microarrays, and qPCR.

In this chapter, we provide stepwise protocols for using the TRAP method in the frog *Xenopus laevis* along with a description of the bioinformatic steps involved in analyzing the transcriptome for *Xenopus laevis*. The latter is made more challenging because of the allotetraploid nature of the *X. laevis* genome. While we do not provide in-depth protocols for generating the transgenic TRAP frog lines, we do provide an overview of the workflow involved in validating newly generated TRAP lines [7]. Since our initial studies [7, 8], several aspects of the original TRAP protocol [4] were updated primarily as a means to increase the total mRNA quality and yield and provide results from a side-by-side comparison of fresh vs. frozen tissue [5]. We also provide a discussion of the experimental design and necessary controls and highlight challenging critical procedural steps along with problem-solving methods.

2 Materials

Buffers required for the TRAP assay are provided in this section. Please note that all reagents must be kept RNase-free and solutions must be made using RNase-free water. Any glassware and all benchtops, pipets, and tube racks are washed with RNase decontamination solution and rinsed with RNase-free water (*see* **Notes 1** and **2**). It is practical to prepare a sufficient volume of stocks to repeat experiments several times using RNase-free tested reagents.

2.1 TRAP Supplies and Reagents

1. Transgenic TRAP frogs (*see* **Notes 3** and **4**).
2. Silicone plates for tissue dissection.
3. Streptavidin-coated magnetic beads (e.g., Dynabeads MyOne Streptavidin T1, Invitrogen) (*see* **Note 5**).
4. Monoclonal anti-green fluorescent protein (anti-GFP) antibody (*see* **Note 6**).
5. Fluorescence-based RNA quantitation kit (e.g., Quant-iT RiboGreen RNA assay) (*see* **Note 7**).
6. RNA extraction kit with in-column DNase digestion (e.g., Absolutely RNA Nanoprep kit; QIAGEN RNeasy) (*see* **Note 8**).

7. **RNA stock:** Purify total RNA from a tissue. Dilute RNA to 100 $\mu\text{g}/\text{mL}$ using RNase-free water and aliquot into single-use tubes; store at $-80\text{ }^{\circ}\text{C}$. The RNA will be used to make a concentration curve for the fluorescence-based RNA quantitation kit. Note: Commercial kits may come with pre-diluted RNA standards.
8. Certified DNase/RNase-free plasticware (50 mL tubes; 15 mL tubes; 1.7 mL microfuge tubes; 0.5 mL microfuge tubes).
9. Barrier tips for P1000; P200; P10; P2 (RNase-free).
10. Magnetic particle concentrator (*see Note 9*).
11. End-over-end microfuge tube rotator.
12. Potter-Elvehjem PTFE Pestle Tissue Grinder and glass holder (*see Note 10*).
13. Motorized homogenizer (*see Note 10*).
14. Large rectangular 9 L ice pan or Styrofoam container to hold samples and reagents.
15. Refrigerated microcentrifuge.
16. Mini microcentrifuge (e.g., Nanofuge).
17. Instrumentation for assessing RNA quality (e.g., Bioanalyzer Instrument) (*see Note 11*).
18. Fluorescence microplate reader (*see Note 12*).
19. Protease inhibitor cocktail tablets (e.g., Roche cOmplete ULTRA EDTA-free tablets).
20. Nuclease-free water.
21. DNase I—1500 Kunitz units of RNase-free lyophilized DNase I.
22. RNase decontamination solution (e.g., RNase AWAY, RNase ZAP).
23. Ribonuclease inhibitor—a broad-spectrum recombinant RNase inhibitor sensitive to denaturation; store with enzymes at $-20\text{ }^{\circ}\text{C}$, preferably in a benchtop cryo-cooler. Add to Tissue Lysis Buffer immediately prior to use, and swirl gently (do not vortex!) (e.g., RNaseOUT, RNasin Ribonuclease Inhibitor).
24. Ribonuclease-inhibitor plus—an RNase inhibitor with increased stability at higher temperature (e.g., SUPERase•In or RNasin Plus Ribonuclease Inhibitor).
25. 96-well, flat bottom, black, polystyrol plates.
26. **Biotinylated protein L:** Reconstitute biotinylated protein L to 1 $\mu\text{g}/\mu\text{L}$ in IgG-free $1\times$ PBS. Aliquot into single-use aliquots; store at $-80\text{ }^{\circ}\text{C}$.

27. **300 mM DHPC** (1,2-diheptanoyl-sn-glycero-3-phosphocholine): Prepare 300 mM DHPC stock using RNase-free water. DHPC is stored in glass ampules or glass vials at -20°C . Prior to adding water, warm the DHPC powder to room temperature. Keep at room temperature, with occasional vortexing for ~ 30 min to produce a solution. Ensure that sufficient time has passed to allow for complete hydration to occur. Once DHPC is fully reconstituted in water, the 300 mM stock can be stored at 4°C and used for up to 7 days. Do not store it in plastic (*see Note 13*).
28. **Cycloheximide stock solution**: Prepare a 100 mg/mL stock of cycloheximide by dissolving 100 mg of cycloheximide in 1 mL of methanol. Store the stock at 4°C for no more than 1 day. Check color before use—do not use if the solution has yellowed.
29. **DNase I stock solution**: Using a nuclease-free syringe, inject 550 μL of RNase-free water into a 1500 Kunitz units vial of DNase I to dissolve lyophilized DNase I without loss. Mix by gently inverting vial. Divide into single-use aliquots and store at -20°C for up to 9 months (do not refreeze). Thawed aliquots can be stored at 4°C up to 6 weeks.
30. **Methanol**.
31. **100% ethanol**: Molecular biology grade.
32. **1 M DTT**: Reconstitute dithiothreitol to 1 M in RNase-free water. Filter-sterilize the solution and store at -20°C in 1 mL, single-use aliquots.
33. **1 M glucose**: Prepare 50 mL of 1 M glucose in RNase-free water. Store at room temperature.
34. **2 M KCl**: Prepare 50 mL of 2 M KCl in RNase-free water. Store at room temperature.
35. **1 M HEPES-KOH**: Prepare 50 mL of 1 M HEPES-KOH, pH 7.4, in RNase-free water. Use KOH pellets to bring the solution to pH 7.4. Store at room temperature.
36. **1 M MgCl_2** : Prepare 50 mL of 1 M MgCl_2 in RNase-free water. Store at room temperature.
37. **5 M NaCl**: Prepare 50 mL of 5 M NaCl in RNase-free water. Store at room temperature.
38. **10% NP-40**: Prepare 50 mL of 10% v/v NP-40 in RNase-free water. Store at room temperature.
39. IgG-free 10 \times PBS (RNase-free).
40. **PBS-BSA buffer**: Using IgG-free 10 \times PBS, prepare a 1 \times PBS containing 3% (weight/volume) IgG and protease-free BSA using RNase-free water. Make fresh prior to use.

41. **20× TE (pH 7.5):** Prepare a 20 mL solution of 0.2 M Tris-HCl and 20 mM EDTA. Store at room temperature. For use with fluorescence-based RNA quantitation kit (some commercial kits supply 20× TE).

2.2 TRAP Buffers (See Note 14)

42. **10× MMR:** 1 M NaCl, 20 mM KCl, 10 mM MgSO₄, 20 mM CaCl₂, 50 mM HEPES. Adjust pH by dropwise addition of concentrated 5 N NaOH to achieve pH = 7.4 (modified from [9]; see Note 15).

43. **0.5× MMR dissection buffer:** Dilute 10× MMR to 0.5× MMR (pH 7.4) with RNase-free water. If the tissue has a high metabolic rate such as the retina, add glucose to a final concentration of 35 mM glucose. Immediately prior to use, add cycloheximide to a final concentration of 100 µg/mL cycloheximide (see Note 16).

44. **Tissue Lysis Buffer:** 20 mM HEPES-KOH [pH 7.4], 10 mM MgCl₂, 150 mM KCl, and 1% (vol/vol) NP-40. Store at 4 °C up to several months. Immediately prior to use, add DTT, cycloheximide, and RNase inhibitor stocks to yield final concentrations of 0.5 mM DTT, 100 µg/mL cycloheximide, 10 µL/mL of RNase inhibitors, and RNase plus inhibitors. In addition, add one tablet of protease inhibitors (EDTA-free) per 10 mLs of Tissue Lysis Buffer (see Note 1).

45. **Low-salt buffer:** 20 mM HEPES-KOH (pH 7.4), 5 mM MgCl₂, 150 mM KCl, 1% NP-40. Store at 4 °C up to several months. Immediately prior to use, add DTT and cycloheximide (final concentrations: 0.5 mM DTT and 100 µg/mL cycloheximide).

46. **High-salt buffer:** 20 mM HEPES-KOH (pH 7.4), 10 mM MgCl₂, 350 mM KCl, 1% NP-40. Store at 4 °C up to several months. Immediately prior to use, add DTT and cycloheximide (final concentrations: 0.5 mM DTT and 100 µg/mL cycloheximide).

47. β-Mercaptoethanol (store at 4 °C after opening).

3 Methods

3.1 Preliminary Experiments

1. Carry out two sets of pilot experiments (see Note 17) to establish the magnetic bead to sample tissue ratio (pilot experiment #1; see Note 18) and to determine the RNA yield from TRAP tissue, reproducibility, nonspecific binding, and the presence of any potential RNA degradation (pilot experiment #2; see Note 19).

2. Carry out comparative experiments using *Xenopus* TRAP lines (see Note 4).

3.2 Pre-experiment Preparations for TRAP

1. Determine the total number of experimental and control samples (*see Note 20*).
2. Pre-label three sets of 1.7 mL microfuge tubes and three sets of 0.5 mL tubes per sample. Cover tubes with plastic wrap and place at 4 °C.
3. Place P1000 and P200 RNase-free barrier tips at 4 °C or in cold room.
4. Place the homogenizer and glass tube in cold room to pre-chill.
5. Aliquot dissection buffer, Tissue Lysis Buffer, and high-salt and low-salt buffers into 50 mL tubes and place at 4 °C (*see Note 14*).
6. Prepare the affinity matrix (proceed to Subheading 3.3) (*see Note 21*).

3.3 Preparation of Affinity Matrix (2.5 h) (See Note 22)

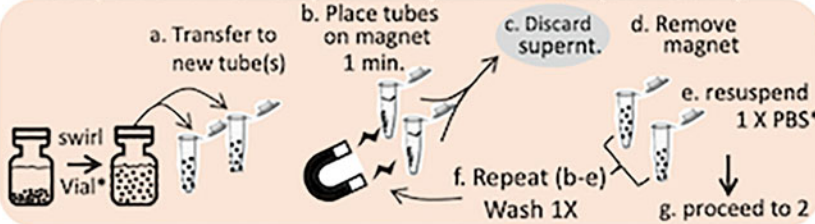
1. Using the optimized affinity matrix component ratio for your specific TRAP tissue (*see Notes 17 and 18*), calculate the total volume of “affinity matrix” required based on the number of experimental TRAP IP samples required for the experiment. Include a no-GFP antibody control sample.
2. On ice, thaw sufficient anti-GFP aliquots equivalent to add 100 µg anti-GFP (*see Note 23*) to each IP sample.
3. Prepare the affinity matrix using the stepwise diagram outlined in Fig. 1.
4. Keep the affinity matrix samples on ice while completing the steps involved in tissue processing (*see Subheadings 3.4, 3.5, and 3.6*).

3.4 Preparatory Steps for Tissue Collection and Homogenization (See Notes 10 and 27)

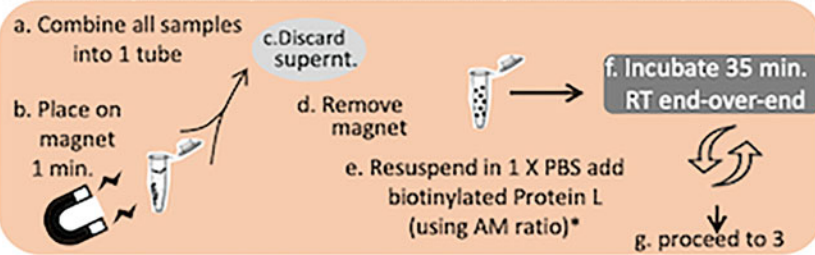
1. Fill two small beakers with dissection buffer with freshly added cycloheximide (final concentration 100 µg/mL), and place in ice bucket (*see Note 28*).
2. Based on the number of samples in the experiment, calculate the amount of buffer needed, and prepare individual 50 mL tubes for the dissection buffer, Tissue Lysis Buffer, low-salt buffer, and high-salt buffers. Place in ice bucket.
3. Add cycloheximide (final concentration 100 µg/mL) to dissection buffer. Place on ice.
4. Add DTT, cycloheximide, and RNase inhibitors to the Tissue Lysis Buffer (final concentrations: 0.5 mM DTT, 100 µg/mL cycloheximide, 10 µL/mL of RNase inhibitors, and RNase plus inhibitors). Add one tablet of protease inhibitors (EDTA-free) per 10 mL of Tissue Lysis Buffer and place on ice.
5. Add DTT and cycloheximide to the low-salt and high-salt buffers (final concentrations: 0.5 mM DTT and 100 µg/mL cycloheximide), and place on ice.
6. Pre-fill the glass homogenizer tube(s) with sufficient ice-cold Tissue Lysis Buffer for one sample and place in ice bucket.

Affinity Matrix (AM) Preparation: Use AM ratio optimized in Pilot expt. 1

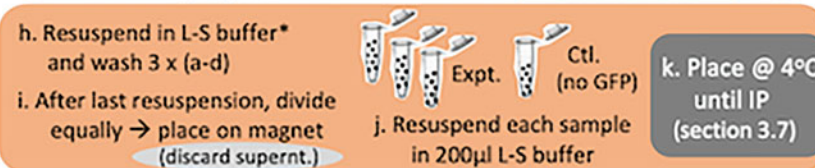
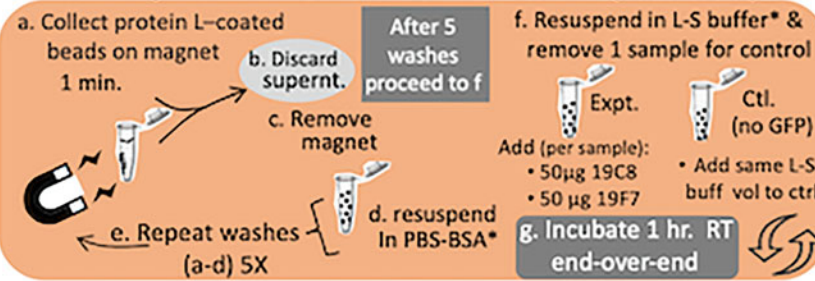
1. Resuspend and wash Streptavidin MyOne-T1 Beads (see Note 24)



2. Coat streptavidin MyOne beads with Biotinylated Protein-L (see Note 25)



3. Bind Biotinylated Protein-L coated-beads to anti-GFP (see Note 26)



* Maintain bead to liquid volume = manufacturer original bead to liquid volume. Within this total volume adjust individual components according to AM ratio

Fig. 1 Stepwise diagram showing details of steps required for preparing the affinity matrix. Preparing the affinity matrix (AM) and control affinity matrix (AM-ct) requires sequentially binding the three affinity matrix components [Streptavidin MyOne T1 magnetic beads (beads), the biotinylated protein L (BP-L), and 100 µg of Htz anti-GFP antibody (mAb) lots (50 µg of 19C8 and 50 µg of 19F7)] in three distinct steps (1–3). The relative ratio of the affinity matrix components needs to be optimized for distinct TRAP-extracted tissues during preliminary pilot experiments (see **Notes 18, 19** and **20**). The overall volume of liquid to beads should be the same as the volume in which beads arrive from manufacturer (see asterisk and **Note 24**). Handle beads gently; all resuspension steps are performed by slowly and gently pipetting up and down four times using a P1000 (*do not introduce air bubbles; do not vortex*) (1e; 2e; 3d; 3j). Following binding of anti-GFP to the biotinylated protein L-coated beads (3g), wash the AM (beads–BP-L–mAB) and AM-ct (beads–BP-L) three times with low-salt buffer (L-S buffer; 3h). After the third and final L-S buffer wash (3h, i), divide the affinity matrix into pre-labeled tubes corresponding the total number of IP samples, and place individual samples on magnet (3i). Discard supernatant and resuspend each sample containing either the AM or AM-ct in final 200 µL volume of L-S buffer (3j). Place samples on ice until sample lysates are ready to be immunoprecipitated (3k). Beads can be prepared up to 2 weeks prior to use (see **Note 22**)

3.5 Tissue Collection and Homogenization—Work on Ice/Keep Samples Cold (See Notes 10 and 27)

1. Quickly dissect the tissue of interest in ice-cold dissection buffer with freshly added 100 µg/mL cycloheximide (*see* Notes 29 and 30).
2. Use forceps to briefly and sequentially rinse TRAP-extracted tissue in beakers containing pre-chilled dissection buffer for 2–5 s (*see* Note 28).
3. Quickly transfer pooled tissue into the glass homogenizer tube pre-filled with volume of ice-cold Tissue Lysis Buffer for one sample (*see* Note 30).
4. Immediately homogenize the tissue for each set of pooled tissues before dissecting next sample by plunging the Teflon pestle to the bottom of the tube.
5. Once the plunger is fully immersed, turn on the homogenizer to 300 rpm, and gradually increase the speed to 900 rpms for 12 strokes (*see* Note 10).
6. Turn off homogenizer while pestle is submerged and remove the plunger while keeping the sample on ice.
7. Transfer the homogenized lysate using pre-chilled P1000 barrier tips to a pre-labeled, pre-chilled microfuge tube.
8. Keep homogenized lysates on ice until all the samples have been sequentially collected and homogenized (*see* Note 31).

3.6 Lysate Preparation—Work on Ice Unless Indicated

1. Centrifuge the homogenized tissue lysates in a refrigerated centrifuge for 10 min at $2000 \times g$.
2. Transfer the supernatant (S2) to new pre-labeled microcentrifuge tube on ice. While transferring the S2 supernatant, record the final supernatant volume (*see* Note 32).
3. Add 1/9 sample volume of 10% NP-40 to S2 for a final sample concentration of 1% NP-40 and mix gently by inversion.
4. Briefly pulse the sample to the bottom of the tube using a mini microcentrifuge and return to ice immediately.
5. Add 1/9 sample volume using the 300 mM DHPC stock for a final sample concentration of 30 mM DHPC. Mix gently by inversion (*see* Note 33).
6. Briefly pulse the sample to the bottom of the tube using a mini microcentrifuge and incubate on ice for 5 min.
7. Centrifuge all samples at 4 °C, 10 min, $20,000 \times g$.
8. Transfer each supernatant (S20) containing the ribosome–RNA complex to a new pre-labeled, pre-chilled microcentrifuge tube on ice, and proceed with immunopurification.

3.7 Immuno-purification

1. Add 50–200 µL freshly prepared affinity matrix or matrix control (*see* Subheading 3.3, step 4) to corresponding S20 samples.

2. Incubate samples and affinity matrix at 4 °C for 16–18 h (overnight) with end-over-end mixing.
3. After binding with affinity matrix, place samples on magnet submerged in ice for 60 s; transfer the supernatant (unbound fraction) to a new pre-chilled tube on ice, and save until RNA isolation step (*see* **Note 34**).
4. Remove the magnet leaving samples on ice. Resuspend beads containing the ribosome–RNA complex in 1 mL of high-salt buffer (0.35 M KCl), and gently pipet up and down four times using the P1000 pipet.
5. Wash each sample three times by placing tubes on magnet for 60 seconds and resuspending in 1 mL of H-S buffer (*see* **Note 35**).
6. After final wash, place samples on magnet, remove and discard the supernatant, and proceed to RNA isolation (*see* Subheading 3.9).

3.8 Preparatory Steps for RNA Isolation (See Note 36)

1. Add 10 µL beta-mercaptoethanol (β-ME) per 1 mL RLT buffer; place at room temperature (*see* **Note 37**).
2. Add 100% ethanol to the concentrated RPE buffer.
3. Thaw aliquot of DNase I stock solution on ice.
4. Prepare the DNase I–RDD buffer by adding 10 µL DNase I stock solution with 70 µL RDD buffer for each sample. Mix gently by gentle tube inversion (do not vortex).
5. Place three new sets of pre-labeled tubes, pre-chilled 0.5 mL tube in ice bucket.

3.9 RNA Isolation (See Notes 8 and 36)

1. After the last wash (*see* Subheading 3.7, step 6), place beads on magnet at room temp and remove all H-S buffer.
2. Add 350 µL RLT buffer with added β-ME to each sample and incubate for 5 min at *room temperature* (*see* **Notes 37 and 38**).
3. Add 250 µL 100% ethanol to the RLT–beads by pipetting up and down five times.
4. Place samples on the magnet and carefully remove RLT and ethanol solution from beads (the supernatant now contains the eluted RNA–ribosome complex).
5. Transfer the supernatant from each sample to an RNeasy spin column placed in a 2 mL collection tube.
6. Centrifuge spin columns for 30 s at 8000 × *g*; discard flow-through.
7. Add 350 µL of RW1 buffer to the RNeasy spin column. Close the lid gently, and centrifuge for 15 s at ≥8000 × *g* to wash the spin column membrane. Discard the flow-through.

8. Reuse the collection tube from **step 7**.
9. Add 80 μL of the DNase I–RDD buffer solution directly to the column membrane of each spin column, and incubate on the benchtop (20–30 $^{\circ}\text{C}$) for 15 min.
10. Add 350 μL RW1 buffer directly to each RNeasy spin column. Close the lid gently, and centrifuge for 15 s at $\geq 8000 \times g$. Discard the flow-through and collection tube.
11. Place spin column in a new 2 mL collection tube. Wash spin columns by adding 500 μL RPE buffer, close the spin column lid gently, and centrifuge for 15 s at $\geq 8000 \times g$. Discard the flow-through.
12. Wash column by adding 500 μL of 80% ethanol, close the spin column lid gently, and centrifuge for 2 min at $\geq 8000 \times g$. Discard the flow-through.
13. To rid spin columns of any residual ethanol, place the RNeasy spin column in a new 2 mL collection tube, leave lid open, and centrifuge at full speed for 5 min. Discard flow-through and spin column.
14. To elute RNA from spin column, place RNeasy spin columns in a new 1.5 mL collection tube, and, depending on the expected yield, add 20–50 μL nuclease-free water. Spin RNeasy columns for 1 min at $8000 \times g$.
15. Reapply eluate from **step 14** directly to the spin column and centrifuge RNeasy columns for 1 min at $8000 \times g$. Discard spin columns (*see Note 39*).
16. Mix eluted RNA by pipetting up and down several times on ice.
17. Immediately transfer 2 μL of RNA into *each* of the *two sets* of 0.5 mL pre-labeled tubes. One set will be used for RNA quantitation; the other set will be used for assessing quality of the RNA (*see Notes 11 and 40*).
18. Flash freeze all samples in liquid nitrogen and store at -80°C (*see Note 41*).

3.10 Assessment of RNA Quantity (See Note 42)

1. Allow all RiboGreen Quant-iT to warm to room temp until the DMSO is thawed.
2. Prepare 20 mLs of $1\times$ TE (1 mL of $20\times$ TE + 19 mL of nuclease-free water).
3. Prepare aqueous Quant-iT RiboGreen working solution optimized for low-range RNA quantification (*see Note 43*).
4. Thaw one set of pre-aliquoted 2 μL samples on ice to determine the concentration of affinity-purified TRAP-extracted RNA.
5. Thaw 1 aliquot of 100 $\mu\text{g}/\text{mL}$ RNA stock on ice. Thaw the 100 $\mu\text{g}/\text{mL}$ RNA stock sample on ice.

6. Prepare a standard curve optimized for a low-range standard curve using serial dilutions of the 100 µg/mL RNA stock to yield a 100 ng/mL working RNA stock (*see Note 43*).
7. Once the standard curve is prepared, prepare duplicate wells for each unknown TRAPed sample by adding the following components to each well:
 - 99 µL of 1× TE
 - 100 µL of low-range Quant-iT solution
 - 1 µL of sample
8. Use the software associated with the fluorescence-based scanner to provide a standard curve and results for the unknown samples.

3.11 Assessment of RNA Quality (See Note 11)

1. Send one set of 2 µL aliquots to a university core facility for analysis using an Agilent Technologies Bioanalyzer.
2. The RNA concentration of affinity-purified TRAP-extracted samples determined in subheading 3.10 will dictate the range required for the Bioanalyzer chip selection (*see Note 11*).
3. Samples with an RNA integrity number (RIN) >8 will yield viable cDNA libraries of sufficient quality to provide good RNA-Seq results.

3.12 cDNA Library Construction and RNA Sequencing

1. Send samples on dry ice to a suitable facility for cDNA library construction and RNA sequencing.

3.13 Data Analysis Overview and Working Environment

In this section we will review an example workflow for analyzing RNA-Seq data obtained from TRAP. At each step we will cover example software solutions or techniques from among the many available. An overview of the individual steps of this data analysis, along with associated terminology and file types, can be found in Fig. 2.

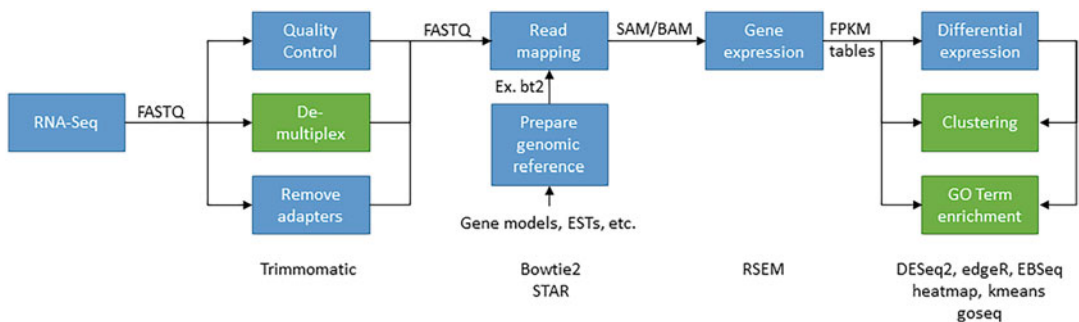


Fig. 2 Schematic diagram of the major stages for data analysis. File formats typically used at each step are shown above the arrows, possibly optional steps shown in green, and software discussed here are listed at the bottom of the figure

In choosing a computing environment to work in, we recommend any popular Linux platform such as Ubuntu or Amazon Linux (Red Hat) for the smoothest experience. Each of the computationally intensive parts of this workflow is independent and easily run in parallel for each of your samples on an in-house high-performance computing cluster or on compute instances provided by a cloud vendor. For scripting, data wrangling, and creating visualizations, we recommend R using the RStudio development environment (<https://rstudio.com/products/rstudio/>) [10], although Python is another popular choice. If you are new to R, we recommend Garrett Golemund and Hadley Wickham’s *R for Data Science* (<https://r4ds.had.co.nz/>) as an excellent place to get started.

3.14 Sequence File Preparation and Quality Control Filtering

If your RNA-Seq vendor is using Illumina sequencing, the input to this workflow will be sequence reads stored in FASTQ files. These files contain both the raw sequences obtained through high-throughput sequencing and quality values for each of the base calls in those reads. It is important at this initial step to understand how your RNA-Seq vendor has supplied these files. For example, if you multiplexed your samples—ran more than one sample in each sequencing lane using unique adapter sequence for each—the FASTQ files you are provided may or may not have already been separated by sample. So, to map sequencing reads to the genome, we will need to, possibly, do several things: (1) demultiplex FASTQ files so that there is one FASTQ for each unique TRAP sample, (2) remove adapter sequences introduced during cDNA library creation, and (3) filter reads to a standardized quality threshold.

To perform these steps, we recommend using Trimmomatic [11]. Trimmomatic is a widely used, well-documented solution that is efficient and has a relatively simple command line interface. It is also multithreaded, so it can take advantage of high-CPU count devices or cloud instances. Trimmomatic is provided by the Usadel lab as a Java “.jar” file (<http://www.usadellab.org/cms/?page=trimmomatic>), so you may need to install a Java VM, such as OpenJDK, in your computing environment to use it. We will run Trimmomatic on each of our input FASTQ files, providing it (1) an input file name, (2) an output file, (3) a SE (single-end) or PE (paired-end) mode setting, (3) information about adapter sequences to be removed (e.g., “TruSeq2” or “TruSeq3”), and (4) a number of optional quality control cutoff values. We recommend experimenting with how different combinations of quality control cutoff settings affect the number of reads that survive the quality control filter (*see Note 44*). Trimmomatic produces log files from each run that are easily parsed to find the percentage of reads that were discarded with a particular combination of quality control settings. We recommend scanning these logs for each of your samples to ensure that none of your samples have an unusually

large number of discarded reads, relative to the others, as this might be a sign of a technical issue with a sequencing lane which could introduce bias in read mapping results.

3.15 Mapping RNA-Seq Reads to the Genome

The next step in our data analysis workflow will be to try to map each of the RNA-Seq reads in our filtered FASTQ files to genomic loci (unique genes). At this stage of the analysis, we will need to choose a resource to use for our genomic reference. We could, for example, align our RNA-Seq reads to a gene model reference, such as the JGI gene models [12]. Or we could align our samples to a set of expressed sequence tags, like those in the NCBI EST database [13]. Although the allotetraploid nature of the *X. laevis* genome has long complicated the construction of a high-quality reference genome, recent advances have significantly improved the resources available. Importantly, when mapping reads to the newer gene models (v9.1 and v9.2), a distinction is made between homeolog pairs that map to large “.L” or small “.S” chromosomes. At present, we would recommend aligning to the JGI v.9.2 gene models mirrored at Xenbase (<ftp://ftp.xenbase.org/pub/Genomics/JGI/>) as a first pass, reverting to EST approach only if a particular gene of interest to your project is not yet present in the gene model set.

One popular software option for performing read alignments is the Bowtie2 package [14], although there are many others with performance advantages and disadvantages (*see Note 45*). Performing read alignments with Bowtie2 comes in two stages: (1) first we will prepare a genome reference from our chosen source (once), and (2) then we will use that reference to align the reads in each of our filtered FASTQ files. The first step creates a number of “.bt2” files that contain the genomic index Bowtie2 we will use, while the second step produces SAM (Sequence Alignment/Map) files that associate each of our successfully mapped sequencing reads with symbols in the reference genome (*see Note 46*). As above, we recommend scanning log files at this stage to ensure that none of your samples exhibited unusually low rates of reads mapped to the reference genome.

With these results in place, we can now estimate levels of gene expression in each of our samples, counting the number of times we found a match between an RNA-Seq read and a gene in the reference genome. Fundamentally, we need to perform two kinds of normalization to make these counts meaningfully comparable between genes and samples. The first is to normalize counts to the coding region length for each gene. The second is to normalize counts within a sample to the number of total reads for that sample. A widely used unit for these normalized counts is FPKM: *fragments per kilobase of exon per million reads* (*see Note 47*).

There are numerous software solutions available that take different approaches to performing this normalization and gene

expression estimation, but we recommend RSEM as a widely used, well-documented, and mature option (<https://github.com/deweylab/RSEM>) (*see Note 48*) [15].

3.16 Higher-Order Analysis

The first question we usually want to ask once we have normalized gene expression estimates for each of our TRAP samples is which genes appear to be up- or downregulated when we compare our experimental groups. There is a daunting variety of software options and algorithmic approaches to choose from when performing differential gene expression on RNA-Seq data. This diversity of options has been extensively reviewed (e.g., [16–20]). The best choice for any project hinges on the nature of the experimental design, including the number of biological replicates, and the downstream questions of interest. As a first pass, we recommend considering DESeq2, edgeR, or EBSeq as widely used and well-maintained software projects with documented strengths and weaknesses (*see Note 49*). We also recommend experimenting with at least a few algorithmically distinct approaches to ensure that differential expression estimates for genes of particular interest to your project are robust across different approaches.

Hierarchical clustering is a popular method for visualizing sets of up- or downregulated genes in RNA-Seq data. These visualizations can be created using either FPKM values from gene expression estimation or log₂ ratios generated during differential gene expression analysis. Hierarchical clusters can be created in R using the base “heatmap” function. We recommend pairing hierarchical clustering with other clustering methods that have distinct strengths and weaknesses, such as k-means clustering. This can be done using the “kmeans” function in R (*see Note 50*). Pairwise distance analysis is a nice way to get a high-level overview of the relationships between samples. A matrix of distances between each of your samples can be calculated using a measure like Pearson correlation (the “cor” function in R), or Euclidean distance. The “geom_tile” function in the “ggplot2” R package is a good option for creating visualizations of these distance matrixes [21].

The last popular analysis technique we will touch on here is to search for Gene Ontology (GO) terms that are overrepresented in a set of up- or downregulated genes [22]. In GO databases, graphs of biological terms (e.g., “splicing” or “translation”) are associated with gene symbols in a model organism’s genome. There are numerous packages available that will provide an estimation of the likelihood that terms are overrepresented in a given set of genes, usually generated by gene expression estimates that suggest a group of factors are up- or downregulated in response to an experimental condition. In R, we recommend the “goseq” package [23]. Xenbase hosts a number of useful files for performing GO analysis. First, the “GenePagesGoTerms.txt” table associates GO terms with Xenbase “gene pages.” These are the webpages for each gene in the genome

that include, where relevant, gene symbols for both the large (“L”) and small (“S”) homeolog pairs and *X. tropicalis* gene symbols. Coupled with the “XenbaseGenepageToGeneIdMapping.txt,” it is quite easy to generate the input needed to run “goseq” on a *X. laevis* gene set.

4 Notes

1. *Inhibiting RNases*: RNases are resilient enzymes prevalent in most tissues and on all surfaces. Presence of RNases can lower both the yield and the quality of the RNA. Before carrying out any experiments, clean all surfaces, pipets, and microfuge tube racks with an RNase decontamination solution (e.g., RNase-Zap, RNase AWAY), and use certified RNase-free disposable barrier tips. Keeping samples, buffers, and tips as cold as possible will also help lower RNase activity. Tissues from older animals, such as retinas from older frogs, can be highly vascularized. The blood of older animals tends to be more oxidized and has increased levels of RNases. In such cases, it may be worth briefly rinsing freshly dissected tissues in two sequential ice-cold dissecting buffer baths and removing excess liquid before placing tissue into homogenizer tube containing ice-cold lysis buffer. Use of pre-cooled barrier pipet tips to transfer the post-homogenized lysate into pre-chilled, pre-labeled microfuge tubes on ice is also advised. SUPERase•In and RNasin will inhibit RNase A, B, and C. SUPERase•In will also inhibit RNase 1 and T1. These enzymes need to be handled gently (do not vortex) and added to buffers immediately prior to use. While I only used RNasin and had good RNA integrity (RIN >8) in my TRAP assays, the Heiman Lab [5] recommends adding both RNase inhibitors.
2. If this assay will be performed frequently, commercially available RNase decontamination solution is available in bulk (5 gallons) and can be used to fill small spray bottle.
3. Use of all animal experiments should be carried out in accordance with procedures approved by the Institutional Animal Care and Use Committee (IACUC). Published clones and TRAP transgenic frog lines are available upon request either from the author [8] or by purchase (available in 2022) through the National Xenopus Resource (NXR, RRID:SCR_013731, <http://www.mbl.edu/xenopus>).
4. *Considerations when using established or creating new TRAP transgenic lines in Xenopus*: Relatively few labs have created transgenic lines for *Xenopus laevis* owing to their allotetraploid genome and long life cycle (8–12 months to reach sexual maturity). However, frogs can lay several hundred embryos at

one time making REMI transgenesis and the more novel CRISPR/Cas methods excellent tools for generating transgenic *Xenopus laevis* lines [24, 25]. Standard amplification and cloning methods can be used to create the EGFP-L10a transgene that can subsequently be subcloned into an expression vector under control of a cell-type-specific promoter. *Xenopus laevis* TRAP lines were created using the RPL10a ORF (Xenbase.org and Open Biosystems, IMAGE: 4684157) for *Xenopus laevis* fused to an enhanced green fluorescent protein (EGFP) by way of a linker made of two tandem copies of a serine followed by four glycines (SGGGG)₂ [7]. The glycine linker was added to enhance protein folding. Our established TRAP frog lines are driven by two distinct cell-type-specific promoters and a third ubiquitously expressed promoter: Xop promoter [26] to drive the EGFP-L10a transgene in rods Tg(*Xop*:EGFP-L10a); Isl2b promoter [27] to drive EGFP-L10a expression in RGCs Tg(*islet2b*: EGFP-L10a); and Blbp to drive EGFP-L10a expression in Müller cells Tg(*Blbp*: EGFP-L10a) [7]. Both the rod-specific *XOP* and RGC-specific *islet2b* promoters are allowed for cell-type-specific enrichment of the retina [7]. The *islet2b* promoter also drives expression in the Rohon–Beard neurons and the dorsal root ganglia, two types of spinal sensory neurons, as well as neurons in the trigeminal ganglia (unpublished). While we have not isolated TRAPed RNAs from these sensory cells, their visible expression pattern indicates they could be used for TRAP experiments. Since the Tg(*Blbp*: EGFP-L10a) frog lines showed high levels of expression in retinal pigment epithelial (RPE) layer and progenitor cells along with a low and ubiquitous expression level in all the major retinal cell types, this transgenic line is most useful as a non-cell-type-specific control [7]. Results from our initial experiments showed that the quantity of RNA isolated and the background noise can vary between different TRAP transgenic founder lines underscoring the importance of carrying out careful analysis of transgene integration and expression analysis for each F₀ founder line [24]. Because embryos from F₀ founder lines are heterozygous, tadpoles must be screened for EGFP using a fluorescence dissecting microscope. The RPE and chromatophores can obscure the ability to screen for EGFP using the epifluorescent dissecting microscope. Therefore, it is critical to complete screening of tadpoles prior to the appearance of the darkened RPE (Stage 36). While comparative TRAP experiments could be carried out using progeny from different TRAP founder (F₀) lines, we advise against this approach due to differences in the EGFP-L10a transgene expression levels between individual frog lines that may be attributable to transgene integration site and copy number [7]. Given that EGFP-

L10a expression levels per cell are variable and can impact the translational profiling of different cell types and contribute to the experimental variability, we recommend using the F₁ progeny from individual established F₀ hemizygous founder lines with single integration [7].

To establish founder TRAP lines, it is necessary to verify that (a) the EGFP-L10a protein is expressed in the correct location within the cell, (b) the expression is cell-type-specific, and (c) TRAPed mRNAs are enriched in the targeted cell types. To localize the transgene expression pattern within and between cells, harvest and fix tissue from a single TRAP animal, cryosection tissues, stain nuclear DNA with DAPI, and image the sections using confocal microscopy. Results should show a Nissl-like staining pattern of EGFP-L10a in the cytoplasm as well as a diffuse staining in the nucleus along with an area of punctate staining in the nucleolus, the site of ribosomal assembly. To show the EGFP-L10a transgene is cell-type-specific, co-stain these tissue sections with an antibody marker specific to the targeted cell type. Likewise, the expression of the transgene for each line should be tested using cell-type-specific qPCR primers for genes expected to be expressed at low, mid, and high expression levels. As a measure of non-cell-type-specific background noise, include qPCR primers for genes not expected to be expressed in the TRAPed RNA samples from retina [7]. To show expression of the EGFP-L10a protein product, harvest tissues from a single TRAP animal, a wild-type animal (negative control) and, if available, a non-TRAP GFP transgenic animal (positive control), homogenize tissue in protein lysis buffer, and run protein samples on a protein gel. Western blotting using a commercial anti-GFP antibody should show GFP expression of the correct size for the non-TRAP GFP sample (~27KD) and for the EGFP-L10a transgene (~57KD) in appropriate lanes. Finally, to determine whether TRAPed mRNAs are enriched in the targeted cell type relative to other cell types present in the tissue lysate, collect and save the first supernatant removed following sample incubation with the affinity matrix. Using this unbound fraction, it is possible to estimate the level of mRNA enrichment relative to the unbound fraction containing nonspecific mRNAs (total unbound RNA less the TRAPed mRNAs). Comparing the TRAPed mRNAs to total non-TRAPed mRNAs will also provide a measure of cell-type-specific enrichment.

5. Streptavidin-coated magnetic beads. The reagents in this step have changed considerably since the protocol was originally published [4]. The Magnetic Streptavidin MyOne T1 Dynabeads coupled with biotinylated protein L replaces the Dynal Protein G magnetic beads. The Streptavidin MyOne T1

Dynabeads consist of 1- μ M-diameter supermagnetic beads surrounded by a monolayer of streptavidin, a tetroid molecule that binds to biotin with high affinity. Biotinylated protein L binds the IgG constant region without interfering with the mAb antigen-binding site. The “affinity matrix” is prepared by incubating the protein L-coated MyOne T1 Dynabeads matrix to the anti-GFP mAb. Because of the affinity of biotin for IgG, it is critical that all washes be carried out in IgG-free 1 \times PBS. To ensure sufficient affinity matrix is present to capture all the tagged RNA, the following ratio of individual components provided is recommended [5]: 300 μ L streptavidin-coated magnetic beads: 120 biotinylated protein L: 100 μ g anti-GFP [5]. This ratio is deemed sufficient to capture all tagged ribosomes in 50–200 mg of cerebral tissues. However, because the amount of affinity matrix varies based on factors such as the cell type and its abundance, the translational state, and the amount of TRAP-extracted tissue collected, carrying out preliminary experiments is highly recommended (*see* **Notes 18, 19 and 20**). It is worth noting that in a side-by-side comparison of the protein L-coated Streptavidin MyOne T1 Dynabeads with the original Protein G Dynabeads, the Protein G Dynabeads produced a better RNA yield (L. Fague, UC Davis, CA).

6. Anti-GFP monoclonal antibodies are available from the Memorial Sloan Kettering Monoclonal Antibody Facility Contact Dr. Frances Weis-Garcia (f-weis-garcia@ski.mskcc.org). Order equal amounts of “bioreactor supernatant” purity: 50 μ g HtzGFP_04 (clone19F7) and 50 μ g HtzGFP_02 (clone 19C8). It is highly recommended that the antibodies be obtained directly from Sloan Kettering. If antibodies arrive frozen, store at -80°C until ready to aliquot; then thaw on ice to aliquot. If antibodies arrive thawed, store at 4°C for a few days until ready to aliquot or use in experiment. Before aliquoting, spin mAb in refrigerated microcentrifuge at maximum speed ($>13,000 \times g$) for 10 min, and transfer supernatants containing the antibody to new tubes on ice. Based on the concentration of batches, aliquot the volume necessary for making single-use 50 μ g antibody aliquots in 0.5 mL tubes for each of the two anti-GFP (19C8 and 19F7). Flash freeze by immersing tubes in liquid nitrogen and storing at -80°C . As part of a series of initial control experiments, a side-by-side comparison of the recommended monoclonal HtzGFP (50 μ g 19F7 and 50 μ g 19C8) antibody mixture was performed using two different commercial anti-GFP antibodies known to work well for Western immunoblots, immunoprecipitations (IPs), and/or immunostaining. In our hands, neither commercial antibodies yielded any significant polysomal TRAPed RNA isolates. Concentration range of available anti-

GFP mAb from Sloan Kettering is 0.5–4.5 mg/mL and varies by batch. Purchasing sufficient amounts of both antibodies (19F7 and 19C8) to complete any comparative studies is recommended as our experiments found variability between different mAb batches. Record mAb batch numbers/concentrations for re-ordering.

7. Use of fluorescence-based RNA quantification methods such as the RiboGreen kit (or similar) provides the best way to quantify low concentrations of RNA. The columns in most commercial RNA kits shed silica debris that can scatter light and lead to inaccurate RNA readings for samples with RNA yields below ~10 ng/ μ L. Therefore, use of spectrophotometer-based methods should only be used for RNA concentrations above 10–50 ng/ μ L. The Bioanalyzer 2100 or 6000 (or similar) can also assess RNA yield and concentration. However, this value has not been deemed reliable for RNA quantification.
8. Many different commercial total RNA extraction kits are available and the instructions for individual kits should be followed. In the methods section, we provide instructions for the QIAGEN micro-RNeasy kit. However, because kit components and instructions may be updated or changed over time, users are advised to verify that these instructions are current for their specific RNA extraction kit.
9. Magnetic particle concentrator. Several labs have made homemade versions of a magnetic particle concentrator by gluing a strong magnet to the side of a microfuge tube holder. The magnet strength needs to be sufficient to quickly pull the magnetic beads against the side of the microfuge tubes in ~30–60 s. Commercially available versions are available. Since speed is an important factor in minimizing RNA degradation, use of a magnetic particle concentrator that can be placed in ice and accommodate all experimental samples at the same time is recommended.
10. **Tissue homogenization:** In our experience, the homogenization step was the most important determinant affecting RNA yield. The method for homogenizing tissue is determined by the type of tissue to be homogenized. For instance, plant seeds have a protective case and insects have tough exoskeleton that is difficult to shear [28]. Cryogenic grinding with a ceramic pestle and mortar followed by manual grinding using a glass-on-glass manual homogenizer has been used in *Arabidopsis* plant seedlings [29], a multidirectional fast-speed bead grinder has been used in *Drosophila* [30], a motor-driven homogenizer coupled to a PTFE Teflon pestle [4, 5, 8] or coupled to a sawtooth grinder [31] has been used in mouse tissues, and both a manual glass-on-glass homogenizer and a motorized

Teflon–glass homogenizer have been used to grind *Xenopus* tissue [7, 8]. Extreme care should be taken at this step because many of these methods rely on high-speed frequencies that can heat samples leading to RNase degradation and/or introduce air leading to protein denaturation [28]. Initially, we used a glass-on-glass (Wheaton) Potter-Elvehjem manual homogenizer whereby the glass pestle is submerged to the bottom of the tube and manually twisted as the piston is raised and lowered for a total of 12 strokes. Twisting the pestle 360° ensures all sides of the sample become exposed to grinding. To disrupt the sample effectively, the fit between the mortar and pestle in glass tissue grinders should be tight so the pestle can grab and then shear the tissue between the glass pestle and tube wall [28]. The effectiveness of the grinding was directly correlated with the fit of the glass pestle in the tube: the tighter the fit, the better the homogenization of the tissue (out of six glass Potter-Elvehjem homogenizers we ordered, only one had an adequate fit). We eventually used a motor-driven homogenizer with a Teflon (PTFE) pestle to mechanically shear the tissue. To effectively homogenize the tissue, submerge the PTFE pestle to the bottom of the tube, turn on the homogenizer at ~300 rpm, and then gradually increase the speed to ~900 rpm while plunging the pestle up and down slowly for 12 strokes. On the downstroke, make sure to plunge the pestle all the way to the bottom of the tube, while on the upstroke, avoid the air–liquid interface so as not to create air bubbles. To maintain samples as cold as possible, homogenize the tissue in a walk-in cold room, and place the glass homogenizer tube on ice while homogenizing as the grinding generates heat within the sample. To achieve reproducibility between technical samples, it was critical to limit the use of one pestle that had a tight fit to two homogenizer tubes. By working in the cold room, we could effectively clean the homogenizer tubes and pestle between samples by submerging the pestle in a cold RNase decontamination solution (e.g., RNase AWAY), rinsing multiple times with RNase-free water, and carrying out a final rinse in Tissue Lysis Buffer. It was critical to limit any side-to-side wobbling, even to the extent of designing an adapter using the 3D printer to limit any side-to-side pestle movement (L. Fague UC Davis, CA). Attention to the manner in which the tissue is homogenized combined with technical skills acquired through experience is likely to be the key to optimizing this step.

11. Qualitative RNA assessment is critical for downstream application of cDNA library construction and RNA sequencing. Agilent Technologies Bioanalyzer 2100 or 6000 is optimized to determine the integrity of extremely low levels of RNA. Results from the fluorescence-based RNA quantification (Subheading

3.10) will inform which chip should be used for assessing the quality: the nano-chip is used to assess the quality of total RNA in the 25–500 ng/ μ L range and mRNA in the 25–500 ng/ μ L range, while the pico-chip can be used to assess the quality of total RNA in the 50–5000 pg/ μ L and mRNA in the 250–5000 pg/ μ L range. To outsource RNA quality, send one set of 2 μ L aliquots on dry ice to a core facility for analysis using an Agilent Technologies Bioanalyzer. Each chip can process 12 μ L samples. Bioanalyzer results include a slab gel analysis, RNA concentration, rRNA ratios, and the RNA integrity number. The RNA integrity number (RIN) is based on an algorithm designed to assess the highly prevalent ribosomal 28S and 18S RNA peaks relative to other peaks (noise) present in the samples. A RIN of 10 (highest rating) will typically only have the two 28S and 18S ribosomal peaks, while a RIN of 3 has multiple additional peaks and indicates the sample may be degraded. The amount of rRNAs in the samples is much more prevalent than that of mRNAs, but these rRNAs are subtracted during the bioinformatic analysis. The RIN was developed to standardize the interpretation of the results and provides a reliable tool to assess RNA integrity. Sample RINs for cDNA library construction and RNA sequencing should be above 8, preferably in the 8.5–10 range.

12. The fluorometric measurement of nucleic acids is based upon the use of fluorogenic dyes that bind selectively to DNA or RNA. A commercially available fluorescence microplate reader is required to allow detection and quantification of small amounts of low concentrations of RNA.
13. Order powdered form (e.g., Avanti Polar Lipids 07:0 PC) with a request for special packaging (5 \times 50 mg) as the glass ampules cannot be resealed.
14. Estimate and aliquot the approximate volume of each buffer required to carry out the experiment in its entirety. RNase inhibitors, cycloheximide, DDT, and/or protease inhibitors will be added to the cold aliquoted buffers immediately prior to use. Keep all buffers ice-cold and work in cold room or if no walk-in cold room is available, maintain samples and reagents on ice at all times.
15. Although MMR (Marc's Modified Ringer's solution) preparations often include EDTA, we exclude it here because EDTA chelates magnesium, an important component of the TRAP assay.
16. To accommodate the physiological saline of frogs, dissect tissues in 0.5 \times MMR dissection buffer (see TRAP buffers) with cycloheximide added fresh to a final concentration of 100 μ g/mL. The cycloheximide stalls polysomes on the mRNA and

keeps the ribosome–mRNA complexes from dissociating. For tissues with a high metabolic rate, e.g., retinas, add glucose to a final concentration of 35 mM to help quench metabolism. Since blood represents a source of RNases, highly vascularized tissues should be rinsed sequentially (twice) in dissection buffer prior to being lysed. Tissue can also be collected and flash frozen (*see* **Note 29**).

17. Early studies reported low RNA yields from TRAP-extracted tissue. This protocol has been updated to reflect methods optimized for increased total RNA yield [5]. RNA yields can vary as a function of (1) promoter activity driving the EGFP-L10a transgene and number of cells processed, (2) the affinity matrix to tissue ratio used to tag the EGFP-L10a, (3) the efficiency of the tissue homogenization step, and (4) RNA degradation. To optimize the RNA yield, a series of pilot experiments using the experimental TRAP tissues is recommended. Pilot experiments, discussed below, will inform the criteria required for designing the comparative TRAP studies, number of technical replicates, and animal usage.
18. **Pilot experiment #1:** While maintaining the ratio of individual components constant, vary the amount of streptavidin-coated magnetic beads to determine the amount of “affinity matrix ratio” relative to the TRAP tissue for your planned experiments. Prepare the “affinity matrix” by incubating the streptavidin-coated magnetic bead matrix to the anti-GFP mAb. Because of the affinity of biotin for IgG, it is critical that all washes be carried out in IgG-free 1× PBS. To ensure sufficient affinity matrix is present to capture all the tagged RNA in a given tissue, use the following ratio of individual components [5]: 300 μL streptavidin-coated magnetic beads: 120 biotinylated protein L: 100 μg anti-GFP. This ratio is deemed sufficient to capture all the tagged ribosomes in 50–200 mg of cerebral tissues [5]. The amount of affinity matrix per tissue type can vary substantially. For instance, using the Protein G Dynabeads, we used 100 μL magnetic beads per sample containing 10 post-metamorphic *Xenopus* retinas (2.6×10^6 RGCs) [8] or 14–20 tadpole retinas per 67 μL of beads [7] which represents ten-fold fewer cells yet only a third less affinity matrix. Given that the scaling is non-linear, it is important to optimize the affinity matrix to ensure sufficient affinity matrix exists to capture all the ribosomes and associated mRNAs in your particular tissue.

Due to the cost of these reagents, an oversaturation of beads is not typically used. To optimize the affinity ratio relative to your tagged tissue, prepare the affinity matrix (Subheading 3.3), and vary the amounts of beads by 0.5X and 2X while maintaining the individual components constant.

- A. Collect and pool sufficient tissue from TRAP animals for three samples.
 - B. Divide sample into three tubes to ensure the amount of starting material is the same in all three samples.
 - C. Follow methods for collecting, homogenizing, and processing TRAP samples (Subheadings 3.4, 3.5 and 3.6). To immunoprecipitate (Subheading 3.7), add differing affinity matrix ratios to each sample (*see example below*). *Note*: If starting with smaller tissue sample sizes, use the same component ratios but with less volume, e.g., 150 μL beads: 60 μL biotinylated protein L: 50 μg anti-GFP.
 - Sample 1 (0.5X): 150 μL beads: 120 biotinylated protein L: 100 μg anti-GFP
 - Sample 2 (1X): 300 μL beads: 120 biotinylated protein L: 100 μg anti-GFP
 - Sample 3 (2X): 600 μL beads: 120 biotinylated protein L: 100 μg anti-GFP
 - D. Compare the amount of TRAP-extracted RNA from the samples to establish the proper ratio components suitable for TRAP tissue.
19. **Pilot experiment #2:** To establish the background noise and reproducibility and between RNA extraction efficiency (technical replicates) and between individual tissues (biological replicates), compare the total RNA yield, quality of RNA (RNA degradation), and homogenization efficiency. Using the amount of affinity matrix ratio optimized in pilot experiment #1, run a minimum of three experimental IP samples per tissue type, and include a no antibody matrix-only control to establish the level of background noise:
- A: Technical Replicate:** Collect and pool tissues from three different sets of TRAP animals and homogenize samples. Divide pooled tissue homogenate into three different tubes. In parallel, carry out the binding, immunoprecipitation, and RNA extraction protocol of all three samples. Compare total RNA yields, RNA concentration, rRNA, and RIN values to inform your planned TRAP experiments. If the RIN value is <8 , results from these samples will provide a measure of technical error and/or RNase contamination.
 - B: Biological Replicate:** Collect tissues from one set of TRAP animals and proceed through to the homogenization step; place on ice. Collect tissues and proceed to homogenization step for two additional sets of TRAP animals (do not pool samples). Compare total RNA yields, RNA concentration, rRNA, and RIN values to inform your planned

TRAP experiments. If the RIN value is above 8 but there is significant variability between samples, then variability is not likely due to RNA degradation but most likely due to insufficient or inadequate tissue homogenization (*see Note 12*). Note: It may be worth waiting to carry out the biological replicates until an acceptable amount of variability between the technical replicates is achieved.

C: Nonspecific Control: Tissue from non-transgenic (wild-type) animals—homogenize and TRAP samples individually—since these animals do not have a ribotag, a comparison of these samples with the biological replicates will provide a measure of the nonspecific background.

D: Matrix-Only Control: Incubate transgenic tissue with a protein L-coated beads-only control (no anti-GFP)—homogenize and TRAP samples (if more than one) individually—this sample will provide a measure of the background level related to the matrix.

20. The experimental samples refer to the number of samples that will be immunoprecipitated (also referred to as IP or TRAP-extracted). The control samples (Ctl) refer to the number of samples that will be immunoprecipitated with the control affinity matrix not bound with the anti-GFP antibody. Knowing the total number of samples is required for estimating the volume required for each buffer, preparation of the affinity matrix, and labeling and pre-chilling the correct number of tubes.
21. The “affinity matrix” refers to a ratio of three components: streptavidin-coated magnetic beads coated in biotinylated protein L and bound with anti-GFP antibody. The control affinity matrix refers to affinity matrix without addition of the anti-GFP antibody. To optimize the ratio of individual affinity matrix components relative to the TRAP-extracted tissue, carry out pilot experiment #1 (*see Note 19*). To help determine your RNA yield, reproducibility, nonspecific binding, and any potential RNA degradation, carry out pilot experiment #2 (*see Note 20*).
22. Preparing the affinity matrix (AM) and control affinity matrix (AMctl) takes approximately 2.5 h and can be prepared fresh prior to collecting and processing the TRAP-extracted or control tissues. Alternately, with the addition of 0.02% sodium azide, the affinity matrix can be prepared up to 2 weeks prior to the experiment and stored at 4 °C. If using pre-prepared affinity matrix, the affinity matrix must be washed to remove all traces of sodium azide. This can be done by placing the affinity matrix on an end-over-end tube rotator at 4 °C overnight. Immediately prior to use, carry out three sequential washes in

- low-salt buffer (*do not vortex!*), and aliquot equally by dividing into the numbers of tubes that correspond to each IP or control sample (Fig. 1h).
23. If you are using the anti-GFP antibody mixture from Sloan Kettering as outline in **Note 6**, use 50 μg 19F7 and 50 μg 19C8.
 24. The Dynabeads are packaged by the manufacturer in a set volume of buffer. It is important to maintain the beads in the same total volume as when the beads arrive from the manufacturers. Calculate the volume of beads needed for each IP sample and multiply by the number of total IP samples in the experiment + control. The total volume of liquid to bead ratio should not be changed even though the ratio of buffers that make up this volume is maintained according to the optimized affinity matrix ratio.
 25. This step allows the biotinylated protein L to bind to the beads. The beads should be maintained in a volume approximating that which is specified by the manufacturer. Each 1 mL of resuspended beads transferred from the manufacturer's bottle into a tube should be washed once in 1 mL of $1\times$ PBS, placed on magnet, and resuspended in 1 mL of PBS minus the appropriate volume of biotinylated protein L. *For example*, for samples using an affinity matrix ratio of 300 μL streptavidin-coated magnetic beads: 120 biotinylated protein L: 100 μg anti-eGFP, resuspend the 1 mL of beads–streptavidin using 600 μL of $1\times$ PBS and 400 μL of biotinylated protein L.
 26. Binding of the anti-GFP antibody to the biotinylated protein L-coated beads is carried out in low-salt buffer in a volume that corresponds to the initial affinity matrix ratio. For example, using an affinity matrix ratio of 300 μL streptavidin-coated magnetic beads: 120 biotinylated protein L: 100 μg anti-GFP, if the combined 100 μg (50 μg 19F7 + 50 μg 19C8) of GFP antibody = 40 μL , then resuspend the protein L-coated beads for one sample in 260 μL of low-salt buffer, and add 40 μL of the combined GFP antibody. For the no antibody control sample, add 300 μL of low-salt buffer.
 27. The recommended tissue to lysis buffer ratio is 25–50 mg tissue: 1 mL lysis buffer [5]. Scale accordingly. For example, we homogenized ten adult frog retinas in 300 μL of Tissue Lysis Buffer. The tissue to lysis buffer ratio should be optimized in pilot experiments (*see Notes 18 and 20*).
 28. Rinsing the dissected tissues is particularly important in highly vascularized tissues from older animals as they can harbor higher amounts of RNases. Work on ice, fill two small shallow (5–10 mL) beakers with ice-cold dissection buffer, and add 100 $\mu\text{g}/\text{mL}$ cycloheximide (the opening of the beaker should

be sufficiently wide to allow the forceps holding the tissue to be fully immersed). To remove RNase contaminants, briefly immerse tissue in two sequential baths containing ice-cold dissection buffer with added cycloheximide. Remove excess liquid by pressing tissue against the edge of the beaker before placing tissues into the homogenizer tube containing ice-cold lysis buffer.

29. *Tissue collection:* Using freshly harvest tissues for TRAP is optimal. However, a side-by-side comparative analysis showed that flash freezing tissue in liquid nitrogen, storing it at -80°C for several months, and then homogenizing the tissue in Tissue Lysis Buffer while the tissue is still frozen led to a 46.2% loss in overall RNA yield [5]. Importantly, since the quality (RIN) of the TRAPed RNA was sufficient to perform RNA-Seq TRAP studies, if you plan on freezing tissue, the use of additional animals may be required [5]. Because of the difference in RNA yields, it is not recommended to mix frozen and fresh tissues within a single comparative studies as there may be unanticipated artifacts [5].
30. If dissecting retinas, remove the entire eyes rapidly by cutting the optic nerve quickly and cleanly, and place the whole eyes in ice-cold dissection buffer with freshly added cycloheximide to a final concentration of $100\ \mu\text{g}/\text{mL}$. Then transfer individual eyes to a fresh clean silicone plate, remove and discard the lens, and cleanly extract the retina from the sclera and retinal pigment epithelium (RPE).
31. To reduce RNA degradation, collect the tissue for an individual sample and proceed through the sample homogenization step. If possible, several individuals can work together in an assembly-line style where one individual extracts the tissue of interest from the TRAP animal and another refines the dissection and brings the tissue to a third individual who carries out the homogenization step. Ideally, the homogenization step should be carried out by the same individual and carried out in the cold room (*bring a hat and warm jacket!*).
32. The first centrifugation step removes the cellular debris (pellet) from the ribosomes and associated RNAs. The final volume is recorded because some sample may become lost during the homogenization and transfer steps. Recording the volume is critical as the next two steps will involve adding $1/9$ volume of NP-40 and $1/9$ volume of DHPC to the lysate. To account for any loss of volume and streamline the process, readjust the volume using tissue lysis buffer so the volume in all samples is equal.
33. The estimated sample volume for DHPC should include the volume of NP-40 added at **step 3**. DHPC is used at low

concentrations (10–40 mM) as this concentration has been shown to preserve the native three-dimensional structural conformation and activity of solubilized proteins.

34. The unbound fraction consists of the total RNA minus the RNA–ribosome complex that bound to the affinity matrix. Save the unbound fraction and either flash freeze, store at -80°C , and extract using commercial RNA extraction kits at a later date or place on ice and isolate the RNA after the IP samples have been extracted. Note that the total RNA yield can be quite high, so it is advisable to use RNA extraction kits with increased binding capacity suitable for higher total RNA yields (e.g., mini or midi RNeasy kit). If the concentration of the unbound fraction exceeds 10–50 ng/mL, these samples can be quantified using standard spectrophotometer-based RNA quantitation methods.
35. To wash the sample, aspirate/pipet off supernatant and discard, remove magnet, and resuspend beads in 1 mL of *high*-salt buffer by gently titrating up and down four times using a P1000. Be gentle and avoid introducing air bubbles.
36. Here we provide an example of QIAGEN's RNeasy extraction kit. However, these steps and the reagents in commercial kits are frequently updated. Therefore we recommend using the instructions that come with the kit. The in-column DNase digestion is necessary to remove any residual DNA. Not digesting the DNA can result in a lower-quality RNA (as measured by the RIN value).
37. This step will depend on which commercial RNA extraction kit is used. The QIAGEN RNeasy kit uses a proprietary buffer (RLT buffer) which contains a high concentration of guanidine isothiocyanate designed to support the binding of RNA to the spin column silica membrane. If using other commercial RNA extraction kits, substitute corresponding buffer. The beta-mercaptoethanol (β -ME) irreversibly denature RNases by reducing disulfide bonds and destroying the native conformation required for enzyme functionality.
38. Unlike the recommendation in [5], resuspending the beads in RLT– β -ME buffer while still in the cold room and then immediately placing at room temperature for the 5 min incubation did not appear to have any effect. Because β -ME irreversibly denatures RNases, extracting the RNA–ribosome complex from the beads at room temperature will not degrade the RNA.
39. Following the affinity purification of TRAP-extracted RNA, the yield is low. To increase to total RNA, repeat the elution using the eluate from first elution (**step 14**).
40. Collect two aliquots of 2 μL of TRAPed RNA for each sample because the yield of affinity-purified TRAP-extracted RNA is

low (do not carry out the RNA quantitation in triplicate). This will provide two 1 μ L replicates for each sample. One set will be used for RNA quality assessment and generate the RNA RIN, while the other set will be used for RNA quantitation using a fluorescence-based RNA quantitation kit.

41. To prevent ice crystals from growing in the sample during the slow freezing process, we use extra long forceps to immerse samples in a dewer containing liquid nitrogen until frozen. Immediately store frozen samples at -80°C .
42. The concentration of the RNA in the TRAP-extracted samples tends to be low. Thus, spectrophotometer-based RNA analysis typically used for quantitation should only be used to quantify column-purified RNA samples with a yield that exceeds 10–50 ng/ μ L. Instead, a fluorescence-based RNA quantitation method should be used to accurately quantify the concentration and yield of the TRAPed samples. Many commercially available fluorescence-based kits can be used to detect and quantify nucleic acids. Because this method utilizes advanced fluorophores that fluoresce upon binding to RNA, the silica shed from the columns in the commercial RNA extraction kits will not interfere with RNA quantitation. We provide the steps for the RiboGreen Quant-iT kit. If using a different fluorescence-based quantitation kit, follow the manufacturer's instructions.
43. Preparation of the standard curve for low-range RNA quantitation:
 - (a) The standard curve should include triplicate samples for concentrations that will bracket the concentration of unknown TRAPed RNA samples. Typical range for the low standards includes the following concentrations: 0 (blank), 1, 2, 5, 15, 25, and 50 ng/mL.
 - (b) Prepare a 10 mL aliquot of a 1:2000 dilution of Quant-iT by adding 5 μ L Quant-iT RiboGreen solution and 9.95 mL of $1\times$ TE.
 - (c) Use a known RNA sample available as part of the RiboGreen Quant-iT kit or use the RNA stock purified unbound fraction. Use a spectrophotometer to calculate the RNA concentration based on the O.D. 260 and 280 absorbance.
 - (d) For the standard curve, using the 100 μ g/mL RNA stock, prepare a fresh 1 mL RNA working stock with a concentration of 100 ng/mL (1:1000 \times dilution using 2 serial dilutions of 1:10).

44. In mapping reads to the *X. laevis* genome, we recommend paying particularly close attention to the “LEADING,” “TRAILING,” and “MINLEN” settings.
45. Another software solution we recommend considering is STAR (<https://github.com/alexdobin/STAR>) [32]. STAR’s particular strength is in splice-isoform analysis, but its implementation also has some performance and resource requirement implications when compared to Bowtie2. When running, Bowtie2 reads from genome reference files kept on disk, while STAR loads its genome reference data into memory. This means STAR runs can be significantly faster than Bowtie2 but also requires significantly more memory overhead than Bowtie2. This may create constraints depending on the computing resources available.
46. SAMs (Sequence Alignment/Maps) are flat text files. You can optionally choose to output results as BAM files, which are simply the compressed binary equivalent, so much smaller in size. The Samtools (<http://www.htslib.org/>) package provides a variety of useful utility functions for converting between these formats and viewing or manipulating their contents.
47. FPKM and RPKM, where “Reads” is substituted for “Fragments,” are often used interchangeably. When performing single-end reads, they are the same value. The difference comes when performing pair-end reads where a match to a reference symbol can come from either one or two RNA-Seq reads. TPM is an alternative, newer, method that is becoming popular.
48. Although we’ve separated our discussion of performing read alignments and gene expression estimation here, RSEM provides convenient command line options for chaining these two operations together in one step with popular aligners like Bowtie2 or STAR.
49. In our own experience, DESeq2 and edgeR generally perform more conservatively, while EBSeq is notable for its flexibility in handling complex experimental designs.
50. The “RowSideColors” argument to the “heatmap” function provides an easy way to visualize k-means clusters alongside a hierarchical cluster.

Acknowledgments

Many thanks to Nicholas Marsh-Armstrong and Lindsay Fague (University of California, Davis, CA) for their helpful edits and insight on the manuscript.

References

- Emery B, Barres BA (2008) Unlocking CNS cell type heterogeneity. *Cell* 135:596–598
- Okaty BW, Sugino K, Nelson SB (2011) Cell type-specific transcriptomics in the brain. *J Neurosci* 31:6939–6943
- Tebaldi T, Re A, Viero G, Pegoretti I, Passerini A, Blanzieri E et al (2012) Widespread uncoupling between transcriptome and translational variations after a stimulus in mammalian cells. *BMC Genomics* 13:220
- Heiman M, Schaefer A, Gong S, Peterson JD, Day M, Ramsey KE et al (2008) A translational profiling approach for the molecular characterization of CNS cell types. *Cell* 135:738–748
- Heiman M, Kulicke R, Fenster RJ, Greengard P, Heintz N (2014) Cell type-specific mRNA purification by translating ribosome affinity purification (TRAP). *Nat Protoc* 9:1282–1291
- Dougherty JD (2017) The expanding toolkit of translating ribosome affinity purification. *J Neurosci* 37:12079–12087
- Watson FL, Mills EA, Wang X, Guo C, Chen DF, Marsh-Armstrong N (2012) Cell type-specific translational profiling in the *Xenopus laevis* retina. *Dev Dyn Off Publ Am Assoc Anat* 241:1960–1972
- Whitworth GB, Misaghi BC, Rosenthal DM, Mills EA, Heinen DJ, Watson AH et al (2017) Translational profiling of retinal ganglion cell optic nerve regeneration in *Xenopus laevis*. *Dev Biol* 426:360–373
- Sive HL, Grainger R, Harland RM (2010) Early development of *Xenopus laevis*: a laboratory manual. Cold Spring Harbor, N.Y.: Cold Spring Harbor Laboratory Press. ISBN: 978-087969942-0
- R Core Team (2015) R: a language and environment for statistical computing [Internet]. Vienna, Austria: R Foundation for Statistical Computing. Available from <https://www.R-project.org/>
- Bolger AM, Lohse M, Usadel B (2014) Trimmomatic: a flexible trimmer for Illumina sequence data. *Bioinformatics* 30:2114–2120
- Session AM, Uno Y, Kwon T, Chapman JA, Toyoda A, Takahashi S et al (2016) Genome evolution in the allotetraploid frog *Xenopus laevis*. *Nature* 538:336–343
- Karpinka JB, Fortriede JD, Burns KA, James-Zorn C, Ponferrada VG, Lee J et al (2015) Xenbase, the *Xenopus* model organism database; new virtualized system, data types and genomes. *Nucleic Acids Res* 43:D756–D763
- Langmead B, Salzberg SL (2012) Fast gapped-read alignment with Bowtie 2. *Nat Methods* 9:357–359
- Li B, Dewey CN (2011) RSEM: accurate transcript quantification from RNA-Seq data with or without a reference genome. *BMC Bioinf* 12:323
- Zhang ZH, Jhaveri DJ, Marshall VM, Bauer DC, Edson J, Narayanan RK et al (2014) A comparative study of techniques for differential expression analysis on RNA-Seq data. *PLoS One* 9:e103207
- Schurch NJ, Schofield P, Gierliński M, Cole C, Sherstnev A, Singh V et al (2016) How many biological replicates are needed in an RNA-seq experiment and which differential expression tool should you use? *RNA N Y N* 22:839–851
- Li X, Brock GN, Rouchka EC, Cooper NGF, Wu D, O'Toole TE et al (2017) A comparison of per sample global scaling and per gene normalization methods for differential expression analysis of RNA-seq data. *PLOS ONE Public Library of Science* 12:e0176185
- Osabe T, Shimizu K, Kadota K (2019) Accurate classification of differential expression patterns in a bayesian framework with robust normalization for multi-group RNA-Seq count data. *Bioinforma Biol Insights [Internet]* [cited 2021 Feb 22];13. Available from <https://www.ncbi.nlm.nih.gov/pmc/articles/PMC6614939/>
- Li X, Cooper NGF, O'Toole TE, Rouchka EC (2020) Choice of library size normalization and statistical methods for differential gene expression analysis in balanced two-group comparisons for RNA-seq studies. *BMC Genomics* 21:75
- Wickham H (2009) ggplot2: elegant graphics for data analysis. Springer, New York
- Ashburner M, Ball CA, Blake JA, Botstein D, Butler H, Cherry JM et al (2000) Gene ontology: tool for the unification of biology. The Gene Ontology Consortium. *Nat Genet* 25:25–29
- Young MD, Wakefield MJ, Smyth GK, Oshlack A (2010) Gene ontology analysis for RNA-seq: accounting for selection bias. *Genome Biol* 11:R14
- Kroll KL, Amaya E (1996) Transgenic *Xenopus* embryos from sperm nuclear transplantations reveal FGF signaling requirements during gastrulation. *Development* 122:3173–3183
- Feehan JM, Chiu CN, Stanar P, Tam BM, Ahmed SN, Moritz OL (2017) Modeling

- dominant and recessive forms of retinitis pigmentosa by editing three rhodopsin-encoding genes in *Xenopus Laevis* using Crispr/Cas9. *Sci Rep* 7:6920
26. Batni S, Scalzetti L, Moody SA, Knox BE (1996) Characterization of the *Xenopus* rhodopsin gene. *J Biol Chem* 271:3179–3186
 27. Pittman AJ, Law M-Y, Chien C-B (2008) Pathfinding in a large vertebrate axon tract: isotypic interactions guide retinotectal axons at multiple choice points. *Dev Camb Engl* 135:2865–2871
 28. Burden DW (2008) Guide to the disruption of biological samples – 2012. Random Primer [Internet]. [Cited 2021 Mar 1]. Available from <https://opsdiagnostics.com/applications/samplehomogenization/homogenizationguidepart1.html>
 29. Thellmann M, Andersen TG, Vermeer JE (2020) Translating ribosome affinity purification (TRAP) to investigate *Arabidopsis thaliana* root development at a cell type-specific scale. *JoVE J Vis Exp*:e60919
 30. Bertin B, Renaud Y, Aradhya R, Jagla K, Junion G (2015) TRAP-rc, translating ribosome affinity purification from rare cell populations of *drosophila* embryos. *JoVE J Vis Exp* 103: e52985
 31. Moran P, Guo Y, Yuan R, Barnekow N, Palmer J, Beck A, et al (2019) Translating ribosome affinity purification (TRAP) for RNA isolation from endothelial cells in vivo. *J Vis Exp* 147 59624
 32. Dobin A, Davis CA, Schlesinger F, Drenkow J, Zaleski C, Jha S et al (2012) STAR: ultrafast universal RNA-seq aligner. *Bioinformatics* 29: bts635



LCM-Seq for Retinal Cell Layer-Specific Responses During Optic Nerve Regeneration

Wesley Speer and Matthew B. Veldman

Abstract

LCM-seq is a powerful tool for gene expression analysis from individual or groups of cells that can be spatially isolated. Within the visual system, retinal ganglion cells (RGCs), the cells that connect the eye to the brain through the optic nerve, reside in the retinal ganglion cell layer of the retina. This well-defined location provides a unique opportunity to harvest RNA by laser capture microdissection (LCM) from a highly enriched cell population. Using this method, it is possible to explore transcriptome-wide changes in gene expression following optic nerve injury. In the zebrafish model, this method can be used to identify molecular events driving successful optic nerve regeneration in contrast to mammals that fail to regenerate axons in the central nervous system. Here we provide a method for LCM from the different retinal layers of zebrafish following optic nerve injury and during the process of optic nerve regeneration. Purified RNA from this protocol is sufficient for RNA-seq or other downstream analysis.

Key words LCM-seq, Microdissection, Retina, Optic nerve, Regeneration, RNA-seq, Retinal ganglion cell layer, Inner nuclear layer, Outer nuclear layer, Zebrafish

1 Introduction

Axon regeneration within the central nervous system of adult mammals is extremely limited, while anamniotes, fish and frogs, exhibit a robust regenerative response and can recover lost function after brain or nerve injury. Given the genetic similarities and differences between the species, it is likely that understanding the molecular genetic events underlying the pro-regenerative response in anamniotes will provide insight into the failure of axon regeneration in mammals and suggest ways to overcome this deficit. A powerful method to identify genome-wide changes in gene expression during axon regeneration is RNA-seq. Measuring mRNA abundance in uninjured control samples and regenerating samples over the complete time course of regeneration can identify differ-

entially expressed genes and be further bioinformatically analyzed to discover known and novel signaling pathways that may be mediating the regenerative process [1–7].

When considering RNA-seq experiments, high-quality sample preparation is key to success. Purified RNA should be intact with little degradation. Additionally, for the highest experimental sensitivity, samples should be enriched for the cell type of interest. This is especially relevant for the study of axon regeneration where neuronal somas are distant from the site of injury and commonly intermingled with more abundant interneurons, glia, and other support cells. Laser capture microdissection (LCM) provides an ideal method to isolate high-quality RNA from minimally processed tissue samples with the spatial resolution to enrich for specific cells of interest [8]. A major advantage of this method is that samples are acutely dissected and then flash frozen leaving little time for RNA degradation or changes in mRNA composition that can accompany other methods of cell purification. LCM coupled to RNA-seq (LCM-seq) provides a sensitive method to assay changes in gene expression from spatially defined cell populations. When applied to models of axon regeneration *in vivo*, the LCM-seq method enables gene expression analysis of defined cells at selected anatomical locations throughout the time course of regeneration.

The visual system provides an ideal system in which to study CNS axon regeneration. The optic nerve is experimentally accessible and almost completely composed of axons running from the retinal ganglion cells (RGCs) of the eye to the brain. The layered structure of the retina delineates the location of its known cell types: RGCs and displaced amacrine cells are in the retinal ganglion cell layer (GCL); amacrine, bipolar, horizontal cells and Muller glia are in the inner nuclear layer (INL); and photoreceptors are in the outer nuclear layer (ONL). In whole retina, RGCs only make up 1–2% of the total cell population [9]. However, purification by LCM of the GCL enriches the sample >50-fold for RGCs. Additionally, the other layers of the retina can be similarly purified and processed by LCM-seq to sensitively assay for gene expression changes in non-RGCs that might support axon regeneration.

We have previously used LCM coupled to microarray analysis to identify novel genes mediating optic nerve regeneration in the RGCs of zebrafish [6]. Here we present our updated protocol for optic nerve crush injury (Subheading 3.1), tissue dissection (Subheading 3.2), cryosectioning (Subheading 3.3), cresyl violet staining (Subheading 3.4), LCM (Subheading 3.5), and RNA purification (Subheading 3.6) for the purpose of RNA-seq from retinal tissue of zebrafish during optic nerve regeneration. This protocol for tissue preparation should be broadly applicable for LCM-seq from fresh tissue samples from any species.

2 Materials

2.1 Zebrafish Optic Nerve Crush Surgery, Tissue Dissection, and Cryosectioning

1. Tricaine-S solution: Dissolve Tricaine-S (MS-222) at a concentration of 0.033% w/v solution in fish system water; bring the pH to 7.0 using 1 M Tris-HCl pH 9.0.
2. Sponge with groove for holding fish.
3. Dissecting microscope.
4. Two #5 forceps.
5. Vannas spring scissors with 2.5 mm cutting edge.
6. Razor blades.
7. Aluminum foil cups (*see Note 1*).
8. Optimum cutting temperature (OCT) compound.
9. Dry ice (*see Note 2*).
10. Cryostat.
11. Low profile disposable cryostat blades.
12. RNase decontamination spray or wash (*see Note 3*).
13. Carl ZeissTM MembraneSlide: NF 1.0 PEN (D) (*see Note 4*).
14. Biosafety cabinet with UV lamp.
15. Paintbrush, round size 4 (3/32").

2.2 Cresyl Violet Staining

1. RNase-free disposable nitrile gloves.
2. Coplin jars.
3. Paper towels.
4. RNase-free water.
5. 70% ethanol: Prepared by mixing 7 volumes 100% ethanol to 3 volumes RNase-free water.
6. 100% ethanol.
7. 100% xylene (*see Note 5*).
8. Chemical fume hood.
9. 1% cresyl violet solution: Dissolve solid cresyl violet acetate powder at a concentration of 1% (w/v) in 50% EtOH at room temperature with agitation/stirring for several hours to overnight. Vacuum filter the staining solution to remove undissolved powder. Cresyl violet solution can be reused up to three times.
10. 0.22 μm pore size polyethersulfone vacuum filter (*see Note 6*).
11. Desiccator jar.
12. Desiccant.

**2.3 Laser Capture
Microdissection**

1. Zeiss PALM MicroBeam LCM system (*see Note 7*).
2. Zeiss AdhesiveCap 200.

**2.4 RNA Purification
and Quality Control**

1. Vortex mixer.
2. Microcentrifuge.
3. Small sample RNA purification kit (e.g., Takara NucleoSpin RNA XS kit or equivalent; *see Note 8*), including RNA purification spin column, spin column collection tubes, RA1 buffer, TCEP, membrane desalting buffer, rDNase, rDNase buffer, A2 buffer, RA3 buffer, and RNase-free water.
4. 1.5 mL nuclease-free collection tube.
5. RNA quality analysis system (e.g., Agilent 4200 TapeStation System or equivalent; *see Note 9*).

3 Methods
**3.1 Zebrafish Optic
Nerve Crush Surgery**

1. Anesthetize adult fish by immersion in Tricaine-S solution (*see Note 10*).
2. Place fish on a sponge soaked in fish system water under a dissecting microscope.
3. Using a #5 forceps, pull the right eye slightly from the orbit, and cut connective tissue and intraocular muscles with Vannas spring scissors, thereby exposing the optic nerve.
4. Crush the exposed optic nerve with a #5 forceps for 5 s such that a clear separation in the myelin is apparent with no bleeding from the ophthalmic artery.
5. Place the right eye back into the orbit. Leave the left eye intact for use as an uninjured control.
6. Place the fish into an individual tank with fresh aquatic system water to recover (*see Note 11*).
7. Allow fish to recover for 1 h before placing tanks back onto the aquatic facility system.

**3.2 Tissue
Dissection**

1. On the desired day after optic nerve crush surgery, euthanize fish by overdosing with Tricaine-S solution (*see Note 12*).
2. Dissect both eyes from the head. Using #5 forceps and Vannas spring scissors, gently pull each eye out of the orbit, and cut the connective tissue, ocular muscles, and optic nerve from dorsal to ventral to free the eye.
3. Remove the lenses by making a small cut in the cornea using a razor blade and gently applying downward pressure with forceps until the lens is forced out through the cut.

- Place each eye into 1 cm³ aluminum foil cups filled with OCT compound. These were then placed on a block of dry ice to rapidly freeze from the bottom up. The frozen eyes were stored at -80 °C for up to a month before sectioning without loss of RNA quality (*see* **Note 13**).

3.3 Cryosectioning

- Place the frozen eye into cryostat chamber and allow it to equilibrate to the temperature of the chamber (set at -20 °C) for 30 min.
- Place the number of membrane slides to be activated into a UV-illuminated biosafety cabinet for 30 min, and then place into the cryostat chamber to cool to -20 °C.
- Before sectioning, the specimen disc, blade holder, and surrounding apparatus should be cleaned with RNase decontamination spray followed by 100% ethanol.
- To mount the eye, remove the aluminum foil from the frozen tissue block. A layer of OCT media is placed around the base of the specimen disc, and the frozen block of OCT with the eye is pressed firmly in place and allowed to freeze onto the disc. The block should be oriented with dorsal side of the eye up and the ventral side closest to the specimen disc (*Fig. 1a*).
- The specimen disc containing the frozen eye is placed into the specimen head and locked into place with the anterior eye facing the blade. The block is trimmed until the black dorsal surface of the eye appears. From this point we regularly trim the top 500 μm off the top of the eye to only collect sections from the central portion of the retina (*Fig. 1b*).

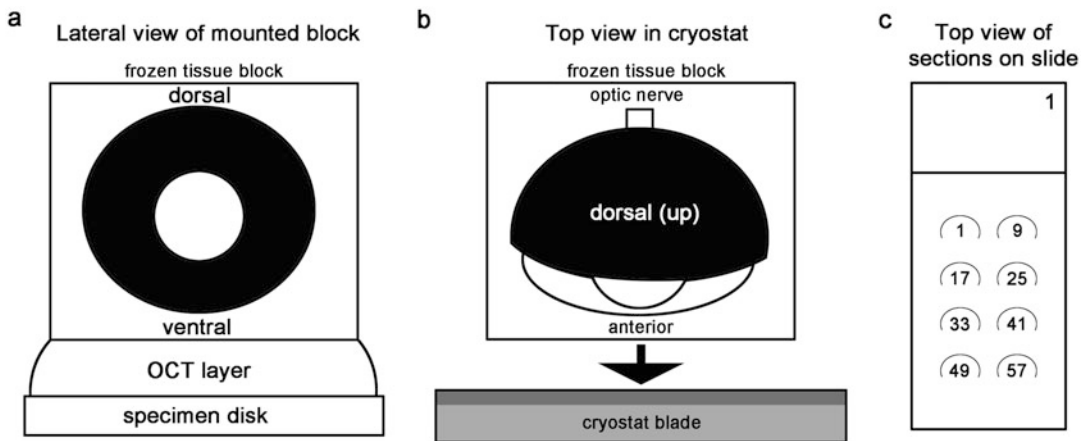


Fig. 1 Preparing the tissue block for sectioning and sampling the sections on the slide. **(a)** Mounting the frozen tissue block on the specimen disc. **(b)** Orientation of tissue to the cryostat blade during sectioning. **(c)** Tissue section sampling on the slide. Every section is mounted on consecutive slides returning to the first slide after the 8th section to evenly distribute 64 sections across 8 slides equally representing the dorsal to ventral distribution of sections. Numbers denote section numbers

6. Set the cryostat to cut 10- μ m-thick sections.
7. Cut a section using the glass anti-roll plate to prevent rolling of the sections.
8. After waiting a few seconds for the section temperature to stabilize, lift the anti-roll plate, and use a paintbrush if needed to hold the sections down on the collection plate.
9. To collect the section on the membrane slide, quickly but carefully place a pre-chilled membrane slide, membrane side down, very close to the tissue section, touching it if needed so that it adheres to the slide (*see Note 14*). Take care not to damage the membrane (*see Note 15*).
10. One section is placed onto each slide before returning to the first slide to add a second section, thereby creating an equal dorsal–ventral distribution of the retina on each slide. We commonly collect 64 sections per eye onto 8 slides (Fig. 1c).
11. Wipe the collection plate with an RNase-free wipe after every few sections. Keep the slides inside the cryostat chamber throughout the duration of sectioning.
12. Upon completion, transport slides on crushed dry ice and store at -80°C until ready for staining and LCM (*see Note 16*).

3.4 Cresyl Violet Staining

1. Prepare an RNase-free workstation in a chemical fume hood. Wear RNase-free nitrile gloves or spray RNase wash solution on gloves before beginning. Prepare the necessary solutions using RNase-free water. All solutions, except 1% cresyl violet, should be made fresh immediately before staining. All glass Coplin jars should be cleaned with RNase decontamination spray immediately before staining (*see Note 17*).
2. Obtain frozen tissue sections on membrane slides from -80°C freezer (*see Note 18*).
3. Submerge slides into 70% ethanol for 2 min at room temperature. **Steps 4–7** should also be performed at room temperature.
4. Dip slides for 30 s into filtered 1% cresyl violet solution.
5. Remove excess stain by allowing the solution to drip from slides onto a clean paper towel. This should take about 30 s.
6. Dip slides in 70% ethanol for 30 s.
7. Dip slides in 100% ethanol for 30 s.
8. Dip slides gently in xylene three times.
9. Place slides in fresh xylene for 5 min.
10. Air-dry slides for 1–2 min in fume hood before placing them in a desiccator jar filled with desiccant. Keep the slides in the desiccator jar until LCM commences (*see Note 19*).

3.5 Laser Capture Microdissection

The following instructions are a modification of a previously published protocol [10] using the PALM Laser-MicroBeam System (*see Note 7*).

1. Load a slide onto the stage while wearing RNase-free nitrile gloves.
2. Adjust the condenser at 10 \times magnification to locate the desired location to be sampled within the tissue section.
3. Select higher magnification if desired (we used 20 \times), and load the adhesive capped tube, adjusting the cap so that it hovers just slightly above the tissue section.
4. Center the laser and then outline the region of interest (ROI) within the field of view. The ROI should be as in focus as possible, as this will affect the quality of laser cutting. The size of each ROI should be big enough such that the laser does not destroy it upon cutting but small enough that it can be captured easily onto the adhesive cap (*see Note 20*).
5. Once outlined, turn on the laser and cut each area. Only clearly defined layers of cells in the GCL, INL, and ONL of the retina should be collected (Fig. 2).
6. Examine the cap to determine if its position needs to be changed because of excess tissue in the collection area or non-adhering ROIs before moving onto the next tissue section (*see Note 21*).
7. Once all ROIs are collected from a field of view, move onto the next tissue section, repeating until all the desired cell area is collected from each tissue section on the slide. Repeat this process until the desired area of interest has been captured from each tissue section from each slide.
8. Carefully remove adhesive cap tube and proceed to the RNA purification step.

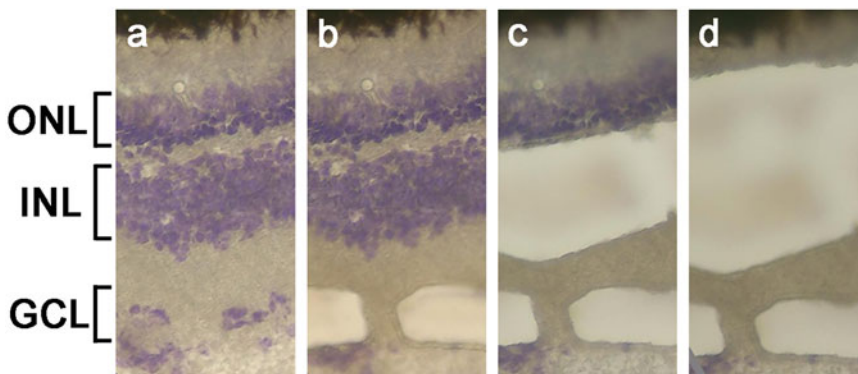


Fig. 2 LCM of defined layers of the retina. (a) Cresyl violet-stained retina section prior to LCM. (b) LCM-mediated collection of the ganglion cell layer (GCL). (c) LCM-mediated collection of the inner nuclear layer (INL). (d) LCM-mediated collection of the outer nuclear layer (ONL)

3.6 RNA Purification

In order to extract the small amounts of RNA present in the LCM sample, we describe our use of a low input RNA purification kit following the manufacturer's protocol (e.g., NucleoSpin RNA XS kit or equivalent; *see Note 22*).

1. Immediately after removing the adhesive cap tube, add 100 μL RA1 buffer plus 2 μL TCEP to the tube and close it. Leave the tube inverted at room temperature while the other samples are collected (*see Note 23*).
2. Vortex the sample(s) 2×5 s to homogenize.
3. Adjust RNA binding condition by adding 100 μL of 70% ethanol to the lysate and mix by pipetting five times. Do not filter the lysate to increase the final yield, and do not add carrier RNA since it will contaminate downstream RNA-seq.
4. Bind the RNA to the spin column by pipetting the sample into the column and centrifuging for 30 s at $11,000 \times g$.
5. Desalt the column by adding 100 μL of membrane desalting buffer to the column and centrifuging for 30 s at $11,000 \times g$.
6. Digest the contaminating DNA bound to the column using freshly prepared rDNase reaction mixture. Add 25 μL of the mixture to the column and incubate for 15 min at room temperature.
7. Wash the column by adding 100 μL of RA2 buffer to the column. Incubate for 2 min at room temperature; then centrifuge for 30 s at $11,000 \times g$.
8. Place the column into a new collection tube and add 400 μL of RA3 buffer to the column. Centrifuge for 30 s at $11,000 \times g$.
9. Discard the flow through and replace the column in the collection tube.
10. Add 200 μL of RA3 buffer to the column and centrifuge 2 min at $11,000 \times g$ to dry the membrane.
11. Place the column in a nuclease-free collection tube (1.5 mL).
12. Elute the RNA by adding 10 μL of RNase-free water to the column. Centrifuge 30 s at $11,000 \times g$.
13. Keep the purified RNA on ice and store it at -80°C .
14. RNA quantity and quality should be assessed using a spectrophotometric or electrophoretic-based system capable of measuring nanogram range samples (*see Note 24*).
15. High-quality RNA that passes quality control can now be submitted for RNA sequencing (*see Note 25*).

4 Notes

1. Aluminum foil cups are made by wrapping the foil around the bottom of an electroporation cuvette with a 1 cm² base or an object of similar size and shape. Carefully avoid punctures in the corners of the foil where OCT compound will leak out.
2. Dry ice should always be properly handled with cryo-gloves and eye protection to prevent cryoinjury.
3. RNase decontamination spray or wash is used to eliminate RNases from surfaces or containers that will touch your samples. This will prevent degradation of your RNA sample and ensure the highest-quality LCM-seq result.
4. If using an LCM system other than the Zeiss PALM Micro-Beam, this material may be different. Please refer to your system's user manual.
5. Xylene is a volatile and toxic chemical. All use should always be restricted to a chemical fume hood with proper precautions and personal protective equipment used.
6. We commonly use a tube top 50 mL vacuum filter to filter the 1% cresyl violet solution.
7. We have successfully used the Zeiss PALM MicroBeam LCM system and report the materials and methods necessary for this system here. This method can be used for other commercially available LCM systems but should be adapted according to the manufacturer's recommendations.
8. Small sample RNA purification kits are available from multiple suppliers. We chose the Takara NucleoSpin RNA XS kit since it was recommended for our downstream sample library preparation.
9. Several commercial systems are available to analyze small nanogram quantities of RNA. We have successfully used the Agilent Bioanalyzer and TapeStation systems in the past.
10. Fish should quickly (~30 s) lose their righting reflex and tip onto their side. Their gill movements should slow significantly. When they are unresponsive to tail pinch with a forceps, they are sufficiently anesthetized to proceed, usually less than 2 min in Tricaine-S solution.
11. Fish gill movement should begin as soon as they are placed in fresh fish water. If not, water can be gently squirted over the head with a transfer pipette to improve water flow over the gills to revive the fish. The animal should rapidly regain its righting ability and begin to swim normally.

12. The same Tricaine-S solution used for anesthesia can be used for euthanasia but increase the incubation time to 5 min. When the animal is unresponsive to tail pinch and gill movements have stopped, it is ready for dissection.
13. It is critical to freeze the block from the bottom up to prevent increased internal pressure and cracking. The block should be completely frozen in less than a minute.
14. Placing a gloved finger on the back of the slide beneath the location where the tissue section will be placed immediately before collecting the section onto the slide (but after cutting) helps the section adhere to the slide due to the temperature difference. Only slight melting of the tissue onto the slide should occur before the slide is placed into the -20°C cryostat chamber again.
15. Damage to the membrane on the slide allows liquid to get underneath the membrane during the staining protocol making drying difficult, if not impossible. The sample needs to be completely dry for efficient laser cutting of the membrane in the LCM step. Avoid scratching the membrane slide against the cryostat blade or cutting surface.
16. Keeping the samples frozen, ideally at -80°C or on dry ice, is key to producing highest-quality RNA following purification.
17. Make sure all RNase-washed surfaces and glassware are dry before adding staining solutions and beginning protocol.
18. Make sure to transport the slides on crushed dry ice and keep there until fixing in the 70% ethanol step.
19. Having completely dry slides is critical for efficient laser cutting of the membrane to harvest the tissue samples. Residual moisture will absorb excess heat and prevent the membrane from cutting.
20. We usually break up retinal layers into five separate fragments per field of view under the $20\times$ objective to efficiently harvest them with the laser.
21. Ensure that cut ROIs are on the adhesive cap by surveying the tissue section at a lower magnification, looking for any cut sections that may be loose on the slide. Be sure to collect all loose sections. Sections may have to be cut more than once if the section is not collected after the first cut with the laser.
22. The small sample RNA purification kit is available from multiple suppliers. We chose the Takara NucleoSpin RNA XS kit since it was recommended for our downstream sample library preparation.
23. Samples are stable for several hours at room temperature in RAI buffer plus TCEP.

24. Several commercial systems are available to analyze the quality and quantity of nanogram quantities of RNA. We have successfully used the Agilent Bioanalyzer and TapeStation systems in the past.
25. Using this protocol, we have obtained high-quality RNA (RNA integrity numbers >8) from individual eyes (~32 sections per eye). Average yields per eye are 1.3 ng from the GCL, 4.3 ng from the INL, and 2.8 ng from the ONL. These amounts are sufficient for RNA-seq following linear amplification of the sample.

Acknowledgments

Funding for this project was provided to MBV by a pilot grant from the Medical College of Wisconsin Research Affairs Committee.

References

1. Belrose JL, Prasad A, Sammons MA et al (2020) Comparative gene expression profiling between optic nerve and spinal cord injury in *Xenopus laevis* reveals a core set of genes inherent in successful regeneration of vertebrate central nervous system axons. *BMC Genomics* 21(1):540
2. Dhara SP, Rau A, Flister MJ et al (2019) Cellular reprogramming for successful CNS axon regeneration is driven by a temporally changing cast of transcription factors. *Sci Rep* 9(1):14198
3. Fuller-Carter PI, Carter KW, Anderson D et al (2015) Integrated analyses of zebrafish miRNA and mRNA expression profiles identify miR-29b and miR-223 as potential regulators of optic nerve regeneration. *BMC Genomics* 16(1):591
4. McCurley AT, Callard GV (2010) Time course analysis of gene expression patterns in zebrafish eye during optic nerve regeneration. *J Exp Neurosci* 4:17–33
5. Saul KE, Koke JR, García DM (2010) Activating transcription factor 3 (ATF3) expression in the neural retina and optic nerve of zebrafish during optic nerve regeneration. *Comp Biochem Physiol A Mol Integr Physiol* 155(2):172–182
6. Veldman MB, Bembien MA, Thompson RC et al (2007) Gene expression analysis of zebrafish retinal ganglion cells during optic nerve regeneration identifies KLF6a and KLF7a as important regulators of axon regeneration. *Dev Biol* 312(2):596–612
7. Whitworth GB, Misaghi BC, Rosenthal DM et al (2017) Translational profiling of retinal ganglion cell optic nerve regeneration in *Xenopus laevis*. *Dev Biol* 426(2):360–373
8. Emmert-Buck MR, Bonner RF, Smith PD et al (1996) Laser capture microdissection. *Science* 274(5289):998–1001
9. Macosko EZ, Basu A, Satija R et al (2015) Highly parallel genome-wide expression profiling of individual cells using nanoliter droplets. *Cell* 161(5):1202–1214
10. Lu JX, Szeto CC (2011) Gene expression using the PALM system. *Methods Mol Biol* 755:47–56



Profiling Dynamic Changes in DNA Accessibility During Axon Regeneration After Optic Nerve Crush in Adult Zebrafish

Sumona P. Dhara and Ava J. Udvardia

Abstract

A time-course series utilizing assay for transposase-accessible chromatin with high-throughput sequencing (ATAC-seq) can be used to detect changes in accessibility of DNA regulatory elements such as promoters and enhancers over the course of regeneration. This chapter describes methods for preparing ATAC-seq libraries from isolated zebrafish retinal ganglion cells (RGCs) following optic nerve crush at selected post-injury time points. These methods have been used for identifying dynamic changes in DNA accessibility that govern successful optic nerve regeneration in zebrafish. This method may be adapted to identify changes in DNA accessibility that accompany other types of insults to RGCs or to identify changes that occur over the course of development.

Key words CNS axon regeneration, Chromatin accessibility, Optic nerve regeneration, ATAC-seq, Zebrafish

1 Introduction

Adult mammals such as mice and humans have a limited ability to regenerate axonal connections between the retina and the brain after optic nerve injury. Unlike mammals, severe damage to axons in teleost fish and urodele amphibians stimulates the re-expression of regeneration-associated genes and robust axonal regeneration to fully restore visual function [1–3]. Cis-regulatory DNA elements such as promoters and enhancers, along with the trans-activating factors that bind them, play an instructive role in regulating regeneration-associated gene regulation in response to injury. Previously, purely computational approaches applied to the identification of shared *cis*-regulatory elements in mammalian peripheral neurons focused on putative transcription factor binding sites located within DNA sequences situated 1–5 kb from the transcriptional start site of axon growth-associated genes [4, 5]. Such approaches considered promoter proximal sequences an arbitrary

distance from the transcriptional start sites of genes with the assumption that they would be accessible to transcription factor binding. They also disregard the role of gene enhancers located more distal to transcriptional start sites that have been demonstrated to play prominent roles in mediating gene expression changes that accompany changes in cell state [6, 7]. ATAC-seq enables the identification of putative gene promoters and enhancers based on chromatin accessibility and overcomes both of the aforementioned complications [1].

Retinal ganglion cells (RGCs) are the sole output neurons of the eye that convey detected light information to the brain via their axons that bundle together within the optic nerve. To specifically evaluate injury-induced changes in chromatin accessibility within RGCs, we employ the transgenic zebrafish *Tg(Tru.gap43:egfp)*. Within the retina, these fish express green fluorescent protein (GFP) specifically in developing and regenerating RGCs [8]. These transgenic fish allow for the isolation of GFP-positive RGCs following optic nerve lesion at selected post-injury time points. The protocol that follows includes detailed instructions for conducting optic nerve crush on adult zebrafish, retina dissection, dissociation of retinal tissue, GFP-positive RGC isolation by fluorescence-activated cell sorting (FACS), and the subsequent preparation and quality assessment of ATAC-seq libraries.

2 Materials

2.1 Adult Optic Nerve Crush and Retina Dissection (See Note 1)

1. Wild-type zebrafish strain (*see Note 2*).
2. A transgenic reporter fish expressing a fluorescent marker in the retinal ganglion cells (RGCs) (*see Note 3*).
3. Molecular biology-grade nuclease-free water.
4. 3.5 cm polystyrene petri dishes.
5. 10 cm polystyrene petri dishes.
6. 0.2 mL DNase-/RNase-free PCR tubes.
7. Round Watchmaker's forceps.
8. #5 forceps with 0.005 mm × 0.025 mm tips × 2.
9. Micropipette 1000 µL, 10 µL.
10. Fish holder: 7 cm × 5 cm sponge that is 3 cm thick with a 4 cm 45° angle slit and placed on a 10 cm polystyrene petri dish (*see Note 4*).
11. Phosphate-buffered saline (PBS) without calcium and magnesium: 2.67 mM KCl, 1.76 mM KH₂PO₄, 136.9 mM NaCl, 8.1 mM Na₂HPO₄·7H₂O in distilled, deionized water. Adjust pH to 7.2 with 1 N NaOH.

12. Thermocycler.
13. Dissection microscope with fiber-optic lamp.
14. Tabletop centrifuge with fixed angle rotor for 1.5 mL tubes; swinging-bucket rotor for 5 mL polystyrene round bottom tubes.
15. Fishnet.
16. Recovery tank filled with fish system water.
17. Fluorescent microscope with 488 nm channel.
18. 30% Danieau solution: 17.4 mM NaCl, 0.21 mM KCl, 0.12 mM MgSO₄ (7H₂O), 0.18 mM Ca(NO₃)₂ (4H₂O), 150 mM HEPES in distilled, deionized water. Adjust pH to 7.6 with 1 N NaOH.
19. Anesthetic solution: Dissolve 0.3 g tricaine (MS222) in 600 mL 30% Danieau; adjust pH to 7.2 with sodium bicarbonate. This should be prepared fresh and pre-chilled on ice before each use.
20. Euthanasia solution: Dissolve 0.5 g tricaine (MS222) in 600 mL 30% Danieau; adjust pH to 7.2 with sodium bicarbonate.
21. Instrument sterilizer (*see Note 5*).
22. Dark chamber (*see Note 6*).

2.2 Retina Dissociation and Cell Sorting

1. Twenty-four-well polystyrene plate.
2. 5 mL polystyrene round bottom tube with cell strainer cap, sterile.
3. 5 mL polystyrene round bottom tube with snap cap, sterile.
4. Cell dissociation solution (e.g., Accumax, Sigma; *see Note 7*).
5. Quenching buffer: 20% fetal calf serum in Dulbecco's Modified Eagle Medium with Nutrient Mixture F-12 (DMEM/F12). Sterile filter the buffer through a 0.22 μm PVDF filter. Prepare the buffer fresh for each use.
6. Nutating mixer for 24-well plates or 1.5 mL tubes.
7. 5× protease inhibitor cocktail (PIC) (*see Note 8*).
8. Cell viability stain (*see Note 9*).
9. Fluorescent-activated cell sorter equipped with 100 μm nozzle (*see Note 10*).

2.3 ATAC-Seq Library Preparation and Quality Assessment

1. Cell lysis buffer: 10 mM Tris-HCl pH 8.1, 10 mM NaCl, 1.5 mM MgCl₂, and 0.5% IGEPAL CA-630, 1× PIC in 50 mL nuclease-free water. Add PIC before each use and store at 4 °C for up to 48 h. Store the cell lysis buffer without PIC at RT for up to 3 months.

2. Nuclear lysis buffer: 50 mM Tris–HCl pH 8.1, 5 mM EDTA, 1% SDS, 1× PIC in 50 mL nuclease-free water. Add PIC before each use and store at 4 °C for up to 48 h. Store the nuclear lysis buffer without PIC at RT for up to 3 months.
3. DNA elution buffer: 10 mM Tris–HCl pH 8.5, 0.1 mM EDTA in nuclease-free water.
4. 2× tagmentation buffer (e.g., Illumina; *see Note 11*).
5. Tn5 transposase enzyme 1 U/μL (e.g., Illumina; *see Note 11*).
6. DNA clean and concentrator kit (*see Note 12*).
7. 2× SYBR Green PCR Master Mix.
8. ATAC-seq primers (*see Note 13*).
9. PCR cleanup kit (*see Note 14*).
10. Clean, dry, lint-free lab wipe (e.g., Kimwipes).
11. Fluorescent-based double-stranded DNA quantification kit (e.g., Invitrogen Qubit kit; *see Note 15*).
12. Kit for chip-based capillary electrophoresis DNA analysis to detect 5–500 pg/μL concentrations of DNA (e.g., Agilent High Sensitivity DNA Assay; *see Note 16*).
13. Real-time PCR detection system (e.g., BioRad CFX96 Touch).
14. Microvolume spectrophotometer (e.g., Nanodrop ND2000).
15. Fluorometric quantitation platform (e.g., Qubit 2.0).
16. Chip-based capillary electrophoresis platform (e.g., Agilent 2100 Bioanalyzer).

3 Method

3.1 *Adult Optic Nerve Crush*

1. Presoak the fish holder in the chilled anesthetic solution and place it on a 10 cm petri dish.
2. Use the fishnet to transfer the adult fish from the tank into the anesthetic solution until the fish is motionless and does not respond to touch (*see Note 17*).
3. Position the anesthetized fish on the anesthetic-soaked fish holder so that the head and eyes are accessible but the rest of the body is secure within the slit and the left eye is angled up under a dissecting microscope (*see Note 18* and Fig. 1b).
4. Under the dissecting microscope, gently move the superfine forceps between the eyeball and socket to loosen the connective tissue.
5. Gently lift the eyeball out of the socket and expose the optic nerve with Watchmaker's round forceps.

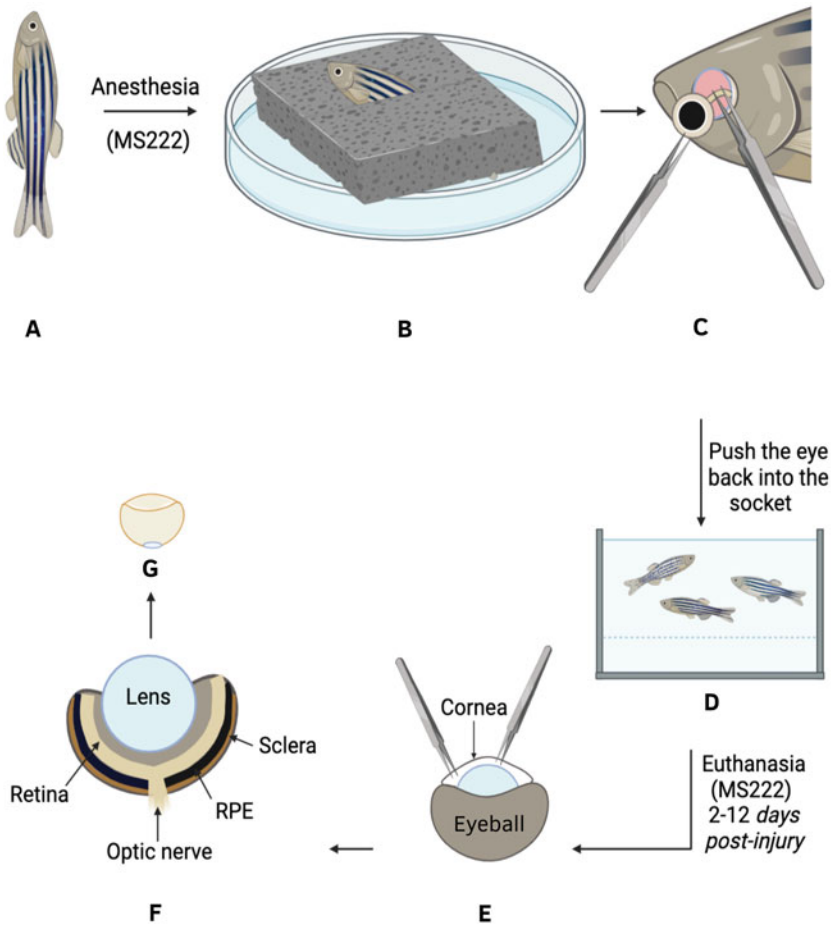


Fig. 1 Schematic of optic nerve crush and retina dissection of adult zebrafish. **(a)** Adult Fish. **(b)** Place the fish in pre-soaked fish holder with the head and left eye. **(c)** Gently lift the eyeball out of the socket & crush the left optic nerve. **(d)** Return the fish in recovery tank. **(e)** Dissect out the eyeball from the socket & puncture the cornea. **(f)** Peel away the sclera & RPE, remove the lens

6. Using light pressure, crush the optic nerve directly behind the orbit by pinching it between the superfine forceps for 10 s, taking care to avoid the ophthalmic artery (*see* Fig. 1c and Note 19).
7. Gently use the flat edge of your closed forceps to push the eye back into the socket.
8. Revive the fish by immediately returning it to a recovery tank containing fish system water (*see* Note 20 and Fig. 1d). Monitor the fish's swimming and eating behavior during the post-injury period (*see* Note 21).
9. Fish are euthanized between 2 and 12 days post-injury (dpi) to harvest retinas for RGC isolation using FACS (*see* Note 22 and Fig. 2).

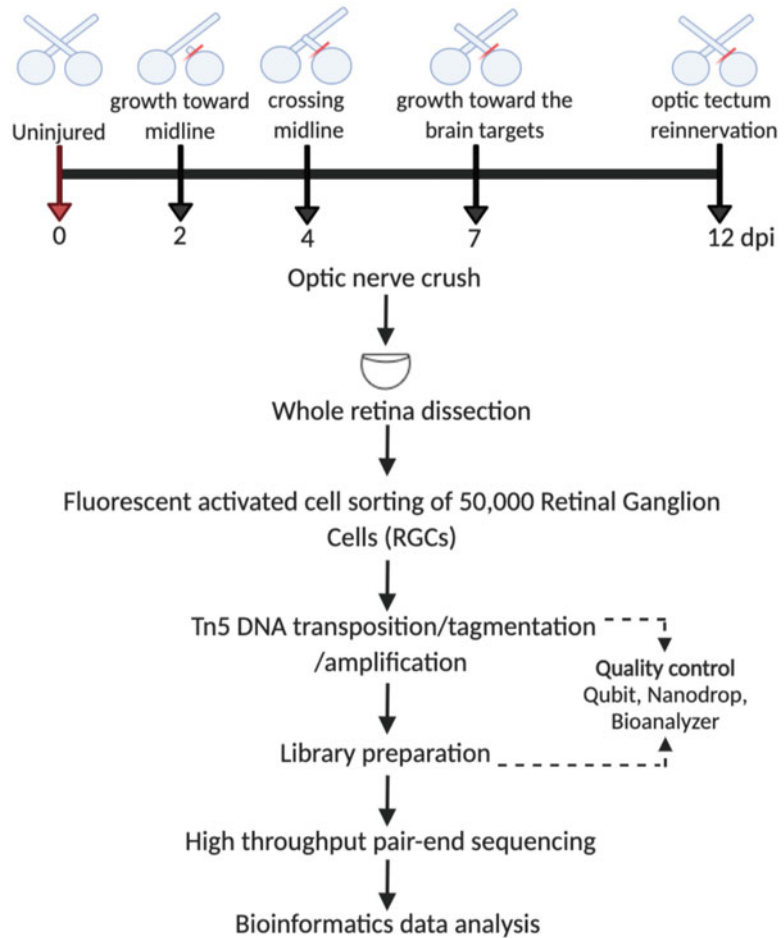


Fig. 2 Workflow of ATAC-seq library preparation to assess changes in chromatin accessibility over the course of optic nerve regeneration in zebrafish. Chromatin extraction from nuclei isolated from purified RGCs of *Tg (Tru.gap43:egfp)* fish after optic nerve injury. For constructing ATAC-seq libraries, 50,000 RGCs were isolated using fluorescent-activated cell sorting (FACS). The transposition and library preparation were performed using Nextera Tn5 transposase kit. Libraries were sequenced at UWBC—Madison genomic center. Three biological replicates were sequenced per time point (except for 7 dpi, one replicate sample was below the cutoff criteria and therefore omitted from full sequencing and subsequent data analysis)

3.2 Retina Dissection

1. At least 2 h prior to dissection, place the tank of operated fish in the dark chamber (*see Note 23*).
2. Place the fish in euthanasia solution until the fish stops moving its gills (*see Note 24*).
3. Prior to retina dissection, place the fish on a glass slide, and quickly examine the left and right eyes of the surgery fish under fluorescence microscope with 488 nm channel to verify GFP expression in the operated eye (*see Note 25*).

4. Once fully euthanized, place the fish onto an anesthetic-soaked fish holder under the dissecting microscope with the left eye facing upward.
5. Release the connective tissue surrounding the eyeball and remove the eye from the socket with a superfine forceps.
6. Disconnect the eye from the optic nerve by severing it with a Watchmaker's forceps, and transfer the eye to a 3.5 cm petri dish filled with ice-cold PBS.
7. Using the superfine forceps, puncture the cornea to expose the lens (Fig. 1e).
8. Peel away the sclera, the retinal pigmented epithelium (RPE), and other supporting tissues around the eyecup (Fig. 1f).
9. Remove the lens from the retina by carefully pinching it out from the retinal cup and discard it.
10. Transfer the translucent retina cup to a second 3.5 cm petri dish filled with ice-cold PBS to rinse off any remaining vitreous fluid (Fig. 1g).
11. Repeat **steps 4–9** for the right eye which will serve as the uninjured control (label accordingly).
12. Keep the dissected retinas on ice-cold PBS until proceeding to dissociation step (*see Note 26*).

3.3 Retina Dissociation into Single-Cell Suspensions

1. Transfer each dissected retina into one well of a 24-well plate filled with 500 μ L cell dissociation solution.
2. Gently rock on a nutating mixer for 70 min at room temperature.
3. After 70 min in cell dissociation solution, add 500 μ L quenching buffer.
4. Gently triturate samples with a 1000 μ L micropipette at least ten times while avoiding foaming (*see Note 27*).
5. Remove larger, undigested tissue fragments with a 10 μ L micropipette (*see Note 28*).
6. Transfer the cell suspension to a 1.5 mL tube and avoid foaming.
7. Centrifuge the cell suspension in a fixed angle rotor at 300 $\times g$ for 3 min at 4 $^{\circ}$ C.
8. Pipette off and discard the supernatant without disturbing the cell pellet.
9. Resuspend the cell pellet in 500 μ L of fresh quenching buffer.
10. Keep the samples on ice until you have six retinas ready to pool.
11. Pool the cell suspensions from six retinas by passing the suspension through a 5 mL polystyrene round bottom tube with a cell strainer cap. Repeat for each of the injury time points and uninjured control.

3.4 Fluorescence-Activated Cell Sorting (FACS) of GFP-Positive RGCs

1. Centrifuge in a swinging-bucket rotor at $200\times g$ for 3 min at 4°C . Remove the quenching buffer supernatant with a pipette to a final volume of $\sim 250\ \mu\text{L}$. Keep the tube on ice until you are ready for cell sorting.
2. Add $10\ \mu\text{L}$ of diluted cell viability stain to each sample prior to FACS analysis.
3. Begin the FACS session by analyzing dissociated retinal cells from wild-type fish (EK) to set up the gates (it is not necessary to collect cells used for this step). Create an experiment file, set wild-type sample on the sample station, and run.
4. Plot forward scatter-height (FSC-H) vs. FL2-H (Fig. 3a) and set the gate for live cells using the freehand gating tool against cell viability stain as Gate 1.

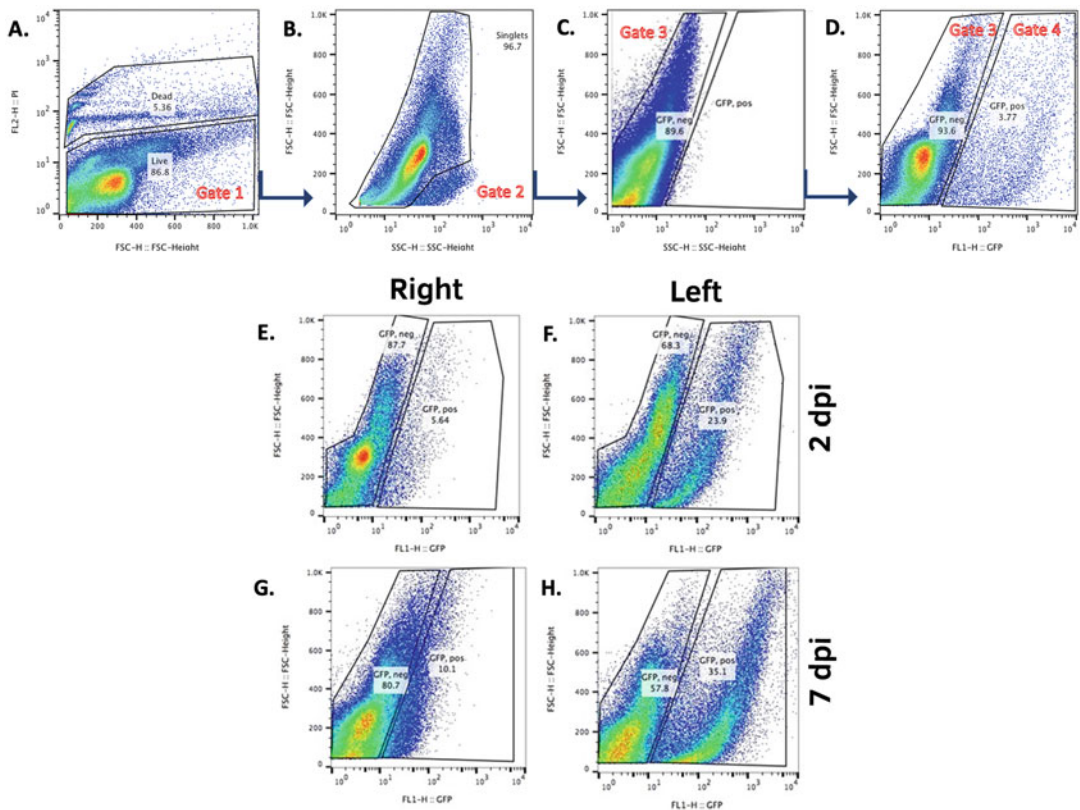


Fig. 3 Gating strategy for GFP+ retinal ganglion cells (RGCs) represented by flow cytometry plots. Gates were set based on negative samples (EK). Gating strategies were defined such as cell size (forward scatter, FSC-H) (a) vs. granularity (side scatter, SSC-A) (b) to exclude cellular debris and clumps or doublets of cells that may give erroneous fluorescent readings. Fluorescence scatter is used to separate cells according to the GFP fluorescence intensity by setting Gate 3 for GFP-negative (c) and Gate 4 for GFP-positive cell populations (d). The resultant plots show a positive correlation between fluorescence intensity of GFP+ retinal ganglion cells and post-injury time points. This is illustrated by injury-induced GFP expression at 0 days post-injury (dpi) from the uninjured right eye control (e, g) and injured left eyes from the same fish at 2 dpi and 7 dpi, respectively (f, h)

5. Set Gate 2 (Fig. 3b) to exclude cell aggregates or doublets and include single-cell populations in the side scatter-height (SSC-H) plot.
6. Set Gate 3 to exclude cells that are negative for GFP (Fig. 3c).
7. Place the dissociated cell suspension from the uninjured control (0 dpi) and/or post-injury time points on the sample station and run. Set Gate 4 to include GFP-positive, live RGCs (Fig. 3d).
8. After setting up the gates, put 4 mL of cold quenching buffer into the collection tube and place it on the sample collection port.
9. Collect sorted cells from GFP-positive fractions into the collection tube (*see* representative data in Fig. 3e–h and **Note 29**).
10. Perform “Clean Flow Cell” procedure three times between each sample (*see* **Note 30**).
11. Transfer the collection tube with at least 50,000 sorted GFP-positive cells on ice. Proceed immediately to nuclear isolation.

3.5 Nuclear Isolation and Transposase Reaction

1. Pellet the collected cells in a swinging-bucket rotor of a centrifuge at $200\times g$ for 3 min at 4 °C. Carefully remove the supernatant with a pipette and discard.
2. Resuspend the pellet in 100 μ L of ice-cold cell lysis buffer and transfer to a 1.5 mL microcentrifuge tube.
3. Microcentrifuge samples at $300\times g$ for 3 min at 4 °C.
4. Remove supernatant with a micropipette and resuspend in 50 μ L ice-cold nuclear lysis buffer.
5. Microcentrifuge immediately at $500\times g$ for 10 min at 4 °C and discard the supernatant. Keep the remaining nuclear pellet on ice while you prepare the transposition reaction mix.
6. Gently resuspend the cell pellet in transposition reaction mix: 25 μ L $2\times$ tagmentation buffer, 2.5 μ L Tn5 transposase enzyme, and 22.5 μ L nuclease-free water.
7. Transfer the contents to 0.2 mL PCR tubes and incubate the transposition reaction at 37 °C for 30 min in a thermocycler (*see* **Note 31**).
8. Purify the transposed DNA using a clean and concentrator kit (Zymo).

3.5.1 Transposed DNA Cleanup

1. Mix the transposed DNA from **step 8** with 5 volumes of binding buffer in a 1.5 mL tube. Proceed to **step 2**.
2. Transfer the sample to the center of a spin column (supplied by the manufacturer) without touching the walls of the column.

3. Microcentrifuge at $10,000\times g$ for 1 min at room temperature.
4. Wash twice with wash buffer by spinning at $10,000\times g$ for 1 min at room temperature and discard the flow-through.
5. Add 15 μL DNA elution buffer to the center of the column; allow to sit at room temperature for 5 min.
6. Microcentrifuge at $10,000\times g$ for 30 s at room temperature.
7. Store transposed samples at $-20\text{ }^{\circ}\text{C}$ for up to 6 months or proceed directly to library amplification (*see* Subheading 3.6).

3.6 Library Amplification

1. Set up amplification reactions in DNase-/RNase-free 0.2 mL tubes.
2. Library amplification reaction conditions are as follows (50 μL final reaction volume): 25 μL 2 \times SYBR Green PCR Master Mix, 10 μL nuclease-free water, 2.5 μL Universal Primer Ad1 (25 μM), 2.5 μL barcoded customized PCR primer (*see* Table 1 [1]) (25 μM), and 10 μL transposed DNA from Subheading 3.5.1, **step 7**.
3. Partially amplify ATAC-seq libraries using a thermocycler (5 min at $72\text{ }^{\circ}\text{C}$, 30 s at $98\text{ }^{\circ}\text{C}$ followed by four cycles of 10 s at $98\text{ }^{\circ}\text{C}/30\text{ s}$ at $63\text{ }^{\circ}\text{C}/1\text{ min}$ at $72\text{ }^{\circ}\text{C}$, and final hold at $4\text{ }^{\circ}\text{C}$).
4. Set up a side reaction using 5 μL of partially amplified library from **step 3** to perform real-time PCR to determine how many additional PCR cycles are needed.
5. Perform real-time PCR (10 μL reaction volume): 5.5 μL 2 \times SYBR Green Master Mix, 0.25 μL Universal Primer Ad1 (Nextera) (25 μM), 0.25 μL barcoded customized PCR primer (*see* Table 1 [1]) (25 μM), and 5 μL 4 \times partially amplified transposed DNA from **step 4**.
6. The transposed DNA samples can be quantified using a real-time PCR detection system (30 s at $98\text{ }^{\circ}\text{C}$ followed by 19 cycles of 10 s at $98\text{ }^{\circ}\text{C}/30\text{ s}$ at $63\text{ }^{\circ}\text{C}/1\text{ min}$ at $72\text{ }^{\circ}\text{C}$, and final hold at $4\text{ }^{\circ}\text{C}$).
7. In order to prevent overamplification of samples, calculate the number of additional PCR cycles needed for each sample, by calculating the number of cycles that corresponds to $\frac{1}{4}$ maximum fluorescent intensity (round to the nearest cycle number) (*see* Fig. 4 and **Note 32**).
8. Continue amplification on the remaining 45 μL of the partially amplified library from **step 3** for the appropriate number (n) of cycles.
9. Purify the fully amplified library using a PCR cleanup kit (QIAquick).

Table 1
Sequences for custom primers used in generating ATAC-seq libraries for multiplex short-read sequencing

Primer 2 options	Sequence	Index
1	CAAGCAGAAGACGGCATAACGAGATTGCCTTAGTCTCG TGGGCTCGGAGATGT	Ad2.1_TAAGGCGA
2	CAAGCAGAAGACGGCATAACGAGATTTCTGCCTGTCTCG TGGGCTCGGAGATGT	Ad2.3_AGGCAGAA
3	CAAGCAGAAGACGGCATAACGAGATGTAGAGAGGTCTCG TGGGCTCGGAGATGT	Ad2.7_CTCTCTAC
4	CAAGCAGAAGACGGCATAACGAGATCAGCCTCGGTCTCG TGGGCTCGGAGATGT	Ad2.10_CGAGGCTG
5	CAAGCAGAAGACGGCATAACGAGATTGCCTCTTGTCTCG TGGGCTCGGAGATGT	Ad2.11_AAGAGGCA
6	CAAGCAGAAGACGGCATAACGAGATTCCTCTACGTCTCG TGGGCTCGGAGATGT	Ad2.12_GTAGAGGA
7	CAAGCAGAAGACGGCATAACGAGATGCTCAGGAGTCTCG TGGGCTCGGAGATGT	Ad2.4_TCCTGAGC
8	CAAGCAGAAGACGGCATAACGAGATAGGAGTCCGTCTCG TGGGCTCGGAGATGT	Ad2.5_GGACTCCT
9	CAAGCAGAAGACGGCATAACGAGATCATGCCTAGTCTCG TGGGCTCGGAGATGT	Ad2.6_TAGGCATG
10	CAAGCAGAAGACGGCATAACGAGATCCTCTCTGGTCTCG TGGGCTCGGAGATGT	Ad2.8_CAGAGAGG
11	CAAGCAGAAGACGGCATAACGAGATAGCGTAGCGTCTCG TGGGCTCGGAGATGT	Ad2.9_GCTACGCT
12	CAAGCAGAAGACGGCATAACGAGATATCACGACGTCTCG TGGGCTCGGAGATGT	Ad2.13_GTCGTGAT
13	CAAGCAGAAGACGGCATAACGAGATACAGTGGTGTCTCG TGGGCTCGGAGATGT	Ad2.14_ACCACTGT
14	CAAGCAGAAGACGGCATAACGAGATCAGATCCAGTCTCG TGGGCTCGGAGATGT	Ad2.15_TGGATCTG

3.6.1 ATAC-Seq Library Cleanup

1. Mix the amplified library with 5 volumes of the Buffer PB and transfer it in the provided silica membrane-based column.
2. Microcentrifuge at $10,000\times g$ for 1 min at room temperature and discard the flow-through.
3. Add 25 μL DNA elution buffer to the center of the column; there is dead volume of 2 μL ; adjust accordingly.
4. Allow to stand at room temperature for 1 min.

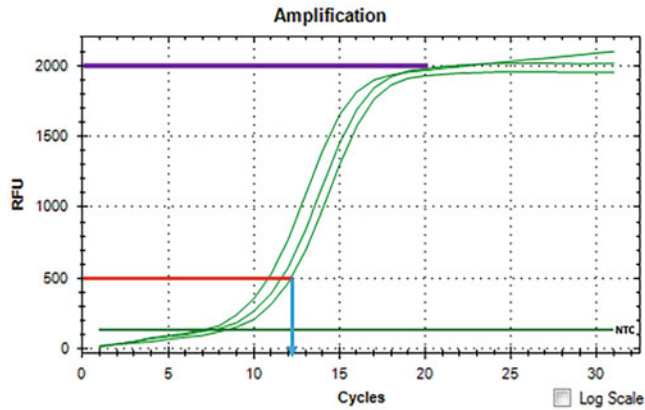


Fig. 4 Calculation of the number of cycles needed for ATAC-seq library amplification. qPCR amplification curves for three different ATAC-seq libraries are shown in green. A non-template control (NTC) is shown as the lower green line. The purple line indicates maximum fluorescence (2000 RFU), the red line indicates one 1/4 fluorescence ($2000/4 = 500$), and the blue line indicates the number of cycles. In this example, the sample furthest to the right underwent 12 additional cycles. X-axis, cycle number. Y-axis, relative fluorescence units (RFU)

5. Microcentrifuge at $10,000\times g$ for 1 min at room temperature.
6. Aliquot 3 μL of the purified ATAC-seq library to use for quality assessment (Subheading 3.7).
7. Store the remainder of the purified ATAC-seq library at -80°C until ready for sequencing.

3.7 Library Quality Control

3.7.1 NanoDrop Directions

1. Determine sample purity by measuring the A_{260}/A_{280} of the samples on a microvolume spectrophotometer (*see Note 33*).
1. Clean the upper and lower surfaces of the pedestal of microvolume spectrophotometer with nuclease-free water on a clean, dry, lint-free lab wipe.
2. Open the NanoDrop software and select the Nucleic Acid application. Use a 10 μL micropipette to perform a blank measurement by dispensing 1 μL of DNA elution buffer onto the lower optical pedestal surface. Lower the lever arm and select "Blank" in the Nucleic Acid application.
3. Clean both optical surfaces with a clean, dry, lint-free lab wipe after blank measurement.
4. Dispense 1 μL of purified ATAC-seq library sample from Subheading 3.6.1, step 6, onto the lower optical pedestal.

5. Close the lever arm and select “Measure” in the application software. The software automatically calculates the DNA concentration and purity ratios with a spectral image to assess sample quality.
6. Assess the total DNA concentration of ATAC libraries on a fluorometric quantitation platform (*see Note 34*).

3.7.2 Fluorometric Quantitation Platform Directions

1. Set up the required number of Qubit assay tubes for samples and two standards.
2. Prepare the Qubit working solution by diluting the Qubit dsDNA HS reagent in Qubit buffer (1:2).
3. Add Qubit working solution to each assay and standard tube.
4. Add the corresponding volume of samples and standard DNA to make the final volume 200 μ L.
5. Mix by vortexing and incubate at room temperature for 2 min.
6. Read the standards to calibrate the fluorometric quantitation platform (Qubit 2.0) followed by reading the samples.
7. Assess the nucleosomal laddering using a chip-based capillary electrophoresis platform (*see Note 35*).

3.7.3 Size Selection Using Chip-Based Capillary Electrophoresis Platform Directions

1. Briefly, mix the gel–dye mix by adding the dye concentrate to gel matrix.
2. Put 9 μ L of the gel–dye mix into the marked wells of (DNA) chip placed on a priming station (supplier provided).
3. Pipette the marker in sample and ladder wells followed by the addition of HS DNA ladder.
4. Finally, add 1 μ L of sample in the wells.
5. Vortex for 1 min and run the chip on Agilent 2100 platform.
6. Use the libraries with appropriate nucleosomal patterning and electropherogram trace for high-throughput sequencing (*see representative result, Fig. 5*).
7. Good-quality samples are ready for sending out to a sequencing center.
8. Estimate the sequencing depth by running a small-scale MiSeq run, and omit any samples that were below the cutoff criteria before running the full-genome sequencing.
9. Each remaining indexed library is subsequently sequenced on four lanes of the Illumina HiSeq2000 device with pair-end 50 bp sequencing to obtain approximately 25 million reads/sample.

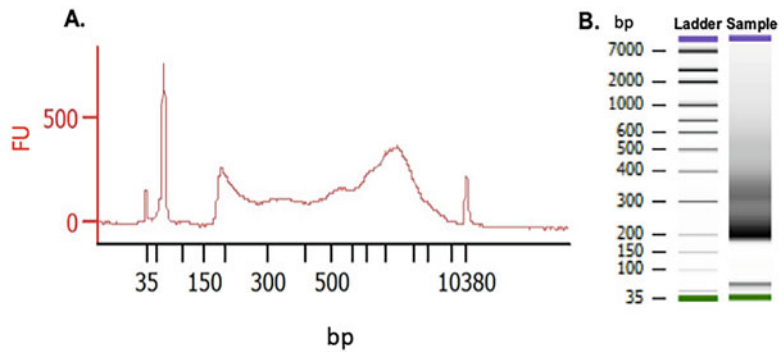


Fig. 5 An ideal ATAC-seq library quality analysis obtained with Bioanalyzer. (a) Electropherogram trace. (b) Nucleosomal patterning. The band sizes correspond to the expected nucleosomal pattern (200 bp) obtained by chromatin tagmentation of regenerating RGCs. *FU* fluorescence units, *bp* base pair

4 Notes

1. Use detergent- and bleach-free beakers for making solutions that encounter zebrafish, i.e., soap should never be used on any zebrafish equipment.
2. We use the *Ekkwill* (EK) wild-type fish. Typically, two (uninjured/naïve) retinas from one fish are used to set the gates on the cell sorter.
3. This method can be used for any transgenic animal. Here, we use the transgenic strain *Tg(Tru.gap43:egfp)* that expresses green fluorescent protein (GFP) under the regulation of the fugu GAP-43 promoter/enhancer in the RGCs in the EK background. We use 6 retinas from 6 transgenic animals (1 injured eye/fish) for a post-injury time point to acquire 50,000 cells for preparation of ATAC-seq libraries.
4. We use spongy packing material of medium stiffness rather than sponges used for cleaning, which may be impregnated with detergents. The sponge should be stiff enough to firmly hold the fish in place without crushing it. The sponge should be thoroughly rinsed with deionized water and autoclave in a 13 × 25 cm sterilization pouch.
5. Use heat for sterilizing forceps in between surgeries on different animals to avoid any cross-contamination between the animals. Alternatively, have a pair of autoclaved forceps for each animal. We use the BactiZapper MicroSterilizer (Benchmark Scientific); however, several options exist for small instrument heat sterilization. We set the BactiZapper to 400 °F for 10 min prior to starting the surgeries. Forceps are placed in the cylindrical sterilization area for 5 s and then placed on a prepared sterile area to cool for 10 s before use.

6. A light-tight inverted cardboard box placed over the fish tank serves as the dark chamber.
7. There are several commercially available cell dissociation solutions that may be used to dissociate dissected retinas to a single-cell state for subsequent fluorescence-activated cell sorting (FACS). The volume of dissociation solution and dissociation times described in this protocol were optimized using Accumax (Sigma). We conducted a series of retina dissociations varying the volume of dissociation solution and the incubation time. We analyzed cell dissociation under the different conditions using flow cytometry to determine the conditions that maximized single-cell suspension in the shortest period of time while minimizing the rate of cell death. We recommend similarly optimizing the dissociation parameters for the dissociation solution of your choice.
8. We use a commercially available protease inhibitor cocktail, Pierce™ Protease Inhibitor Tablets, EDTA-free (ThermoFisher A32965) containing aprotinin, bestatin, E64, leupeptin, and pepstatin A. To make a 5× solution, dissolve one tablet in 10 mL distilled, deionized water and vortex intermittently. Store 1 mL aliquots of the 5× PIC at −20 °C. Dilute 5× PIC in cell lysis and nuclear lysis buffer to make a final concentration of 1×.
9. Because cell dissociation can damage cells, we use a fluorescent stain that cannot enter live cells, but easily permeates compromised cells. This allows us to gate on the live cells and avoid dead or dying cells during the cell sorting steps. There are many fluorescent counterstains that are impermeable to live cells that can be used. We use SYTOX Green nucleic acid stain, 5 mM in DMSO (ThermoFisher) diluted 1/80 in quenching buffer.
10. The optimal nozzle size may differ depending on the type of cells you are sorting. We tested the 30, 70, and 100 μm nozzles on the Becton Dickinson FACS Aria™ III sorter and determined that the best cell viability was achieved using the 100 μm nozzle.
11. 2× tagmentation buffer is provided with the Tn5 transposase enzyme and is available through multiple suppliers. Our experience is with the Nextera DNA Library Prep Kit (FC-121-1030).
12. Kits for purifying and concentrating microscale DNA samples are available through a variety of suppliers. This protocol is written based on our experience with the Zymo Chromatin Immunoprecipitation (ChIP) DNA Clean & Concentrator (D5201). Alternatively, you may use standard method of phenol–chloroform extraction with ethanol precipitation.

13. A primer Ad1: AATGATACGGCGACCACCGAGATCTA CACTCGTCGGCAGCGTCAGATGTG along with customized PCR indexed primer is used for subsequent multiplex sequencing (*see* Table 1). Care should be taken to ensure that each sample is indexed appropriately for multiplex sequencing. The indexing strategy includes hyperactive (Tn5) transposase enzyme that catalyzes in vitro DNA fragmentation and adaptor insertion simultaneously of Primer 1 and any one of the available Primer 2 per sample. This unique dual indexing enables running multiple samples across four lanes of Illumina sequencing chip and post-sequencing deconvolution.
14. Kits for purifying amplified PCR samples are available through a variety of suppliers. This protocol is written based on our experience with the QIAquick PCR Purification Kit.
15. Kits optimized for quantifying double-stranded (ds) DNA samples using fluorometric quantitation platform (e.g., Qubit 2.0) are available through a variety of suppliers (e.g., Lumiprobe QuDye assay kit, Invitrogen Qubit kit). Two measurement ranges of the DNA quantification kits include broad range (100 pg/ μ L to 1000 ng/ μ L) and high sensitive (HS) range (10 pg/uL to 100 ng/uL). This protocol is written based on our experience with the Invitrogen Qubit dsDNA HS kit measuring DNA concentration of the prepared ATAC-seq libraries.
16. A proprietary kit for the separation-based sizing and quantification of dsDNA using the chip-based capillary electrophoresis platform (e.g., Agilent 2100 Bioanalyzer) uses Agilent DNA kits and reagents. Depending on the quantification and size range, the Bioanalyzer DNA kits are available in two different varieties, for example, DNA 12000 kit (25–50 ng/ μ L sensitivity, size range 100–12,000 bp) and DNA HS kit (0.5–4 ng/ μ L sensitivity, 50–7000 bp size range). This protocol is written based on our experience with the Agilent HS DNA kit.
17. Be attentive after putting the fish in anesthesia solution; fish not responding to touch happens quickly, approximately within 15 s. Prolonged exposure to anesthesia can result in increased recovery time or death.
18. To standardize our procedure, we always perform surgeries on the left eye. The damage is done unilaterally leaving the right nerve as a naïve control. Optic nerve crush of both eyes may be possible if the procedure is approved by your Institutional Animal Care and Use Committee (IACUC) guidelines and regulations.
19. Optic nerve crush with the superfine forceps results in breaking the axonal connection within the nerve without disrupting the meningeal nerve sheath.

20. Fish normally start swimming within a few seconds upon their return to water. Fish that do not immediately revive upon returning to the water will be aided by irrigating their gills with system water using a transfer pipette.
21. Observe fish to ensure they are swimming properly before their tanks are returned to the recirculating rack system. Any fish that show eye bleeding, gill inflammation, or erratic swimming patterns during the post-surgery observation period are sacrificed promptly. Subsequently monitor the fish daily until the experiment is terminated.
22. You may use the following regeneration timeline in choosing time points. At 2 dpi, regenerating axons have crossed the original site of injury. At 4 dpi, regenerating axons are crossing the chiasm. At 7 dpi, regenerating axons have reached the optic tectum. At 12 dpi, regenerating axons are undergoing synaptogenesis.
23. Dark adaptation reduces the interaction between RPE and photoreceptor cells, thereby facilitating the easy removal of the RPE from the retina.
24. Overdose with tricaine (MS222) by prolonged immersion in the euthanasia solution for at least 10 min. Following cessation of opercular movement, dissect out the eye, and dispose of fish carcasses in accordance with the requirements of handling and euthanizing animals of the institutional ethics committee of your respective research institute.
25. When using *Tg(Tru.gap43:egfp)*, GFP is robustly induced in response to optic nerve injury and can be easily visualized through the lens of intact animals. Bright green fluorescence can be observed in operated eyes compared to naïve eyes, making this a quick verification step for optic nerve injury prior to retina dissection. Discard any animals that do not display induced GFP expression in the left eye compared to the right eye. This step is only applicable when using transgenic strains like *Tg(Tru.gap43:egfp)* in which the GFP fluorescence is induced upon regeneration and not in animals that display constitutive GFP expression in RGCs.
26. We try to minimize the time between retina dissection and cell dissociation by moving samples to the dissociation steps after dissecting retinas from three fish. It takes us less than 2 min to dissect out three retinas from left injured eyes and three retinas from right uninjured eyes. We then move all six retinas to the dissociation steps (*see* Subheading 3.3) before dissecting retinas from the next three fish.
27. Visualize the pieces of retina under a dissecting microscope while pipetting up and down with a 1000 μ L pipette set to 500 μ L.

28. Take care to only remove the undigested tissue and not the solution with dissociated cells.
29. A typical sort of a 250 μL sample takes 10–15 min, thereby limiting the time during which transcriptional changes in the isolated cells could occur in the nuclei.
30. Between samples, we typically perform a quick cleaning of the flow cell with distilled water. This clears the fluidics lines and helps decrease the occurrence of clogs during sample sorting.
31. Disable the lid heating. Preheat the block and pause it until you are ready to load the transposed samples.
32. If two samples have similar cycle threshold (Ct) values but differ in fluorescent intensities, calculate the cycle number using the sample with lower fluorescent intensity.
33. Purity can be determined by the A260/A280 ratio. A ratio of ≥ 1.8 is generally acceptable.
34. Typically, a pool of six retinas yields 10–25 ng/ μL transposed DNA.
35. An Agilent Bioanalyzer or similar instrument can be used to check the size and integrity. Alternatively, perform gel-based size selection if chip-based electrophoresis platform is unavailable.

References

1. Buenrostro JD, Wu B, Chang HY, Greenleaf WJ (2015) ATAC-seq: a method for assaying chromatin accessibility genome-wide. *Curr Protoc Mol Biol* 109:21 29 21–21 29 29. <https://doi.org/10.1002/0471142727.mb2129s109>
2. Dhara SP, Rau A, Flister MJ, Recka NM, Laiosa MD, Auer PL, Udvadia AJ (2019) Cellular reprogramming for successful CNS axon regeneration is driven by a temporally changing cast of transcription factors. *Sci Rep* 9(1):14198. <https://doi.org/10.1038/s41598-019-50485-6>
3. Whitworth GB, Misaghi BC, Rosenthal DM, Mills EA, Heinen DJ, Watson AH, Ives CW, Ali SH, Bezold K, Marsh-Armstrong N, Watson FL (2017) Translational profiling of retinal ganglion cell optic nerve regeneration in *Xenopus laevis*. *Dev Biol* 426(2):360–373. <https://doi.org/10.1016/j.ydbio.2016.06.003>
4. Chandran V, Coppola G, Nawabi H, Omura T, Versano R, Huebner EA, Zhang A, Costigan M, Yekkirala A, Barrett L, Blesch A, Michaelovski I, Davis-Turak J, Gao F, Langfelder P, Horvath S, He Z, Benowitz L, Fainzilber M, Tuszyński M, Woolf CJ, Geschwind DH (2016) A systems-level analysis of the peripheral nerve intrinsic axonal growth program. *Neuron* 89(5):956–970. <https://doi.org/10.1016/j.neuron.2016.01.034>
5. Michaelovski I, Segal-Ruder Y, Rozenbaum M, Medzihradzky KF, Shalem O, Coppola G, Horn-Saban S, Ben-Yaakov K, Dagan SY, Rishal I, Geschwind DH, Pilpel Y, Burlingame AL, Fainzilber M (2010) Signaling to transcription networks in the neuronal retrograde injury response. *Sci Signal* 3(130):ra53. <https://doi.org/10.1126/scisignal.2000952>
6. Frank CL, Liu F, Wijayatunge R, Song L, Biegler MT, Yang MG, Vockley CM, Safi A, Gersbach CA, Crawford GE, West AE (2015) Regulation of chromatin accessibility and Zic binding at enhancers in the developing cerebellum. *Nat Neurosci* 18(5):647–656. <https://doi.org/10.1038/nn.3995>
7. Velasco S, Ibrahim MM, Kakumanu A, Garipler G, Aydin B, Al-Sayegh MA, Hirsekorn A, Abdul-Rahman F, Satija R, Ohler U, Mahony S, Mazzone EO (2017) A

multi-step transcriptional and chromatin state cascade underlies motor neuron programming from embryonic stem cells. *Cell Stem Cell* 20(2):205–217 e208. <https://doi.org/10.1016/j.stem.2016.11.006>

8. Udvardia AJ (2008) 3.6 kb genomic sequence from *Takifugu* capable of promoting axon growth-associated gene expression in developing and regenerating zebrafish neurons. *Gene Expr Patterns* 8(6):382–388. <https://doi.org/10.1016/j.gep.2008.05.002>



Quantitative Proteomics of Nervous System Regeneration: From Sample Preparation to Functional Data Analyses

Dasfne Lee-Liu and Liangliang Sun

Abstract

Mammals have a limited regenerative capacity, especially of the central nervous system. Consequently, any traumatic injury or neurodegenerative disease results in irreversible damage. An important approach to finding strategies to promote regeneration in mammals has been the study of regenerative organisms like *Xenopus*, the axolotl, and teleost fish. High-throughput technologies like RNA-Seq and quantitative proteomics are starting to provide valuable insight into the molecular mechanisms that drive nervous system regeneration in these organisms. In this chapter, we present a detailed protocol for performing iTRAQ proteomics that can be applied to the analysis of nervous system samples, using *Xenopus laevis* as an example. The quantitative proteomics protocol and directions for performing functional enrichment data analyses of gene lists (e.g., differentially abundant proteins from a proteomic study, or any type of high-throughput analysis) are aimed at the general bench biologist and do not require previous programming knowledge.

Key words Quantitative proteomics, Spinal cord regeneration, Nervous system, iTRAQ, *Xenopus*, Non-model organisms, Functional enrichment analysis, Axon regeneration, Data analysis, Bioinformatics

1 Introduction

Most mammals are unable to regenerate their central nervous system, which results in irreversible functional loss after both traumatic events and neurodegenerative disease. As opposed to mammals, amphibians and teleost fish have a remarkable capacity for functional regeneration after traumatic injury to the nervous system (e.g., spinal cord injury) [1, 2]. The mechanisms that drive central nervous system regeneration in these nonmammalian organisms are starting to be elucidated, and high-throughput technologies are playing a key role in this process [3]. Quantitative proteomics allows obtaining a global profile of all the proteins present in a nervous system sample [4]. We used this technique on *Xenopus laevis*, which has a high capacity to regenerate the spinal

cord during larval stages (highest at stages (st) 49–51) and gradually loses this capacity during metamorphosis, where the larva transforms into a juvenile non-regenerative froglet (st 66). In this chapter, we present a detailed protocol to perform iTRAQ proteomics of nervous system samples, using, as an example, our previous quantitative proteomics analysis of spinal cord samples after sham and spinal cord injury surgery, comparing samples from regenerative (stages (st) 49–51) and non-regenerative (st 66) *X. laevis*, to identify the proteins that show differential abundance changes in response to injury [5]. The differences in regenerative and non-regenerative proteomes provide an extensive database of candidate proteins and biological processes and pathways that are starting to help elucidate the mechanisms that explain why *X. laevis* larvae regenerate, in contrast to the non-regenerative froglet, leading ultimately to an understanding of how to activate the regenerative program in a non-regenerative model. This protocol should be generally applicable to quantitative proteomics of any nervous system sample. We included a description of sample obtention, protein extraction, and labeling with iTRAQ reagents, followed by reversed-phase liquid chromatography (RPLC)–electrospray ionization (ESI)–tandem mass spectrometry analysis. Then, we describe how to analyze raw data from the mass spectrometer to determine differential protein abundance. Finally, we included a section on functional data analysis of differentially abundant proteins, including functional enrichment of gene ontology, biological pathways, and protein–protein interaction, among others. These tools can be applied to any type of gene list originating from proteomics, transcriptomics, or any high-throughput analysis. The tools we included in this chapter are aimed at the bench biologist, and do not require previous programming knowledge. We hope this chapter will be a useful guideline to anyone planning an experiment of quantitative proteomics of the nervous system and provide tools to extract the most significant information from the global proteomic landscape.

2 Materials

2.1 Acquisition of Tissue Samples

1. Liquid nitrogen and an appropriate tabletop container (e.g., small vacuum flask).
2. Floating foam microfuge tube rack that fits inside tabletop liquid nitrogen container.
3. Dissection instruments (e.g., iridectomy scissors and fine forceps; *see Note 1*).
4. 10× Barth’s stock solution: 88 mM sodium chloride, 1 mM potassium chloride, 2.4 mM sodium bicarbonate, 10 mM HEPES, 0.82 mM magnesium sulfate, 3.3 mM calcium nitrate,

0.41 mM calcium chloride, pH 7.6. In a large beaker, dissolve 52 g NaCl, 0.75 g KCl, 2 g NaHCO₃, and 23.8 g HEPES in 800 mL of deionized water. Then, add 2 g MgSO₄·7H₂O, 0.8 g Ca(NO₃)₂·4H₂O, and 0.6 g CaCl₂·2H₂O, and mix until dissolved. Adjust the pH to 7.6 with 10 M NaOH, and complete the volume to 1 L. Transfer the solution to an appropriate autoclavable bottle, autoclave, and store at 4 °C.

5. 0.1× Barth's: Dilute 10 mL of 10× Barth's stock solution in deionized water to a final volume of 1 L for 0.1× working solution. Use immediately and discard the remaining solution.
6. Glass Petri dish with lid for anesthetizing animals and to use as dissecting surface.
7. Stock anesthetic solution: 1% (w/v) ethyl 3-aminobenzoate methanesulfonate (MS-222). Dissolve 0.5 g MS-222 in 50 mL deionized water and store at 4 °C in a dark bottle.
8. Anesthetic solution: Measure 2 mL of the stock anesthetic solution and bring the volume up to 100 mL using 0.1× Barth's solution. Use immediately and discard the remaining solution.

2.2 Protein Extraction

(See **Note 2** before starting the remaining steps in the Materials section.)

1. Tris-HCl buffer: 100 mM Tris-HCl solution in deionized water, pH 7.6. Dissolve 1.6 g Tris hydrochloride in 100 mL deionized water. Use concentrated HCl to adjust pH to 7.6.
2. Lysis buffer: 2% (w/v) sodium dodecyl sulfate (SDS), 100 mM Tris-HCl, and 5× cComplete Protease Inhibitor Cocktail (Roche; see **Note 3**), pH 7.6. Weigh 200 mg SDS per 10 mL Tris-HCl buffer, dissolve, and then add one tablet of the protease inhibitor cocktail, and dissolve completely. The pH does not need to be further adjusted when using the previously prepared pH 7.6 Tris-HCl buffer.
3. Microcentrifuge, room temperature, minimum 10,000× *g*.
4. Probe sonifier, 200 W, line voltage 115 V, amplitude control 10–100% of power supply output voltage, operation at room temperature.
5. 100 mM ammonium bicarbonate: 100 mM ammonium bicarbonate in deionized water, pH 8. Prepare the required volume of 100 mM ammonium bicarbonate by dissolving the salt in deionized water. The resulting pH will be 8 and no further adjustment is needed.
6. 100 mM DTT: 100 mM dithiothreitol, 100 mM ammonium bicarbonate. Dissolve 1.6 mg DTT in 100 μL ammonium bicarbonate solution. Sonicate for 1 min to dissolve.

7. 100 mM IAA: 100 mM iodoacetamide (IAA), 100 mM ammonium bicarbonate. Dissolve 1.8 mg IAA in 100 μ L 100 mM ammonium bicarbonate. Sonicate for 1 min to dissolve.
8. Thermoregulated water bath.
9. 80% ACN/0.1% formic acid solution. 80% (v/v) acetonitrile and 0.1% (v/v) formic acid. Mix 100 μ L formic acid with 80 mL pure acetonitrile and complete the volume to 100 mL using deionized water.
10. 0.1% formic acid solution. 0.1% (v/v) formic acid. Use 100 μ L formic acid per 100 mL of deionized water.

2.3 Cleanup and Tryptic Digestion

1. 8 M urea solution: 8 M urea, 100 mM ammonium bicarbonate, pH 8. Dissolve 4.8 g urea in approximately 6 mL of 100 mM ammonium bicarbonate and complete the volume to 10 mL.
2. 30 kDa molecular weight cutoff centrifugal filter unit (e.g., Microcon®, Merck, #11750403; *see Note 4*).
3. TPCK-treated trypsin: 1 mg/mL L-(tosylamido-2-phenyl) ethyl chloromethyl ketone (TPCK)-treated trypsin (Sigma-Aldrich, #4370285; *see Note 4*). Dissolve 1 mg TPCK-treated trypsin in 1 mL 100 mM ammonium bicarbonate.
4. Concentrated formic acid.
5. C18 solid phase extraction (SPE) columns (e.g., Waters, #WAT023590; *see Note 4*).
6. Vortexer.
7. Vacuum concentrator.

2.4 iTRAQ 8-Plex Labeling

1. iTRAQ 8-plex labeling kit (e.g., AB Sciex, #4390811; *see Note 4*).
2. 2% ACN solution: Dilute 2 mL of pure acetonitrile in deionized water, for a final volume of 100 mL. Increase volumes proportionately as needed.
3. 0.5% formic acid/2% ACN solution: 0.5% (v/v) formic acid, 2% (v/v) acetonitrile. Dilute 500 μ L formic acid in 100 mL of 2% ACN solution. Increase volumes proportionately as needed.

2.5 Strong Cation-Exchange Fractionation of iTRAQ Labeled Peptides

1. HPLC system (e.g., Waters Alliance; *see Note 4*).
2. Zorbax 300-SCX separation column (2.1 mm i.d. \times 150 mm length, 5 μ m particles) (e.g., Agilent, #883700-714; *see Note 4*).
3. SCX trap column (4.6 mm i.d. \times 12.5 mm length) (Agilent, #820950-904; *see Note 4*).
4. SCX buffer A: 8 mM KH_2PO_4 , 20% acetonitrile, pH 2.8. Dissolve 1.1 g KH_2PO_4 in 400 mL deionized water, and adjust

the pH to 2.8 using concentrated phosphoric acid (concentrated), followed by 100 mL of acetonitrile, for a final volume of 500 mL.

5. SCX buffer B: 0.8 M KCl in SCX buffer A, pH 2.8. Dissolve 6 g KCl in 100 mL SCX buffer A.
6. 0.1% formic acid/2% ACN solution: 0.1% (v/v) formic acid, 2% (v/v) acetonitrile. Dilute 100 μ L formic acid in 100 mL of 2% acetonitrile solution. Increase volumes proportionately as needed.

2.6 Reversed-Phase Liquid Chromatography (RPLC)–Electrospray Ionization (ESI)–Tandem Mass Spectrometry (MS/MS) Analysis

1. Ultrahigh performance liquid chromatography system (e.g., nanoACQUITY UltraPerformance LC®, Waters, Milford) (*see Note 5*).
2. RPLC buffer A: 0.1% (v/v) formic acid in HPLC-grade water.
3. RPLC buffer B: 0.1% (v/v) formic acid in pure acetonitrile.
4. Peptide BEH C18 reversed-phase column: 100 μ m \times 100 mm, 1.7- μ m-diameter particle, column temperature 40 °C (e.g., Waters, #186008802; *see Note 4*).
5. Capillary tip for electrospray (e.g., New Objective, PicoTip Nanospray Emitters, SilicaTip™; *see Note 4*).
6. Quadrupole ion trap mass spectrometer (e.g., Q-Exactive HF, Thermo Fisher Scientific, Waltham; *see Note 4*).

2.7 Software Packages for Identification, Quantification, Differential Abundance Analysis, and Functional Analysis of Proteins

1. MaxQuant software (*see Note 6*).
2. Perseus software (*see Note 7*).
3. g:Profiler (*see Note 8*).
4. Cytoscape, with stringApp installed (*see Note 9*).
5. DAVID Bioinformatics Resources (*see Note 10*).
6. BioVenn (*see Note 11*).

3 Methods

3.1 Acquisition of Tissue Samples

1. Before starting the dissection, prepare a small appropriate container of liquid nitrogen to keep on your bench (e.g., a small vacuum flask) and a small floating foam microfuge tube rack that fits inside this container. This will allow you to flash freeze the dissected tissue, as well as pool tissues of the same experimental condition into a single microfuge tube (*see Fig. 1* for a workflow summary from acquisition of tissue samples to protein identification and quantification and differential protein abundance analysis).

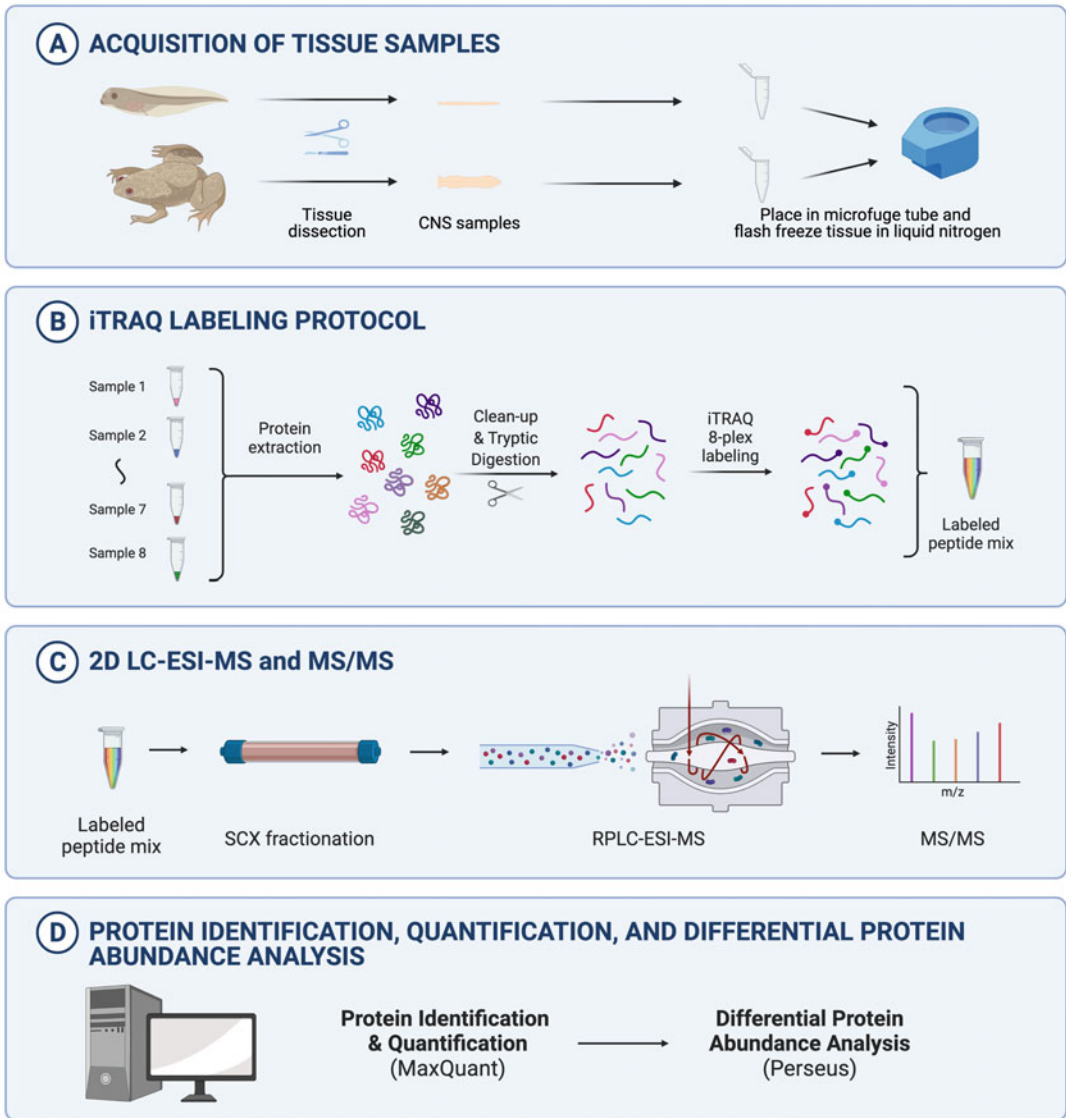


Fig. 1 Workflow summary of the protocol (part I). (a) Summary of acquisition of tissue samples, from tissue dissection to flash freezing them in liquid nitrogen. (b) iTRAQ labeling protocol of peptides, from protein extraction to iTRAQ 8-plex labeling. (c) Schematic design of the SCX–RPLC–ESI–MS/MS (strong cation exchange–reversed-phase liquid chromatography–electrospray ionization–tandem mass spectrometry). (d) Protein identification and quantification and differential protein abundance analysis, performed using MaxQuant and Perseus

- For *Xenopus laevis* stage 49–51 larvae (regenerative stage), anesthetize animals by completely submerging them in a Petri dish containing anesthetic solution for 1–2 min (verify anesthesia by lightly touching the tail using forceps—there should be no movement response). Euthanize animals by using

iridectomy scissors to decapitate the animal at the hindbrain–spinal cord junction, and proceed to dissect the tissue or tissue segment of interest as described in **step 4**, below (*see Note 12*).

3. For *X. laevis* stage 66 froglets (non-regenerative stage), anesthetize animals by completely submerging in anesthetic solution, also in a Petri dish (covered, to keep froglets from jumping out), for 5–10 min. Verify anesthesia by lightly touching the hind limbs and ensure lack of response. Euthanize animals by making a cut at the hindbrain–spinal cord junction.
4. Immediately after euthanizing animals, proceed to dissect the tissue or tissue segment of interest (e.g., spinal cord segment or brain region). Stage 49–51 larvae can be dissected on an inverted Petri dish, keeping the tissue always submerged in a large drop of anesthetic solution (*see Note 13*). Stage 66 froglets can also be dissected on an inverted Petri dish, taking care to frequently wet the tissue during dissection with anesthetic solution to preserve tissue integrity. As soon as it is possible, continue the dissection by submerging the tissue completely in a large drop of anesthetic solution.
5. Keep a drop of 0.1× Barth's without anesthetic separately on the same dissecting dish, so that once you isolate the tissue or segment of interest, you can quickly submerge it into the anesthetic-free drop and then remove as much liquid from the tissue by sliding it away from the drop. Perform the following processes as quickly as possible. Transfer the tissue into a 1.5 mL microfuge tube by adhering it to the wall of the tube. Close the tube, place it on the floating rack, and handle using large forceps to submerge into the liquid nitrogen container for flash freezing (*see Note 14* for pooling samples).
6. Samples can be stored at –80 °C until used.

3.2 Protein Extraction

1. Keep the samples on ice and let them thaw. Pulse spin tubes in a microcentrifuge to keep the samples at the bottom of the microfuge tubes.
2. Resuspend the tissue samples in an appropriate volume of lysis buffer (*see Note 15*). Then homogenize the samples in the lysis buffer on ice for 1 min using a handheld homogenizer.
3. Sonicate samples for 10 min on ice using a sonifier and then keep samples on ice for 1 additional hour (*see Note 16*).
4. Centrifuge samples at 15,000× *g* for 10 min.
5. Carefully transfer the supernatant to a new tube. Set aside a small aliquot (check the requirements for the bicinchoninic acid (BCA) assay kit already in your laboratory to determine the volume you will need) to determine protein concentration using the BCA assay according to the manufacturer's procedure.

6. Transfer the required amount of protein (usual range: 10–100 μg) to a new tube and denature samples at 90 °C for 15 min (*see* **Note 17**).
7. Add 2 μL of 100 mM DTT per 100 μg protein solution for protein reduction and incubate at 60 °C in a water bath for 1 h. Adjust the volume of 100 mM DTT proportionally according to the mass of proteins in the sample.
8. Add 5 μL of 100 mM IAA per 100 μg protein solution for protein alkylation and incubate at room temperature for 30 min in the dark. Adjust the volume of 100 mM IAA proportionally according to the mass of proteins in the sample.

3.3 Cleanup and Tryptic Digestion

1. Mix 8 M urea solution with each protein solution (v/v 1:1) via gentle vortexing. Load the mixture onto the filter membrane integrated in the Microcon® 30 kDa filter unit. Centrifuge at 14,000 $\times g$ for 15 min and discard the flow-through.
2. To remove the SDS, wash the membrane by adding 200 μL of 8 M urea solution, centrifuge at 14,000 $\times g$ for 15 min, and discard the flow-through. Repeat for a total of five times.
3. Then, to remove the urea, add 200 μL of 100 mM ammonium bicarbonate, centrifuge at 14,000 $\times g$ for 15 min, and discard the flow-through. Repeat once more.
4. Add 50 μL of 100 mM ammonium bicarbonate onto the membrane, and vortex gently to resuspend the proteins.
5. Add 3.3 μL of TPCK-treated trypsin onto the membrane that held the 100 μg proteins and incubate overnight at 37 °C. The protein-to-trypsin ratio should be 30:1 (w/w). The amount of trypsin should be adjusted proportionally to the amount of protein on the membrane.
6. Centrifuge each filter unit at 18,000 $\times g$ for 15 min and collect the flow-through, which now contains the peptides.
7. Add an additional 50 μL of 100 mM ammonium bicarbonate onto the membrane. Centrifuge at 18,000 $\times g$ for 15 min to collect the flow-through and pool it with the one obtained in **step 6**.
8. Add concentrated formic acid to obtain a final formic acid concentration of 0.5% (v/v) to acidify the sample.
9. To desalt the samples, first activate required C18 SPE columns using 3 mL of 80% ACN/0.1% formic acid solution.
10. Equilibrate the column using 0.1% formic acid solution.
11. Load each sample to the C18 SPE column, and wash it using 3 mL 0.1% formic acid solution to desalt it.
12. Elute the analyte from the column using 1.5 mL of 80% ACN/0.1% formic acid solution.

3.4 iTRAQ 8-Plex Labeling

1. Add the appropriate volume of dissolution buffer (*see Note 18*) included in the iTRAQ 8-plex labeling kit (AB Sciex, Foster City) to the lyophilized sample to resuspend the sample.
2. Add the corresponding iTRAQ reagent (*see Note 18*) and incubate at room temperature for 2 h. Label each sample with a different channel of the iTRAQ 8-plex reagent.
3. Block excess iTRAQ reagent with 100 μ L Tris-HCl buffer in each tube.
4. Combine the eight samples labeled with different iTRAQ 8-plex channels and lyophilize the pooled samples.
5. Redissolve the samples in formic acid solution via vortexing and sonication to obtain a final 0.5–1 mg/mL protein concentration. Desalt the peptide samples in C18 SPE columns and lyophilize them (*see Note 19*).
6. Redissolve the samples in 0.5% formic acid/ACN solution for a final 0.5–1 mg/mL peptide concentration if possible.

3.5 Strong Cation-Exchange Fractionation of iTRAQ Labeled Peptides

7. For this step, use an HPLC system with the mobile phase flow rate at 0.3 mL/min and the Zorbax 300-SCX separation column (*see Notes 4 and 20*).
8. Generate the mobile phase gradient using the SCX buffers A and B.
9. Load samples onto the SCX column, followed by 20 min washing with 100% SCX buffer A to remove the excess iTRAQ reagent.
10. Separate peptides by a 60 min linear gradient from 100% SCX buffer A to 100% SCX buffer B.
11. Collect an appropriate number of fractions per sample (*see Note 21*) during the 60 min gradient separation. Lyophilize the fractions and redissolve them in 0.1% formic acid/ACN solution. Desalt each fraction and lyophilize it. Redissolve each fraction in an appropriate volume of 0.1% formic acid/ACN solution for MS analysis.

3.6 Reversed-Phase Liquid Chromatography (RPLC)–Electrospray Ionization (ESI)–Tandem Mass Spectrometry (MS/MS) Analysis

1. For this step, use an appropriate ultra performance liquid chromatography (UPLC) system.
2. Use the following buffers as mobile phases for gradient separation: RPLC buffer A and RPLC buffer B.
3. Automatically load peptides onto a commercial C18 reversed-phase column (Waters, 100 μ m \times 100 mm, 1.7- μ m-diameter particle, BEH130C18, column temperature 40 $^{\circ}$ C; *see Note 4*) with 2% buffer B for 14 min at a flow rate of 0.7 μ L/min, followed by a three-step gradient separation: 1 min from 2% to 8% RPLC buffer B and flow rate from 0.7 μ L/min to 0.6 μ L/min, 84 min to 28% RPLC buffer B at a flow rate of 0.6 μ L/

min, and 1 min to 80% RPLC buffer B and flow rate from 0.6 $\mu\text{L}/\text{min}$ to 0.7 $\mu\text{L}/\text{min}$ and maintained at 80% RPLC buffer B for 5 min with a flow rate of 0.7 $\mu\text{L}/\text{min}$. Equilibrate the column for 14 min with 2% B at a flow rate of 0.7 $\mu\text{L}/\text{min}$ before analyzing the next sample.

4. Pump eluted peptides from the C18 column through a capillary tip for electrospray, which are then analyzed by a Q-Exactive HF mass spectrometer (*see Note 4*). Load the appropriate volume of peptides onto the column (*see Note 22*).
5. Perform data acquisition using a TopN data-dependent acquisition (DDA) method. The MS and MS/MS parameters depend on the mass spectrometer used (*see Note 23*).

3.7 Protein Identification and Quantification

1. Analyze the raw files with MaxQuant software [6] (*see Note 24* on how to install).
2. Load the raw data files by going to the “Raw data” tab and pressing “Load.”
3. Select or upload the protein reference database for your model organism. In our experiment, we used the protein reference database (*see Note 25*) from the *X. laevis* genome v7.1 for database searching.
4. Go to the “Group-specific parameters” tab for this and the next two steps. First, select the “Modifications” button, and add the appropriate modifications for your experiment. For example, we selected the following as variable modifications: acetyl (protein N-term), deamidation (NQ), and oxidation (M). We set carbamidomethyl (C) as a fixed modification.
5. Select the “Digestion” button and choose the enzyme(s) you used (e.g., we selected “Trypsin”).
6. Select the “Type” button, and below, the first scroll down menu will be set as “Standard.” For iTRAQ 8-plex labeling quantification, change it to “Reporter ion MS2,” and then click on the “8plex iTRAQ button,” which by default will contain the following labels: iTRAQ 8plex-Lys 113–121 and iTRAQ 8plex-Nterm 113–121. Set other iTRAQ related parameters as follows: reporter mass tolerance as 0.01 Da and filter by precursor intensity fraction (PIF) with minimal reporter PIF as 0.75. We left the remaining parameters as default settings.
7. Download the protein reference database for your model organism as a FASTA file (*see Note 25*). Then, in the “Global parameters” tab in MaxQuant, select “Sequences,” and next to “Fasta files,” select “Add” to load your protein reference database.
8. The *X. laevis* genome v7.1 reference database contained 54,130 protein sequences at the time, and we used the

following parameters, which you can set in the “Global parameters” tab → “MS/MS analyzer”: set the “maximum number of allowed missed cleavages for database search” at two; “mass tolerance for parent ions” at 20 ppm for the first search and 4.5 ppm for the main search; and “mass tolerance for fragment ions” at 20 ppm. The common contaminants were included in the database for search (*see Note 26*).

9. In “Global parameters” → “Identification,” leave the parameters at default values, which should filter the database searching results with false discovery rates (FDRs) less than 1% on both peptide and protein levels.

3.8 Differential Protein Abundance Analysis

1. Load the export file of MaxQuant software into the Perseus [7] software, and filter the data to remove the proteins identified from reverse database and contaminant proteins.
2. In the following steps, we will describe what we did for our experiment, which should be adapted accordingly to your own experimental design.
3. For our experiment, we had three experimental conditions: uncut (duplicate), sham surgery (triplicate), and spinal cord transection (triplicate). We averaged the reporter ion intensity of the biological duplicate of uncut samples for both regenerative and non-regenerative stages.
4. We then normalized the reporter ion intensity of transected and sham-operated samples to the averaged uncut samples for both stages to get the protein abundance ratios compared with uncut samples.
5. This was followed by bias correction for protein quantitation results in Perseus with the “divide” function. We corrected the median protein ratio in each biological condition (biological triplicates of transected and sham-operated) to unity and applied this factor to all quantitation results in each corresponding biological condition.
6. Differential abundance analyses were then performed in Perseus to compare the protein expression in transected and sham-operated samples using the “Two-sample tests” function. Select Welch’s t-test in “Test,” using $S0 = 0$, Side = Both, and “p-value” in the “Use for truncation” option, with a 0.05 threshold. Remaining parameters were kept at default.
7. Once you obtain the results of your differential abundance analysis, you can filter the proteins having significant changes at your desired p-value or corrected p-value (usually <0.05) and with the additional fold-change filter you determine (*see Note 27*).

3.9 Finding the Human or Mouse Ortholog of Your Gene List Using an Ortholog Converter Tool (See Note 28)

1. Access the g:Profiler website at <https://biit.cs.ut.ee/gprofiler/gost>. It will automatically load on the g:GOST functional profiling tab (*see Note 29*).
2. Click on the “g:Orth Orthology search” tab.
3. Copy and paste your gene list directly (each term can be separated by a white space or new line to be identified as a separate term, and queries are case-insensitive).
4. Select your origin species in the “Organism” drop-down menu in the “Options” section on the right. Below, in “Target,” select “Homo sapiens” or “Mus musculus.” In “Numeric IDs treated as,” leave it at default, unless you are using WikiGene accession numbers.
5. Click “Run query.”
6. The results will appear on a table underneath, and you can click “Export to CSV” to download the results in a file you can open in Microsoft Excel (*see Note 30*).
7. After obtaining your human or mouse orthologs, you can continue with the functional enrichment analyses.

3.10 Finding the Human or Mouse Ortholog by Transforming Your Identifiers to Their Official Gene Symbols (See Note 31)

1. Access DAVID Bioinformatics Resources at <https://david.ncifcrf.gov/home.jsp>.
2. Click on “Start analysis” in the top menu.
3. Click on the “Upload” tab, and then copy and paste your gene list in the “A: Paste a list” box.
4. In “Step 2: Select Identifier,” select the identifier in which your list is.
5. In “Step 3: List Type,” select “Gene list.”
6. Click on “Submit list.”
7. In the resulting window, click on the “Gene ID conversion tool.”
8. In the next window, select “OFFICIAL_GENE_SYMBOL” in the drop-down menu.
9. Type the name of your species in the “For species” box and select it when it appears among the options. Then click “Submit to conversion tool.”
10. A pop-up window with the results will appear. Right-click on the “Download File” link, and click on the “Download linked file” option (if using macOS, or equivalent option in your operating system).
11. You can open this file in MS Excel, where the “To” column will contain your gene list in official gene symbol format (*see Note 32*). You can then proceed to use this gene list in any mouse or human search engine. Most gene symbols will be the same across species (*see Notes 33 and 34*).

3.11 Obtaining All Functional Annotations for Your Gene Sets

1. Upload your gene list of interest as indicated in Subheading 3.10.
2. Click the “Functional Annotation Tool” link or go to the drop-down menu at “Shortcut to DAVID tools” and click on “Functional Annotation.”
3. Select the annotation type(s) you want to download by checking on the boxes below “Annotation Summary Results” by pressing the plus (+) buttons and checking the desired boxes.
4. Click on the “Functional Annotation Table” button and a new window will pop up. In this window, on the top right, you can download the data as a .txt file. This can be opened in MS Excel, and for each gene, it will have a different column with all the information you selected in the previous step.

3.12 Functional Enrichment Using the g:Profiler Tool (See Note 35)

1. Choose your gene list of interest to analyze that has already been transformed to human or mouse orthologs. These may be, for example, the upregulated proteins in your experimental condition, or all differentially abundant proteins in response to your experimental stimulus, depending on the kind of conclusion you would like to obtain from your data.
2. Access the g:Profiler website at <https://biit.cs.ut.ee/gprofiler/gost>. It will automatically load on the g:GOST functional profiling tab.
3. You may copy and paste your gene list directly (each term may be separated by a white space or new line to be identified as a separate term, and queries are case-insensitive).
4. Next to the input space, there is an “Options” section, where you can select the organism. We recommend leaving the rest of the parameters as default.
5. If there are ambiguous query genes, a yellow box will appear before the results, where you can manually select the ID that corresponds to your gene and then press “Rerun query” to include the ambiguous IDs.
6. The output will appear in three different tabs. The “Results” tab is a summarized display of the results represented in a Manhattan plot that shows the enrichment results, with the adjusted p-value on the Y-axis, and the different functional terms, grouped and color-coded by database. Scrolling above the circles on the plot will display the details of each term and clicking on them will select them to be displayed on a table below the plot. You may export the plot with the table below as a PNG file.
7. The “Detailed Results” tab will contain all enriched functional terms in descending adjusted p-value, separated by database. The top box allows you to filter your results for specific search

terms, e.g., type “mitochondria” to find all functional terms with the word mitochondria in them, and then export them as a CSV file that can be opened in MS Excel or any worksheet reader. Using the default values and no filter, the resulting CSV file will contain a list of all functional terms with their associated adjusted p-value and genes.

8. The “Query info” tab contains the query parameters and the original identifiers that were included in the analysis (and the ones that were not found in the database).

3.13 Cytoscape and STRING Protein-Protein Network

1. Download and install Cytoscape with the stringApp (*see Note 36*).
2. Use your human or mouse ortholog gene list in official gene symbol format. We have noticed that this identifier is best recognized by the STRING database.
3. Go to File → Import → Network from Public Databases.
4. In the pop-up window, at Data Source, select “STRING: protein query.” In species, select the species you converted your list to (*Homo sapiens* or *Mus musculus*), and in the box enter your official gene symbol list, separating each ID by a new line.
5. Select the “Load enrichment data box” so that the stringApp can perform a functional enrichment analysis that can be complementary to the one performed using g:Profiler. Leave remaining parameters as default.
6. The displayed STRING network can be customized using either the “STRING” panel at the right or the “Style” tab at the left. To use the latter, you need to uncheck all the options in the “STRING” panel at the right first. For example, a useful addition is to color each node in the network according to the fold change. To achieve this, generate an Excel file with two columns: the first containing the official gene symbol ortholog in your gene list and the second containing the fold change. You can then export this file as a .txt file. Make sure that both columns have a name (e.g., “Gene_symbol” and “Fold_change”).
7. In the node table (bottom part of Cytoscape), press the “Import Table from File...” button, select your file, and in the pop-up window, in “Key Column for Network,” select “query term,” and uncheck the “Case Sensitive Key Values” box. Leave remaining parameters as default and click “OK.” Your node table should now have an extra column named “Fold_change” (or whichever name you used).
8. Then, in the “Style” tab, you can select “Fill color,” and in “Column,” select the “Fold_change” column. In “Mapping type,” select “Continuous Mapping,” and double-click the

color scale to customize it as desired. While this example was for introducing fold-change values, you may use it to introduce any additional column and customize any of the other criteria in the network (e.g., label size, node shape, size, etc.).

9. The resulting network can be exported in File → Export → Network to image.

3.14 Generating Venn Diagrams

1. Access BioVenn at <https://www.biovenn.nl> (see Note 37).
2. Edit the “Title” and “Subtitle” boxes as desired.
3. Enter the names of each set or list into the “x title,” “y title,” and “z title” boxes. You can modify the format on the options at the right.
4. Copy and paste each ID list into the “ID Set X/Y/Z” boxes, or upload file with IDs by pressing the “Choose file” button. You can choose the color of each set in the options at the right. If you only have two sets, leave the third one blank.
5. Check the box “print numbers” if you want to the resulting Venn diagram to contain this information, which can be in absolute numbers (“absolute nrs”) or “percentages.”
6. You may also modify the image size in the “image width/height” boxes below.
7. Press Embedded SVG to obtain an embedded image in the white panel at the right where the text and numbers can be dragged and positioned. The “Embedded PNG” will result in an unmodifiable image that can be downloaded, and the “SVG/PNG only” buttons will open a new window with the image.
8. Underneath the main panel, there is a “Current Image Statistics” panel, where you can press the numbers to obtain (in a pop-up window) a list of the identifiers found in each area of the Venn diagram. For example, x-y total overlap will give you a list of the intersection between sets X and Y.
9. In the pop-up window, you can right-click “File with IDs” to download a .txt file with the identifiers in that list.

4 Notes

1. Gather dissection tools suitable for your specific preparation. For example, for *Xenopus* spinal cord dissections, fine forceps and iridectomy scissors are required.
2. Reagents used for Subheading 2.2 onward should be HPLC grade.

3. We have listed Roche's cOMplete Protease Inhibitor Cocktail because it is the only one we have used and the composition is proprietary of the manufacturer. You are welcome to use another one that has worked for you.
4. We have included the brand and supplier details here because we have not tried using other brands in our experiments. However, this does not mean the experiment will not work with other brands or vendors.
5. We list this equipment in particular because it is the one we used for our experiment, but you may try a similar system with the following characteristics: stable nanoliters per minute flow rate that can be used at a high pressure (i.e., 8000 psi), which will allow high-resolution separation.
6. MaxQuant software (<https://www.maxquant.org/maxquant/>) [6] allows analysis of raw data obtained when performing mass spectrometry-based proteomics. It is used to map the generated spectra against a reference peptide database using Andromeda, the included peptide database search engine.
7. Once peptide and protein abundance has been determined using MaxQuant, Perseus software (<https://www.maxquant.org/perseus/>) [7] allows performing statistical analyses to determine differential protein abundance.
8. g:Profiler (<https://biit.cs.ut.ee/gprofiler/gost>) [8, 9] is a web-accessible program that includes (1) a functional enrichment analysis tool (g:GOST); (2) a gene ID conversion tool that allows converting between different gene and protein identifiers (g:Convert); (3) a tool to find orthologs between organisms based on information from the Ensembl database (g:Orth); and (4) a tool that maps human single nucleotide polymorphism (SNP) rs codes to gene names (g:SNPense).
9. Cytoscape (<https://cytoscape.org>) [10] is a bioinformatics package that allows biological network visualization and data integration and has various apps that have been developed to perform further analyses, such as the stringApp [11], which integrates the STRING database. STRING is a comprehensive database that integrates information on different levels of protein-protein association, ranging from direct or physical interactions to indirect or functional interactions that are specific and biologically meaningful [12]. STRING has an online platform that allows performing analyses, but we will describe how to use the tool in Cytoscape, using the stringApp [11], which contains more functionalities.
10. DAVID Bioinformatics Resources (<https://david.ncifcrf.gov/home.jsp>) [13, 14] is also a web-accessible program containing a powerful set of functional annotation tools, including an ID converter. The only caveat is that annotations are not updated

as frequently as g:Profiler (at least for Gene Ontology annotations; see <https://david.ncifcrf.gov/content.jsp?file=release.html> for details on the version history of the database). This is why we recommend using g:Profiler for gene ontology enrichment analyses. However, for those working on *Xenopus laevis*, it does present the advantage that the genes from this species are very well annotated, allowing identifier conversion for *X. laevis*. In addition, it contains a very useful tool that the other databases do not: the generation of a functional annotation table containing all functional annotations in the database for each gene.

11. Venn diagrams are a useful tool when working with any -omics type of data. You may want to find the intersection between differentially expressed genes across different conditions, or when faced with very long lists of enriched functional categories, finding which are different across experimental conditions can provide valuable information. Here we describe how to use BioVenn (<https://www.biovenn.nl>) [15], which generates area-proportional Venn diagrams.
12. Here, we describe the protocol for euthanasia and tissue dissection for *X. laevis* stage 49–51 larvae and stage 66 froglets, but the anesthetic solution, protocol, and dissection instrumentation should be optimized for the model organism you are using. MS-222 is the anesthetic routinely used for *X. laevis*, and 0.1× Barth's solution is the medium used for animal growth and maintenance while also providing buffering for the pH change caused by MS-222. See Edwards-Faret et al. (2017) [16] for more details on *X. laevis* spinal cord regeneration protocols.
13. For *X. laevis*, dissection of any region of the central nervous system takes 3–5 min per animal, for which the complete procedure can be performed at room temperature. If the dissection will take longer, it is recommended to perform the dissection on ice, using a previously chilled dissection solution.
14. To pool samples from different animals of the same experimental condition into a single microfuge tube, place the first sample in the tube, transfer tube to the floating rack, and quickly submerge it in your liquid nitrogen container. Leave tube and rack inside the container during the dissection of the following sample. Once you have obtained it, retrieve the floating rack holding the tube with the previous sample using large forceps, and take it out of the liquid nitrogen. Introduce the new sample, close the tube, and return to the rack for flash freezing again. Repeat this procedure as many times as needed. The samples can be placed on any part inside the tube, because the tube will be centrifuged before lysis.

15. In our experiment, we pooled 5 stage 49–51 *X. laevis* caudal spinal cord segments, obtaining 6 μg protein per spinal cord for a total of 30 μg protein, which were lysed in 100 μL of lysis buffer. For stage 66 *X. laevis* froglets, we pooled 3 spinal cord segments per sample, obtaining 20 μg protein per spinal cord, for a total of 60 μg protein, which were lysed in 150 μL of lysis buffer. Therefore, we recommend a range of 3–4 μg protein per 10 μL of lysis buffer. The volume of the lysis buffer is dependent on the estimated protein mass in the sample. It is advisable to keep the protein concentration as high as possible by keeping the volume of lysis buffer as low as possible, and, if needed, samples can be readily diluted afterward.
16. Sonication time can vary depending on the samples, but usually 10 min is enough. Use approximately 70% of the amplitude and set it to 50 on–off cycles.
17. The required protein quantity per sample depends on the iTRAQ reagent. Usually, 10–100 μg protein per sample is sufficient for iTRAQ labeling. When labeling eight different samples in one iTRAQ 8-plex experiment, it is important to label the same protein quantity across all samples, to reduce variations during sample preparation.
18. Pay special attention to the volume of dissolution buffer used for resuspending the peptides. You need to consider two things. First, make sure the final peptide concentration is in 0.5–1 mg/mL range during the iTRAQ labeling. Second, make sure the final organic solvent (i.e., ethanol) concentration is higher than 60%. The ethanol is used to solubilize the iTRAQ reagents. Typically, for 100 μg peptides, use 35 μL of dissolution buffer to dissolve the peptides, and add 70 μL of the iTRAQ reagent in ethanol. See Table 1 for guidance.
19. Do not dry the peptide samples completely (i.e., do not “over-dry” them), as this will make it extremely difficult to redissolve them later.
20. There are several options for the SCX column for fractionation. Choose an appropriate flow rate based on the manufacturer’s instructions. If necessary, add an additional SCX trap column before the separation column for protection.
21. The number of fractions collected for LC–MS analysis can vary, mostly depending on the available MS time. More fractions in general will produce more protein quantification. When re-dissolving the labeled peptides in 0.1% (v/v) formic acid in 2% acetonitrile for LC–MS analysis, aim for a peptide concentration between 0.5 and 1 mg/mL.
22. The peptide sample volume loaded onto the C18 column for LC–MS analysis is dependent on protein concentration:

Table 1
Reagent ratios for iTRAQ labeling

Peptide quantity range (μg)	Dissolution buffer volume (μL)	iTRAQ labeling reagent volume (μL)
100	35	70
20	10	20
10	5	10

peptide amount loaded onto the column should be close to 1 μg . For example, if the peptide concentration is 0.5 mg/mL, the injection volume should be 2 μL .

23. For our experiment, we used the following parameters (considering we used the Q-Exactive HF mass spectrometer): The electrospray voltage was set at 2 kV and the ion transfer tube temperature at 300 °C. The S-Lens RF level was 60.00. We acquired full MS scans in the Orbitrap mass analyzer over m/z 350–1800 range with a resolution of 60,000 (m/z 200) and the number of microscans set to 1. The target value was 3.00E+06. For MS/MS scans, the 12 (for stage 66 *X. laevis* froglets) or 5 (for stage 49–51 *X. laevis* larvae) most intense peaks with charge state ≥ 2 were sequentially isolated and further fragmented in the higher-energy-collisional-dissociation (HCD) cell following one full MS scan. The isolation window was set at 1.2 m/z . The normalized collision energy was 30%, and tandem mass spectra were acquired in the Orbitrap mass analyzer with a resolution of 60,000 (m/z 200). The fixed first mass was m/z 100.0. The target value was 1.00E+05 and maximum injection time was 110 ms (for stage 66 froglets) or 200 ms (for stage 49–51 larvae). The number of microscans was 1 and the ion selection threshold was 1.0E+05 counts. Dynamic exclusion was set at 60 s.
24. To download the MaxQuant software, you need to visit the <https://www.maxquant.org/> website, press the “Download” button, and enter your data. You will shortly receive an e-mail containing a download link. Once you have downloaded the file, decompress it, open the folder, and run the software directly by double-clicking the MaxQuant icon. In the same website, you can select Perseus and request the download link by entering your data. Like with MaxQuant, you will shortly receive an e-mail with the download link. MaxQuant and Perseus do not require installation. Once you download them, double-click on the MaxQuant or Perseus icon and the program will load directly.
25. For *Xenopus* (both *X. laevis* and *X. tropicalis*), the protein reference databases are available at Xenbase [17] (<http://www.xenbase.org/>), in the “Genomes” tab \rightarrow “Download

Xenopus Genomes” → “Sequences.” There is a list of options which include the Xenbase protein database as well as the one from NCBI, both of which can be downloaded as a FASTA file. For other species, you may download the databases directly from RefSeq at the NCBI site <https://www.ncbi.nlm.nih.gov/refseq/>.

26. These parameters are usually the default ones, since the raw file from the mass spectrometer contains the details from the mass analysis, and MaxQuant reads them and sets the parameters.
27. At this step you will have obtained a list of the proteins that change their abundance in your experimental conditions, e.g., in response to spinal cord injury. It is of great interest to determine whether they are related to each other in functional groups. For example, they may participate in similar biological processes or signaling pathways, or they could belong to a group of proteins that are functionally connected. In Subheadings 3.10, 3.11, 3.12, 3.13, and 3.14, we provide a set of tools that can be used to perform functional analysis of any gene list. These tools are freely available and user-friendly for the bench biologist and do not require previous programming knowledge (see Fig. 2 for a workflow summary on the use of these tools).
28. Functional annotation databases have the highest amount of information for mouse and human, for which it is convenient to convert your gene list into mouse or human orthologs before performing functional enrichment analyses.
29. While g:Profiler is a comprehensive database, it does not contain data for *Xenopus laevis*. Please see Subheading 3.10 for alternatives to find mouse or human orthologs for *X. laevis*.
30. For some identifiers, you will obtain more than one ortholog. This will require manual curation of the list according to the gene symbol or gene description to obtain the desired final list. Please note that it is possible that the database will not find orthologs for all your genes. It is important to take note of which ones do not appear, and see if you can manually find the ortholog, for example, directly at the NCBI website.
31. For less annotated organisms, using the method in Subheading 3.10 can yield a low number of orthologs. Also, there are some organisms, like *X. laevis*, that are not included in the g:Profiler database. For this and other cases, an alternative is to convert your gene list identifiers into the official gene symbol (e.g., the official gene symbol for *uncoupling protein 2* is *ucp2*). To achieve this, you can use the DAVID Bioinformatics Resources website [13].
32. If you are using *X. laevis*, the resulting official gene symbols will contain information on the homeolog of the gene (short or long chromosome, e.g., *cfb.L* corresponds to the L homeolog

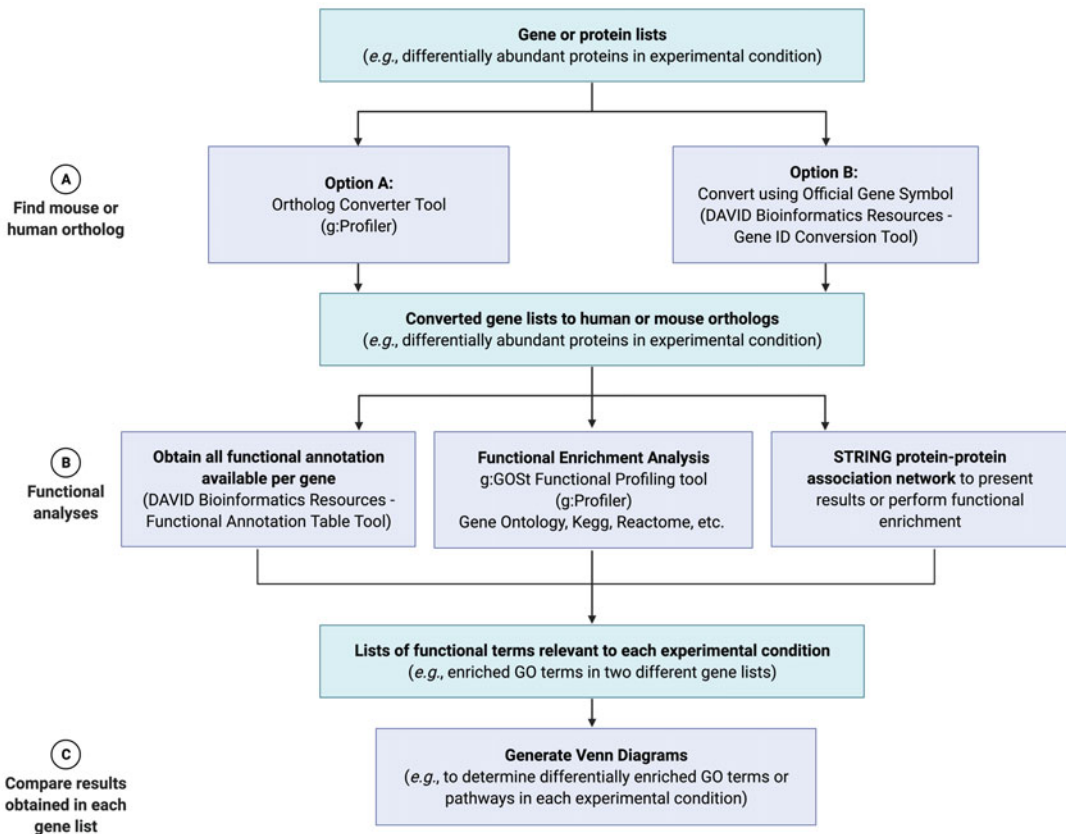


Fig. 2 Workflow summary of the protocol (part II). Schematic workflow of the functional analyses that can be performed once differential abundance gene or protein lists are obtained. These include, if needed, finding the human or mouse ortholog for better functional annotation (a), different types of functional analyses, including obtaining all functional annotation available per gene, functional enrichment analysis, and STRING protein–protein association network representation of results (b). Resulting functional analysis terms may be further compared among samples using Venn diagrams (c)

of the *cfb* (complement factor B)). Since this information will interfere when using the gene list in a mouse or human database, an easy way to remove it without requiring programming is the following: In MS Excel, generate a new spreadsheet, and go to File → Import. In the pop-up window, select “Text file” and click on “Import.” On the next window, make sure the “Delimited” option is selected, and then click “Next.” In the “Delimiters options,” select “Other” and in the box type a period (“.”). Click “Finish.” The resulting table will have a column with all your gene symbols without the .L or .S that you can now use as input in any mouse or human database search engine.

33. While we recommended above to perform your analysis using human or mouse orthologs, it is possible to use your original

gene list in the species you are working with (if available in the g:Profiler database). You can perform both analyses and compare the results, to see which one delivers better information.

34. Another option for finding human or mouse orthologs for *X. laevis* is available in the Xenbase website. Access it at <http://www.xenbase.org>, and then go to Download → Download Xenbase data. In the “Data Reports” section, click on the “+” button next to “Orthology,” where you can download files with the orthologs between *Xenopus* genes and human and mouse, among others.
35. g:Profiler is one of the gene ontology enrichment tools recommended by the Gene Ontology Consortium because its annotations are up to date with the original consortium database and analysis results include the version of the gene ontology database being used at the time. It provides annotation from databases from the following categories: (1) Gene Ontology [18, 19], (2) biological pathways (KEGG [20, 21], Reactome [22], WikiPathways [23]), (3) regulatory motifs in DNA (TRANSFAC [24], miRTarBase [25]), (4) protein databases (Human Protein Atlas [26], CORUM [27]), and (5) Human Phenotype Ontology [28].
36. Download Cytoscape for your operating system from the link, <https://cytoscape.org>, and install it. Then, open Cytoscape, and go to Apps → App Manager, and in the search box, type “stringApp.” Select it and press “Install.”
37. BioVenn allows you to obtain area-proportional Venn diagrams for up to three lists. Input lists can be made of gene or protein identifiers, gene ontologies, KEGG pathways, or any element separated by a new line. Please note that the analysis is case-sensitive.

Acknowledgments

This work was funded by FONDECYT Postdoctoral 3180180 (DLL). Figures 1 and 2 were created with BioRender.com.

References

1. Lee-Liu D, Edwards-Faret G, Tapia VS, Larrain J (2013) Spinal cord regeneration: lessons for mammals from non-mammalian vertebrates. *Genesis* 51(8):529–544. <https://doi.org/10.1002/dvg.22406>
2. Lee-Liu D, Mendez-Olivos EE, Munoz R, Larrain J (2017) The African clawed frog *Xenopus laevis*: a model organism to study regeneration of the central nervous system. *Neurosci Lett* 652:82–93. <https://doi.org/10.1016/j.neulet.2016.09.054>
3. Tedeschi A, Popovich PG (2019) The application of omics technologies to study axon regeneration and CNS repair. *F1000Res* 8. <https://doi.org/10.12688/f1000research.17084.1>

4. Hosp F, Mann M (2017) A primer on concepts and applications of proteomics in neuroscience. *Neuron* 96(3):558–571. <https://doi.org/10.1016/j.neuron.2017.09.025>
5. Lee-Liu D, Sun L, Dovichi NJ, Larrain J (2018) Quantitative proteomics after Spinal Cord Injury (SCI) in a regenerative and a non-regenerative stage in the frog *Xenopus laevis*. *Mol Cell Proteomics* 17(4):592–606. <https://doi.org/10.1074/mcp.RA117.000215>
6. Tyanova S, Temu T, Cox J (2016) The MaxQuant computational platform for mass spectrometry-based shotgun proteomics. *Nat Protoc* 11(12):2301–2319. <https://doi.org/10.1038/nprot.2016.136>
7. Tyanova S, Temu T, Sinitcyn P, Carlson A, Hein MY, Geiger T, Mann M, Cox J (2016) The Perseus computational platform for comprehensive analysis of (prote)omics data. *Nat Methods* 13(9):731–740. <https://doi.org/10.1038/nmeth.3901>
8. Raudvere U, Kolberg L, Kuzmin I, Arak T, Adler P, Peterson H, Vilo J (2019) g:Profiler: a web server for functional enrichment analysis and conversions of gene lists (2019 update). *Nucleic Acids Res* 47(W1):W191–W198. <https://doi.org/10.1093/nar/gkz369>
9. Reimand J, Kull M, Peterson H, Hansen J, Vilo J (2007) g:Profiler—a web-based toolset for functional profiling of gene lists from large-scale experiments. *Nucleic Acids Res* 35(Web Server issue):W193–W200. <https://doi.org/10.1093/nar/gkm226>
10. Shannon P, Markiel A, Ozier O, Baliga NS, Wang JT, Ramage D, Amin N, Schwikowski B, Ideker T (2003) Cytoscape: a software environment for integrated models of biomolecular interaction networks. *Genome Res* 13(11):2498–2504. <https://doi.org/10.1101/gr.1239303>
11. Doncheva NT, Morris JH, Gorodkin J, Jensen LJ (2019) Cytoscape StringApp: network analysis and visualization of proteomics data. *J Proteome Res* 18(2):623–632. <https://doi.org/10.1021/acs.jproteome.8b00702>
12. Szklarczyk D, Morris JH, Cook H, Kuhn M, Wyder S, Simonovic M, Santos A, Doncheva NT, Roth A, Bork P, Jensen LJ, von Mering C (2017) The STRING database in 2017: quality-controlled protein-protein association networks, made broadly accessible. *Nucleic Acids Res* 45(D1):D362–D368. <https://doi.org/10.1093/nar/gkw937>
13. Huang da W, Sherman BT, Lempicki RA (2009) Systematic and integrative analysis of large gene lists using DAVID bioinformatics resources. *Nat Protoc* 4(1):44–57. <https://doi.org/10.1038/nprot.2008.211>
14. Huang DW, Sherman BT, Tan Q, Kir J, Liu D, Bryant D, Guo Y, Stephens R, Baseler MW, Lane HC, Lempicki RA (2007) DAVID Bioinformatics Resources: expanded annotation database and novel algorithms to better extract biology from large gene lists. *Nucleic Acids Res* 35(Web Server issue):W169–W175. <https://doi.org/10.1093/nar/gkm415>
15. Hulsen T, de Vlieg J, Alkema W (2008) BioVenn – a web application for the comparison and visualization of biological lists using area-proportional Venn diagrams. *BMC Genomics* 9:488. <https://doi.org/10.1186/1471-2164-9-488>
16. Edwards-Faret G, Munoz R, Mendez-Olivos EE, Lee-Liu D, Tapia VS, Larrain J (2017) Spinal cord regeneration in *Xenopus laevis*. *Nat Protoc* 12(2):372–389. <https://doi.org/10.1038/nprot.2016.177>
17. Karpinka JB, Fortriede JD, Burns KA, James-Zorn C, Ponferrada VG, Lee J, Karimi K, Zorn AM, Vize PD (2015) Xenbase, the *Xenopus* model organism database; new virtualized system, data types and genomes. *Nucleic Acids Res* 43(Database issue):D756–D763. <https://doi.org/10.1093/nar/gku956>
18. Gene Ontology C (2021) The Gene Ontology resource: enriching a GOLD mine. *Nucleic Acids Res* 49(D1):D325–D334. <https://doi.org/10.1093/nar/gkaa1113>
19. Ashburner M, Ball CA, Blake JA, Botstein D, Butler H, Cherry JM, Davis AP, Dolinski K, Dwight SS, Eppig JT, Harris MA, Hill DP, Issel-Tarver L, Kasarskis A, Lewis S, Matese JC, Richardson JE, Ringwald M, Rubin GM, Sherlock G (2000) Gene ontology: tool for the unification of biology. The Gene Ontology Consortium. *Nat Genet* 25(1):25–29. <https://doi.org/10.1038/75556>
20. Kanehisa M, Goto S (2000) KEGG: Kyoto encyclopedia of genes and genomes. *Nucleic Acids Res* 28(1):27–30. <https://doi.org/10.1093/nar/28.1.27>
21. Kanehisa M (2019) Toward understanding the origin and evolution of cellular organisms. *Protein Sci* 28(11):1947–1951. <https://doi.org/10.1002/pro.3715>
22. Jassal B, Matthews L, Viteri G, Gong C, Lorente P, Fabregat A, Sidiropoulos K, Cook J, Gillespie M, Haw R, Loney F, May B, Milacic M, Rothfels K, Sevilla C, Shamovsky V, Shorser S, Varusai T, Weiser J, Wu G, Stein L, Hermjakob H, D’Eustachio P (2020) The reactome pathway knowledgebase. *Nucleic Acids Res* 48(D1):D498–D503. <https://doi.org/10.1093/nar/gkz1031>
23. Martens M, Ammar A, Riutta A, Waagmeester A, Slenter DN, Hanspers K,

- Miller RA, Digles D, Lopes EN, Ehrhart F, Dupuis LJ, Winckers LA, Coort SL, Willighagen EL, Evelo CT, Pico AR, Kutmon M (2021) WikiPathways: connecting communities. *Nucleic Acids Res* 49(D1):D613–D621. <https://doi.org/10.1093/nar/gkaa1024>
24. Matys V, Fricke E, Geffers R, Gossling E, Haubrock M, Hehl R, Hornischer K, Karas D, Kel AE, Kel-Margoulis OV, Kloos DU, Land S, Lewicki-Potapov B, Michael H, Munch R, Reuter I, Rotert S, Saxel H, Scheer M, Thiele S, Wingender E (2003) TRANSFAC: transcriptional regulation, from patterns to profiles. *Nucleic Acids Res* 31(1): 374–378. <https://doi.org/10.1093/nar/gkg108>
25. Hsu SD, Lin FM, Wu WY, Liang C, Huang WC, Chan WL, Tsai WT, Chen GZ, Lee CJ, Chiu CM, Chien CH, Wu MC, Huang CY, Tsou AP, Huang HD (2011) miRTarBase: a database curates experimentally validated microRNA-target interactions. *Nucleic Acids Res* 39(Database issue):D163–D169. <https://doi.org/10.1093/nar/gkq1107>
26. Thul PJ, Akesson L, Wiking M, Mahdessian D, Geladaki A, Ait Blal H, Alm T, Asplund A, Bjork L, Breckels LM, Backstrom A, Danielsson F, Fagerberg L, Fall J, Gatto L, Gnann C, Hober S, Hjelmare M, Johansson F, Lee S, Lindskog C, Mulder J, Mulvey CM, Nilsson P, Oksvold P, Rockberg J, Schutten R, Schwenk JM, Sivertsson A, Sjostedt E, Skogs M, Stadler C, Sullivan DP, Tegel H, Winsnes C, Zhang C, Zwahlen M, Mardinoglu A, Ponten F, von Feilitzen K, Lilley KS, Uhlen M, Lundberg E (2017) A subcellular map of the human proteome. *Science* 356(6340). <https://doi.org/10.1126/science.aal3321>
27. Giurgiu M, Reinhard J, Brauner B, Dunger-Kaltenbach I, Fobo G, Frishman G, Montrone C, Ruepp A (2019) CORUM: the comprehensive resource of mammalian protein complexes-2019. *Nucleic Acids Res* 47(D1): D559–D563. <https://doi.org/10.1093/nar/gky973>
28. Robinson PN, Kohler S, Bauer S, Seelow D, Horn D, Mundlos S (2008) The Human Phenotype Ontology: a tool for annotating and analyzing human hereditary disease. *Am J Hum Genet* 83(5):610–615. <https://doi.org/10.1016/j.ajhg.2008.09.017>



Live Cell Imaging of Dynamic Processes in Adult Zebrafish Retinal Cross-Section Cultures

Manuela Lahne and David R. Hyde

Abstract

Following retinal injury, zebrafish possess the remarkable capacity to endogenously regenerate lost retinal neurons from Müller glia-derived neuronal progenitor cells. Additionally, neuronal cell types that are undamaged and persist in the injured retina are also produced. Thus, the zebrafish retina is an excellent system to study the integration of all neuronal cell types into an existing neuronal circuit. The few studies that examined axonal/dendritic outgrowth and the establishment of synaptic contacts by regenerated neurons predominantly utilized fixed tissue samples. We recently established a flatmount culture model to monitor Müller glia nuclear migration in real time by two-photon microscopy. However, in retinal flatmounts, z-stacks of the entire retinal z-dimension have to be acquired to image cells that extend through parts or the entirety of the neural retina, such as bipolar cells and Müller glia, respectively. Cellular processes with fast kinetics might thus be missed. Therefore, we generated a retinal cross-section culture from light-damaged zebrafish to image the entire Müller glia in one z-plane. Isolated dorsal retinal hemispheres were cut into two dorsal quarters and mounted with the cross-section view facing the coverslips of culture dishes, which allowed monitoring Müller glia nuclear migration using confocal microscopy. Confocal imaging of cross-section cultures is ultimately also applicable to live cell imaging of axon/dendrite formation of regenerated bipolar cells, while the flatmount culture model will be more suitable to monitor axon outgrowth of ganglion cells.

Key words Zebrafish, Retina, Regeneration, Confocal microscopy, Live cell imaging, Retinal slice culture, Interkinetic nuclear migration

1 Introduction

The zebrafish offers a unique opportunity to study both the regeneration of retinal neurons produced from Müller glia-derived neuronal progenitors and the concomitant outgrowth and integration of axons into an existing neuronal network [1–4]. A few studies investigated the reestablishment of dendritic and axonal projections and the reinnervation patterns after killing specific cell types using a genetic cell ablation approach, ouabain to injure inner retinal

neurons, or intense light to damage photoreceptors [1, 4–7]. The dendritic and/or axonal/synaptic patterning were predominantly investigated using immunohistochemical approaches, except for Yoshimatsu et al. (2016; [1]), who employed two-photon live cell imaging of zebrafish larvae to examine whether surviving H3 horizontal cells adapted their innervation pattern following UV cone photoreceptor ablation. Larval zebrafish lend themselves to monitoring reinnervation of neurons or axon regeneration in vivo [1, 8]. However, larval fish retinas rapidly grow and remodel their axons and dendrites [9, 10]. Thus, it is unclear whether developmentally expressed factors contribute to a regenerative response in larval fish. In contrast to larval fish, in vivo retinal imaging approaches in adult zebrafish are currently limited to spectral domain optical coherence tomography (SD-OCT) or confocal scanning laser ophthalmoscopy (cSLO; [11–15]). While SD-OCT can detect aberrations within the different retinal layers following retinal damage, this technique cannot resolve details at a cellular level [11, 12, 15]. In contrast, cellular structures, such as microglial or Müller glial processes, and cell bodies, as well as cones and blood vessels, could be visualized in vivo in fluorescent reporter-expressing transgenic zebrafish lines using cSLO [14, 15]. Unfortunately, both SD-OCT and cSLO require anesthetized fish to be mounted without being immersed in water, and thus, these techniques are only viable to perform short-term imaging over a period of less than 10 min (including anesthetizing and mounting; [15]). However, the same fish can be revived and reimaged on consecutive days to obtain snapshots of cells/cellular structures over an extended period [11, 15].

Culturing adult zebrafish retinal flatmounts in tissue culture inserts immersed in six-well plates established that adult zebrafish retinal tissue can be maintained ex vivo [16]. However, retinal explants mounted in culture inserts are not amenable to confocal/multiphoton live cell imaging. We recently developed an approach to culture flatmounted dorsal retinal explants from adult zebrafish on glass bottom dishes and established conditions to perform two-photon microscopy. Using this approach, we monitored the migration of Müller glia nuclei along the apicobasal axis in phase with the cell cycle (interkinetic nuclear migration) following light damage-induced photoreceptor injury [17, 18]. However, imaging of retinal flatmounts has some limitations: (1) light scattering occurs in deeper layers, which requires adjusting laser/gain intensities, or imaging is prevented when using dim-fluorescing transgenic lines and (2) cellular processes with fast dynamics, such as calcium signaling events, might be missed in Müller glia, which extend throughout the entire thickness of the retina. Therefore, this requires imaging of the entire z-stack, which consequently takes several minutes depending on image settings. In contrast, a

retinal cross-section view would allow imaging of Müller glia in one z-plane, thereby reducing the acquisition time and enabling imaging of cellular processes with faster kinetics. Acute retinal slices from different species have been employed for patch clamp and short imaging experiments [19–24]. Recently, a retinal slice culture model from postnatal mice was also developed to facilitate live cell imaging [25]. Thus, we developed an approach to produce a retinal cross-section preparation using a scalpel blade [19, 26] to cut a dorsal retinal hemisphere mounted in agarose into two quarters, which were subsequently mounted with the cross-section view facing the bottom of a glass culture dish or a coverslip of a two-well chamber. We utilized this culture system to monitor interkinetic nuclear migration in retinal cross-sections from light-damaged *Tg[glap:nGFP]mi2004*; *Tg[her4.3:dRFP]knu2* double transgenic zebrafish (35-h light damage) using a confocal microscope equipped with 488 and 561 nm lasers and a Perfect Focus System to prevent focal drift. While multiphoton microscopy has the advantage of reduced photobleaching/phototoxicity and an extended z-imaging range, we chose the confocal microscope for several reasons: (1) an ability to image different fluorescent reporters including RFP, which is not efficiently possible on all multiphoton systems, (2) the ability to employ the Perfect Focus System (PFS) to overcome drift issues, which utilizes a 870 nm infrared laser, thus preventing imaging using 910 nm laser light as previously published [17, 18], and (3) the general availability/pricing of confocal microscopes versus multiphoton microscopes.

The establishment of culture and imaging conditions for both retinal flatmounts and slices not only enables investigating the mechanisms underlying interkinetic nuclear migration but also provides options to examine different newly generated neurons live during retinal regeneration. The imaging approaches will be amenable to examining axonal and dendritic outgrowth in the regenerating zebrafish retina if suitable transgenic lines, for example, those required for cell type specification, are employed [7]. As an example, axonal outgrowth of ganglion cells and their fasciculation could be assessed in retinal flatmount cultures from *Tg[atoh7:GFP]rw21* zebrafish [7], as imaging of only a few z-planes or a relatively small z-stack might be required. In contrast, retinal slice cultures may be better suited to investigate bipolar cell behavior, as these cells expand from the outer plexiform layer to the different strata of the inner plexiform layer. While exact conditions to examine axonal/dendritic outgrowth will have to be established, the development of imaging capabilities provides promising avenues to examine neuronal behavior live in the regenerating retina in the future.

2 Materials

2.1 Chemicals/ Solutions

1. 70% ethanol in double distilled water. Use the 70% ethanol to sterilize the tissue culture hood and to subsequently spray the wrapped serological pipettes, syringes, syringe filters, tubes, etc. before transferring the tools into the tissue culture hood.
2. System water: Aquarium salt (e.g., Crystal Sea, Marinemix) dissolved in reverse osmosis (RO) purified water—conductivity, 500–800 $\mu\text{S}/\text{cm}$. Adjust pH to 6.8–7.2 with sodium bicarbonate powder.
3. 0.2% 2-phenoxyethanol in system water.
4. 1 M CaCl_2 : Prepare 10 mL of 1 M CaCl_2 in double distilled water. Sterilize the outside of the 15 mL conical tube containing the 1 M CaCl_2 , before transferring it into the sterile tissue culture hood. Use a 0.2 μm pore-size syringe filter attached to a 10 mL syringe to sterilize the 1.0 M CaCl_2 solution, transferring it to a new sterile 15 mL conical tube. Store at 4 °C until use.
5. 1 M MgCl_2 : Prepare 10 mL of 1 M MgCl_2 in double distilled water and sterilize as described for CaCl_2 under Subheading 2.1, **item 4**. Store at 4 °C until use.
6. HBSS (CM): In the sterilized tissue culture hood, add sterile CaCl_2 and sterile MgCl_2 at a final concentration of 1 mM each to 1 \times Hank's balanced salt solution (HBSS) without calcium, magnesium, and phenol red. Store at 4 °C until use.
7. Culture medium: 50% 1 \times minimum essential medium (1 \times MEM) without phenol red, 25% HBSS (CM), 25% heat-inactivated horse serum, 10 units/mL penicillin, and 10 $\mu\text{g}/\text{mL}$ streptomycin (*see Note 1*).
8. 1% low melting point agarose: On the day of culturing, prepare a 1% agarose solution by melting 0.1 g low melting point agarose in 10 mL of 1 \times MEM without phenol red using a microwave. Make sure that the agarose is fully transparent and that all agarose particles have melted (*see Note 2*).

2.2 Dissection Tools/ Equipment

1. Binocular dissection microscope equipped with a dual gooseneck light source.
2. #5 forceps (e.g., Dumont).
3. Tweezers #5B, 11 cm, 45-degree-angled, 0.05 \times 0.01 mm tips (e.g., Dumont).
4. 1 \times McPherson-Vannas scissors, 7 cm, curved, 3 mm blade.
5. Carbon Steel Scalpel Blades, number 10, sterile (*see Note 3*).
6. Scalpel handle.

7. Chattaway spatula.
8. Lid of a 100 × 15 mm Petri dish (*see Note 4*).
9. 100 mL beaker.
10. Plastic spoon.
11. Paper towel.

2.3 Culturing

1. Glass bottom cell culture dishes (e.g., FluoroDishes, 35 mm, 23 mm well) or TC-treated, sterile cell imaging cover glasses with two chambers.
2. Tissue culture hood.
3. Tissue culture incubator set at 32 °C, 5% CO₂/air environment.
4. Serological pipettes (5 mL, 10 mL, 25 mL; sterile, single wrapped).
5. Pipette controller.
6. 1 mL pipette.
7. 200 µL pipette.
8. 10 µL pipette.
9. Sterile 1 mL pipette tips.
10. Sterile 200 µL pipette tips.
11. Sterile 10 µL pipette tips.

2.4 Confocal Microscopy

1. Confocal microscope equipped with 488 and 561 nm lasers and corresponding excitation and emission filters.
2. Heat and gas adjustable equilibration slide chamber with the option to exchange inserts.
3. Insert for round culture dishes or cover glass chambers.
4. Extra dishes/cover glass chambers to fill all the positions of the holder to prevent gas from escaping into the room.
5. Type A refractive index oil (*see Note 5*).

3 Methods

3.1 Light Damage Paradigm

1. Place transgenic *albino* zebrafish into an environment devoid of light for 14 days. The number of fish to be dark-adapted depends on the number of cultures required for the experiment and the technical skills of the experimenter. We typically use two to three fish. Maintain the temperature at 28.5 °C according to standard housing conditions [27] and continue normal feeding protocols (*see Notes 6 and 7*).

2. Place a tank with system water between two fluorescent lights (2800 lux [2, 17, 28]) to equilibrate the water temperature to reach 31–33 °C.
3. Transfer the dark-adapted transgenic *albino* zebrafish into the prewarmed tank and expose the zebrafish to constant intense light for 35 h (*see Note 8*).
4. Regularly monitor the zebrafish and ensure that the temperature is maintained at 31–33 °C.

3.2 Preparations on the Day of Culturing

1. Sterilize the tissue culture hood with 70% ethanol. Subsequently, sterilize the components/tools that are transferred into the tissue culture hood (e.g., bottles containing MEM and HBSS, pipettes, sterile pipette tips, etc.) also with 70% ethanol (*see Note 9*).
2. Let the solutions used for culturing acclimate to room temperature.

3.3 Retinal Isolation, Mounting, and Culturing

1. Euthanize one light-damaged transgenic zebrafish in a beaker containing 0.2% 2-phenoxyethanol (*see Note 10*).
2. Transfer the zebrafish onto a dry paper towel with a plastic spoon, positioning the fish in a lateral view with one eye accessible. Using a stereomicroscope, place the angled tips of the curved pair of forceps (#5, 45° angle) at the nasal and temporal sides of the eye, push them into the socket behind the eye, and cut the optic nerve to remove the eye. Transfer the eye onto the lid of a 100 mm Petri dish (*see Note 11*).
3. Under the stereomicroscope, position the eye with the pupil facing the bottom of the Petri dish lid, so that the optic nerve at the back of the eye can be accessed (Fig. 1a, b).
4. Cut the optic nerve close to the back of the eye with a pair of McPherson-Vannas scissors while holding/stabilizing the eye with a straight pair of #5 forceps (Fig. 1b, c). Use McPherson-Vannas scissors to remove excessive connective tissue covering the sclera.
5. With the back of the eye still facing upward, hold the eye between its dorsal and ventral sides using a pair of #5 forceps. To obtain the dorsal side of the eye, make an incision with the McPherson-Vannas scissors at the optic stalk, inserting one blade into the lamina cribrosa, and cut the eye (sclera + retina) along both the nasal and temporal axes of the eye (dotted line, Fig. 1c).
6. Using one pair of #5 forceps, hold the dorsal side of the retina at the cut edge where the cornea connects the ventral and dorsal retina. Place a second pair of #5 forceps on the ventral side and pull both hemispheres apart. Discard the ventral side

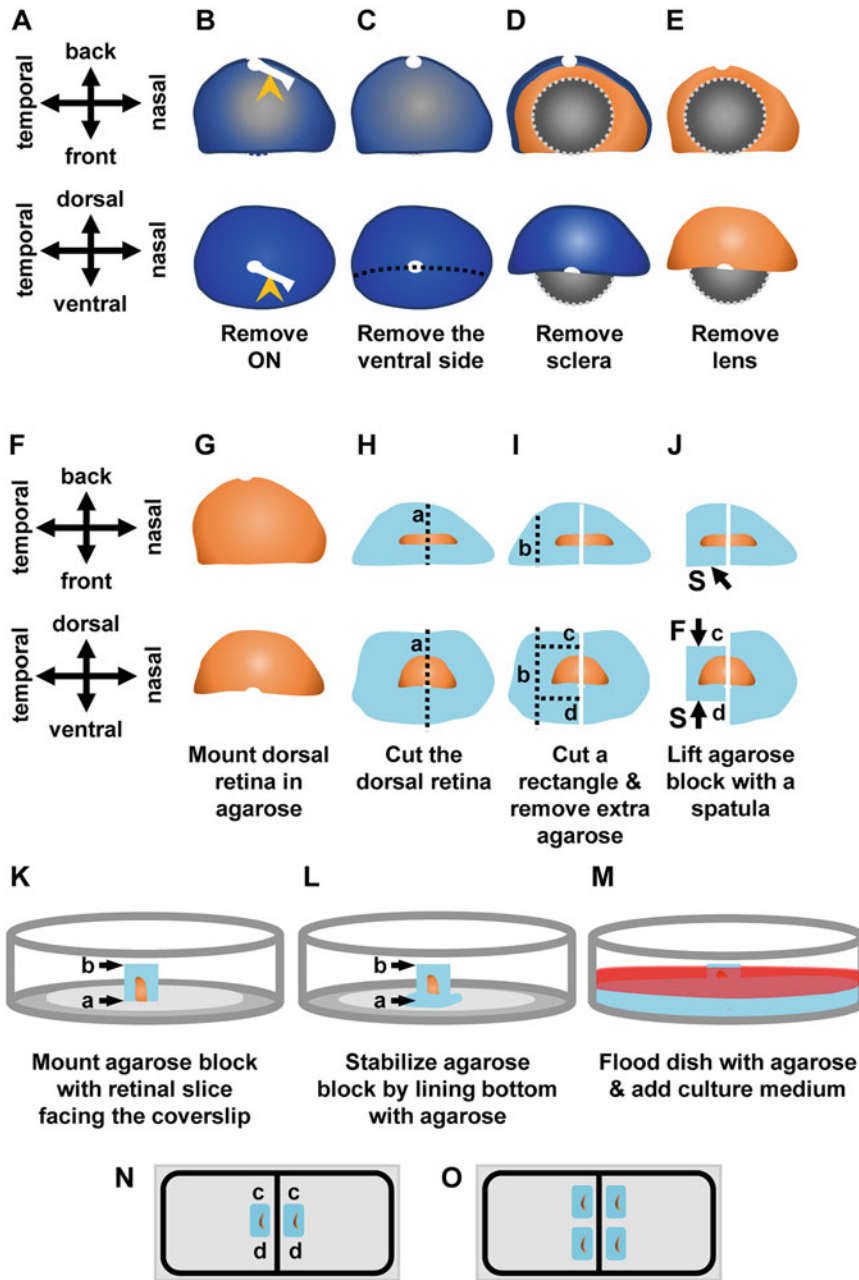


Fig. 1 Schematic of retinal isolation and preparation of retinal slice culture. (a, f) Arrows indicate the orientation of the eye/retina. (b–e, g) The zebrafish eye (blue, b–d)/retina (brown, e, g) is oriented with the front of the eye downward (top row) or viewing the back of the eye with the optic nerve (yellow arrowhead, bottom row). The optic nerve (ON, b) is cut, which reveals the lamina cribrosa/optic stalk (white disc, c). The ventral hemisphere is removed by cutting along the nasal and temporal axis (dotted line, c, bottom row), revealing the dorsal hemisphere with the lens visible (d). Subsequently, the dorsal retina is separated from the sclera (e) and lens (g) and flatmounted in agarose (h). The dorsal hemisphere is cut into two dorsal quarters from the dorsal margin toward the optic stalk (h, dotted line = cut side “a”). The agarose containing one dorsal quarter is cut into a rectangular shape (i, dotted lines = cut sides “b–d”) and the residual agarose is removed (j). The agarose block containing a dorsal quarter is lifted with a Chattaway spatula (“S” next to the

- and continue with the dorsal hemisphere (Fig. 1d). Alternatively, the cornea can be cut to remove the ventral hemisphere (*see Note 12*).
7. Hold the lens with a pair of #5 forceps to stabilize the attached retinal tissue in one place while removing the sclera with another set of #5 forceps (Fig. 1d, e).
 8. Carefully, without inflicting retinal damage, cut behind the lens with the McPherson-Vannas scissors to separate the lens from the retina (Fig. 1e–g). If the lens separated from the retina during an earlier dissection step, use one pair of straight #5 forceps to hold the retina at the cut edge, while the sclera is carefully pulled away with a second pair of straight #5 forceps.
 9. Flatten the dorsal retina on the Petri dish lid and add 300–500 μL of warm melted 1% low melting point agarose around and on top of the retina. It is ok that the retina lifts, as it is ideally positioned in the middle and center of the agarose, horizontally aligning with the bottom of the Petri dish lid (Fig. 1h). To position the retina within the agarose, use a pair of curved #5 forceps (45° angle), place the blades of the curved forceps at the nasal and temporal edges of the dorsal hemisphere, and carefully move the retina. If the retina remains at the bottom of the Petri dish, carefully lift the retina with the tips of the curved #5 forceps. While the agarose sets, the retina might need to be repositioned several times to remain in a horizontal position relative to the Petri dish lid. The pair of curved forceps may have to be held in position until the agarose begins setting (*see Notes 13–16*).
 10. While the agarose properly sets, isolate the retina of the opposite eye and mount it in the way described for the first retina (*see Note 17*).
 11. Once the retina of the second eye has been isolated and mounted, the agarose is typically well set and ready for cutting (*see Note 18*).
 12. Perform one cut using a rounded #10 scalpel blade, from the dorsal margin of the retina toward the optic stalk, splitting the dorsal hemisphere into two quarters (*see Fig. 1h*, dotted line

Fig. 1 (continued) arrow indicates the position of the spatula at cut site “d,” **j**), while a pair of forceps indicated by an arrow that is labeled with “F” (**j**) is used to stabilize the agarose block at cut side “c.” The agarose block is transferred to a tissue culture glass bottom dish and turned 90° to mount, so that the cut side of the retina (“a”) faces the cover glass (**k**). A small amount of agarose is added to attach the agarose block to the cover glass (**l**). Subsequently, agarose is added to the entire bottom of the culture dish and once set, culture medium is added (**m**). (**n**, **o**) Mounting suggestion for cover glass chambers when multiple retinal slices/agarose blocks are imaged during one time-lapse experiment. Letters in panels **k**, **l**, and **n** correspond to the cut sides indicated by the labeled dotted lines in **h** and **i**

labeled with “a”; [19, 26]). Ensure that you initially position the blade at an angle of at least 45° in relation to the agarose block and roll its rounded edge downward to the bottom of the dish, thereby carefully cutting the agarose and the tissue (*see* Fig. 1h, dotted line, and **Notes 19–21**).

13. For the first agarose half containing the retina, cut a rectangular/square agarose block (*see* Fig. 1i, dotted lines “b–d,” and **Notes 22 and 23**).
14. Remove the cut agarose pieces lacking retinal tissue to access the agarose block containing a dorsal retinal quarter. Slide the bent side of the Chattaway spatula underneath the agarose block (cut side “d”; Fig. 1i, j) while pushing the agarose against the sides of the #5 forceps positioned at cut side “c” (Fig. 1i, j) for stabilization.
15. Lift the agarose block and transfer it to the culture dish, turning the agarose block 90°, so that the retinal cross section faces the bottom of the cover glass of the culture dish (Fig. 1k) or the coverslip of the two-well culture chamber for use on an inverted microscope. A pair of forceps can be used to push the agarose block off the spatula and to adjust the position of the block (*see* **Notes 24 and 25**).
16. Add 10 µL of 1% agarose around the bottom of the agarose block to stabilize the position of the block. Repeat this several times to seal the bottom of the entire agarose block (*see* Fig. 1l and **Note 26**).
17. Once the agarose is set, cover the entire glass bottom culture dish or cover glass well chamber with 1% low melting point agarose. Let the agarose solidify and then carefully add 1.5 mL of culture medium (*see* Fig. 1m and **Notes 27–29**).
18. Transfer the retinal slice culture into an incubator with a 5% CO₂/air supply, which is set at 32 °C. Maintain the retinal slice culture in the incubator for 12 h to allow the retina to adapt to the culture conditions and to recover from the isolation (*see* **Note 30**).
19. Repeat **steps 13–17** for the second dorsal retinal quarter and **steps 12–17** for the opposite eye (*see* **Note 31**).

3.4 Imaging Interkinetic Nuclear Migration with an Inverted Confocal Microscope (See Note 32)

1. Insert the correct holder for either Petri dishes (glass bottom dishes) or slides (cover glass chambers) into the environmental chamber. To prevent gas leakage into the room, insert empty Petri dishes or cover glass chambers into the corresponding holder, while the chamber equilibrates to achieve a 5% CO₂/air atmosphere prior to imaging. Set the temperature to 32 °C.
2. Turn on the confocal microscopy system and, if the Perfect Focus System (PFS) is employed, move the dichroic mirror

slider (located next to the objective turret) to the “IN” position. Open the NIS-Elements image acquisition software and within it the “TiPad,” “A1 Compact GUI,” “ND acquisition,” “Scan Area,” and “LUT” windows, which are required to set up timelapse imaging of z-stacks.

3. In the “SETTING” field within the “A1 Compact GUI” window, select the correct filter combinations according to the fluorescent proteins expressed in the retinal sections or fluorescent probes employed. For example, for retinal slice cultures from *Tg[gfap:nGFP]mi2004*; *Tg[her4.3:dRFP]knu2* double transgenic zebrafish, select the 405/488/561 for the first dichroic mirror, and choose the 525/50 and 595/50 band-pass filters to acquire GFP and RFP fluorescence, respectively.
4. Set up the software for initial screening for adequate retinal slice cultures as follows: 512×512 images and a scan speed of 1 frame/second. Select “NORMAL” in the “A1 compact GUI” to image without averaging. Choose “CHANNEL SERIES” in the “A1 Compact GUI” to avoid bleed through between the different channels imaged (*see Note 33*).
5. After equilibration of the environmental chamber is completed, add refractive index liquid onto the $40\times$ plan-fluor oil immersion objective (N.A. 1.3) (*see Notes 34 and 35*).
6. Exchange the empty glass bottom dish/cover glass chambers in the equilibrated environmental chamber with those containing retinal slice cultures. Ideally, orient the glass bottom dishes, so that retinal slices are ultimately positioned either vertically or horizontally within the image field of view. Move the stage to coarsely position the agarose block containing the retinal slice into the light path using bright-field light. Subsequently, fluorescent light will more easily enable focusing on cells of interest within the retinal slice.
7. Initially, view the retinal slice through the eyepieces using epifluorescent light to briefly assess its overall integrity (*see Note 36*). Determine whether (1) the cells look healthy (*see Note 37*), (2) the slice is cut at the correct angle (*see Note 38*), (3) the surface of the slice is even (*see Note 39*), and (4) cells fluoresce according to the expected brightness (*see Note 40*). If the integrity of the slice is not satisfactory, move to a different retinal slice to assess its integrity.
8. Once an adequate retinal slice has been identified, scan a 512×512 image at a scan speed of 1 frame/second, and roughly adjust the *laser power*, gain (HV), and *pinhole* within the “A1 Compact GUI.” Confirm that the integrity of the retinal slice is satisfactory while focusing at different z-levels according to the criteria given under Subheading 3.4, **step 7**, and **Notes 37–40**.

9. To overcome focal drift during long-term imaging, the Perfect Focus System (PFS) can be employed. The PFS utilizes an 870 nm laser to maintain the focal position in relation to a reference plane, which corresponds to the refractive index boundary at the interface of the coverslip and the medium in which the specimen is immersed. However, the PFS has a limited working range and, therefore, it needs to be checked whether the mounted retinal slice is in the PFS range (*see Note 41*). Ensure that the PFS dichroic mirror is in the “IN” position. Focus the specimen close to the surface of the coverslip and then press the “ON” button at the front of the Nikon Eclipse Ti microscope. This might change the level at which the retinal slice is focused. Using the PFS offset controller (*see Note 42*), refocus if necessary, on the surface of the sample, and then assess the z-range that the slice can be imaged. If the tissue is out of the PFS range, check whether it works for a different retinal slice culture (*see Note 43*).
10. Once an adequate retinal slice is identified, reduce the frame size to 512×256 in the “Scan Area” window, choosing the “BAND SCAN AREA” function, which allows the width or height to be adjusted. If the retinal section is positioned at a diagonal or vertical angle, rotate (function located in the “Scan Area” window) the frame so that the maximal amount of the retinal cross section is imaged; however, image rotation may result in a smaller field of view that can be imaged (*see Notes 44–46*).
11. Adjust the laser power, gain, and pinhole settings. Utilize the “PIXEL SATURATION” function located in the “LUT” window to prevent over- and undersaturation of pixel intensities. Set different colors for over- and undersaturated pixels, which will only show in the image when pixels are either over- or undersaturated, respectively (*see Note 47*). For information on laser power, gain, and pinhole settings used for monitoring interkinetic nuclear migration, *see legends of Figs. 2 and 3*.
12. To set up the z-stack limits, choose the “Z” tab in the “ND acquisition” window and click the “RESET” button. When using the PFS, choose either the “SYMMETRIC” or “ASYMMETRIC” function in the “Z” tab. For the “SYMMETRIC” function, focus on the z-plane that resembles the center position of the z-stack in the region that you want to acquire, and click the “HOME” button and then the “RELATIVE” button (*see Note 48*). Set the range in the left “RANGE” field in the “Z” tab and choose the “STEP” size (*see Notes 49 and 50*). To check that the z-levels are satisfactory, double-click on the fields with the numbers next to the “VOLUME VIEW” in the “Z” tab, which correspond to the top, middle, and bottom focal planes of the z-stack (*see Note 51*).

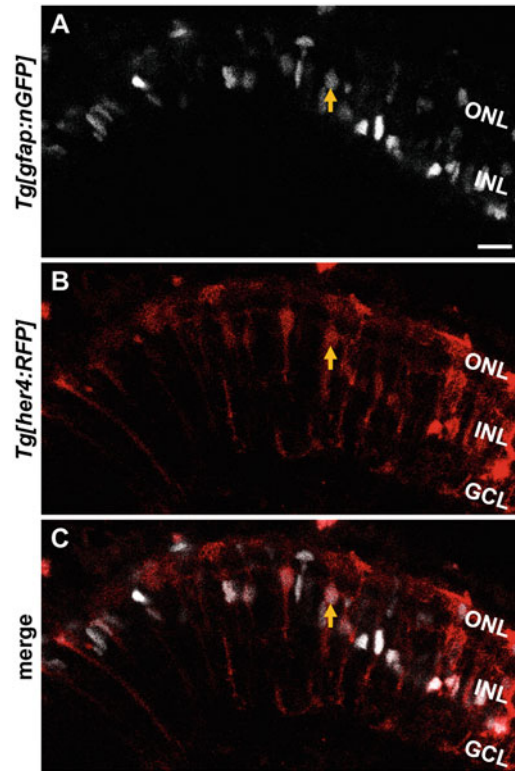


Fig. 2 Retinal slice culture from light-damaged *Tg[gfap:nGFP]mi2004; Tg[her4.3:dRFP]knu2* double transgenic zebrafish. (a, c) Expression of GFP in Müller glia nuclei from the *gfap* promoter and (b, c) a subset of these Müller glia express *her4.3*-driven RFP in retinal slice cultures prepared at 35 h of light treatment and cultured for 12 h. Images were acquired by confocal microscopy using a 40× oil objective and the following settings: 488 nm laser power, 0.5; HV (gain), 110; 561 nm laser power, 0.7; HV (gain), 121; pinhole, 3 airy units. Yellow arrows indicate the cell undergoing interkinetic nuclear migration displayed in Fig. 3. *GCL* ganglion cell layer, *INL* inner nuclear layer, *ONL* outer nuclear layer. Scale bar, 20 μm

13. Optional: Apply z-intensity correction to overcome pixel intensity loss in deeper z-layers (for instructions *see* Subheading 3.5 and Note 52).
14. In the “ND acquisition” window, select the “TIME” tab. Choose the “DURATION” and “INTERVAL” according to your experiment (*see* Notes 53 and 54).
15. If acquiring timelapse images of z-stacks in multiple positions, check the “XY POS” tab in the “ND acquisition” window. Initially, clear all previous positions (red “X”). Move to the XY position of interest and use the “+ ADD” button to set the first position. Subsequently, move to the next position of interest and push the “+ ADD” button again. If the position

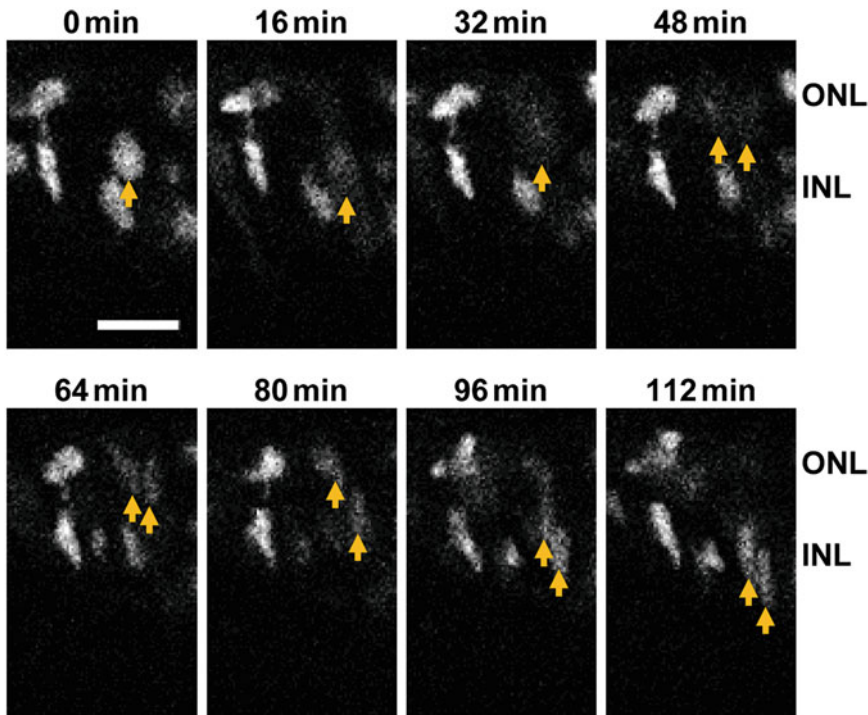


Fig. 3 Confocal time-lapse imaging of Müller glia nuclei in a retinal slice culture. Müller glia interkinetic nuclear migration (yellow arrows) was monitored in a retinal slice culture from *Tg[gfap:nGFP]mi2004; Tg[her4.3:dRFP]knu2* double transgenic zebrafish light-damaged for 35 h and subsequently cultured for 12 h before imaging. The yellow arrows mark the Müller glia nucleus that is undergoing mitosis to produce two neuronal progenitor cell nuclei. Note: Nuclear envelope breakdown, i.e., the onset of mitosis, begins based on the distribution of GFP throughout the cytoplasm, while the Müller glia is still located in the INL (16 min). However, the subsequent division into two neuronal progenitor cell nuclei occurs in the ONL (48 min), and these newly arising nuclei return to the basal INL (112 min). Live cell imaging was performed by confocal microscopy using a 40× oil objective (NA, 1.3), a 488 nm laser with the power set to 0.5 and the HV (gain) at 110, and the pinhole set to 3 airy units. *INL* inner nuclear layer, *ONL* outer nuclear layer. Scale bar, 20 μm

requires adjusting, move to the desired position and click the arrow in the table column “POINT NAME” for the selected position (*see Note 55*).

16. In the “A1 Compact GUI,” switch from “NORMAL” to line averaging twice (button: “∅ 2x”) (*see Note 56*).
17. Double-check that all the subwindows in the “ND acquisition” window are ticked (e.g., timelapse, z-stack, etc.) before starting the acquisition by clicking the “RUN NOW” button in the “ND acquisition” window. If the “z-intensity correction” function is employed, then click the “RUN z-CORRECTION” in the “ND acquisition” window instead.
18. Regularly monitor the sample as it is being imaged. If the power and gain levels require adjusting due to photobleaching, repeat **step 11**, or if z-intensity correction was applied, *see* Subheading 3.5, steps 3–5.

19. If the image plane shifts horizontally, pause or stop the image acquisition and refocus on the region of interest. Test if the z-position also needs to be readjusted (*see* Subheading 3.4, **step 12**). Importantly, as long as “RELATIVE z-CORRECTION” was set up initially, laser power and gain do not require readjusting in the “z-intensity correction” window, except if the sample was extensively photobleached.

3.5 Z-Intensity Correction to Overcome Pixel Intensity Loss in Deeper Z-Layers (See Note 52)

1. Open the “z-intensity correction” window by right-clicking into the software background. Choose “ACQUISITION CONTROLS” and then “z-intensity correction.”
2. First, the z-stack range needs to be imported or set. As the z-stack limits were set up according to the instructions under Subheading 3.4, **step 12**, choose “FROM ND” within the “z-intensity correction” window, which will transfer the z-stack data for the top, middle, and bottom planes. Note: Additional planes can be added according to need.
3. In the table of the “z-intensity correction” window, click on the bottom focal plane, which corresponds to the topmost layer and thus the brightest layer. In the “AI Compact GUI” window, choose the laser intensity and gain according to the desirable brightness, keeping in mind to maintain the laser power as low as possible to avoid photobleaching and phototoxicity.
4. Confirm the adjusted values for the chosen focal plane by clicking the “ARROW” next to the “z-VALUES” in the “z-intensity correction” window. The new values are displayed in the table under “DEVICE SETTINGS” within the “z-intensity correction” window.
5. Increase the laser power and gain for the middle and top planes and if applicable for those that were added.
6. Choose “RELATIVE INTENSITY CORRECTION” in the “z-intensity correction” window.

4 Notes

1. Phenol red autofluoresces and thereby adversely affects imaging by decreasing the signal to noise ratio [29]. Additionally, phenol red can modulate cell signaling pathways [30, 31].
2. Do not prepare large volumes of agarose as ion concentrations change due to fluid evaporation following repeated reheating. Additionally, larger volumes will take longer to cool to a usable temperature. A water bath set at 37–40 °C can be used to maintain the melted low melting point agarose at a constant temperature.

3. It is important that the blade has a rounded tip to improve the manipulations.
4. Both the lid and the bottom of the Petri dish can be used; however, because the lid has a smaller lip, the dissection tools can be held at a shallower angle.
5. Type B refractive index oil (e.g., from Cargill) is useful for imaging multiple positions.
6. Zebrafish in an *albino* background are used as photoreceptors are reliably damaged and die following exposure to constant intense light [2, 32]. Photoreceptor cells are more vulnerable in response to constant intense light exposure following dark-adapting zebrafish.
7. Transgenic zebrafish should be chosen according to the research question. For example, to image interkinetic nuclear migration, *Tg[gfap:nGFP]mi2004; Tg[her4.3:dRFP]knu2* double transgenic zebrafish were used that express GFP in the nuclei of all Müller glia and RFP in the cytoplasm of a subset of reprogrammed Müller glia. Nuclear expression of GFP allows tracking the nuclei in phase with the cell cycle, while the cytoplasmic localization of RFP allows the visualization of the entire Müller glia and gives an outline of the cross-section view.
8. The 35-h timepoint was chosen because the first Müller glia commence interkinetic nuclear migration at this time [17]. The timepoint, as well as the damage paradigm, can be adjusted according to the research question being investigated.
9. For culturing retinal explants, we expect that the experimenter possesses basic knowledge and experience in sterile culturing techniques and, therefore, we do not describe exact details of sterilization procedures in this protocol.
10. Euthanize only one fish at the time to obtain the most viable retinal slice cultures.
11. We do not transfer the eye into fluid to reduce the possibility that (1) fluid pockets develop when the dorsal retina is mounted in agarose and (2) fluid mixes with the agarose in localized areas, thereby locally reducing the agarose concentration. Both can affect successful cutting/slicing of the retina.
12. Only the dorsal hemisphere is kept because exposure to constant intense light damages the dorsal retina, while the ventral side remains predominantly intact [32, 33]. However, other damage paradigms such as exposure to NMDA or ouabain do not cause localized cell death, and consequently, the entire retina could be utilized for experiments (Hyde lab, unpublished observation).
13. Do not position the retina at the bottom of the lid or at the top of the agarose, as it will likely be pulled out of the agarose while slicing or transferring the retinal slice/agarose block into the culture dish.

14. If the agarose concentration is below 1%, the agarose is too soft and the retina pulls out of the agarose during slicing. Similarly, when the agarose concentration is too high, the agarose becomes too firm, and the pressure applied during slicing might damage the retina or also push it out of the agarose. It is possible to go up to 1.1% or 1.2% to stabilize the retina during slicing.
15. If the agarose is too fluid, i.e., too hot, then it will spread out, and the agarose mount becomes thin, which will make it more difficult to maintain an upright position of the agarose block (thickness ~0.4–0.7 cm) during mounting, which is described under Subheading 3.3, step 15.
16. If the retina is not positioned horizontally in regard to the nasal–temporal axis, the slice will be cut at an angle. In contrast, it is not as critical that the axis from the dorsal margin to the optic nerve head is aligned horizontally to the lid, as the agarose block can be rotated during mounting to position it within the culture dish.
17. If the isolation of the first retina takes a long time, the second eye might start to deteriorate, and it will be difficult to dissect the retina and to obtain usable slice cultures.
18. Make sure that the agarose does not dry out too much if the isolation procedure of the second retina takes too long.
19. For each experimental day, use a new scalpel blade. If many slice preparations are produced during one session, it might be advisable to change the scalpel blade.
20. The cut surface (cut side “a”; Fig. 1h) needs to be straight to obtain a cross-section view of the retina that is not at an angle.
21. Only cut the dorsal hemisphere once, as the retinal section is often pulled out of the agarose when cutting multiple (two to three) times.
22. The inside height of the culture dish has to be considered. For example, the height of the FluoroDish rim is 7.8 mm. Thus, the width between cut sides “a” and “b” (Fig. 1h, i) should be between 5 and 7 mm, as this represents the axis that is mounted upright. Additionally, when cutting sides “c” and “d” of the agarose block (Fig. 1i), it is advisable to not cut it too thin as the block might not be stable when turned upright.
23. If an upright microscope is used, cut side “b” (Fig. 1i) is the side that is mounted onto the coverslip and therefore has to be cut straight to ensure that the retinal cross section is not mounted at an angle.
24. The agarose block should not be adjusted too much by sliding it across the coverslip as that might render the position of the

retinal explant surface or pull the retina out of the agarose block.

25. When using an upright microscope, retinal slice cultures should only be mounted in culture dishes and not in coverslip chambers as the water dipping objective will not fit into the wells of the coverslip chambers and thereby prevent focusing on the tissue. Furthermore, the agarose blocks should be mounted in the middle of the culture dish to avoid the objective hitting the rim of the culture dish. Additionally, when cut “b” (Fig. 1i, dotted line b) is performed, two aspects have to be considered: (1) the height of the agarose block, i.e., the distance between cut sides “a” and “b” (Fig. 1h, i), in relation to the height of the culture dish to ensure that the retina can be covered with culture medium (*see* Subheading 3.3, step 17) and (2) the water dipping objective will displace some fluid when focusing on the sample, which could lead to fluid overflow if the fluid level is too high.
26. The agarose should not be too fluid/hot as it will run under the agarose block and that will reduce the visibility while imaging and decrease the range that can be used for imaging with the Perfect Focus System (PFS) function.
27. If the agarose did not properly solidify, then the addition of culture medium will rupture the agarose layer or lift the entire layer, rendering the culture unusable for imaging as pieces will float and thereby prevent maintaining the focal plane while imaging. Similarly, make sure that the agarose does not dry out.
28. The height of the culture dish needs to be considered when cutting the agarose mount in position “b” (Fig. 1i, dotted line “b”) to ensure that the retina is covered once culture medium is added.
29. Carefully add culture medium to the mounted retinal slices, which face away from the coverslip for use on an upright microscope. Avoid adding fluid directly onto the slice as the force might dislodge the retinal slice.
30. The temperature of 32 °C was chosen as zebrafish are maintained at this temperature during the light treatment.
31. Multiple agarose blocks containing a retinal slice preparation can be mounted in one glass bottom dish. For example, the two slice blocks from one dorsal retina if not even the four slice blocks from one fish can be mounted in one glass bottom dish. This however depends on how fast and careful the experimenter works. It is important that enough space is left between individual slice blocks so that they are not tipped over or slide together when adding 1% low melting point agarose with the 10 µL pipette. If multiple blocks are mounted, steps 17 and 18 under Subheading 3.3 will have to be omitted until the last

agarose block has been mounted. Reduce the amount of agarose added to cover the entire dish according to the number of slice blocks.

32. To image interkinetic nuclear migration of Müller glia/neuronal progenitor cells in retinal slice cultures from light-damaged *Tg[gfap:nGFP]mi2004; Tg[her4.3:dRFP]knu2* double transgenic zebrafish (Figs. 2 and 3), we used a Nikon A1R confocal microscope equipped with a 40× plan-fluor oil immersion objective and 488 and 561 nm lasers to acquire GFP and RFP, respectively. The functions employed in these experiments are common to other current confocal microscopes, though they may be named differently.
33. If there is no bleed through between two different channels, then the “CHANNEL SERIES” function is not required, which allows faster imaging if necessary, as both channels are acquired simultaneously. The ability to acquire light emitted from two spectrally different fluorophores simultaneously is an advantage when capturing processes with faster kinetics. Note: For the images presented in Figs. 2 and 3, we did not apply “CHANNEL SERIES.”
34. When alternating the imaging position to monitor multiple retinal slices at the same time, the use of higher viscosity refractive index oil (e.g., Type B refractive index oil, Cargill) should be considered to avoid separation of the oil between the objective and the cover glass while the XY position repeatedly changes between different slice preparations during timelapse imaging. It is advisable to test whether the use of the higher viscosity refractive index oil causes chromatic or focal aberrations in conjunction with the objective of choice on the experimenter’s microscope.
35. To reduce the possibility that the oil separates between the objective and the coverslip, the slices should be positioned as close as possible while considering the potential problems described in **Note 31**. When using coverslip chambers with two compartments, it is advisable to mount the slice/agarose blocks next to the chamber divider so that both slice cultures are positioned as close as possible (Fig. 1n, o).
36. Checking slice cultures for their overall integrity should be performed as quickly as possible to avoid photobleaching.
37. The loss of basal processes in retinal explants from undamaged or light-damaged *Tg[gfap:EGFP]nt11* (not used here) or *Tg[her4.3:dRFP]knu2* indicates that Müller glia might be unhealthy.
38. Indicators of slice cultures at an inappropriate angle are (1) the appearance of short interrupted Müller glial basal processes that cannot be scanned in the same focal plane, (2) Müller

glial processes surrounding more than one row of ganglion cells in the same focal plane, and (3) thickened ONL (not applicable for light-damaged retinas).

39. Accumulation of agarose under the agarose block during mounting can lead to the sample being mounted at an angle. This might, however, only become visible when scanning multiple z-planes and it will have to be assessed whether the retinal slice is acceptable for imaging.
40. Accumulation of agarose under the agarose block during mounting can lead to samples fluorescing dimly.
41. If multiple retinal slice cultures are imaged simultaneously, it needs to be checked that all of them are in PFS range.
42. The microscope focus controls are not working when the PFS is switched “ON.”
43. If the PFS “ON” button flickers on and off, adjust the focal level with the microscope focal control wheel until the PFS locks in and the button stays on continuously. At that point, only the external PFS offset controller works.
44. Typically, if the retina is cut at an optimal angle, the cross section of the retina will fit into the 512×256 frame.
45. Imaging the retinal slice at 512×256 will enable faster image acquisition.
46. If culture dishes are used, the position of the dish can be rotated within the environmental chamber to obtain an optimal angle that allows imaging the maximal image field of view. In glass coverslip chambers, the retinal slice cultures are ideally mounted with the slice positioned at a 90° angle relative to the chamber divider or in parallel (Fig. 1n, o).
47. The laser power should be as low as possible to avoid phototoxicity and photobleaching. Set the gain as high as possible without producing too much noise. Opening the pinhole is another way to allow additional light to pass and thereby reduce the laser intensity; however, confocality is lost, and hence more out of focus light is imaged (*see* Figs. 2 and 3 for settings).
48. Choosing the “RELATIVE” button will allow readjustments of the position during the timelapse run in case a horizontal shift occurs.
49. The step size depends on the size of the pinhole. For optimal 3D reconstructions, the suggested z-step size should be chosen; however, for some research questions, a larger z-step will provide sufficient information for analysis. A larger z-step size reduces the number of focal planes imaged and thereby the exposure of the specimen to laser light. Acquiring fewer z-planes also allows faster imaging, which might be useful when investigating cellular processes with faster dynamics.

50. We imaged a 30 μm z-stack at a step size of 1.5 μm (optimal step size: 1.025).
51. Avoid imaging the top of the slice that was cut and rather focus a few μm below the surface of the retinal slice.
52. To overcome loss of pixel intensity in deeper z-layers due to light scattering, the z-intensity correction functions can be applied.
53. We acquired 512×256 images approximately every 8 min for 4 h in two positions. The 8-min timeframe was chosen based on previous experiments using the two-photon microscope to image interkinetic nuclear migration of Müller glia/neuronal progenitor cells in retinal flatmounts [17, 18] and to reduce photobleaching.
54. We previously acquired images every 30 min of Müller glia undergoing interkinetic nuclear migration to reduce phototoxicity. However, using this acquisition interval, we often missed either the nuclear envelope breakdown, the cell division, or both. Consequently, it was difficult to identify with certainty the newly formed nuclei and to perform analysis of certain features of interkinetic nuclear migration, such as division type or velocities (Lahne & Hyde, unpublished data).
55. Do not set XY positions for multiple glass bottom dishes. The cover glass of the dishes is offset to the bottom of the metal place holder they sit on, and the objective remains in the same z-plane when switching between different positions. Consequently, if the position is switched, the objective will drive into the metal rim and thereby become damaged. Instead, image multiple slices within one glass bottom dish or, alternatively, utilize cover glass chambers. Besides two-well cover glass chambers, four- and eight-well cover glass chambers are also available.
56. Line averaging twice will reduce noise. While there are options to average more often, the experimenter will have to decide whether the kinetics of the process investigated will allow averaging more often. The experimenter also has to keep in mind that averaging more often will increase the likelihood of photobleaching and phototoxicity.

Acknowledgments

We thank the Freimann Life Sciences staff for their relentless efforts in caring and maintaining our zebrafish stocks, especially under the strenuous conditions we recently experienced. We appreciate the support provided by the current and previous members of the Optical Microscopy Core within the NDIIF, especially Sara Cole for feedback provided on aspects of this manuscript.

Funding

This study was supported by a grant from the National Eye Institute of NIH to DRH (R01-EY018417 and U01-EY027267) and the Center for Zebrafish Research, University of Notre Dame, Notre Dame, IN.

References

1. Yoshimatsu T, D'Orazi FD, Gamlin CR et al (2016) Presynaptic partner selection during retinal circuit reassembly varies with timing of neuronal regeneration in vivo. *Nat Commun* 7: 10590. <https://doi.org/10.1038/ncomms10590>
2. Kassen SC, Ramanan V, Montgomery JE et al (2007) Time course analysis of gene expression during light-induced photoreceptor cell death and regeneration in albino zebrafish. *Dev Neurobiol* 67(8):1009–1031. <https://doi.org/10.1002/dneu.20362>
3. Bernardos RL, Barthel LK, Meyers JR et al (2007) Late-stage neuronal progenitors in the retina are radial Muller glia that function as retinal stem cells. *J Neurosci* 27(26): 7028–7040. 27/26/7028 [pii]
4. McGinn TE, Mitchell DM, Meighan PC et al (2018) Restoration of dendritic complexity, functional connectivity, and diversity of regenerated retinal bipolar neurons in adult zebrafish. *J Neurosci* 38(1):120–136. <https://doi.org/10.1523/JNEUROSCI.3444-16.2017>
5. D'Orazi FD, Zhao XF, Wong RO et al (2016) Mismatch of synaptic patterns between neurons produced in regeneration and during development of the vertebrate retina. *Curr Biol* 26(17):2268–2279. <https://doi.org/10.1016/j.cub.2016.06.063>
6. McGinn TE, Galicia CA, Leoni DC et al (2019) Rewiring the regenerated zebrafish retina: reemergence of bipolar neurons and cone-bipolar circuitry following an inner retinal lesion. *Front Cell Dev Biol* 7:95. <https://doi.org/10.3389/fcell.2019.00095>
7. Lahne M, Brecker M, Jones SE et al (2021) The regenerating adult zebrafish retina recapitulates developmental fate specification programs. *Front Cell Dev Biol* 8:617923. <https://doi.org/10.3389/fcell.2020.617923>
8. Harvey BM, Baxter M, Granato M (2019) Optic nerve regeneration in larval zebrafish exhibits spontaneous capacity for retinotopic but not tectum specific axon targeting. *PLoS One* 14(6):e0218667. <https://doi.org/10.1371/journal.pone.0218667>
9. Mumm JS, Williams PR, Godinho L et al (2006) In vivo imaging reveals dendritic targeting of laminated afferents by zebrafish retinal ganglion cells. *Neuron* 52(4):609–621. S0896-6273(06)00801-4 [pii]
10. Schroeter EH, Wong RO, Gregg RG (2006) In vivo development of retinal ON-bipolar cell axonal terminals visualized in *nyx::MYFP* transgenic zebrafish. *Vis Neurosci* 23(5): 833–843. S0952523806230219 [pii]
11. Bailey TJ, Davis DH, Vance JE et al (2012) Spectral-domain optical coherence tomography as a noninvasive method to assess damaged and regenerating adult zebrafish retinas. *Invest Ophthalmol Vis Sci* 53(6):3126–3138. <https://doi.org/10.1167/iovs.11-8895>
12. Weber A, Hochmann S, Cimalla P et al (2013) Characterization of light lesion paradigms and optical coherence tomography as tools to study adult retina regeneration in zebrafish. *PLoS One* 8(11):e80483. <https://doi.org/10.1371/journal.pone.0080483>
13. DiCicco RM, Bell BA, Kaul C et al (2014) Retinal regeneration following OCT-guided laser injury in zebrafish. *Invest Ophthalmol Vis Sci* 55(10):6281–6288. <https://doi.org/10.1167/iovs.14-14724>
14. Bell BA, Yuan A, DiCicco RM et al (2016) The adult zebrafish retina: in vivo optical sectioning with confocal scanning laser ophthalmoscopy and spectral-domain optical coherence tomography. *Exp Eye Res* 153:65–78. S0014-4835(16)30315-3 [pii]
15. Bell BA, Xie J, Yuan A et al (2014) Retinal vasculature of adult zebrafish: in vivo imaging using confocal scanning laser ophthalmoscopy. *Exp Eye Res* 129:107–118. <https://doi.org/10.1016/j.exer.2014.10.018>
16. Kustermann S, Schmid S, Biehlmaier O et al (2008) Survival, excitability, and transfection of retinal neurons in an organotypic culture of mature zebrafish retina. *Cell Tissue Res* 332(2):195–209. <https://doi.org/10.1007/s00441-008-0589-5>
17. Lahne M, Li J, Marton RM et al (2015) Actin-cytoskeleton- and rock-mediated INM are

- required for photoreceptor regeneration in the adult zebrafish retina. *J Neurosci* 35(47):15612–15634. <https://doi.org/10.1523/JNEUROSCI.5005-14.2015>
18. Lahne M, Gorsuch RA, Nelson CM et al (2017) Culture of adult transgenic zebrafish retinal explants for live-cell imaging by multiphoton microscopy. *J Vis Exp* 120. <https://doi.org/10.3791/55335>
 19. Boos R, Schneider H, Wässle H (1993) Voltage- and transmitter-gated currents of all-amacrine cells in a slice preparation of the rat retina. *J Neurosci* 13(7):2874–2888
 20. Tian N, Hwang TN, Copenhagen DR (1998) Analysis of excitatory and inhibitory spontaneous synaptic activity in mouse retinal ganglion cells. *J Neurophysiol* 80(3):1327–1340. <https://doi.org/10.1152/jn.1998.80.3.1327>
 21. Frech MJ, Perez-Leon J, Wässle H et al (2001) Characterization of the spontaneous synaptic activity of amacrine cells in the mouse retina. *J Neurophysiol* 86(4):1632–1643. <https://doi.org/10.1152/jn.2001.86.4.1632>
 22. Tamalu F, Chiba C, Ishida AT et al (2000) Functional differentiation of ganglion cells from multipotent progenitor cells in sliced retina of adult goldfish. *J Comp Neurol* 419(3):297–305. [10.1002/\(SICI\)1096-9861\(20000410\)419:33.0.CO;2-X](https://doi.org/10.1002/(SICI)1096-9861(20000410)419:33.0.CO;2-X) [pii]
 23. Yu CJ, Gao Y, Willis CL et al (2007) Mitogen-associated protein kinase- and protein kinase A-dependent regulation of rhodopsin promoter expression in zebrafish rod photoreceptor cells. *J Neurosci Res* 85(3):488–496. <https://doi.org/10.1002/jnr.21157>
 24. Giarmarco MM, Cleghorn WM, Hurley JB et al (2018) Preparing fresh retinal slices from adult zebrafish for ex vivo imaging experiments. *J Vis Exp* 135. <https://doi.org/10.3791/56977>
 25. Barrasso AP, Wang S, Tong X et al (2018) Live imaging of developing mouse retinal slices. *Neural Dev* 13(1):23–018–0120-y. <https://doi.org/10.1186/s13064-018-0120-y>
 26. Perez-Leon J, Frech MJ, Schroeder JE et al (2003) Spontaneous synaptic activity in an organotypic culture of the mouse retina. *Invest Ophthalmol Vis Sci* 44(3):1376–1387. <https://doi.org/10.1167/iovs.02-0702>
 27. Kimmel CB, Ballard WW, Kimmel SR et al (1995) Stages of embryonic development of the zebrafish. *Dev Dyn* 203(3):253–310. <https://doi.org/10.1002/aja.1002030302>
 28. Conner C, Ackerman KM, Lahne M et al (2014) Repressing Notch signaling and expressing TNF α are sufficient to mimic retinal regeneration by inducing Müller glial proliferation to generate committed progenitor cells. *J Neurosci* 34(43):14403–14419. <https://doi.org/10.1523/JNEUROSCI.0498-14.2014>
 29. Coutu DL, Schroeder T (2013) Probing cellular processes by long-term live imaging – historic problems and current solutions. *J Cell Sci* 126(Pt 17):3805–3815. <https://doi.org/10.1242/jcs.118349>
 30. King BF, Liu M, Townsend-Nicholson A et al (2005) Antagonism of ATP responses at P2X receptor subtypes by the pH indicator dye, Phenol red. *Br J Pharmacol* 145(3):313–322. 0706187 [pii]
 31. Berthois Y, Katzenellenbogen JA, Katzenellenbogen BS (1986) Phenol red in tissue culture media is a weak estrogen: implications concerning the study of estrogen-responsive cells in culture. *Proc Natl Acad Sci U S A* 83(8):2496–2500. <https://doi.org/10.1073/pnas.83.8.2496>
 32. Thomas JL, Nelson CM, Luo X et al (2012) Characterization of multiple light damage paradigms reveals regional differences in photoreceptor loss. *Exp Eye Res* 97(1):105–116. <https://doi.org/10.1016/j.exer.2012.02.004>
 33. Vihtelic TS, Soverly JE, Kassen SC et al (2006) Retinal regional differences in photoreceptor cell death and regeneration in light-lesioned albino zebrafish. *Exp Eye Res* 82(4):558–575. S0014-4835(05)00257-5 [pii]



PCNA Staining of Retinal Cryosections to Assess Microglial/Macrophage Proliferation

Anna G. Lovel and Diana M. Mitchell

Abstract

Detection of the protein PCNA (proliferating cell nuclear antigen) is used to identify cells in the S phase of the cell cycle to indicate cellular proliferation. Here we describe our method to detect PCNA expression by microglia and macrophages in retinal cryosections. We have used this procedure with zebrafish tissue, but this procedure could be applied to cryosections from any organism. Retinal cryosections are subjected to a heat-mediated antigen retrieval step in Citrate Buffer, then immunostained with antibodies to label PCNA and microglia/macrophages, and counterstained for cell nuclei. After fluorescent microscopy, the number of total and PCNA+ microglia/macrophages can be quantified and normalized to compare across samples and groups.

Key words Microglia, Cell cycle, Proliferation, PCNA, Retina, Damage, Regeneration, Zebrafish, Cryosections, Immunostaining

1 Introduction

Many researchers using the zebrafish, as well as other animal models, will desire to detect microglial proliferation in response to retinal tissue and neuronal damage, as well as during subsequent tissue regeneration. PCNA (proliferating cell nuclear antigen) staining can be used to detect cells in S phase of the cell cycle directly in tissue samples to indicate cellular proliferation. Several anti-PCNA antibodies, produced in a variety of animal hosts, are commercially available. PCNA detection provides an alternative or parallel approach to that of nucleotide analog incorporation and detection using reagents such as EdU (5-ethynyl-2'-deoxyuridine) and/or BrdU (5-bromo-2'-deoxyuridine) to assess cellular proliferation. Staining for PCNA can be performed in conjunction with a microglia marker to visualize proliferating microglia, which can then be quantified in subsequent image analysis.

For immunodetection of PCNA in fixed tissues, an epitope/antigen retrieval step is required. The idea behind the need for antigen retrieval procedures to detect certain proteins is based on the thought that the epitopes of interest are often inaccessible (or masked) in the endogenous or post-fixation state of the tissue. By exposing the tissue to certain buffers and/or heat, the antigen conformation is changed such that the epitope is now exposed for antibody binding. Various procedures for antigen retrieval have been developed and may involve heat, acidic or basic buffers, enzymatic treatments, or combinations thereof. Each method of antigen retrieval poses unique challenges in regard to temperature maintenance, buffer toxicity/hazards, and the costs of reagents. We have had reliable success using the heat-mediated Citrate Buffer antigen retrieval procedure detailed here with zebrafish retinal cryosections to label PCNA in combination with a microglial marker. This has allowed us to visualize and to quantify microglial/macrophage proliferation in response to retinal damage [1] and during subsequent retinal regeneration [2] (Fig. 1). Of note, we have been able to reliably perform this procedure using a laboratory hot plate as the heat source, with no need for a pressure cooker, steamer, or specialized equipment. This facilitates monitoring of solution temperature and minimizes issues from solution boilover and evaporation. In addition, the Citrate Buffer Solution is relatively simple and economical to prepare.

The microglial marker of choice for co-label with PCNA needs to show a staining pattern that sufficiently labels the cytoplasm/cell body of microglial cells, so that individual PCNA+ nuclei can be assigned to individual microglia during image analysis. Two types of antibodies have been used most predominantly to detect microglia in zebrafish retinal tissue: antibodies to L-plastin (expressed in all leukocytes, including microglia) [1–5] and the antibody 4C4 (specific for a previously unknown antigen expressed by microglia, recently suggested to be Lgals3bp) [5–10]. Unfortunately, to date, not all antibodies used in published studies to label microglia are available commercially. Alternatives to using antibodies specific to endogenous molecules expressed by microglia include the use of transgenic zebrafish reporter lines in which microglia express fluorescent reporters. For example, transgenic lines that can be used in this manner include *mpeg1:GFP* and *mpeg1:mCherry* [11], both available from the Zebrafish International Resource Center (ZIRC). We and others have shown that *mpeg1*-driven reporters can be used to label microglia in zebrafish retina [1–3, 12]. However, it is worth noting that to date, zebrafish markers to distinguish microglia from infiltrating macrophages have not yet been identified or characterized. This is true for both the antibodies noted above and the *mpeg1* reporter lines. This should be thoughtfully

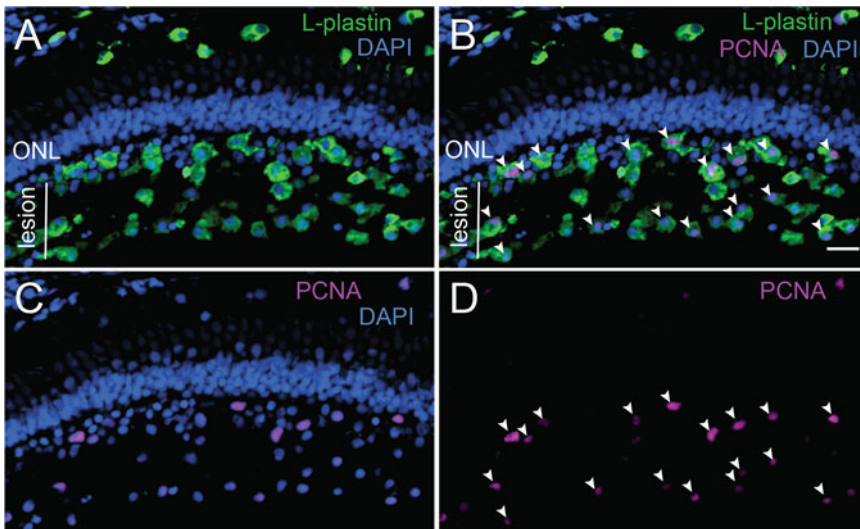


Fig. 1 Representative results from PCNA staining with the leukocyte marker L-plastin, using cryosections from damaged retinal tissue. Zebrafish retinas were lesioned by intraocular injection with 2 μ M of the neurotoxin ouabain, which leads to an injury response by microglia and macrophages, as previously shown in [1, 2]. This cytotoxic lesion results in death of neurons in the inner retina (indicated in **a** and **b** as “lesion”) while leaving the outer nuclear layer (ONL) intact. Whole zebrafish eyes were collected at 48 h post-lesion and processed to generate retinal cryosections. Following the procedure outlined in this chapter, retinal cryosections were stained for PCNA (magenta), the leukocyte marker L-plastin (to label microglia/macrophages, green), and DAPI (blue). Images were acquired by confocal microscopy. Images show (**a**) L-plastin and DAPI staining and (**b**) three-color merge to show PCNA localization to individual cell nuclei. (**c**) shows PCNA and DAPI, to demonstrate PCNA localization to cell nuclei. (**d**) shows PCNA signal only. Assignment of PCNA-positive microglia/macrophages is indicated by white arrowheads in **b** and **d**. Scale bar in **b** is 20 microns—applies to all images

considered by the investigator when designing and interpreting results of experiments. As discussed for antibody staining, when choosing a reporter line, it is important that the fluorescent reporter is cytoplasmic or located in the cell in a manner that will allow assignment of PCNA+ nuclei to microglia. In our experience, the heat-mediated Citrate Buffer antigen retrieval protocol described here destroys endogenous fluorescence from these reporter molecules, but commercially available antibodies to detect GFP and mCherry (or other fluorescent reporters) can be used to then co-label with anti-PCNA antibody during the immunofluorescence procedure.

Each investigator will need to determine the appropriate combination of antibodies to use in their study, which will depend on the availability to the investigator, the species used to produce the antibody, the choice of microglial label, as well as other factors.

2 Materials

Prepare all solutions using ultrapure water. Use analytical-grade chemicals. Note that some solutions can be made ahead of time and stored as indicated; others should be made fresh upon use.

2.1 Antigen Retrieval

1. 1× Citrate Buffer Solution: 10 mM sodium citrate with 0.05% Tween 20, pH 6.0 (*see Note 1*). Measure 950 mL of water in a graduated cylinder, and transfer to a glass bottle. Weigh out 1.921 g anhydrous citric acid and 0.8 g NaOH and add to the glass bottle. Mix until dissolved, using a stir bar. Bring pH to 6.0; then bring the total volume up to 1 L. Mix, then add 0.5 mL of Tween 20, and mix again. Smaller volumes can be prepared accordingly. Make the 1× solution fresh for each use.
2. Tall form heat-safe 200 mL glass beaker with slide rack.
3. Slides containing frozen retinal cryosections, prepared from tissue fixed in 4% paraformaldehyde (PFA) in sucrose solution, cut at 5–10 μm thickness. Store slides at –20 °C until use and bring to room temperature just before proceeding (*see Note 2*).
4. Thermometer, glass, with temperature range covering ~85–110 °C.
5. Laboratory hot plate with temperature control, stirrer not required. Alternatively, water bath that accurately maintains 95–100 °C temperature may be used.
6. Microwave oven.
7. Hot mitt, for handling the hot beakers.

2.2 Immunostaining of Cryosections

1. Humidified chamber(s) with slide holders (*see Note 3*).
2. Anti-PCNA antibody (e.g., mouse anti-PCNA clone PC10 (SantaCruz) or rat anti-PCNA (clone 16D10, ChromoTek).
3. Anti-L-plastin antibody (*see Note 4*).
4. Anti-GFP (ab13970, Abcam).
5. Anti-mCherry (GTX128508, GeneTex).
6. Secondary antibodies (F(ab')₂ format from Jackson ImmunoResearch, conjugated to selected fluorophore to detect the primary antibody species).
7. Antibody blocking buffer: In a 50 mL conical tube, add 5 mL 10× phosphate-buffered saline (PBS), 10 mL normal goat serum or normal donkey serum (*see Note 5*), and mix. Weigh out; then add 0.05 g sodium azide. Bring to 50 mL total volume with water. Mix well, then add 25 μL Triton X-100, and mix again. Store at 4 °C.

8. Antibody dilution buffer: Prepare in a 50 mL conical tube. Add 5 mL 10× phosphate-buffered saline (PBS), 0.5 mL normal goat serum or normal donkey serum (*see Note 5*), and mix. Weigh out; then add 0.05 g sodium azide. Bring to 50 mL total volume with water. Mix well; then add 250 μL Triton X-100. Mix well. Store at 4 °C.
9. 1× PBST wash buffer: 0.5% Triton X-100. Add 100 mL of 10× PBS and 895 mL of water to a 1 L glass bottle and mix. Add 5 mL Triton X-100 and mix. Store at 4 °C.
10. Coplin jars for slide washing.
11. DAPI stock solution of 1 μg/mL (*see Note 6*), for nuclear stain.
12. Coverslips, 60 x 22 mm size, 0.13–0.17 mm thickness.
13. Mounting medium: Several choices exist (*see Note 7*).
14. Forceps for handling slides.
15. Paper towels.
16. Laboratory tissues, e.g., Kimwipes.
17. Orbital mixer.
18. Liquid blocker pen (aka PAP pen; *see Note 8*).

2.3 Microscopy

A fluorescent microscope system with appropriate excitation and detection capabilities, with acquisition software. For thin sections (~5 microns), epifluorescence microscopy can be used for imaging, but sections thicker than 5 microns will need to be imaged using confocal microscopy (or other method) that can optically resolve individual cells.

3 Methods

3.1 Heat-Mediated Antigen Retrieval in Citrate Buffer

1. If using the hot plate method, determine the hot plate temperature setting (*see Notes 8 and 9*). This is best done before beginning the procedure.
2. Preheat the hot plate to pre-determined temperature that will maintain the hot 1× Citrate Buffer Solution at 95–100 °C. Alternatively, if using a water bath, bring the water bath to 95–100 °C and allow temperature to stabilize (*see Notes 9 and 10*).
3. Fill the glass tall form beaker with the 1× Citrate Buffer Solution and bring to a boil in the microwave. Handle the hot beaker with a hot mitt. Use the thermometer to check the temperature of the solution, microwaving again until the solution is 95–100 °C. Transfer the beaker with hot buffer to the heat plate (or, if using a water bath, transfer the beaker to the water bath and ensure the lip remains above the water level).

There may be a very small boil. Wait a few minutes, and use the thermometer to ensure that the temperature of the 1× Citrate Buffer Solution in the beaker is stabilized at 95–100 °C.

4. When the temperature is stabilized, remove slides with cryosections from the freezer and select those to use. Lay them flat, facing up on a paper towel and allow them to come to room temperature for approximately 10 min (*see Note 11*). Then, transfer them to the slide rack that fits into the tall form beaker.
5. Place the slide rack holding the glass slides containing cryosections into the beaker of hot 1× Citrate Buffer Solution. Ensure cryosections on slides are fully submerged. Also insert the thermometer into the beaker to monitor solution temperature. Incubate for 20 min and make sure to maintain the temperature at 95–100 °C. You may need to adjust the setting on the heat block occasionally, in order to maintain correct temperature.
6. After the heat incubation, remove the beaker from the heat plate or water bath (use the hot mitt to handle the beaker), and allow the solution to cool at room temperature for at least 20 min.
7. Proceed immediately with the immunofluorescence staining procedure.

3.2 Immuno-fluorescent Staining with Antibodies to Detect PCNA and Microglia

1. Transfer slides from the room temperature 1× Citrate Buffer Solution onto a clean paper towel. Wick away excess liquid on the slide surface; then use a PAP pen to draw a hydrophobic barrier around the slide border or tissue sections. Then, transfer the slides to the slide holders/supports within the humidified chamber.
2. Perform the blocking step: Add antibody blocking buffer to top of each slide so that sections are covered in liquid (~200–250 µL per slide). Put the lid securely on the humidified chamber and incubate at room temperature for 1 hour. Alternatively, blocking can be performed overnight at 4 °C.
3. Prepare dilutions of primary antibody to PCNA and primary antibody to detect microglia, in antibody dilution buffer (*see Note 11*). Calculate and prepare the volume of diluted antibody required using the estimate of ~200 µL of solution per slide. We use the following dilutions of primary antibodies: mouse anti-PCNA (1:200), rat anti-PCNA (1:200), chicken anti-GFP (1:1000), rabbit anti-mCherry (1:1000), and rabbit anti-L-plastin (gifted 1:10,000, GeneTex 1:50).
4. Gently pick up each slide using forceps and touch the slide corner to a dry paper towel to wick excess blocking buffer. Then, place each slide back on the holder/support in the chamber. Ensure slides are lying face up and flat.

5. Add the primary antibody solution to each slide (~200 μL per slide). Ensure that the liquid covers the slide surface. Take care that the container is lying flat in order to prevent the solution from running off of the slides. If desired, a small piece of parafilm cut to the size of the slide surface can be placed on top of the solution. Close the lid of the chamber securely and incubate overnight at 4 $^{\circ}\text{C}$.
6. Remove the unbound primary antibody as follows: Add 1 \times PBST wash buffer to Coplin jar(s). Remove the humidified chamber holding the slides from 4 $^{\circ}\text{C}$. Use the forceps to gently pick up each slide and touch the slide corner to paper towel, to wick excess buffer. Then, transfer each slide to the Coplin jar washing container; ensure slides are completely submerged. Place the Coplin jar with slides on an orbital mixer (set at ~50 rpm) for 30 min (minimum, can be up to a few hours) at room temperature.
7. Remove slides from the wash container using forceps or gloved hands; touch slide corners to paper towel to wick away excess wash buffer; then transfer each slide back to the chamber face up.
8. Prepare dilutions of secondary fluorophore-conjugated antibodies in antibody dilution buffer. We typically use secondary antibodies at 1:200 dilution (*see Note 12*). In addition, you may wish to include a nuclear counterstain in this solution mixture (*see Note 6*). We regularly use DAPI at 1:1000 dilution from a 1 $\mu\text{g}/\text{mL}$ stock at this step.
9. Add the diluted secondary antibody/nuclear stain mixture to slides (~200 μL per slide). Again, parafilm can be used to cover the liquid on the surface of the slide. Make sure slides and the container are lying flat. Close the lid on the chamber securely and protect from light at this step. You may place the container in a flat, dark location, or cover the container entirely with foil. Incubate for 1 hour at room temperature, or overnight at 4 $^{\circ}\text{C}$.
10. Repeat the wash step above (**step 6**), with fresh PBST. After the wash, remove slides from the wash container; touch corners to paper towel to wick; then transfer onto a clean paper towel on the lab benchtop.
11. Add mounting medium to the slide surface and coverslip (*see Note 13* for details and suggestions). Avoid air bubbles. If you are using a non-curing medium, seal the edges of the slide/coverslip border with clear nail polish.
12. Transfer the coverslipped slides on top of paper towels to a flat tray and place in a drawer (or other dark, level place) to dry at room temperature. For hardening mounting medium, sufficient curing generally takes 2–3 hours, but slides can be left in the dark for longer. Also consider time for drying of nail

polish if you used it to seal your slides, as well as storage conditions based on recommendations from the mounting medium supplier (*see Note 14*).

13. When ready to image, clean the slides by gently rinsing and wiping the back of the slide (not the coverslip!) with 70% ethanol and wiping with Kimwipes (*see Note 15*).

3.3 Imaging and Analysis

1. Use fluorescent microscopy to image your stained slides, detecting fluorescence based on the secondary antibodies used in the staining procedure, and to detect the nuclear counterstain. Prior to imaging, consider the thickness of your sections as well as regions of retina that you will image and analyze (*see Note 16*).
2. Using image analysis software (*see Note 17*), such as Fiji/ImageJ, open the individual image files. Brightness/contrast adjustments can be made to best visualize signal in each channel.
3. Determine a region for counting that can be standardized across all images or samples and/or that can be used for normalization (*see Note 16*).
4. In each image and the region chosen for quantification, count the number of DAPI-positive (DAPI+) nuclei within microglial cell bodies to determine the total number of microglia in the region of interest. Microglial cell bodies are determined by signal from the marker/label used to visualize microglia. Counting can be performed manually, though most image analysis software will have a feature/plugin for this purpose (e.g., cell counter plug-in available in Fiji/ImageJ).
5. Count the number of DAPI+ and PCNA+ nuclei within the microglial cells counted previously within the standardized region of interest.
6. Determine the fraction of PCNA+ microglia by dividing the number of PCNA+ microglia by the number of total microglia. Before determining this fraction, you may wish to first normalize the cell counts based on area, curvilinear distance, or other parameter.

4 Notes

1. We frequently make the 1× Citrate Buffer Solution for each use from a 10× stock of 100 mM sodium citrate solution, pH 6.0. The stock solution can be stored at room temperature for up to 6 months. Note that the 10× stock solution does not contain Tween 20; you will need to add the appropriate volume to achieve 0.05% Tween 20 final concentration to the 1× solution prior to use.

2. We have performed this heat-mediated Citrate Buffer antigen retrieval procedure and PCNA staining on retinal cryosections prepared from zebrafish whole eye tissue fixed in 4% paraformaldehyde (PFA) in sucrose phosphate solution. After cryopreservation and embedding, whole eye tissue was cryosectioned and adhered to glass slides. Slides containing retinal cryosections should be stored at -20°C until use. We have used this procedure with retinal cryosections ranging from 5 to 20 microns in thickness.
3. A chamber can be made from a Tupperware container with a flat bottom and tight-fitting lid, using water-soaked paper towels on each end to maintain humidity. Slides need to remain elevated from the bottom of the container and flat throughout all incubations. We have repurposed bamboo skewers for this use (placed in parallel on the bottom of the container), as well as plastic embedding base molds that can hold individual slides (similar to the 27,147 series from Ted Pella, Inc.). Alternatively, staining can be performed in Coplin jars filled with antibody solutions. This uses considerably larger volumes and therefore more antibody and is therefore substantially more expensive. Some labs have reported re-using the solutions over multiple procedures, but we have not tried this.
4. For labeling microglia, we have used gifted rabbit anti-L-plastin (from Dr. Michael Redd, University of Utah, not commercially available) with great success. We have had some success with rabbit anti-L-plastin available commercially (Cat. # GTX124420, GeneTex). Alternatively, one may find another source of antibody to label microglia in zebrafish.
5. Chose serum species based on the secondary antibody species to minimize background. For example, if secondary antibodies are generated in goat, then use normal goat serum. However, in practice, we have had success using goat serum with secondary antibodies produced in donkey and vice versa.
6. Alternatively, one may choose to include a counterstain in the mounting medium format (*see* **Note 7**). However, we have the most reliable nuclear staining results when we add the DAPI stain during **step 8** (Subheading **3.2**). Another option is to add the nuclear stain during the second wash step (Subheading **3.2**, **step 10**), though this results in a larger volume of hazardous waste to manage.
7. Choices for mounting medium include several options. We most frequently use VECTASHIELD Vibrance, in the hardening form without counterstain (e.g., VECTASHIELD Hard-Set, Vector Laboratories), which is self-curing and does not require sealing coverslip edges. In our experience, this product preserves fluorescent signal and slides can be stored in the dark

for several months for re-imaging later. There are many other mounting mediums from various suppliers that preserve signal but do not cure, so one must seal the edges of the coverslips on slides. In addition, several formats come with a nuclear counterstain, if desired. Glycerol can be used, but in our experience does not preserve signal; in addition, one must seal edges of coverslips on slides. Clear nail polish (not strengthener, which contains proteins that can increase autofluorescence) can be used for sealing, if needed.

8. PAP pens are used to draw a hydrophobic barrier around the slide edges, which keeps the solutions pooled and prevents liquid dripping off of the sides of the glass slides during incubation steps. These are available in different tip widths; we generally prefer the 5 mm width for edging the slides. If desired, one can draw a circle around the actual piece of tissue on the glass slide, rather than around the entire slide edge.
9. Maintaining an accurate temperature range and full saturation/submersion of the slides, during the heat-mediated antigen retrieval step, is necessary for good results. After pre-heating in the microwave, you will need to maintain the 1× Citrate Buffer Solution at 95–100 °C. We have found that it was worthwhile to purchase a tall form beaker with slide rack for this purpose (as noted in the material list). This also allows for a good number of slides to be processed together in the same batch. Alternatively, you can heat/submerge slides in a heat-safe glass beaker, keeping them separated, or use a heat-safe Coplin jar.
10. If using the hot plate method, then before starting the procedure, you will need to determine the hot plate settings that work best with your lab's equipment. The temperature setting can be determined with some trial and error beforehand, in which the pre-heated solution is placed on the hot plate and monitored for maintaining a 95–100 °C temperature range. It is also important to make sure that the slides with cryosections remain submerged in the solution and do not adhere to each other. Some solution will evaporate off during the procedure.
11. You may attempt using a PAP pen to create a hydrophobic border around the slide edge or sections, but the hot 1× Citrate Buffer Solution will cause most of it to fall off of the slide. Instead, you can add this barrier just before the blocking step (*see* Subheading 3.2, **step 1**) by using Kimwipes to wick away excess liquid and then drawing the border using the PAP pen.
12. Antibody dilutions for staining are determined based on supplier guidelines, information in the literature, as well as an individual investigator basis. You may need to determine the optimal dilution of each antibody if this information is not available.

13. You may attempt this in various ways. One method is to add ~3 small drops of mounting medium distributed across the slide surface (1 left, 1 middle, 1 right) and then gently place a coverslip on top. The mounting medium will move out and cover the slide surface under the coverslip. Another method is to place the coverslips on a paper towel, add the mounting medium dropwise to the coverslip, and then invert the slide with sections onto the coverslip. Regardless of method, avoid air bubbles and be careful not to use too much (can leak and stick to slide/coverslip surface) or too little (tissue sections will dry out) of the mounting medium.
14. Stained slides can be stored in a slide box, protected from light, before or after imaging. The length and duration of storage will depend on the mounting medium used and individual investigator's experience; follow the manufacturer's guidelines.
15. We often use a lab marker to circle the location of sections to find them more quickly when imaging. Circles are drawn on the coverslip.
16. There are several considerations prior to imaging and analysis. If your cryosections were cut thicker than 5 microns, you may need to use confocal microscopy (or another appropriate method) to resolve fluorescence from individual cells by acquiring a z-series to cover the tissue thickness and/or imaging single planes of focus. You may wish to quantify microglia along a curvilinear distance of the retina, and all or distinct retinal cell layers. Alternatively, or in addition, you may wish to count within a defined area of a region of interest, or in a particular retinal cell layer. You may be able to image entire, intact cryosections from the same region of the retina. In any case, you must be able to compare counts standardly across your samples and normalize counts in some way (such as per unit distance, unit area, or per entire cryosection). This needs to be considered before image acquisition as well as during image analysis.
17. Image analysis can be performed using suitable image analysis software. Fiji/ImageJ is freely available.

Acknowledgments

This work was supported by funding from Idaho INBRE NIH Grant P20 GM103408 and NIH Grant R01EY030467 to DMM. We thank Dr. Deborah Stenkamp for review of previous versions of the chapter.

References

1. Mitchell DM, Lovel AG, Stenkamp DL (2018) Dynamic changes in microglial and macrophage characteristics during degeneration and regeneration of the zebrafish retina. *J Neuroinflamm* 15:163. <https://doi.org/10.1186/s12974-018-1185-6>
2. Mitchell DM, Sun C, Hunter SS, New DD, Stenkamp DL (2019) Regeneration associated transcriptional signature of retinal microglia and macrophages. *Sci Rep-uk* 9:4768. <https://doi.org/10.1038/s41598-019-41298-8>
3. Blume ZI, Lambert JM, Lovel AG, Mitchell DM (2020) Microglia in the developing retina couple phagocytosis with the progression of apoptosis via P2RY12 signaling. *Dev Dynam* 249:723–740. <https://doi.org/10.1002/dvdy.163>
4. Conedera FM, Pousa AMQ, Mercader N, Tschopp M, Enzmann V (2019) Retinal microglia signaling affects Müller cell behavior in the zebrafish following laser injury induction. *Glia* 67:1150–1166. <https://doi.org/10.1002/glia.23601>
5. Walsh CE, Hitchcock PF (2017) Progranulin regulates neurogenesis in the developing vertebrate retina. *Dev Neurobiol* 77:1114–1129. <https://doi.org/10.1002/dneu.22499>
6. Rovira M, Misericocchi M, Montanari A, Hammou L, Chomette L, Pozo J, Imbault V, Bisteau X, Wittamer V (2022) Zebrafish Galectin 3 binding protein is the target antigen of the microglial 4C4 monoclonal antibody. *Dev Dyn*. <https://doi.org/10.1002/dvdy.549>
7. Craig SEL, Calinescu A-A, Hitchcock PF (2008) Identification of the molecular signatures integral to regenerating photoreceptors in the retina of the zebra fish. *J Ocular Biology Dis Informatics* 1:73. <https://doi.org/10.1007/s12177-008-9011-5>
8. Bernardos RL, Barthel LK, Meyers JR, Raymond PA (2007) Late-stage neuronal progenitors in the retina are radial Müller glia that function as retinal stem cells. *J Neurosci* 27:7028–7040. <https://doi.org/10.1523/jneurosci.1624-07.2007>
9. Silva NJ, Nagashima M, Li J, Kakuk-Atkins L, Ashrafzadeh M, Hyde DR, Hitchcock PF (2020) Inflammation and matrix metalloproteinase 9 (Mmp-9) regulate photoreceptor regeneration in adult zebrafish. *Glia* 68:1445–1465. <https://doi.org/10.1002/glia.23792>
10. Raymond PA, Barthel LK, Bernardos RL, Perkowski JJ (2006) Molecular characterization of retinal stem cells and their niches in adult zebrafish. *BMC Dev Biol* 6:36. <https://doi.org/10.1186/1471-213x-6-36>
11. Ellett F, Pase L, Hayman JW, Andrianopoulos A, Lieschke GJ (2011) mpeg1 promoter transgenes direct macrophage-lineage expression in zebrafish. *Blood* 117:e49–e56. <https://doi.org/10.1182/blood-2010-10-314120>
12. White DT, Sengupta S, Saxena MT, Xu Q, Hanes J, Ding D, Ji H, Mumm JS (2017) Immunomodulation-accelerated neuronal regeneration following selective rod photoreceptor cell ablation in the zebrafish retina. *Proc National Acad Sci* 114:E3719–E3728. <https://doi.org/10.1073/pnas.1617721114>



***Drosophila* Laser Axotomy Injury Model to Investigate RNA Repair and Splicing in Axon Regeneration**

Qin Wang, Shannon Trombley, Mahdi Rashidzada, and Yuanquan Song

Abstract

The limited axon regeneration capacity of mature neurons often leads to insufficient functional recovery after damage to the central nervous system (CNS). To promote CNS nerve repair, there is an urgent need to understand the regeneration machinery in order to develop effective clinical therapies. To this aim, we developed a *Drosophila* sensory neuron injury model and the accompanying behavioral assay to examine axon regeneration competence and functional recovery after injury in the peripheral and central nervous systems. Specifically, we used a two-photon laser to induce axotomy and performed live imaging to assess axon regeneration, combined with the analysis of the thermnociceptive behavior as a readout of functional recovery. Using this model, we found that the RNA 3'-terminal phosphate cyclase (Rtca), which acts as a regulator for RNA repair and splicing, responds to injury-induced cellular stress and impedes axon regeneration after axon breakage. Here we describe how we utilize our *Drosophila* model to assess the role of Rtca during neuroregeneration.

Key words Axon regeneration, Rtca, *Drosophila*, Sensory neurons, Behavioral assay, Functional recovery

1 Introduction

1.1 RNA Repair and Axon Regeneration

RNA posttranscriptional modification is a critical eukaryotic mechanism for regulating mRNA levels and increasing molecular diversification [1–3]. In neurons, it is a highly dynamic and conserved system, contributing to neuronal activity and plasticity [4–7]. Previous studies have revealed that regulating RNA repair and splicing is a powerful strategy for cells to respond to cellular stress [8–10] and that this machinery is activated after nerve injury [11, 12]. In 2015, the RNA ligase RNA 2',3'-cyclic phosphate and 5'-OH ligase (Rtcb) was reported to inhibit neuroregeneration after axon injury in *C. elegans* [13]. More recently, we showed that the RNA 3'-terminal phosphate cyclase (Rtca), which converts the RNA 3'-phosphate back to 2',3'-cyclic phosphate after RNA damage or splicing, is also implicated in axon regeneration in fly and mouse

[14]. We hypothesize that after axon injury, *Rtca* impedes axon regrowth by counteracting the *Rtcb* and *Archease* (its catalyst)-dependent RNA repair/splicing, with the cellular stress sensor *Xbp1* acting as their substrate [14, 15]. Reduction of *Rtca* via mutation or RNAi efficiently increases the regenerative capacity of axons, making it a potential target for treating central nervous system (CNS) injury. This finding reveals that the RNA repair and splicing pathway is important in mediating the injury-induced cellular stress and implicated in regulating axon regeneration. However, a broader picture of the link between RNA repair/splicing and nerve repair after traumatic injury remains poorly understood and warrants further study.

1.2 *Drosophila* Sensory Neuron Injury Model

Previous work has demonstrated that the axon regeneration programs, like many other fundamental physiological processes, are evolutionarily conserved from *Drosophila* to mammals [14, 16, 17]. The fruit fly *Drosophila melanogaster* is thus an ideal model to screen for and further study key genes that play a role in neuroregeneration, which may be targeted to improve functional restoration. Therefore, we have established a *Drosophila* sensory neuron injury model [17, 18]. *Drosophila* dendritic arborization (da) sensory neurons can be subdivided into four classes by their morphology, from class I to class IV [19, 20]. With their cell bodies and dendrites located in the periphery, all da neurons project their axons all the way through peripheral tissues to form synaptic connections in the ventral nerve cord (VNC), which is part of the CNS in flies. This pattern shares a high degree of similarity with the way dorsal root ganglion (DRG) neurons project their axons into the spinal cord in vertebrates. To gain spatial precision, we use a two-photon laser to induce sensory neuron axon breakage in fly larvae, thus restricting injury to a small point and preventing diffusive damage. Prior work from our lab revealed that these da neurons exhibit class-specific regeneration potential. While class IV da (C4da) sensory neurons (labeled by *ppk-CD4tdGFP*) are capable of regenerating in the periphery, class III da (C3da) sensory neurons (labeled by *19-12-Gal4 > CD4-tdGFP* or *nompC-QF > CD4tdGFP*) display limited regeneration potential after injury [17]. Notably, even for C4da neurons, their regeneration competence is significantly reduced if their axons are injured within the CNS. In this chapter, we describe how we utilize our *Drosophila* sensory neuron injury model to determine the role *Rtca* plays in axon regeneration.

2 Materials

2.1 Equipment

1. Stereomicroscope for screening larvae.
2. 25 °C incubator with light/dark cycle and humidity control for fly culture.

3. Confocal imaging system equipped with two-photon laser for axon injury and imaging (*see Note 1*).
4. Fume hood for larval anesthetization.
5. Forceps for picking and holding larvae (e.g., Dumont AA – Epoxy Coated).
6. Computer equipped with ImageJ and a statistics software package (e.g., GraphPad) (*see Note 2*).
7. Glass slides (75 × 25 mm) and coverslips (50 × 22 × 0.16–0.19 mm).
8. 6 oz square bottom *Drosophila* stock bottles.
9. Rayon balls (for wide vials).
10. 35 mm tissue culture dish (35 × 10 mm).
11. 60 mm tissue culture dish (60 × 15 mm).
12. 60 mm glass culture dish (60 × 15 mm).
13. Tissue paper (e.g., Kimwipes).
14. Heat probe with the temperature control unit.

2.2 Reagents

1. 0.5% propionic acid solution: Combine 5 mL of propionic acid with 995 mL H₂O.
2. Grape juice agar plates: Combine 200 mL grape juice, 10 g agar power, and 192 mL H₂O. Boil the solution until the agar is dissolved (about 5 min). Mix periodically and remove from heat when necessary to prevent boiling over. Naturally cool down to about 60 °C; then add 4.2 mL 95% ethanol and 4.0 mL glacial acetic acid. Mix solution thoroughly and add 3–4 mL to each 35 mm tissue culture dish. Dishes may be prepared in advance and stored under refrigeration for about a month.
3. Halocarbon 27 Oil.
4. Diethyl ether (≥99.0% pure) for larval anesthetization.
5. Yeast paste: Dissolve the active dry yeast powder in 0.5% propionic acid solution to make a paste. Gradually add 0.5% propionic acid until all yeast is dissolved, typically about a 1:1 acid to yeast ratio. Keep paste refrigerated when not in use and store for 2–3 weeks.
6. Vacuum grease.
7. CO₂ for adult fly anesthetization and collection, administered from compressed gas cylinders onto CO₂ pads or through CO₂ blowguns.

3 Methods

3.1 Collection of Larvae for Injury

1. Cut a hole in the wall (about 1/2" wide) of a 6 oz square bottom *Drosophila* bottle and fill the hole with a piece of a rayon ball. Carefully transfer five male flies together with ten virgin females into the bottle (*see Note 3*). Seal the bottle with a grape juice agar plate with a smear of yeast paste (yeast should cover about 1/5 of the grape juice agar plate's surface). Tape the agar plate into place.
2. Place the culture bottle bottom-up in the 25 °C incubator and exchange the agar plate with a fresh one every day (*see Note 4*). To change plates, gently tap the bottle on a hard surface until the flies fall to the bottom, quickly remove the tape, and use the adhesive of the tape to lift the plate from the bottle and replace with the new plate.
3. Prepare a 60 mm petri dish that contains 1/4 a piece of tissue paper soaked with 0.5% propionic acid (*see Note 5*). Place the older agar plate that was just removed into the petri dish. The fly embryos should be visible on the agar plate, typically around the yeast paste.
4. Cover and label the petri dish, and continue to incubate the plates at 25 °C for 48 h (*see Note 6*).

3.2 Laser Axotomy

1. Turn on the microscope and the two-photon laser; then open the imaging software. While using GFP to label the C4da neurons, set the two-photon laser at 930 nm. Set the maximum laser power to ~2000 mW.
2. Select the acquisition mode; maximize the scanning speed and pinhole. Set the laser intensity to 20% (~400 mW) and set gain to ~750.
3. Prior to injury, pick third instar larvae (*see Note 7*) from the plate, and transfer them to a clean grape juice agar plate without the yeast paste (*see Note 8*). It is best to lift larvae from the side or the posterior end. Let the larvae stay in the new plate for a while (about 2–3 min) until their skin is clean of yeast.
4. In the fume hood, place half a piece of tissue paper in a 60 mm glass dish and place a grape juice agar plate in the middle of the tissue.
5. Gradually add diethyl ether drop by drop into the glass dish until the paper is soaked with ether and liquid ether is visible in the dish, being careful to avoid spilling ether onto the agar plate.
6. Gently transfer a larva onto the plate; then cover the dish with a glass lid. Wait until the whole larva is motionless (including its mouth hooks) (*see Note 9*). Anesthetization will typically take anywhere from 30 s to about 5 min. Add more ether if

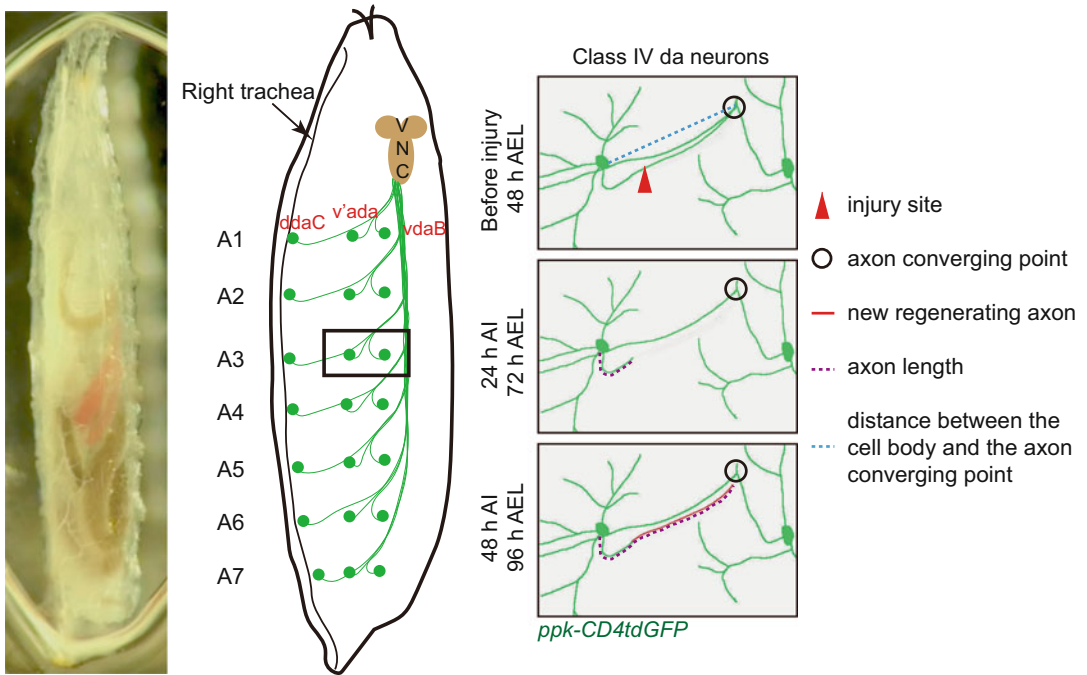


Fig. 1 The C4da neuron peripheral injury model. For C4da neuron injury, the larvae should be positioned on the microscope slide as shown, with the v'ada and vdaB neurons forming two columns down the middle of the larva. When injuring, use the crop function to target the area of the axon intended for injury, as shown by the red arrow. When imaging, capture the v'ada cell body, the entirety of the v'ada axon, and the converging point, as shown by the black circle. Images should look similar to the representative drawings of the 24 and 48 h AI timepoints

anesthetization time is long and the liquid ether has evaporated and is no longer visible in the dish.

7. Place a drop of halocarbon oil in the middle of a clean glass slide.
8. Place a small amount of vacuum grease in each of the four corners of the slide.
9. Carefully transfer the anesthetized larva to the slide. To injure the lateral C4da neurons v'ada, mount the larva ventral side up, with the right trachea barely seen on the left (*see Fig. 1* and **Note 10**).
10. Carefully place down a clean coverslip. Press lightly to make contact with the larva but be careful not to crush it (*see Note 11*). Do not press the coverslip flush with the slide because it becomes difficult to remove the coverslip after injury without killing the larva.
11. Place the slide under the microscope and locate the larva under the 10× objective. If needed, adjust the position of the larva by gently pushing the coverslip to make the v'ada neurons align slightly to the left of the middle line of the larva.

12. Turn to the 40× objective for injury. Because the larval tail is more sensitive to pain, it is highly recommended to injure the neurons in a posterior–anterior order.
13. Use the live scan mode to locate the *v*'ada neuron in the abdominal A7 body segment (*see Note 12*); then use crop to focus the scan window onto the target axon (typically 20–40 μm from the cell body) (*see Note 13*). The crop window should cover the width of the axon to ensure full transection, but not be so large as to cause excessive injury (*see Note 14*). Once cropped, open a new imaging tab.
14. Sever the axon, using a low scan speed (3–5) under the continuous mode, beginning with a laser intensity of 30% (~600 mW). Utilizing the continuous mode, wait until bright green lines are observed, which are an indicator of successful axon injury (*see Note 15*).
15. Return to the prior imaging tab and click “reuse.” Use the live mode to confirm that the target axon is completely transected (*see Notes 16 and 17*).
16. Once the A7 neuron is injured, move to the A6 body segment and repeat **steps 13–15** to injure the *v*'ada C4da neuron in this segment.
17. After injuring all the seven neurons (body segment A7–A1), carefully remove the coverslip, and place the larva in a new grape juice agar plate supplied with a small amount of yeast paste (much less than used for the cross, covering about 1/20 of the plate) (*see Note 18*). Make grooves in the agar to help keep the larva in the plate (*see Note 19*).
18. Put the plate in a 60 mm petri dish containing a piece of tissue paper soaked with 0.5% propionic acid.
19. Culture the larva at room temperature (*see Note 20*).

3.3 Post-injury Imaging

1. Prepare larvae for imaging by gently washing each larva to remove any yeast residue on the skin. Place the larva in a clean petri dish filled with PBS. Swirl the dish carefully and remove the larva using forceps (*see Note 21*).
2. Continue preparation of larvae for imaging by following **steps 4–10** of Subheading **3.2**.
3. Use the argon laser at 488 nm and adjust the gain to 700. For the pinhole, use 1–2 airy units (AU) (*see Note 22*).
4. Locate neurons using the 10× objective. If necessary, roll the larva into the correct position (*v*'ada neurons slightly to the left of the midline) by gently pushing the coverslip.
5. Once the neurons are positioned, switch to the 25× objective.

6. Image using the live scan and setting the Z stack first and last positions. Make sure to capture the v'ada cell body, the entirety of the v'ada axon, and the point where the ddaC axon converges with the ventral C4da neuron vdaB axon (the converging point) (*see* Fig. 1 and **Notes 23, 24, and 25**). Set the pixel dimensions to 1024×1024 , maximize the scanning speed, and click “start experiment.” If a neuron is not successfully injured, there is no need to image and this neuron should be excluded from analyses.
7. After imaging at 24 h AI (hours after injury), return the larva to its individual agar plate in the 60 mm petri dish. Culture at room temperature.
8. Repeat **steps 1–6** at the 48 h AI timepoint (*see* **Notes 26 and 27**).

3.4 Axon Regeneration Quantification

1. In ImageJ, open the images of the same neuron taken at 24 h and 48 h AI.
2. Use the segmented line tool to outline and measure (using the analyze drop-down menu or Ctrl + M) the length of injured axons (from the cell body to axon tip) and the distance between the cell body of the injured neuron and the axon converging point. The latter value is used to normalize the increased axon length to larval growth.
3. Calculate the regeneration index, defined as the increased axon length normalized to the distance between the cell body and the axon converging points, using the following formula: $\text{regeneration index} = \frac{L2}{D2} - \frac{L1}{D1}$, where $L1$ = axon length at 24 h AI; $L2$ = axon length at 48 h AI; $D1$ = the distance from the cell body of injured neuron to the axon converging point at 24 h AI; and $D2$ = the distance from the cell body of injured neuron to the axon converging point at 48 h AI (Figs. 1 and 2).
4. Calculate the regeneration percentage, defined as the percentage of neurons showing significantly elongated axons at 48 h AI compared with 24 h AI out of all the injured neurons. We assess whether an axon has regenerated visually, and, if needed, use dendrites as a reference (*see* **Notes 28, 29, and 30**).

3.5 Nociceptive Behavior Test

See **Note 31** before commencing the following steps.

1. As described previously, carefully place five male flies and ten virgin females into a culture bottle, and seal the bottle with a grape juice agar plate with a smear of yeast paste (*see* **Note 32**). Culture the bottles bottom up at 25 °C and change the agar plates daily.

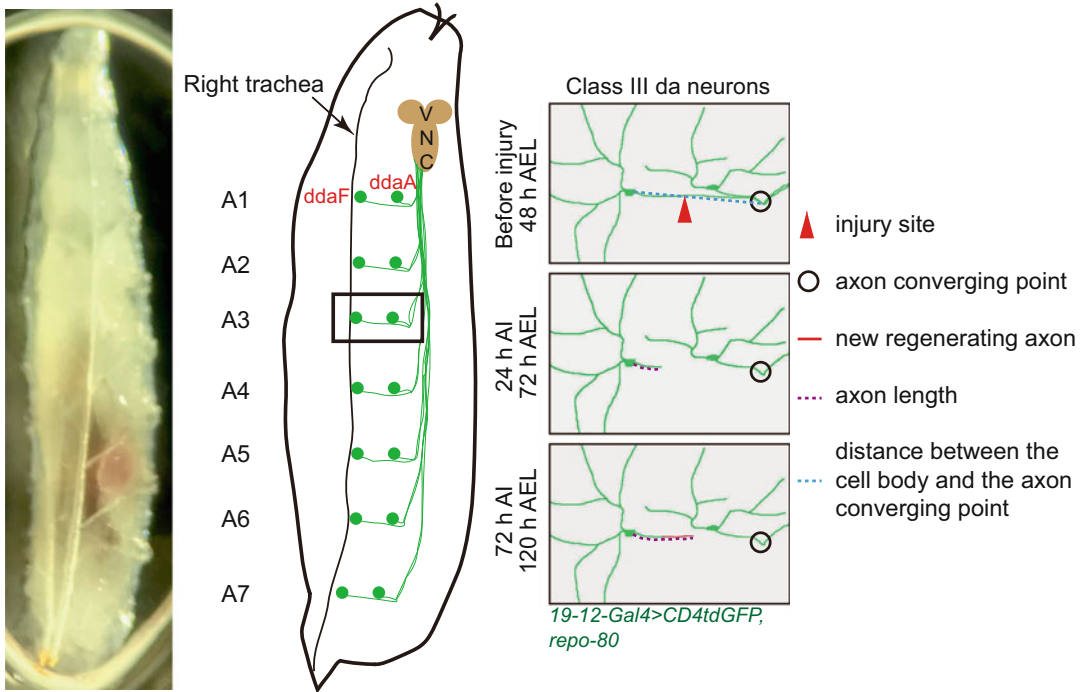


Fig. 2 The C3da neuron peripheral injury model. For C3da neuron injury, the larvae should be positioned on the microscope slide as shown, with the *ddaF* and *ddaA* positioned in the middle of the larva. When injuring, use the crop function to target the area of the axon intended for injury, as shown by the red arrow. When imaging, capture the *ddaF* cell body, the entirety of the *ddaF* axon, and the converging point, as shown by the black circle. Images should look similar to the representative drawings of the 24 and 72 h AI timepoints

2. Pick male larvae at 96 h after egg laying (h AEL) and transfer it to a slide ventral side up after anesthetization (Fig. 3).
3. In larvae, da sensory neurons project their axons into VNC and form a ladder-like structure in an anterior–posterior pattern, with each pair of axon bundles corresponding to one body segment (Fig. 3). Locate and injure the four axon bundles corresponding to A7 and A8 body segments, as described in Subheadings 3.2, steps 13–15. After injury, transfer the larva to a new agar plate supplied with a small amount of yeast paste, covering about 1/20 of the agar plate.
4. At 24 h AI, pick the larva from the plate and hold it up by the middle of its body with a pair of forceps (Fig. 4).
5. Perform a training session to allow the larva to acclimate to the stimulation paradigm. Apply a 47 °C heat probe onto the A7 and A8 body segments twice, each time for a duration of 5 seconds (s). Wait for ~10 s before proceeding.
6. Repeat three consecutive trials for each larva. In each trial, the 47 °C heat probe is applied at A7 and A8 body segments for 5 s. The interval between trials is 15 s.

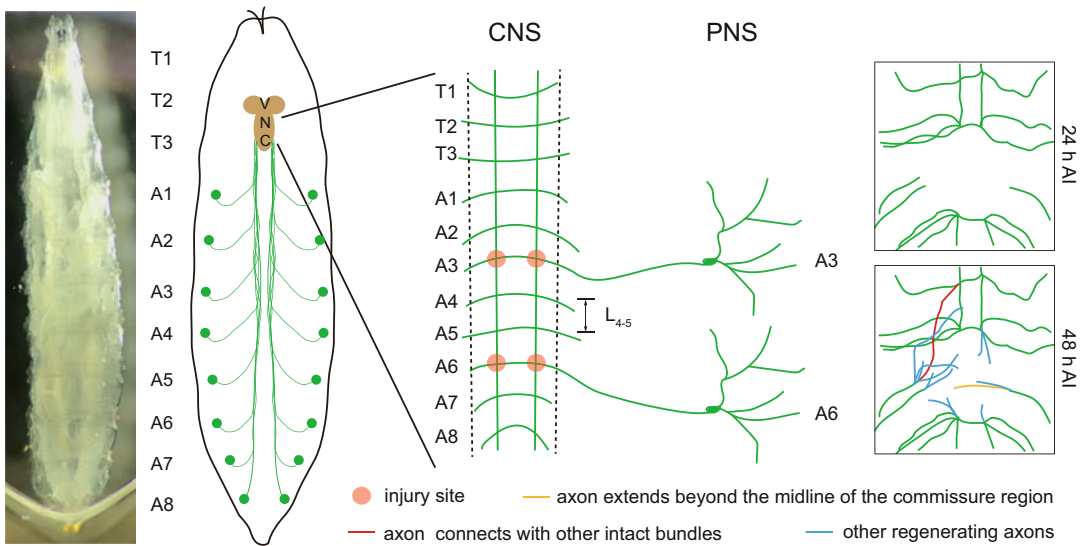


Fig. 3 The C4da neuron CNS injury model. For C4da neuron CNS injury, the larvae should be positioned on the microscope slide ventral side up so that the VNC will be positioned closest to the microscope lens. When injuring, use the crop function to target the area of the axon intended for injury, as indicated by the red circles. When imaging, capture three to four commissure segments that contain the injured segment. Images should look similar to the representative drawings of the 24 and 48 h AI timepoints

7. Score each trial as follows: Upon heat stimulation, if the larva's head rolls in a corkscrew-like way for more than two cycles, score the trial as "1." Otherwise score the trial as "0." Sum the scores of the three trials. If the A7 and A8 bundles are successfully ablated, the combined score should be below 1 at 24 h AI. If the larva has a combined score of 1 or higher, the A7 and A8 bundles were not successfully ablated, and the larva should be excluded from future calculations.
8. Repeat another three consecutive trials, this time with the same heat probe applied at the body segments A4 and A5. This is to ensure that all the uninjured larvae exhibit normal nociceptive responses to the heat probe when applied to intact body segments. If a larva gives no response to the heat probe in this part of the test, it should be excluded.
9. Return the larva to the agar plate. Repeat **steps 5–7** at 48 h AI. A larva is defined as recovered only when its combined score is below 1 at 24 h AI and increases to 2 or 3 at 48 h AI. Those failing to exhibit such improvement at 48 h AI are defined as unrecovered.
10. Calculate the recovery percentage. Recovery percentage = $\frac{\text{recovered larvae}}{(\text{recovered} + \text{unrecovered larvae})}$ (see **Note 33**).

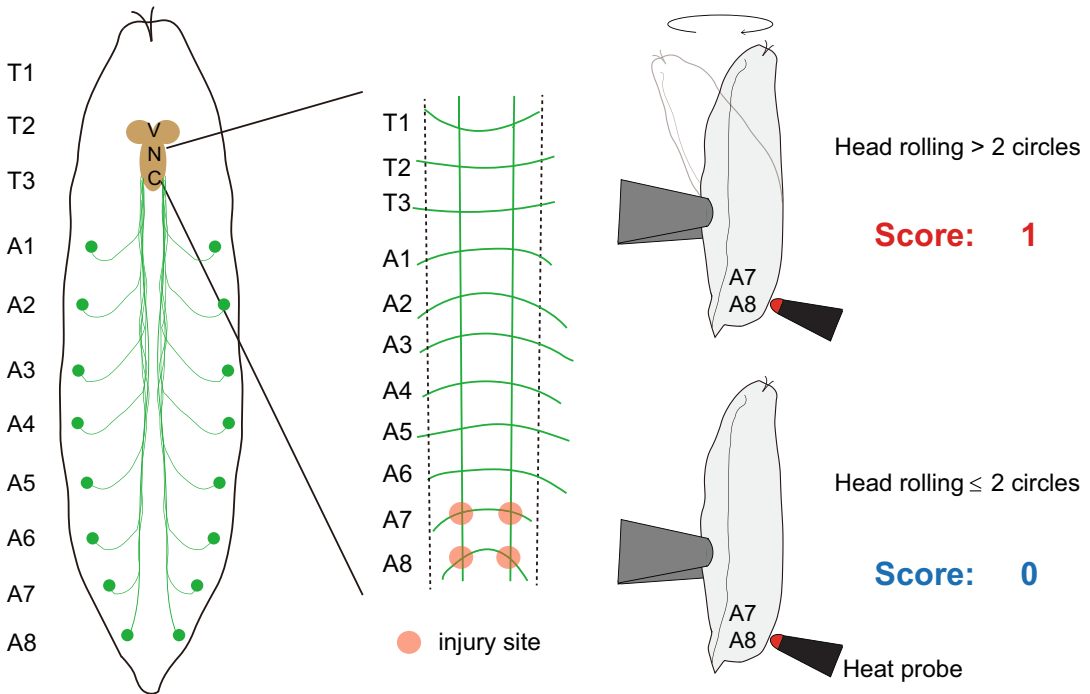


Fig. 4 Behavioral assay. For the behavioral assay, the four axon bundles corresponding to A7 and A8 (indicated by the red circles) of the larva's VNC should be injured at 96 h AEL. At 24 h AI, perform the training session and three consecutive trials. A response of head rolling behaviors for more than two cycles receives a score of 1, whereas two or less instances of head rolling behaviors receive a score of 0. Repeat these trials at A4 and A5, excluding any larvae that do not exhibit head rolling behavior. Repeat the trials for A7 and A8 at 48 h AI. A larva is considered recovered if they received a summed score of <1 at 24 h AI and it increases to 2 or 3 at 48 h AI

4 Notes

1. We use the Zeiss LSM 880 upright confocal microscope with the 488 nm argon laser and the Coherent Chameleon Ultra two-photon laser. The microscope is equipped with the following objectives: 10 \times /0.30 air, 25 \times /0.8 oil, and 40 \times /1.3 oil. The imaging software is Zen.
2. ImageJ is an image processing system that can also be used for quantification of regeneration. Fiji, the distribution of ImageJ needed for the purposes described in this protocol, can be downloaded at <https://imagej.net/Fiji/Downloads>. GraphPad is an analysis and graphing program used to run the following statistical tests: Fisher's exact test for comparing percentages (Fig. 5b, e, h, j), unpaired t-test between two groups (Fig. 5c, f, i), or two-way ANOVA among multiple groups (Fig. 5k).

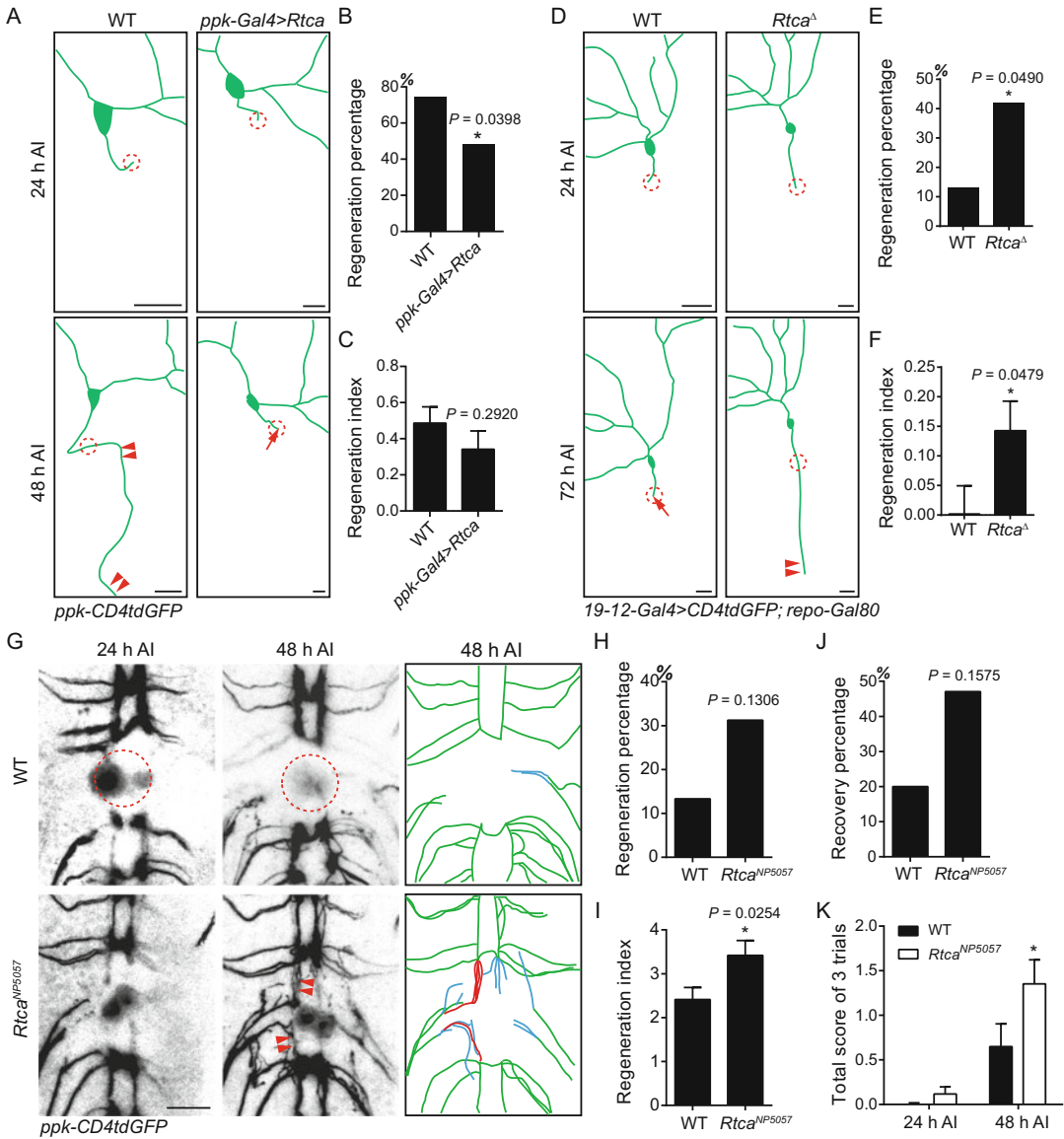


Fig. 5 *Rtca* inhibits axon regeneration. (a–c) C4da neuron-specific overexpression of *Rtca* causes decreased axon regeneration. $N = 36$, 27 neurons. Scale bar: 20 μm . (d–f) Axon regrowth is significantly increased in C3da neurons of *Rtca* mutant larvae. $N = 23$, 23 neurons. (g–i) *Rtca*^{NP5057} mutants exhibit enhanced axon regeneration in the CNS. $N = 30$, 32 commissure segments. Scale bar: 20 μm . (j–k) Reduction of *Rtca* promotes functional regeneration after CNS injury. $N = 20$, 17 larvae. The injury sites are marked by the dashed circles and regenerating axons are marked by arrowheads. Non-regenerating axons are labeled by arrow. Data are mean \pm SEM and analyzed by Fisher’s exact test (b, e, h, j), unpaired t-test (c, f, i), or two-way ANOVA followed by Sidak’s multiple comparisons test (k), $*P < 0.05$

3. The fly stocks we used to investigate the RNA splicing regulator *Rtca* in axon regeneration are listed as follows: (1) *UAS-Rtca*—the coding sequence of *Rtca* was cloned into the pACU2 vector; then the construct was injected into fly embryos. In the transgenic fly, *Rtca* is expressed under the control of the UAS-Gal4 system; (2) *Rtca*^{NP5057}, a loss of function allele of *Rtca* [14]; and (3) *Rtca*^Δ, a deletion allele [14]. To specifically label C4da sensory neurons and their axons, we cross the *Rtca*^{NP5057} or *Rtca*^Δ flies to *ppk-CD4tdGFP* [21]. *ppk* (*pickpocket*) encodes a sodium channel which is restricted to C4da neurons in flies; thus GFP will only highlight C4da neurons. For *UAS-Rtca* flies, we cross them to *ppk-CD4tdGFP*; *ppk-Gal4* [22] instead to express *Rtca* in C4da neurons at the same time. Similarly, we use *19-12-Gal4 > CD4tdGFP* [23], or *nompC-QF > CD4tdGFP* [24] to label C3da neurons. An example of a C3da cross would be crossing five *19-12-Gal4*, *UAS-CD4tdGFP*, *repo-Gal80/TM6B* males together with ten *Rtca*^Δ virgin females. A separate wild-type (WT) control cross will need to be made to compare each experimental group. Generally, we use *w1118* flies as WT. For the C4da control, cross five *ppk-CD4tdGFP*; *ppk-Gal4* males or five *ppk-CD4tdGFP* and ten *w1118* virgin females. For the C3da control, cross five *19-12-Gal4*, *UAS-CD4tdGFP*, *repo-Gal80/TM6B* males and ten *w1118* virgin females. When selecting females, try to pick flies that appear younger and healthier, as they are more likely to lay eggs and produce viable larvae. It is permissible if numbers of each sex vary slightly, but note that less larvae will be available with fewer virgin females utilized in the cross.
4. When collecting larvae, to ensure the larvae are of the same developmental stage, the plate can be changed every 2 h.
5. The propionic acid solution is used to maintain humidity in the dish and avoid the growth of mold.
6. To increase survival rate, we typically use 1 day older larvae for CNS injury than peripheral nervous system (PNS) injury, which means that after harvest, the plates need to be cultured at 25 °C for 72 h, rather than 48 h.
7. Third instar larvae are larvae that have emerged from eggs laid about 72 h prior and are about 1–2 mm long. These larvae are strong enough to survive injury, but are not so old that they will turn into pupae before the final imaging timepoint. If utilizing the C3da *Rtca*^Δ cross or the C4da *Rtca*^{NP5057} cross, male larvae must be used as the *Rtca* gene is located on the X chromosome and males are thus hemizygous for the *Rtca*^Δ allele by inheriting a single X chromosome from their mother. Male larvae can be distinguished by gonads, which are two translucent disc organs on the lower abdominal segments.

8. Selecting larvae that are too large can allow them to develop into pupae before the final imaging timepoint, while selecting larvae that are too small decreases their chances of survival.
9. The timing of anesthetization is very important. While precise site injury requires the larva to be still, excessive exposure to ether is harmful and even lethal. For peripheral injury, wait until the mouth hooks of the larva are motionless. For CNS injury, it is necessary to wait a little longer until the trachea is still, which indicates deeper anesthetization. However, to increase the survival rate, the anesthetization at 24 h AI needs to be brief. The larva can be imaged once its body stops moving.
10. If injuring C3da neurons instead, the positioning will be slightly different. The ddaF C3da neurons are positioned close to the trachea, so the larvae should be mounted dorsal side up, with the right trachea coinciding with the middle line of the larva (Fig. 2). If injuring the CNS, position the larvae ventral side up to place the CNS as close to the lens as possible (Fig. 3).
11. Occasionally, the larva will curl up in response to the ether and you will not be able to correctly position the larva with the forceps. In this case, get the larva as close to the correct position as possible, place the coverslip on as described, and gently roll the larva into the correct position.
12. The purpose of utilizing the live scan mode in this step is to locate the region of interest and find the neuron/axon we wish to injure, rather than taking the best quality image. Therefore, use the minimal settings sufficient to visualize the target area to avoid overexposure or photobleaching (typically a laser power of 20%, maximized scanning speed, and the pixel dimensions of 512×512).
13. When injuring C3da neurons, again begin in the A7 body segment and injure 20–40 μm from the cell body. For CNS injury, we injure different axon bundles for different purposes. For the regeneration assessment assay, we injure the A3 and A6 bundles for better assessment of axon regrowth while leaving A4 and A5 intact. The distance between A4 and A5 axon bundles will be measured to normalize axon regeneration to larval growth at 48 h AI (*see* Fig. 3). In the behavioral assay, we sever the two consecutive axon bundles at A7 and A8 to ensure the probe would not touch other parts of the larval body (*see* Fig. 4).
14. If possible, avoid injuring the axon from the dorsal C4da neuron ddaC, which travels in parallel to the v'ada axon.



Fig. 6 The autofluorescence is correlated with injury extent. Under the “Continuous” mode for axon injury, the appearance of a single (for peripheral axon injury) or a few (for CNS injury) green lines often indicates that the injury is successfully restricted to a small point, while multiple bright green lines may be caused by excessive injury and diffusive damage. The absence of any bright green line is associated with mistargeted or under injury

15. The laser power used for injury is dependent on the position of the neuron, the intensity of fluorescence, the condition of the larva’s skin surface, and many other factors. Therefore, each time when injuring a new larva, it is recommended to begin with a lower laser intensity, typically around 30%. Additionally, C4da sensory neurons are responsible for nociception, so they are more sensitive to pain and may twitch out of the way when attempting to injure the axons. Usually, we need to use a higher laser power to sever C4da neurons. On the other hand, C3da neurons are responsible for mechanosensation, thus they are less sensitive, and using a lower intensity (~20%) of the laser is possible for complete transection. As mentioned, C3da neurons exhibit limited regeneration capacity after injury and could be used to test pro-regeneration factors.

During injury, the appearance of the green lines (fluorescence spike) is due to autofluorescence at the injury site. When utilizing the continuous mode to injure the axon, over injury will be indicated by an excess of bright green lines, while under injury is indicated by an absence of any bright green line (Fig. 6). Each larva, and to an extent each neuron, will need a bit of trial and error to determine which laser power is appropriate for complete injury without excess. Starting with a lower laser power and gradually increasing it prevents over injury, thus increasing chances of survival. Typically for peripheral injury, a laser power of 30–40% is sufficient for injury, and rarely will a laser power higher than 55% be needed. However, compared with sensory neuron axons in the periphery, CNS axons in the VNC lay deeper in the tissue, so a higher intensity of the laser is needed to completely transect the axons. To avoid diffusive damage to the VNC, typically we start with ~50% intensity of the laser and then gradually increase the intensity until the axon bundle is completely ablated. For CNS injury, we commonly use 50–70% of the laser power, and even 100% is possible if needed.

16. If the axon is not injured or only partially severed, repeat **step 14** of Subheading 3.2, increasing the laser intensity increments of 5–10% with each attempt at injury. We typically do not attempt to injure a single neuron more than three or four times to improve chances of larva survival. In CNS injury, the laser is usually not sufficient to fully ablate the whole axon bundles in one attempt, so a second or even third scan is necessary. In this case, always use lower intensity (~40% intensity of laser) on subsequent scans to prevent damage to the surrounding tissue, which may decrease the chance of survival.
17. A good indication of successful injury is the appearance of a small crater, ring-like structure, or localized debris right at the injury site. In the case that the laser power is too high, a large damaged area will be visible in the post-injury live scan image. Too much injury may cause the death of the larva. Always be sure to assess the extent of injury in the live scan, and reposition your crop window in between each attempt at injury to avoid mistargeted injury.
18. Injured larvae are often much weaker than uninjured larva. Therefore, only a very tiny amount of yeast is necessary on the agar plate after injury and after 24 h imaging. Using large amounts of yeast can cause the larva to get stuck and decrease chances of survival.
19. After injury, it is permissible to keep two to three injured larvae in the same agar plate. After 24 h imaging, each larva should be kept in its own agar plate in separate petri dishes to easily keep track of each larva and compare 24–48 h images.
20. Leaving the larva at room temperature (~22 °C) after injury will allow the larva to remain in the larval stage for approximately an extra day compared to at 25 °C, increasing the chances for successful imaging at 48 h AI.
21. Be careful when removing the larva to not squeeze them. Try to lift the larvae from the PBS through adhesion, lifting from the posterior end.
22. Although a higher AU will increase the intensity of the fluorescence, it will also decrease the resolution of the image. For this reason, we try not to exceed 2 AU for imaging.
23. Axons may regenerate dorsally or ventrally and may also penetrate deep into the larvae, so be careful to capture the entire axon when cropping and setting the Z stack positions. Additionally, if the ddaC axon was accidentally injured, approximate the convergence point based on the curve in the vdaB axon.
24. For C3da neurons, when imaging, make sure to capture the ddaF cell body, the entirety of the ddaF axon, and the turning of the axon of neighboring C3da neuron ddaA (the converging

point) (Fig. 2). For CNS injury, we need to trace all regenerating axons. In most cases, the axons will regrow within the original commissure segment, so capturing A2–A7 axon bundles is enough. But occasionally, new axons will extend along the VNC and join upper axon bundles.

25. Because of the close proximity of the target injury area to the *ddaA* cell body in C3da injuries, the *ddaA* cell may often not survive injury. In this case, use the measurement from a neighboring *ddaF* cell and its converging point to normalize the regeneration length for this axon.
26. The regeneration competence of C3da neurons is much poorer than C4da neurons, so the larvae are imaged at 24 and 72 h AI to assess axon regeneration. If performing C3da injuries, note that anywhere in the protocol referencing 48 h AI will be the 72 h AI timepoint for these neurons.
27. The neurons are imaged at 24 h AI to verify complete transection of the axon, as well as for quantification purposes. The neurons are imaged at 48 h AI (C4da and CNS) and 72 h AI (C3da) to visualize and assess regeneration.
28. We define significantly elongated axons as axons that at 48 h AI have clearly regenerated beyond its initial length at 24 h AI, rather than axons that have simply grown in proportion with the larva's growth or shifted due to slight changes in positioning the larva. Examples of this may include clear elongation dorsally or ventrally or branching of the axons that had not previously been present. A useful way to visually assess regeneration is by utilizing dendrites as a reference. Dendrites grow proportionately with the larvae, so check if the regenerating axon has extended beyond dendrite branching that it had not previously at 24 h AI to determine if the axon is regenerating beyond normal larval growth. This method is most easily utilized with C4da neurons as they have widespread dendrite branches. An alternative way to assess regeneration or confirm your qualification is by evaluating the regeneration index after measuring the axon length at 24 and 48 h AI. A regenerating axon will have a regeneration index well over 0, and a non-regenerating axon will have an index close to, equal to, or below 0 (retracting axon). For example, a regeneration index of 0.3 or 0.4 shows significant regeneration, while a regeneration index of 0.02 would likely be considered a non-regenerating axon.
29. For CNS injuries, regenerating axons and regeneration index are defined and calculated differently. At 48 h AI, a commissure segment can be defined as regenerated only when at least one axon extends beyond the midline of the commissure region or joins into other intact bundles. Every commissure region is

evaluated as a whole and independent of each other. To quantify the extent of regrowth, we measure the length of all the regrown axons and normalize the sum to the distance between A4 and A5 axon bundles ($L4-5$ in Fig. 3).

$$\text{Regeneration index} = \frac{\sum \text{length of all regrown axons}}{L4-5}$$

30. Expected outcomes for each previously mentioned cross are as follows: *Rtca* overexpression impairs the regeneration competence in C4da neurons. At 48 h AI, although the regeneration index was comparable between WT and *Rtca* overexpressing neurons, the percentage of regenerating axons was significantly decreased to less than 50% in *Rtca* overexpressing neurons from the 70% of WT neurons capable of regenerating (Fig. 5a–c) [14]. Removal of *Rtca* enhances axon regrowth in the PNS. Loss of *Rtca* significantly promotes C3da axon regeneration (Fig. 5d–f) [14]. Compared with WT, in which only 13.00% neurons succeeded in regenerating, the regeneration percentage in *Rtca*^Δ C3da neurons was significantly higher, at 42.00%. Notably, the regeneration index also showed a remarkable increase, implying that *Rtca* is an intrinsic inhibitor to C3da axon regeneration. Reduction of *Rtca* promotes regeneration in the CNS. In WT, 13.30% of injured commissure segments displayed remarkable regrowth, while in *Rtca* mutants the percentage increased to 31.25%. Correspondingly, the regeneration index of the *Rtca*^{NP5057} larvae was significantly elevated compared with the WT (Fig. 5g–i), suggesting that removal of *Rtca* promotes axon regrowth in the CNS.
31. The nociceptive behavior test is used to assess functional recovery of regenerating neurons in the CNS through utilization of larval thermonociception [25]. C4da neurons are essential for larval thermonociception. Therefore, injuring A7 and A8 axon bundles in the VNC will cause an impaired nociceptive response to the heat probe at body segments A7 and A8, while the other body segments remain sensitive to the probe and will produce a stereotypical head rolling behavior upon stimuli.
32. An example cross would be five male *ppk-CD4tdGFP* flies and ten *Rtca*^{NP5057} virgin females. This cross allows us to evaluate the inhibitory role of *Rtca* in axon regeneration in the CNS, and subsequently functional recovery, by utilizing a loss of function allele of *Rtca*, *Rtca*^{NP5057}. This genotype has shown an increase in regeneration after injury in the CNS. A control will also need to be set up: cross five *ppk-CD4tdGFP* males and ten *w1118* virgin females into a separate bottle.
33. Expected results for the behavioral test of *Rtca* mutants are as follows: *Rtca* mutants display accelerated recovery from CNS injury. In the behavioral test, WT larvae picked up their

thermonociception slowly as they showed limited response to the heat probe at 48 h AI. In comparison, substantial recovery was observed in the *Rtca* mutant larvae. Their combined score of three trials at 48 h AI was significantly higher than that of the WT, and the percentage of larvae exhibiting behavioral recovery also showed a modest increase (Fig. 5j, k). Altogether, these results corroborate that the reduction of *Rtca* not only promotes axon regeneration after injury but also benefits functional recovery.

Acknowledgments

We thank members of the Song lab for helpful discussions. Y.S. is a recipient of the National Institute of Neurological Disorders and Stroke (NINDS) Pathway to Independence Award. This work was supported by an IDDRRC New Program Development Award (CHOP/Penn), an NINDS K99/R00 award (R00NS088211), an NIH grant (1R01NS107392), and a Craig H. Neilsen Foundation research grant to Y.S.

References

1. Dredge BK, Polydorides AD, Darnell RB (2001) The splice of life: alternative splicing and neurological disease. *Nat Rev Neurosci* 2(1):43–50. <https://doi.org/10.1038/35049061>
2. Matlin AJ, Clark F, Smith CW (2005) Understanding alternative splicing: towards a cellular code. *Nat Rev Mol Cell Biol* 6(5):386–398. <https://doi.org/10.1038/nrm1645>
3. Lareau LF, Inada M, Green RE, Wengrod JC, Brenner SE (2007) Unproductive splicing of SR genes associated with highly conserved and ultraconserved DNA elements. *Nature* 446(7138):926–929. <https://doi.org/10.1038/nature05676>
4. Zheng S (2020) Alternative splicing programming of axon formation. *Wiley Interdiscip Rev RNA* 11(4):e1585. <https://doi.org/10.1002/wrna.1585>
5. Su CH DD, Tarn WY (2018) Alternative splicing in neurogenesis and brain development. *Front Mol Biosci* 5:12. <https://doi.org/10.3389/fmolb.2018.00012>
6. Mao S, Zhang S, Zhou Z, Shi X, Huang T, Feng W, Yao C, Gu X, Yu B (2018) Alternative RNA splicing associated with axon regeneration after rat peripheral nerve injury. *Exp Neurol* 308:80–89. <https://doi.org/10.1016/j.expneurol.2018.07.003>
7. Raj B, Blencowe BJ (2015) Alternative splicing in the mammalian nervous system: recent insights into mechanisms and functional roles. *Neuron* 87(1):14–27. <https://doi.org/10.1016/j.neuron.2015.05.004>
8. Takechi H, Hosokawa N, Hirayoshi K, Nagata K (1994) Alternative 5' splice site selection induced by heat shock. *Mol Cell Biol* 14(1):567–575. <https://doi.org/10.1128/mcb.14.1.567>
9. Chandler DS, Singh RK, Caldwell LC, Bitler JL, Lozano G (2006) Genotoxic stress induces coordinately regulated alternative splicing of the p53 modulators MDM2 and MDM4. *Cancer Res* 66(19):9502–9508. <https://doi.org/10.1158/0008-5472.CAN-05-4271>
10. Meshorer E, Erb C, Gazit R, Pavlovsky L, Kaufer D, Friedman A, Glick D, Ben-Arie N, Soreq H (2002) Alternative splicing and neuritic mRNA translocation under long-term neuronal hypersensitivity. *Science* 295(5554):508–512. <https://doi.org/10.1126/science.1066752>
11. Hu Y, Park KK, Yang L, Wei X, Yang Q, Cho KS, Thielen P, Lee AH, Cartoni R, Glimcher LH, Chen DF, He Z (2012) Differential effects of unfolded protein response pathways on axon injury-induced death of retinal ganglion cells. *Neuron* 73(3):445–452. <https://doi.org/10.1016/j.neuron.2011.11.026>

12. Chen L, Liu Z, Zhou B, Wei C, Zhou Y, Rosenfeld MG, Fu XD, Chisholm AD, Jin Y (2016) CELF RNA binding proteins promote axon regeneration in *C. elegans* and mammals through alternative splicing of Syntaxins. *eLife* 5. <https://doi.org/10.7554/eLife.16072>
13. Kosmaczewski SG, Han SM, Han B, Irving Meyer B, Baig HS, Athar W, Lin-Moore AT, Koelle MR, Hammarlund M (2015) RNA ligation in neurons by RtcB inhibits axon regeneration. *Proc Natl Acad Sci U S A* 112(27): 8451–8456. <https://doi.org/10.1073/pnas.1502948112>
14. Song Y, Sretavan D, Salegio EA, Berg J, Huang X, Cheng T, Xiong X, Meltzer S, Han C, Nguyen TT, Bresnahan JC, Beattie MS, Jan LY, Jan YN (2015) Regulation of axon regeneration by the RNA repair and splicing pathway. *Nat Neurosci* 18(6):817–825. <https://doi.org/10.1038/nn.4019>
15. Vargas EJM, Matamoros AJ, Qiu J, Jan CH, Wang Q, Gorczyca D, Han TW, Weissman JS, Jan YN, Banerjee S, Song Y (2020) The microtubule regulator ringo functions downstream from the RNA repair/splicing pathway to promote axon regeneration. *Genes Dev* 34(3–4): 194–208. <https://doi.org/10.1101/gad.331330.119>
16. Song Y, Li D, Farrelly O, Miles L, Li F, Kim SE, Lo TY, Wang F, Li T, Thompson-Peer KL, Gong J, Murthy SE, Coste B, Yakubovich N, Patapoutian A, Xiang Y, Rompolas P, Jan LY, Jan YN (2019) The mechanosensitive ion channel Piezo inhibits axon regeneration. *Neuron* 102(2):373–389 e376. <https://doi.org/10.1016/j.neuron.2019.01.050>
17. Song Y, Ori-McKenney KM, Zheng Y, Han C, Jan LY, Jan YN (2012) Regeneration of *Drosophila* sensory neuron axons and dendrites is regulated by the Akt pathway involving Pten and microRNA bantam. *Genes Dev* 26(14): 1612–1625. <https://doi.org/10.1101/gad.193243.112>
18. Li D, Li F, Guttipatti P, Song Y (2018) A *Drosophila* in vivo injury model for studying neuroregeneration in the peripheral and central nervous system. *J Vis Exp* 135. <https://doi.org/10.3791/57557>
19. Grueber WB, Jan LY, Jan YN (2002) Tiling of the *Drosophila* epidermis by multidendritic sensory neurons. *Development* 129(12): 2867–2878
20. Shimono K, Fujimoto A, Tsuyama T, Yamamoto-Kochi M, Sato M, Hattori Y, Sugimura K, Usui T, Kimura K, Uemura T (2009) Multidendritic sensory neurons in the adult *Drosophila* abdomen: origins, dendritic morphology, and segment- and age-dependent programmed cell death. *Neural Dev* 4:37. <https://doi.org/10.1186/1749-8104-4-37>
21. Han C, Jan LY, Jan YN (2011) Enhancer-driven membrane markers for analysis of non-autonomous mechanisms reveal neuron-glia interactions in *Drosophila*. *Proc Natl Acad Sci U S A* 108(23):9673–9678. <https://doi.org/10.1073/pnas.1106386108>
22. Grueber WB, Jan LY, Jan YN (2003) Different levels of the homeodomain protein cut regulate distinct dendrite branching patterns of *Drosophila* multidendritic neurons. *Cell* 112(6): 805–818. [https://doi.org/10.1016/s0092-8674\(03\)00160-0](https://doi.org/10.1016/s0092-8674(03)00160-0)
23. Xiang Y, Yuan Q, Vogt N, Looger LL, Jan LY, Jan YN (2010) Light-avoidance-mediating photoreceptors tile the *Drosophila* larval body wall. *Nature* 468(7326):921–926. <https://doi.org/10.1038/nature09576>
24. Petersen LK, Stowers RS (2011) A Gateway MultiSite recombination cloning toolkit. *PLoS One* 6(9):e24531. <https://doi.org/10.1371/journal.pone.0024531>
25. Li F, Sami A, Noristani HN, Slattery K, Qiu J, Groves T, Wang S, Veerasammy K, Chen YX, Morales J, Haynes P, Sehgal A, He Y, Li S, Song Y (2020) Glial metabolic rewiring promotes axon regeneration and functional recovery in the central nervous system. *Cell Metab* 32(5):767–785 e767. <https://doi.org/10.1016/j.cmet.2020.08.015>



Assessing Rewiring of the Retinal Circuitry by Electroretinogram (ERG) After Inner Retinal Lesion in Adult Zebrafish

Lindsey M. Barrett, Peter C. Meighan, Diana M. Mitchell, Michael D. Varnum, and Deborah L. Stenkamp

Abstract

Adult zebrafish respond to retinal injury with a regenerative response that replaces damaged neurons with Müller glia-derived regenerated neurons. The regenerated neurons are functional, appear to make appropriate synaptic connections, and support visually mediated reflexes and more complex behaviors. Curiously, the electrophysiology of damaged, regenerating, and regenerated zebrafish retina has only recently been examined. In our previous work, we demonstrated that electroretinogram (ERG) recordings of damaged zebrafish retina correlate with the extent of the inflicted damage and that the regenerated retina at 80 days post-injury exhibited ERG waveforms consistent with functional visual processing. In this paper we describe the procedure for obtaining and analyzing ERG recordings from adult zebrafish previously subjected to widespread lesions that destroy inner retinal neurons and engage a regenerative response that restores retinal function, in particular the synaptic connections between photoreceptor axon terminals and the dendritic trees of retinal bipolar neurons.

Key words Electroretinogram, Regeneration, Retina, Zebrafish, Ouabain, Lesion, Central nervous system, Photoreceptor, Retinal bipolar neuron, Eye

1 Introduction

The field of regenerative medicine seeks to develop treatments for damaged or diseased tissues by replenishing with new, functional tissues. For example, the National Eye Institute (NEI) announced in 2013 the Audacious Goals Initiative, “to replace cells of the retina that have been damaged by disease or injury and to restore their connections to the visual centers of the brain.” Approaches to achieve these goals range from the *in vitro* growth of retinal tissues for transplantation [1] to the stimulation of endogenous retinal stem cells to create progenitors capable of repopulating the retina

with new neurons [2]. The hallmark features of a successful regenerative approach are that the new retinal neurons will have appropriate functional connections with other retinal neurons and that the output neurons of the retina, the retinal ganglion cells, will have functional connections with their targets in the brain [3].

Efforts to induce endogenous regenerative responses in mammalian retina, which normally does not display such responses, are largely modeled from retinas of other vertebrates that are known to exhibit a functional regenerative capacity (reviewed by [4–7]). In particular, regenerative studies involving zebrafish have been highly informative, revealing that the stem cell sources of regenerated retina are the Müller glia [8–12], in addition to identifying a number of intrinsic and extrinsic factors necessary for regeneration [13–22]. Less well understood are the mechanisms underlying the re-establishment of functional neuronal circuitry within the retina [23–25] and the extent to which, and timing of when, visual function is restored [24, 26, 27].

Loss and recovery of visual function after a widespread chemical lesion to the retina have now been demonstrated in goldfish and in zebrafish by examining (i) visually mediated reflexes such as the dorsal light reflex [26, 28] and optokinetic nystagmus [28]; (ii) visually mediated behaviors, including the escape response [26], place-preference behaviors [27], and responses to visual stimuli using a classical conditioning approach [28]; and (iii) retinal physiology through the measurement of the electroretinogram (ERG) [24, 29]. The ERG is a minimally invasive method to evaluate the electrical responses initiated in the outer retina (primarily photoreceptors and bipolar neurons) in response to a visual stimulus, generally a light flash [30]. The ERG has seen broad use in aquatic vertebrates including zebrafish, for functional studies of models of retinal disease (e.g., [31–35]), but only minimal applications to date toward the study of retinal regeneration [24, 29]. The ERG shows considerable promise, however, for future studies of retinal regeneration, to more deeply analyze the restoration of photoreceptor–bipolar neuron connectivity [24, 36, 37], color sensitivity and processing [38, 39], photoresponse kinetics [40], adaptation, and other features of visual function [41]. Such future analyses will help to fill a large knowledge gap regarding the essential functionality of regenerated retina and to identify potential limitations and challenges of regenerative approaches for treating retinal disease. We have begun to address this knowledge gap through evaluation of ERG responses in adult zebrafish subjected to widespread damage of inner retinal layers and a period of regeneration [24]. Here we describe the ERG procedure used in these studies to obtain and analyze recordings from adult zebrafish.

2 Materials

2.1 Solutions

1. Anesthetic solution: Prepare fresh 200 mg/L tricaine methane sulfonate (MS-222) by adding 4.0 mL of thawed, 10 g/L Tris-buffered MS-222 (*see Note 1*) to a 250 mL glass beaker reserved only for zebrafish handling. Glassware used with live animals should be washed only with bleach and hot water, no detergent. Bring to 200 mL with zebrafish system water.
2. Intubation (gill perfusion) solution: Prepare fresh intubation solution by adding to a 50 mL conical, sterile centrifuge tube and 1 mL MS-222 stock +50 μ L rocuronium bromide stock (0.1 mg/mL; *see Note 2*); bring to 50 mL with system water.
3. Electrode solution (E3 medium): Prepare fresh E3 medium by diluting 16.5 mL 60 \times stock solution (*see Note 3*) with 983.5 mL ultrapure water, in a 1.0 L container.
4. 4% paraformaldehyde in sucrose phosphate solution: In a sterile 50 mL conical centrifuge tube, combine one ampule of 10 mL 16% paraformaldehyde with 4 mL 10 \times PO₄ buffer (pH 7.4) and 2 g sucrose. Bring volume to 40 mL with ultrapure water. Make aliquots of 750 μ L in 1.5 mL tubes to be stored in the freezer until needed. Thoroughly thaw, in a 65 °C water bath, one aliquot per extracted zebrafish eye (two per fish). Before using fixative, ensure that it is well mixed with no visible precipitate. This solution is only required if you wish to conduct post-ERG histological analysis on fixed eye tissues.
5. Zebrafish system water: Collected from the zebrafish aquatic housing system.

2.2 Supplies

1. Plastic bags: Polyethylene (3–4 mil) live fish shipping bags, 6 $\frac{1}{4}$ in X 21 in for each fish.
2. Fish-safe beakers: These are reserved only for zebrafish handling (have been washed only with bleach and hot water, no detergent).
3. Glass capillary tubes for pipette fabrication: 1.2/0.68 mm (outer diameter/inner diameter) borosilicate glass capillary tubes.
4. Microfil flexible needle or similar.
5. Sapphire blade microknife (double-edged lancet, 0.75 mm wide, 60°).
6. Nitrile gloves.
7. Wet recording bed: Thoroughly moistened and folded Kim-wipes or sponge with anesthetic solution.
8. Tool to transfer fish from anesthetization solution to ERG chamber: A plastic spoon with holes drilled into it so liquid can drain, or a plastic transfer pipette cut in half to be used as a scoop.

2.3 Equipment

1. The ERG setup consists of an isolated recording chamber located on a low-vibration table (Kinetic Systems) surrounded by a Faraday cage. A Nikon SMZ645 stereomicroscope is used for positioning fish and placing recording electrode under red light. For light stimulation, we use a Solis-3C High-Power White LED (Thorlabs) as our light source, located outside the Faraday cage, and a fiber-optic pathway directed at the zebrafish eye; light intensity control is accomplished using neutral density filters with defined log unit attenuation. Evoked electrical events are recorded with a Ag/AgCl electrode in ESW-M12N microelectrode holder (Warner Instruments) and an AC differential amplifier/headstage system (Model 1800, A-M Systems) and digitized using a computer interfaced PowerLab acquisition system with LabChart Pro software (AD Instruments). Electrode positioning is achieved using MX1680R manipulator (Siskiyou Instruments). Reference and ground disc electrodes (8 mm × 1 mm disc, A-M Systems) are placed under the zebrafish and outside of direct light to avoid possible light stimulus artifacts. Platinum lead extension cables (Natus) are connected to disc electrodes via solderless male pins (AMP INC) to minimize system noise. This setup is similar to that of [30]. As an alternative to our custom ERG setup, off-the-shelf systems can be purchased (*see* **Note 4**).
2. P-97 Micropipette Puller (Sutter Instruments) with trough heating filament.
3. Regulated oxygen air source including plastic tubing and air-stone diffuser to oxygenate gill perfusion (intubation) solution.
4. Vacuum supply for periodic aspiration of media from recording chamber.
5. Darkroom light.
6. Zebrafish perfusion apparatus: A gravity drip system to perfuse the gills of adult zebrafish with oxygenated media. For our system we use a glass separating funnel fitted with an IV administrative set that includes a roller clamp and drip chamber for flow-rate control.

3 Methods

3.1 Dark Adaptation and Recording Preparation

1. Assess retinal damage prior to recording (optional) (*see* **Note 5**).
2. Dark-adapt the zebrafish: Fill a plastic bag with about 3 inches of system water and use the transfer net to transfer the zebrafish to the bag. Tie the top of the bag, leaving at least 3 inches of airspace to protect the fish during transport and to ensure

sufficient oxygen. Ensure knot is tight to prevent air loss during transport. Place bagged fish into a Styrofoam cooler with a tight-fitting lid to maintain a dark interior. Zebrafish should be dark-adapted for at least 30 min prior to recording (*see Note 6*).

3. Transport cooler(s) to room containing the ERG setup and other equipment, and place in dark cabinet to further ensure dark adaptation.
4. Pull a glass capillary tube using P-97 Micropipette Puller, and subsequently break the tip of the micropipette with fine forceps to achieve a tip opening diameter of 15–25 μm (*see Note 7*). Fill with E3 medium, using the Microfil flexible needle and position on recording electrode holder.
5. Add intubation solution to the perfusion system and begin lightly oxygenating. The intubation solution should be continuously oxygenated throughout the duration of the recordings.
6. Line the bottom of the recording chamber with a Kimwipes wiper that has been moistened with anesthetic solution. This can be positioned over the reference electrode (e.g., Ag/AgCl pellet assembly).

3.2 Preparation of Zebrafish for Recording

1. Turn off all regular room lighting and turn on darkroom (red) light. Place the red filter over the light source (stimulation light) of the ERG setup.
2. Using a fish transfer net, transfer a dark-adapted zebrafish to the anesthetic solution (MS-222), and allow it to remain there until spontaneous movement has ceased, opercular movement is not evident, and the fish shows no startle response (does not move in response to tapping the beaker). The fish should be anesthetized within 30 s.
3. Transfer the fish to the MS-222-soaked tissue bed within the ERG chamber. The first fish to be tested should have at least one undamaged eye for validation of the setup. This eye should be positioned upward toward the light source.
4. Place the perfusion tube within the fish's mouth, such that gills will be perfused with the anesthetic and muscle relaxant solution at a flow rate of approximately 1 mL/min. Ensure that the intubation medium is flowing over the gills.
5. Using the sapphire microknife (the sharpest edge is marked with a black dot; *see Note 8*), make an incision in the cornea, parallel with the dorsal–ventral axis of the eye, with the midpoint of the incision between the center of the eye and the most nasal point of the eye. The incision must be deep enough to penetrate the zonule fibers/tissues separating the anterior and posterior chambers but must not damage the retina itself (*see Note 9*).

6. Insert the recording electrode into the vitreous chamber through the incision, and position the tip of the electrode in the small space between the lens and the retina. The electrode tip should not touch the lens as this introduces noise into the recording.
7. Turn off the stimulation light and remove the red filter. Monitor the fish for several minutes to ensure the stability of the intubation and electrode placement and that the fish is deeply anesthetized and immobilized.

3.3 Light Stimulation and ERG Recording

1. Select appropriate light stimulus duration (*see Note 10*) and interstimulus interval (ISI; *see Note 11*) based on the ERG features to be examined. Begin a series of test recordings with these settings and monitor the amplitudes and topographical features of the evoked responses (*see Note 12*). Record 5–10 ERG waveforms (“sweeps”) to evaluate consistency of the response and for signal averaging, depending on the signal-to-noise ratio. To isolate cone-driven responses, a constant (rod-saturating) background light can be imposed prior to bright light stimuli. This can be accomplished via a secondary light source at approximately 60 lux [30].
2. To determine the sensitivity of the regenerating retina, it is useful to assess the light intensity–response relationship. This can be accomplished by using a series of neutral density filters of logarithmically graded optical density. Begin by collecting responses with maximal light attenuation, and then replace with successively lower optical density filters until the evoked responses achieve saturation. This approach can also reveal the threshold light stimulus level needed to elicit a reproducible ERG response above background noise.
3. Remove the recording electrode and gently turn the fish over to the opposite side—such that the eye with retinal damage or regeneration is facing the light source. Repeat **steps 4–6** under Subheading 3.2 (Preparation of Zebrafish for Recording), ensuring that the intubation and electrode placement are stable (*see Note 13*). Be sure to aspirate liquid from the recording chamber between recordings from each eye. Too much liquid in the chamber can introduce noise into the recording.
4. Repeat **steps 1–2** (*see Note 14*).
5. Gently extubate the fish and transfer to a clean work surface or a dissecting microscope. Proceed to Subheading 3.4 (Post-ERG Acquisition Steps) for that fish.
6. If additional zebrafish are to be evaluated on the same day, repeat **steps 1–5** for each fish (*see Note 15*). Aspirate liquid from the recording chamber between fish.

3.4 Post-ERG Acquisition Steps

1. Use an OLAW-approved method to ensure zebrafish death (*see Note 16*). Based on AVMA 2020 Guidelines on Euthanasia, fish are exposed to buffered MS-222 for at least 30 min after the cessation of opercular movement, or euthanized by ice water bath exposure for 10 min after cessation of opercular movement, followed by decapitation.
2. If collecting retinal tissues for histological analyses, enucleate eyes and process for fixation (*see Note 17*).
3. Offline analysis: Digitized waveforms can be imported into one of a number of data-analysis software packages (e.g., Prism, Igor, MATLAB). If present, the b-wave amplitudes can be extracted as the difference between the peak of the b-wave and subsequent trough. For stimulus response curves, b-wave amplitudes as a function of light intensity can be fit with the Naka–Rushton function: $\frac{V}{V_{\text{MAX}}} = \frac{I^n}{I^n + K^n}$, where V is the b-wave amplitude, V_{MAX} is the maximum b-wave amplitude, I is the illuminance, K is the illuminance at half-maximal amplitude, and n is a coefficient relating to the slope of the relationship. Note that extensive damage of inner retinal neurons can result in the absence of a detectable b-wave. This necessitates alternative analytical strategies to compare damaged vs. control ERG waveforms (*see Note 18*).

4 Notes

1. 50 mL of 10 g/L MS-222 stock solution is made by adding 0.5 g pharmaceutical-grade MS-222 to 1 mL 1 M Tris–HCl buffer in ultrapure water. In fish-safe container, bring to 50 mL with ultrapure water; adjust pH to 7.0 using 1 M NaOH added dropwise. Prepare 4.0 mL aliquots and freeze for future use. Preparation of MS-222 stock from the crystalline solid requires the use of nitrile gloves, protective clothing, chemical safety goggles, and an N95 mask and should be done in a fume hood or sealed container.
2. To make 0.1 mg/mL rocuronium bromide stock solution, add 0.1 mg rocuronium bromide powder to ultrapure water, for a final volume of 1.0 mL. This stock solution can be made in a 1.5 mL microcentrifuge tube. The presence of a paralytic agent in the intubation solution means that for the recording portion of the procedure, depth of anesthesia is more difficult to monitor. However, we have carried out identical recordings over the same length of time but in the absence of the paralytic agent. Under those conditions we observed that anesthesia is maintained as expected; however opercular and gill motor activities contaminate the ERG recordings. Remember to replenish the solution between recordings and make more as needed.

3. To make 60× stock E3 solution, dissolve 34.8 g NaCl, 1.6 g KCl, 5.8 g CaCl₂•2H₂O, and 9.78 g MgCl₂•6H₂O in 1.95 L ultrapure water. Adjust pH to 7.2 adding 0.1 M NaOH dropwise. Adjust volume to 2.0 L using ultrapure water and autoclave.
4. Alternative off-the-shelf ERG systems include ColorDome LabCradle (Diagnosys), which uses a Ganzfeld-type light stimulator and Diagnosys Espion software and is suitable for zebrafish and other small species.
5. The day before a planned ERG recording, intended damage outcomes and regeneration can be verified in numerous ways. The use of transgenic reporter lines with fluorescent proteins in targeted retinal cell types will allow the investigator to examine the retina of a live, anesthetized zebrafish with an epifluorescence stereomicroscope [24, 25, 42]. For example, the *smx2:mCherry; nyx::mYFP* dual transgenic [43, 44] can be examined for the presence of the row mosaic of mCherry+ blue-sensitive cones and absence of YFP+ bipolar neurons to verify selective damage to the inner retina (vs. the presence of both types of neurons in an undamaged contralateral eye). Damage outcome may also be verified through behavioral assays such as a place-preference assay [27, 45] or escape-response assay [26]; however, these approaches require that both retinas be damaged. Alternatively, unilateral retinal damage can be verified by the presence of an abnormal dorsal light reflex (DLR)—the zebrafish will swim in a “tilted” manner such that the damaged eye appears to look upward toward a source of downwelling light [26]. This approach is easier to incorporate when using non-shoaling, less active, and larger-bodied fish such as goldfish [28, 29].
6. We have found that the optimal time of day for obtaining ERG recordings of adult zebrafish appears to be in early to mid-afternoon local time. The zebrafish are otherwise maintained on a light–dark cycle such that light onset in the fish facility is 8:00 AM and light offset at 10:00 PM.
7. It is essential that the tip opening is even (i.e., non-jagged). It may require a few attempts to produce a suitable recording electrode.
8. The tip of the sapphire microknife is delicate and extremely sharp and should only touch the zebrafish eye. Avoid contact with other objects.
9. The preferred site of incision can be investigator-specific, with some investigators favoring the temporal approach (*see Note 13*).
10. The stimulus duration can vary depending on ERG features of interest. An advantage of using a long-duration stimulus (e.g.,

greater than 500 ms) is that it will produce a prominent b-wave (associated with the ON response) and subsequent d-wave (associated with the OFF response). A short-duration stimulus (e.g., 10 ms) is sufficient to produce a robust b-wave (ON response); however the d-wave (OFF response) is absent. An advantage of using a short-duration stimulus is that less recovery time is needed between stimuli.

11. To ensure complete recovery between flashes, we use a minimum interstimulus interval (ISI) of 10 s. It may be necessary to increase the ISI up to 30 s at saturating stimulus intensities (e.g., ND filter = 0).
12. A typical ERG waveform obtained from an adult zebrafish (undamaged) eye is characterized by several prominent waves, most notably a transient and downward-deflecting a-wave, indicating photoreceptor activity in response to light, followed by a larger magnitude, upward-deflecting b-wave, indicating the activity of ON-bipolar neurons [30]. A representative recording is presented in Fig. 1a. Figure 1b shows an example of a recording in which ongoing fish movement results in regular deflections that do not represent electrophysiological activity within the retina.

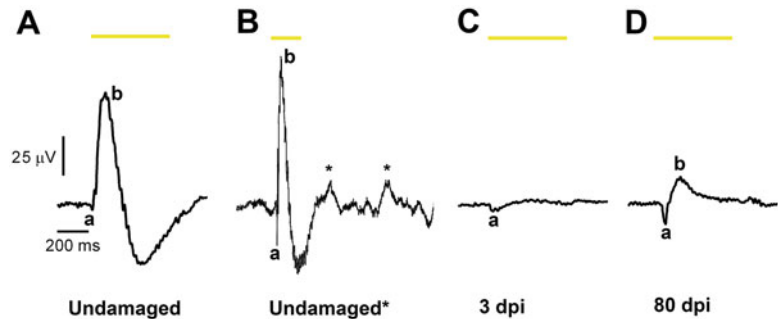


Fig. 1 Examples of ERG recordings from live, anaesthetized adult zebrafish. (a) Representative recording from an undamaged eye, showing a- and b-wave waveforms (labeled a, b). (b) Recording from an undamaged eye of an anesthetized fish with insufficient immobilization, such that residual motor activities result in deflections (some indicated by *s) not related to retinal physiology. (c) Representative recording from an eye subjected to a selective lesion of inner retinal neurons, at 3 days post-injury (3 dpi), showing an a-wave representing photoreceptor responses but a highly reduced/absent b-wave due to damage/death of bipolar neurons. (d) Representative recording from an eye subjected to selective lesion, but following 80 days of recovery/regeneration, showing an ERG waveform containing both an a-wave and a b-wave, consistent with the restoration of retinal function. Yellow horizontal lines indicate duration of light flash (500 ms for a, c, and d; 200 ms for b). (Panels a, c, and d were modified from Fig. 12 of [24], with permission)

13. Eyes containing retinas that have been recently damaged using intraocular toxin injection (e.g., 3 days post-injury; dpi) are extremely fragile, and so the investigator must use extreme caution in making this incision. The cornea is weak near the site of the previous incision (which was used to inject the neurotoxin), and so minimal force is needed to puncture the cornea. If the previous incision site is visible, it may be reused. Otherwise, the pressure exerted on the cornea while making the new incision can result in rupture of the previous incision, causing unnecessary tissue trauma and corneal damage. Eyes containing retinas that have regenerated (e.g., 80 dpi) also remain fragile. Consequently, the previous incision site can be reused in this case if possible. Additional consideration in recording from regenerated retinas is that the response to damage within the fish eye is not limited to the retina. These responses result in abnormalities such as an opaque lens, a duplicated (double) lens, and/or growth of the iris to cause a decrease in pupillary size [26, 29]. Any of these features can result in reduced light reaching the retina and should be taken into consideration when interpreting the ERG results.
14. ERG waveforms obtained from an adult zebrafish eye that has been recently damaged by intraocular injection of ouabain exhibit an altered waveform topography [24]. In the case of “selective” damage to the inner retina, waveforms display an a-wave that appears slightly exaggerated in comparison to that of undamaged retina (Fig. 1c), indicating that photoreceptors remain responsive to light. The b-wave, however, is highly reduced in amplitude or eliminated (Fig. 1c), indicating that the function, synaptic connection to, and/or presence of ON-bipolar cells has been greatly reduced [24]. Absence of the voltage-positive b-wave response essentially un.masks more of the voltage-negative a-wave response. ERG waveforms obtained from an adult zebrafish eye that has regenerated following this “selective” damage to inner retinal neurons, in contrast, have features more similar to that of undamaged retina (Fig. 1d) [24]. These features include an a-wave component and a b-wave component that displays a waveform similar to that of a normal b-wave response (when scaled to the normal waveform; [24]) but reduced in amplitude (Fig. 1d).
15. When obtaining ERGs from fish with one undamaged and one damaged/regenerated retina, there is a risk of bias if the recordings are always obtained from the undamaged retina prior to the injured retina. Therefore, we recommend recording from four to six fish and alternating the recording sequence (1, “damaged-then-undamaged”; 2, “undamaged-then-damaged”; etc.).

16. Recording of ERGs from live, anesthetized adult zebrafish may offer the potential for fish recovery following recording [30, 46], and thus the opportunity to obtain longitudinal ERG data over a time-course of retinal damage and regeneration, within individual fish. However, in our experience the length of time during which the fish are under anesthesia appears incompatible with this strategy. It is possible that future modifications of the procedure will ultimately allow repeated ERG recordings over the span of retinal regeneration in the same fish. Corneal placement of the recording electrode (rather than intravitreal) facilitated repeated measurements from the same fish, with intervening recovery times [46]. However, our approach provides robust information about waveform features and kinetics during regeneration, along with longer recording sessions for each fish.
17. If desired, whole eyes can be removed from humanely sacrificed zebrafish after ERG recordings, to process for directly correlating histological condition of the retina with physiology. Place eyes in freshly prepared 4% paraformaldehyde in phosphate-buffered (pH 7.4) 5% sucrose, and follow the procedure of [47]. Fixation times exceeding their recommended 1 h in paraformaldehyde at room temperature can still result in good histological outcomes (Fig. 2) and may be needed if a single investigator is collecting ERG recordings from multiple fish on a single day. If this is the case, fixation should initially be done on ice and can be continued overnight at 4 °C prior to the next step of the procedure.
18. A scaled sum-of-squares test can be used to assess whether the retinal-damage protocol produces ERG waveforms that are topographically distinct from controls. This entails scaling the “damaged” ERG trace such that its amplitude is equivalent to a grand average of the control waveform and calculating the sum-of-squared deviations between the control and “damaged” waveforms [24].

Acknowledgments

ERG studies of damaged and regenerated retinas in our laboratories using the approaches described have been supported by NIH R01 EY012146 (DLS), NIH R01 EY030467 (DMM), NIH R21 EY026814 (DLS and DMM), and NIH R21 AA028106 (MDV). We are also grateful for the support in the form of pilot grants and other funding from Idaho INBRE (NIH P20 GM103408) and the ADARP at Washington State University. We thank past and present members of the Stenkamp and Mitchell laboratories, particularly

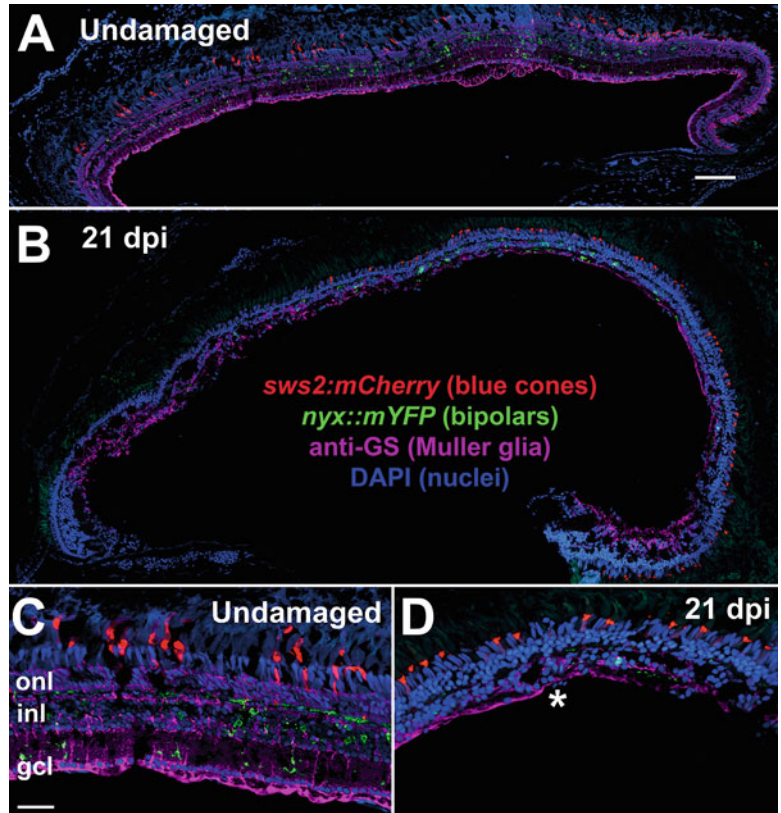


Fig. 2 Examples of histological preparations of retinal tissues following ERG recordings. (a) Sectioned undamaged retina following ERG recording. Labeling is for blue-sensitive cones (*sws2:mCherry* reporter [48]), a subpopulation of bipolar neurons (*nyx::mYFP* reporter [44]), anti-glutamine synthetase (GS; Müller glia [49]), and DAPI (nuclei). (b) Retinal cryosection of eye subjected to selective lesion of inner retinal neurons, with ERG recording obtained at 21 days post-injury (dpi); then the eye was fixed for histological processing. (c) Higher magnification view of retinal histology of undamaged retina after ERG recording (onl, outer nuclear layer; inl, inner nuclear layer; gcl, ganglion cell layer). (d) Higher magnification view of retinal histology of 21 dpi retina after ERG recording. Asterisk (*) lies beneath a region showing a “laminar fusion” in which nuclei occupy locations in the inner plexiform layer and there is little distinction between the inl and gcl, a feature typical of regenerated inner retina [27]. Scale bar in a (applies to b) = 100 μm ; scale bar in C (applies to D) = 50 μm

Ruth Frey for zebrafish husbandry. We also thank Kemal Donlic in the Varnum laboratory for the input on ERG setup design improvements. Transgenic lines *sms2:mCherry* and *nyx::mYFP* (in Fig. 2) were the kind gifts of Drs. Pamela Raymond and Rachel Wong, respectively.

References

1. Uyama H, Mandai M, Takahashi M (2021) Stem-cell-based therapies for retinal degenerative diseases: current challenges in the establishment of new treatment strategies. *Develop Growth Differ* 63(1):59–71. <https://doi.org/10.1111/dgd.12704>
2. Eastlake K, Lamb WDB, Luis J, Khaw PT, Jayaram H, Limb GA (2021) Prospects for the application of Muller glia and their derivatives in retinal regenerative therapies. *Prog Retin Eye Res*:100970. <https://doi.org/10.1016/j.preteyeres.2021.100970>
3. Angueyra JM, Kindt KS (2018) Leveraging zebrafish to study retinal degenerations. *Front Cell Dev Biol* 6:110. <https://doi.org/10.3389/fcell.2018.00110>
4. Massoz L, Dupont MA, Manfroid I (2021) Zebra-fishing for regenerative awakening in mammals. *Biomedicine* 9(1). <https://doi.org/10.3390/biomedicines9010065>
5. Gao H, Luodan A, Huang X, Chen X, Xu H (2021) Muller glia-mediated retinal regeneration. *Mol Neurobiol*. <https://doi.org/10.1007/s12035-020-02274-w>
6. Lahne M, Nagashima M, Hyde DR, Hitchcock PF (2020) Reprogramming Muller glia to regenerate retinal neurons. *Annu Rev Vis Sci* 6:171–193. <https://doi.org/10.1146/annurev-vision-121219-081808>
7. Konar GJ, Ferguson C, Flickinger Z, Kent MR, Patton JG (2020) miRNAs and Muller glia reprogramming during retina regeneration. *Front Cell Dev Biol* 8:632632. <https://doi.org/10.3389/fcell.2020.632632>
8. Yurco P, Cameron DA (2005) Responses of Muller glia to retinal injury in adult zebrafish. *Vis Res* 45(8):991–1002
9. Fausett BV, Goldman D (2006) A role for alpha1 tubulin-expressing Muller glia in regeneration of the injured zebrafish retina. *J Neurosci* 26(23):6303–6313
10. Bernardos RL, Barthel LK, Meyers JR, Raymond PA (2007) Late-stage neuronal progenitors in the retina are radial Muller glia that function as retinal stem cells. *J Neurosci* 27(26):7028–7040
11. Thummel R, Kassen SC, Montgomery JE, Enright JM, Hyde DR (2008) Inhibition of Muller glial cell division blocks regeneration of the light-damaged zebrafish retina. *Dev Neurobiol* 68(3):392–408
12. Nagashima M, Barthel LK, Raymond PA (2013) A self-renewing division of zebrafish Muller glial cells generates neuronal progenitors that require N-cadherin to regenerate retinal neurons. *Development* 140(22):4510–4521. <https://doi.org/10.1242/dev.090738>
13. Fausett BV, Gumerson JD, Goldman D (2008) The proneural basic helix-loop-helix gene *ascl1a* is required for retina regeneration. *J Neurosci* 28(5):1109–1117
14. Qin Z, Barthel LK, Raymond PA (2009) Genetic evidence for shared mechanisms of epimorphic regeneration in zebrafish. *Proc Natl Acad Sci U S A* 106(23):9310–9315
15. Ramachandran R, Reifler A, Parent JM, Goldman D (2010) Conditional gene expression and lineage tracing of tubal1a expressing cells during zebrafish development and retina regeneration. *J Comp Neurol* 518(20):4196–4212. <https://doi.org/10.1002/cne.22448>
16. Ramachandran R, Zhao XF, Goldman D (2011) *Ascl1a*/Dkk/beta-catenin signaling pathway is necessary and glycogen synthase kinase-3beta inhibition is sufficient for zebrafish retina regeneration. *Proc Natl Acad Sci U S A* 108(38):15858–15863
17. Powell C, Grant AR, Cornblath E, Goldman D (2013) Analysis of DNA methylation reveals a partial reprogramming of the Muller glia genome during retina regeneration. *Proc Natl Acad Sci U S A* 110(49):19814–19819. <https://doi.org/10.1073/pnas.1312009110>
18. Powell C, Elsaedi F, Goldman D (2012) Injury-dependent Muller glia and ganglion cell reprogramming during tissue regeneration requires Apobec2a and Apobec2b. *J Neurosci* 32(3):1096–1109. <https://doi.org/10.1523/JNEUROSCI.5603-11.2012>
19. Nelson CM, Ackerman KM, O'Hayer P, Bailey TJ, Gorsuch RA, Hyde DR (2013) Tumor necrosis factor-alpha is produced by dying retinal neurons and is required for Muller glia proliferation during zebrafish retinal regeneration. *J Neurosci* 33(15):6524–6539. <https://doi.org/10.1523/JNEUROSCI.3838-12.2013>
20. Lenkowski JR, Qin Z, Sifuentes CJ, Thummel R, Soto CM, Moens CB, Raymond PA (2013) Retinal regeneration in adult zebrafish requires regulation of TGFbeta signaling. *Glia* 61(10):1687–1697. <https://doi.org/10.1002/glia.22549>
21. Wan J, Zhao XF, Vojtek A, Goldman D (2014) Retinal injury, growth factors, and cytokines converge on beta-catenin and pStat3 signaling to stimulate retina regeneration. *Cell Rep* 9(1):

- 285–297. <https://doi.org/10.1016/j.celrep.2014.08.048>
22. Nagashima M, D’Cruz TS, Danku AE, Hesse D, Sifuentes C, Raymond PA, Hitchcock PF (2020) Midkine-a is required for cell cycle progression of Muller glia during neuronal regeneration in the vertebrate retina. *J Neurosci* 40(6):1232–1247. <https://doi.org/10.1523/JNEUROSCI.1675-19.2019>
 23. D’Orazi FD, Zhao XF, Wong RO, Yoshimatsu T (2016) Mismatch of synaptic patterns between neurons produced in regeneration and during development of the vertebrate retina. *Current Biology: CB* 26(17):2268–2279. <https://doi.org/10.1016/j.cub.2016.06.063>
 24. McGinn TE, Mitchell DM, Meighan PC, Partington N, Leoni DC, Jenkins CE, Varnum MD, Stenkamp DL (2018) Restoration of dendritic complexity, functional connectivity, and diversity of regenerated retinal bipolar neurons in adult zebrafish. *J Neurosci* 38(1):120–136. <https://doi.org/10.1523/JNEUROSCI.3444-16.2017>
 25. McGinn TE, Galicia CA, Leoni DC, Partington N, Mitchell DM, Stenkamp DL (2019) Rewiring of the regenerated zebrafish retina: Reemergence of bipolar neurons and cone-bipolar circuitry following an inner retinal lesion. *Front Cell Dev Biol* 7:95. <https://doi.org/10.3389/fcell.2019.00095>
 26. Sherpa T, Fimbel SM, Mallory DE, Maaswinkel H, Spritzer SD, Sand JA, Li L, Hyde DR, Stenkamp DL (2008) Ganglion cell regeneration following whole-retina destruction in zebrafish. *Dev Neurobiol* 68(2):166–181. <https://doi.org/10.1002/dneu.20568>
 27. Sherpa T, Lankford T, McGinn TE, Hunter SS, Frey RA, Sun C, Ryan M, Robison BD, Stenkamp DL (2014) Retinal regeneration is facilitated by the presence of surviving neurons. *Dev Neurobiol* 74(9):851–876. <https://doi.org/10.1002/dneu.22167>
 28. Lindsey AE, Powers MK (2007) Visual behavior of adult goldfish with regenerating retina. *Vis Neurosci* 24(3):247–255
 29. Mensinger AF, Powers MK (1999) Visual function in regenerating teleost retina following cytotoxic lesioning. *Vis Neurosci* 16(2):241–251
 30. Makhankov YV, Rinner O, Neuhauss SC (2004) An inexpensive device for non-invasive electroretinography in small aquatic vertebrates. *J Neurosci Methods* 135(1–2):205–210. <https://doi.org/10.1016/j.jneumeth.2003.12.015>
 31. Lewis A, Wilson N, Stearns G, Johnson N, Nelson R, Brockerhoff SE (2011) *Celsr3* is required for normal development of GABA circuits in the inner retina. *PLoS Genet* 7(8):e1002239. <https://doi.org/10.1371/journal.pgen.1002239>
 32. Stearns G, Evangelista M, Fadool JM, Brockerhoff SE (2007) A mutation in the cone-specific *pde6* gene causes rapid cone photoreceptor degeneration in zebrafish. *J Neurosci* 27(50):13866–13874
 33. Schlegel DK, Glasauer SMK, Mateos JM, Barmettler G, Ziegler U, Neuhauss SCF (2019) A new zebrafish model for CACNA2D4-dysfunction. *Invest Ophthalmol Vis Sci* 60(15):5124–5135. <https://doi.org/10.1167/iovs.19-26759>
 34. Dona M, Slijkerman R, Lerner K, Broekman S, Wegner J, Howat T, Peters T, Hetterschijt L, Boon N, de Vrieze E, Sorousch N, Wolfrum U, Kremer H, Neuhauss S, Zang J, Kamermans M, Westerfield M, Phillips J, van Wijk E (2018) Usherin defects lead to early-onset retinal dysfunction in zebrafish. *Exp Eye Res* 173:148–159. <https://doi.org/10.1016/j.exer.2018.05.015>
 35. Ali Z, Zang J, Lagali N, Schmitner N, Salvenmoser W, Mukwaya A, Neuhauss SCF, Jensen LD, Kimmel RA (2020) Photoreceptor degeneration accompanies vascular changes in a zebrafish model of diabetic retinopathy. *Invest Ophthalmol Vis Sci* 61(2):43. <https://doi.org/10.1167/iovs.61.2.43>
 36. Moyano M, Porteros A, Dowling JE (2013) The effects of nicotine on cone and rod b-wave responses in larval zebrafish. *Vis Neurosci* 30(4):141–145. <https://doi.org/10.1017/S0952523813000187>
 37. Wong KY, Gray J, Hayward CJ, Adolph AR, Dowling JE (2004) Glutamatergic mechanisms in the outer retina of larval zebrafish: analysis of electroretinogram b- and d-waves using a novel preparation. *Zebrafish* 1(2):121–131. <https://doi.org/10.1089/zeb.2004.1.121>
 38. Nelson RF, Singla N (2009) A spectral model for signal elements isolated from zebrafish photopic electroretinogram. *Vis Neurosci* 26(4):349–363
 39. Meier A, Nelson R, Connaughton VP (2018) Color processing in zebrafish retina. *Front Cell Neurosci* 12:327. <https://doi.org/10.3389/fncel.2018.00327>
 40. Renninger SL, Gesemann M, Neuhauss SC (2011) Cone arrestin confers cone vision of high temporal resolution in zebrafish larvae. *Eur J Neurosci* 33(4):658–667. <https://doi.org/10.1111/j.1460-9568.2010.07574.x>

41. Chrispell JD, Rebrik TI, Weiss ER (2015) Electroretinogram analysis of the visual response in zebrafish larvae. *J Vis Exp* 97. <https://doi.org/10.3791/52662>
42. Duval MG, Chung H, Lehmann OJ, Allison WT (2013) Longitudinal fluorescent observation of retinal degeneration and regeneration in zebrafish using fundus lens imaging. *Mol Vis* 19:1082–1095
43. Sifuentes CJ, Kim JW, Swaroop A, Raymond PA (2016) Rapid, dynamic activation of Muller glial stem cell responses in zebrafish. *Invest Ophthalmol Vis Sci* 57(13):5148–5160. <https://doi.org/10.1167/iovs.16-19973>
44. Schroeter EH, Wong RO, Gregg RG (2006) In vivo development of retinal ON-bipolar cell axonal terminals visualized in *nyx::MYFP* transgenic zebrafish. *Vis Neurosci* 23(5):833–843. <https://doi.org/10.1017/S0952523806230219>
45. Sherpa T, Hunter SS, Frey RA, Robison BD, Stenkamp DL (2011) Retinal proliferation response in the buphthalmic zebrafish, *bugeye*. *Exp Eye Res* 93(4):424–436. <https://doi.org/10.1016/j.exer.2011.06.001>
46. Nadolski NJ, Wong CXL, Hocking JC (2021) Electroretinogram analysis of zebrafish retinal function across development. *Doc Ophthalmol* 142(1):99–109. <https://doi.org/10.1007/s10633-020-09783-y>
47. Barthel LK, Raymond PA (1990) Improved method for obtaining 3-microns cryosections for immunocytochemistry. *J Histochem Cytochem* 38(9):1383–1388
48. Salbreux G, Barthel LK, Raymond PA, Lubensky DK (2012) Coupling mechanical deformations and planar cell polarity to create regular patterns in the zebrafish retina. *PLoS Comput Biol* 8(8):e1002618. <https://doi.org/10.1371/journal.pcbi.1002618>
49. Peterson RE, Fadool JM, McClintock J, Linser PJ (2001) Muller cell differentiation in the zebrafish neural retina: evidence of distinct early and late stages in cell maturation. *J Comp Neurol* 429(4):530–540. [https://doi.org/10.1002/1096-9861\(20010122\)429:4<530::aid-cne2>3.0.co;2-c](https://doi.org/10.1002/1096-9861(20010122)429:4<530::aid-cne2>3.0.co;2-c)



Analysis of Visual Recovery After Optic Nerve Crush in Adult Zebrafish

An Beckers, Steven Bergmans, Annelies Van Dyck, and Lieve Moons

Abstract

Zebrafish can successfully regenerate axons after optic nerve crush (ONC). Here, we describe two different behavioral tests to map visual recovery: the dorsal light reflex (DLR) test and the optokinetic response (OKR) test. The DLR is based on the tendency of fish to orient their back to a light source, and it can be tested by rotating a flashlight around the dorsolateral axis of the animal or by measuring the angle between the left/right body axis and the horizon. The OKR, in contrast, consists of reflexive eye movements triggered by motion in the visual field of the subject and is measured by placing the fish in a drum on which rotating black-and-white stripes are projected.

Key words Axonal regeneration, Optic nerve crush, Retinotectal system, Retina, Zebrafish, Visual recovery, Behavioral test, Dorsal light reflex, Optokinetic response, Neurobiology

1 Introduction

Adult zebrafish subjected to optic nerve crush (ONC) represent a valuable model system to investigate axonal regeneration, as outlined in chapter 9. Here, we will describe two behavioral assays to (1) map visual recovery after ONC, or after any other model affecting visual performance, or (2) study visual ability in mutant fish with reduced sight. Both tests allow a longitudinal follow-up of the same (group of) fish at multiple time points. The first method is the DLR test, which is based on the fact that fish equalize light input in both eyes by orienting their back toward incoming light in order to maintain a horizontal swimming position [1, 2]. A first way to perform a DLR test is to place the fish in a tight tube containing water and then spin a light source from the dorsal side of the fish to the lateral side (*see* Subheadings 3.1 and 3.2). The zebrafish will tilt and turn its back toward the direction of the light if that eye receives light input. In contrast, the animal will retain its original position if the optic nerve is damaged [1, 3]. The DLR can

also be evaluated by recording the swimming position and more specifically by quantification of the dorsoventral axis of the animal (*see* Subheadings 3.3 and 3.4). The normal horizontal position indeed shifts toward a slightly oblique one immediately after ONC, when the fish is blind, in an attempt to balance the amount of light entering both eyes [1, 4]. The second behavior-based visual recovery protocol is the OKR test. Similar as for the DLR, OKR testing in adult zebrafish is performed while restricting the fish in a small tube, but here the animal will be surrounded with a black-and-white stripes-containing rotating drum (*see* Subheadings 3.5, 3.6, 3.7, and 3.8). Due to the movement of these stripes, an OKR is evoked, which consists of (1) a slow and smooth eye movement to follow the stripes and (2) a subsequent fast reset of the eye position in the opposite direction. This reflexive behavior is innate to humans and virtually all vertebrates. After ONC, zebrafish are not able to distinguish the black-and-white stripes, so no OKR is triggered, but soon after injury it reappears. Changing the thickness of the stripes and thereby changing the spatial frequency of the stimulus enables to thoroughly measure the visual acuity of the fish as thicker stripes are more easily observed than thinner ones [1, 2].

2 Materials

2.1 DLR Test Method 1

1. Zebrafish of similar size and age.
2. Aquarium fishnet.
3. Flashlight with a focused light beam.
4. Cylindrical glass container with one closed and one open end. The length should be approximately 50 mm and the diameter 12 mm, to restrain an individual adult zebrafish.
5. Funnel with an opening that fits on the opening of the cylindrical container.
6. Parafilm.
7. Black pieces of paper.
8. One extra person for assistance.

2.2 DLR Test Method 2

1. Video camera.
2. Translucent plastic container ($2.7 \times 17.5 \times 20.0$ cm), filled with 400 mL of aquarium system water. It is important that the width of the container is small so that enough video frames in which the fish swims toward the camera are obtained.
3. Fiji software program.

2.3 OKR Test

1. Tricaine stock solution: 0.3% w/v ethyl 3-aminobenzoate methanesulfonate salt–tricaine powder (MS-222), 20.6 mM

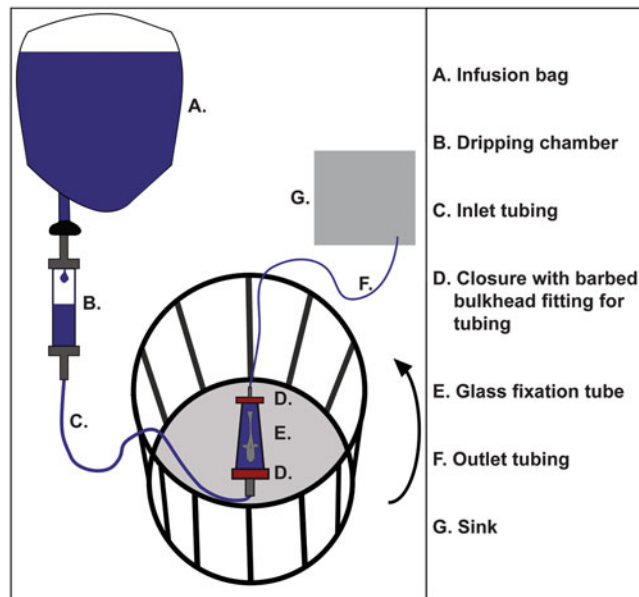


Fig. 1 Overview of the OKR setup. The infusion bag (A) is connected to the dripping chamber (B), necessary to provide water to the fish via the inlet tubing (C). The fish is restrained inside a glass fixation tube (E), closed with barbed bulkhead fitting (D). Water will be discarded via the outlet tubing (F) in the sink (G)

Tris-HCl, pH 7 (adjusted with 1M HCl) in ultrapure water. The 0.3% tricaine stock can be stored at 4 °C up to 6 weeks if kept in the dark.

2. Tricaine working solution: Dilute 7 mL of the tricaine stock solution in 93 mL aquarium system water in a 250 mL glass beaker (0.02% tricaine). Diluted tricaine can be kept at 4 °C maximally for 1 week when kept in the dark.
3. Small fish holder: Plastic Pasteur pipette (3 mL) from which half of the upper part (pipette bulb) is removed by making a longitudinal cut using scissors. In this way a convenient small fishnet/holder is created to take out fish from a narrow beaker. A tiny fishnet can be used as well, if available.
4. Optokinetic monitoring system (*see Note 1*).
5. Infusion bag (5 L), filled with ± 5 L aquarium system water (*see Fig. 1*, material A).
6. Support stand for infusion bag.
7. Burette clamp.
8. Infusion set with drip chamber and roller clamp (*see Fig. 1*, material B).
9. PVC tubing (*see Fig. 1*, materials C and F).

10. Two closures with barbed bulkhead fitting for tubing (*see* Fig. 1, material D).
11. Glass tube with double head screw cap (inner diameter ± 1.5 cm) (*see* Fig. 1, material E).
12. Hook-and-loop fasteners.
13. Tape.
14. Parafilm.
15. Waste container (at least 5 L) (*see* Fig. 1, material F).
16. Transparent stand made out of plexiglass ($15 \times 15 \times 15$ cm) with a hook-and-loop fastener (± 3 cm²) attached to the center of the stand.
17. Sponge.

3 Methods

3.1 DLR Method 1 Test Subject Preparation

1. Fill the cylindrical glass container with aquarium system water and hold it vertically.
2. Put the funnel on top of the open part of the container and place the fish gently in the center of the funnel. In this way the fish will fall into the glass container (*see* **Note 2**).
3. Close the container with parafilm.
4. Gently place the closed container horizontally on the black paper (*see* **Note 3**). In 80% of the cases, the fish is spontaneously oriented with its head toward the closed part of the glass container, which is ideal to perform the DLR test. Tilt the container to evoke a 180° turn, if the fish is oriented with its head faced to the parafilm (*see* **Note 4**).
5. Turn off the light in the room.

3.2 DLR Method 1 Testing and Quantification

1. This assay requires two people: one person to manipulate the flashlight movement and one person to focus on the position of the fish, and more specifically the eyes.
2. Make sure that nobody enters the room during the testing period.
3. Perform the DLR test first on the uncrushed, right eye. Keep a distance of ± 60 cm between the light source and the fish. Slowly rotate the flashlight from the dorsal (0°) to the right lateral side of the fish (90°), ultimately giving sole input to the right eye. The duration of flashlight rotation is 5–10 s. Because the right optic nerve is uninjured, fish show an inclination of their dorsoventral axis in this setup, or a “full DLR” (*see* below). Testing the DLR of the uninjured eye therefore serves as a control step.

4. Perform the DLR test for the left, injured eye in the same way as for the right eye (*see Note 5*).
5. The response of the adult fish is divided into three categories, based on the position of the light-exposed eye relative to the non-light-exposed eye at the end of the DLR, when the light source is positioned completely lateral (90°): (1) a “full” DLR which corresponds to a fish where the body axis completely follows the movement of the light bundle, resulting in a position of the light-exposed eye below the non-light-exposed eye, when drawing a fictive horizontal line through both eyes, (2) a “partial” DLR when the fish does show body axis tilting but maximally tilted in such a way that the targeted eye is not completely located beneath the non-targeted eye, and (3) “no DLR” in case the fish does not respond to the moving light influx at all and thus not tilt its body axis, indicative for a lack in basic visual perception.
6. Analyze the DLR data using chi-square statistics.

3.3 DLR Method

2 Test Subject Preparation

1. Fill the plastic container with 400 mL aquarium system water and place it on a black paper on a bench.
2. Position the camera facing the smallest side of the container.
3. Zoom in until the container fills the complete field of view.
4. Let the fish swim freely in the container for 5 min.

3.4 DLR Method

2 Testing and Quantification

1. Make sure that nobody enters the room during the testing period.
2. After the habituation period, take a video record of approximately 2 min.
3. Out of all the video frames, select three separate takes in which the fish swims in a straight line toward the camera, thus with its rostral–caudal body axis parallel to the base of the container.
4. Using Fiji, measure the angle between the horizon (0°), starting from the lowest positioned eye, and the left/right body axis, measured using a straight line through the eyes. Upon ONC, zebrafish swim in a slightly oblique position (approximately 10°), which reverses gradually during the regeneration process.
5. Test the data regarding the body axis angle using a one-way analysis of variance (ANOVA) repeated measurement test.

3.5 OKR Test

Equipment Setup

1. Fill the infusion bag with aquarium system water and connect the closed infusion set (*see Note 6*) (*see Fig. 1*, materials A–B).
2. Replace the screw caps from the glass tube with the two closures with barbed bulkhead fitting for tubing (*see Note 7*) (*see Fig. 1*, materials D–E). Place a small sieve at the distal end of

the glass tube, the furthest point from the infusion bag, to prevent the fish from getting stuck in the outlet tubing.

3. Add a hook-and-loop fastener around the most proximal closure, as well as to the transparent stand (the transparent stand is not shown in Fig. 1 for clarification).
4. Connect the infusion set to the most proximal closure with barbed bulkhead fitting for tubing (*see* Fig. 1, material C) while connecting a drainage tube to the distal closure. Fix the drainage/outlet tube to a waste container (or sink) with some tape (*see* Fig. 1, materials F–G), located beneath the OptoMotry system to avoid stationary water.
5. Seal all connection points with parafilm to avoid leakage.
6. Hang the infusion bag filled with aquarium system water near the OptoMotry equipment using a support stand with the burette clamp (not shown in Fig. 1).
7. Slowly open the scroll clamp from the infusion set to completely fill the water flow system with aquarium system water. Set the water flow to one droplet per s during the complete duration of the OKR test.
8. Adhere the glass tube to the transparent stand (using the hook-and-loop fastener) and place in the center of the OptoMotry setup.
9. Place a sponge between the lid of the OptoMotry setup to avoid squeezing of the tubes when closing the lid and thus obstruction of water flow (*see* **Note 8**).

3.6 OptoMotry Software

1. Turn on the computer and run the OptoMotry software. A two-panel program will open consisting of an “OptoMotry Controller” and “Camera” panel.
2. Adjust the spatial frequency, contrast, and drift speed of the stimulus (rotating black-and-white stripes) within the “Stimulus” window, “Gratings” tab. Set these to 0.042 c/d, 100%, and 010.0 d/s, respectively. Leave “Calibration” tabs untouched since this is accurately calibrated by CerebralMechanics Inc.
3. If a video recording of the OKR test is required, adjust preference for magnification, frame rate, etc., within the different tabs of the “Camera” window (*see* **Note 9**). Leave the “Calibration” tab untouched.
4. Specify the OKR test approach in the “Testing” window. Set the psychophysical method, directions, and threshold within the “Psychophysics” tab as follows: simple staircase (*see* **Note 10**), manual/combine, and frequency. For fish there is a maximum of “Seven Reversals” and a termination at 1.00%. In the “Option” tab, a “Yes/No” and “End of Run” feedback is

required when having “Yes/No Buttons” as a response. The options are “reserved.” After each measurement the system is reset to “100% Contrast” and “Min Preset Freq.” Turn off all other settings. Set “Trial Duration” to 5.0 s, “Tracking Blank” to “Gray,” and “Ref Frequency” to 0.100 c/d. Use the “Presets” described in “Prusky et al., 2004” for rodents and [5] and adapt for zebrafish (*see Note 11*). We set the “Highest Frequency” to 0.450 c/d. However, this parameter may vary between different zebrafish lines and should be determined before starting an experiment. Set the “Lowest Frequency” to 0.042 c/d with an “amount of six Frequencies.”

5. In the OptoMotry Menu Bar, a movie file can be prepared within the “Movie” tab, “New Movie File.” Within the “Camera” panel (where your fish is depicted), “start/record” the movie using Button 1 in the sidebar, or “Pause” the movie using Button 2. Click the “Center Platform” button in the sidebar to center the camera feed. Turn on the “Center Tracking Cursor” and “Stimulus Direction” while performing a test to see the moving lines of the projected stimulus and their direction.
6. Click in between the eyes of the fish on the camera feed to start the stimulus and to enable the computational lines to rotate with the eyes of the fish as the center.
7. Save a movie/recording using the “Movie” tab in the OptoMotry Menu Bar and click on “Close Movie File” (*see Note 12*).

3.7 OKR Test Habituation

1. One day before testing, habituate fish to the OptoMotry setup to minimize stress during the actual measurements. Catch a fish and anesthetize in 0.02% tricaine working solution.
2. Transfer the sedated fish to the glass fixation tube with water flow (briefly stop the water flow by closing the roller clamp) using the small fish holder. Orient the fish against the current (head pointing toward the inlet tubing).
3. Place the fish positioned in the glass tube, in the OptoMotry system while presenting a white screen. Allow the fish to recover from the sedation by providing a continuous water flow (one droplet per s) before starting the test (*see Note 13*).
4. Display the stimulus for 3 min when the fish is fully conscious, followed by an additional 2 min of a white screen.

3.8 OKR Testing

1. Place a fish in the glass fixation tube (*see steps 1–3* of the OKR habituation) (*see Note 14*).
2. Once fully conscious, start testing by presenting the black-and-white-striped stimulus (*see Note 15*). Click anywhere on the computer screen where the camera feed is projected (preferable

in between the two eyes of the fish), or click the “Stimulus” button in the bottom bar of the “OptoMotry Controller” panel. Center the stimulus directions around the eyes of the subject using the “Center Tracking Cursor” button.

3. For every single frequency that is presented during the staircase approach, a minimum of three positive responses is required to proceed to a higher frequency (by clicking “Yes”). A response is defined positive when (1) the eyes of the fish follow the direction of the stimulus until it exits the field of view and (2) this is subsequently followed by an abrupt counter-direction movement of the eyes (*see Note 16*). Absence of a positive response for 1 min is defined as a negative response (click “No”), resulting in further testing of a lower spatial frequency following the staircase approach. Of note, in between positive responses, the direction of the stimulus is automatically changed, to exclude the occurrence of random eye movements.
4. When reaching the maximum spatial frequency and thus maximum visual acuity of the tested fish, the OptoMotry software will play the sound “Done” (*see Note 17*). Write down the maximum spatial frequency and click on “Done.” Before starting a new fish, click on “reset” and start the next test. Total time spent per fish should not exceed 15 min to minimize stress.

4 Notes

1. In the host lab, we use the OptoMotry setup of CerebralMechanics Inc., so all software settings are specifically intended to use for this system. Additional systems are commercially available or you can use a custom-made device.
2. If no funnel with an appropriate opening size is available, a funnel can be made with your hands.
3. The black paper is used to minimize light reflection, as this disturbs the DLR testing.
4. Positioning the fish with its head toward the closed part of the glass container can only take ± 90 s. After this time period, it is better to put the fish back in its tank and restart after several minutes to avoid stress. It is important that the head of the fish faces the closed (made of glass) part of the container as this gives a clear view on the eyes of the fish.
5. In our hands, zebrafish remain fairly calm inside the glass container during the DLR test. As they are not stressed, they are able to focus on the light input, which makes the DLR test trustable. Nevertheless, some fish do react on being placed in the narrow tube and make efforts to escape, e.g., swim toward

the ends or turn their bodies. In this case, let the fish first relax for ± 60 s before performing the DLR. If the test still fails because the fish is not focused on the light source, repeat the DLR after the fish had some recovery time in a tank. A last option is to remove the fish from the experiment, although normally a reliable DLR test can be performed for every zebrafish on every time point.

6. To easily fill the 5 L infusion bag, remove a spike from an infusion set and attach to a tube. This combination can be connected to a tap with aquarium system water maintaining a temperature ranging between 27.5 and 30 °C. Ideally, the complete setup is located in a thermoregulated room. We also advise to use an infusion set with dripping chamber to easily regulate water flow.
7. We use a custom-made glass fixation tube, simplifying the complete setup as we experienced that finding a glass tube with the correct inner diameter and the possibility to connect tubes from both ends is challenging.
8. Since the lid of the OptoMotry system cannot be fully closed, measurements should be carried out in a dark room.
9. In the host lab, settings in the “Video in” tab are set as follows while recording: max frame rate, auto display, 144% magnification, and 58 iSight focus. Within the “Overlay” tab, compass size is put to 154%, while cursor size, tick spacing, tick size, and blind mask are set to 70%, 85°, 5°, and 214%, respectively.
10. During a staircase approach, stimuli are presented in a bidirectional ascending and descending way regarding the tested spatial frequencies, meaning that when a stimulus is positively perceived, the frequency increases, while it decreases when a fish is not able to distinguish the black from the white lines. This will be repeated until the maximum perceived spatial frequency is reached.
11. Here, all settings are depicted for a functional OKR test in zebrafish. The majority of these settings are identical to an OKR test for mice which is described by Prusky et al. [5], except for some adjustments.
12. Due to the large amount of data created by recording the OKR test for all fish, we prefer to keep a written data log of the maximum spatial frequency of each fish, as an alternative. This is depicted in the “OptoMotry Controller” panel, “Stimulus” window, “Gratings tab” underneath the “Spatial Frequency”. The use of the written data log implies that the two first buttons in the “Camera” panel are not needed.
13. By increasing the water flow (within tolerable limits for the fish), the recovery time in the glass cylinder can be shortened.

14. In contrast to the DLR test, a bilateral crush is needed to evaluate visual acuity via the OKR test in fish. If a unilateral crush is performed, the OKR of the injured eye is influenced by the visual input in the uninjured eye, leading to false positive results. To avoid any visual input of a spared eye, which will influence the OKR, a standardized bilateral crush must be performed.
15. Immediately switching from the white screen to the stimulus might spook the fish leading to insufficient concentration/focus. Presenting a gray screen (for around 10 s) just before turning on the stimulus increases focus and simplifies testing.
16. During a positive response, both eyes will react simultaneously and similarly toward the presented stimulus. In order to distinguish this positive response from a random movement (due to a lack of focus), changing the direction of the stimulus is crucial. A positive response will reverse upon changing stimulus direction. To provoke attention when the fish is unfocused, one can quickly switch between “Gray screen/Black screen” and “Stimulus screen,” as well as change the direction of the stimulus or the frequency using the “Higher frequency” button in the “OptoMotry Controller” panel. Keep in mind to turn it off while measuring.
17. The OptoMotry system is equipped with audio, supporting an investigator while performing a OKR test. An audio file is played for every “Yes,” “No,” and “Done.”

Acknowledgments

We thank the present and former lab members of the Neural Circuit Development and Regeneration (NCDR) group, especially the ones forming the zebrafish research team, who have helped to develop these techniques over the years. This work was financially supported by fellowships and project grants from the Research Foundation Flanders (FWO), FWO Flanders-Quebec bilateral research grant, the KU Leuven Research Council, and L’Oréal-UNESCO (For Women in Science).

References

1. Bollaerts I, Veys L, Geeraerts E et al (2018) Complementary research models and methods to study axonal regeneration in the vertebrate retinofugal system. *Brain Struct Funct* 223: 545–567
2. Van houcke J, Bollaerts I, Geeraerts E et al (2017) Successful optic nerve regeneration in the senescent zebrafish despite age-related decline of cell intrinsic and extrinsic response processes. *Neurobiol Aging* 60:1–10. <https://doi.org/10.1016/j.neurobiolaging.2017.08.013>
3. Beckers A, Van Dyck A, Bollaerts I et al (2019) An antagonistic axon-dendrite interplay enables efficient neuronal repair in the adult zebrafish central nervous system. *Mol Neurobiol* 56:

- 3175–3192. <https://doi.org/10.1007/s12035-018-1292-5>
4. Diekmann H, Kalbhen P, Fischer D (2015) Active mechanistic target of rapamycin plays an ancillary rather than essential role in zebrafish CNS axon regeneration. *Front Cell Neurosci* 9: 251. <https://doi.org/10.3389/fncel.2015.00251>
 5. Prusky GT, Alam NM, Beckman S, Douglas RM (2004) Rapid quantification of adult and developing mouse spatial vision using a virtual optomotor system. *Investig Ophthalmol Vis Sci* 45: 4611–4616. <https://doi.org/10.1167/iovs.04-0541>

INDEX

A

- Adeno-associated virus (AAV) 95
- Animal models
- axolotl 237–245
 - Drosophila* 298, 401–418
 - mouse 2–5, 12, 20, 40, 44, 46, 48, 67, 89–92, 96, 97, 118, 148, 156, 170, 259, 280, 298, 354, 355, 362–364, 392, 394, 401
 - rat 392, 394
 - Xenopus 206, 279–308, 343, 348, 357, 359, 361, 362, 364
 - zebrafish 264
- Antibodies
- 5HT 88, 94
 - cholera toxin subunit B (CTB) 44–49, 51, 52
 - GFAP 88, 95
 - GFP 14, 45, 88, 94, 95, 98, 147, 150, 156, 159, 200, 205, 207, 212, 218, 286, 296, 304, 324, 328, 330, 331, 336, 339, 378, 379, 381, 384, 391, 404, 412
 - L-plastin 390, 391
 - MAP 2 166, 179
 - mCherry 147, 150, 391
 - PCNA 389–399
 - PSD-95 166, 175, 179, 182
 - pStat3 88, 94, 96, 98
 - synaptotagmin 2 164, 166, 179, 182
 - Thy1 4, 5, 8, 12
- Axon v, vi, 1, 20, 43, 102, 145, 164, 191, 205, 222, 247, 263, 311, 323, 401
- Axonal dynamics 247–260
- Axonal protein synthesis 155
- Axonal translation 148
- Axon regeneration v, 1–16, 19–41, 43, 86, 93, 102, 247, 248, 259, 260, 311, 312, 323–340, 368, 401–418
- Axotomy .v, 20, 101, 102, 118, 120, 247–260, 401–418

B

- Behavioral assay
- dorsal light reflex (DLR) 231, 422, 428, 437, 438
 - nociceptive behavior test 407–409, 417

- optokinetic response (OKR) test 438, 441–443
- Bioinformatics 279–308, 347, 354, 358, 362
- Brain v, 2, 40, 56, 60, 61, 66, 67, 80, 82, 85, 95–98, 164, 165, 173–177, 181, 182, 185, 187, 207, 210, 221, 248, 311, 312, 323, 324, 349, 421, 422

C

- Cell cycle 368, 381, 389
- Central nervous system (CNS) v, 1, 2, 19, 85, 86, 93, 97, 98, 163, 164, 206, 221, 238, 247, 279, 311, 343, 359, 402, 409, 411–417
- Chromatin accessibility 324, 328
- CNS axon regeneration v, 312
- Confocal microscopy 11, 51, 296, 371, 374, 378, 379, 391, 393, 399
- Cortical neuronal activity 55–69
- Cryosections 67, 93, 164, 175, 179, 181, 183, 187, 296, 389–399, 432

D

- Data analysis 151, 290–292, 328, 343–364, 427
- Dendritic remodeling 188
- Dorsal root ganglia (DRG) 101–142, 146, 148–153, 157, 158, 295, 402

E

- Electroretinogram 421–432
- Epigenetics vi, 101, 102, 222
- Euthanasia 5, 8, 320, 325, 328, 339, 359, 427
- Expression profiling 4, 280
- Eye 3, 8, 48, 56, 57, 60, 66, 87, 89, 90, 108, 116, 118, 171–176, 182, 183, 192, 193, 195, 198–200, 205–207, 209, 210, 212, 213, 215–218, 224–231, 253, 259, 305, 312, 314–316, 319, 321, 324, 326–330, 336, 338, 339, 372–375, 381, 382, 391, 397, 421, 423–432, 437–439, 441, 443, 444, 446

F

Fluorescence activated cell sorting (FACS).....3, 4, 6, 7, 9–15, 280, 324, 327, 328, 330, 331, 337
 Fluorescence recovery after photobleaching (FRAP).....146–155, 157, 158
 Fractionation43–52, 146, 346, 351, 360
 Functional enrichment analysis 354, 356, 358, 362, 363
 Functional recoveryv, 85, 86, 92, 98, 164, 222, 241, 263, 417, 418

G

Gene function..... 263–276
 Glaucoma.....4, 166, 206

H

Hyper-interleukin-6 (hIL-6) 86–88, 92, 94–96

I

Immediate early genes (IEGs)..... 14, 55–69
 Immunohistochemistry (IHC)..... 3, 7, 13, 55, 59
 Immunomagnetic separation..... 44
 Immunostaining..... 11, 93, 94, 166, 179, 192, 193, 196, 199, 297, 392, 393
 Injury models
 buccal optic nerve crush (*Xenopus laevis*)..... 209
 dorsal column axotomy (DCA)..... 101, 102, 118, 120
 intraocular optic nerve crush (zebrafish, mouse) .. 164
 larval zebrafish nerve transection models (optic nerve and spinal cord)..... 191
 laser axotomy in zebrafish and *Drosophila*..... v, 248, 401–418
 monocular enucleation 56, 57, 60
 sciatic nerve axotomy (SNA)..... 101, 102, 105, 118, 120, 128
 spinal cord contusion injury (axolotl)..... 238
 spinal cord crush 237–245
 ventral optic nerve crush (*Xenopus laevis*).... 206, 207
 In situ hybridization (ISH)55, 56, 64, 65, 67
 Interkinetic nuclear migration..... 368, 369, 374, 377–379, 381, 384, 386
 Intracortical injection86, 91, 92, 95, 96
 Intravitreal injection.....225
 Islet 2b 205
 iTRAQ 344, 346–348, 351, 352, 360, 361

L

Lesion 2, 93–95, 98, 101, 102, 104, 105, 118, 222, 224–228, 230–232, 239, 242, 263, 269, 271, 272, 274–276, 324, 391, 421–432

Live cell imaging 148, 151, 153, 158, 368, 369, 379
 Localized protein synthesis..... 146, 153, 156

M

Machine learning..... 40
 Microglia..... 3, 222, 231, 389–391, 394, 395, 397, 399
 Monocular enucleation56, 57, 60
 mRNA translation145, 146, 148, 155
 Müller glia 3, 222, 229, 368, 369, 378, 379, 381, 384, 386, 422, 432

N

Neurodegeneration205
 Neuronal resilience..... 1–16, 19–41
 Neuroprotection 1–16, 19–41
 Non-coding RNAs
 circRNA72–78, 80, 82
 miRNA..... 72, 74, 78–80, 82
 Non-model organisms 343

O

Optic nerve v, 2–4, 14, 20, 40, 43, 44, 47–49, 56, 164–166, 171–176, 180–183, 191, 192, 195, 199, 205–207, 209–213, 215–218, 229, 247, 305, 312, 314, 323–340, 372, 373, 382, 437, 439
 Optokinetic response (OKR) 438, 439, 441–443, 445, 446
 Ouabain 222–232, 367, 381, 391, 430

P

Peripheral nervous system (PNS).....v, 85, 158, 412, 417
 Photoreceptor 3, 4, 165, 182, 227, 229, 230, 312, 339, 368, 381, 422, 429, 430
 Proliferation..... 389–399

Q

Quantitative proteomics 343–364

R

R..... 22, 40, 291, 293
 Raphe 86, 95, 96
 Real time quantitative PCR (qRT-PCR) 72, 76–79
 Recovery56, 66, 86, 109, 118, 120, 140, 146, 148, 153–155, 158, 159, 167, 172, 173, 179, 184, 206, 208, 209, 211–214, 217, 223, 226, 227, 241, 256, 263, 325, 327, 338, 409, 417, 418, 422, 429, 431, 445
 Regulatory RNAs71–82

Retina..... v, 2, 3, 5, 8, 9, 12,
 14, 20, 164–166, 176, 179, 180, 182, 184, 185,
 193, 197, 198, 200, 206, 212, 216, 217, 221,
 222, 225, 228–231, 282, 294–296, 301, 304,
 305, 312, 315–317, 323–325, 327–329, 336,
 337, 339, 340, 368, 369, 372–375, 381–383,
 385, 390, 391, 395, 399, 421, 422, 425, 426,
 428–432
 Retinal ganglion cell (RGC)
 RGC purification.....4–7, 10
 Retinal slice culture.....369, 373, 375–379,
 381, 383–385
 Retinotectal system.....164, 165
 RNA 3'-terminal phosphate cyclase (Rtca).....401, 402,
 411, 412, 417, 418
 RNA isolation.....72, 109, 281, 288, 289
 RNA repair.....401–418

S

Sensory neurons.....101, 248, 295,
 402, 408, 412, 414
 Sequencing
 assay for transposase accessible chromatin
 (ATAC-seq).....102, 105, 106,
 115–117, 135, 143, 324–326, 328, 332–334,
 336, 338
 chromatin immunoprecipitation (ChIP-seq).....101
 laser capture microscopy-sequencing
 (LCM-seq).....311–321
 RNA-seq.....101–104,
 109–111, 120, 142, 143, 279–308

 single-cell RNA-sequencing (scRNA-seq).....vi, 2–4,
 8, 9, 11, 14–16, 19–21, 25, 40
 Single-cell dissociation.....5–9, 13
 Somatosensory.....248
 Spinal cord.....v, 85–98, 101,
 102, 108, 118, 120, 139, 175, 177, 191, 192,
 221, 237–245, 247, 251, 257–260, 263–276,
 343, 344, 349, 353, 357, 359, 360, 362, 402
 Spinal cord lesion.....85, 265, 266
 Splicing.....293, 401–418
 Supervised classification.....20, 21, 27, 28, 30
 Surgery.....2, 66, 89, 91, 97,
 102, 108, 116, 118–120, 183, 206–209, 212,
 214, 216–218, 314, 328, 336, 338, 344, 353

T

Thyl-stop-YFP.....4, 5, 8, 12
 Tissue lipid profiles.....43
 Transcription.....14, 77, 78, 81, 82, 86, 104,
 105, 110, 128, 138, 142, 143, 158, 323, 324
 Transient transgenesis.....248
 Translating Ribosome Affinity Purification
 (TRAP).....148, 156, 279–308

V

Vglut2-ires-cre.....4, 5, 12
 Visual recovery.....437, 438

Z

zif268.....56, 57, 59, 65, 66